

# **Structural Investigations on Sequence-Specific “Ant-Pro” Pseudo- $\beta$ -Turn**

**Thesis Submitted to the AcSIR for the Award of  
the Degree of  
DOCTOR OF PHILOSOPHY  
In Chemistry**



**By  
Vijayadas K. N.  
10CC11J26098**

**Under the guidance of  
Dr. G. J. Sanjayan**

**Division of Organic Chemistry  
CSIR-National Chemical Laboratory  
Pune 411008, Maharashtra, India**

**August 2014**

## CANDIDATE'S STATEMENT

I hereby declare that the thesis entitled “**Structural Investigations on Sequence-Specific *Ant-Pro* Pseudo  $\beta$ -Turn**”, submitted for the Degree of Doctor of Philosophy in Chemistry to the Academy of Scientific and Innovative Research (AcSIR), has not been submitted by me to any other university or institution. This work has been carried out at Division of Organic Chemistry, CSIR-National Chemical Laboratory, Pune under the supervision of Dr. G. J. Sanjayan.



**Vijayadas K. N.**



राष्ट्रीय रासायनिक प्रयोगशाला  
(वैज्ञानिक तथा औद्योगिक अनुसंधान परिषद)  
डॉ. होमी भाभा मार्ग पुणे - 411 008. भारत  
**NATIONAL CHEMICAL LABORATORY**  
(Council of Scientific & Industrial Research)  
Dr. Homi Bhabha Road, Pune - 411 008. India.




### CERTIFICATE BY THE SUPERVISOR

Certified that the work incorporated in the thesis entitled “**Structural Investigations on Sequence-Specific *Ant-Pro* Pseudo  $\beta$ -Turn**”, submitted by **Mr. Vijayadas K. N.** for the Degree of **Doctor of Philosophy** was carried out by the candidate under my supervision in the Division of Organic Chemistry, CSIR-National Chemical Laboratory, Pune, India. Materials obtained from other sources have been duly acknowledged in the thesis.

Date: 14 August 2014

**Dr. G. J. Sanjayan**

Communication  
Channels

  
NCL Level DID : 2590  
NCL Board No. : +91-20-25902000  
EPABX : +91-20-25893300  
+91-20-25893400

FAX

Director's Office : +91-20-25893355  
COA's Office : +91-20-25893619  
COS&P's Office : +91-20-25893008

WEBSITE

[www.ncl-india.org](http://www.ncl-india.org)



*Dedications*

*Faith ~ Family ~ Friends*

## Acknowledgement

*During the long period of my research work, I have been acquainted, accompanied and supported by many people. It is a pleasant aspect that I have now the opportunity to express my gratitude for all of them.*

*It is my great privilege to express my deep gratitude to my research supervisor Dr. G. J. Sanjayan for the guidance, unflinching support, timely advices and encouragement during the course of my Ph.D work. He helped me to overcome many difficulties during the reaction chemistry with his stimulating suggestions. I owe to thank my DAC members, Dr. Sudalai, Dr. Rajamohanan, Dr. Alok Sen for their constant guidance and advice. I owe my gratitude to Organic Chemistry Divisional Heads, Dr. Ganesh Pandey, Dr. R. A. Joshi and Dr. Pradeep Tripathi and Directors, Dr. S. Sivaram and Dr. Saurav Pal, for providing the infrastructure to work in this prestigious research institution.*

*I am grateful to Dr. P. R. Rajamohanan for his help in undertaking the 2D NMR studies which was of great help for the completion of my thesis work. I thank Amol, Hilda, and Jima from NMR facility for helping me with the NMR analyses. I thank Dr. Rajesh Gonnade and Dr. Vedavati. G. Puranik for their advices with single crystal X-diffraction studies. I thank Rupesh, Sridhar, Omkar, Archana, Debamithra, Ektha and Pranaya from X-ray facility for helping me with the crystal structure analyses. I express my warm and sincere thanks to Dr. Santhakumari, for helping me in performing the mass analyses.*

*I take this opportunity to express my heartfelt gratitude to my teachers who helped me to learn the basics of Chemistry. They encouraged me with their full support which made me to become more ambitious and practice science as a way of life. I am deeply indebted to them more than they know. I also express my thanks to my fellow class mates and college mates. I feel a deep sense of gratitude to my parents, Sura and Neelakandadas, Lalan and Shylaja, Sabitha, Sanoop, Nia, Aswathy (Achu), Jithin and Anu (my love and life). I also thank all my relatives who encouraged me to come up in life.*

*I would like to thank our NCL group members Pranjali, Sreenivas, Amol, Panchami, Arup, Ramesh, Gowri, Sangram, Roshna, Vijay Thorat, Tukaram, Ganesh, Sachin, Sanjeev, Shiva, Suresh R. Suresh M., Krishna, Adhiti, Kasthuri, Rashid, Jayasree, Raj and labmates Pinak and Ajay Kale for their cheerful company and support. I would like to thank all my friends Ajishettan, Manojettan, Shijochettan, Harichettan, Rajeesh, Suresh, Jijo, Sumesh, Alson, Rajesh, Jijil, Rahul, Mufsir, Sreenidhi, Renny, Reji, Hari, Sreekuttan, Arun, Sarath, Govind, Aneesh, Eldo, Anumon, Rajith, Shoy, Ashwin, Jithesh, Bihag, Bipin, leena, Aany, Manafikka, Shahid and many others. I will thank my all time friends Dil Raj, Balu, Shakti, Jibin, Kannan, Unni, Prabeed, Sanil etc. for their support.*

*I thank DST, DBT and CSIR, New Delhi, for the financial supports.*

*Finally, I would like to thank all those who have contributed to the successful realization of this dissertation as well as expressing my apology that I could not mention personally one by one. Finally I would thank the Almighty.*



**Vijayadas K N**

## Table of Contents

Abbreviations .....	iv
Thesis Abstract.....	vi
General Remarks.....	xiii
List of Publications .....	xiv

## CHAPTER 1

### **The Ant-Pro Reverse-Turn Motif: Structural Modifications around the Folding Core**

#### **PART A: *Significance of Hydrogen-bonding Potential of Ester and Amide Carbonyl in Folding of Ant-Pro Reverse Turn***

1.1 Hydrogen bond .....	2
1.2 Significance of the hydrogen bond in peptide folding .....	3
1.3 Amino acids and secondary structure of proteins .....	6
1.4 Resonance stabilization of a peptide bond .....	7
1.5 Amide to ester modifications .....	8
1.6 Peptide chain end-fraying .....	10
1.7 Absence of sequential hydrogen bonding at the termini .....	11
1.8 Peptide chain end-fraying as a consequence of swapping C-terminal amides with esters: A case study .....	11
1.9 Utilizing Ant-Pro reverse turn for the case study: The design strategy .....	12
1.10 Synthesis .....	13
1.11 Conformational Analyses .....	14
1.11.1 Single crystal X-ray diffraction studies .....	14
1.11.2 Solution state NMR studies .....	16
1.12 Simultaneous display of N-H···O hydrogen bonding and C-H···O interactions .....	19
1.13 Significance of swapping C-terminal amides with thioesters .....	19
1.14 Conclusions .....	20

#### **PART B: *Sulphonamides vs. Carboxamides at the N-Terminus of Ant-Pro Reverse Turn.***

1.15 The geometrical preferences of a sulfonamide bond .....	21
1.16 Objective of present work: Investigating the robustness of Ant-Pro C9 turn .....	21
1.17 Synthesis .....	22
1.18 Conformational analyses .....	23
1.18.1 Single crystal X-ray diffraction studies .....	23
1.18.2 Solution state NMR studies .....	24
1.18.3 Circular Dichroism (CD) studies .....	25
1.19 Conclusions .....	26

1.20 Biological activity studies of Ant-Pro dipeptides .....	26
1.21 Summary .....	27
1.22 Experimental procedures.....	28
1.23 Single crystal X-ray crystallographic data .....	45
1.24 Spectra of compounds .....	51
1.25 References.....	98

## CHAPTER 2

### Orthanilic Acid-Mediated Pseudo $\beta$ -turn Motifs

#### ***Robust Reverse Turn comprising Orthanilic Acid (<sup>S</sup>Ant) and Proline (Pro), featuring C-9 H-bonding***

2.1 Folding in peptides .....	104
2.2 Role of hydrogen bonding in peptide folding .....	104
2.3 Significance of backbone modification in peptides .....	105
2.4 Amino acids and secondary structure propensities .....	108
2.5 Torsion angles of peptide bond .....	109
2.6 Sulfonamides .....	110
2.7 Sulfonamides: A potent bioactive compound .....	111
2.8 Sulfonamides: A connecting element for foldamers or synthetic peptides .....	112
2.9 Sulfonamides vs. carboxamides in peptide folding - the utilization of the geometrical preferences of sulfonamide bond: Present study .....	112
2.10 Objective of present work: Investigating the robustness of <sup>S</sup> Ant-Pro C <sub>9</sub> turn .....	113
2.11 Synthesis .....	114
2.12 Conformational analyses .....	115
2.12.1 Single crystal X-ray diffraction studies .....	115
2.12.2 Solution state 2D NOESY NMR studies .....	115
2.12.3 DMSO- <i>d</i> <sub>6</sub> titration studies of <b>6</b> .....	116
2.12.4 MeOD exchange studies of <b>6</b> .....	116
2.13 The unusual conformational similarity of sulfonamides and carboxamides: Consequence of the robustness of <sup>S</sup> Ant-Pro inter-residual C <sub>9</sub> hydrogen-bond .....	117
2.14 Conformational investigations .....	118
2.14.1 Solid state structural investigations .....	118
2.14.2 Solution state IR dilution studies .....	120
2.15 Role of intra-residual hydrogen-bonding in stabilizing the <sup>S</sup> Ant-Pro turn formation .....	120
2.16 Synthesis .....	120
2.17 Conformational investigations in solid state .....	121
2.18 Stability of methyl ((2-aminophenyl)sulfonyl)prolinate: Formation of thiadiazepinones .....	121

## ***Reverse Turn Formation in <sup>S</sup>Ant-AA Residues: Role of Sulfonamide in Inducing Folding***

2.19 Objective of the work: Role of <sup>S</sup> Ant in <sup>S</sup> Ant-Pro C-9 turn formation .....	123
2.20 Synthesis .....	123
2.21 <sup>S</sup> Ant-NMe-Aib featuring C-9 Turn: Conformational investigations in solid state .....	126
2.22 Crystallization tendency of sulfonamides .....	128
2.23 Conclusions .....	128
2.24 Experimental procedures.....	129
2.25 Single crystal X-ray crystallographic data .....	141
2.26 Spectra of compounds .....	143
2.27 References.....	193

## **CHAPTER 3**

### **Studies Regarding the Role of Ant-Sulfonamide (<sup>S</sup>Ant) as Turn Inducer in Peptides**

#### **PART A: Multifaceted Folding in Orphanic acid (<sup>S</sup>Ant)-Based Reverse Turn Motifs.**

3.1 Non-covalent interactions and drug target receptors .....	200
3.2 Reverse turns - The targeted areas for drug receptors .....	200
3.3 Peptidomimetics - Tool for drug development .....	201
3.4 Multifaceted folding in mesyl-Xaa- <sup>S</sup> Ant-Yaa peptide residues: Present study .....	202
3.5 Objective of the work: Incorporation of <sup>S</sup> Ant in peptide sequences .....	202
3.6 Synthesis .....	202
3.7 Conformational analyses .....	204
3.7.1 Solid-state X-ray and solution state NMR studies .....	204
3.7.2 NMR DMSO- <i>d</i> <sub>6</sub> titration and variable temperature Studies .....	208
3.8 Conclusions .....	210

#### **Part B: Incorporation of <sup>S</sup>Ant in Aib-Pro β-Bends**

3.9 Incorporation of <sup>S</sup> Ant in Aib-Pro β-Bend peptide residues: Present study .....	211
3.10 Objective of the work: Role of conformational restriction on hydrogen bonding .....	211
3.11 Hybrid systems having multiple folds: Design strategy .....	212
3.12 Synthesis .....	213
3.13 Conformational analyses .....	214
3.13.1 Single crystal X-ray analysis .....	214
3.13.2 Solution-state NMR analysis .....	216
3.13.3 NMR titration and variable temperature Studies .....	217
3.14 Conclusions .....	220
3.15 Experimental procedures.....	221
3.16 Single crystal X-ray crystallographic data .....	231
3.17 Spectra of compounds .....	235
3.18 References.....	288



## ABBREVIATIONS

AA	Amino acid
Ac <sub>2</sub> O	Acetic anhydride
Å	Angstrom
AcCl	Acetyl chloride
[α] <sup>24</sup> <sub>D</sub>	Specific rotation
Aib	2-Aminoisobutyric acid
Ala	Alanine
Ant	Anthranilic acid
Arg	Arginine
Asn	Asparagine
Asp	Aspartic acid
Boc, <sup>t</sup> Boc	<i>tert</i> -butyloxycarbonyl
<sup>i</sup> Boc	<i>iso</i> -butyloxycarbonyl
Bn	Benzyl
CD	Circular Dichroism
CDCl <sub>3</sub>	Deuterated Chloroform
COSY	Correlation Spectroscopy
Cys	Cysteine
d	Doublet (NMR)
δ	Chemical shift (NMR)
DBU	1,8-Diazabicyclo[5.4.0]undec-7-ene
DCC	N,N-Dicyclohexylcarbodiimide
DCM	Dichloromethane
DIEA	N,N-Diisopropylethylamine
DMAP	4-Dimethylaminopyridine
DMF	N,N-Dimethylformamide
DMSO	N,N-Dimethylsulfoxide
DMSO- <i>d</i> <sub>6</sub>	Deuterated N,N-Dimethylsulfoxide
EDC.HCl	1-Ethyl-3-(3-dimethylaminopropyl)carbodiimide hydrochloride
ESI MS	ElectroSpray Ionisation mass spectrometry
Et <sub>3</sub> N	Triethylamine
EtOAc	Ethyl acetate
Gln	Glutamine
Gly	Glycine
Glu	Glutamic acid
H-bonding	Hydrogen bonding
HBTU	N,N,N',N'-Tetramethyl- <i>O</i> -(1 <i>H</i> -benzotriazol-1-yl)uronium hexafluorophosphate
HMBC	Heteronuclear Multiple Bond Correlation
His	Histidine
HOBt	Hydroxybenzotriazole
HSQC	Heteronuclear Single-Quantum Correlation
Ile	Isoleucine
IR	Infrared
LC MS	Liquid Chromatography mass spectrometry
Leu	Leucine
Lys	Lysine

m	Multiplet (NMR)
MALDI	Matrix-Assisted Laser Desorption/Ionization
MeCN,	
ACN	Acetonitrile
Mesyl-Cl	Methanesulfonyl chloride
Met	Methionine
MHz	Mega Hertz
MIC	Minimum Inhibition Concentration
mp	Melting point
nm	nanometre
NMR	Nuclear Magnetic Resonance
NOE, nOe	Nuclear Overhauser Effect
NOESY	Nuclear Overhauser Effect spectroscopy
Phe	Phenylalanine
Piv-Cl	Pivaloyl chloride
ppm	Parts per million
Rf	Rate of flow
R-factor	Residual factor
rt, RT	Room temperature
<sup>S</sup> Ant	Orphanic acid
s	Singlet (NMR)
Ser	Serine
t	Triplet (NMR)
TFA	Trifluoroacetic acid
THF	Tetrahydrofuran
Thr	Threonine
TOCSY	Total correlation Spectroscopy
TOF MS	Time of Flight mass spectrometry
Tosyl-Cl	Toluenesulfonyl chloride
Trp	Tryptophan
Tyr	Tyrosine
Val	Valine

## ABSTRACT

Name of the Candidate	<b>Vijayadas K. N.</b>
Name of the Research Guide	<b>Dr. G. J. Sanjayan</b>
Synopsis of the thesis entitled	<b>STRUCTURAL INVESTIGATIONS ON SEQUENCE SPECIFIC ANT-PRO PSEUDO BETA TURN</b>

**Preamble:** Hydrogen bonding plays significant role in rigidifying the conformation of peptide-based drugs, as the reverse turn regions are targeted areas for most of the receptors, particularly G-Protein Couple Receptors (GPCRs). By understanding the basic structural features, one can utilise these turn motifs for different applications, like structural mimicry of bioactive peptides, understanding biopolymer function *etc.*

**Objective:** The primary objective of this work was to investigate the effect of structural and backbone modifications that affect the hydrogen bonding patterns in reverse turns, particularly featuring  $\alpha/\beta$ -conjugated building blocks comprising  $\alpha$ -amino acid (proline) and unnatural  $\beta$ -amino acid (anthranilic acid). We also aimed at investigating the role of orthanilic acid (2-aminobenzenesulfonic acid) in inducing folding when incorporated into peptide sequences.

**Chapter 1:** This chapter deals with structural and backbone modifications around reverse-turn motif, consisting of L-proline and anthranilic acid subunits, that features nine-membered hydrogen bonding. It provides insights into consequences of various structural modifications of amide bond to esters, thioesters and sulphonamides of Ant-Pro reverse turn motif.

A part of the work describes the striking case of comparison of the individual contribution of C-terminal ester *vs.* amide carbonyl as hydrogen bonding acceptor in the folding of peptide secondary structure featuring a closed network of H-bonded ring. Ant-Pro reverse-turn motif, a simple two-residue peptide fold, serves as an easy model, with least interference from other opposing interactions originating from the backbone and / or side chains, in evaluating the extent of individual contribution of C-terminal ester *vs.* amide carbonyl as H-bonding acceptor in the formation of a peptide fold.

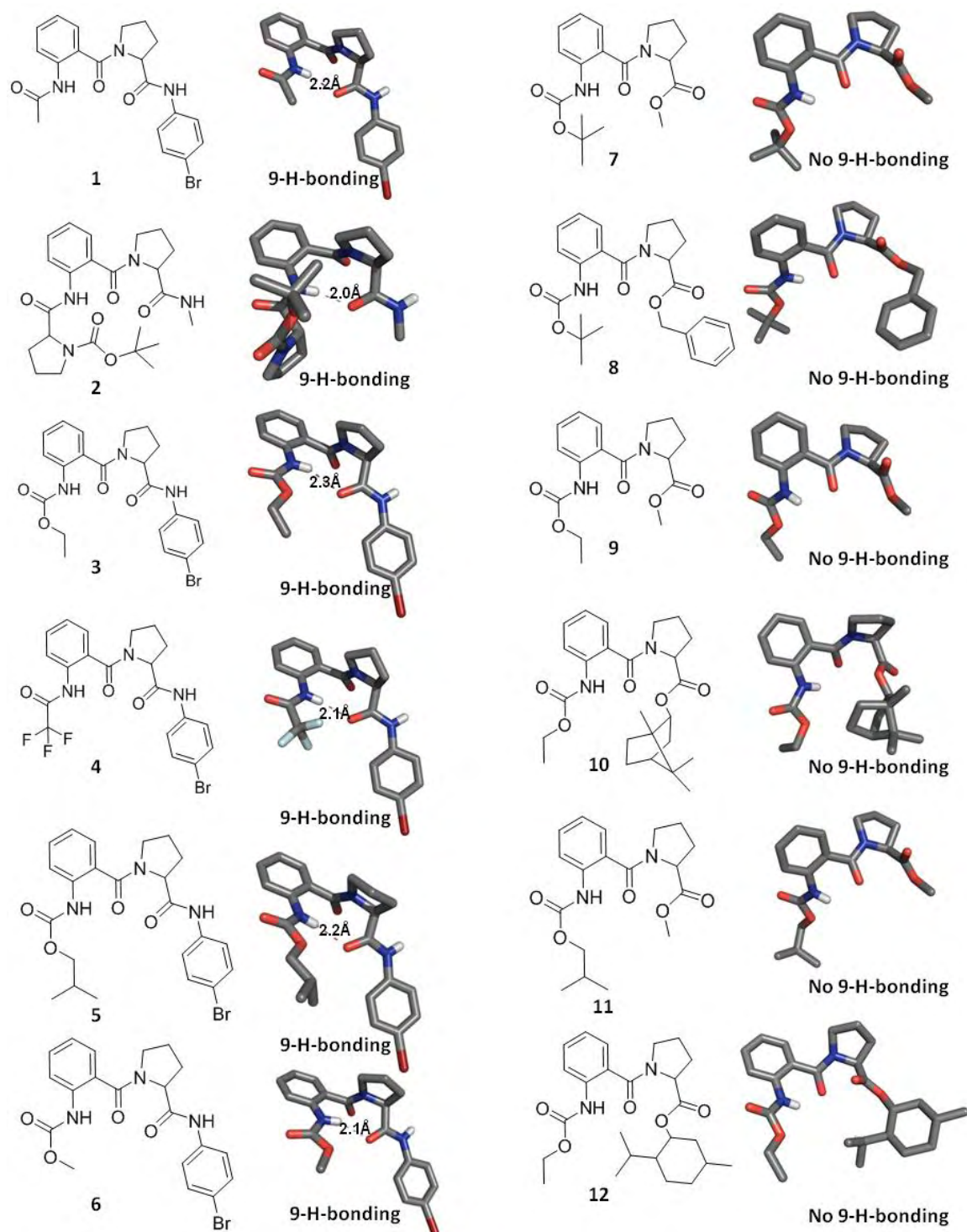


**Figure-1:** Molecular and crystal structures of C-terminal amides **1-6**, (left panel) and C-terminal esters **7-12** (right panel). *Note:* The amides assume folded conformation featuring 9-membered-ring hydrogen bonding (*9-H-bonding*), whilst the esters display fraying (*without 9-H-bonding*). In the crystal structures, all hydrogens, except the polar ones, have been deleted for clarity.

Results from the crystallographic studies of two large sets of C-terminal esters and amides unequivocally reveal the high propensity of the C-terminal amides, when compared to their ester counterparts, to stabilize a folded conformation [Figure 1]. The complete

manifestation of the individual contributions - ester *vs.* amide - in modulating the stability of the hydrogen-bonded network, free from involvement of other effects which would have otherwise noticeable in large oligomer systems, is notable [Figure 2].

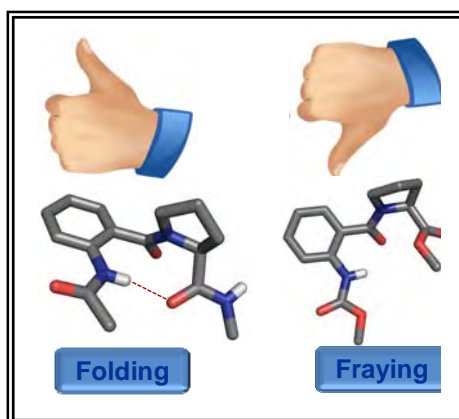


**Figure-2.** Schematic representation of Ant-Pro reverse-turn motif having C-terminal amide undergoing folding featuring nine-membered hydrogen bonding (left) while the C-terminal ester undergoing fraying featuring six-membered H-bonding (right).

[Ester *vs.* amide on folding: a case study with a 2-residue synthetic peptide. **Vijayadas, K. N.**; Nair, R. V.; Gawade, R. L.; Kotmale, A. S.; Prabhakaran, P.; Gonnade, R. G.; Puranik, V. G.; Rajamohanam, P. R.; Sanjayan, G. J.; *Org. Biomol. Chem.*, **2013**, *11*, 8348-8356]

Another part of this chapter deals with the backbone modifications of N-terminal Ant-Pro carboxamides with sulphonamides. Sulphonamides, with distinctly different structural geometry (twisted when compared to planar carboxamide) and hydrogen bonding preferences (two hydrogen bond acceptor oxygen atoms compared with one acceptor oxygen of carboxamide), are known to form unusual hydrogen bonding interactions. Structural modifications of amide to sulphonamide at the N-terminal of Ant-Pro reverse-turn strongly suggests a robust turn motif [Figure 3] raising the possibility of practical utility, particularly in rigidifying peptide backbone.

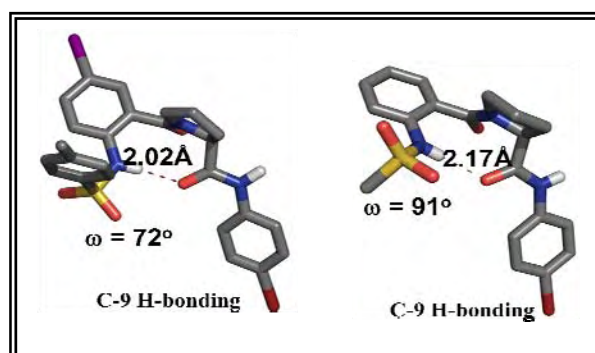


**Figure-3.** Crystal structures of tosyl- (left) and mesyl-Ant-<sup>L</sup>Pro-p(C<sub>6</sub>H<sub>4</sub>)Br (right) revealing stable reverse-turn architecture. (Hydrogens have been removed for clarity).

[The Ant-Pro Reverse-Turn Motif: Structural Features and Conformational Characteristics. Thorat, V. H.; Ingole, T. S.; **Vijayadas, K. N.**; Nair, R. V.; Kale, S. S.; Ramesh, V. V. E.; Davis, H. C.; Prabhakaran, P.; Gonnade, R. G.; Gawade, R. L.; Puranik, V. G.; Rajamohanan, P. R.; Sanjayan, G. J. *Eur. J. Org. Chem.* **2013**, 3529-3542]

**Chapter 2:** This chapter describes the unusual structural and conformational similarity showed by two peptide folds featuring a carboxamide (Ant-Pro turn) and a sulfonamide (<sup>S</sup>Ant-Pro) at the folding core. This observation is unusual for the fact that carboxamides and sulfonamides are known to augment entirely different conformational and geometrical preferences [Figure 4].

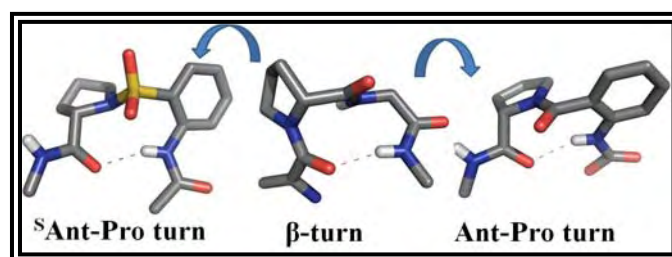


**Figure-4.** Schematic representation showing the structural similarity of Ant-Pro (carboxamide) and <sup>S</sup>Ant-Pro (sulphonamide) reverse-turn motifs to a normal  $\beta$ -turn.

[An unusual conformational similarity of two peptide folds featuring sulfonamide and carboxamide on the backbone. **Vijayadas, K. N.**; Davis, H. C.; Kotmale, A. S.; Gawade, R. L.; Puranik, V. G.; Rajamohanan, P. R.; Sanjayan, G. J. *Chem. Commun.* **2012**, 48, 9747-9749]

This chapter also details about the robustness of reverse turn motif featured by orthanilic acid (<sup>S</sup>Ant) and proline (Pro). Replacing proline with  $\alpha$ -amino acids showed the absence of folding, confirming the role of a cyclic imino acid (proline) in the turn formation [Figure 5]. N-methylation of the corresponding  $\alpha$ -amino acid residues led to retention of nine-membered hydrogen bonding (C-9 turn) explaining the role of <sup>S</sup>Ant (sulfonamide) in folding [Figure 6].

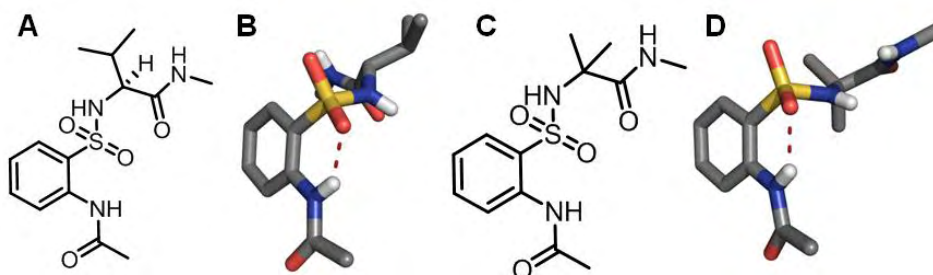


**Figure-5.** <sup>S</sup>Ant-AA motifs showing absence of nine-membered hydrogen bonding.

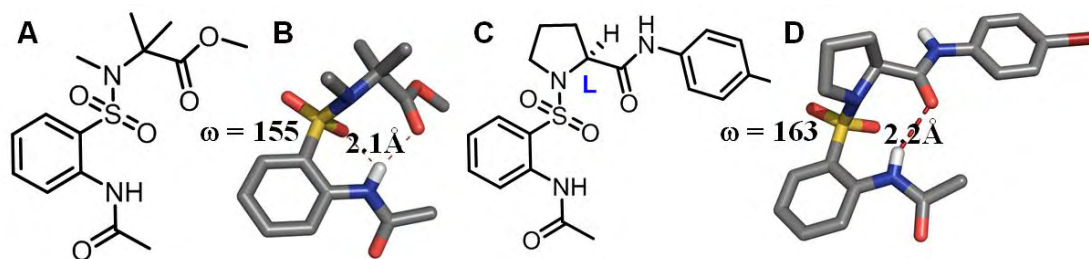


**Figure-6.** Structural similarity observed by Ac-<sup>S</sup>Ant-NMe-AA-OMe (A and B) and Ac-<sup>S</sup>Ant-Pro-NH (C and D) turn motifs featuring nine-membered hydrogen bonding.

**Chapter 3:** This chapter describes the design, synthesis and evaluation of conformational features of turn motifs featuring -Pro-<sup>S</sup>Ant-Pro- units. It also describes the role of <sup>S</sup>Ant in facilitating folding in peptides [Figure 7].

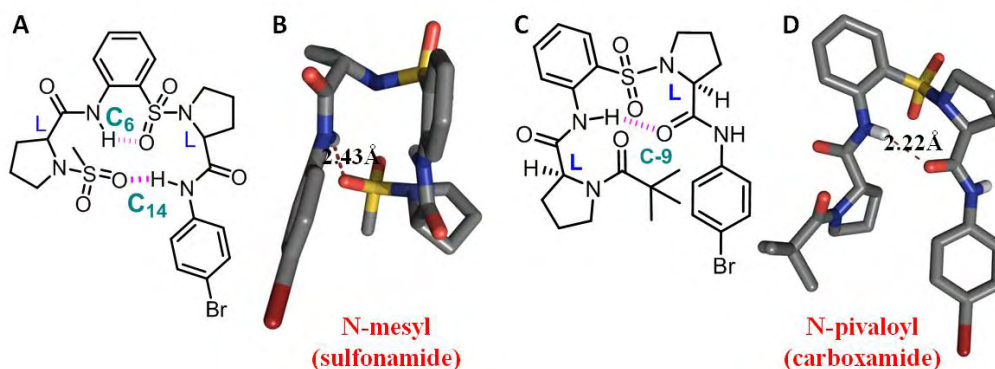


**Figure-7.** Conformational change in Pro-<sup>S</sup>Ant-Pro residues upon changing terminal carboxamide to sulphonamide: Mes-Pro-<sup>S</sup>Ant-Pro featuring C-14 hydrogen bonding (A and B) and Pivaloyl-Pro-<sup>S</sup>Ant-Pro featuring C-9 hydrogen bonding.

Pro-<sup>S</sup>Ant-Pro tripeptide unit, which adopted a nine-membered hydrogen bonding as observed in <sup>S</sup>Ant-Pro reverse turns, formed C-14 membered hydrogen bonding pattern upon converting the terminal carboxamide to sulphonamide [Figure 7]. Replacing one of the proline residues with constrained  $\alpha$ -amino acid like  $\alpha$ -amino isobutyric acid (Aib), as in three-residue folded peptide structures featuring mesyl-Xaa-<sup>S</sup>Ant-Yaa, exhibited folding patterns with diverse types of hydrogen bonding patterns, unlike that of Pro-<sup>S</sup>Ant-Pro residues. The diverse hydrogen bonding patterns were dependent on the terminal amino acid residues ( $i$  and  $i+2$ ) and presence of sulphonamide bond between the residues [Figure 7, 8]. This work also illustrates the versatility in the folding behaviour of <sup>S</sup>Ant-based foldamers to adopt unique conformational behaviour aided by C-6 residual hydrogen bonding and amide to sulphonamide modifications.

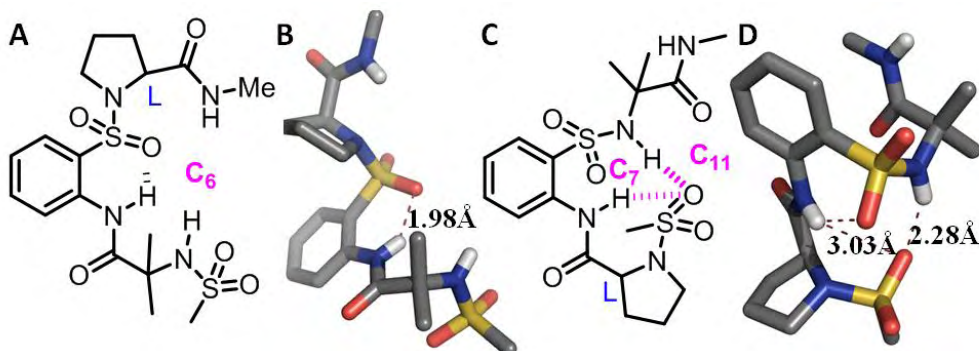


**Figure-8.** Mesyl-*Xaa*-<sup>S</sup>Ant-*Yaa* with multi-faceted folding: Mesyl-Aib-<sup>S</sup>Ant-Pro featuring C-6 hydrogen bonding (A and B) and mesyl-Pro-<sup>S</sup>Ant-Pro featuring C-10 hydrogen bonding (C and D).

[Multifaceted folding in mesyl-*Xaa*-<sup>S</sup>Ant-*Yaa* peptide turn motifs. Vijayadas, K. N.; Sanjayan, G. J. *Manuscript under preparation*]

A part of this chapter also deals with the synthesis and conformational investigations of orthanilic acid (2-aminobenzenesulfonic acid, <sup>S</sup>Ant)-based hybrid peptide sequences featuring multiple folds [Figure 9, 10]. The former system exists featuring a combination of a  $\beta$ -turn (Aib-Pro C<sub>10</sub> - between '*i*' and '*(i+3)*' amino acid residues) and an extended  $\beta$ -turn (Pro-<sup>S</sup>Ant-NHR C<sub>11</sub> - between '*i*' and '*(i+3)*' amino acid residues) [Figure 9]. The latter one failed to form the expected combination of a  $\beta$ -turn (Aib-Pro C<sub>10</sub> - between '*i*' and '*(i+3)*' amino acid residues) and a *pseudo*  $\beta$ -turn (<sup>S</sup>Ant-Pro C<sub>9</sub> - between '*(i-1)*' and '*(i+2)*' amino acid residues) [Figure 10] due to the conformational restriction offered by C-6 H-bonding of <sup>S</sup>Ant.

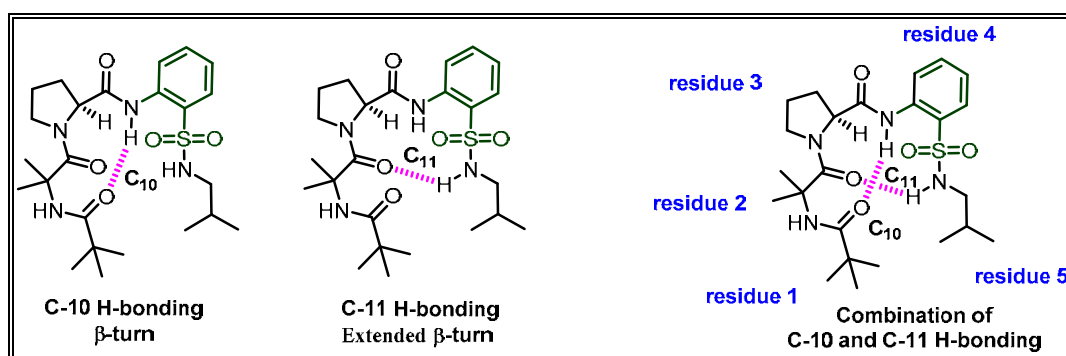


**Figure-9.** Piv-Aib-Pro-<sup>S</sup>Ant-NH<sup>i</sup>Bu featuring a combination of C-10 (Aib-Pro  $\beta$ -turn) and C-11 H-bonding (Pro-<sup>S</sup>Ant-NH<sup>i</sup>Bu extended  $\beta$ -turn).



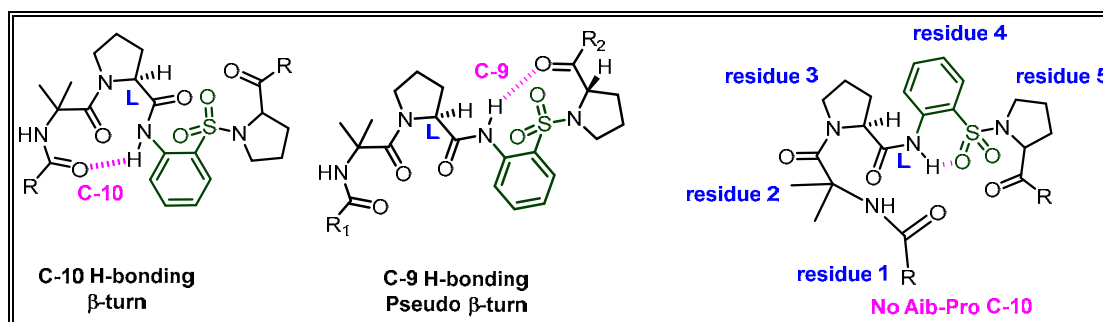


**Figure-10.** Piv-Aib-Pro-<sup>S</sup>Ant-Pro showing absence of C-10 H-bonding ( $\beta$ -turn) and C-11 H-bonding (pseudo  $\beta$ -turn).

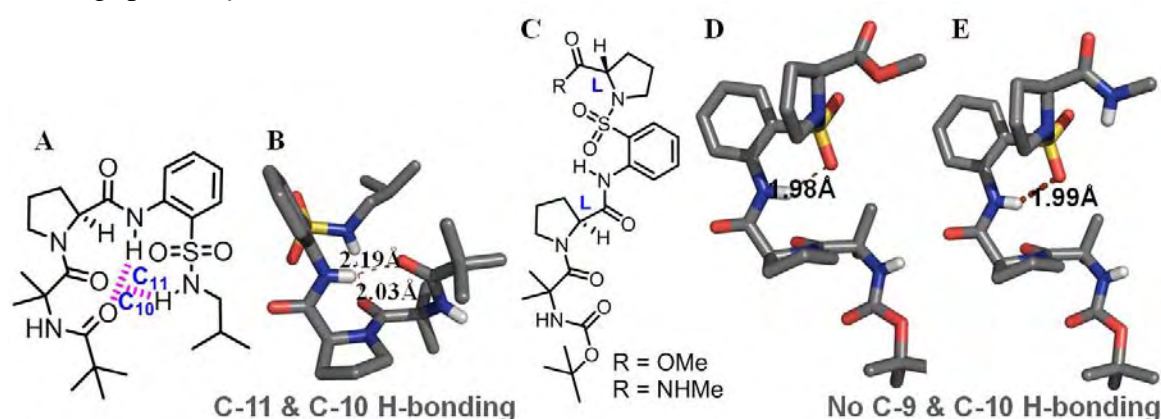


**Figure-11.** Piv-Aib-Pro-<sup>S</sup>Ant-NHiBu (A and B) showing Aib-Pro C-10  $\beta$ -bent structure. The  $\beta$ -bent C-10 H-bonded structure was absent in Boc-Aib-Pro-<sup>S</sup>Ant-Pro turn motifs (C-E).

[Orthanilic-based foldamer motifs featuring co-operative folding. **Vijayadas, K. N.;** Sanjayan, G. J. *Manuscript under preparation*]

Structural investigations, including solid-state crystal structure and solution-state NMR studies, revealed that the Aib-Pro C-10 hydrogen bonded structure got disrupted by the conformational restriction offered by the C-6 *intra-residual* hydrogen bonding of <sup>S</sup>Ant [Figure 11]. The case study is analogous to the instances in peptide systems, which are being subjected to adopt/evade multiple folds. It also provides the opportunity to understand multiple factors affecting the conformation of peptides.

## GENERAL REMARKS

- ✚ Unless otherwise stated, all the chemicals and reagents were obtained commercially.
- ✚ Required dry solvents and reagents were prepared using the standard procedures.
- ✚ All the reactions were monitored by thin layer chromatography (TLC) on precoated silica gel plates (Kieselgel 60F254, Merck) with UV, I<sub>2</sub>, bromo-cresol, or ninhydrin solution as the developing reagents in the concerned cases.
- ✚ Column chromatographic purifications were done with 100-200 Mesh Silica gel or with flash silica gel (230-400 mesh) in special cases.
- ✚ Melting points were determined on a Buchi Melting Point B-540 and are uncorrected.
- ✚ IR spectra were recorded in nujol or CHCl<sub>3</sub> using Shimadzu FTIR-8400 spectrophotometer.
- ✚ NMR spectra were recorded in CDCl<sub>3</sub> on Ac 200 MHz, AV 400 MHz, Jeol 400 or DRX-500 MHz Bruker NMR spectrometers. All chemical shifts are reported in  $\delta$  ppm downfield to TMS and peak multiplicities as singlet (s), doublet (d), quartet (q), broad (br), broad singlet (bs) and multiplet (m).
- ✚ Elemental analyses were performed on a Elementar-Vario-EL (Heraeus Company Ltd.; Germany).
- ✚ ElectroSpray Ionization (ESI) Mass Spectrometric measurements were done with API QSTAR Pulsar mass Spectrometer and MALDI-TOF mass spectrometric measurements were done on Voyager-DE STR mass spectrometer.
- ✚ Single crystal X-ray data were collected on a *Bruker SMART APEX* CCD Area diffractometer with graphite monochromatized (Mo K $\alpha$  = 0.71073Å) radiation at room temperature.

## LIST OF PUBLICATIONS

### **(1) Conformationally Rigid Aromatic Amino Acids as Potential Building Blocks for Abiotic Foldamers**

Veera V. E. Ramesh, Arup Roy, **Kuruppanthara N. Vijayadas**, Amol M. Kendhale, Panchami Prabhakaran, Rajesh Gonnade, Vedavati G. Puranik and Gangadhar J. Sanjayan

*Org. Biomol. Chem.*, **2011**, 9, 2, 367-369. (Front Cover)

### **(2) Concurrent display of both $\alpha$ - and $\beta$ -turns in a Model Peptide**

Deekonda Srinivas, **Kuruppanthara N. Vijayadas**, Rajesh Gonnade, Usha D. Phalgune,

Pattuparambil R. Rajamohanan and Gangadhar J. Sanjayan

*Org. Biomol. Chem.*, **2011**, 9, 2, 5762-5765.

### **(3) An Unusual Conformational Similarity of Two Peptide Folds Featuring Sulfonamide and Carboxamide on the Backbone**

**Kuruppanthara N. Vijayadas**, Hilda C. Davis, Amol S. Kotmale, Rupesh L. Gawade, Vedavati G. Puranik, Pattuparambil R. Rajamohanan and Gangadhar J. Sanjayan

*Chem. Commun.*, **2012**, 9, 78, 5762-5765. Won **NCL-RF NANAI NATU AWARD-2012**)

### **(4) The Ant-Pro Reverse-Turn Motif: The Structural Features and Conformational Characteristics**

Vijaykumar H. Throat, Tukaram S. Ingole, **Kuruppanthara N. Vijayadas**, Roshna V. Nair, Sangram S. Kale, Veera V. E. Ramesh, Hilda C. Davis, Panchami Prabhakaran, Rajesh Gonnade, Rupesh L. Gawade, Vedavati G. Puranik, Pattuparambil R. Rajamohanan and Gangadhar J. Sanjayan

*Eur. J. Org. Chem.*, **2013**, *Foldamer Special Issue*, 17, 3529-3542.

### **(5) Switching the H-bonding Network of a Foldamer by Modulating the Backbone Chirality and Constitutional Ratio of Aminoacids**

Veera V. E. Ramesh, **Kuruppanthara N. Vijayadas**, Amol S. Kotmale, Rajesh G. Gonnade, Pattuparambil R. Rajamohanan and Gangadhar J. Sanjayan

*Org. Biomol. Chem.*, **2013**, 11, 41, 7072-7075.

### **(6) Ester vs. amide on folding: a case study with a 2-residue synthetic peptide**

**Kuruppanthara N. Vijayadas**, Roshna V. Nair, Rupesh L. Gawade, Amol S. Kotmale, Panchami Prabhakaran, Rajesh Gonnade, Vedavati G. Puranik, Pattuparambil R. Rajamohanan and Gangadhar J. Sanjayan

*Org. Biomol. Chem.*, **2013**, 11, 48, 8348-8356.

**(7) Heterogenous Foldamers from Aliphatic-Aromatic Amino Acid Building Blocks: Current Trends and Future Prospects**

Roshna V. Nair, **Kuruppanthara N. Vijayadas**, Arup Roy, and Gangadhar J. Sanjayan

*Eur. J. Org. Chem.*, **2014**, DOI: 10.1002/ejoc.201402877.

**(8) Reversal of H-bonding Direction by N-Sulfonation: A Case Study With a Synthetic Reverse-Turn Peptide Motif**

**Kuruppanthara N. Vijayadas**, Amol S. Kotmale, Shridhar H. Thorat, Rajesh G. Gonnade, Roshna V. Nair, Pattuparambil R. Rajamohanan and Gangadhar J. Sanjayan

*Org. Biomol. Chem.*, **2014**, *accepted for publication*

**(9) Conformationally Rigid Orthanic acid (2-amino benzene sulfonic acid <sup>S</sup>Ant), as a Potential Amino acid Residue for Heterogeneous Foldamers**

**Kuruppanthara N. Vijayadas**, Rupesh L. Gawade, Rajesh G. Gonnade, Pattuparambil R. Rajamohanan and Gangadhar J. Sanjayan

*Manuscript under preparation*

**(10) Aromatic Amino acids in Foldamer Design**

**Kuruppanthara N. Vijayadas**, Ganesh S. Jedhe, Roshna V. Nair, Arup Roy, and Gangadhar J. Sanjayan

*Manuscript under preparation*

**(11) Removal of  $\beta$ -turns Upon Reversing the Neighbouring Sequential H-bonding Direction: A Case Study With Synthetic Peptide Motifs**

**Kuruppanthara N. Vijayadas**, Tukaram S. Ingole, Rupesh L. Gawade, Rajesh G. Gonnade, Pattuparambil R. Rajamohanan and Gangadhar J. Sanjayan

*Manuscript under preparation*

**POSTERS, SYMPOSIA & CONFERENCES**

**(1) Unveiling the H-bonding Potential of Ester and Amide Carbonyl in Peptide Folding Using the Two-residue Ant-Pro Reverse Turn: *Poster***

*Venue*: CSIR-National Chemical Laboratory, *Event*: National Science Day, 2012

**(2) An Unusual Conformational Similarity of Two Peptide Folds Featuring Sulfonamide and Carboxamide on the Backbone: *Poster***

*Venue*: CSIR-National Chemical Laboratory, *Event*: National Science Day, 2013

**(3) Certification Course on "Patents for Scientists and Engineers": Seven-Day Workshop**

*Venue:* CSIR-National Chemical Laboratory Venture Centre, *Event:* conducted by IPFACE, February 2014

**(4) Switching the Hydrogen-bonding of a Foldamer by Modulating the Backbone Chirality, Constitutional Ratio of Amino acids and C-terminal Amide to Ester Mutations: Poster**

*Venue:* CSIR-National Chemical Laboratory, *Event:* National Science Day, 2014

## AWARDS AND FELLOWSHIPS

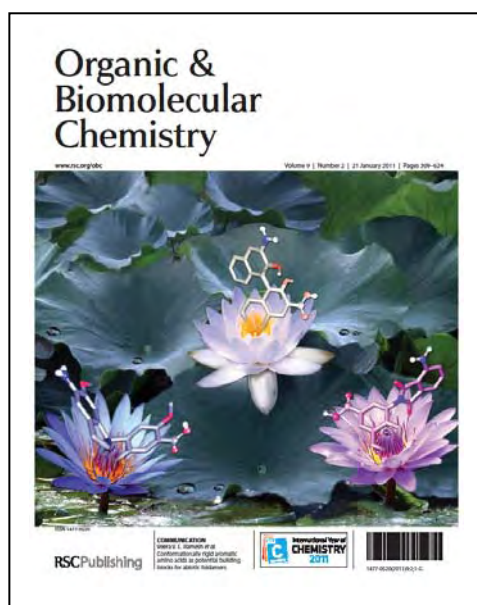
**(1) GRADUATE APTITUDE TEST in ENGINEERING (GATE-2007)** for chemistry: by Ministry of Human Resource Development, Government of India

**(2) SENIOR RESEARCH FELLOWSHIP (SRF-2012):** by Council of Scientific and Innovative Research (CSIR).

**(3) NCL-RF NANAI NATU AWARD FOR RESEARCH SCHOLARS:** For Best Published Research Paper in Organic Chemistry with Second Highest Impact Factor of the Year, 2012

*Citation:* An Unusual Conformational Similarity of Two Peptide Folds Featuring Sulfonamide & Carboxamide on the Backbone, by CSIR-National Chemical Laboratory Research Foundation, NCL.

## COVERS



*Org. Biomol. Chem.*, 2011, 9, 367-369

Chapter 1:  
The Ant-Pro Reverse-Turn Motif: Structural  
Modifications around the Folding Core

## Part A: Significance of Hydrogen Bonding Potential of Ester and Amide Carbonyl in Folding of Ant-Pro Reverse Turn

**1.1 Hydrogen Bond:** Hydrogen bond is a non-covalent interaction involving three atoms i.e. a donor electronegative atom (D), Hydrogen (H) attached to the donor and an acceptor atom (A) in close proximity.<sup>1-3</sup> The proximity of acceptor atom 'A' to partially positively charged hydrogen causes charge separation. In short, a hydrogen atom involved in hydrogen-bonding shares its electron density around two electronegative atoms. This can be represented as.



Hence, hydrogen bonding acts as a non-covalent force having higher interaction energy than van der Waals interactions. Hydrogen-bonding explains the dimerization of carboxylic acids in their vapor state, crystal formation of ice and its consequent low density compared to liquid water, strength of nylon, self-assembly and consequent insolubility of cellulose molecules, double helical structure of DNA (Deoxyribose Nucleic Acid), folded structure of proteins and many other natural self-assemblies.

Dramatically higher boiling points of  $\text{NH}_3$  (ammonia),  $\text{H}_2\text{O}$  (water), and HF (hydrogen fluoride) compared to the heavier analogues  $\text{PH}_3$  (phosphine),  $\text{H}_2\text{S}$  (hydrogen sulfide), and HCl (hydrogen chloride) are some of the phenomena caused due to hydrogen-bonding. Increase in the melting point, boiling point, solubility, and viscosity of many compounds like anhydrous phosphoric acid and of glycerol, hexamer formation in hydrogen-fluoride, which occur even in the gas phase, resulting in gross deviations from the ideal gas law are also due to hydrogen-bonding. The pentamer formation of water and alcohols in apolar solvents, high water solubility of many compounds such as ammonia, negative azeotropy of mixtures of HF (hydrogen fluoride) and water are some of the other phenomena which are explained by hydrogen bonding. The deliquescence of NaOH (sodium hydroxide) is caused in part by reaction of  $\text{OH}^-$  (hydroxyl ion) with moisture to form hydrogen bonded  $\text{H}^3\text{O}^{2-}$  (hydronium ion) species. An analogous process happens between  $\text{NaNH}_2$  (sodamide) and  $\text{NH}_3$  (ammonia), and between NaF (sodium fluoride) and

HF. Wool, a protein fiber, is another example which is held together by hydrogen bonds causing it to recoil when stretched. Washing at high temperatures permanently breaks the hydrogen bonds and a garment may lose its shape.

**1.2 Significance of the hydrogen-bond in peptide folding:** In peptides or proteins, hydrogen bonds are formed between the amide 'NH' and carbonyl 'O' where 'N' is the donor atom and 'O' is the acceptor atom. Although the energy of the hydrogen bond (~12 kJ/mol) is fairly weak when compared to covalent interactions, together can contribute a significant amount of energy and stability to protein conformation. A protein which is folded into a highly complex three dimensional structure uses intra-molecular hydrogen bonding, while at the surface it interacts with water or other proteins through intermolecular hydrogen bonding. The intra-molecular hydrogen bonding is the major factor which facilitates proteins to adopt a particular shape and is always enveloped or stabilized by hydrophobic interactions of amino acid side chains.<sup>4-7</sup> Various secondary structures of proteins like  $\alpha$ -helix,  $\beta$ -sheets, turns etc are stabilized by *intra-molecular* hydrogen bonding interactions.

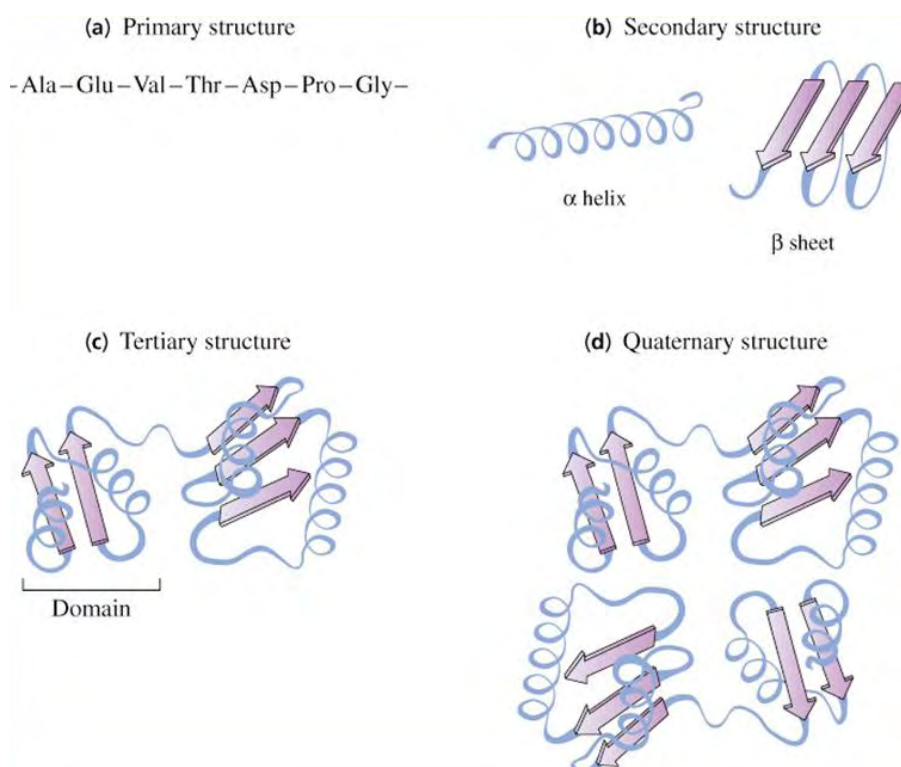


**Fig. 1.1:** Four levels of protein structure.



**$\alpha$ -helix:** By model, Linus Pauling (1951) guessed that the  $\alpha$ -helix, a right-handed helix with 3.6 residues per turn, would be the most stable secondary structure. The hydrogen bonding in the backbone is completely satisfied with *intra-molecular* bonds characterized by  $\phi$  angle  $60^\circ$  and  $\psi$  angle of  $45^\circ$ . Myoglobin (oxygen storage protein) and camodulin (activator of calcium sensitive enzymes) are two proteins which contain  $\alpha$ -helical structure.

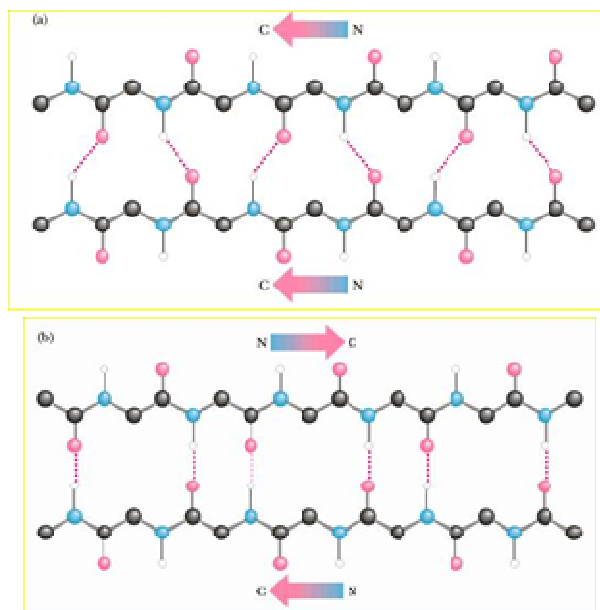


**Fig. 1.2:** Representations of parallel  $\beta$ -sheets (a) and anti-parallel  $\beta$ -sheets (b), seen in peptides.

**$\beta$ -pleated sheets:** Pauling and Corey in 1951 predicted the existence of sheet structure of proteins. Two polypeptide chains called  $\beta$ -strands run alongside each other and are linked together by hydrogen bonds to form a  $\beta$ -sheet. Immunoglobulins and green fluorescent proteins are two proteins which contain predominantly  $\beta$ -sheet structures (fig. 1.2). They are of two types; parallel (a) and anti parallel (b). Parallel  $\beta$ -sheets are less prevalent and less stable where as anti-parallel  $\beta$ -sheets occur frequently and are highly stable.

**Peptide  $\beta$ -hairpins:** The  $\beta$ -hairpin (sometimes also called  $\beta$ -ribbon or  $\beta$ - $\beta$  unit) is the simple protein structural motif involving two  $\beta$ -strands that look like a hairpin. The motif consists of two strands that are adjacent in primary structure oriented in an anti-parallel direction (the N-terminus of one sheet is adjacent to the C-terminus of the next) and are linked by a short loop of two to five amino acids.  $\beta$ -hairpins can occur in isolation or as part of a series of hydrogen bonded strands that collectively comprise a  $\beta$ -sheet.

**Loops:** These are the connectors of two secondary structures which are often located at the surface of folded protein. Loops varying in length and shapes are important structural entity in biological recognition process.

**Turns:** Turns are regions in peptide chain where a chain reversal occurs.<sup>8-10</sup> They can be classified into  $\alpha$ ,  $\beta$ ,  $\gamma$ ,  $\pi$  etc.<sup>11</sup> and are represented by the following diagram (fig. 1.3).

**$\gamma$ -turn:** If the carbonyl of first amino acid forms a 7-membered ring hydrogen bond with NH of third amino acid, then it is called a  $\gamma$ -turn.<sup>12-14</sup>

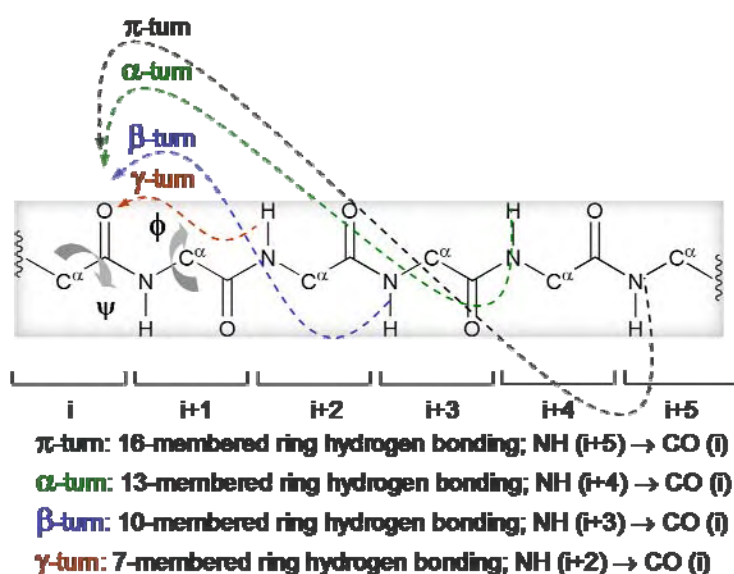


Fig. 1.3: Representations of various types of turns, seen in peptides.

**$\beta$ -turn:** The most common turn motif, where the carbonyl of first amino acid forms a 10-membered ring hydrogen bond with NH of fourth amino acid, is the  $\beta$ -turn.  $\beta$ -turns are found abundantly in biological systems, which are further classified into type-I, type-II (fig. 1.4) and so on, depending on their dihedral angle preferences ( $\psi$  and  $\phi$ ).<sup>15-16</sup>

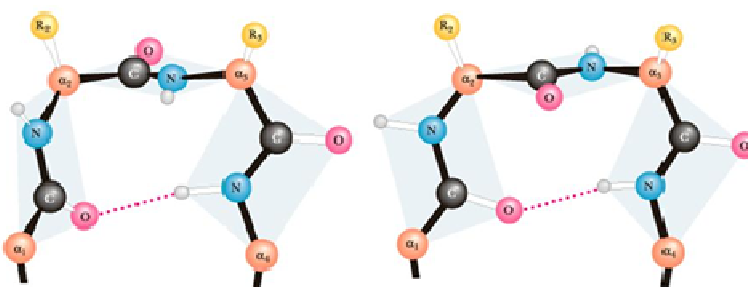


Fig. 1.4: Representations of type I  $\beta$ -turn (left) and type II  $\beta$ -turn (right).

$\beta$ -turns differ in the backbone conformational angles ( $\phi, \psi$ ) at the two residues ( $i + 1, i + 2$ ) yielding turns which have distinctive influences on polypeptide chain folding. The type I/III structures ( $\phi(i+1) = -30^\circ, \psi(i+1) = -60^\circ, \phi(i+2) = -60^\circ/90^\circ, \text{ and } \psi(i+2) = -30^\circ/0^\circ$ ) upon repetition form helices, while the type II structures ( $\phi(i+1) = -60^\circ, \psi(i+1) = 120^\circ, \phi(i+2) = 80^\circ, \text{ and } \psi(i+2) = 0^\circ$ ) facilitate reversal of chain direction. In sequences that contain all L-amino acids, insertion of a type II' turn (enantiomer of type II) forming segment promotes anti-parallel array of the nearby strands, thereby stabilizing  $\beta$ -hairpins.

$\beta$ -Turns provide conformational rigidity to the bio-active peptide sequences and are useful for the development of drugs with improved pharmaco-kinetic properties. They form the active site of enzymes and hence can act as enzyme mimics. Hence, they catalyze several organic reactions and thus find their application in organic catalysis.<sup>17-20</sup> One of the most common and important secondary structures found in peptide hormones that stimulate GPCRs is the  $\beta$ -turn.<sup>21</sup> G-Protein-Coupled Receptors (GPCRs) form the largest group of signal transduction proteins in vertebrates. They comprise a large protein family of trans-membrane receptors that sense molecules outside the cell and activate inside signal transduction pathways and, ultimately, cellular responses. They are involved in many diseases, and are also the target of approximately 40% of all modern medicinal drugs.<sup>21</sup> The pioneer work, which gave an understanding of the function of GPCRs, was awarded Nobel Prize in Chemistry (2012) done by Brian Kobilka and Robert Lefkowitz.<sup>22-26</sup>

**$\alpha$ -turn:** In this case, the carbonyl of first amino acid forms a 13-membered ring hydrogen bond with NH of fifth amino acid.<sup>27-29</sup>  $\alpha$ -turn motif is likely to be one of the crucial structural factors effecting specific molecular recognition processes including the recently isolated Asian scorpion toxin (BmK 17[4]).<sup>30</sup>

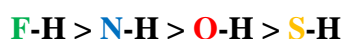
**$\pi$ -turn:** A 16-membered ring hydrogen bonded ring formed between the carbonyl of first amino acid and the NH of sixth amino acid.

### 1.3 Amino acids and secondary structure of proteins

The secondary structures of proteins can be predicted by the side chains of the amino acid residues present in the structure. Amino acids like glutamine, methionine, alanine are often associated with  $\alpha$ -helix, while isoleucine, valine, tyrosine, phenyl alanine, leucine, tryptophan are found in the strands of the  $\beta$ -sheets. Proline, glycine, aspartic acid *etc.* are found in the turn region of the secondary structure.

Enormous research has been undertaken during the past decades to understand the role of hydrogen-bonding in peptide folding.<sup>31</sup> Hydrogen bonding codes like NH and CO have been varied in the peptide backbone to understand their significance. 'NH' in the peptide bond has been substituted with oxygen atom, as in esters, or with sulfur atom, as in thioesters, while carbonyl 'O' has been substituted with sulfur. Other substitutions involve swapping of carboxamides with moieties like sulfonamides, thioamides, sulfonamides, *etc.* The effect of sulfonamide modifications will be discussed in the later part of this thesis. In all those *isosteric* replacements, there arises a huge difference in the folding propensities owing to the diversity in the strength of donor and acceptor atoms in participating in the hydrogen bonding.<sup>32</sup> Hydrogen bonds can vary in strength from very weak ( $1-2 \text{ kJ mol}^{-1}$ ) to extremely strong ( $161.5 \text{ kJ mol}^{-1}$  in the ion  $\text{HF}^{-2}$ ).<sup>33</sup>

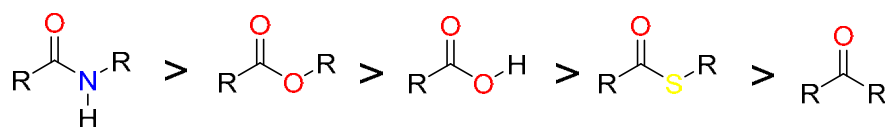
**Hydrogen-donor capacity of D:** The hydrogen donor capacity of donor follows the order for various donor atoms.



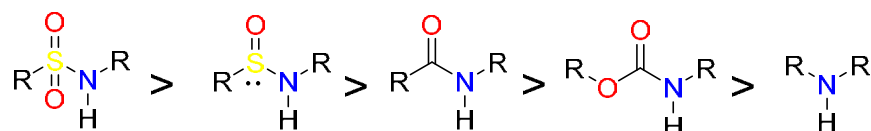
**Hydrogen-acceptor capacity of A:** The hydrogen acceptor capacity of acceptor atoms follows the order.



**Hydrogen-acceptor capacity of CO:** The hydrogen acceptor capacity of the oxygen of the carbonyl varies with the atoms connected to the carbonyl.



**Acidity of NH:** The donor capacity of nitrogen depends on the acidity of the NH which varies in turn with the type of the amide bond.



**1.4 Resonance stabilization of a peptide bond:** The peptide bond is a resonance hybrid of three canonical forms (fig. 1.5). The planarity of the peptide bond originates from the delocalization of the nitrogen lone pair into the antibonding orbital ( $\pi^*$ ) of the carbonyl

group, which is reflected in resonance structure (fig. 1.5). This delocalization is mainly responsible for the rotational barrier between the peptide bond, which can limit the rate of protein folding. The oxygen lone pairs in the amide bond are not only located in degenerate  $sp^2$  hybrid orbitals, but are considerably  $\sigma$ -rich and directed along the C=O bond, whereas the other higher energy lone pair ( $n\pi$ ) is  $\pi$ -rich and located orthogonal to the C=O bond. In many protein secondary structures, the C=O $\cdots$ H-N hydrogen bond between two amide groups involves the delocalization of the  $\sigma$ -rich lone pair ( $n\sigma$ ) into the anti-bonding orbital ( $\sigma^*$ ) of the N-H bond. The other,  $\pi$ -rich lone pair ( $n\pi$ ) delocalizes into the anti-bonding orbital of the adjacent carbonyl group to give rise to a carbonyl-carbonyl interaction, which we term as an  $n\rightarrow\pi^*$  interaction. In esters, the lone pair of oxygen 'O' delocalizes into the anti-bonding orbital ( $\pi^*$ ) of the ester carbonyl group, as analogous to amidic resonances. The lower rotational barrier in esters (11 kcal mol $^{-1}$ ) compared with that of amides (20 kcal mol $^{-1}$ ) is attributed to the weaker charge transfer from the bridging oxygen (O) to the carbonyl group. Peptide bonds between all *proteinogenic* amino acids, except proline, can both donate and accept hydrogen bonds. Esters cannot donate a hydrogen bond and are only weak hydrogen-bond acceptors. On the other hand, the large size of sulfur, longer C=S bond, and skewed hydrogen bonding capacity alter the conformational feature of peptides containing thioamides.<sup>35-37</sup>

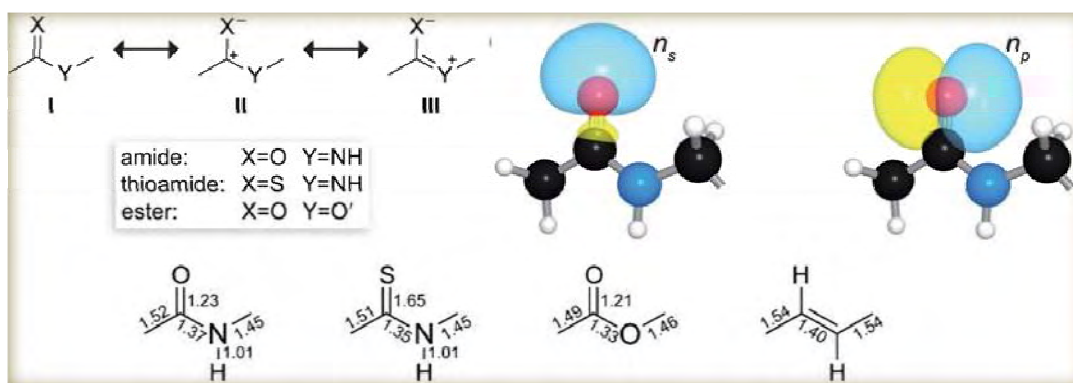


**Fig. 1.5:** Resonance stabilization of a peptide bond (Raines *et. al.*)<sup>32</sup>.

**1.5 Amide to ester modifications:** Amide to ester modifications affect the folding of peptides in two ways. A hydrogen bonding donor is eliminated by replacing an amide NH with ester oxygen and a hydrogen bond acceptor is weakened by replacing an amide carbonyl with an ester carbonyl (fig. 1.6).<sup>38</sup>

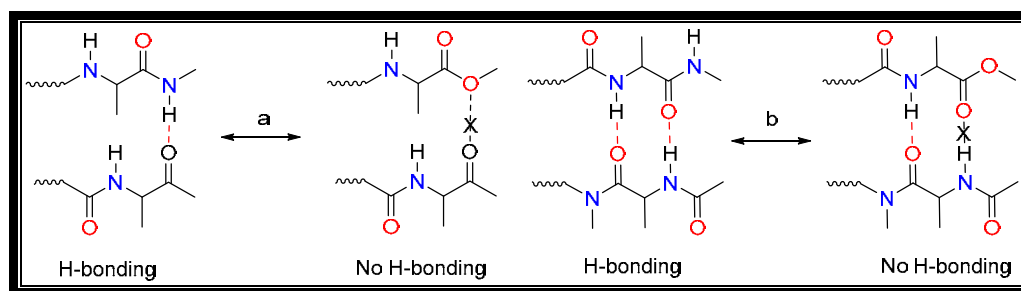


**Fig. 1.6:** Representations of peptides having the end terminals where, H-bonding donor is eliminated (a) and H-bonding acceptor is weakened (b).

The elimination of donor not only abolishes the hydrogen bond but also creates repulsion between the two donor atoms (i.e. the ester and carbonyl oxygens) in esters resulting in destabilization. The second case in which a weakening of the hydrogen bonding acceptor capacity or basicity of the carbonyl (linked to oxygen as in esters) can abolish the formation of a hydrogen bond (fig. 1.6). This effect is observed in various peptide secondary structures like helices,  $\beta$ -sheets, turns,  $\beta$ -hairpins *etc.*

Amide to ester mutations were done in real peptide backbones by replacing 'NH' with 'O', resulting in elimination of hydrogen bonding.<sup>39-40</sup> In an effort to understand the contribution of backbone hydrogen bonds to the folding kinetics and thermodynamics of a small  $\beta$ -sheet protein, PIN WW domain was investigated by Kelly and co-workers by individually replacing its backbone amides with esters.<sup>41-42</sup> Here, a site-specific amide-to-ester mutations were done, which perturbed backbone hydrogen bonds in the overall folding of the  $\beta$ -sheet protein. The degree of destabilization due to the absence of hydrogen bonding was strongly dependent on the location of the amide bond replaced. Hydrogen bonds near turns or at the ends of  $\beta$ -strands were less influential than hydrogen bonds that are protected within a hydrophobic core.<sup>42</sup>

Energetic evaluation studies to differentiate the destabilization of proteins, which contain amide groups mutated by ester groups in backbone core, significantly explained the differences created by ester to amide mutations. The contribution of backbone hydrogen bonds in  $\alpha$ -helices to the overall stability of a protein was examined experimentally by replacing several backbone amide linkages in  $\alpha$ -helix 39-50 of T4 lysozyme with ester linkages by Schultz and co-workers.<sup>43</sup> Similar studies in the *Chymotrypsin inhibitor 2* (CI2), a small 64 residue protein consisting of an  $\alpha$ -helix sandwiched by four  $\beta$ -strands, showed a destabilization of protein folding by 2.93

kcal/mol compared to the protein containing all-amide protein.<sup>44</sup> Dawson and coworkers analyzed such effects in GCN4 coiled coil domain, a stable  $\alpha$ -helical dimer that possesses a well-packed hydrophobic core, explaining backbone engineering through ester substitution as an useful approach for probing the relative strength of backbone hydrogen bonds.<sup>45</sup> Mutational analysis of backbone amide bonds to a weaker hydrogen bond acceptor ester carbonyl, in a  $\beta$ -sheet secondary structure in *Staphylococcal Nuclease* by Schultz, showed a 1.5-2.5 kcal/mol decrease in protein stability, similar to those values reported for the deletion of a protein side chain-side chain interaction.<sup>46</sup> Similar mutagenesis was analyzed at the turn region of *Staphylococcal Nuclease*, where there is an absence of side chain-side chain interactions, explained clearly the backbone destabilization of the protein by amide to ester modification.<sup>46</sup> The energetic contribution of backbone hydrogen bonds to the thermodynamic stability of a hyperstable P22 Arc Repressor mutant was studied by Fitzgerald.<sup>47</sup> Fitzgerald described a total chemical synthesis and biophysical characterization in *4-oxalocrotonate tautomerase* (4OT) to furnish such mutagenesis.<sup>48</sup> Such ester to amide mutations were performed at the  $\beta$ -turn regions of *Staphylococcal Nuclease*, by Schultz *et al.*<sup>38</sup> A recent study involving the amide to ester mutations in the postsynaptic density 95/discs large/zonula occludens 1 (PDZ) domain of mammalian cells, was carried out first by Per Jemth and co-workers.<sup>49</sup>

**1.6 Peptide chain end-fraying:** Peptide chain “end-fraying” is defined as the non-participation of hydrogen bonding sites at the termini causing peptide chains to fray apart from the secondary structure formation. This phenomenon is predominantly observed at the termini of secondary structures of proteins like  $\beta$ -hairpins,  $\beta$ -sheets, helices etc.<sup>50-56</sup> Aromatic-aromatic ring  $\pi$ - $\pi$  interactions, NH- $\pi$  interactions, solvent competition for backbone hydrogen bonding, chirality of amino-acids at the turn or hairpin region, bulkiness of groups at the end terminals, absence of amide groups at peptide end terminals, temperature or enthalpy changes *etc.* are the various reasons discussed in the literature about the fraying phenomenon.<sup>52-53,57-58</sup> But, the role of a C-terminal ester causing the terminals to fray-apart to disrupt hydrogen bonding has not been intensely scrutinized.

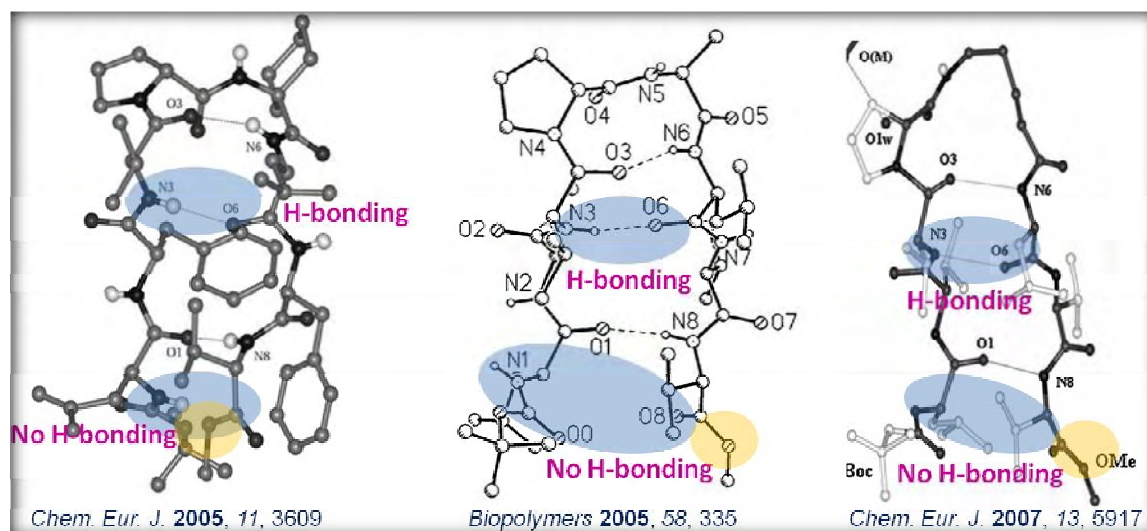


**Fig. 1.7:** Crystal structures of  $\beta$ -sheet peptides showing fraying. Closer examinations of the structures show that the hydrogen bonding is absent at the termini containing ester carbonyls.

**1.7 Absence of sequential hydrogen bonding at the termini:** This is also generally termed as fraying and is usually observed in helices in which the hydrogen bonding which stabilizes the helix is absent at the termini.<sup>59-60</sup> A tetrapeptide featuring Boc-Aib-Gpn-Aib-Gpn-NHMe features three C-12 hydrogen bonding interactions, but fails to form the third end hydrogen bonding in absence of donor NH as seen in Boc-Aib-Gpn-Aib-Gpn-OMe.<sup>59</sup> In some other cases, it results in the formation of new *inter*-molecular hydrogen bonds.

### 1.8 Peptide chain end-fraying as a consequence of swapping C-terminal amides with esters: A case study.

Esters are often found at the C-terminus of peptides and synthetic oligomers (foldamers), owing to the synthetic ease with which they are obtained using protected peptide coupling and further oligomerization. As ester carbonyls, being poorer hydrogen bonding acceptor, deviate from regularity in forming the hydrogen bonding interactions at the termini, peptide chains tend to “fray apart”. Owing to the diverse competing effects originating from large peptide chains, which cause end-fraying in peptides, the individual contribution of C-terminal esters in causing peptide chain end-fraying goes often unnoticed. There are a large number of examples of peptide-based systems known in the literature wherein the C-terminal esters are not seen participating in *intra*-molecular hydrogen bonding that would strengthen the stability of the secondary structure. In fact, the terminal hydrogen bond that connects the N- and the C-termini of the peptide is



absent in most of the peptide hairpin crystal structures as a result of strand fraying. Once “frayed”, the exposed termini may interact with solvent molecules for hydrogen bonding and when the hydrogen bonding solvents are not available, peptides may aggregate by intermolecular hydrogen bonding interactions.

In large peptides, including the synthetic oligomers called foldamers, it would often be a tough task to identify the individual role of the C-terminal esters in causing end-fraying. This is particularly due to the competing diverse effects originating at the peptide termini such as:  $\pi$ - $\pi$  interactions, NH- $\pi$  interactions, chirality of amino-acids at the turn or hairpin region, temperature effects and bulkiness of groups at the end terminals, which are known to cause peptide chain end-fraying. Employing a simple 2-residue reverse turn motif with least interference from other effects, as mentioned above, we could demonstrate how minute structural changes can have remarkable consequences on the folding propensities at the peptide termini.

The ester to amide mutation studies were performed at the  $\beta$ -turn regions of *Staphylococcal Nuclease* by Schultz and co-workers.<sup>38</sup> The present study described herein shows the clear distinction of such amide to ester mutagenic studies, by solid state crystallography and solution state NMR studies. The non-natural Ant-Pro reverse turn unit (a foldameric unit) is acting here as a stable entity in order to understand the folding behavior of peptides or proteins.

### 1.9 Utilizing Ant-Pro reverse turn for the case study: The design strategy

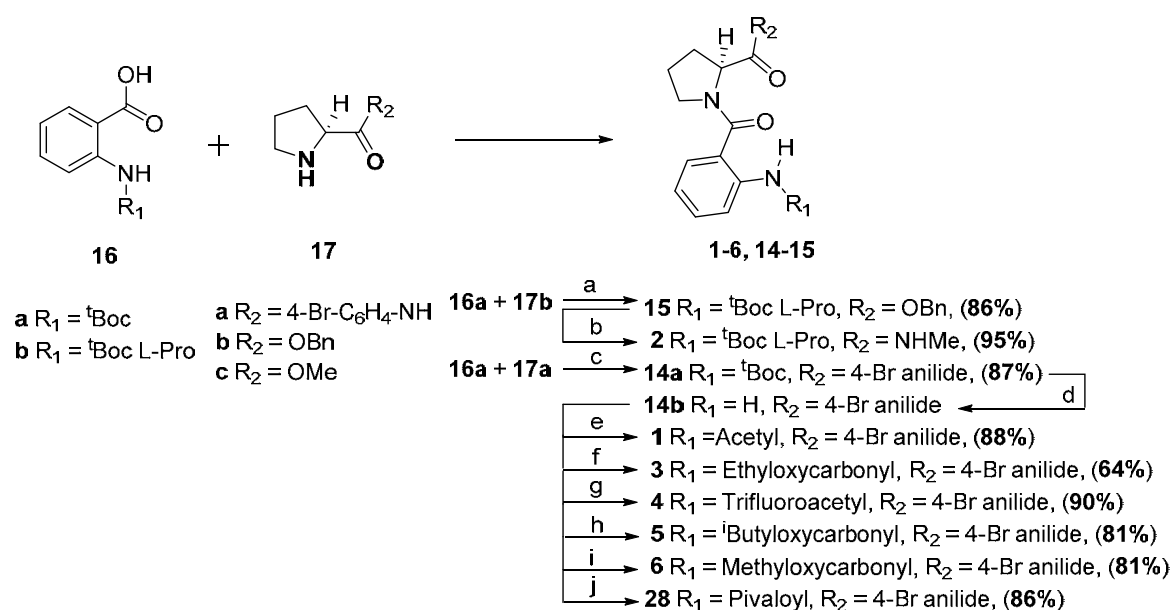
The helical conformation displayed by Ant-Pro *hetero*-oligomers show repeating segments of 9-membered-ring hydrogen bonded networks.<sup>61</sup> While investigating the conformational characteristics of the Ant-Pro oligomers, we were caught upon the finding that the C-terminal peptide esters did not show the folded C9-turn conformation with closed hydrogen bonded ring, although its corresponding C-terminal amides did show the expected folding. Fascinated by this finding, we synthesized diversely substituted dipeptide sets of Ant-Pro C-terminal esters and amides at both N-and C-termini to compare the individual contribution of C-terminal ester *vs.* amide carbonyl as hydrogen bonding acceptor in the formation of a folded structure featuring a closed network of 9-membered hydrogen bonded ring. Using a simple two-residue reverse-turn mimic, we investigated the consequences on swapping C-terminal amides with esters on the overall folding ability of a peptide.

## 1.10 Synthesis

In order to unequivocally establish the individual contribution of amide and ester carbonyls in modulating the folding propensity, syntheses were carried out using the normal peptide coupling strategy to furnish both categories of diversely substituted C-terminal amides and esters.

<sup>t</sup>Boc-Ant-OH was coupled with H-<sup>L</sup>Pro-AniBr using EDC.HCl and HOBT in DCM to obtain compound **14a**. The compound **14a** upon deprotection of <sup>t</sup>Boc group using TFA and acylation using acetyl chloride, pivaloyl chloride, ethyl chloroformate, trifluoroacetic anhydride, isobutyl chloroformate and methyl chloroformate furnished compounds **1**, **3-6** and **28**, respectively.

**Scheme 1.1:** Synthesis of C-terminal amides

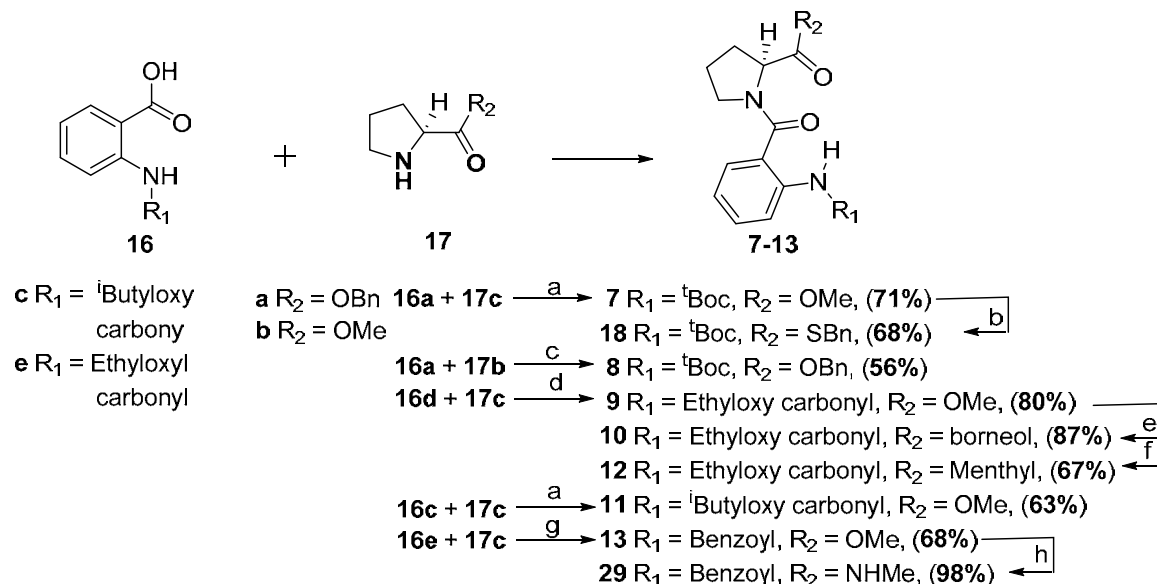


**Reagents and Conditions:** (a) DCC, HOBT, DCM, rt, 12h; (b) methanolic MeNH<sub>2</sub>, rt, 3h; (c) EDC.HCl, HOBT, DCM, rt, 12h; (d) TFA, DCM, rt, 3h; (e) AcCl, Et<sub>3</sub>N, DCM, rt, 12h; (f) ethyl chloroformate, Et<sub>3</sub>N, DCM, rt, 12h; (g) trifluoroacetic anhydride, Et<sub>3</sub>N, DCM, rt, 12h; EDC.HCl, HOBT, DCM, rt-12h; (h) isobutyl chloroformate, Et<sub>3</sub>N, DCM, rt, 12h; (i) methyl chloroformate, Et<sub>3</sub>N, DCM, rt, 12h; (j) pivaloyl chloride, Et<sub>3</sub>N, DCM, rt, 12h.

<sup>t</sup>Boc-<sup>L</sup>Pro-Ant-OH was coupled with H-<sup>L</sup>Pro-OBn and subsequent amidation using methylamide to obtain tripeptide unit **2**. <sup>t</sup>Boc/<sup>i</sup>Boc or ethyloxycarbonyl-Ant-OH was coupled with H-<sup>L</sup>Pro-OMe/ H-<sup>L</sup>Pro-OBn using representative coupling agents (see, scheme 1.2) in DCM to afford compounds **7-12**. The compound **13**, on the other hand, was obtained from benzoxazinone<sup>62-64</sup> using the nucleophilic ring opening using H-<sup>L</sup>Pro-OMe in presence of DBU and molecular sieves in DMF.<sup>65</sup> Compound **13** was amidated

with methylamine to furnish amide **29**. The thioester analogue was synthesized from **7** using benzylmercaptan.

**Scheme 1.2:** Synthesis of C-terminal esters



*Reagents and Conditions:* (a) EDC.HCl, DMAP, DCM, rt, 12h; (b) (i) LiOH.H<sub>2</sub>O, MeOH, H<sub>2</sub>O, rt, 12h, (ii) DCC, DMAP, benzylthiol, rt, 12h; (c) DCC, HOBT, DCM, rt, 12h; (d) HBTU, DIEA, MeCN, rt, 12h; (e) (i) LiOH.H<sub>2</sub>O, MeOH, H<sub>2</sub>O, rt, 12h, (ii) DCC, DMAP, borneol, rt, 12h; (f) DCC, DMAP, menthol, rt, 12h; (g) (i) Na<sub>2</sub>CO<sub>3</sub>, BzCl, THF, rt, 12h, (ii) DBU, DMF, 4 Å MS, rt, 3h; (h) methanolic MeNH<sub>2</sub>, rt, 3h.

## 1.11 Conformational Analyses

The conformational investigations in the solid state were carried out using single crystal X-ray studies of compounds **1-13**. NMR studies were carried out in the solution state to evaluate the conformational features in solution state.

**1.11.1 Single crystal X-ray diffraction studies:** In order to have a better comparison, two sets of crystal structures - five each from both categories of diversely substituted C-terminal amides **1-6** (fig. 1.8, left panel) and esters **7-12** (fig. 1.8, right panel) were analysed. Substituents around the folding segment have been varied extensively at both termini of the amides and esters in order to clearly explain the role of substituent effects in hydrogen bonding interactions.

Comparison of all crystal structures of the C-terminal amides **1-6** clearly revealed that folding, aided by robust 9-membered ring hydrogen bonding involving the <sup>1</sup>Ant NH and <sup>2</sup>Pro carbonyl hydrogen bonding codes was clearly seen throughout.

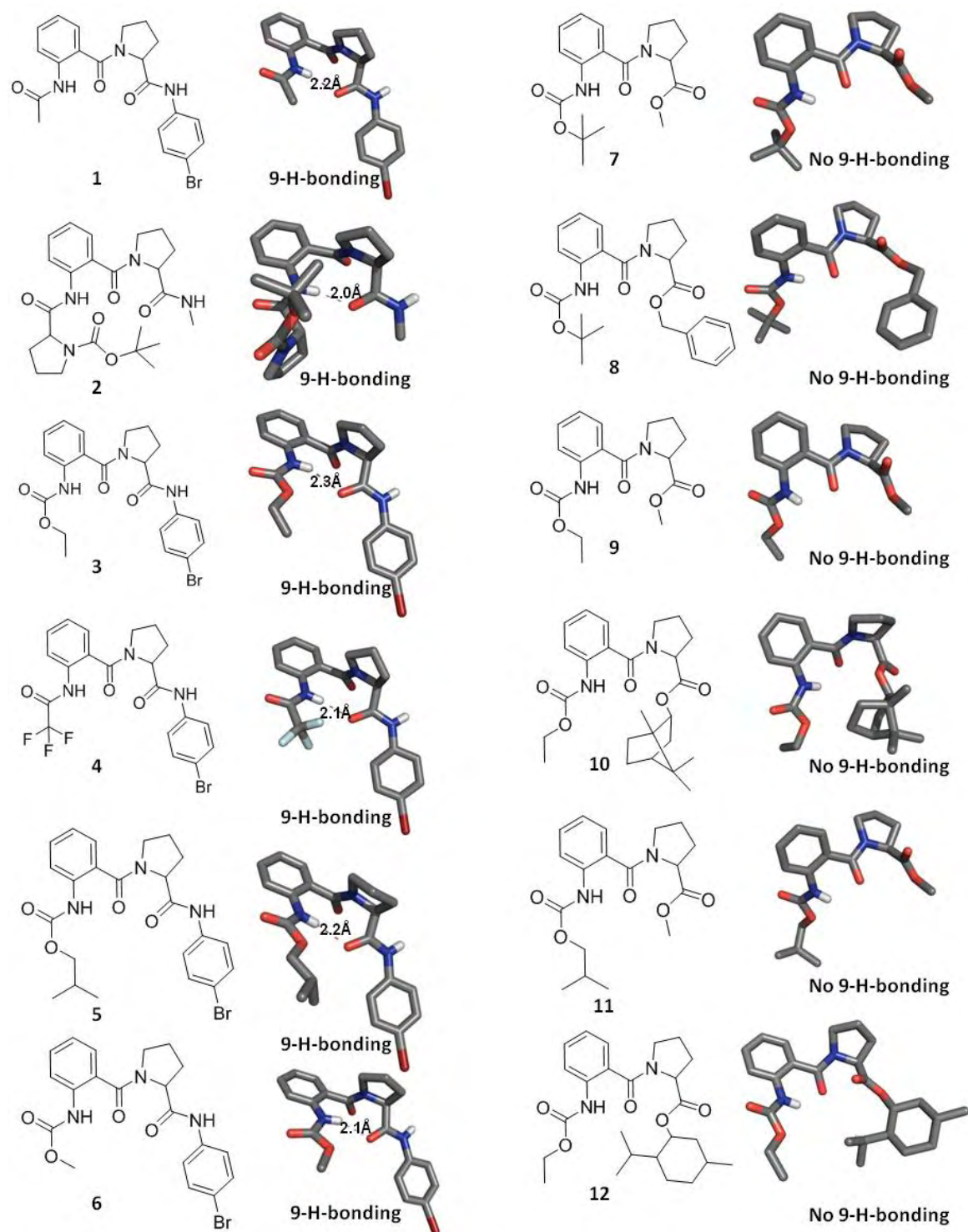


**Fig. 1.8:** Molecular and crystal structures of C-terminal amides **1-6**, (left panel) and C-terminal esters **7-12** (right panel). *Note:* The amides assume folded conformation featuring 9-membered-ring hydrogen bonding (*9-H-bonding*), whilst the esters display fraying (*without 9-H-bonding*). In the crystal structures, all hydrogens, except the polar ones, have been deleted for clarity.

The hydrogen bonding parameters are: hydrogen bonding distances [ $\Delta(\text{N}\cdots\text{O}) = 2.881 - 3.080\text{\AA}$ , and  $\Delta(\text{H}\cdots\text{O}) = 2.030 - 2.268\text{\AA}$ ]. In stark contrast, all the C-terminal esters **7-12** showed absence of folding involving 9-membered ring hydrogen bonding

between the  $^1\text{Ant}$  NH and  $^2\text{Pro}$  carbonyl. As the ester carbonyls in **7-12** moved away causing fraying of ends with the absence of nine-membered hydrogen bonding, the  $^1\text{Ant}$  NH formed only 6-membered-ring hydrogen bonding. The consequences of end-fraying of the termini resulted in lack of folding which was readily visible from the high  $\psi$  torsion angles of the Ant residues in the esters **7-12** ( $\psi_{av} = 145^\circ$ ), when compared to that of the amides **1-6** ( $\psi_{av} = 68^\circ$ , table 1.1). The reluctance of the C-terminal ester carbonyl in participating in hydrogen bonding was actually due to its poorer hydrogen bonding acceptor potential leading to fraying.

**Table 1.1:** Torsion angles and hydrogen bonding parameters of compounds **1-13**

Compound No.	Torsion angles (Deg.)				Hydrogen bonding Parameters			
	Ant		Pro		Distances (Å)		Angles (Deg.)	
	$\phi$	$\psi$	$\phi$	$\psi$	O...H	N...O	C=O..N	NH..O
<b>Amides</b>								
<b>1</b>	173.40	-65.37	-55.97	164.59	2.173	3.025	127.28	170.80
<b>2</b>	170.23	-69.58	-60.64	174.04	2.030	2.881	131.10	169.81
<b>3</b>	-172.38	-70.08	-58.82	164.32	2.259	3.075	123.31	158.34
<b>4</b>	176.23	-72.66	-55.94	166.62	2.108	2.960	132.15	171.33
<b>5</b>	166.51	-71.89	-56.49	162.41	2.178	3.033	127.17	172.17
<b>6</b>	170.54	-68.86	-60.21	169.85	2.098	2.946	129.12	169.22
<b>Esters</b>								
<b>7</b>	153.97	150.75	-61.60	-139.47	5.263	5.842	65.58	128.93
<b>8</b>	-177.80	140.07	-69.70	153.71	5.452	5.930	72.70	120.03
<b>9</b>	-144.62	146.41	-57.70	135.55	5.237	5.790	64.08	125.28
<b>10</b>	167.51	-144.35	-56.68	-38.27	4.737	5.552	48.65	156.00
<b>11</b>	-138.63	146.28	-59.04	134.8	5.366	5.874	62.70	122.65
<b>12</b>	155.54	-145.540	-59.54	155.11	3.781	4.314	103.88	122.52
<b>13</b>	-177.28	-130.50	-59.62	156.72	3.177	4.510	111.12	148.44

**1.11.2 Solution state NMR studies:** Conformational investigations by solution state NMR studies (500 MHz) revealed that the solid-state conformational features of the C-terminal amides were clearly preserved in the solution-state as well, as evidenced from 2D NOESY studies. The 9-membered hydrogen bonding networks that lead to folding in the case of the C-terminal amides prevailed in the solution-state as well from the solvent titration experiments.<sup>66-67</sup> However, the potential involvement of 6-membered hydrogen bonding, in the absence of 9-membered hydrogen bonding, made it difficult to clearly distinguish the nature of the hydrogen bonded rings of the C-terminal esters in the solution-state.

**2D-NOESY NMR studies:** Extensive solution-state NMR studies were undertaken to verify the nature of the hydrogen bonding interactions in the amide and esters.

Conformational investigations by solution-state 2D NOESY studies (500 MHz, CDCl<sub>3</sub>) revealed that the solid-state conformational features of the C-terminal amides were clearly preserved in the solution-state as well.<sup>20aa</sup> The significant nOes observed: C20 vs. C19H and NH1 vs. C12H supported their spatial proximity, suggesting the folded conformation for the amide **1**, as observed in their solid-state by crystal structure studies (fig. 1.9A).

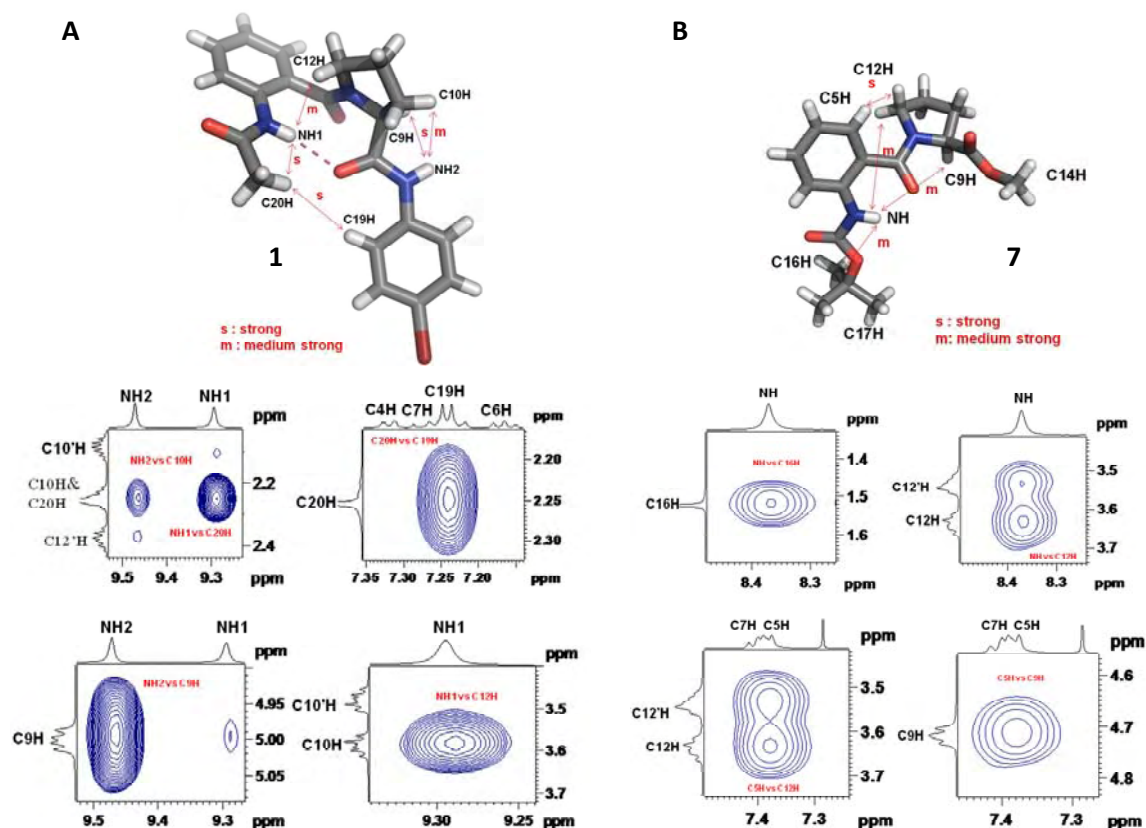


Fig. 1.9: 2D NOESY extracts of amide **1** and ester **7** (400MHz, CDCl<sub>3</sub>)

The characteristic nOes observed for **6** which supported its folded conformation in the solution-state include: C24H vs. C19H, C24H vs. C18H and NH1 vs. C12H (fig. 1.10C). However, similar characteristic nOes were weakened or absent in the case of esters, suggesting significant fraying, as observed in the solid-state (crystal structures). It is also noteworthy that the characteristic NH1 vs. C12H nOe interaction that is suggestive of folding, as observed in the amide **1**, got significantly weakened in the ester counterpart **7** (fig. 1.9B). The NOE interactions like C24H vs. C19H and C24H vs. C18H in amide **1** were absent in its ester counterpart **7**. On the other hand, esters (**7** and **12**) displayed strong NOE involving the interactions between  $\delta$ -hydrogens of proline and aromatic hydrogens of Ant (i.e. C12H vs. C5H), suggestive of fraying. These differences in the

conformational features of ester and amide model systems can be attributed to the differences in their hydrogen bonding patterns.

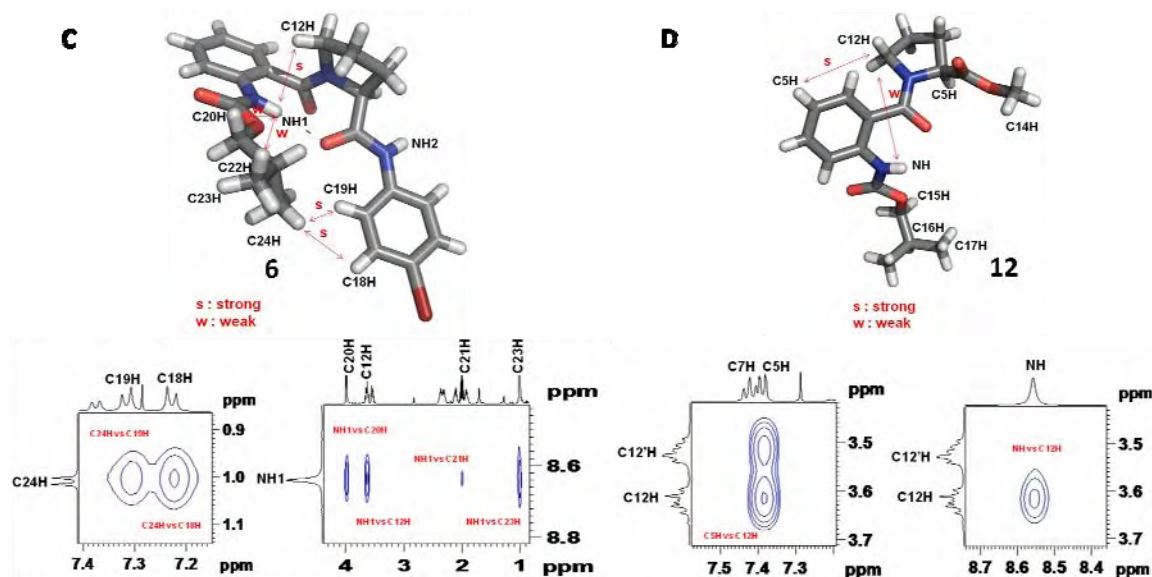


Fig. 1.10: 2D NOESY extracts of amide **6** and ester **12** (400MHz, CDCl<sub>3</sub>)

**NMR titration studies with DMSO-*d*<sub>6</sub>:** The 9-membered-ring hydrogen bonding that lead to folding in the case of the C-terminal amides were retained in the solution-state, as evidenced from the solvent titration experiments (fig. 1.11).

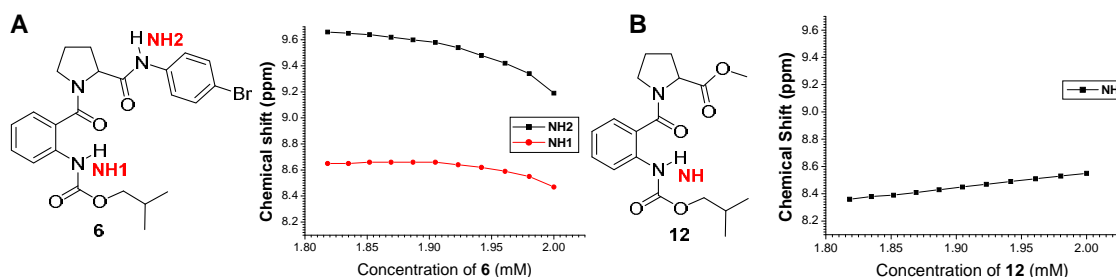
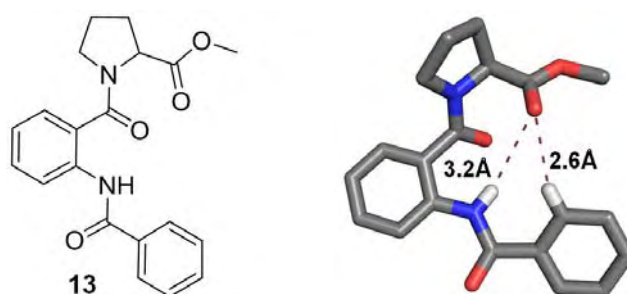


Fig. 1.11: Titration study of **6** (left) and **12** (right) in CDCl<sub>3</sub> with DMSO-*d*<sub>6</sub> (Volume of DMSO-*d*<sub>6</sub> added at each addition = 5  $\mu$ l)

DMSO-*d*<sub>6</sub> titration studies of **6** and **12** were performed to understand the strength of C-9 hydrogen bonding that clearly distinguishes *inter vs. intra*-molecular hydrogen-bonding patterns. The experiments were performed in 2mM concentration of compound in CDCl<sub>3</sub>. The potential intervention of C-6 hydrogen bonding, in place of C-9 hydrogen-bonding in esters, made the exact hydrogen bonding analysis difficult. It was observed that the NH of Ant undergoes signal splitting due to rotamer formation - an effect due to the *cis-trans* inter-conversion of <sup>t</sup>Boc group.<sup>68</sup>

### 1.12 Simultaneous display of N-H...O hydrogen bonding and C-H...O interactions

On investigating the effects of substituent on the structural feature of the folded conformation, we noticed an anomalous example of an ester **13** that purportedly formed a very weak C-9 hydrogen bonding [d(N-H...O): 3.17), d(N...O): 4.51)] (fig. 1.12). Closer investigation of its crystal structure revealed that the N-terminus benzoyl group restricted the C-terminus ester group from fraying, apparently mediated through a C-H...O interaction.<sup>9</sup>



**Fig. 1.12:** Molecular and crystal structure of a C-terminal ester **13** showing intra-molecular C-H...O interaction.

### 1.13 Significance of swapping C-terminal amides with thioesters

Thioesters are one of the good *isosteric* replacements of amides and esters. The hydrogen bonding acceptor potential of a thioester carbonyl is weaker than that of an ester.<sup>32,69</sup> Though the electron withdrawing power of sulfur is less than that of oxygen, the hydrogen bonding potential of the carbonyl oxygen in thioesters are weakened due to the delocalization of electron density around the carbonyl oxygen to vacant *d*-orbitals of sulfur resulting in the reduction of hydrogen bonding acceptor capacity.<sup>32,69-70</sup>

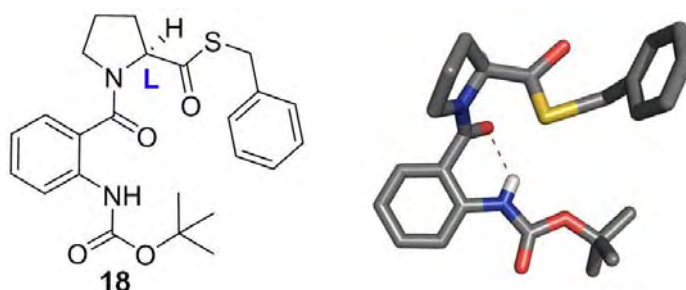


**Fig. 1.13:** Molecular and crystal structure of Ant-Pro C-terminal thioester **18** showing C-6 hydrogen bonding

In order to understand the hydrogen bonding propensities, Ant-Pro C-terminal thioesters were synthesized. Further investigation has been envisaged by the single crystal



X-ray analysis of **18**. The crystallographic analysis of **18** showed the C-6 hydrogen bonding of Ant, in *lieu* of the Ant-Pro C-9 hydrogen bonding (fig. 1.13).

### 1.14 Conclusions

The present study described a striking case of a comparison of the individual contribution of C-terminal ester *vs.* amide carbonyl as hydrogen bonding acceptor in the folding of a peptide secondary structure featuring a closed network of hydrogen bonded ring. A simple two-residue peptide fold served as easy model, with least interference from other opposing interactions originating from the backbone and / or side chains, in evaluating the extent of individual contribution of C-terminal ester *vs.* amide carbonyl as hydrogen bonding acceptor in the formation of a peptide fold. Results from the crystallographic studies of two large sets of C-terminal esters and amides clearly revealed the high tendency of the C-terminal amides, when compared to their ester counterparts, to stabilize a folded conformation. The complete manifestation of the individual contributions - ester *vs.* amide - in modulating the stability of the hydrogen bonded network, free from involvement of other effects which would have otherwise noticeable in large oligomer systems, is remarkable.

## Part B: Sulphonamides vs. Carboxamides at the N-Terminus of Ant-Pro Reverse Turn.

**1.15 The geometrical preferences of a sulfonamide bond:** A sulfonamide bond is one of the efficient *isosteric* replacements of a carboxamide. The superior stability of a sulfonamide bond towards hydrolysis makes it a better isostere for a carboxamide against proteolysis. The presence of an additional acceptor oxygen atom attached to a sulfur atom increases the hydrogen-bonding preference of a sulfonamide. The sulfonamide NH is relatively more acidic and thus is a strong hydrogen bond donor than a carboxamide. The exceptionality of a sulfonamide bond showing a major twist that occurs from the reduction of the dihedral angle ' $\omega$ ' from  $\sim 180^\circ$  (carboxamide) to  $\sim 90^\circ$  (sulfonamide;  $\pm 20$ ) explains why sulfonamide has a twisted conformation (non-planar), while an amide bond is planar. The role of sulfonamides in inducing folding in peptides has been studied in detail in the following chapters. The present study here attempts to examine the outcome of the amide modification to sulfonamide at the N-terminus of Ant-Pro turn unit, considering the significant differences between sulfonamides and carboxamides.<sup>71-77</sup>

### 1.16 Objective of present work: Investigating the robustness of Ant-Pro C<sub>9</sub> turn

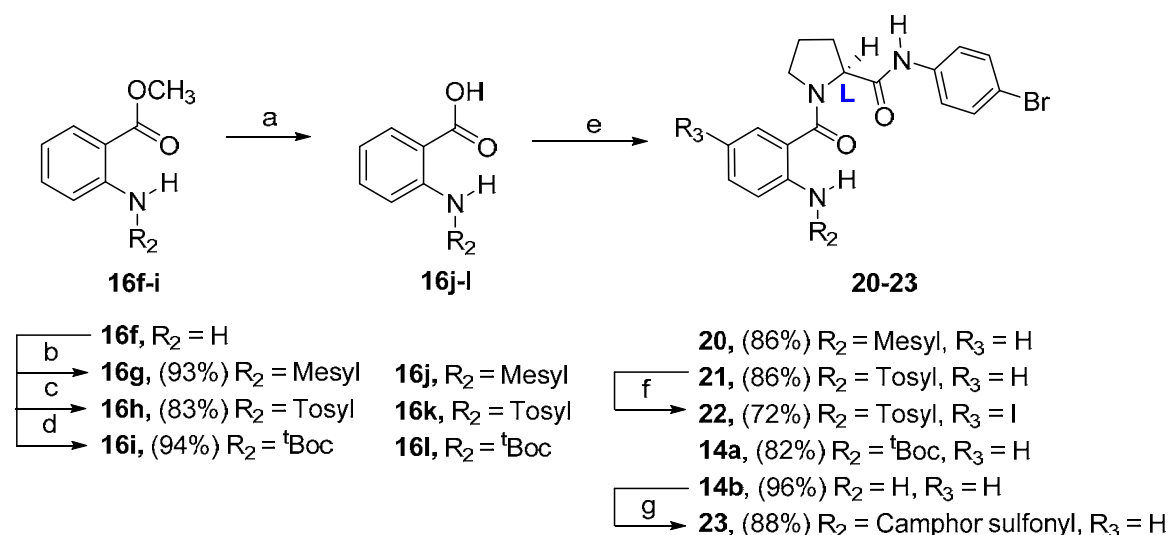
The two-residue Ant-Pro motif adopts a robust *pseudo*  $\beta$ -turn conformation featuring a strong 9-membered-ring hydrogen bonding, formed in the forward direction of the sequence 1 $\rightarrow$ 2.<sup>61</sup> The steric clash between the rings, anthranilic acid (Ant) and proline (Pro) coerces them to adopt an anti-periplanar arrangement breaking the six-membered hydrogen bond of Ant and leading to the formation of a closed nine-membered hydrogen bonded network.<sup>61</sup> Considering the substantial geometrical, hydrogen bonding and conformational differences of carboxamides and sulfonamides, as noted earlier, the robustness of the turn is tested by the introduction of sulfonamides around the Ant-Pro reverse turn unit. Although there is a significant difference in the hydrogen bonding and dihedral angle preferences for carboxamide and sulfonamide, we anticipated a similar conformational feature owing to the fact that a sulfonamide NH is much more acidic than a carboxamide. The swapping of carboxamide with sulfonamide was carried out at the N-terminus where the NH is involved in C<sub>9</sub> hydrogen bonding. The NH when protected by a sulfonamide may involve in strong C-9 bond formation. On the other hand, the

sulfonamide modification creates the possibility of the involvement of sulfonamide oxygens for hydrogen bonding.

### 1.17 Synthesis

In order to study the effect of introducing a sulfonyl group at N-terminus, we prepared various N-sulfonylated 'Ant-Pro' dipeptide units, which would feature the C (9) turn. Anthranilic acid methyl ester was sulfonylated using mesyl and tosyl chloride in presence of Et<sub>3</sub>N as a base to obtain **16f** and **16g**, respectively. In tosylation reaction, 1 mL of DBU was added in order to activate the reaction. The sulfonylated anthranilic methyl ester was subjected to ester hydrolysis using LiOH to obtain the N-sulfonylated anthranilic acid **2** which was coupled with L-Proline 4-Br anilide to obtain the **20** and **21**. The idea of coupling the C-terminus of proline with 4-Bromo aniline was to induce crystallinity as bromo systems are known for their high tendency for halogen contacts. As the tosyl analogue **21** failed to crystallize, it was subjected to iodination using DMAP and ICl in ACN as solvent to furnish **22**. Compound **23** was obtained by treating **14b** with (1S)-camphor sulfonyl chloride, in presence of Et<sub>3</sub>N as base. (1S)-Camphor sulfonyl chloride was obtained by heating (1S)-camphor sulfonic acid with thionyl chloride at 60°C for 2h.

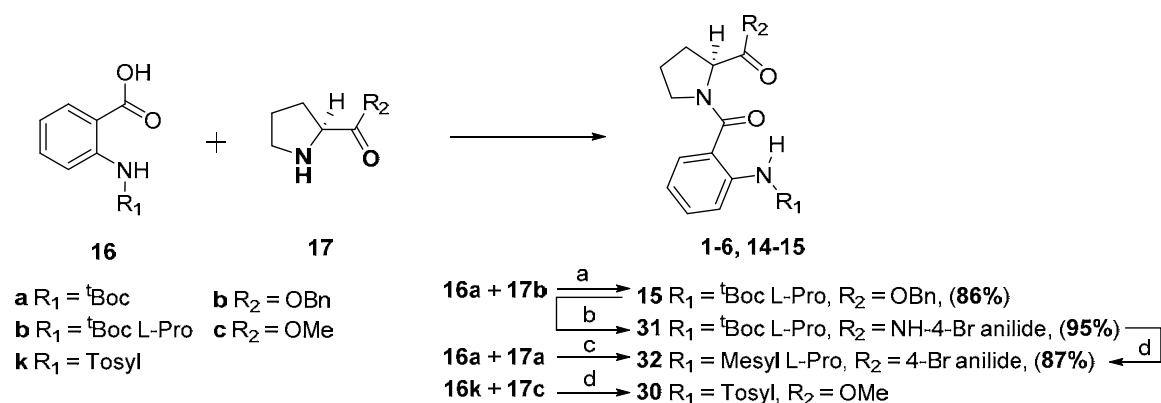
**Scheme 1.3:** Synthesis of N-terminal sulfonamides



*Reagents and Conditions* (a) LiOH.H<sub>2</sub>O, THF, H<sub>2</sub>O, rt, 4h; (b) mesyl-Cl, Et<sub>3</sub>N, DCM, rt, 6h; (c) tosyl-Cl, Et<sub>3</sub>N, DBU, DCM, rt, 6h; (d) <sup>t</sup>Boc anhydride, NaOH, dioxane, H<sub>2</sub>O; (e) HBTU, H-L-Pro-p(C<sub>6</sub>H<sub>4</sub>) Br, DIEA, ACN, rt, 12h, (f) ICl, DMAP, ACN, rt, 2h; (g) (1S)-camphor sulfonyl chloride, Et<sub>3</sub>N, DCM, rt, 6h.

Compound **16k** was coupled with H-L-Pro-OMe using HBTU and DIEA to obtain methyl ester analogue of compound **21**, *i.e.* compound **30**. Compound **15** was subjected to saponification reaction using LiOH to obtain free acid which was further coupled with *p*-bromo aniline using HBTU and DIEA in DCM to obtain compound **31**. Compound **31** was subjected to <sup>t</sup>Boc deprotection using TFA and DCM to obtain the free amine which was sulfonylated using mesyl chloride to obtain compound **32**.

**Scheme 1.4:** Synthesis of N-terminal sulfonamides



*Reagents and Conditions* (a) DCC, HOBt, DCM, rt, 12h; (b) HBTU, *p*-bromo aniline, DIEA, ACN, rt, 12h, (c) HBTU, DIEA, *p*-bromo aniline, DCM, rt, 12h; (d) HBTU, DIEA, DCM, rt, 12h.

## 1.18 Conformational analyses

Conformational analyses were carried out using single crystal X-ray diffraction studies of **20** and **22** and the solution state conformation of **20** was determined using 2D NOESY studies.

**1.18.1 Single crystal X-ray diffraction studies:** Conformational analysis of compounds **20** and **22** showed the presence of C<sub>9</sub> turn by N-terminal swapping of carboxamides with sulfonamides.

The 'ω' value of the sulfonamide bond close to 90° (*i.e.* 91° in **20** and 72° in **22**) in both the compounds showed the characteristic of a sulfonamide bond. Closer examination of the crystal structures of **20** and **22** showed that the folding (twist) induced by the sulphonamide bond at the end terminals makes the C<sub>α</sub> carbons to fray apart. On the other hand the C-9 hydrogen bonding distances were found to be closer than that observed in the case of N-terminal carboxamides, suggesting the increase in the acidity of Ant NH involved in hydrogen bonding.

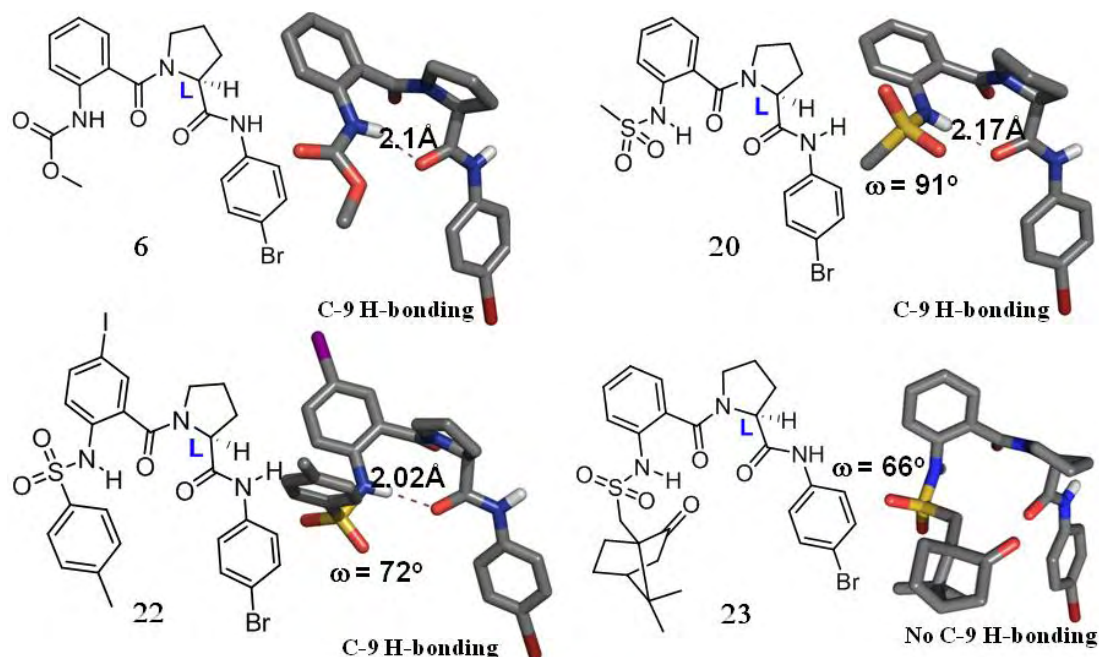


**Fig. 1.14:** Molecular structures and crystal structures of reverse turns featuring sulphonamide bonds (compounds **20** and **22**), showing C-9 turn and the camphor sulfonyl analogue (compound **23**) which is devoid of C-9 turn

Analogue **23**, which contained the Ant NH protected by a bulky camphor sulfonyl group, failed to form the C-9 turn due to the steric factors. The bulky nature of camphor sulfonyl group interacted at the folding region of Ant-Pro dipeptide. Here, it resulted in the absence of C-9 turn and resulted in the involvement of Ant NHs in C-6 *intra*-residual hydrogen bonding of Ant. Apart from C-6 hydrogen bonding, the carbonyl of camphor sulfonyl moiety was seen to be involved in CH $\cdots$ O interactions with prolyl carbonyl in its solid-state conformation.

**1.18.2 Solution state NMR studies:** Conformational investigations by solution state NMR studies of **20** revealed that the solid-state conformation of the N-terminal sulfonamides remained clearly preserved in the solution-state as well, as evidenced from 2D-NOESY studies.

NH1 *vs.* C11H and C6H *vs.* C10H were the two major NOE interactions, which supported the folded structure of **20**. The persistence of 9-membered-ring hydrogen bonding that led to folding, was determined from the solvent titration experiment of **20**. DMSO-*d*<sub>6</sub> titration studies were performed to understand the strength of C-9 hydrogen bonding, which clearly distinguished *inter* and *intra*-molecular hydrogen bonding patterns. NH1, which is involved in *intra*-molecular C-9 hydrogen bonding underwent

negligible shift (value), while the NH2 involved in inter-molecular hydrogen bonding underwent significant shift.

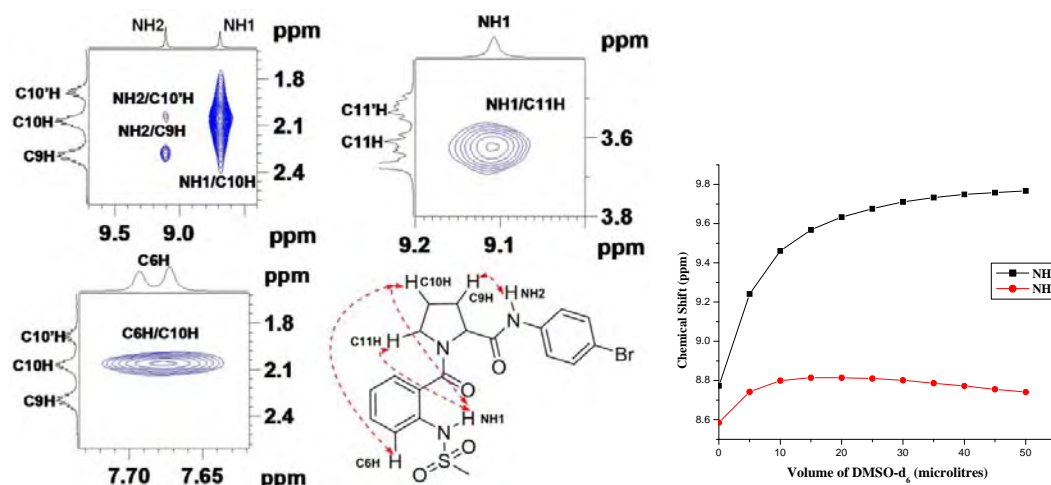


**Fig. 1.15:** 2D extracts of compound **20** (500MHz, CDCl<sub>3</sub>) and titration study of **20** in CDCl<sub>3</sub> (10 mmol) with DMSO-*d*<sub>6</sub> (volume of DMSO-*d*<sub>6</sub> added at each addition = 5  $\mu$ l).

On comparing the NH chemical shift values of various N-substituted Ant-Pro aniline bromide systems, it was noted that the chemical shift values of NHs came in the range of  $\delta$ 8-10. The characteristic chemical shifts of the Ant amide NHs involved in the 9-membered-ring hydrogen bonded network serve as a good reference to test the presence of 9-membered-ring hydrogen bonding.

**1.18.3 Circular Dichroism (CD) studies:** Circular Dichroism is a technique for studying the conformational behavior of peptides or proteins.<sup>78-79</sup> The CD spectra for the compounds **20**, **21** and **23** showed cotton effects and also showed peaks at 280-290 nm due to the presence of aromatic residues (fig 1.16).

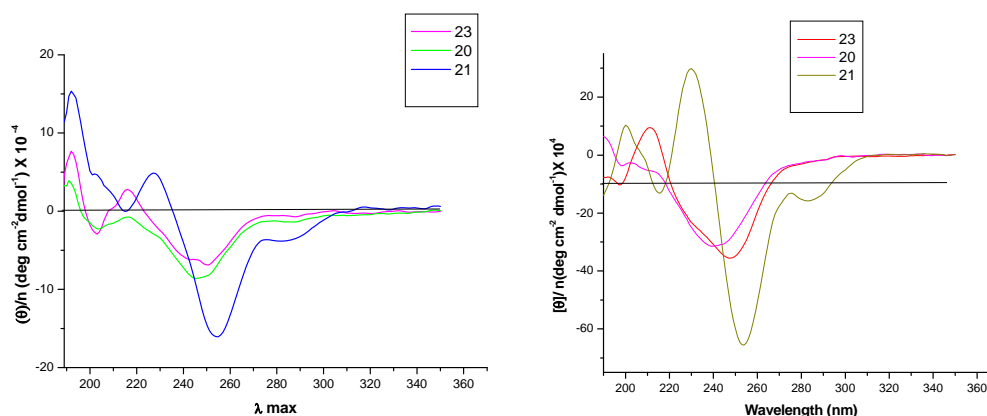


**Fig. 1.16:** Figure showing the CD Spectra for compounds **20**, **21** & **23** in acetonitrile (left) and trifluoroethanol (right).

## 1.19 Conclusions

Sulfonamides, with distinctly different structural geometry (twisted when compared to planar carboxamide) and hydrogen bonding preferences (two hydrogen-bond acceptor oxygen atoms compared with one acceptor oxygen of carboxamide) are known to form unusual hydrogen bonding interactions. The results obtained from the investigation of crystal structures and their NMR studies strongly suggested that the Ant-Pro assumed a folded reverse-turn-like structure, raising its possibility in practical utility, particularly in rigidifying peptide backbone. In one case, where the N-terminus was protected by camphor sulphonyl group, showed absence of folded structure featuring C-9 hydrogen bonding, suggesting the intricacies in folding interactions.

## 1.20 Biological activity studies of Ant-Pro dipeptides

Ant-pro dipeptides were shown to possess antibacterial activity against a group of bacteria, *Streptomyces Aureus sp. nov.*<sup>87</sup>

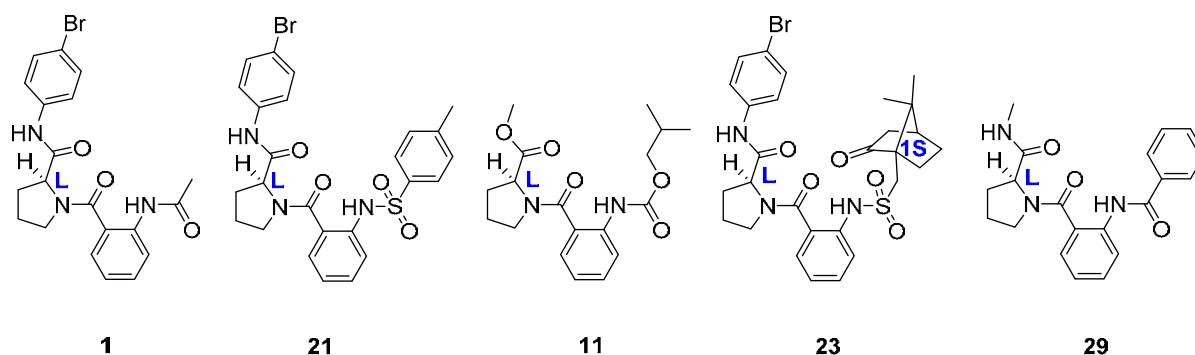


**Fig. 1.17:** Anti-bacterial Ant-Pro dipeptides

**Table 1.2:** Anti-bacterial profiles of Ant-Pro dipeptides

No:	Compound	<i>Strep.</i> -MIC ( $\mu\text{g/mL}$ )	<i>EA</i> - MIC ( $\mu\text{g/mL}$ )
1	<i>Streptomycin</i>	5-10	5-10
2	<b>1</b>	5-10	5-10
3	<b>21</b>	2.5-5	2.5-5
4	<b>29</b>	5-10	5-10
5	<b>23</b>	5-10	5-10
6	<b>11</b>	5-10	5-10

Compounds **1**, **11**, **21**, **23** and **29**, were found to be active against the antibacterial inhibition at an MIC at the range of 5-10  $\mu\text{g/mL}$ . After a series of screening studies, compound **21** was found to be the lead candidate showing MIC (Minimum Inhibition Concentration) of 2.5-5  $\mu\text{g/mL}$ . Although, the other Ant-Pro dipeptides were found to be inhibiting the bacterial growth, MIC was not observed to be that significant. Antibacterial studies (MIC) of dipeptides are summarized in table (table 1.2, *vide infra*).

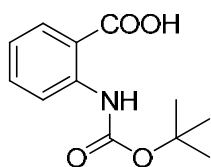
### 1.21 Summary

Crystallographic studies of Ant-Pro dipeptide turn units with diverse substitution patterns at both terminals revealed the structural and conformational features of Ant-Pro reverse turn. Two large sets of C-terminal esters (6 nos) and amides (6 nos) of Ant-Pro dipeptide units clearly exposed the high tendency of the C-terminal amides, when compared to their ester counterparts, to stabilize a folded conformation. In the absence of C-9 hydrogen bonding, ester analogues assumed the absence of folded structure, satisfying the *intra*-residual C-6 hydrogen bond of Ant oligomers. Crystal structures (2 nos) of Ant-Pro dipeptide units having the NH protected with sulfonyl group showed the presence of C-9 turn despite the fact that sulfonamides have entirely different geometrical and hydrogen bonding propensities, when compared to normal amides. The solid state behavior was also reflected in its solution state studies. It was also observed that the Ant-Pro reverse turns were disturbed by steric factors. On the other hand, the C-6 hydrogen bonding of Ant was found to be stable in the systems without the C-9 hydrogen bonding interactions. Besides, Ant-Pro dipeptides were shown to exhibit anti-bacterial properties. The robustness of the Ant-Pro reverse turn raises the prospect of practical applications, particularly in rigidifying peptide backbones by inserting the Ant-Pro reverse turn motifs into their backbone - a work that is in progress in our laboratory.



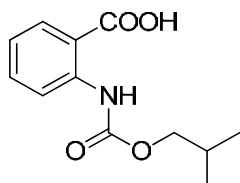
## 1.22 Experimental procedures

### 2-(Tert-butoxycarbonylamino)benzoic acid, **16a**:



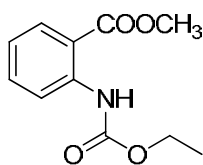
To a solution of anthranilic acid (1g, 6.6mmol) in dioxane (15mL) and water (7.5mL), NaOH (0.528, 13.2 mmol) was added followed by the addition of <sup>t</sup>Boc-anhydride (1.7g, 7.9mmol). The reaction mixture was stirred at room temperature for 3 hours. The solvents were evaporated under reduced pressure. The residue was acidified with saturated potassium bisulphate solution, followed by extraction with DCM (10mL x 3). Evaporation under reduced pressure afforded the crude product **16a**, which was used for further reactions, without purification.

### 2-((Isobutoxycarbonyl)amino)benzoic acid, **16c**:



To a solution of anthranilic acid (1g, 6.6mmol) in dioxane (15mL) and water (7.5mL), NaOH (0.528, 13.2 mmol) was added followed by the addition of isobutyl chloroformate (1.7g, 7.9mmol). The reaction mixture was stirred at room temperature for 3 hours, after which the solvents were evaporated under reduced pressure. The residue was acidified with saturated potassium bisulphate solution, followed by extraction with DCM (10mL x 3). Evaporation under reduced pressure afforded the crude product **16c**, which was used for further reactions, without purification.

### Methyl 2-((ethoxycarbonyl)amino)benzoate, **16d**:

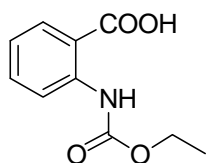


To a solution of anthranilic methyl ester (0.5g, 3.3mmol) in dry DCM (10mL) containing DIEA (1.25g, 1.7mL, 9.92 mmol) was added ethyl chloroformate (0.43g, 3.92 mmol), drop wise with vigorous stirring. The reaction mixture was stirred at room temperature for 12 h. The reaction mixture was diluted with DCM and the organic layer was washed sequentially with saturated sodium bicarbonate, potassium bisulphate and water. The organic layer was dried over anhydrous Na<sub>2</sub>SO<sub>4</sub> solution and evaporated under reduced pressure to furnish the crude product which was purified by column chromatography, (85:15 pet. ether/ethyl acetate, R<sub>f</sub>: 0.5) affording **16d** as a white solid (0.63g, 93%), mp: 60-61°C; IR (CHCl<sub>3</sub>, ν (cm<sup>-1</sup>): 3310, 3021, 1731, 1694, 1591, 1529, 1453, 1315, 1245, 1216; <sup>1</sup>H NMR (CDCl<sub>3</sub>/200MHz): δ ppm 10.47 (s, 1H), 8.42-8.46 (d,

$J=8.23\text{Hz}$ , 1H), 7.97-8.01 (dd,  $J=7.98\text{Hz}$ ,  $J=1.63\text{Hz}$  1H), 7.47-7.56 (m, 1H), 6.96-7.05 (m, 1H), 4.17-4.27 (m, 2H), 3.90 (s, 3H), 1.28-1.35 (t, 1H,  $J=7.07$ ),  $^{13}\text{C}$  NMR ( $\text{CDCl}_3$ , 125MHz):  $\delta$  ppm 168.4, 153.6, 141.8, 134.5, 130.8, 121.3, 118.7, 114.3, 61.1, 52.1, 14.4; LC-MS: 247.06 ( $\text{M}+23$ )<sup>+</sup>; Elemental analysis calculated for  $\text{C}_{11}\text{H}_{13}\text{NO}_4$ : C, 59.19; H, 5.87; N, 6.27; Found: 58.65; H, 5.16; N, 5.94.

### Representative procedure for ester hydrolysis:

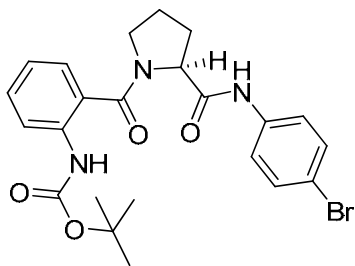
#### 2-((Ethoxycarbonyl)amino)benzoic acid, **16e**



To a solution of **16d** (0.5g) in methanol (5mL), LiOH (0.18, 0.01mmol) in water (5mL) was added. After stirring for 12h, the reaction mixture was stripped of the solvent under reduced pressure, acidified using saturated  $\text{KHSO}_4$  solution and then extracted with ethyl acetate (3x5mL). The organic layer was evaporated under reduced pressure to obtain the free acid **16e** which was used for next reaction, without further purification.

**Representative procedure for peptide coupling** (see schemes for specific coupling agents):

#### (S)-tert-butyl 2-(2-(4-bromophenylcarbamoyl)pyrrolidine-1-carbonyl)phenylcarbamate, **14a**:

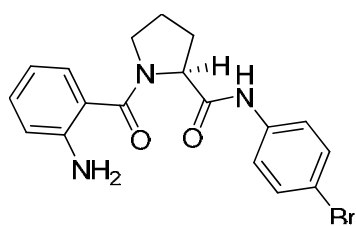


To a solution of **17a** (0.25g, 0.99mmol) in dry DCM (5mL), Boc-Ant-OH (0.5g, 1.9mmol), EDC.HCl (0.286g, 1.492) and HOBT (0.062g, 25wt %) were added. After stirring at room temperature for 12 hours, the reaction mixture was diluted with DCM and washed sequentially with saturated sodium bicarbonate, potassium bisulphate solution and water. The washings were extracted with DCM (10mLx2) and dried with anhydrous  $\text{Na}_2\text{SO}_4$  and evaporated under reduced pressure. The crude residue thus obtained was purified by column chromatography, (50:50 pet ether/ethyl acetate,  $R_f$ : 0.5) furnishing **14a** as a white solid (0.4181g, 87%), mp: 97-101°C;  $[\alpha]_D^{28}$ : -28.89° ( $c = 1.066$ ,  $\text{CHCl}_3$ ); IR ( $\text{CHCl}_3$ ,  $\nu$  ( $\text{cm}^{-1}$ ): 3279, 3018, 1730, 1681, 1614, 1537, 1429, 1367, 1300, 1247, 1159, 1074;  $^1\text{H}$  NMR ( $\text{CDCl}_3$ /500MHz):  $\delta$  ppm 9.59 (s, 1H), 8.46(s, 1H), 8.26-8.28 (d,  $J=8.26\text{Hz}$ , 1H), 7.43 (t,  $J=7.43\text{Hz}$ , 1H), 7.36-7.37 (d,  $J=7.43\text{Hz}$ , 1H), 7.25-7.26 (d,

$J=8.8\text{Hz}, 2\text{H}$ ), 7.15-7.16 (d, 2H,  $J=8.8\text{Hz}$ ), 7.07 (t, 1H,  $J=7.43\text{Hz}$ ), 5.01-5.04 (m, 1H), 3.60-3.65 (m, 1H), 3.49-3.53(m, 1H), 2.23-2.37 (m, 2H) 2.03-2.11 (m, 1H) 1.85-1.93 (m, 1H) 1.55(s, 9H);  $^{13}\text{C}$  NMR ( $\text{CDCl}_3, 125\text{MHz}$ ):  $\delta$  ppm 169.7, 153.1, 137.2, 136.7, 131.3, 131.1, 126.8, 123.9, 122.0, 120.8, 120.1, 116.1, 80.6, 60.7, 50.5, 28.9, 25.1; ESI-MS: 490.3465 ( $\text{M}+2\text{H}$ )<sup>+</sup>; 510.3085 ( $\text{M}+\text{Na}$ )<sup>+</sup>; 528.2927 ( $\text{M}+\text{K}$ )<sup>+</sup>; Elemental analysis calculated for  $\text{C}_{23}\text{H}_{26}\text{BrN}_3\text{O}_4$ : C, 56.56; H, 5.37; N, 8.60; Found: C, 56.18; H, 5.87; N, 8.10.

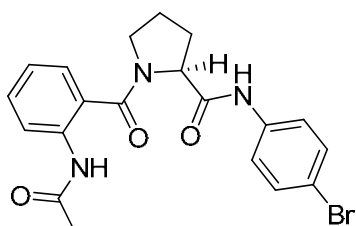
### Representative procedure for <sup>t</sup>boc deprotection:

#### (S)-1-(2-aminobenzoyl)-N-(4-bromophenyl)pyrrolidine-2-carboxamide, **14b**:



To a solution of **14a** (0.1, 0.26mmol) in DCM (1mL) maintained at 0°C, trifluoroacetic acid (1 mL) was added drop wise. The reaction mixture was stirred at 0°C for 10 minutes and then at RT for 3 h. The residue obtained after evaporating the volatiles was neutralized using saturated solution of sodium bicarbonate and extracted repeatedly using DCM (3x5mL). The organic layer was dried over anhydrous  $\text{Na}_2\text{SO}_4$  and evaporated under reduced pressure to obtain the amine **14b** which was used for next reaction, without further purification.

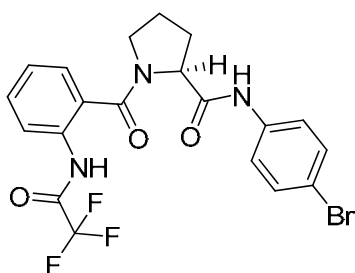
#### (S)-1-(2-acetamidobenzoyl)-N-(4-bromophenyl)pyrrolidine-2-carboxamide, **1**:



To a solution of **14b** (0.1 gm, 0.26mmol) in DCM (5 mL),  $\text{Et}_3\text{N}$  (0.11mL, 0.78mmol) and acetyl chloride (0.03mL, 0.39mmol) were added. After stirring for 12 hours, the reaction mixture was diluted with DCM (5 mL) and the organic layer was washed with saturated sodium bicarbonate (5mL), potassium bisulphate (5mL) and water (5mL). The organic layer was dried over anhydrous  $\text{Na}_2\text{SO}_4$  solution and evaporated under reduced pressure to get the crude product which was purified by column chromatography, (20:80 pet. ether/ethyl acetate,  $R_f$ : 0.5) affording **1** as a white solid (0.98g, 88%), crystallized from a solution of methanol and dichloromethane, mp: 226-229°C;  $[\alpha]_D^{24}$ : -90° ( $c = 0.4$ ,  $\text{CHCl}_3$ ); IR ( $\text{CHCl}_3$ )  $\nu$  ( $\text{cm}^{-1}$ ) 3261, 3020, 2401, 1716, 1697, 1683, 1653, 1647, 1635, 1620;  $^1\text{H}$  NMR( $\text{CDCl}_3/200\text{MHz}$ ):  $\delta$  ppm 9.47 (s, 1H), 9.29 (s, 1H), 8.35-8.39 (d, 1H,  $J=8.06\text{Hz}$ ), 7.38-7.47 (dd, 1H,  $J=15.62\text{ Hz}$ ,  $J=1.59\text{ Hz}$ ), 7.11-7.32 (m, 6H), 4.95-5.01 (m, 1H), 3.39-3.63 (m, 2H), 2.24 (s, 3H), 1.87-2.46 (m, 4H),  $^{13}\text{C}$  NMR ( $\text{DMSO}-d_6, 100\text{MHz}$ ):  $\delta$  ppm

171.3, 168.9, 167.5, 138.4, 135.0, 131.9, 129.9, 128.5, 126.8, 123.9, 121.9, 121.5, 115.4, 60.4, 49.3, 30.2, 24.9, 24.1; LC-MS: 454.05 (M+Na)<sup>+</sup>; Elemental analysis calculated for C<sub>20</sub>H<sub>20</sub>BrN<sub>3</sub>O<sub>3</sub>: C, 55.83; H, 4.68; N, 9.77; Found: C, 57.36; H, 5.14; N, 8.96.

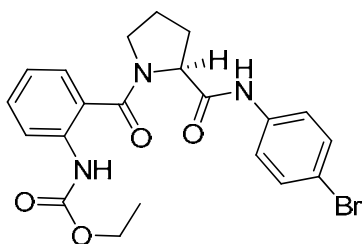
**(S)-1-(2-Trifluoroacetamidobenzoyl)-N-(4-bromophenyl)pyrrolidine-2-carboxamide, 4:**



Compound **4**, obtained by following the procedure used for preparation of **1** (*vide supra*), except using trifluoroacetic anhydride as the acylating agent, was purified by column chromatography (20:80 pet. ether/ethyl acetate, R<sub>f</sub>: 0.5), white solid (0.112g, 90%), crystallized from methanol, mp: 210-217°C; [α]<sub>D</sub><sup>27</sup>: -199° (*c* = 0.1, CHCl<sub>3</sub>);

IR (CHCl<sub>3</sub>) ν (cm<sup>-1</sup>) 3310, 3020, 1733, 1698, 1621, 1531, 1422, 1215; <sup>1</sup>H NMR(CDCl<sub>3</sub>/200MHz): δ ppm 10.63 (s, 1H), 9.04 (s, 1H), 8.33-8.38 (d, 1H, *J*=8.03Hz), 7.52-7.60 (m, 2H), 7.26-7.42 (m, 6H), 4.90-4.97 (m, 1H), 3.61-3.80 (m, 2H), 1.87-2.55 (m, 4H), <sup>13</sup>C NMR (50 MHz, CDCl<sub>3</sub>) δ : ppm 169.6, 168.7, 136.8, 134.5, 131.9, 131.7, 128.1, 125.0, 124.4, 122.3, 121.2, 116.8, 61.0, 51.2, 27.8, 25.4; ESI-MS: 508.6183 (M+Na)<sup>+</sup>; 524.6121 (M+K)<sup>+</sup>. Elemental analysis calculated for C<sub>20</sub>H<sub>17</sub>BrF<sub>3</sub>N<sub>3</sub>O<sub>3</sub>: C, 49.60; H, 3.54; N, 8.68; Found: C, 47.37; H, 6.46; N, 8.16.

**(S)-ethyl 2-(2-(4-bromophenylcarbamoyl)pyrrolidine-1-carbonyl)phenylcarbamate, 3:**



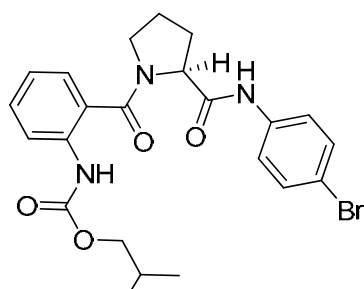
Compound **3**, obtained by following the procedure used for preparation of **1** (*vide supra*), except using ethyl chloroformate as the acylating agent, was purified by column chromatography (30:70 pet. ether/ethyl acetate, R<sub>f</sub>: 0.5), white solid (0.076g, 64%), crystallized from a solution of methanol and dichloromethane, mp: 201-

203°C; [α]<sub>D</sub><sup>26</sup>: -141° (*c* = 0.1, CHCl<sub>3</sub>); IR (CHCl<sub>3</sub>, ν (cm<sup>-1</sup>): 3421, 3020, 1733, 1687, 1616, 1541, 1427, 1398, 1302, 1215; <sup>1</sup>H NMR (CDCl<sub>3</sub>/400MHz): δ ppm 9.58 (s, 1H), 8.66(s, 1H), 8.25-8.27 (d, *J*=8.18Hz, 1H), 7.43-1.47 (t, *J*=7.77Hz, 1H), 7.38-7.39 (d, *J*=7.40Hz, 1H), 7.25-7.27 (d, *J*=8.7Hz, 2H), 7.15-7.18 (d, 2H, *J*=8.51Hz), 7.08-7.12 (t, 1H, *J*=7.40Hz), 5.00-5.03 (m, 1H), 4.22-4.27 (m, 2H), 3.60-3.70 (m, 1H), 3.50-3.56 (m,

1H), 2.23-2.39 (m, 2H), 2.04-2.14 (m, 1H) 1.84-1.94 (m, 1H), 1.32-1.35 (t, 3H,  $J=7.15$ );  $^{13}\text{C}$  NMR ( $\text{CDCl}_3$ , 125MHz):  $\delta$  ppm 169.8, 153.9, 137.2, 136.5, 131.3, 131.2, 126.8, 123.9, 122.3, 120.8, 120.3, 116.2, 61.3, 60.9, 50.7, 28.9, 25.1, 14.4; LC-MS: 482.08 ( $\text{M}+\text{Na}$ ) $^+$ ; Elemental analysis calculated for  $\text{C}_{21}\text{H}_{22}\text{BrN}_3\text{O}_4$ : C, 54.79; H, 4.82; N, 9.13; Found: C, 58.16; H, 4.38; N, 8.92.

### (S)-Isobutyl 2-(2-(4-bromophenylcarbamoyl)pyrrolidine-1-carbonyl)phenyl

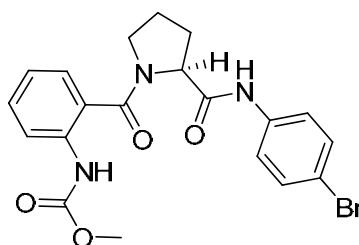
#### Carbamate, 5:



Compound **5**, obtained by following the procedure used for preparation of **1** (*vide supra*), except using isobutyl chloroformate as the acylating agent, was purified by column chromatography (30:70 pet. ether/ethyl acetate,  $R_f$ : 0.55), white solid (0.102g, 81%), mp: 200-203°C;  $[\alpha]_D^{27}$ : -142° ( $c = 0.1$ ,  $\text{CHCl}_3$ ); IR ( $\text{CHCl}_3$ ,  $\nu$  ( $\text{cm}^{-1}$ ): 3316,

3020, 1734, 1686, 1617, 1541, 1457, 1398, 1302, 1215;  $^1\text{H}$  NMR ( $\text{CDCl}_3$ /200MHz):  $\delta$  ppm 9.45 (s, 1H), 8.61 (s, 1H), 8.19-8.23 (d,  $J=8.27\text{Hz}$ , 1H), 6.99-7.41 (m, 7H), 4.91-4.97 (m, 1H), 3.89-3.92 (d, 1H,  $J=6.54$ ), 3.36-3.61 (m, 2H), 1.75-2.25 (m, 5H), 0.91-0.94 (d, 6H,  $J=6.54$ );  $^{13}\text{C}$  NMR ( $\text{CDCl}_3$ , 125MHz):  $\delta$  ppm 169.7, 153.1, 137.2, 136.7, 131.3, 131.1, 126.8, 123.9, 122.0, 120.8, 120.1, 116.1, 80.6, 60.7, 50.5, 28.9, 25.1; ESI-MS: 488.4006 ( $\text{M}+\text{H}$ ) $^+$ ; 510.2612; ( $\text{M}+\text{Na}$ ) $^+$ ; Elemental analysis calculated for  $\text{C}_{23}\text{H}_{26}\text{BrN}_3\text{O}_4$ : C, 56.56; H, 5.37; N, 8.60; Found: C, 56.19; H, 5.85; N, 8.98.

### (S)-Methyl 2-(2-(4-bromophenylcarbamoyl)pyrrolidine-1-carbonyl)phenylcarbamate, 6

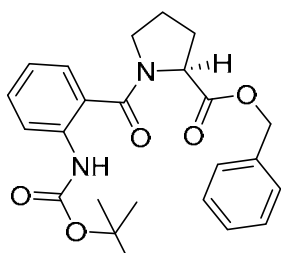


Compound **6**, obtained by following the procedure used for preparation of **1** (*vide supra*), except using methyl chloroformate as the acylating agent, was purified by column chromatography, (30:70 pet. ether/ethyl acetate,  $R_f$ : 0.5) to afford **6** as a white solid (0.076g, 64%) which was later crystallized from a solution of methanol and

dichloromethane. mp: 216-220°C;  $[\alpha]_D^{27}$ : -23° ( $c = 0.1$ ,  $\text{CHCl}_3$ ); IR ( $\text{CHCl}_3$ ,  $\nu$  ( $\text{cm}^{-1}$ ): 3020, 1732, 1686, 1616, 1541, 1427, 1398, 1302, 1215;  $^1\text{H}$  NMR ( $\text{CDCl}_3$ /200MHz):  $\delta$  ppm 9.50 (s, 1H), 8.67(s, 1H), 8.25-8.21 (d,  $J=8.26\text{Hz}$ , 1H), 7.38-7.56 (m, 2H), 7.23-7.31

(m, 4H), 7.08-7.18 (m, 2H), 4.96-5.03 (t,  $J=6.69$ , 1H), 3.80 (s, 3H), 3.43-3.71 (m, 2H), 2.27-2.37 (m, 2H), 2.05-2.20 (m, 1H), 1.83-2.00 (m, 1H);  $^{13}\text{C}$  NMR ( $\text{CDCl}_3$ , 50MHz):  $\delta$  ppm 169.7, 169.6 154.1, 137.1, 136.4, 131.3, 127.0, 126.8, 123.7, 122.4, 120.9, 120.4, 116.3, 60.9, 52.4, 50.7, 28.6, 25.2; LC-MS: 470.08 ( $\text{M}+\text{Na}^+$ ); Elemental analysis calculated for  $\text{C}_{20}\text{H}_{20}\text{BrN}_3\text{O}_4$ : C, 53.82; H, 4.52; N, 9.42; Found: C, 52.22; H, 5.01; N, 8.79;

**(S)-Benzyl 1-(2-(tert-butoxycarbonylamino)benzoyl)pyrrolidine-2-carboxylate, 8:**

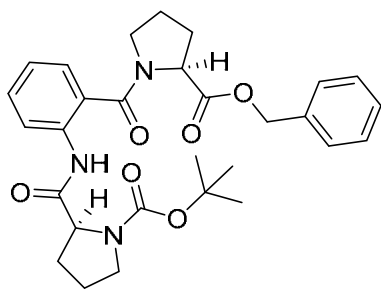


To an ice cold solution of Boc-Ant-OH **8** (3 g, 12.7 mmol, 1 equiv.) and proline benzyl ester (2.6 g, 12.7 mmol, 1 equiv.) in dichloromethane (20 ml) was added DCC (3.13 g, 15.1 mmol, 1.2 equiv.) and DMAP (cat. amount). The reaction mixture was allowed to stir at  $0^\circ\text{C}$  for 10 minutes and for 12 h at room temperature. The reaction mixture was filtered to remove DCU,

diluted with more dichloromethane and the organic layer was washed sequentially with potassium hydrogen sulphate solution, saturated sodium bicarbonate and water. The crude product obtained after the removal of solvent under reduced pressure was purified by column chromatography to afford **8** (3 g, 56%). White solid which was later crystallized from a mixture of ethyl acetate and pet. ether; mp:  $95-96^\circ\text{C}$ ;  $[\alpha]_{\text{D}}^{24}$ :  $-90$  ( $c = 0.4$ ,  $\text{CHCl}_3$ ); IR ( $\text{CHCl}_3$ )  $\nu$  ( $\text{cm}^{-1}$ ) 3356, 3016, 2980, 1717, 1626, 1591, 1520, 1454, 1416, 1215, 1159, 1051, 1026;  $^1\text{H}$  NMR(400 MHz,  $\text{CDCl}_3$ ) d: 8.41 (s, 1H), 8.22-8.18 (d,  $J = 8.37$  Hz, 1H), 7.41-7.34 (m, 7H), 7.05-6.98 (t,  $J = 7.57$  Hz, 1H), 5.24 (s, 2H), 4.78-4.74 (m, 1H), 3.64-3.38 (m, 2H), 2.45-2.28 (m, 1H), 2.07-1.84 (m, 3H), 1.50 (s, 9H);  $^{13}\text{C}$  NMR (100 MHz,  $\text{CDCl}_3$ ) d : 171.9, 168.9, 153.1, 137.4, 135.7, 131.0, 128.6, 128.3, 128.1, 127.3, 123.5, 121.6, 120.2, 80.3, 66.98, 59.1, 50.0, 29.3, 28.3, 25.3; ESI-MS: 425.21 ( $\text{M}+\text{H}^+$ ); 447. 23 ( $\text{M}+\text{Na}^+$ ); 463.24 ( $\text{M}+\text{K}^+$ ).

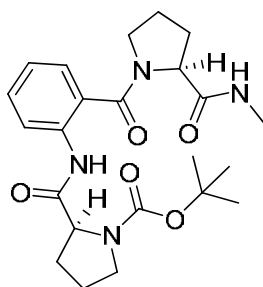
**(S)-tert-Butyl 2-(2-((S)-2-(benzyloxycarbonyl)pyrrolidine-1-carbonyl)phenyl carbamoyl)pyrrolidine-1-carboxylate, 15**

Compound **15**, obtained by following the coupling procedure used for the preparation of **8** (*vide infra*) using **16b** as acid, was purified by column chromatography (50% ethyl acetate/pet. ether,  $R_f$ : 0.4), waxy liquid (1.34 g, 86%);  $[\alpha]_{\text{D}}^{26}$ :  $-74.6^\circ$  ( $c$  0.34,  $\text{CHCl}_3$ ); IR ( $\nu$ ) neat ( $\text{cm}^{-1}$ ) 3307, 3066, 2978, 1743, 1692, 1627, 1596, 1525, 1404, 1215, 1165, 1121,



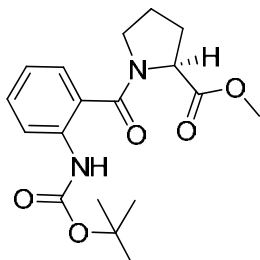
1088, 1031;  $^1\text{H}$  NMR (400 MHz,  $\text{CDCl}_3$ )  $\delta$ : 9.76<sub>rotamer</sub> (0.55H), 9.67<sub>rotamer</sub> (0.45H), 8.50-8.35 (m, 1H), 7.5-7.0 (m, 8H), 5.28-5.19 (m, 1H), 4.78-4.75 (m, 1H), 4.43<sub>rotamer</sub> (0.55H), 4.26<sub>rotamer</sub> (0.45H), 3.80-3.42 (m, 4H), 2.38-1.8 (m, 8H), 1.48<sub>rotamer</sub> (4.3H), 1.40<sub>rotamer</sub> (4.7H);  $^{13}\text{C}$  NMR (100 MHz,  $\text{CDCl}_3$ )  $\delta$ : 171.6, 171.3, 168.1, 154.7, 153.7, 136.6, 135.97, 135.3, 130.9, 130.5, 128.2, 127.98, 127.7, 127.1, 126.9, 124.4, 123.3, 122.9, 122.5, 122.8, 122.5, 121.3, 120.6, 79.5, 66.7, 66.6, 61.9, 61.1, 58.7, 49.8, 49.6, 46.8, 46.4, 31.0, 29.9, 28.8, 28.1, 27.9, 24.8, 24.0, 23.5; ESI MS: 522.5042 ( $\text{M}+\text{H}$ )<sup>+</sup>, 544.5149 ( $\text{M}+\text{Na}$ )<sup>+</sup>, 560.5602 ( $\text{M}+\text{K}$ )<sup>+</sup>; Elemental analysis calculated for  $\text{C}_{29}\text{H}_{35}\text{N}_3\text{O}_6$ : C, 66.78; H, 6.76; N, 8.06; Found: C, 67.01; H, 6.93; N, 7.69.

**(S)-tert-butyl 2-(2-((S)-2-(methylcarbamoyl)pyrrolidine-1-carbonyl) phenyl carbamoyl)pyrrolidine-1-carboxylate, 2:**



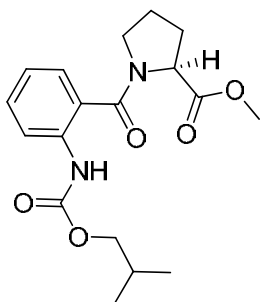
The ester **15** (0.45 g, 0.86 mmol) was converted into its corresponding methyl amide **2** by stirring the compound in methanolic methyl amine at room temperature. After completion of the reaction (3 h), the solvent was stripped off and the product was taken in dichloromethane, washed with water and the organic layer was dried over anhydrous sodium sulfate. Evaporation under reduced pressure and purification by column chromatography afforded **2** (5% methanol /ethyl acetate,  $R_f$ : 0.5), 0.36 g, 95%, ; mp: 185-187 °C;  $[\alpha]_D^{26}$ : -120° ( $c$  0.2,  $\text{CHCl}_3$ ); IR (v) nujol ( $\text{cm}^{-1}$ ): 3273, 2726, 1698, 1655, 1618, 1586, 1460, 1377, 1307, 1215, 1156;  $^1\text{H}$  NMR (400 MHz,  $\text{CDCl}_3$ )  $\delta$ : 10.01<sub>rotamer</sub> (0.5H), 9.71-9.56<sub>rotamer</sub> (0.5H), 8.44-8.13 (m, 1H), 7.41 (b, 2H), 7.13-7.09 (t,  $J = 7.41$  Hz, 1H), 6.70 (bs, 1H), 4.7-4.63 (b, 1H), 4.42<sub>rotamer</sub> (0.4H), 4.29<sub>rotamer</sub> (0.6H), 3.8-3.4 (m, 4H), 4.85-4.84 (d,  $J = 4.72$  Hz, 3H), 2.4-1.8 (m, 8H), 1.48<sub>rotamer</sub> (s, 4H), 1.38<sub>rotamer</sub> (s, 5H);  $^{13}\text{C}$  NMR (100 MHz,  $\text{CDCl}_3$ )  $\delta$ : 172.2, 171.9, 171.8, 169.2, 168.9, 155, 154.2, 136.6, 136.0, 135.3, 131.1, 130.5, 130.3, 126.8, 123.9, 123.5, 123.3, 122.9, 122.5, 120.9, 80.1, 79.9, 62.0, 60.96, 60.1, 50.3, 49.7, 47.1, 46.7, 31.8, 31.3, 29.9, 28.9, 28.2, 26.2, 25.1, 24.3, 23.7, 22.8; ESI MS: 445.3834 ( $\text{M}+\text{H}$ )<sup>+</sup>, 467.3785 ( $\text{M}+\text{Na}$ )<sup>+</sup>, 483.36 ( $\text{M}+\text{K}$ )<sup>+</sup>; Elemental analysis calculated for  $\text{C}_{23}\text{H}_{32}\text{N}_4\text{O}_5$ : C, 62.14; H, 7.26; N, 12.60; Found: C, 61.86; H, 7.14; N, 12.98.

**(S)-Methyl 1-(2-(tert-butoxycarbonylamino)benzoyl)pyrrolidine-2-carboxylate, 7:**



Compound **7**, obtained by following the coupling procedure used for the preparation of **14a** (*vide supra*), was purified by column chromatography (30:70 pet. ether/ethyl acetate,  $R_f$ : 0.5), 3.7 g, 71%, white solid, crystallized from a solution of methanol and dichloromethane; mp: 94-96 °C;  $[\alpha]^{27}_D$ : -91° ( $c = 0.1$ ,  $\text{CHCl}_3$ ); IR ( $\text{CHCl}_3$ )  $\nu$  (cm<sup>-1</sup>) 3368, 3020, 2982, 1724, 1625, 1596, 1522, 1454, 1414, 1216, 1159, 1052, 1026; <sup>1</sup>H NMR (200 MHz,  $\text{CDCl}_3$ )  $\delta$ : 8.33 (s, 1H), 8.13-8.18 (d,  $J = 8.36$  Hz, 1H), 7.32-7.39 (m, 2H), 6.95-7.03 (t,  $J = 7.22$  Hz, 1H), 4.63-4.70 (m, 1H), 3.77 (s, 3H) 3.40-3.65 (m, 2H), 2.25-2.42 (m, 1H), 1.79-2.10 (m, 3H), 1.48 (s, 9H); <sup>13</sup>C NMR (50 MHz,  $\text{CDCl}_3$ )  $\delta$ : 172.4, 168.7, 152.9, 137.2, 130.9, 128.6, 127.1, 123.3, 121.5, 120.0, 80.2, 59.0, 52.3, 49.9, 29.2, 28.2, 25.2; LC-MS: 371.02 ( $\text{M}+\text{Na}$ )<sup>+</sup>; Elemental analysis calculated for  $\text{C}_{18}\text{H}_{24}\text{N}_2\text{O}_5$ : C, 62.05; H, 6.94; N, 8.04; Found: C, 61.99; H, 7.07; N, 8.58.

**(S)-Methyl 1-(2-(iso-butoxycarbonylamino)benzoyl)pyrrolidine-2-carboxylate, 11:**

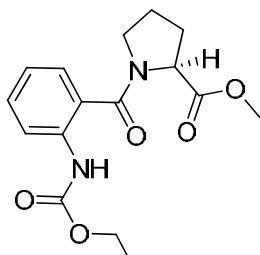


Compound **11**, obtained by following the coupling procedure used for the preparation of **14a** (*vide supra*), was purified by column chromatography (35:65 pet. ether/ethyl acetate,  $R_f$ : 0.5), 0.32g, 63%, white solid, crystallized from a solution of diethyl ether and pet-ether; mp: 76-80 °C;  $[\alpha]^{27}_D$ : -92° ( $c = 0.1$ ,  $\text{CHCl}_3$ ); IR ( $\text{CHCl}_3$ )  $\nu$  (cm<sup>-1</sup>) 3366, 3020, 2959, 1733, 1625, 1597, 1524, 1456, 1415, 1216, 1113, 1058; <sup>1</sup>H NMR (400 MHz,  $\text{CDCl}_3$ )  $\delta$ : 8.54 (s, 1H), 8.17-8.21 (d,  $J = 8.28$  Hz, 1H), 7.31-7.43 (m, 2H), 7.00-7.08 (m, 1H), 4.66-4.73 (m, 1H), 3.91-3.95 (m, 2H), 3.79 (s, 3H), 3.42-3.65 (m, 2H), 2.27-2.44 (m, 1H), 1.78-2.16 (m, 4H), 0.95-0.98 (d,  $J=6.61$ , 6H); <sup>13</sup>C NMR (50 MHz,  $\text{CDCl}_3$ )  $\delta$ : 172.6, 168.7, 153.9, 136.9, 131.1, 127.1, 123.7, 121.9, 120.1, 71.2, 59.0, 52.4, 49.9, 29.3, 27.9, 25.2, 18.9; LC-MS: 371.11 ( $\text{M}+\text{Na}$ )<sup>+</sup>; Elemental analysis calculated for  $\text{C}_{18}\text{H}_{24}\text{N}_2\text{O}_5$ : C, 62.05; H, 6.94; N, 8.04; Found: C, 62.37; H, 6.67; N, 8.35.

**(S)-Methyl 1-(2-(Ethylloxycarbonylamino)benzoyl)pyrrolidine-2-carboxylate, 9:**

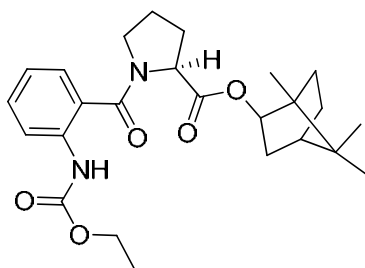
Compound **9**, obtained by following the coupling procedure used for the preparation of **14a** (*vide supra*), was purified by column chromatography (50:50 pet. ether/ethyl acetate,  $R_f$ : 0.5), 0.32g, 80%, white solid, crystallized from a solution of ethyl acetate and pet-





ether; mp: 76-80 °C;  $[\alpha]^{26}_D$ : -103° ( $c = 0.1$ ,  $\text{CHCl}_3$ ); IR ( $\text{CHCl}_3$ )  $\nu$  ( $\text{cm}^{-1}$ ) 3378, 3020, 1732, 1626, 1597, 1525, 1416, 1215;  $^1\text{H}$  NMR (200 MHz,  $\text{CDCl}_3$ )  $\delta$ : 8.49 (s, 1H), 8.14-8.19 (d,  $J = 8.58$  Hz, 1H), 7.33-7.41 (m, 2H), 6.98-7.05 (t,  $J = 7.20$  Hz, 1H), 4.63-4.70 (m, 1H), 4.12-4.23 (m, 2H), 3.77 (s, 3H), 3.40-3.64 (m, 2H), 2.25-2.46 (m, 1H), 1.79-2.10 (m, 3H), 1.23-1.30 (t,  $J=7.18$ , 3H);  $^{13}\text{C}$  NMR (50 MHz,  $\text{CDCl}_3$ )  $\delta$ : 172.4, 168.6, 153.7, 136.8, 131.0, 127.1, 123.4, 121.9, 120.0, 61.01, 59.0, 52.3, 49.9, 29.3, 25.2, 14.3; LC-MS: 343.06 ( $\text{M}+\text{Na}$ )<sup>+</sup>; Elemental analysis calculated for  $\text{C}_{16}\text{H}_{20}\text{N}_2\text{O}_5$ : C, 59.99; H, 6.24; N, 8.74; Found: C, 59.37; H, 5.67; N, 9.12.

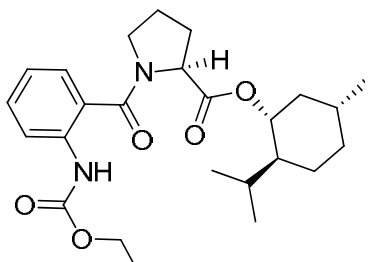
**(2S)-((2R)-1,7,7-trimethylbicyclo[2.2.1]heptan-2-yl) 1-(2-(ethoxycarbonylamino)benzoyl)pyrrolidine-2-carboxylate, 10:**



Compound **8** (0.2 g, 0.625 mmol) was first subjected to ester hydrolysis following the general procedure (*vide supra*). The free acid thus obtained was subjected to peptide coupling as mentioned in the representative procedure for **14a** (70:30 pet. ether/ethyl acetate,  $R_f$ : 0.5) to afford **10** (0.242g, 87%) as a white solid, crystallized from a solution of ethyl acetate and pet-ether; mp: 127-128 °C;  $[\alpha]^{27}_D$ : -93° ( $c = 0.1$ ,  $\text{CHCl}_3$ ); IR ( $\text{CHCl}_3$ )  $\nu$  ( $\text{cm}^{-1}$ ) 3448, 3020, 1726, 1626, 1597, 1524, 1455, 1418, 1216;  $^1\text{H}$  NMR (200 MHz,  $\text{CDCl}_3$ )  $\delta$ : 8.70 (s, 1H), 8.13-8.29 (m, 1H), 7.36-7.43 (m, 2H), 6.93-7.06 (m, 1H), 4.99-5.06 (m, 1H), 4.67-4.83 (m, 1H), 4.13-4.23 (m, 2H), 3.48-3.86 (m, 2H), 2.28-2.47 (m, 2H), 1.85-2.11 (m, 4H), 1.63-1.82 (m, 3H), 1.12-1.40 (m, 5H), 0.84-0.91 (m, 9H);  $^{13}\text{C}$  NMR (50 MHz,  $\text{CDCl}_3$ )  $\delta$ : 172.2, 168.5, 153.8, 137.3, 131.1, 127.2, 123.2, 121.7, 120.0, 80.7, 61.0, 59.5, 50.0, 49.0, 47.9, 44.8, 36.4, 29.3, 27.9, 27.1, 25.3, 19.6, 18.7, 14.4, 13.5; LC-MS: 465.23 ( $\text{M}+\text{Na}$ )<sup>+</sup>, 481.21 ( $\text{M}+\text{K}$ )<sup>+</sup>; Elemental analysis calculated for  $\text{C}_{25}\text{H}_{34}\text{N}_2\text{O}_5$ : 67.85; H, 7.74; N, 6.33; Found: 67.69; H, 7.52; N, 6.52.

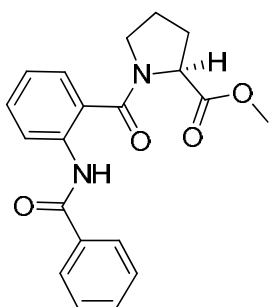
**(S)-((1R,2S,5R)-2-isopropyl-5-methylcyclohexyl) 1-(2-(ethoxycarbonylamino)benzoyl)pyrrolidine-2-carboxylate 12:**

Compound **8** (0.2 g, 0.625 mmol) was subjected to ester hydrolysis following the general procedure for ester hydrolysis. The free acid was dissolved in dry DCM (5 ml), borneol



(0.096 g, 0.625 mmol) was added followed by DCC (0.129 g, 0.625 mmol) and DMAP (25% wt., 0.05g). The reaction mixture was allowed to stir at 0 °C for 10 minutes and 12h at rt. The reaction mixture was filtered and the filtrate was diluted with dichloromethane, and the organic layer was washed sequentially with potassium hydrogen sulphate solution, saturated sodium bicarbonate, and finally with water. The crude product obtained after the removal of solvent under reduced pressure was purified by column chromatography (70:30 pet. ether/ethyl acetate,  $R_f$ : 0.5) to afford **12** (0.22g, 79%) as a white solid which was later crystallized from a solution of ethyl acetate and pet-ether; mp: 58-61 °C;  $[\alpha]^{25}_D$ : -42° ( $c = 0.1$ ,  $\text{CHCl}_3$ ); IR ( $\text{CHCl}_3$ )  $\nu$  (cm<sup>-1</sup>) 3436, 3018, 2926, 1725, 1631, 1523, 1420, 1218; <sup>1</sup>H NMR (200 MHz,  $\text{CDCl}_3$ )  $\delta$ : 8.56 (s, 1H), 8.14-8.25 (m, 1H), 7.16-7.41 (m, 2H), 6.89-7.05 (m, 1H), 4.46-4.84 (m, 2H), 4.10-4.25 (m, 2H), 3.32-3.82 (m, 2H), 1.83-2.42 (m, 6H), 1.55-1.70 (m, 3H), 1.34-1.47 (m, 2H), 1.23-1.30 (t,  $J=7.18$ , 2H), 0.74-1.10 (m, 12H); <sup>13</sup>C NMR (50 MHz,  $\text{CDCl}_3$ )  $\delta$ : 171.6, 168.5, 153.8, 137.0, 130.9, 127.1, 123.4, 121.7, 119.9, 75.12, 60.9, 59.2, 49.9, 47.0, 40.5, 34.1, 31.3, 29.2, 26.0, 25.0, 23.2, 21.9, 20.6, 16.1, 14.4; LC-MS: 467.07 ( $\text{M}+\text{Na}$ )<sup>+</sup>; Elemental analyses calculated for  $\text{C}_{25}\text{H}_{36}\text{N}_2\text{O}_5$ : C, 67.54; H, 8.16; N, 6.30; Found: C, 64.73; H, 8.43; N, 6.65;

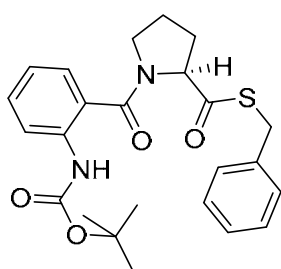
### (S)-Methyl 1-(2-benzamidobenzoyl)pyrrolidine-2-carboxylate, **13**:



To an ice cold solution of 2-phenyl benzoxazinone<sup>3</sup> (1 g, 4.48 mmol) and proline methyl ester (1 g, 5.83 mmol) in dry DMF (20 ml) containing 4Å molecular sieves, DBU (2.05g, 2ml, 13.44mmol) was added drop wise. The reaction mixture was allowed to stir at 0 °C for 10 minutes and then for 3 h at room temperature. The reaction mixture was diluted with DCM, and the organic layer was washed with water and dried using anhydrous  $\text{Na}_2\text{SO}_4$ . The crude product obtained after the removal of solvent under reduced pressure was purified by column chromatography (50:50 pet. ether/ethyl acetate,  $R_f$ : 0.5) to afford **13** (1.08 g, 68%), white solid, crystallized from a solution of diethyl ether and pet-ether; mp: 116-120 °C;  $[\alpha]^{25}_D$ : -50° ( $c = 0.1$ ,  $\text{CHCl}_3$ ); IR ( $\text{CHCl}_3$ )  $\nu$  (cm<sup>-1</sup>) 3337, 3015, 1743, 1668, 1594, 1520, 1416, 1216; <sup>1</sup>H NMR (400 MHz,  $\text{CDCl}_3$ )  $\delta$ : 10.32

(s,1H), 8.53-8.57 (d,  $J = 8.49$  Hz, 1H), 7.90-7.95 (m, 2H), 7.34-7.53 (m, 5H), 7.06-7.13 (m, 1H), 4.61-4.67 (m, 1H), 3.51-3.73 (m, 2H), 3.66 (s, 3H), 2.20-2.38 (m, 1H), 1.73-2.06 (m, 3H);  $^{13}\text{C}$  NMR (50 MHz,  $\text{CDCl}_3$ )  $\delta$  : 172.2, 168.9, 165.2, 162.4, 137.2, 134.3, 131.7, 131.2, 128.4, 127.4, 127.2, 123.6, 122.6, 121.7, 59.1, 52.1, 50.3, 36.3, 31.2, 29.0, 25.0; LC-MS: 375.05 ( $\text{M}+\text{Na}$ ) $^+$ ; Elemental analyses calculated for  $\text{C}_{20}\text{H}_{20}\text{N}_2\text{O}_4$ : C, 68.17; H, 5.72; N, 7.95; Found: C, 68.43; H, 5.43; N, 7.68.

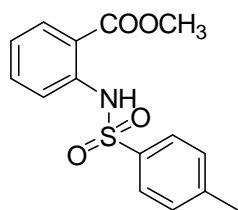
**S-benzyl (S)-1-(2-((tert-butoxycarbonyl)amino)benzoyl)pyrrolidine-2-carbothioate, 18:**



Compound **7** (0.2 g, 0.625 mmol) was subjected to ester hydrolysis following the general procedure for ester hydrolysis. The free acid was dissolved in dry DCM (5 ml), benzylmercaptan (0.096 g, 0.625 mmol) was added followed by DCC (0.129 g, 0.625 mmol) and DMAP (25% wt., 0.05g). The reaction mixture was allowed to stir at 0 °C for 10 minutes and 12h at rt. The reaction mixture was filtered and the filtrate was diluted with dichloromethane, and the organic layer was washed sequentially with potassium hydrogen sulphate solution, saturated sodium bicarbonate, and finally with water. The crude product obtained after the removal of solvent under reduced pressure was purified by column chromatography (70:30 pet. ether/ethyl acetate,  $R_f$ : 0.5) to afford **18** (0.22g, 77%) as a white solid was latter crystallized from a solution of ethyl acetate and pet-ether; mp: 110-112 °C;  $[\alpha]_D^{25}$ : -92° ( $c = 0.1$ ,  $\text{CHCl}_3$ ); IR ( $\text{CHCl}_3$ )  $\nu$  (cm $^{-1}$ ) 3368, 3020, 2933, 1722, 1626, 1520, 1454, 1393;  $^1\text{H}$  NMR (200 MHz,  $\text{CDCl}_3$ )  $\delta$ : 8.52 (s,1H), 8.21-8.25 (m, 1H), 7.27-7.48 (m, 2H), 7.33 (s, 5H), 7.03-7.10 (t,  $J=7.45$ , 1H), 4.97-5.04 (m, 1H), 4.11-4.29 (m, 3H), 3.58-3.71 (m, 3H), 2.33-2.50 (m, 1H), 1.86-2.17 (m, 4H), 1.54 (s, 9H);  $^{13}\text{C}$  NMR (50 MHz,  $\text{CDCl}_3$ )  $\delta$  : 171.8, 168.8, 153.1, 137.3, 135.6, 131.0, 128.5, 128.1, 127.2, 123.4, 121.6, 120.1, 80.32, 66.9, 59.1, 50.0, 29.2, 28.2, 25.3; MALDI-TOF-MS: 463.1967 ( $\text{M}+\text{Na}$ ) $^+$ , 479.1778 ( $\text{M}+\text{K}$ ) $^+$ ; Elemental analyses calculated for  $\text{C}_{24}\text{H}_{28}\text{N}_2\text{O}_4\text{S}$ : C, 65.43; H, 6.41; N, 6.36; Found: C, 64.73; H, 6.83; N, 6.65.

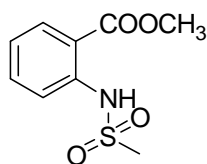
**Methyl 2-(tosylamino) benzoate 16h:**

To a solution of H-Ant-OMe (3.0 g, 18.9 mmol) in dry DCM (20 mL) maintained at 0 °C, dry  $\text{Et}_3\text{N}$  (8.3 mL, 59.55 mmols) and tosyl chloride (4.94 g, 25.8 mmol) were added. The reaction mixture was stirred at 0 °C for 10 min and at room temp for 12 hours. The



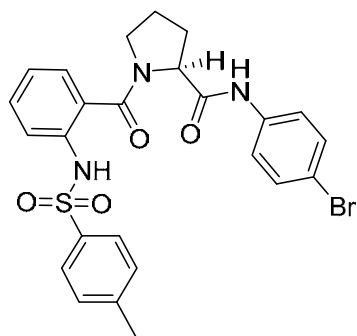
reaction mixture was diluted with DCM (10 mL) and the organic layer was washed sequentially with saturated  $\text{NaHCO}_3$  solution followed by saturated solutions of  $\text{KHSO}_4$  solution, water and brine. The organic layer was dried over anhydrous  $\text{Na}_2\text{SO}_4$  and the crude product was subjected to column purification (80:20 pet. ether/ethyl acetate,  $R_f$ : 0.5) to afford **16h** as a white solid (5.0 g, 83%); mp: 109-111°C; IR ( $\text{CHCl}_3$ )  $\nu$  ( $\text{cm}^{-1}$ ): 3209, 3020, 1869, 1844, 1791, 1772, 1732, 1716, 1697, 1653, 1315, 1215, 1089;  $^1\text{H}$  NMR ( $\text{CDCl}_3$ , 500 MHz)  $\delta$ : 10.63 (s, 1H), 7.90-7.91 (dd,  $J = 7.98$ , 1.38 Hz, 1H), 7.75 (bs, 1H), 7.73 (bs, 1H), 7.67-7.69 (d,  $J = 8.25$  Hz, 1H), 7.44 (t,  $J = 7.44$ , 1H), 7.20-7.22 (d,  $J = 8.26$  Hz, 2H), 7.02 (t,  $J = 7.44$ , 1H), 3.87 (s, 3H), 2.35 (s, 3H);  $^{13}\text{C}$  NMR ( $\text{CDCl}_3$ , 125 MHz)  $\delta$ : 168.3, 143.9, 140.5, 136.4, 134.4, 131.1, 129.6, 127.2, 122.8, 118.9, 115.8, 52.4, 21.5; ESI-MS: 328.2499 ( $\text{M}+\text{Na}$ ) $^+$ , 344.2352 ( $\text{M}+\text{K}$ ) $^+$ ; Elemental Analysis calculated for  $\text{C}_{15}\text{H}_{15}\text{NO}_4\text{S}$ : C, 59.00; H, 4.95; N, 4.59. Found: C, 58.67; H, 5.25; N, 4.19.

#### Methyl 2-(mesylamino) benzoate **16g**:



To a solution of H-Ant-OMe (2.0 g, 13.2mmol) in dry DCM (10mL) maintained at 0 °C,  $\text{Et}_3\text{N}$  (5.5mL, 39.6mmol) and methane sulfonyl chloride (1.6mL, 19.8mmol) were added. The reaction mixture was stirred at 0 °C for 10 min and then at room temperature for 2 h. The reaction mixture was diluted with DCM (5 mL) and the organic layer was washed sequentially with saturated  $\text{NaHCO}_3$  solution followed by saturated solutions of  $\text{KHSO}_4$  solution, water and brine. The organic layer was dried over anhydrous  $\text{Na}_2\text{SO}_4$  and the crude product was subjected to column purification (80:20 pet. ether/ethyl acetate,  $R_f$ : 0.5) to afford **16g** as a white solid (2.81 g, 93%); mp: 87-89°C; IR ( $\text{CHCl}_3$ )  $\nu$  ( $\text{cm}^{-1}$ ): 3203, 3026, 2956, 2850, 1838, 1786, 1693, 1683;  $^1\text{H}$  NMR ( $\text{CDCl}_3$ , 500 MHz)  $\delta$ : 10.46 (s, 1H), 8.04-8.05 (dd,  $J = 7.98$ , 1.37 Hz, 1H), 7.71-7.72 (d,  $J = 7.98$  Hz, 1H), 7.54 (t,  $J = 8.30$  Hz, 1H), 7.11 (t,  $J = 7.93$ , 1H), 3.92 (s, 3H), 3.05 (s, 3H);  $^{13}\text{C}$  NMR ( $\text{CDCl}_3$ , 125 MHz)  $\delta$ : 168.3, 140.7, 134.8, 131.5, 131.4, 122.8, 117.9, 115.3, 52.5, 39.9; ESI-MS: 230.0162 ( $\text{M}+\text{H}$ ) $^+$ ; 252.0270 ( $\text{M}+\text{Na}$ ) $^+$ ; Elemental Analysis calculated for  $\text{C}_9\text{H}_{11}\text{NO}_4\text{S}$ : C, 47.15; H, 4.84; N, 6.11; Found: C, 46.85; H, 5.14; N, 5.88.

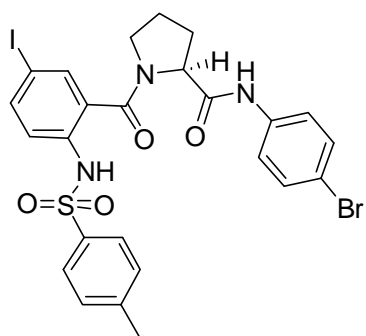
#### N-(4-bromophenyl)-1-(2-(4-methylphenylsulfonamido)-benzoyl)pyrrolidine-2-carboxamide **21**:



To a solution of **16k** (obtained from the saponification of **16h**) in dry MeCN (10 mL) was added proline 4-Br anilide (1.5 g, 5.77 mmol), HBTU (3.3 g, 8.6 mmol) and DIEA (2.2 mL, 12.7 mmol). The reaction mixture was stirred at 0 °C for 15 min and then at room temperature for 12 h. The solvent was evaporated and the residue was dissolved in DCM (15 mL) and the organic layer was

washed sequentially with saturated NaHCO<sub>3</sub> solution followed by saturated solutions of KHSO<sub>4</sub> solution, water and brine. The organic layer was dried over anhydrous Na<sub>2</sub>SO<sub>4</sub> and the crude product was subjected to column purification (25:75 pet. ether/ethyl acetate, *R<sub>f</sub>*: 0.5) furnishing **21** as a white solid (3.24 g, 86.4%). mp: 83-85°C; [α]<sup>29</sup><sub>D</sub>: -23.53° (*c* = 0.3, CHCl<sub>3</sub>); IR (CHCl<sub>3</sub>, ν (cm<sup>-1</sup>): 3315, 3018, 1716, 1697, 1683, 1622, <sup>1</sup>H NMR (DMSO-*d*<sub>6</sub>, 500 MHz) δ: 10.37 (s, 1H) 9.41 (s, 1H) 7.67-7.64 (m, 4H) 7.54-7.52 (m, 2H), 7.38-7.35 (m, 5H), 7.20-7.17 (m, 2H), 4.58-4.55 (m, 1H), 3.23-3.21 (m, 1H), 3.13-3.12 (m, 1H), 3.34 (s, 3H), 2.30-2.29 (m, 1H), 1.97-1.86 (m, 2H), 1.76-1.71 (m, 1H); <sup>13</sup>C NMR (DMSO-*d*<sub>6</sub>, 125 MHz) δ: 170.8, 166.9, 164.8, 143.8, 138.4, 134.5, 131.7, 130.7, 129.8, 128.7, 127.8, 127.1, 124.8, 122.0, 121.4, 115.2, 60.6, 49.5, 39.7, 29.9, 24.8, 21.1; ESI-MS: 542.2380 (M+H)<sup>+</sup>; 564.1860 (M+Na)<sup>+</sup>; Elemental analysis calculated for C<sub>25</sub>H<sub>24</sub>BrN<sub>3</sub>O<sub>4</sub>S: C, 55.35; H, 4.46; N, 7.75. Found: C, 54.95; H, 4.76; N, 7.95.

#### N-(4-bromophenyl)-1-(5-iodo-2-(4-methylphenylsulfonamido)benzoyl)pyrrolidine-2-carboxamide **22**:



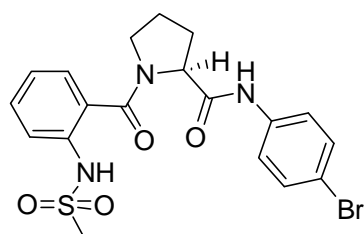
A solution of **21** (0.2 g, 0.35 mmol) in dry MeCN (2 mL) was cooled to 0°C. DMAP (0.298 g, 2.43 mmol) was added followed by the drop-wise addition of iodine monochloride (0.09 mL, 1.742 mmol). The reaction mixture was stirred at room temperature for 2 h. The reaction mixture was quenched by stirring it with a saturated solution containing NaCl, Na<sub>2</sub>S<sub>2</sub>O<sub>8</sub> and KHSO<sub>4</sub>

in 1 mL water for 15 min. The crude product was extracted with DCM (5 mL). The organic layer was dried over anhydrous Na<sub>2</sub>SO<sub>4</sub> and evaporated under reduced pressure. The residue thus obtained was purified by column chromatography, (50:50 pet. ether/ethyl acetate, *R<sub>f</sub>*: 0.5) to afford **22** (0.18g, 72%) as a white solid. mp: 215-217 °C; [α]<sup>29</sup><sub>D</sub>: -13.82° (*c* = 0.5, CHCl<sub>3</sub>); IR (CHCl<sub>3</sub>, ν (cm<sup>-1</sup>): 3321, 3020, 1714, 1681, 1614, 1537, 1489,

1435, 1398, 1338, 1215; 1166;  $^1\text{H}$  NMR ( $\text{CDCl}_3$ , 500 MHz)  $\delta$ : 9.09 (s, 1H), 8.91 (s, 1H), 7.68-7.69 (d,  $J = 7.98$  Hz, 2H), 7.63 (m, 1H), 7.60 (bs, 1H), 7.37 (m, 3H), 7.29 (m, 2H), 7.21-7.22 (d,  $J = 7.98$ , 2H), 4.78 (m, 1H), 3.38-3.35 (m, 1H), 3.21-3.19 (m, 1H), 2.37 (s, 3H), 2.30-2.29 (m, 1H), 2.03-2.00 (m, 1H), 1.79-1.77 (m, 1H);  $^{13}\text{C}$  NMR ( $\text{CDCl}_3$ , 125 MHz)  $\delta$ : 169.4, 167.3, 144.2, 140.0, 136.9, 136.2, 135.8, 135.0, 131.7, 129.7, 128.2, 127.3, 123.2, 116.8; ESI-MS: 668.1056 ( $\text{M}+\text{H}$ ) $^+$ ; 689.9918 ( $\text{M}+\text{Na}$ ) $^+$ ; 705.9593 ( $\text{M}+\text{K}$ ) $^+$ ; Elemental analysis calculated for  $\text{C}_{25}\text{H}_{23}\text{BrIN}_3\text{O}_4\text{S}$ : C, 44.93; H, 3.47; N, 6.29; Found: C, 45.26; H, 3.72; N, 6.59.

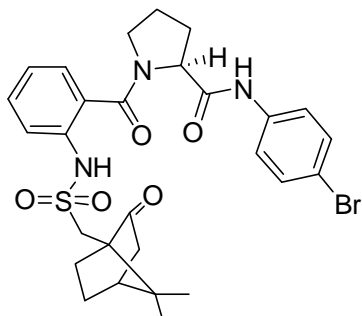
### N-(4-bromophenyl)-1-(2-(methylsulfonamido)benzoyl)pyrrolidine-2-carboxamide

**20:**



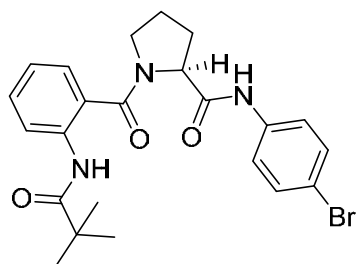
To a solution of **16j** (obtained from the saponification of **16g**) in dry MeCN (10 mL), **3b** (1.0 g, 4.6 mmol), HBTU (2.12 g, 5.6 mmol) and dry DIEA (1.5 mL, 8.208 mmol) were added at 0°C. The reaction mixture was then stirred at room temperature for 12 h. The solvent was evaporated and the residue was dissolved in DCM (10 mL). The organic layer was washed sequentially with saturated  $\text{NaHCO}_3$  solution followed by saturated solutions of  $\text{KHSO}_4$  solution, water and brine. The organic layer was dried over anhydrous  $\text{Na}_2\text{SO}_4$  and the crude product was subjected to column purification (30:70 pet ether/ethyl acetate,  $R_f$ : 0.5) affording **20** as a white solid (1.086, 86%) mp: 178-180°C;  $[\alpha]_D^{28}$ : -22.78° ( $c = 0.3$ ,  $\text{CHCl}_3$ ); IR ( $\text{CHCl}_3$ )  $\nu$  ( $\text{cm}^{-1}$ ): 3020, 1716, 1697, 1683, 1653, 1647, 1635, 1616;  $^1\text{H}$  NMR ( $\text{CDCl}_3$ , 400 MHz)  $\delta$ : 9.69 (s, 1H), 8.80 (s, 1H), 7.57-7.59 (d,  $J = 8.04$  Hz, 2H), 7.48-7.46 (m, 2H), 7.36-7.33 (m, 3H), 7.29-7.27 (m, 3H), 4.75-4.72 (m, 1H), 3.59-3.29 (m, 2H) 2.94 (s, 3H), 2.28-2.27 (m, 1H), 2.10-2.03 (m, 1H), 1.98-1.92 (m, 1H), 1.86-1.78 (m, 1H);  $^{13}\text{C}$  NMR ( $\text{CDCl}_3$ , 100 MHz)  $\delta$ : 170.4, 168.0, 166.6, 137.3, 134.6, 133.6, 131.3, 130.7, 129.1, 128.1, 127.7, 126.7, 124.5, 122.2, 121.1, 116.1, 60.7, 60.1, 49.8, 42.3, 39.6, 39.3, 38.3, 29.3, 24.7, 20.8, 13.9; ESI-MS: 466.0795 ( $\text{M}+\text{H}$ ) $^+$ ; 488.2980 ( $\text{M}+\text{Na}$ ) $^+$ ; Elemental analysis calculated for  $\text{C}_{19}\text{H}_{20}\text{BrN}_3\text{O}_4\text{S}$ : C, 48.93; H, 4.32; N, 9.01; Found: C, 49.26; H, 4.63; N, 8.73.

### N-(4-bromophenyl)-1-(2-((7,7-dimethyl-2-oxobicyclo[2.2.1]heptan-1-yl)methylsulfonamido)benzoyl)pyrrolidine-2-carboxamide **23**



A solution of (1S)-Camphorsulfonicacid (1g, 4,3048mmoles) in 1.6mL of  $\text{SOCl}_2$  (2.56g, 0.022mol) was taken at  $0^\circ\text{C}$ . The reaction mixture was stirred at  $0^\circ\text{C}$  for 30 minutes and 2 hours at  $60^\circ\text{C}$ .  $\text{SOCl}_2$  in reaction mixture was evaporated under vacuum to obtain the (1S)-Camphorsulfonylchloride. A mixture of 2mL TFA and 2mL DCM was added to Compound **14b** (2g, 41.3mmols) taken in 2mL DCM at  $0^\circ\text{C}$  and stirred at rt for 3 hours. TFA was evaporated under reduced pressure and 5mL water was added to the residue. It was then neutralized by saturated sodium bicarbonate solution and aqueous layer was extracted with DCM (5mLx3), dried with anhydrous  $\text{Na}_2\text{SO}_4$  and evaporated under reduced pressure to obtain the free amine. A solution containing the free amine (1g, 2.5840 mmoles) in 20mL dry DCM was cooled to  $0^\circ\text{C}$ . 1.1mL of Dry  $\text{Et}_3\text{N}$  (0.7829g, 7.7519mmoles) was added followed by (1S)-Camphorsulfonylchloride. The reaction mixture was stirred at  $0^\circ\text{C}$  for 10 minutes and rt for 4 hours. Dilute the reaction mixture with 5mL DCM and organic layer was washed with 10mL of sodium bicarbonate, potassium bisulphate and water. The organic layer was dried over anhydrous  $\text{Na}_2\text{SO}_4$  solution and evaporated under reduced pressure to obtain crude product which was purified by column chromatography, (pet. ether/ethyl acetate,  $R_f$ : 0.5) afforded **23** as white solid (1.4g, 90%) which was then crystallized from a solution of methanol. mp: 249-251;  $[\alpha]_D^{29}$ :  $-132.31^\circ$  ( $c = 0.26$ ,  $\text{CHCl}_3$ ); IR ( $\text{CHCl}_3$ ,  $\nu(\text{cm}^{-1})$ ) 3275.24, 3020.63, 1724.42, 1714.77, 1693.56, 1681.98, 1651.12, 1614.47, 1595.18, 1537.32, 1514.17, 1494.88, 1487.17, 1435.09, 1332.86, 1298.14, 1217.12, 1153.47, 1057.03, 929.72, 771.55, 669.32;  $^1\text{H}$  NMR( $\text{CDCl}_3/400\text{MHz}$ ):  $\delta$  ppm 10.41(1H, s), 8.97(1H, s), 7.62(3H, m), 7.51(4H, s), 7.28(m, 1H), 4.64(1H, m), 3.44(2H, m), 2.33(3H, m), 1.93(7H, m), 1.50(1H, m), 1.38(1H, m), 1.23(3H, m), 1.04(3H, s), 0.76(3H, s);  $^{13}\text{C}$  NMR (DMSO- $d_6$ , 100MHz):  $\delta$  ppm 214.46, 170.84, 167.36, 138.51, 135.02, 130.96, 128.55, 127.85, 124.76, 122.36, 121.88, 121.42, 115.23, 60.75, 58.09, 49.97, 48.17, 47.90, 42.20, 30.06, 26.48, 24.91, 19.56, 19.38;  $^{13}\text{C}$  DEPT ( $\text{CDCl}_3, 100\text{MHz}$ ):  $\delta$  ppm 131.75, 130.96, 127.85, 124.76, 122.36, 121.87, 121.42, 60.75, 49.97, 48.16, 42.16, 42.20, 30.26, 26.48, 24.90, 24.85, 19.56, 19.37; ESI-MS: 602.1063 ( $\text{M}+\text{H}$ ) $^+$ ; 624.1148 ( $\text{M}+\text{Na}$ ) $^+$ ; 640.1595 ( $\text{M}+\text{K}$ ) $^+$ ; Elemental analysis calculated for  $\text{C}_{28}\text{H}_{32}\text{BrN}_3\text{O}_5\text{S}$ : C, 55.81; H, 5.35; N, 6.97; Found: C, 56.02; H, 5.67; N, 7.03.

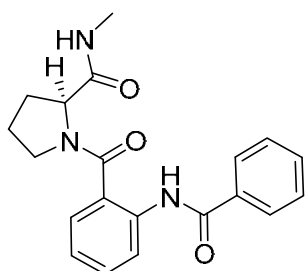
**(S)-N-(4-bromophenyl)-1-(2-pivalamidobenzoyl)pyrrolidine-2-carboxamide, 28**



Compound **28**, obtained by following the procedure used for preparation of **1** (*vide supra*), except using pivaloyl chloride as the acylating agent, was purified by column chromatography, (30:70 pet. ether/ethyl acetate,  $R_f$ : 0.5), white solid (0.076g, 86%). mp: 100-105°C;  $[\alpha]_D^{27}$ : -33° ( $c = 0.1$ , CHCl<sub>3</sub>); IR (CHCl<sub>3</sub>,  $\nu$  (cm<sup>-1</sup>): 3020,

1732, 1686, 1616, 1541, 1427, 1398, 1302, 1215; <sup>1</sup>H NMR (CDCl<sub>3</sub>/200MHz):  $\delta$  ppm 9.37 (s, 1H), 9.06 (s, 1H), 8.27-8.37 (d,  $J=8.34$ Hz, 1H), 7.36-7.49 (m, 6H), 7.07-7.15 (m, 1H), 4.82-4.84 (m, 1H), 3.58-3.71 (m, 2H), 2.47-2.61 (m, 1H), 2.03-2.23 (m, 2H), 1.66-1.96 (m, 3H), 1.26 (m, 9H); <sup>13</sup>C NMR (CDCl<sub>3</sub>, 100MHz):  $\delta$  ppm 177.4, 170.3, 169.1, 137.1, 136.7, 131.7, 131.2, 127.3, 124.5, 123.0, 122.6, 121.2, 116.6, 60.9, 50.8, 39.7, 27.9, 27.3, 25.1; ESI-MS: 494.4207 (M+Na)<sup>+</sup>; Elemental analysis calculated for C<sub>23</sub>H<sub>26</sub>BrN<sub>3</sub>O<sub>3</sub>: C, 58.48; H, 5.55; N, 8.90; Found: C, 47.22; H, 5.31; N, 8.79.

#### (S)-1-(2-benzamidobenzoyl)-N-methylpyrrolidine-2-carboxamide, **29**:



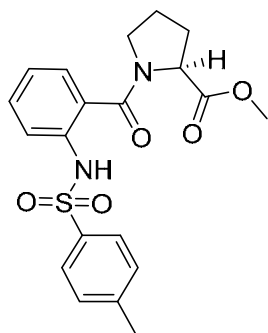
Compound **13** was amidated using methylamine in methanol to obtain **29**. Purified by column chromatography (20:80 pet. ether/ethyl acetate,  $R_f$ : 0.5) (1.28 g, 98%), white solid, mp: 72-75 °C;  $[\alpha]_D^{26}$ : -54.11° ( $c = 0.1$ , CHCl<sub>3</sub>); IR (CHCl<sub>3</sub>)  $\nu$  (cm<sup>-1</sup>) 3336, 3022, 1683, 1668, 1594, 1520, 1416, 1216; <sup>1</sup>H NMR (400 MHz, CDCl<sub>3</sub>)  $\delta$ : 10.34 (s, 1H), 7.87-7.98 (m, 3H),

7.21-7.41 (m, 5H), 7.0-7.07 (t,  $J=7.39$ Hz, 1H), 6.87-6.89 (d,  $J=4.17$ Hz, 1H), 4.55-4.61 (m, 1H), 3.51-3.71 (m, 2H), 2.59-2.62 (d,  $J=4.67$ Hz, 3H), 1.66-2.28 (m, 5H); <sup>13</sup>C NMR (50 MHz, CDCl<sub>3</sub>)  $\delta$ : 171.7, 169.8, 166.1, 136.2, 133.9, 131.9, 131.0, 128.4, 127.4, 126.0, 123.5, 123.1, 60.4, 50.5, 28.8, 26.1, 24.9; LC-MS: 373.98 (M+Na)<sup>+</sup>; Elemental analysis calculated for C<sub>20</sub>H<sub>21</sub>N<sub>3</sub>O<sub>3</sub>: C, 68.36; H, 6.02; N, 11.96; Found: C, 67.97; H, 5.92; N, 11.46.

#### Methyl (2-((4-methylphenyl)sulfonamido)benzoyl)-L-prolinate **30**:

To a solution of **16k** (1g, 3.43mmol) in dry MeCN (10 mL) was added L-proline methylester (1.5 g, 5.31 mmol), HBTU (3.3 g, 8.55 mmol) and DIEA (1.8 mL, 10.29 mmol). The reaction mixture was stirred at 0 °C for 15 min and then at room temperature for 12 h. The solvent was evaporated and the residue was dissolved in DCM (15 mL) and the organic layer was washed sequentially with saturated NaHCO<sub>3</sub> solution followed by

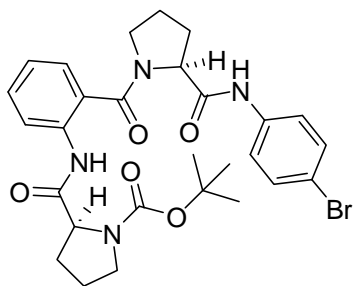




saturated solutions of  $\text{KHSO}_4$  solution, water and brine. The organic layer was dried over anhydrous  $\text{Na}_2\text{SO}_4$  and the crude product was subjected to column purification (50:50 pet. ether/ethyl acetate,  $R_f$ : 0.5) furnishing **30** as colorless viscous liquid (1.24 g, 89.8%).  $[\alpha]_D^{29}$ :  $-32.68^\circ$  ( $c = 0.3$ ,  $\text{CHCl}_3$ ); IR ( $\text{CHCl}_3$ ,  $\nu$  ( $\text{cm}^{-1}$ ): 3315, 3018, 1716, 1697, 1683, 1622,  $^1\text{H}$  NMR ( $\text{CDCl}_3$ , 200 MHz)  $\delta$ : 8.76 (s, 1H) 7.62-7.70 (m, 3H)

7.26-7.36 (m, 2H), 7.17-7.21 (m, 2H), 7.01-7.09 (m, 1H), 4.48-4.55 (m, 1H), 3.80 (s, 3H), 3.03-3.39 (m, 3H), 2.33 (s, 3H), 1.85-2.06 (m, 2H), 1.51-1.81 (m, 1H);  $^{13}\text{C}$  NMR ( $\text{CDCl}_3$ , 50 MHz)  $\delta$ : 172.2, 167.8, 165.2, 143.4, 136.3, 135.6, 131.0, 129.3, 127.2, 125.4, 123.6, 121.6, 58.8, 52.4, 49.6, 38.5, 29.0, 25.0, 21.3; ESI-MS: 424.95 ( $\text{M}+\text{Na}$ ) $^+$ ; Elemental analysis calculated for  $\text{C}_{20}\text{H}_{22}\text{N}_2\text{O}_5\text{S}$ : C, 59.69; H, 5.51; N, 6.96; Found: C, 58.87; H, 5.97; N, 6.25.

**(S)-tert-butyl 2-((S)-2-(4-bromophenylcarbamoyl)pyrrolidine-1-carboxylate)phenylcarbamoylpyrrolidine-1-carboxylate 31:**

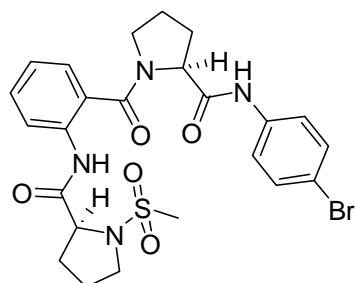


Compound **15** (0.5g, 0.9596 mmol) was subjected to saponification reaction using  $\text{LiOH}$  in aqueous methanol furnishing the crude acid. To a solution containing the crude acid **1c** and p-Br aniline (0.165g, 0.959 mmol) in dry DCM (5mL), HBTU (0.75g, 1.92 mmol) was added followed by the addition of dry DIEA (0.4mL, 0.29g, 2.88

mmol) at  $0^\circ\text{C}$ . The solution was stirred at room temperature for 4 h. The reaction mixture was diluted with DCM (5mL) and washed (5mL each) with saturated solutions of  $\text{KHSO}_4$  solution, water and brine. The organic layer was dried over anhydrous  $\text{Na}_2\text{SO}_4$  and evaporated under reduced pressure to get the crude product which on further purification by flash column chromatography, (pet. ether/acetone 70:30,  $R_f$ : 0.4 ) to afford **31** as a white solid (0.495 g, 88%); mp: 228-229  $^\circ\text{C}$ ;  $[\alpha]_D^{24}$ :  $-206.54^\circ$  ( $c = 0.5$ ,  $\text{CHCl}_3$ ); IR ( $\text{CHCl}_3$ )  $\nu$  ( $\text{cm}^{-1}$ ): 3274, 3210, 2977, 1680, 1614, 1591, 1541, 1490, 1455, 1397, 1367, 1302, 1249, 1162, 1123;  $^1\text{H}$  NMR (400 MHz,  $\text{CDCl}_3$ )  $\delta$ : 10.13 (bs, 1H), 9.60-9.48 (m, 1H), 8.49-8.17 (m, 1H), 7.47-7.31 (m, 6H), 7.14-7.11 (t,  $J = 7.28$  Hz, 1H), 4.96-4.78 (m, 1H), 4.45-4.31 (m, 1H), 3.69-3.37 (m, 4H), 2.28-2.15 (m, 4H), 1.93-1.79 (m, 4H), 1.47-1.38 (m, 9H);  $^{13}\text{C}$  NMR (100 MHz,  $\text{CDCl}_3$ )  $\delta$ : 171.4, 169.7, 168.9, 154.0, 137.0, 131.2, 127.1, 122.5, 120.5, 116.1, 79.8, 61.9, 60.5, 50.3, 46.3, 30.9, 30.5, 28.6, 27.9, 24.8, 23.4;

ESI-MS: 607.6302 (M+Na)<sup>+</sup>; Elemental analysis calculated for C<sub>28</sub>H<sub>33</sub>BrN<sub>4</sub>O<sub>5</sub>: C, 54.44; H, 5.68; N, 9.57; Found: C, 57.08; H, 5.84; N, 9.77.

**(S)-N-(4-bromophenyl)-1-(2-((S)-1-(methylsulfonyl)pyrrolidine-2-carboxamido)benzoyl)pyrrolidine-2-carboxamide 32:**



Compound **32** was synthesized from **31** following the procedure for **20**.

Purification by column chromatography, (pet. ether/acetone 70:30, *R<sub>f</sub>*: 0.4 ) affording **32** as a white solid (0.75 g, 85%); mp: 242-245 °C; [ $\alpha$ ]<sub>D</sub><sup>24</sup>: -226.54° (*c* = 0.5, CHCl<sub>3</sub>); IR (CHCl<sub>3</sub>)  $\nu$  (cm<sup>-1</sup>): 3274, 3210, 2977, 1680, 1614,

1591, 1541, 1490, 1455, 1397, 1367, 1302, 1249, 1162, 1123; <sup>1</sup>H NMR (200 MHz, CDCl<sub>3</sub>)  $\delta$ : 10.14 (s, 1H), 9.19 (s, 1H), 9.26-9.30 (d, *J* = 8.21 Hz, 1H), 7.33-7.49 (m, 6H), 7.10-7.18 (t, *J* = 7.45 Hz, 1H), 4.86-4.92 (m, 1H), 4.27-4.32 (m, 1H), 3.33-3.70 (m, 4H), 2.91 (s, 3H), 1.80-2.44 (m, 10H); <sup>13</sup>C NMR (100 MHz, CDCl<sub>3</sub>)  $\delta$ : 170.1, 169.9, 169.6, 137.4, 135.1, 131.6, 130.8, 126.9, 125.5, 123.6, 121.1, 116.4, 63.0, 61.4, 50.4, 49.5, 34.8, 31.3, 28.1, 25.2, 24.8; LC-MS: 585.00 (M+Na)<sup>+</sup>, 601.10 (M+K)<sup>+</sup>; Elemental analysis calculated for C<sub>24</sub>H<sub>27</sub>BrN<sub>4</sub>O<sub>5</sub>S: C, 51.16; H, 4.83; N, 9.94; Found: C, 52.08; H, 4.74; N, 9.77.

### 1.23 Single crystal X-ray crystallographic data.

Crystal data for the compounds were collected at *T* = 293 K, on SMART APEX CCD Single crystal X-ray diffractometer using Mo KR radiation ( $\lambda$ ) 0.7107 Å. The structures were solved by direct methods using SHELXTL. All the data were corrected for Lorentz polarization and absorption effects. SHELX-97 (ShelxTL) was used for structure solution and full matrix least-squares refinement on *F*<sup>2</sup>. Hydrogen atoms were included in the refinement in the riding mode. The refinements were carried out using SHELXL-97. For reference, see: G. M. Sheldrick, SHELX-97 program for crystal structure solution and refinement, University of Gottingen, Germany, 1997.

**Crystal Data for 1.** Single crystals of **1** were grown by slow evaporation of the mixture of methanol and dichloromethane. Colorless prism crystal of approximate size 0.31 x 0.21 x 0.12 mm, was used for data collection. Temperature = 297 K, wave length = 0.71073 Å, hemisphere acquisition. Total scans = 4, F(000) = 440,  $\theta$  range = 1.90 to 25.00, completeness to  $\theta$  of 25.00° is 99.6 %, SADABS correction applied, goodness-of-

fit on  $F2 = 0.990$ ,  $C_{20}H_{20}Br N_3O_3$ ,  $M = 430.30$ . Crystals belong to monoclinic, space group P21,  $a = 11.1418(8)$ ,  $b = 7.1748(5)$ ,  $c = 12.9148(10)$  Å,  $V = 994.55(13)$  Å<sup>3</sup>,  $Z = 2$ ,  $D_c = 1.437$  mg m<sup>-3</sup>,  $\mu$  (Mo-K $\alpha$ ) = 2.091 mm<sup>-1</sup>, 5062 reflections measured, 2888 unique [ $I > 2\sigma(I)$ ], R value 0.0297, wR2 = 0.0714.

**Crystal Data for 2.** Single crystals of **2** were grown by slow evaporation of the mixture of ethyl acetate and pet. ether. Colorless needle of approximate size 0.17 x 0.12 x 0.12 mm, was used for data collection. Temperature = 295 K, wave length = 0.71073 Å, hemisphere acquisition. Total scans = 3,  $F(000) = 952$ ,  $\theta$  range = 2.11 to 24.99°, completeness to  $\theta$  of 24.99° is 100.0 %. SADABS correction applied, goodness-of-fit on  $F2 = 0.999$   $C_{23}H_{32}N_4O_5$ ,  $M = 444.53$ . Crystals belong to orthorhombic, space group P2<sub>1</sub>2<sub>1</sub>2<sub>1</sub>,  $a = 8.9732(8)$ ,  $b = 10.4292(9)$ ,  $c = 25.653(2)$  Å,  $V = 2400.7(4)$  Å<sup>3</sup>,  $Z = 4$ ,  $D_c = 1.230$  mg m<sup>-3</sup>,  $\mu$  (Mo-K $\alpha$ ) = 0.088 mm<sup>-1</sup>, 12181 reflections measured, 4239 unique [ $I > 2\sigma(I)$ ], R value 0.0467, wR2 = 0.1223.

**Crystal Data for 3.** Single crystals of **3** were grown by slow evaporation of the mixture of methanol and dichloromethane. Colorless plate of approximate size 0.17 x 0.12 x 0.02 mm, was used for data collection. Temperature = 296 K, wave length = 0.71073 Å, Total scans = 4,  $F(000) = 944$ ,  $\theta$  range = 1.62 to 25.00°, completeness to  $\theta$  of 24.99° is 100.0 %. SADABS correction applied, goodness-of-fit on  $F2 = 1.203$ ,  $C_{21}H_{22}BrN_3O_4$ ,  $M = 460.33$ . Crystals belong to orthorhombic, space group P2<sub>1</sub>2<sub>1</sub>2<sub>1</sub>,  $a = 7.1599(7)$ ,  $b = 11.8460(11)$ ,  $c = 25.160(2)$  Å,  $V = 2134.0(4)$  Å<sup>3</sup>,  $Z = 4$ ,  $D_c = 1.433$  mg m<sup>-3</sup>,  $\mu$  (Mo-K $\alpha$ ) = 1.958 mm<sup>-1</sup>, 17385 reflections measured, 3754 unique [ $I > 2\sigma(I)$ ], R value 0.0749, wR2 = 0.1330.

**Crystal Data for 4.** Single crystals of **4** were grown by slow evaporation of the mixture of methanol. Colorless thin plate of approximate size 0.48 x 0.14 x 0.02 mm, was used for data collection. Temperature = 297 K, Wave length = 0.71073 Å, Total scans = 4,  $F(000) = 488$ ,  $\theta$  range = 1.89 to 25.00°, completeness to  $\theta$  of 25.00° is 99.7 %. SADABS correction applied, Goodness-of-fit on  $F2 = 0.985$ ,  $C_{20}H_{17}BrF_3N_3O_3$ ,  $M = 484.28$ . Crystals belong to monoclinic, space group P21,  $a = 11.016(5)$ ,  $b = 7.612(3)$ ,  $c = 12.920(5)$  Å,  $V = 1059.2(7)$  Å<sup>3</sup>,  $Z = 2$ ,  $D_c = 1.518$  mg m<sup>-3</sup>,  $\mu$  (Mo-K $\alpha$ ) = 1.992 mm<sup>-1</sup>, 5304 reflections measured, 3754 unique [ $I > 2\sigma(I)$ ], R value 0.0469, wR2 = 0.0954.

**Crystal Data for 5.** Single crystals of **5** were grown by slow evaporation of the mixture of methanol. Colorless needle of approximate size 0.62 x 0.15 x 0.11 mm, was used for data collection. Temperature = 297 K, wave length = 0.71073 Å, Total scans = 4,  $F(000) =$

504,  $\theta$  range = 2.19 to 25.00°, completeness to  $\theta$  of 25.00° is 98.7 %. SADABS correction applied, goodness-of-fit on  $F_2 = 1.203$ ,  $C_{23}H_{26}BrN_3O_4$ ,  $M = 488.38$ . Crystals belong to monoclinic, space group P21,  $a = 12.8420(19)$ ,  $b = 7.0231(10)$ ,  $c = 13.3863(19)$  Å,  $V = 1207.3(3)$  Å<sup>3</sup>,  $Z = 2$ ,  $D_c = 1.343$  mg m<sup>-3</sup>,  $\mu$  (Mo-K $\alpha$ ) = 1.734 mm<sup>-1</sup>, 9259 reflections measured, 4152 unique [ $I > 2\sigma(I)$ ], R value 0.1045, wR2 = 0.1533.

**Crystal Data for 6.** Single crystals of **6** were grown by slow evaporation of the solution mixture of methanol and dichloromethane. Colorless needle crystal of size 0.55 x 0.15 x 0.12 mm<sup>3</sup>, was used for data collection, temperature = 296 K, wave length = 0.71073 Å, quadrant data acquisition, total scans = 4,  $F(000) = 456$ ,  $\theta$  range = 2.11° to 24.99°, completeness to  $\theta$  of 24.99° is 99.8 %, goodness-of-fit on  $F_2 = 1.059$ ,  $C_{20}H_{20}BrN_3O_4$ ,  $M = 446.30$ . Crystals belong to monoclinic, space group P21,  $a = 11.3493(2)$ ,  $b = 6.9182(1)$ ,  $c = 13.3601(3)$  Å,  $V = 1015.04(3)$  Å<sup>3</sup>,  $Z = 2$ ,  $D_c = 1.460$  g/cc,  $\mu$  (Mo-K $\alpha$ ) = 2.055 mm<sup>-1</sup>, 7581 reflections collected, 3479 unique [ $I > 2\sigma(I)$ ], R value 0.0368, wR<sub>2</sub> = 0.0927, largest diff. peak and hole 0.518 and -0.206 e. Å<sup>-3</sup>, absolute structure parameter = 0.037(9).

**Crystal Data for 7.** Single crystals of **7** were grown by slow evaporation of the mixture of methanol and dichloromethane. Colorless needle of approximate size 1.37 x 0.54 x 0.47 mm, was used for data collection. Temperature = 297 K, wave length = 0.71073 Å, total scans = 4,  $F(000) = 744$ ,  $\theta$  range = 2.28 to 25.00°, completeness to  $\theta$  of 25.00° is 99.8 %. SADABS correction applied, goodness-of-fit on  $F_2 = 1.042$ ,  $C_{18}H_{24}N_2O_5$ ,  $M = 348.39$ . Crystals belong to orthorhombic, space group P2(1)2(1)2(1),  $a = 8.547(5)$ ,  $b = 9.694(5)$ ,  $c = 22.943(12)$  Å,  $V = 1900.9(18)$  Å<sup>3</sup>,  $Z = 4$ ,  $D_c = 1.217$  mg m<sup>-3</sup>,  $\mu$  (Mo-K $\alpha$ ) = 0.089 mm<sup>-1</sup>, 18354 reflections measured, 3348 unique [ $I > 2\sigma(I)$ ], R value 0.0479, wR2 = 0.1257.

**Crystal Data for 8.** Single crystals of **8** were grown by slow evaporation of the mixture of ethylacetate and pet. ether. Colorless rectangular crystal of approximate size 0.43 x 0.31 x 0.14 mm, was used for data collection. Temperature = 296 K, wave length = 0.71073 Å, Total scans = 4,  $F(000) = 904$ ,  $\theta$  range = 2.09 to 25.00°, completeness to  $\theta$  of 25.00° is 100 %. SADABS correction applied, goodness-of-fit on  $F_2 = 1.066$ ,  $C_{24}H_{28}N_2O_5$ ,  $M = 424.48$ . Crystals belong to orthorhombic, space group P2(1)2(1)2(1),  $a = 10.6231(7)$ ,  $b = 10.9569(7)$ ,  $c = 19.5280(12)$  Å,  $V = 2273.0(3)$  Å<sup>3</sup>,  $Z = 4$ ,  $D_c = 1.240$  mg

$\text{m}^{-3}$ ,  $\mu$  (Mo- $K_{\alpha}$ ) = 0.087  $\text{mm}^{-1}$ , 11578 reflections measured, 4004 unique [ $I > 2\sigma(I)$ ], R value 0.0402, wR2 = 0.0946.

**Crystal Data for 9.** Single crystals of **9** were grown by slow evaporation of the mixture of ethylacetate and pet. ether. Colourless thick plate crystal of approximate size 0.50 x 0.27 x 0.22 mm, was used for data collection. Temperature = 173 K, Wave length = 0.71073 Å, Total scans = 4, F(000) = 680,  $\theta$  range = 2.318 to 28.349°, completeness to  $\theta$  of 28.41° is 99.1 %. SADABS correction applied, goodness-of-fit on F2 = 1.031,  $\text{C}_{16}\text{H}_{20}\text{N}_2\text{O}_5$ ,  $M = 320.34$ . Crystals belong to orthorhombic, space group P2(1)2(1)2(1),  $a = 8.111(2)$ ,  $b = 9.756(2)$ ,  $c = 20.126(6)$  Å,  $V = 1592.6(7)$  Å<sup>3</sup>,  $Z = 4$ ,  $D_c = 1.336$  mg  $\text{m}^{-3}$ ,  $\mu$  (Mo- $K_{\alpha}$ ) = 0.100  $\text{mm}^{-1}$ , 8457 reflections measured, 3901 unique [ $I > 2s(I)$ ], R value 0.0353, wR2 = 0.0823.

**Crystal Data for 10.** Single crystals of **10** were grown by slow evaporation of the mixture of ethylacetate and pet. ether. Colorless block crystal of approximate size 0.62 x 0.59 x 0.27 mm, was used for data collection. Temperature = 100 K, wave length = 0.71073 Å, total scans = 4, F(000) = 952,  $\theta$  range = 2.10 to 25.00°, completeness to  $\theta$  of 25.00° is 99.8 %. SADABS correction applied, goodness-of-fit on F2 = 1.090,  $\text{C}_{25}\text{H}_{34}\text{N}_2\text{O}_5$ ,  $M = 442.54$ . Crystals belong to orthorhombic, space group P2(1)2(1)2(1),  $a = 7.4115(4)$ ,  $b = 16.5480(9)$ ,  $c = 19.3577(11)$  Å,  $V = 2374.1(2)$  Å<sup>3</sup>,  $Z = 4$ ,  $D_c = 1.238$  mg  $\text{m}^{-3}$ ,  $\mu$  (Mo- $K_{\alpha}$ ) = 0.086  $\text{mm}^{-1}$ , 17494 reflections measured, 4176 unique [ $I > 2\sigma(I)$ ], R value 0.0442, wR2 = 0.1054.

**Crystal Data for 11.** Single crystals of **11** were grown by slow evaporation of the mixture of ethyl acetate and pet. ether. Colorless plate crystal of approximate size 0.44 x 0.34 x 0.14 mm, was used for data collection. Temperature = 297 K, wave length = 0.71073 Å, total scans = 4, F(000) = 744,  $\theta$  range = 1.77 to 25.00°, completeness to  $\theta$  of 25.00° is 100 %. SADABS correction applied, goodness-of-fit on F2 = 1.062,  $\text{C}_{18}\text{H}_{24}\text{N}_2\text{O}_5$ ,  $M = 348.39$ . Crystals belong to orthorhombic, space group P2(1)2(1)2(1),  $a = 8.3515(8)$ ,  $b = 9.6398(9)$ ,  $c = 22.979(2)$  Å,  $V = 1850.0(3)$  Å<sup>3</sup>,  $Z = 4$ ,  $D_c = 1.251$  mg  $\text{m}^{-3}$ ,  $\mu$  (Mo- $K_{\alpha}$ ) = 0.092  $\text{mm}^{-1}$ , 9400 reflections measured, 3251 unique [ $I > 2\sigma(I)$ ], R value 0.0430, wR2 = 0.1150.

**Crystal Data for 12.** Single crystals of **12** were grown by slow evaporation of the mixture of ethyl acetate and pet. ether. Colorless block crystal of approximate size 0.54 x 0.34 x 0.20 mm, was used for data collection. Temperature = 140(2) K, wave length =

0.71073 Å,  $F(000) = 960$ ,  $\theta$  range = 1.85 to 34.28°, completeness to  $\theta$  of 25.99° is 99.9 %. SADABS correction applied, goodness-of-fit on  $F_2 = 1.061$ ,  $C_{25}H_{36}N_2O_5$ ,  $M = 444.56$ . Crystals belong to orthorhombic, space group  $P2(1)2(1)2(1)$ ,  $a = 8.173(5)$ ,  $b = 13.001(8)$ ,  $c = 17.350(11)$  Å,  $V = 2460.55(9)$  Å<sup>3</sup>,  $Z = 6$ ,  $D_c = 1.200$  mg m<sup>-3</sup>,  $\mu$  (Mo-K $\alpha$ ) = 0.083 mm<sup>-1</sup>, 10048 reflections measured, 8048 unique [ $I > 2\sigma(I)$ ], R value 0.0480, wR2 = 0.1090.

**Crystal Data for 13.** Single crystals of **13** were grown by slow evaporation of the mixture of diethyl ether and pet. ether. Colorless plate crystal of approximate size 0.24 x 0.12 x 0.03 mm, was used for data collection. Temperature = 297 K, wave length = 0.71073 Å, Total scans = 4,  $F(000) = 744$ ,  $\theta$  range = 1.96 to 25.99°, completeness to  $\theta$  of 25.99° is 99.9 %. SADABS correction applied, goodness-of-fit on  $F_2 = 1.117$ ,  $C_{40}H_{40}N_4O_8$ ,  $M = 704.76$ . Crystals belong to orthorhombic, space group  $P2(1)2(1)2(1)$ ,  $a = 8.173(5)$ ,  $b = 13.001(8)$ ,  $c = 17.350(11)$  Å,  $V = 1843.5(19)$  Å<sup>3</sup>,  $Z = 2$ ,  $D_c = 1.270$  mg m<sup>-3</sup>,  $\mu$  (Mo-K $\alpha$ ) = 0.089 mm<sup>-1</sup>, 10075 reflections measured, 3616 unique [ $I > 2\sigma(I)$ ], R value 0.0488, wR2 = 0.1084.

**Crystal data for 18:** Crystals of **18** were grown by slow evaporation of the solution in ethylacetate and pet.ether. Colorless plate crystal of size (0.58 x 0.39 x 0.17 mm) has been used for the data collection. Multiscan acquisition  $C_{24}H_{28}N_2O_4S$ ,  $M = 440.54$ , orthorhombic, space group  $P212121$ ,  $a = 9.6772(3)$  Å,  $b = 11.2638(3)$  Å,  $c = 22.1050(7)$  Å,  $\alpha = \beta = \gamma = 90.00$ ,  $V = 2409.49(12)$  Å<sup>3</sup>,  $F(000) = 936$ ,  $Z = 4$ ,  $D_c = 1.214$  mg m<sup>-3</sup>, goodness of fit = 1.026,  $m = 2.181$  mm<sup>-1</sup> (Mo-K $\alpha$ ,  $\lambda = 0.71073$  Å),  $T = 297(2)$ , K. Total reflections 4251, ( $1.84 \leq \theta \leq 25.0^\circ$ ) were collected yielding 3278 unique data R value 0.0384, wR2 = 0.1011.

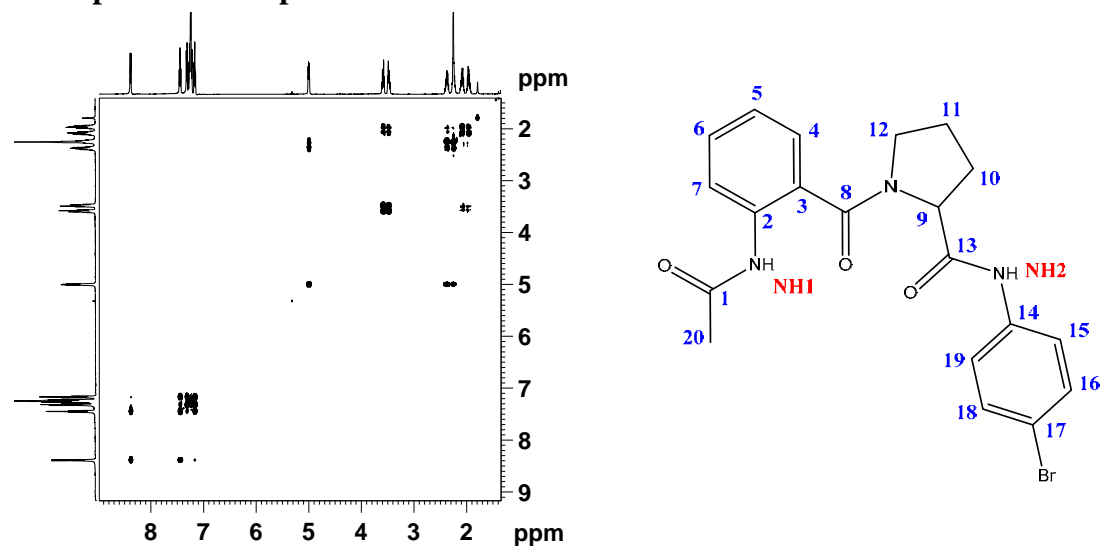
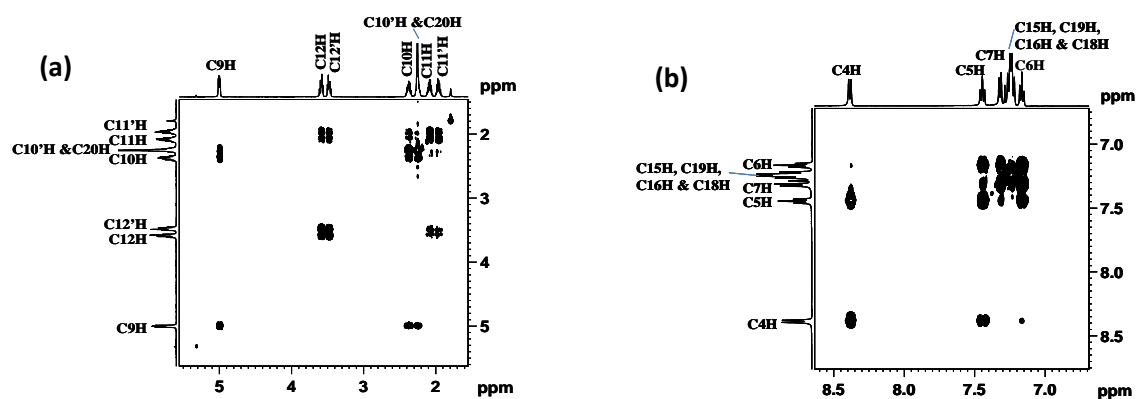
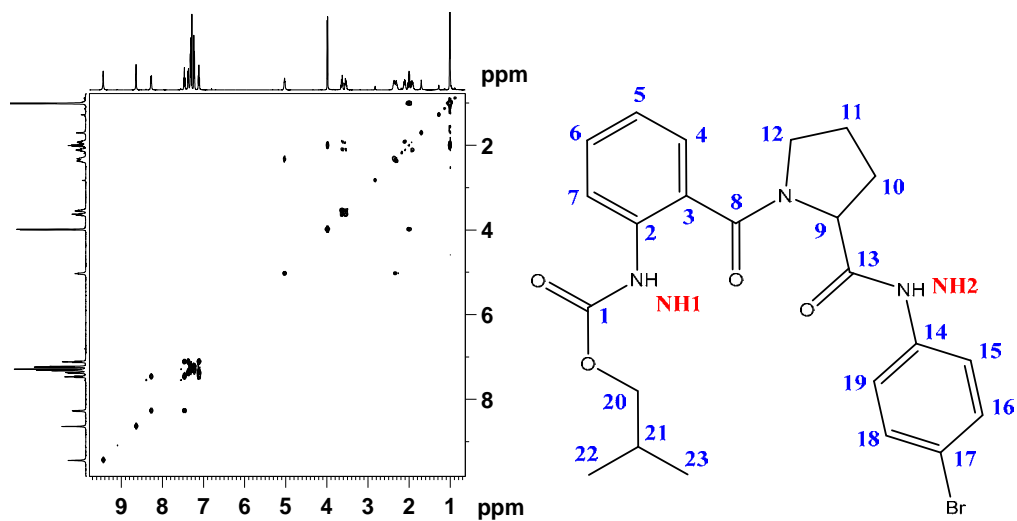
**Crystal data for 20:** Crystals of **20** were grown by slow evaporation of the solution in methanol and DCM. A crystal of size (0.28 x 0.17 x 0.07 mm) has been used for the data collection. Multiscan acquisition  $C_{19}H_{20}BrN_3O_4S$ ,  $M = 466.35$ , monoclinic, space group  $P21$ ,  $a = 11.7287(18)$  Å,  $b = 6.9721(11)$  Å,  $c = 13.389(2)$  Å,  $\alpha = \beta = 90.00$ ,  $\gamma = 113.463(2)$ ,  $V = 1004.3(3)$  Å<sup>3</sup>,  $F(000) = 476$ ,  $Z = 2$ ,  $D_c = 1.542$  mg m<sup>-3</sup>,  $m = 2.181$  mm<sup>-1</sup> (Mo-K $\alpha$ ,  $\lambda = 0.71073$  Å),  $T = 297(2)$ K. 5023 reflections ( $1.66 \leq \theta \leq 25.0^\circ$ ) were collected yielding 3192 unique data R value 0.0328, wR2 = 0.0793. For all data GOF = 1.007.

**Crystal data for 22:** Crystals of **22** were grown by slow evaporation of the solution in methanol and DCM. A crystal of size (0.4 x 0.09 x 0.02 mm) has been used for the data

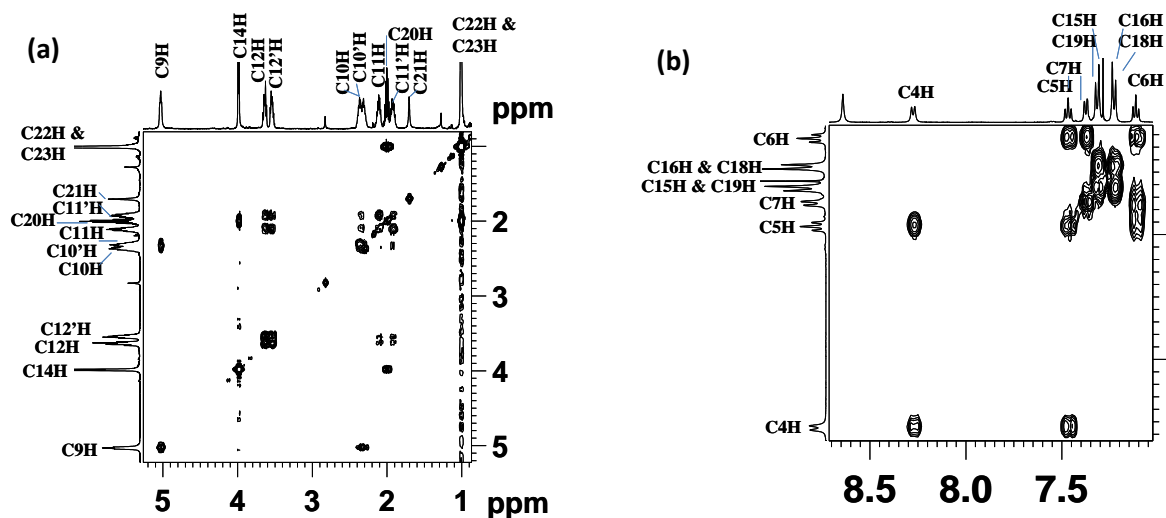
collection. Multiscan acquisition  $C_{25}H_{23}BrIN_3O_4S$ ,  $M = 668.33$ , orthorhombic, space group P212121,  $a = 7.7468(15) \text{ \AA}$ ,  $b = 14.705(3) \text{ \AA}$ ,  $c = 23.523(5) \text{ \AA}$ ,  $\alpha = \beta = \gamma = 90.00$ ,  $V = 2679.7(9) \text{ \AA}^3$ ,  $F(000) = 1320$ ,  $Z = 4$ ,  $D_c = 1.657 \text{ mg m}^{-3}$ ,  $\mu (\text{Mo-K}\alpha) = 2.799 \text{ mm}^{-1}$ ,  $\lambda = 0.71073 \text{ \AA}$ ,  $T = 297(2)\text{K}$ . 19347 reflections ( $1.63 \leq \theta \leq 25.0^\circ$ ) were collected yielding 4725 unique data  $R$  value 0.0569,  $wR2 = 0.1386$ . For all data  $GOF = 1.055$ .

**Crystal data for 23:** Crystals of **23** were grown from ethanol. A crystal of size (0.8 x 0.18 x 0.04 mm) has been used for the data collection. Multiscan acquisition  $C_{28}H_{32}BrN_3O_5S$ ,  $M = 601.12$ , orthorhombic, space group P212121,  $a = 10.6144(15) \text{ \AA}$ ,  $b = 13.0508(18) \text{ \AA}$ ,  $c = 19.690(3) \text{ \AA}$ ,  $\alpha = \beta = \gamma = 90^\circ$ ,  $V = 2727.6(7) \text{ \AA}^3$ ,  $F(000) = 1248$ ,  $Z = 4$ ,  $D_c = 1.657 \text{ mg m}^{-3}$ ,  $\mu (\text{Mo-K}\alpha) = 1.627 \text{ mm}^{-1}$ ,  $\lambda = 0.71073 \text{ \AA}$ ,  $T = 297(2)\text{K}$ . 4793 total reflections ( $1.87 \leq \theta \leq 25.0^\circ$ ) yielding 3626 unique data,  $R = 0.0442$ ,  $wR2 = 0.1313$ .  $GOF = 0.516$ .

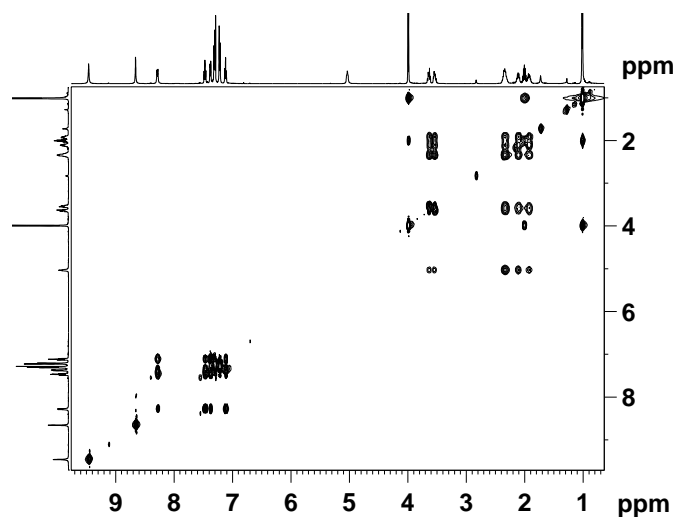
## 1.24 Spectra of compounds.

Figure 1: COSY spectra of amide **1** (400MHz, CDCl<sub>3</sub>)Figure 2: Partial COSY spectra of amide **1** (400MHz, CDCl<sub>3</sub>): aromatic (a) and aliphatic (b) regions.Figure 3: COSY spectra of amide **5** (400MHz, CDCl<sub>3</sub>)





**Figure 4:** Partial COSY spectra of amide **5** (400MHz,  $C_6D_6$ ): aromatic (a) and aliphatic (b) regions.



**Figure 5:** TOCSY spectra of amide **5** (400MHz,  $CDCl_3$ )

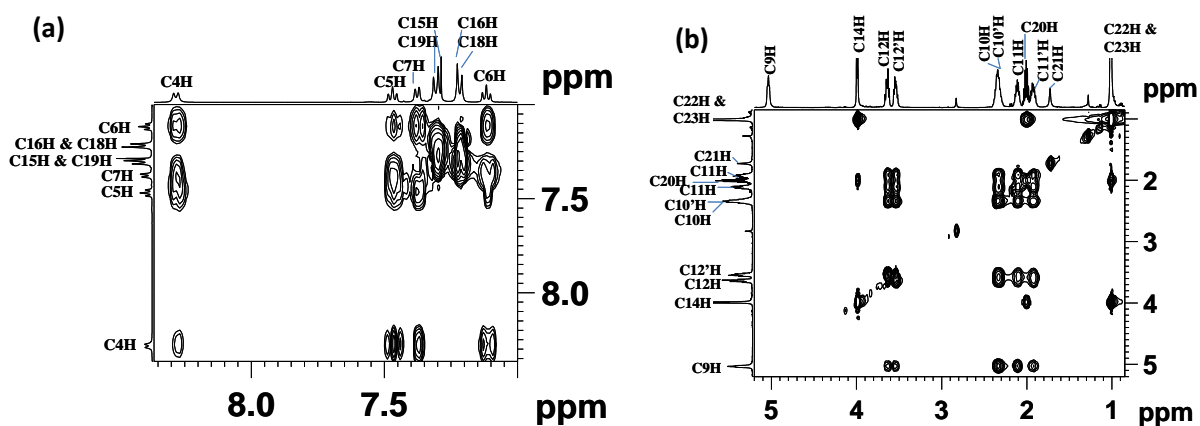


**Figure 6:** Partial TOCSY spectra of amide **5** (400MHz,  $CDCl_3$ ): aromatic (a) & aliphatic (b) regions.

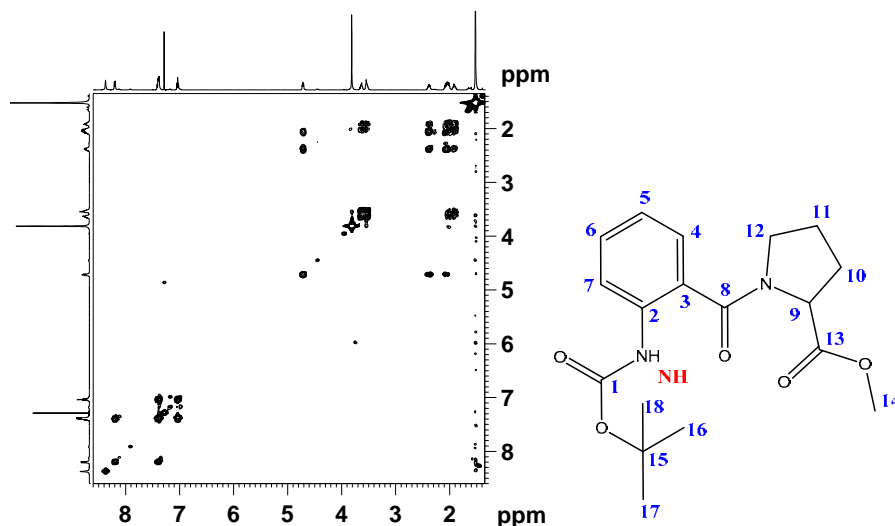


Figure 7: COSY spectra of ester 7 (400MHz, CDCl<sub>3</sub>)

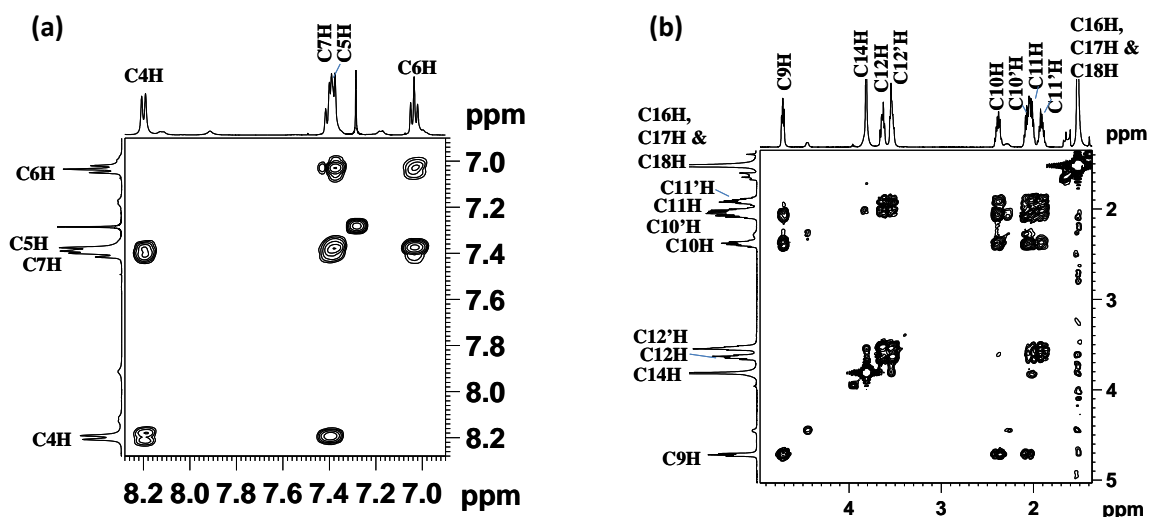


Figure 8: Partial COSY spectra of ester 7 (400MHz, CDCl<sub>3</sub>): aromatic (a) & aliphatic (b) regions.

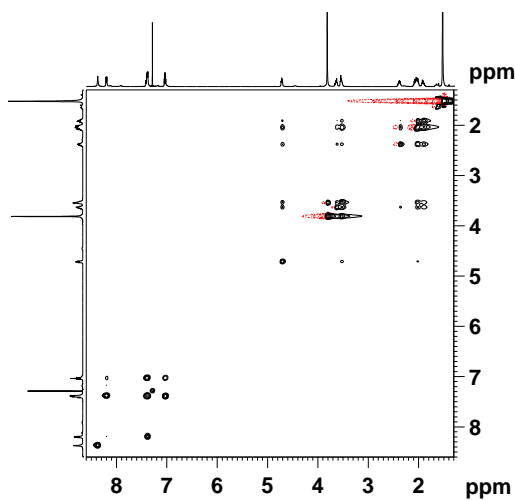
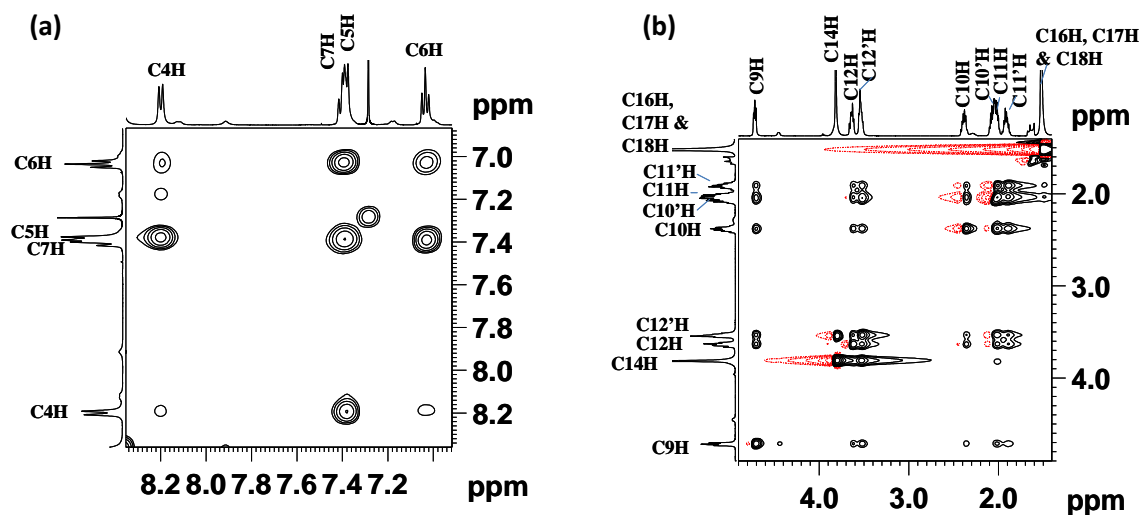
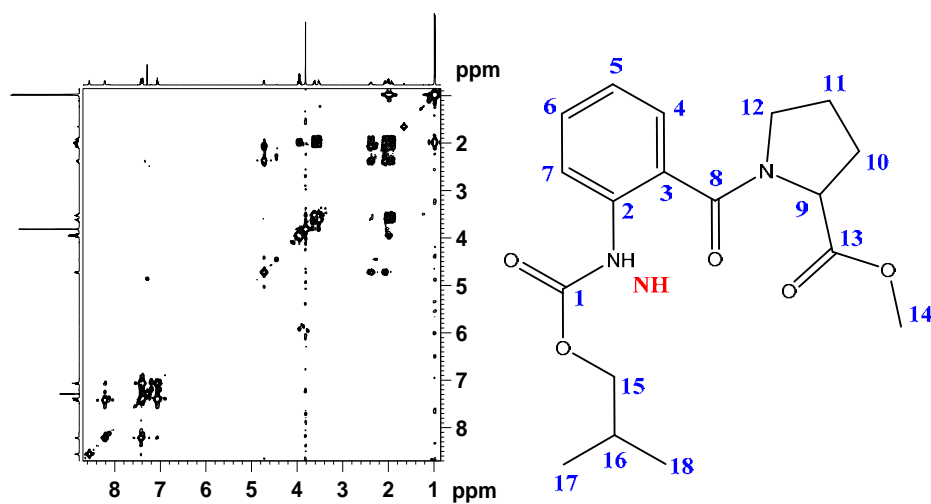


Figure 9: TOCSY spectra of ester 6 (400MHz, CDCl<sub>3</sub>)



**Figure 10:** Partial TOCSY spectra of ester **6** (400MHz,  $\text{CDCl}_3$ ): aromatic (a) & aliphatic (b) regions.



**Figure 11:** COSY spectra of ester **11** (400MHz,  $\text{CDCl}_3$ ):

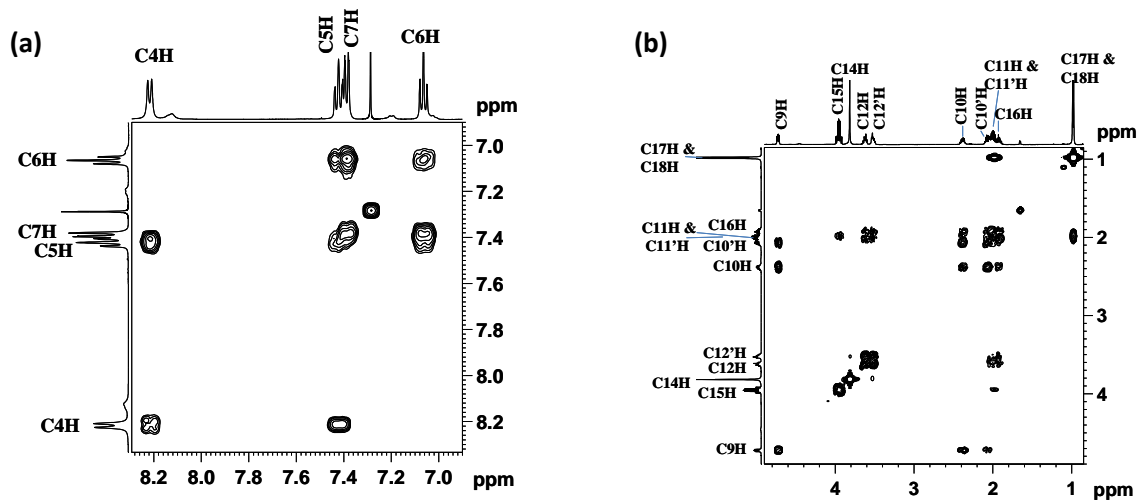


**Figure 12:** Partial COSY spectra of ester **10** (400MHz,  $\text{CDCl}_3$ ): aromatic (a) & aliphatic (b) regions.

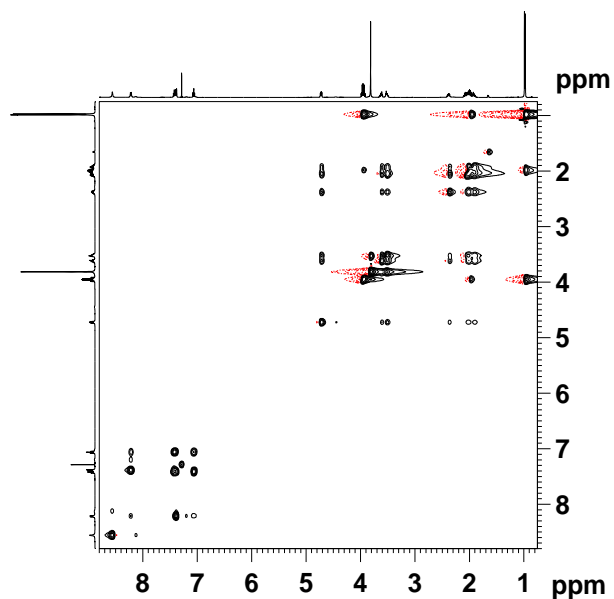


Figure 13: TOCSY spectra of ester **10** (400MHz,  $\text{CDCl}_3$ ):

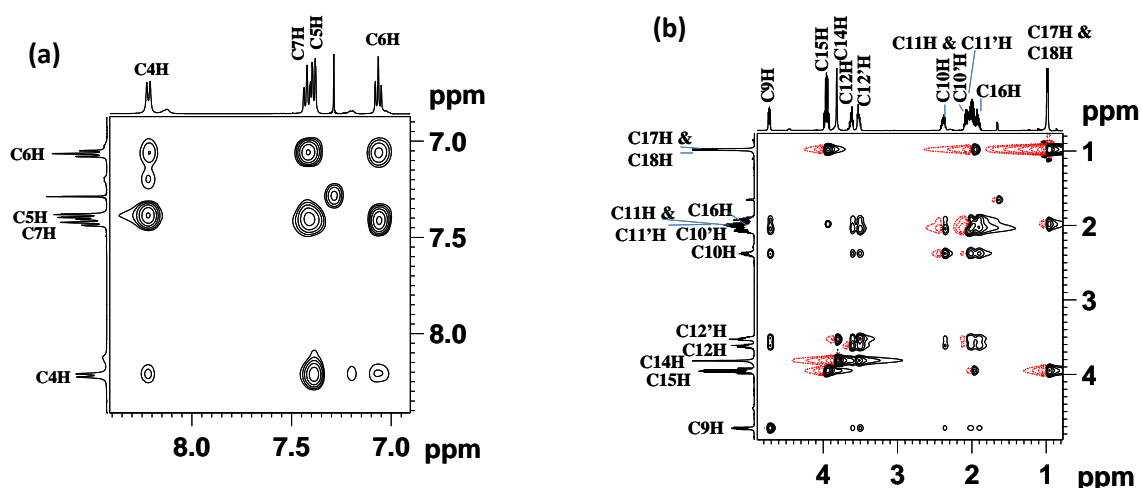


Figure 14: Partial TOCSY spectra of ester **10** (400MHz,  $\text{CDCl}_3$ ): aromatic (a) & aliphatic (b) regions.

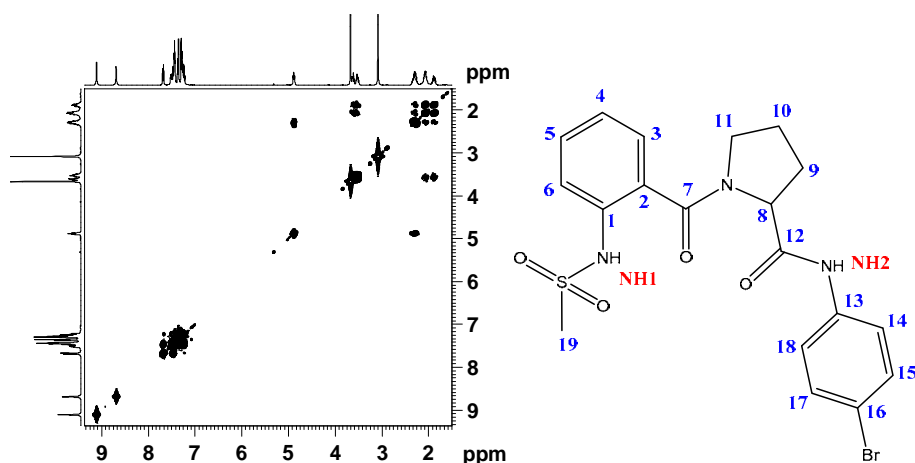
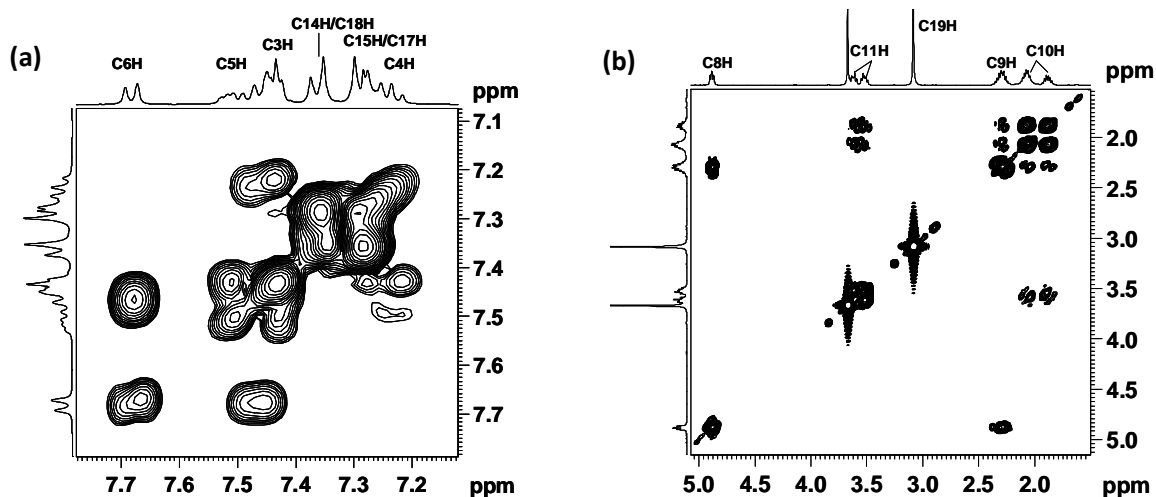
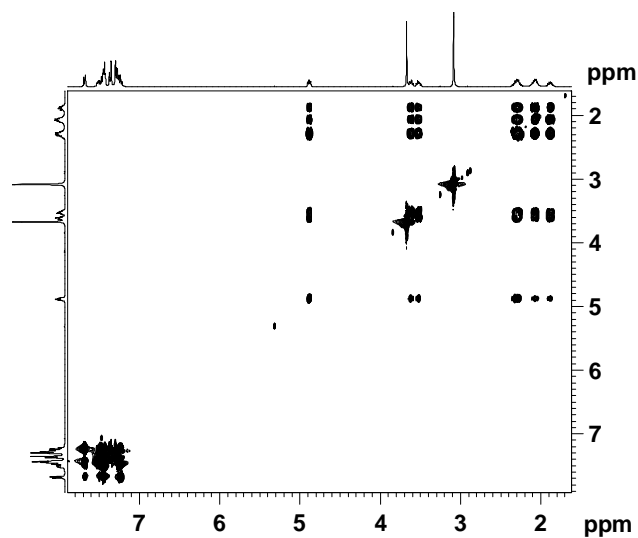


Figure 15: COSY spectra of sulfonamide **20** (400MHz,  $\text{CDCl}_3$ ):



**Figure 16:** Partial COSY spectra of sulfonamide **20** (400MHz,  $\text{CDCl}_3$ ): aromatic (a) & aliphatic (b).



**Figure 17:** TOCSY spectra of sulfonamide **20** (400MHz,  $\text{CDCl}_3$ ):

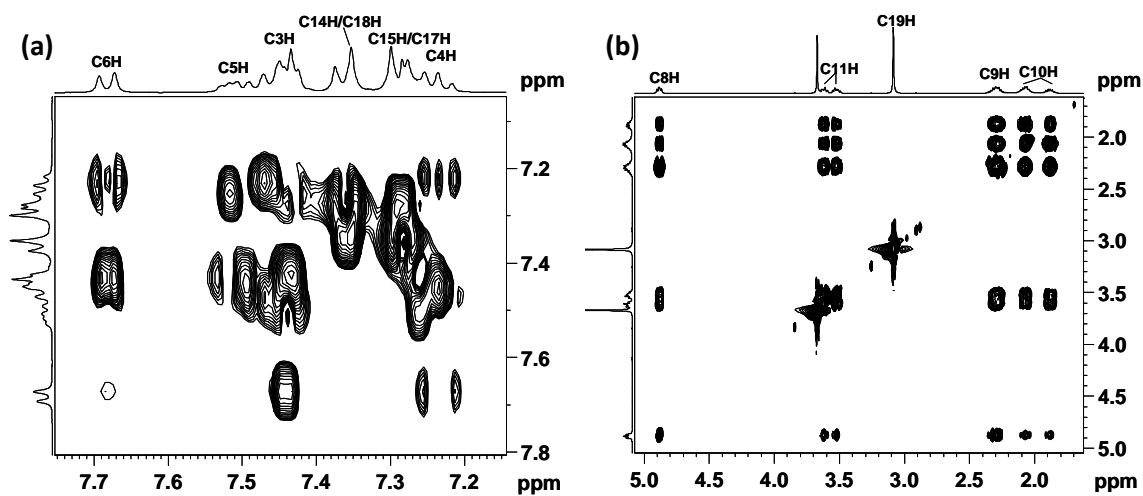


**Figure 18:** Partial COSY spectra of sulfonamide **20** (400MHz,  $\text{CDCl}_3$ ): aromatic (a) & aliphatic (b).

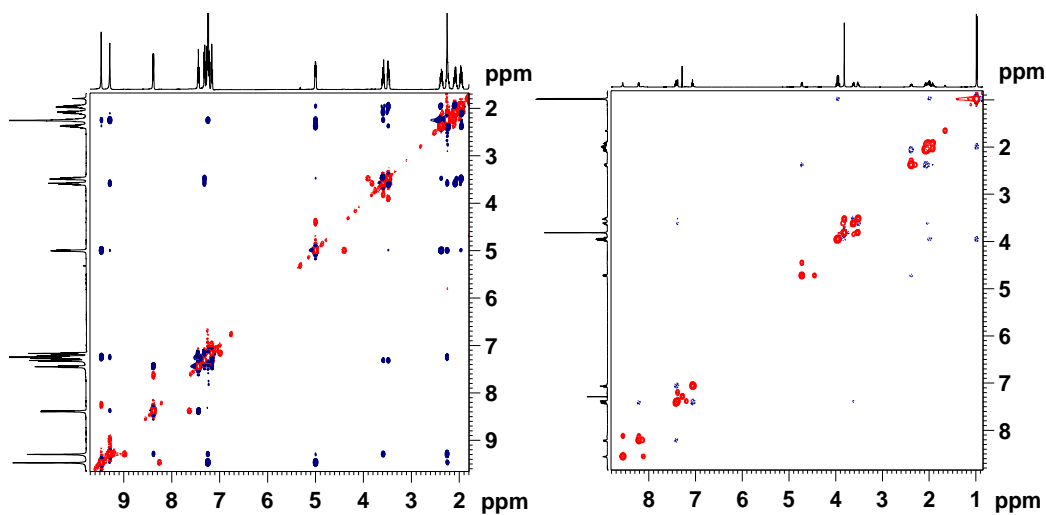


**Figure 19:** NOESY spectra of amide **1** (400MHz,  $\text{CDCl}_3$ ) and amide **6** (400MHz,  $\text{CDCl}_3$ ) respectively.

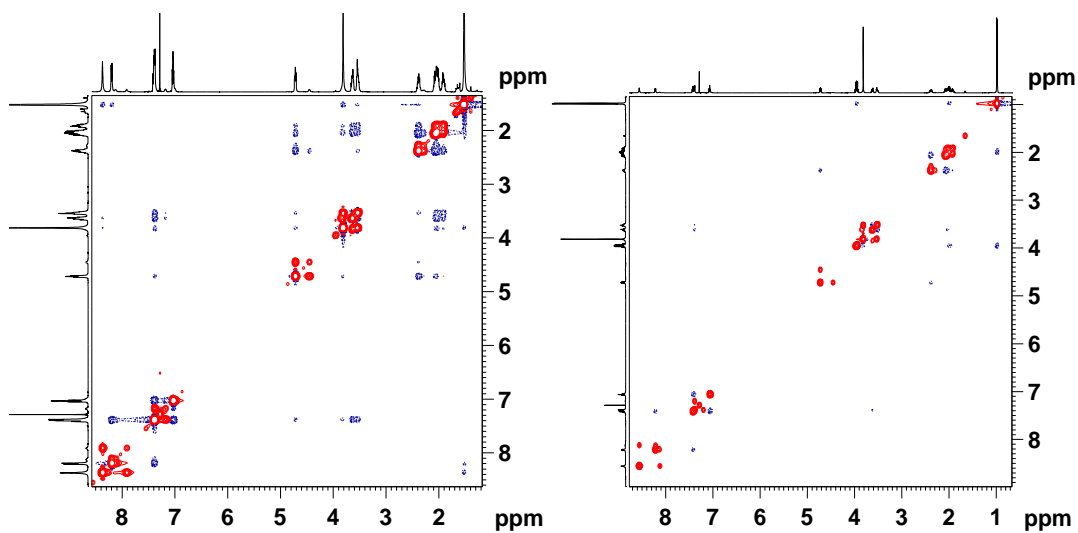


**Figure 20:** 2D NOESY spectra of C-terminal esters **7** (400MHz,  $\text{CDCl}_3$ ) and **11** (400MHz,  $\text{CDCl}_3$ ) respectively.

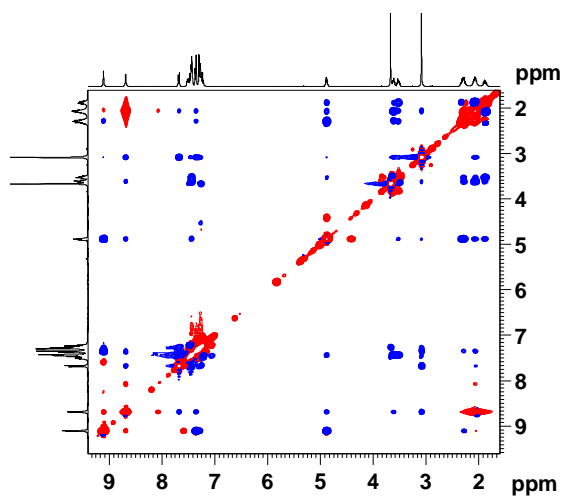


**Figure 21:** 2D NOESY spectra of N-terminal sulfonamide **20** (400MHz,  $\text{CDCl}_3$ ).

**Table 1:** NMR DMSO- $d_6$  titration studies of **1** (5mM, 400MHz, CDCl<sub>3</sub>).

No:	V <sub>DMSO-<math>d_6</math></sub> (in $\mu$ lit)	$\delta$ NH2	$\delta$ NH1
1	0	9.15	9.15
2	5	9.36	9.18
3	10	9.48	9.2
4	15	9.57	9.21
5	20	9.63	9.21
6	25	9.67	9.22
7	30	9.71	9.21
8	35	9.73	9.21
9	40	9.75	9.2
10	45	9.77	9.19
11	50	9.77	9.18

**Table 2:** NMR DMSO- $d_6$  titration studies of **5** (2mM, 400MHz, CDCl<sub>3</sub>).

No:	V <sub>DMSO-<math>d_6</math></sub> (in $\mu$ lit)	$\delta$ NH2	$\delta$ NH1	Concentration in mM
1	0	9.19	8.47	2
2	5	9.34	8.55	1.9802
3	10	9.42	8.59	1.9608
4	15	9.48	8.62	1.9418
5	20	9.54	8.64	1.9231
6	25	9.58	8.66	1.9048
7	30	9.6	8.66	1.8868
8	35	9.62	8.66	1.8692
9	40	9.64	8.66	1.8519
10	45	9.65	8.65	1.8349
11	50	9.66	8.65	1.8182

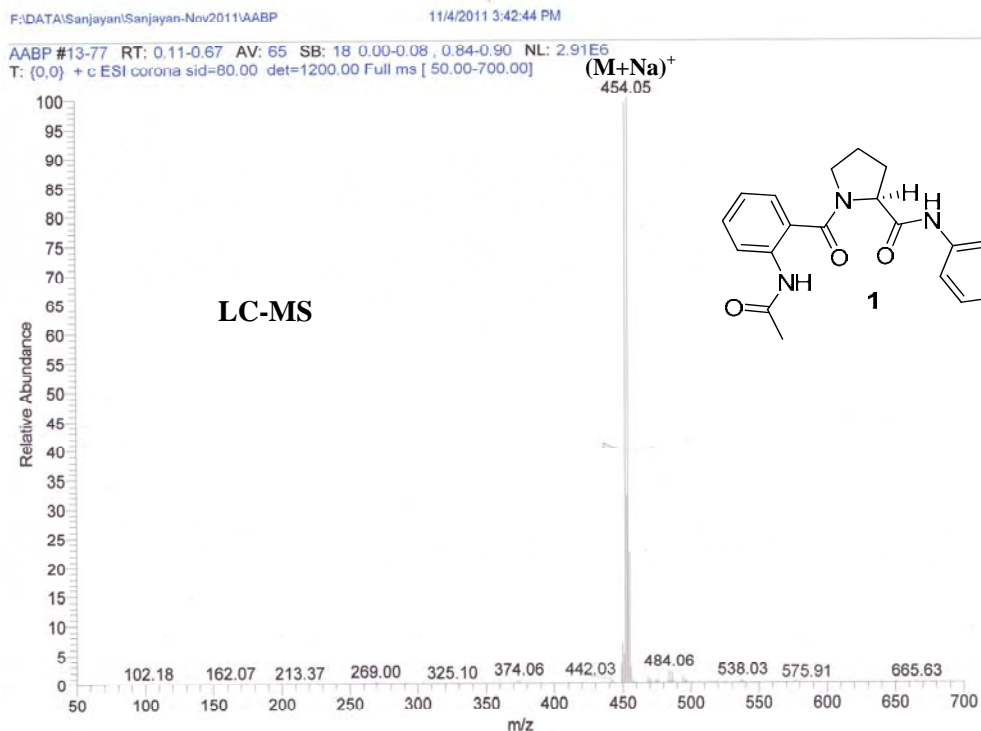
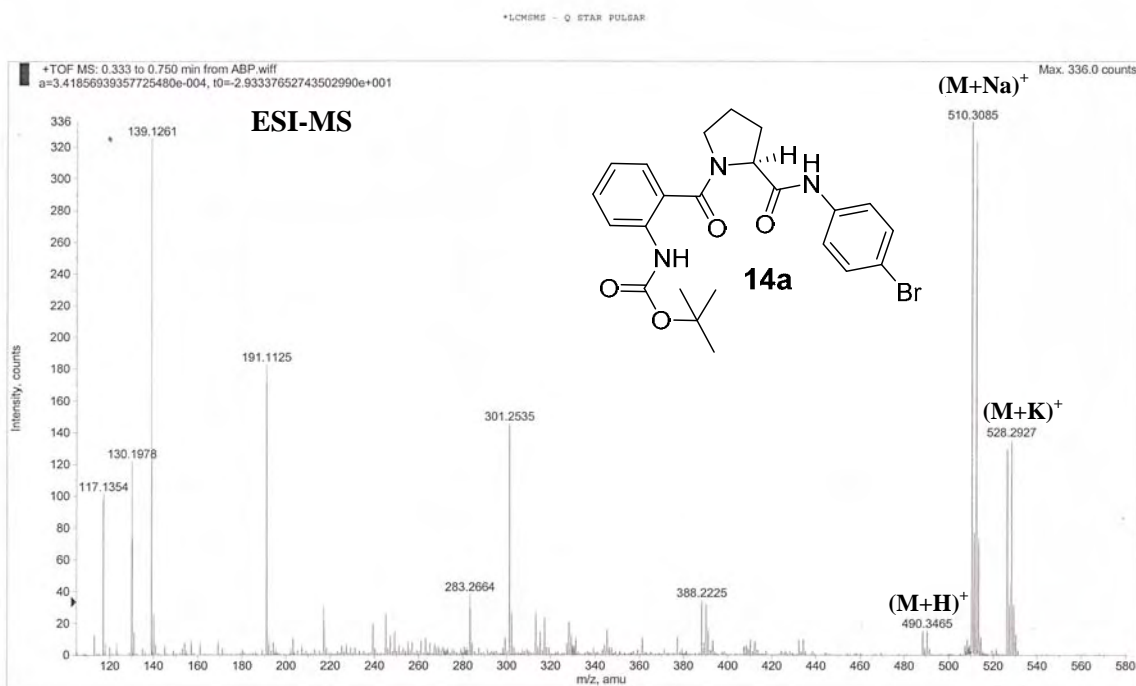
**Table 3:** NMR DMSO-*d*<sub>6</sub> titration studies of **10** (2mM, 400MHz, CDCl<sub>3</sub>).

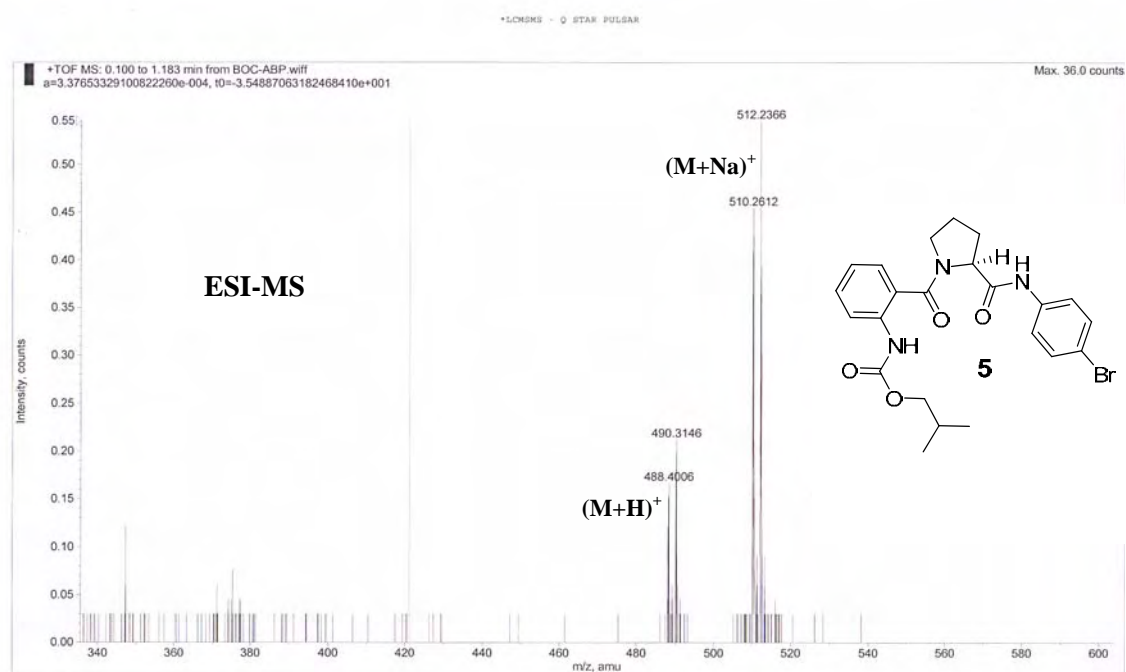
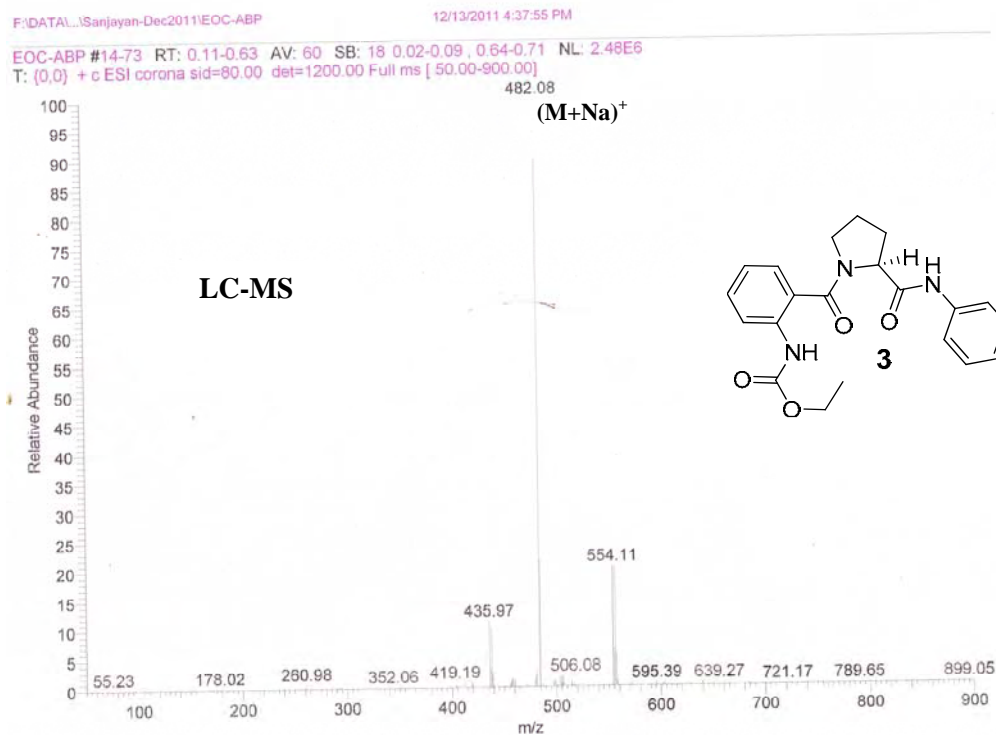
No:	V <sub>DMSO-<i>d</i><sub>6</sub></sub> (in μ lit)	δNH	Concentration in mM
1	0	8.55	2
2	5	8.53	1.9802
3	10	8.51	1.9608
4	15	8.49	1.9418
5	20	8.47	1.9231
6	25	8.45	1.9048
7	30	8.43	1.8868
8	35	8.41	1.8692
9	40	8.39	1.8519
10	45	8.38	1.8349
11	50	8.36	1.8182

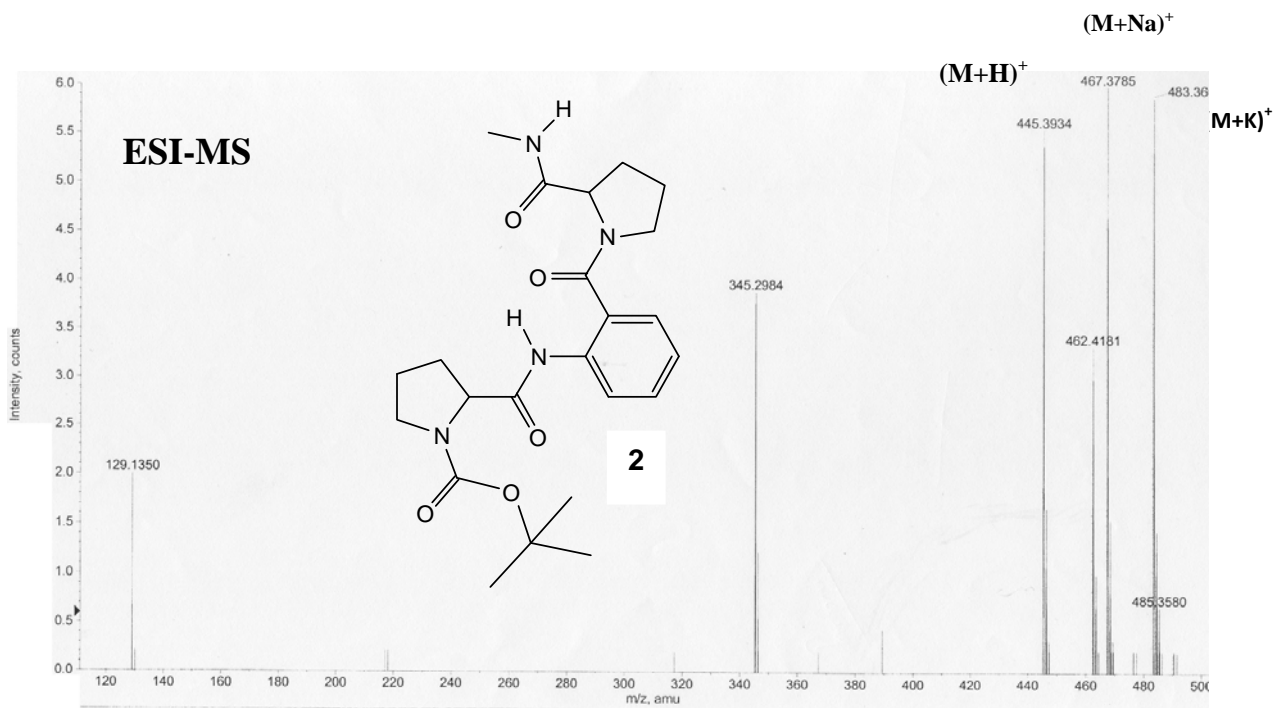
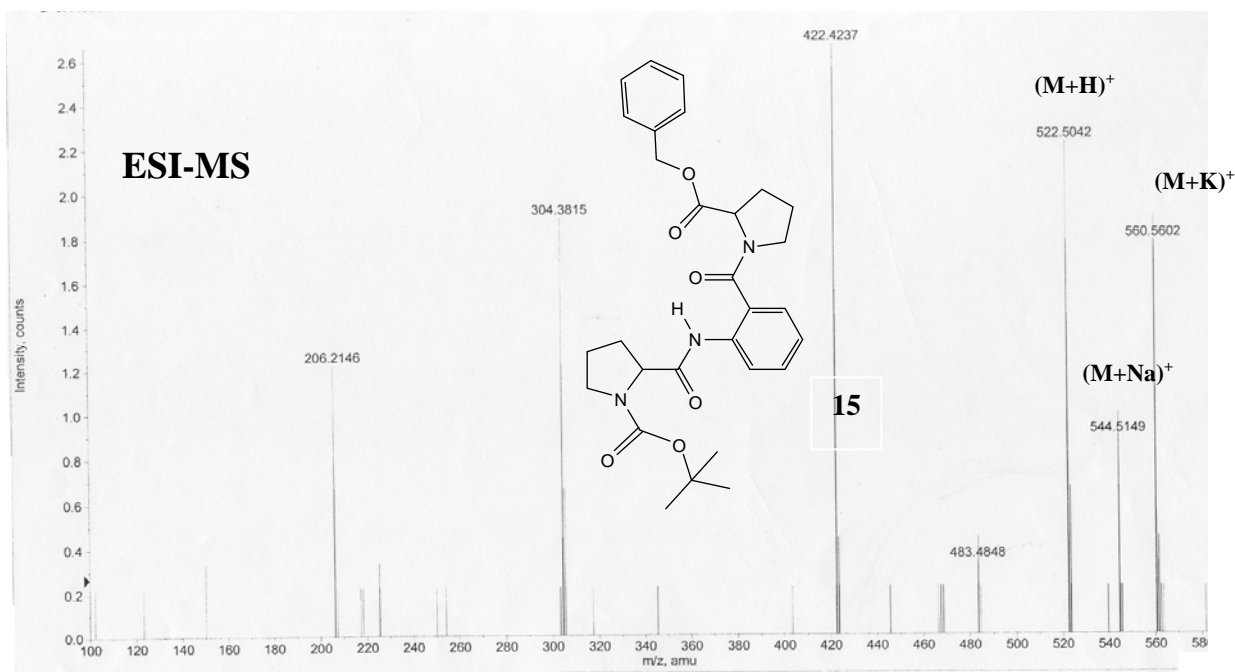
**Table 4:** NMR DMSO-*d*<sub>6</sub> titration studies of **10** (2mM, 400MHz, CDCl<sub>3</sub>).

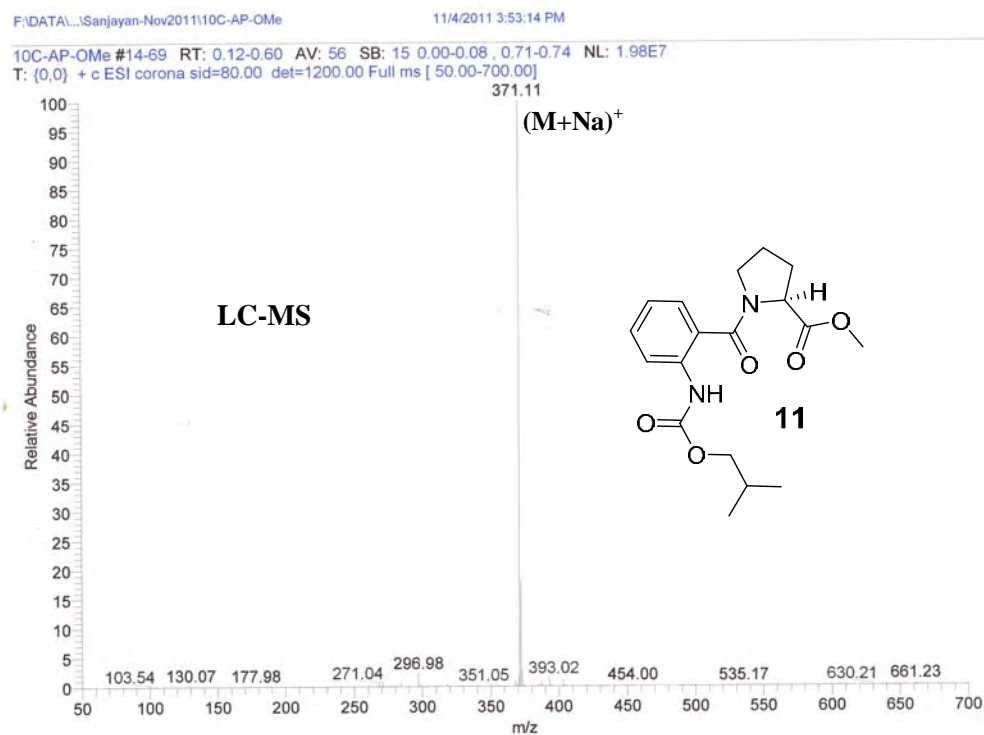
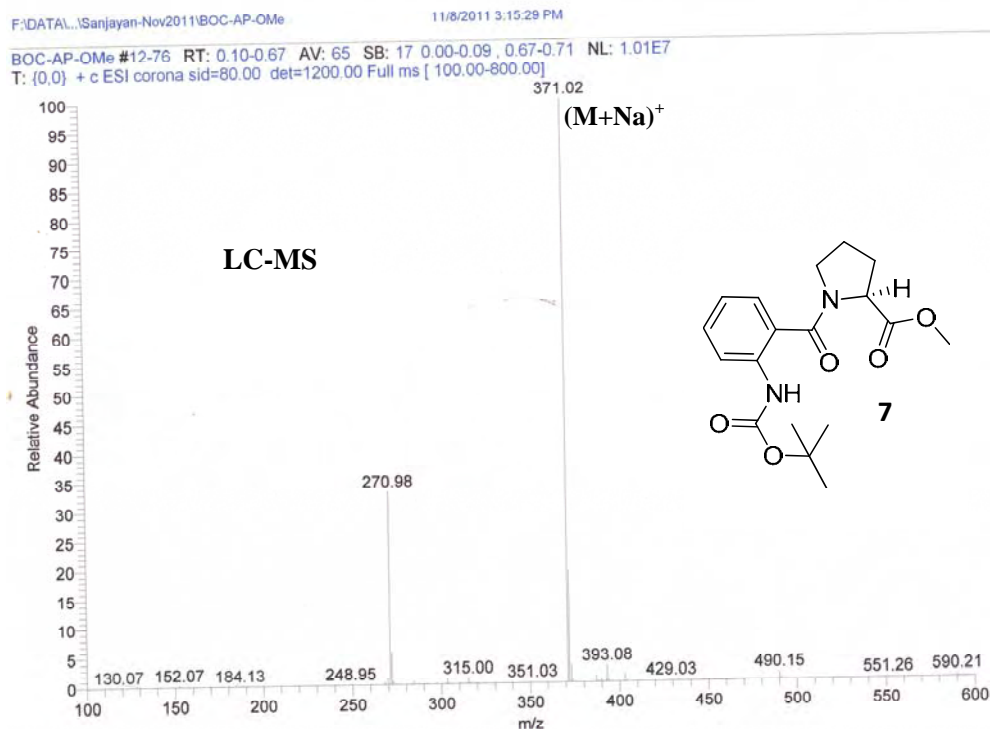
No:	V <sub>DMSO-<i>d</i><sub>6</sub></sub> (in μ lit)	δNH2	δNH1
1	0	8.773	8.585
2	5	9.2413	8.7422
3	10	9.461	8.799
4	15	9.568	8.814
5	20	9.633	8.814
6	25	9.676	8.81
7	30	9.711	8.801
8	35	9.733	8.786
9	40	9.749	8.772
10	45	9.758	8.755
11	50	9.767	8.741









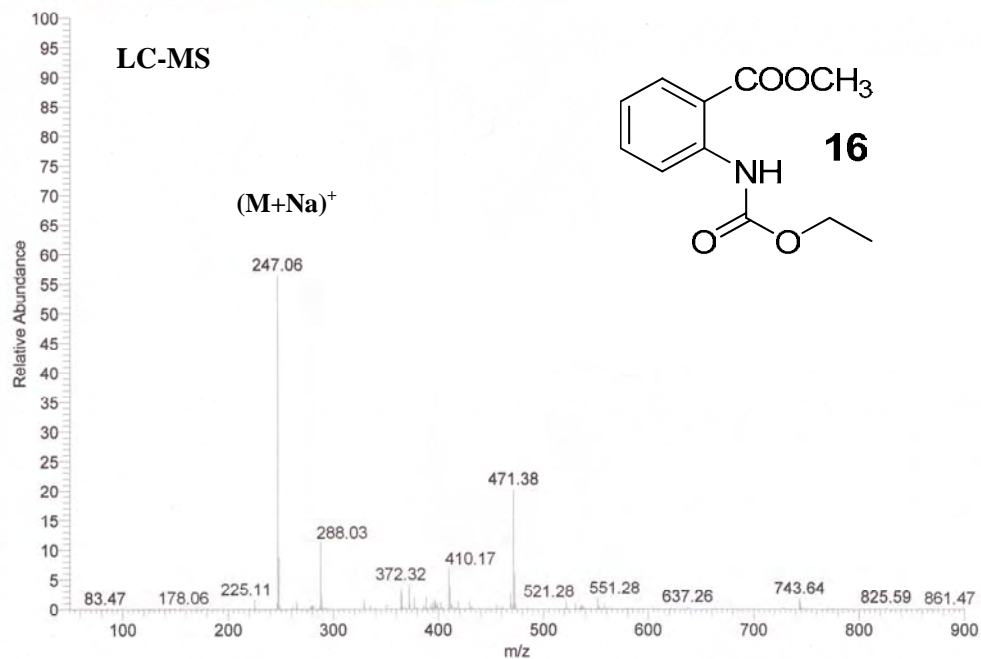


F:\DATA\Sanjayan-Dec2011\EOC-A

12/9/2011 3:58:14 PM

EOC-AP-OTFE #15-52 RT: 0.12-0.45 AV: 38 SB: 17 0.00-0.08, 0.53-0.58 NL: 3.86E6

T: (0,0) + c ESI corona sid=80.00 det=1200.00 Full ms [ 50.00-900.00]

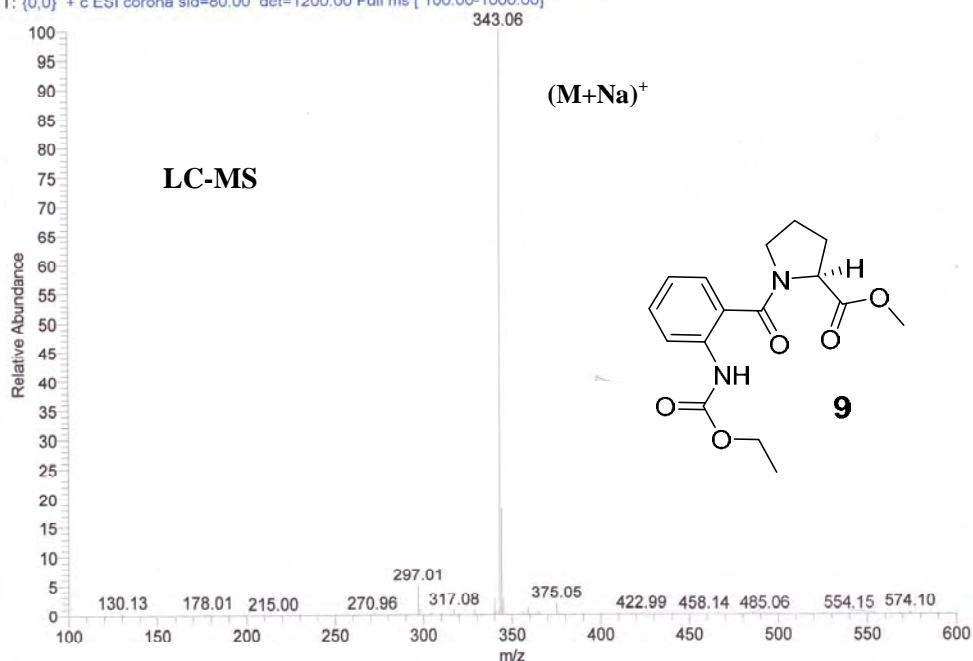


F:\DATA\Sanjayan-Nov2011\EOC-AP-OMe

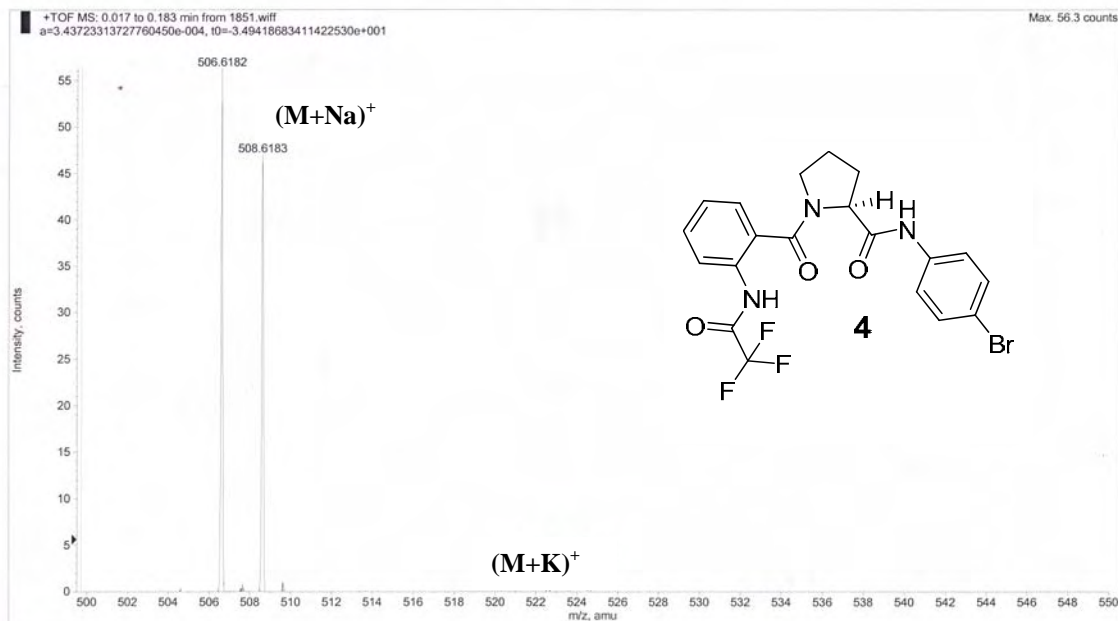
11/3/2011 5:23:55 PM

EOC-AP-OMe #14-61 RT: 0.11-0.53 AV: 48 SB: 15 0.00-0.08, 0.55-0.59 NL: 1.26E7

T: (0,0) + c ESI corona sid=80.00 det=1200.00 Full ms [ 100.00-1000.00]



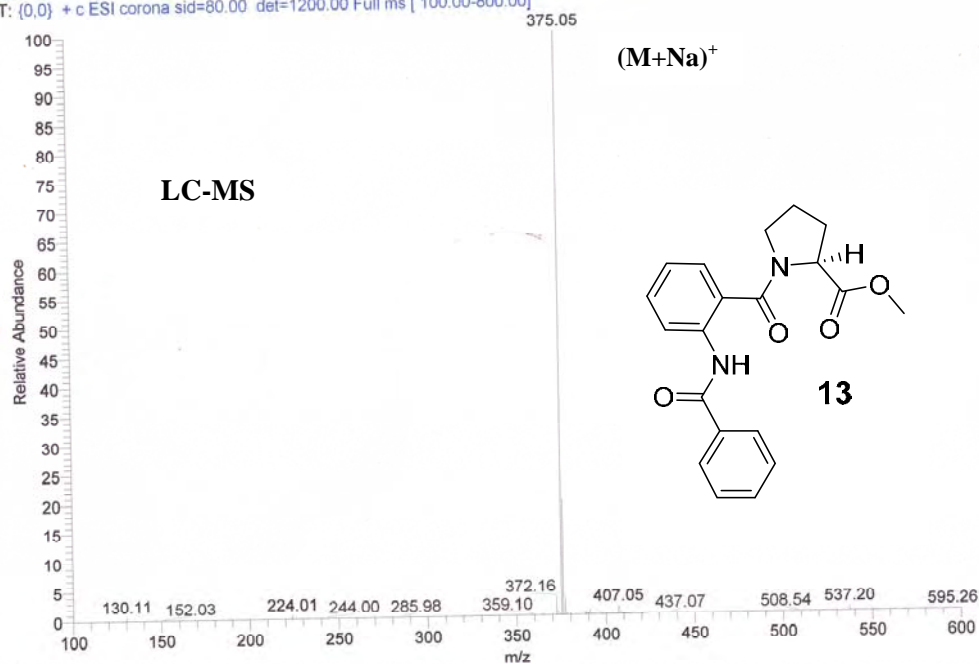
ESI-MS

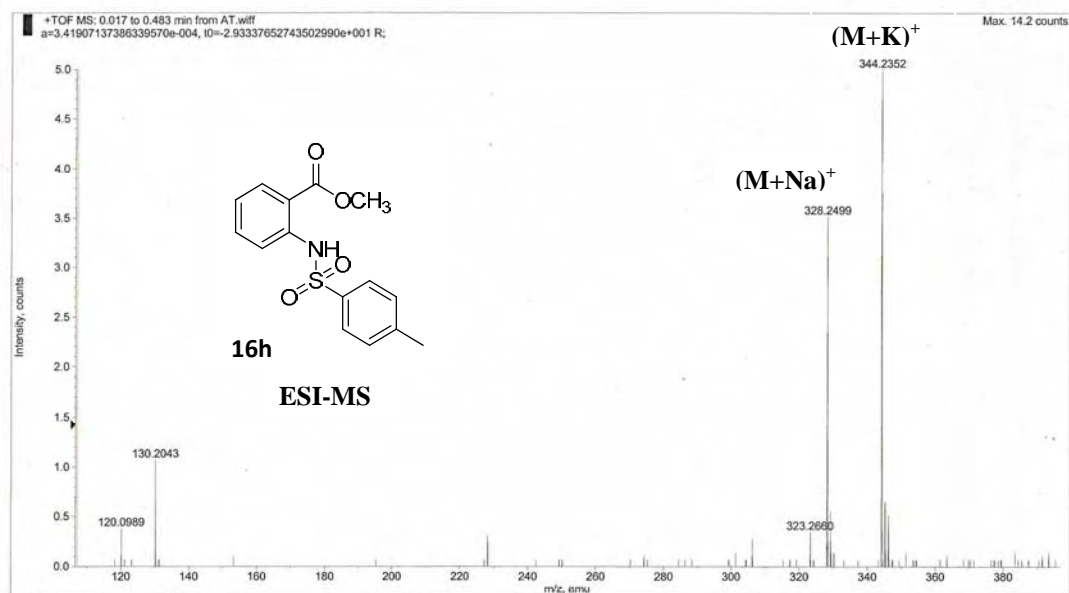
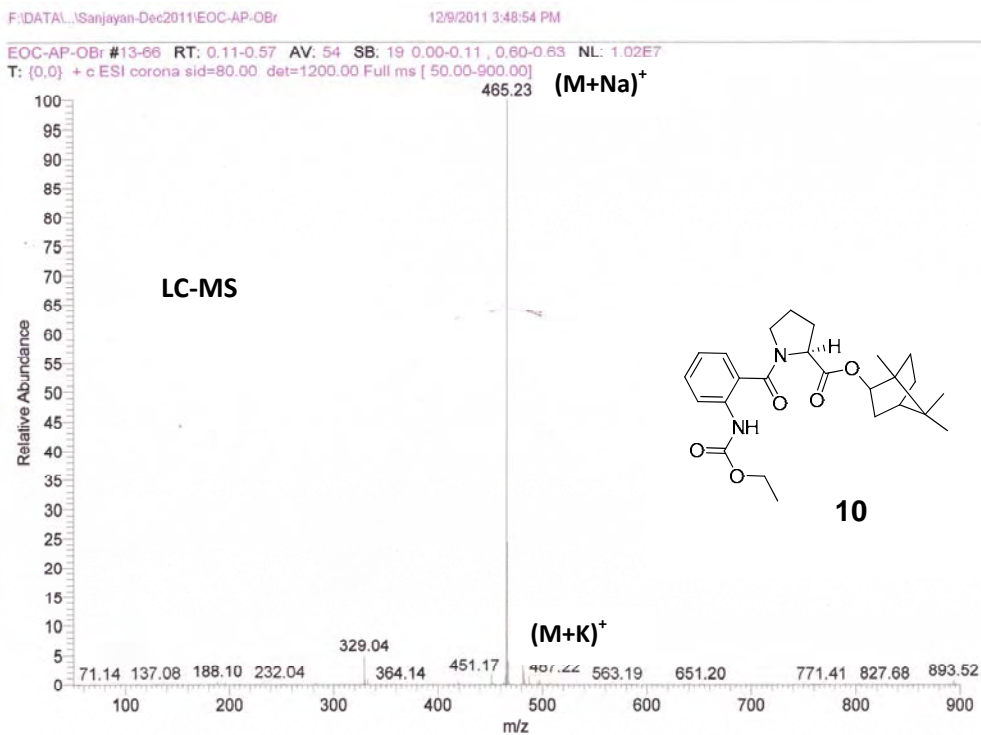


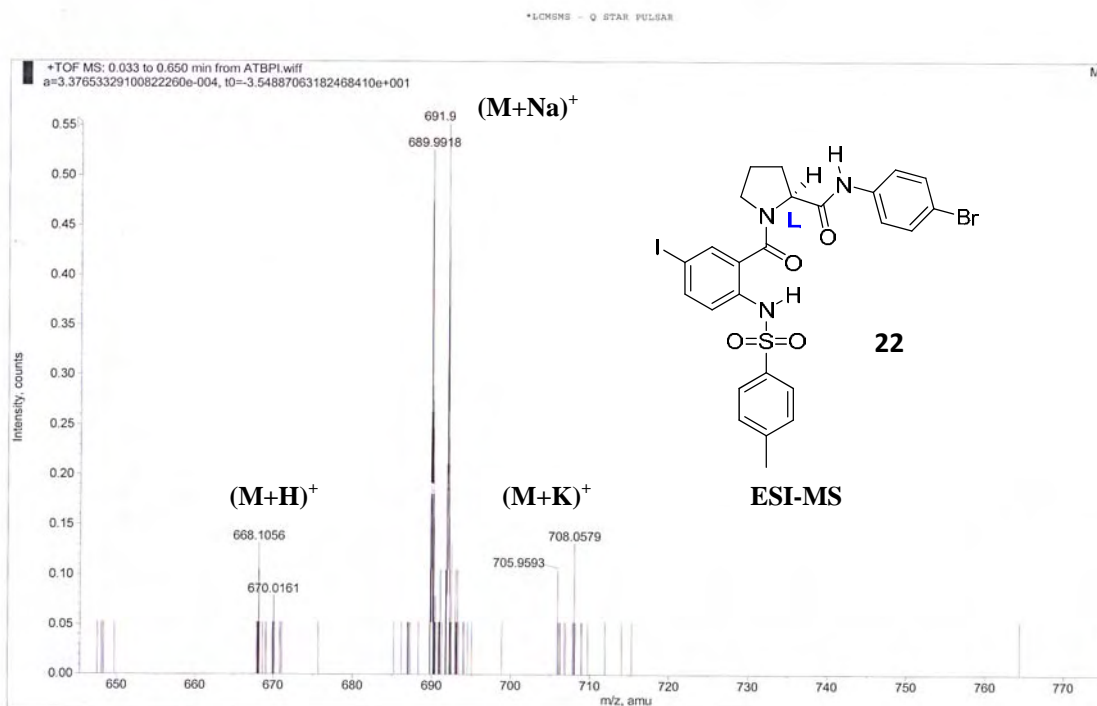
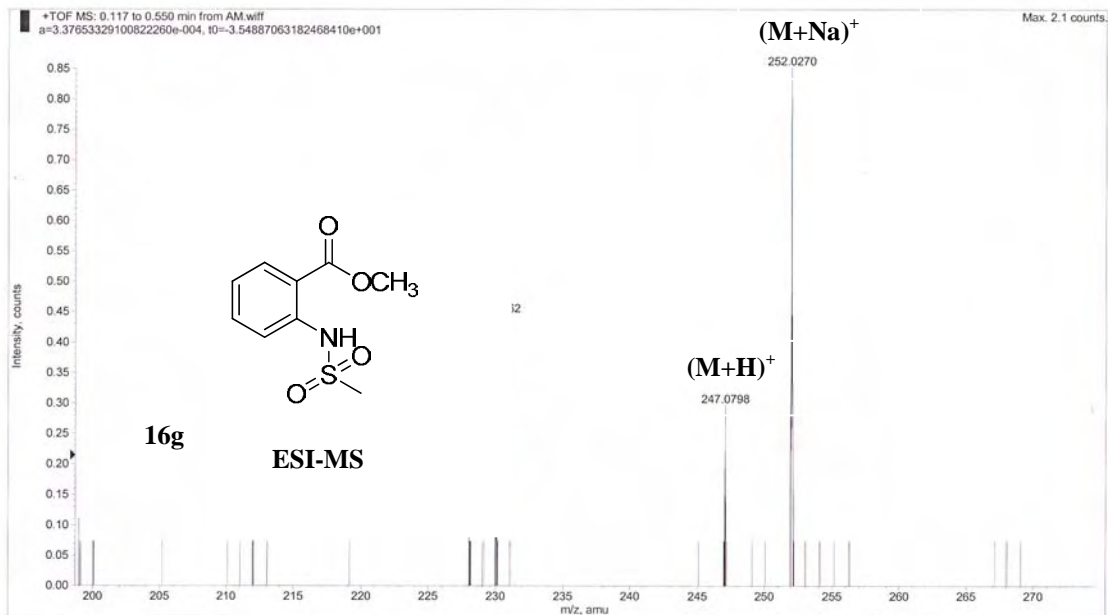
F:\DATA\...\Sanjayan-Nov2011\ABP-OMe

11/0/2011 3:23:59 PM

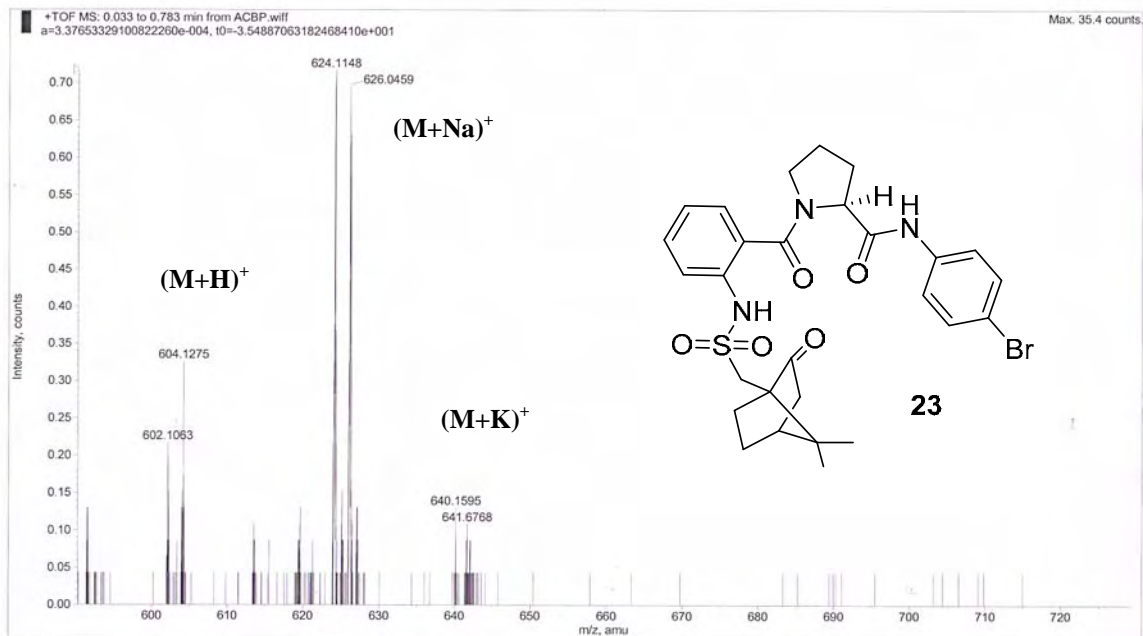
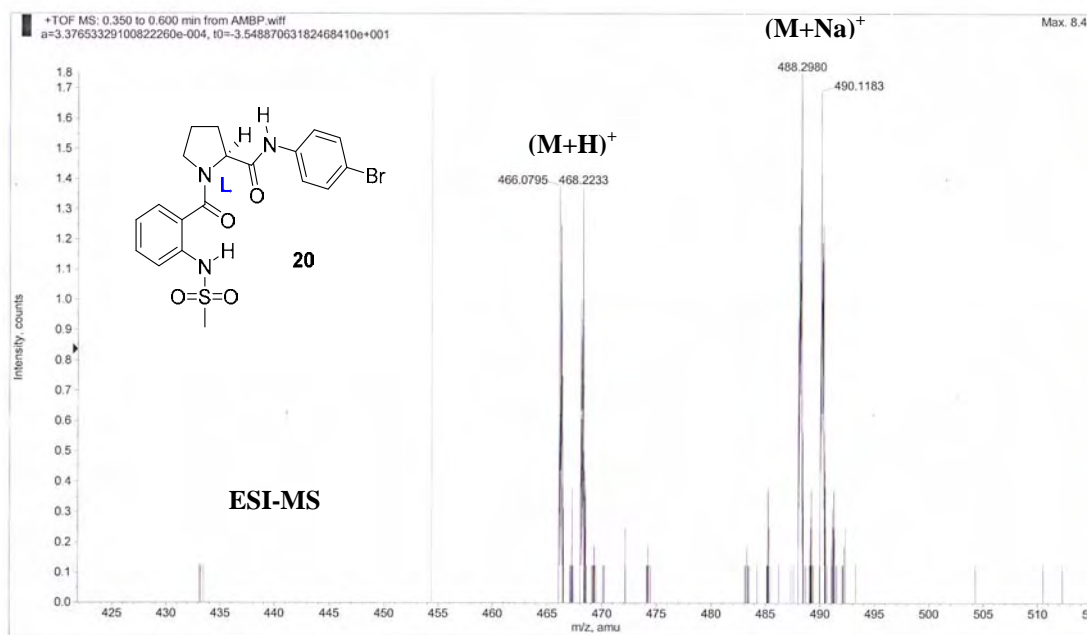
ABP-OMe #14-78 RT: 0.12-0.68 AV: 65 SB: 17 0.02-0.08, 0.80-0.87 NL: 1.22E7  
T: (0,0) +c ESI corona sid=80.00 det=1200.00 Full ms [ 100.00-800.00]

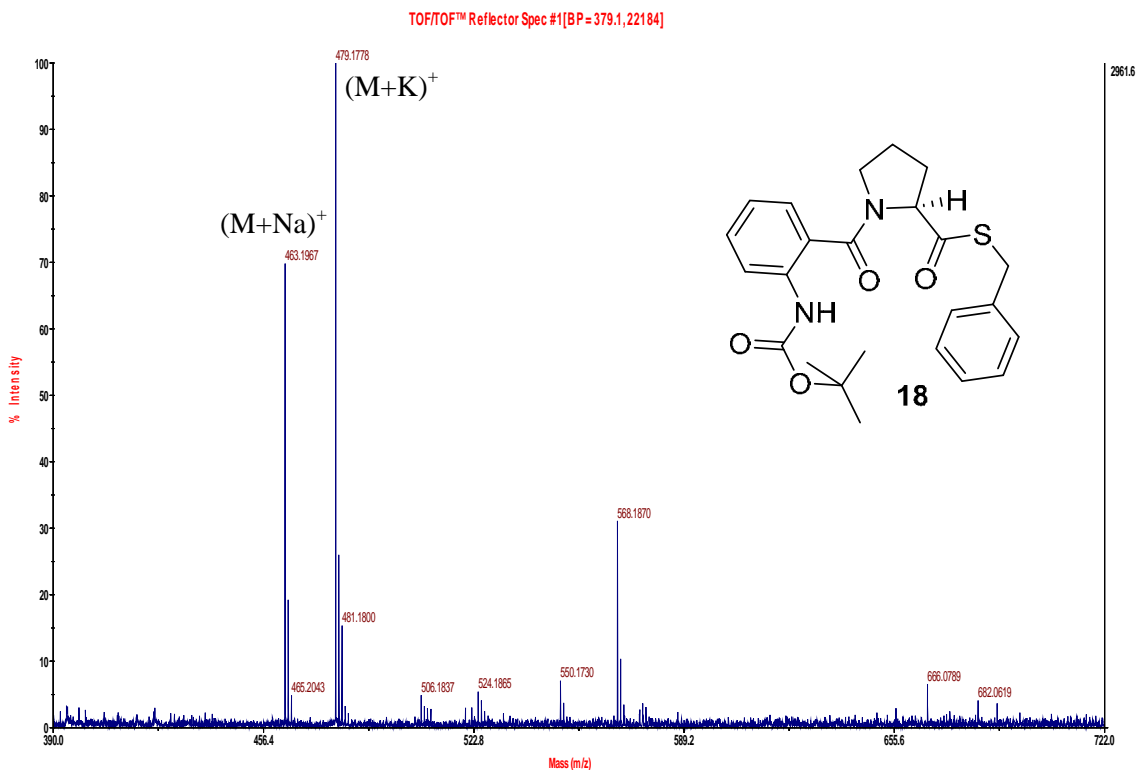
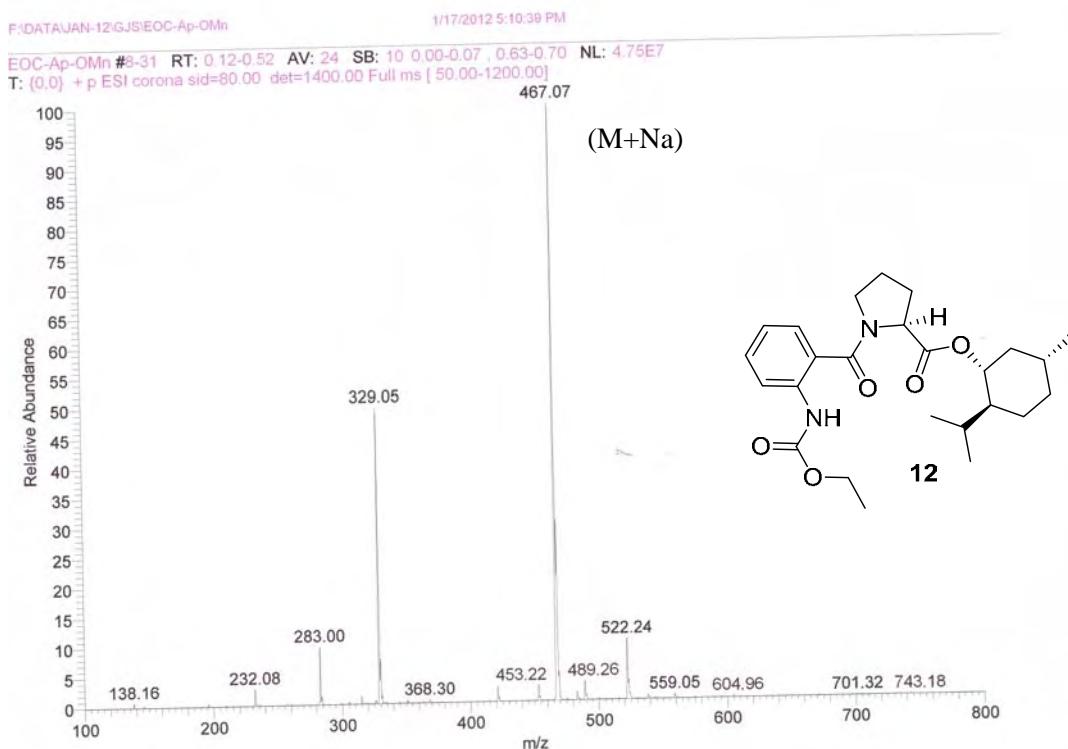


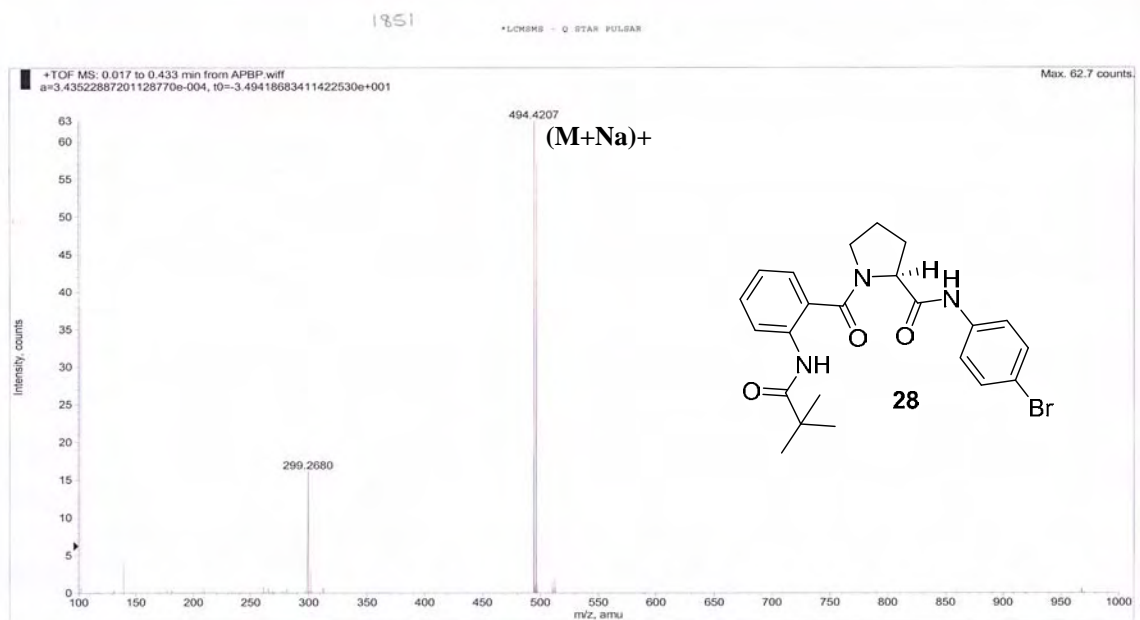
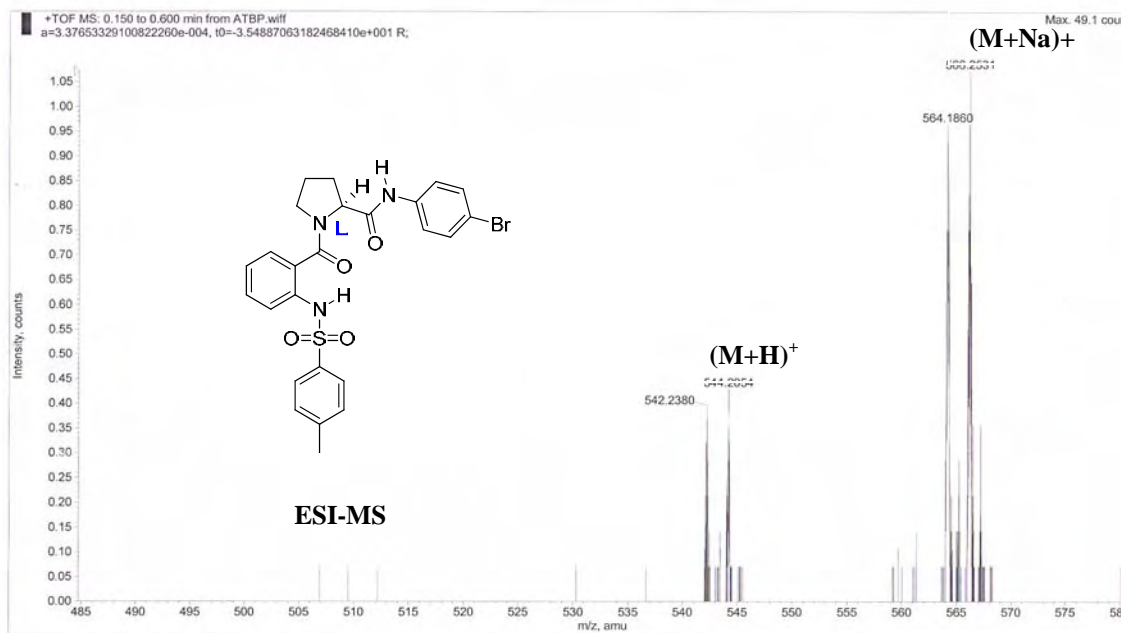


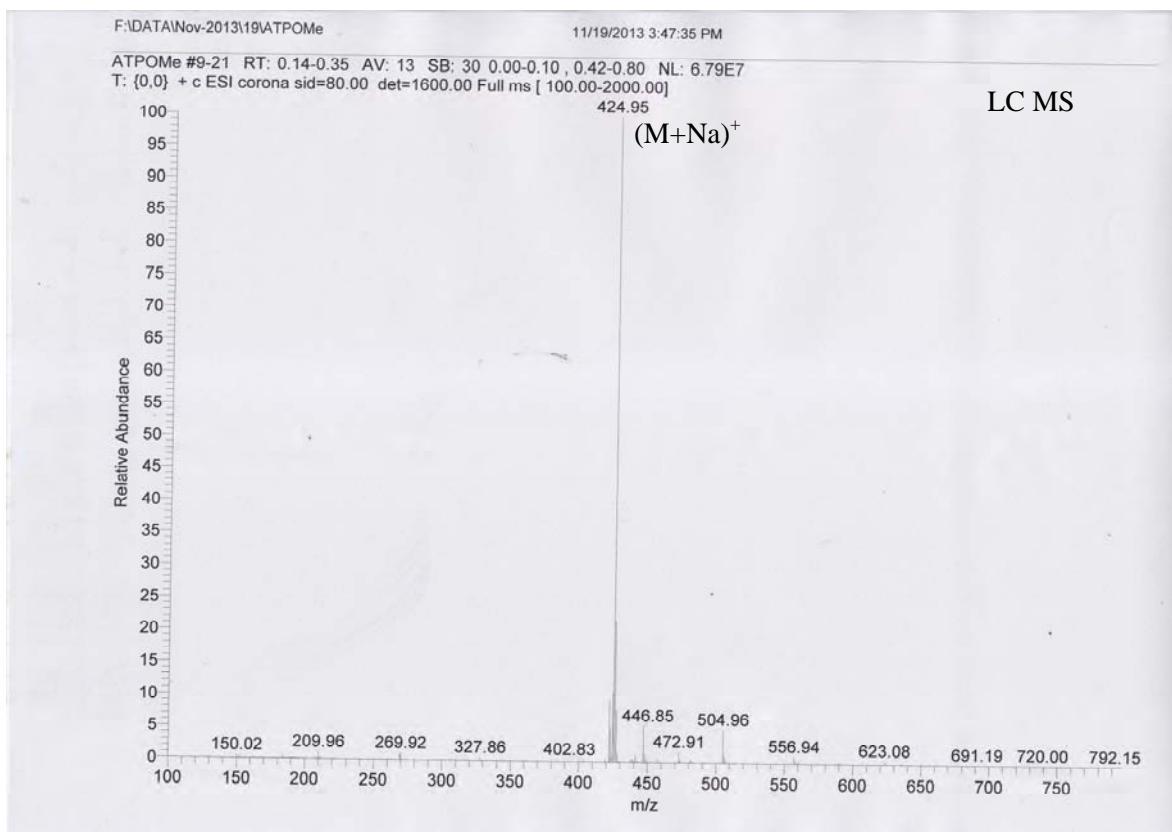
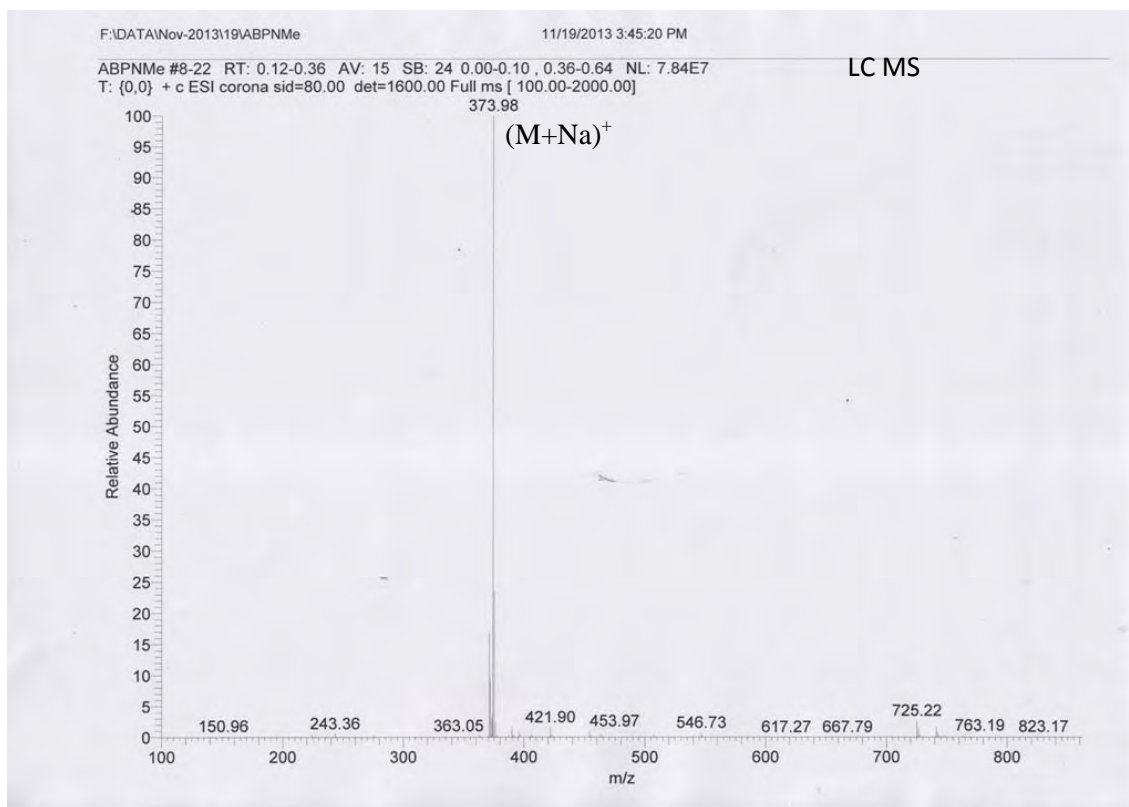


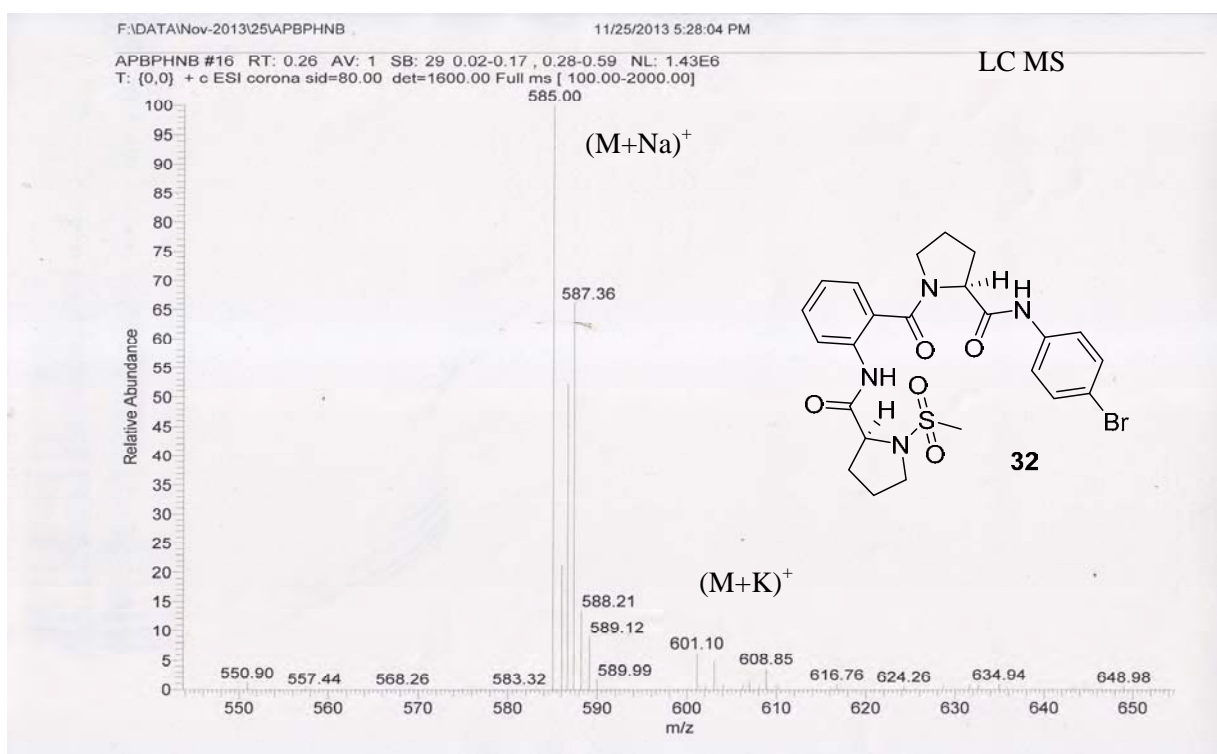
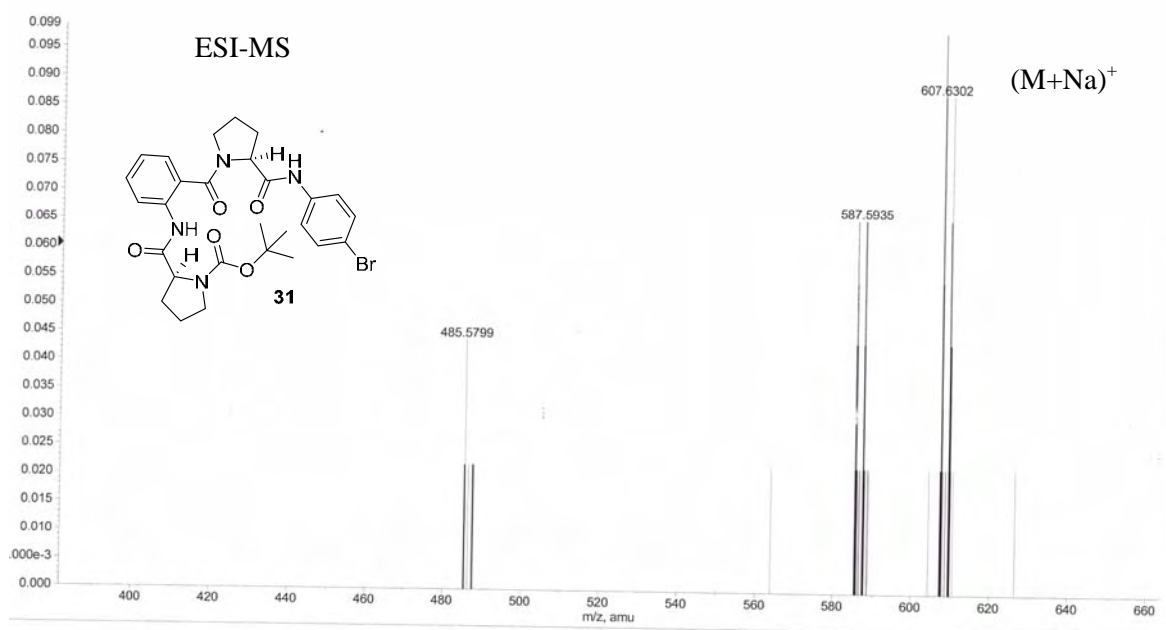


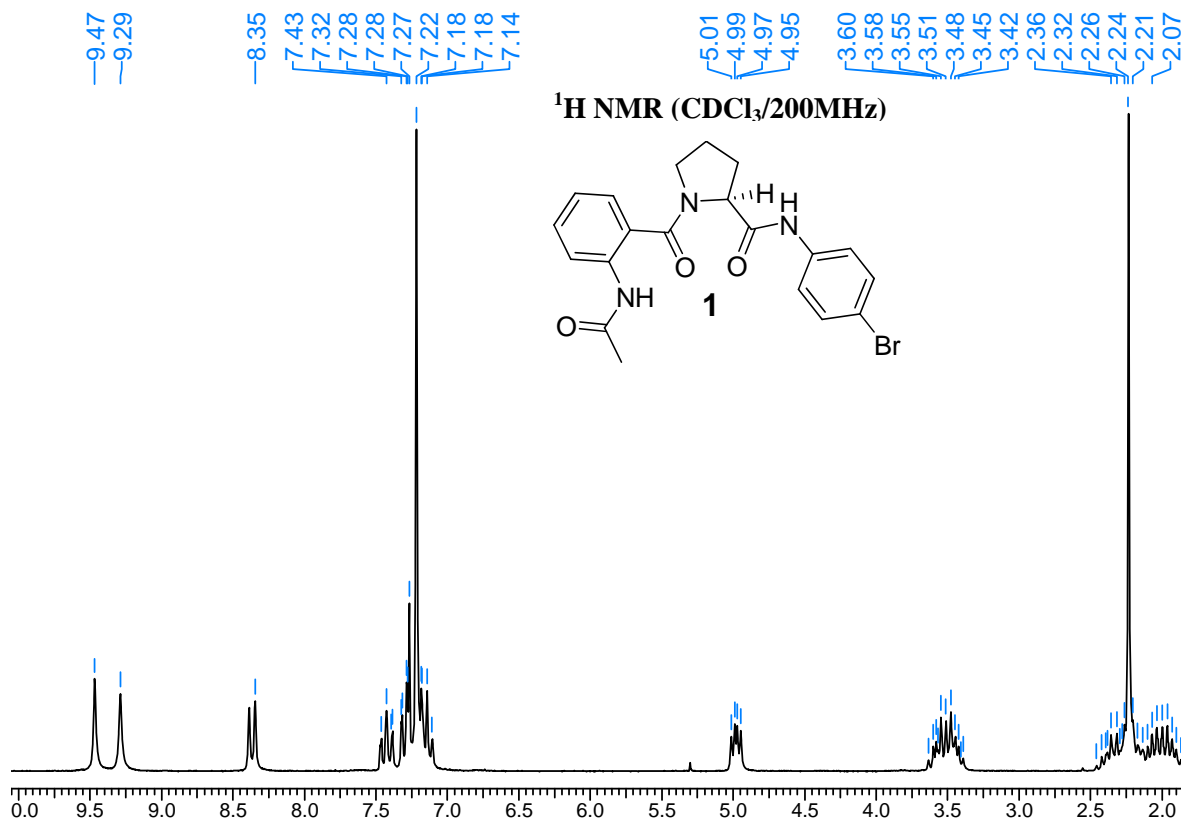
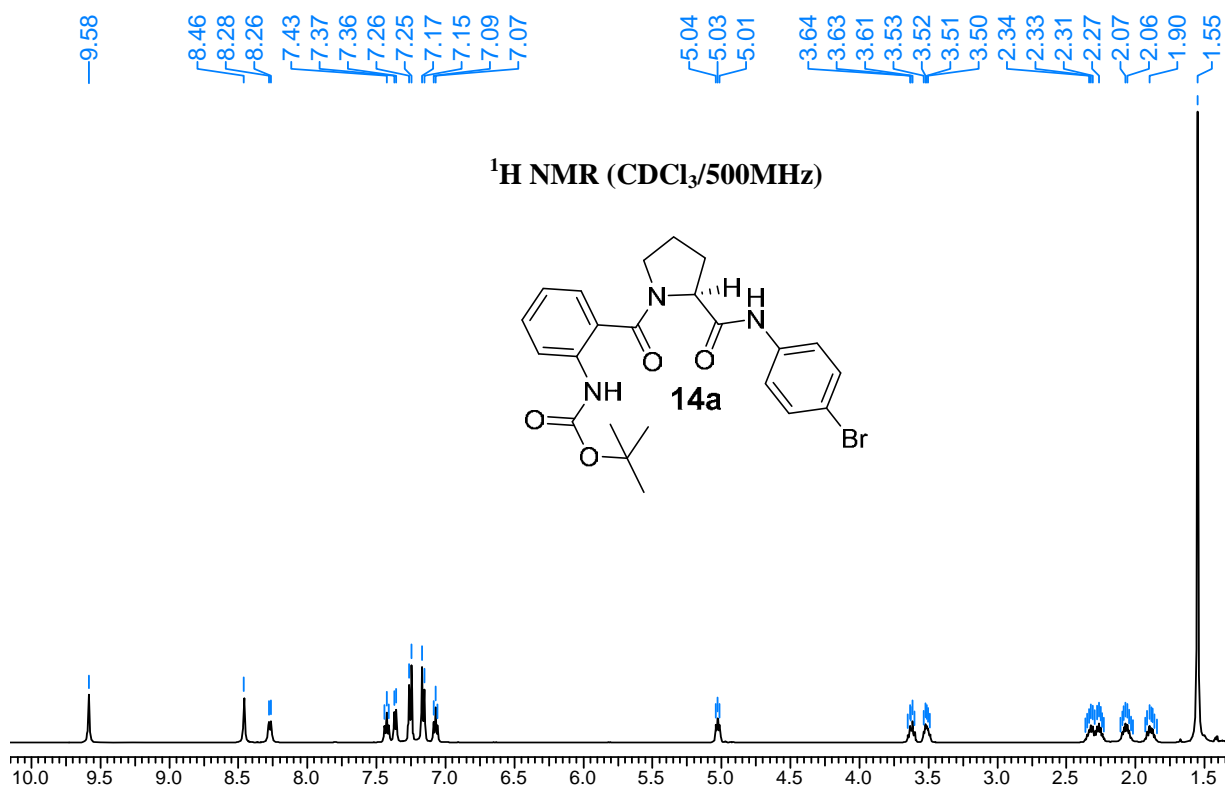


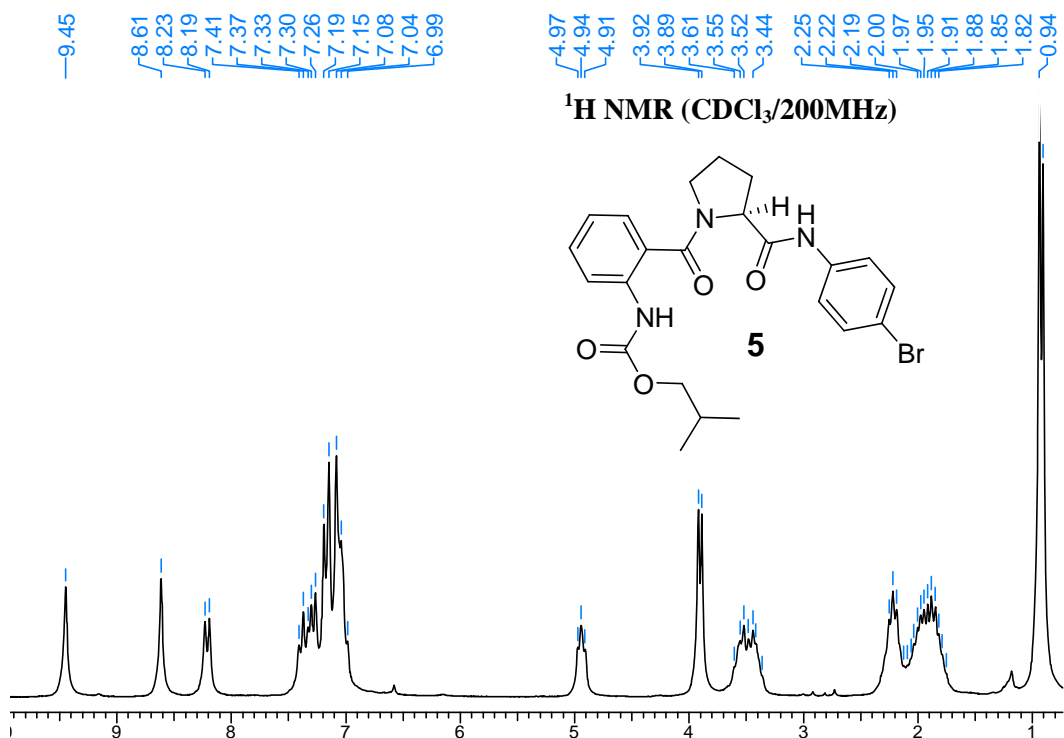
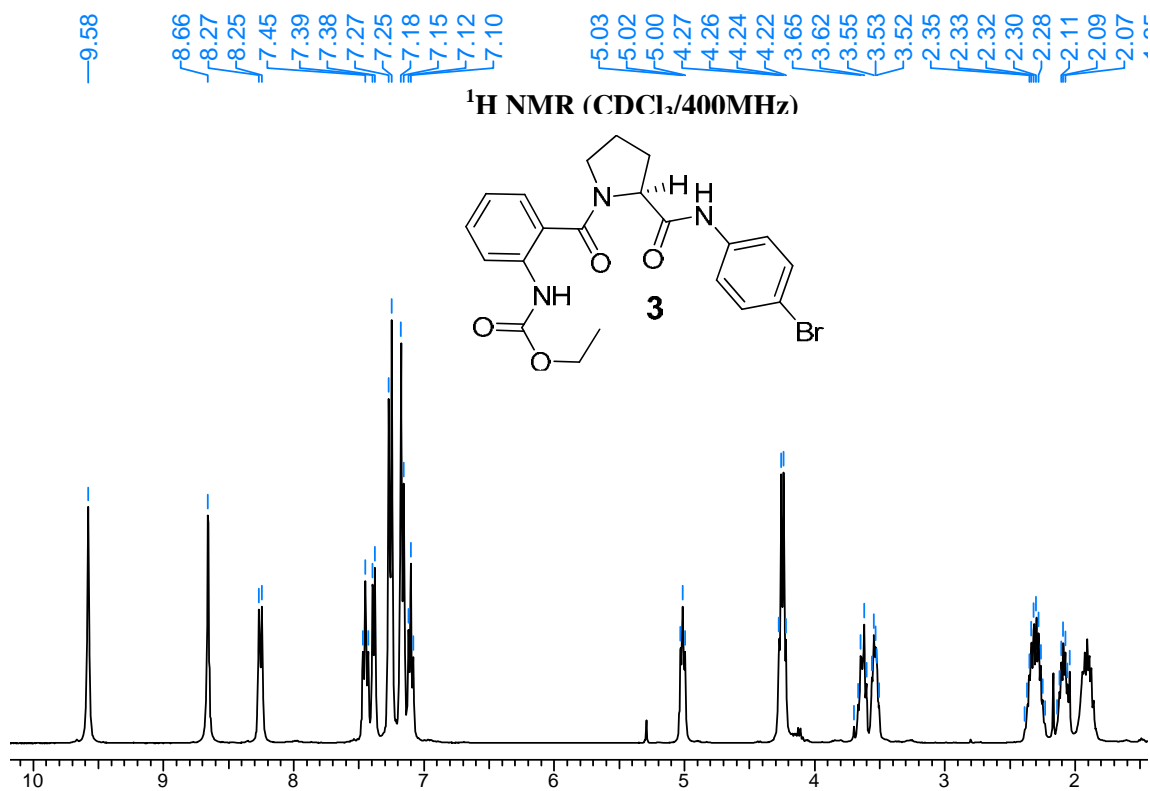


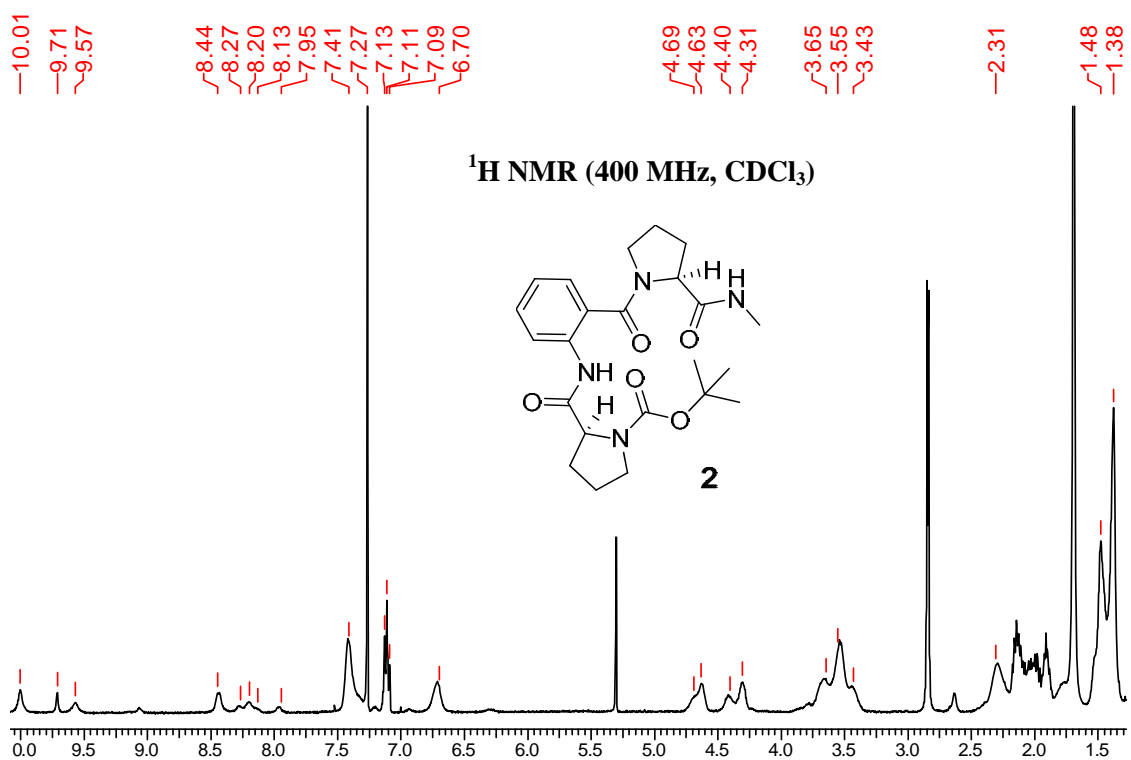
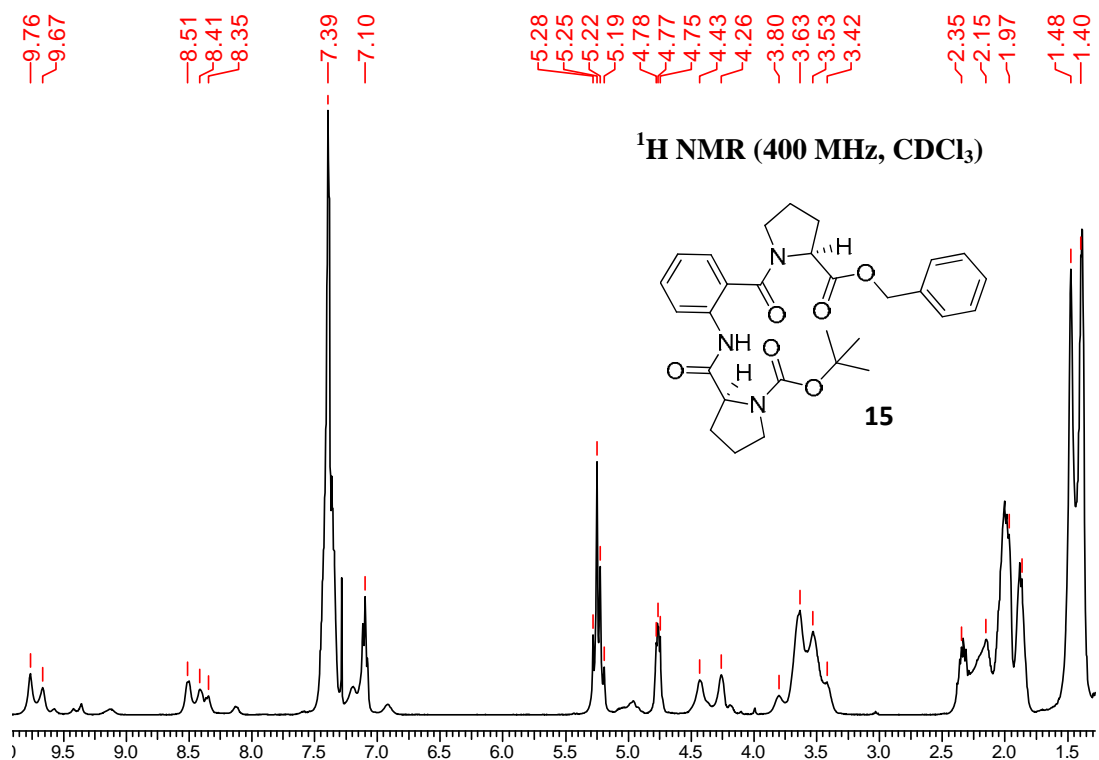




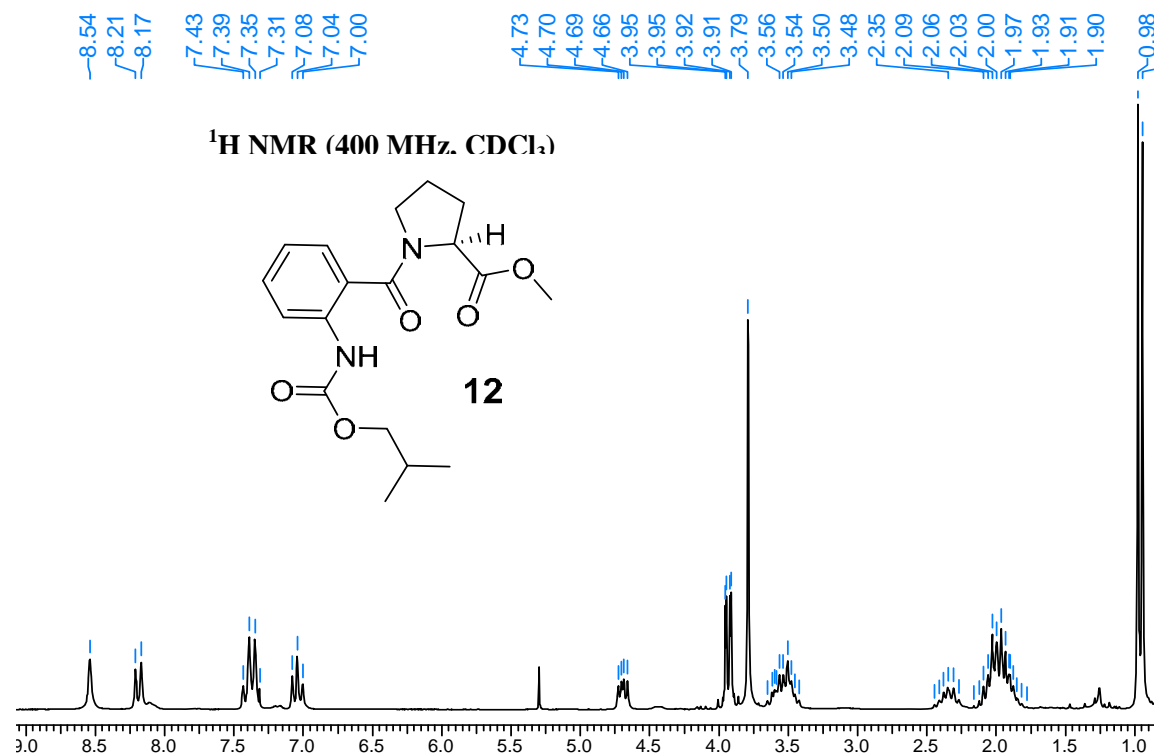
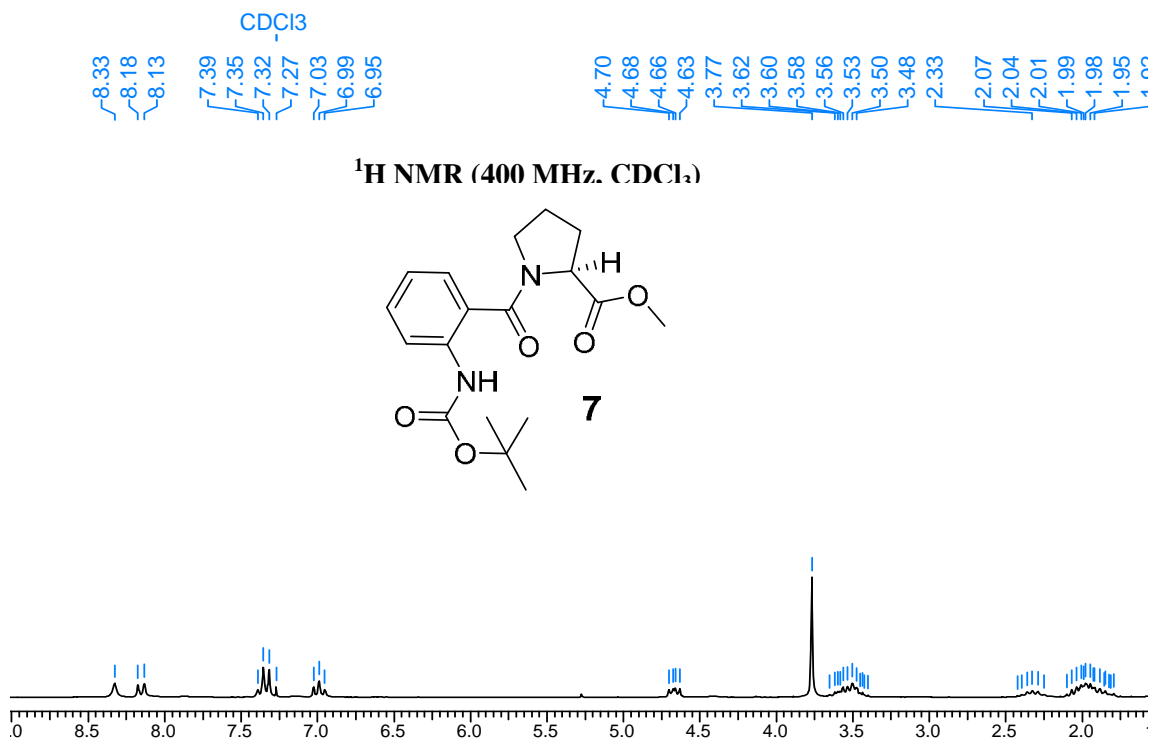


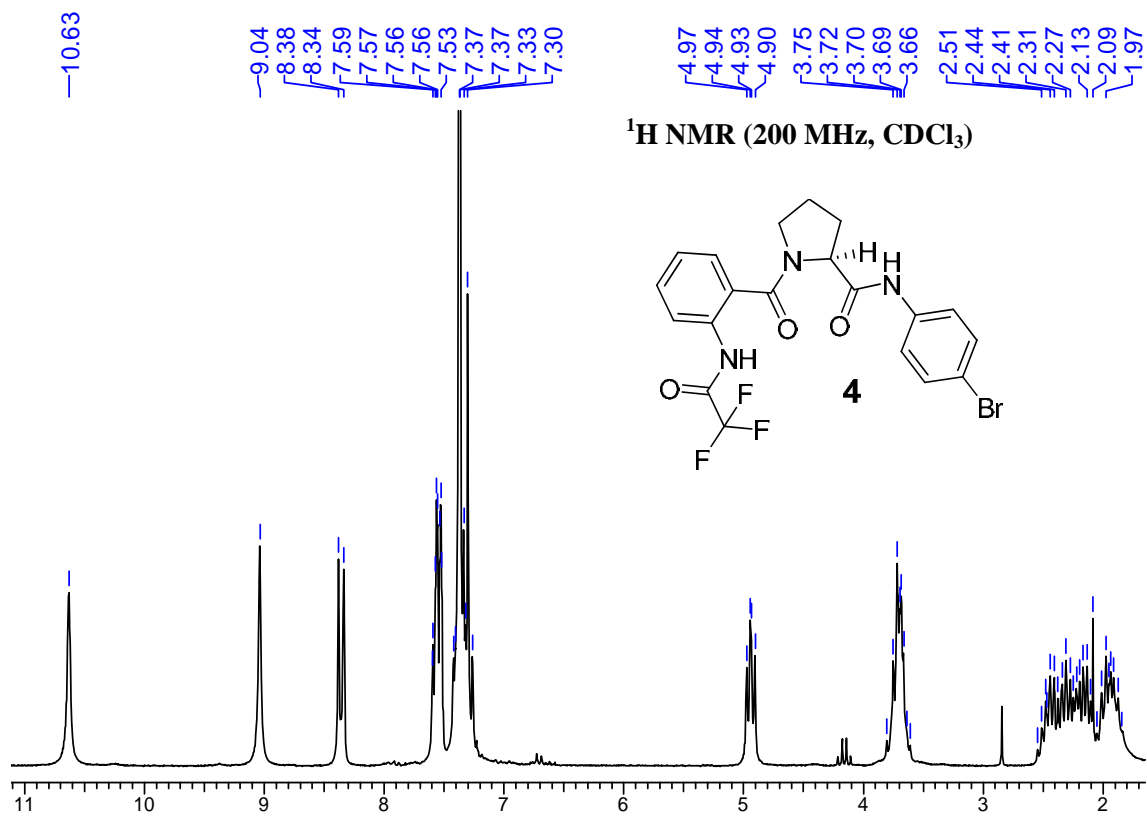
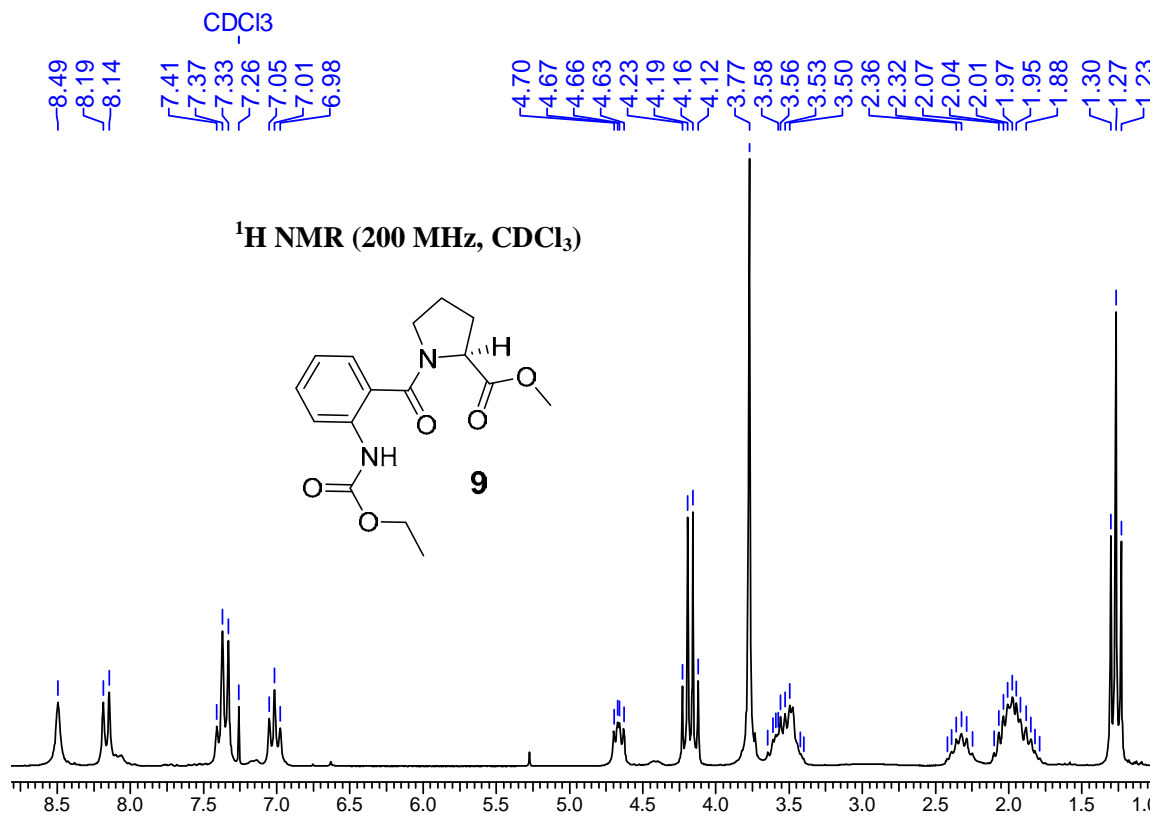


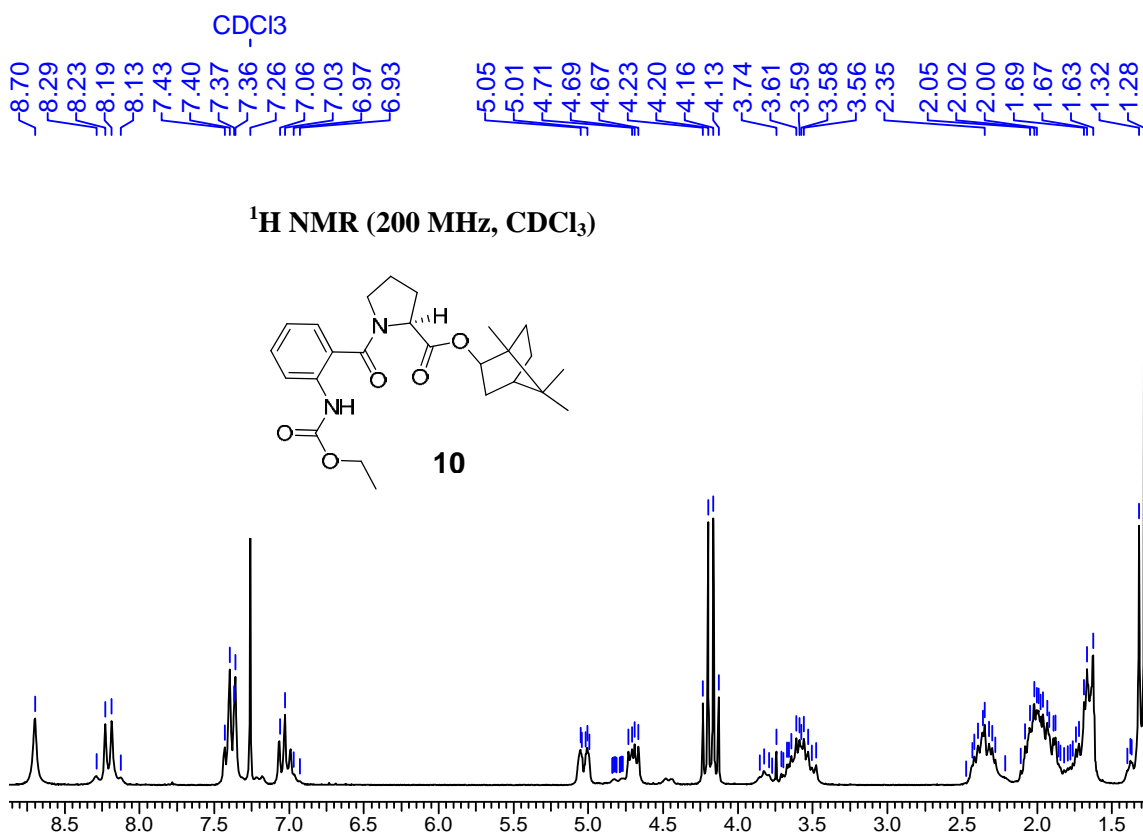
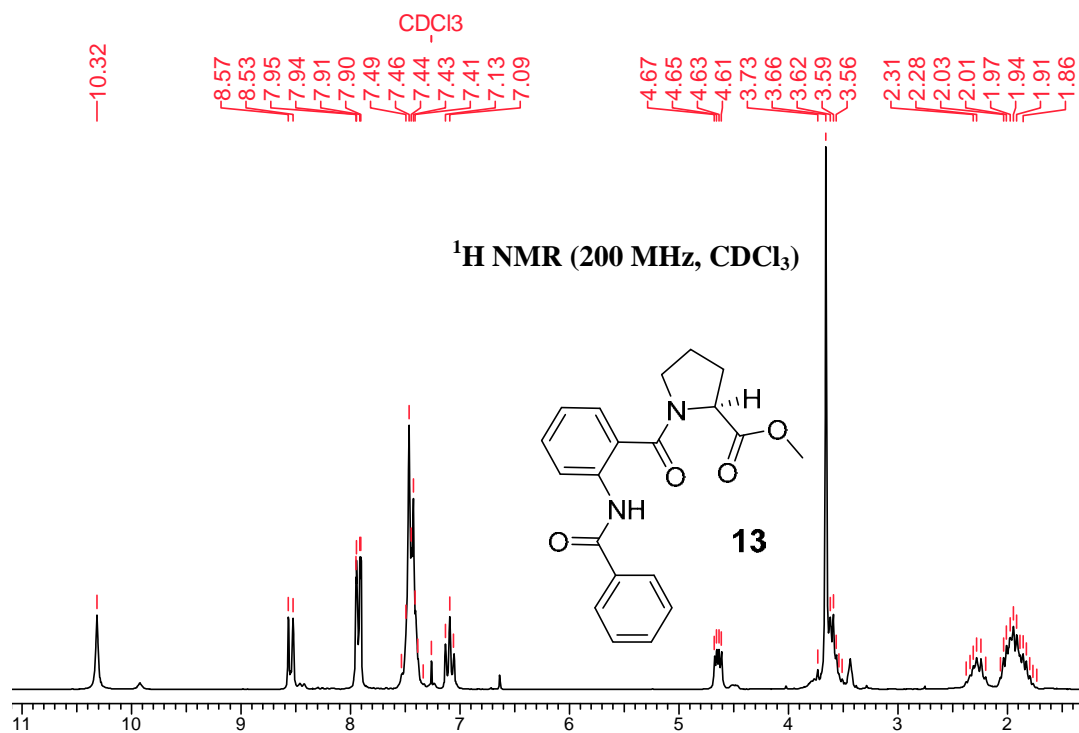


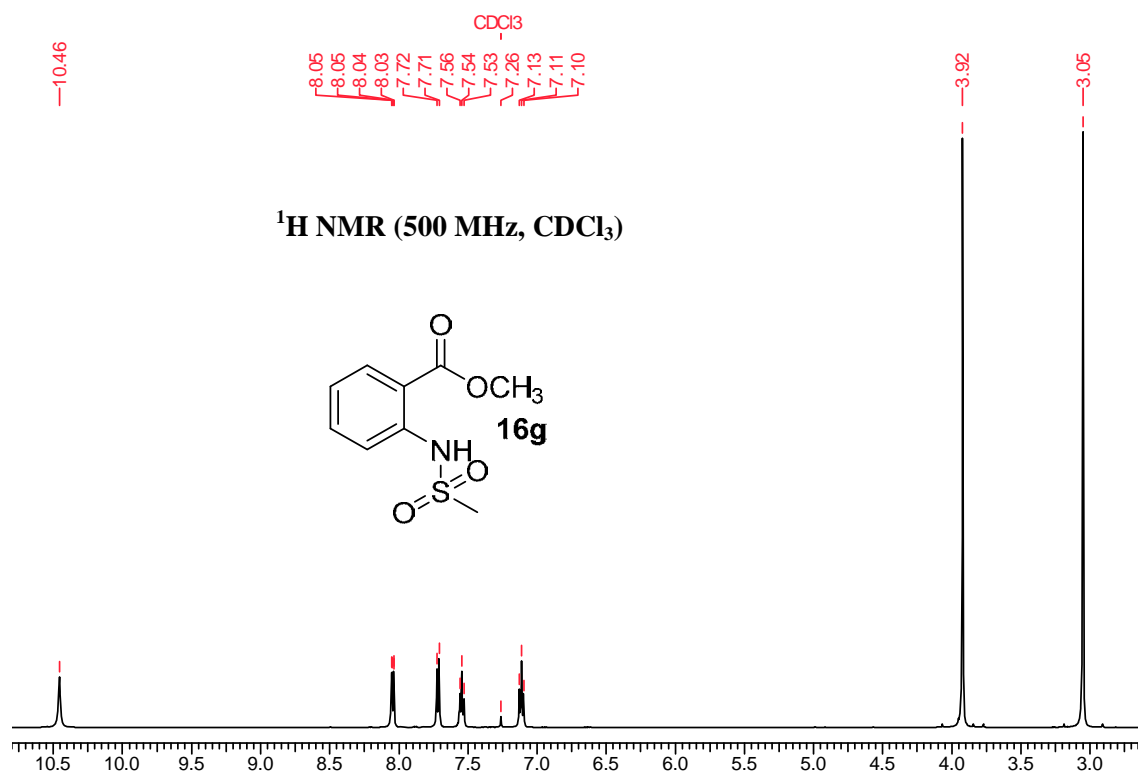
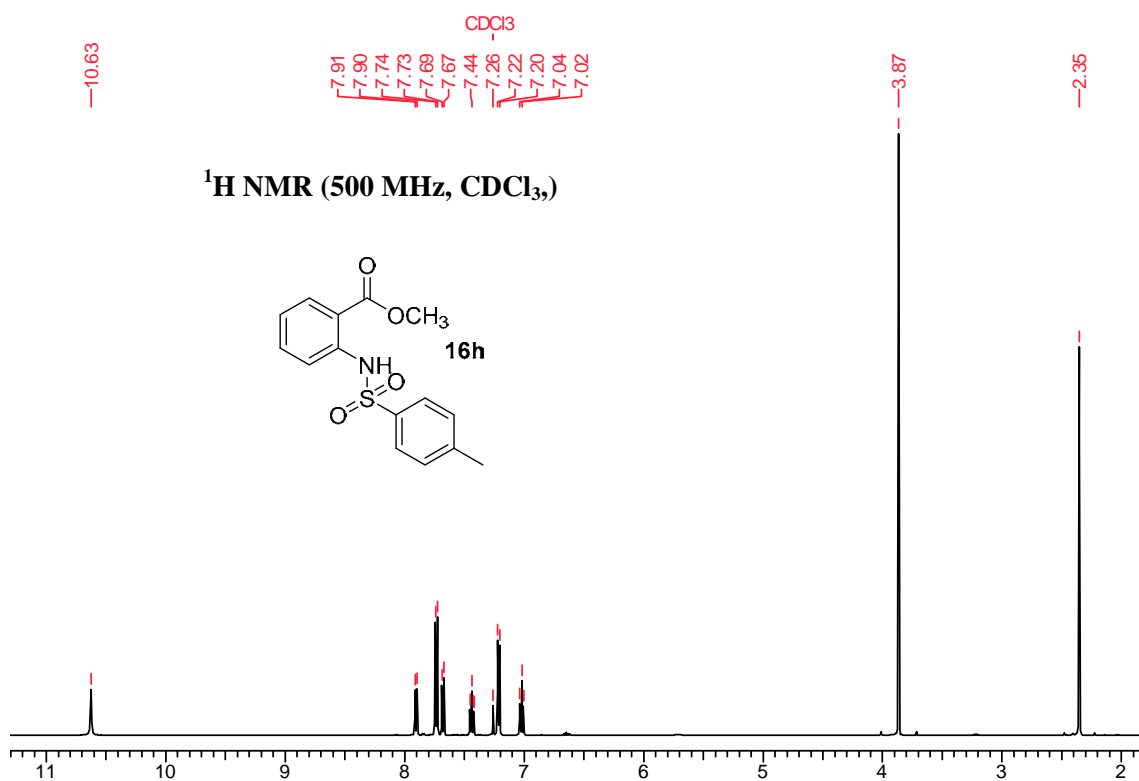


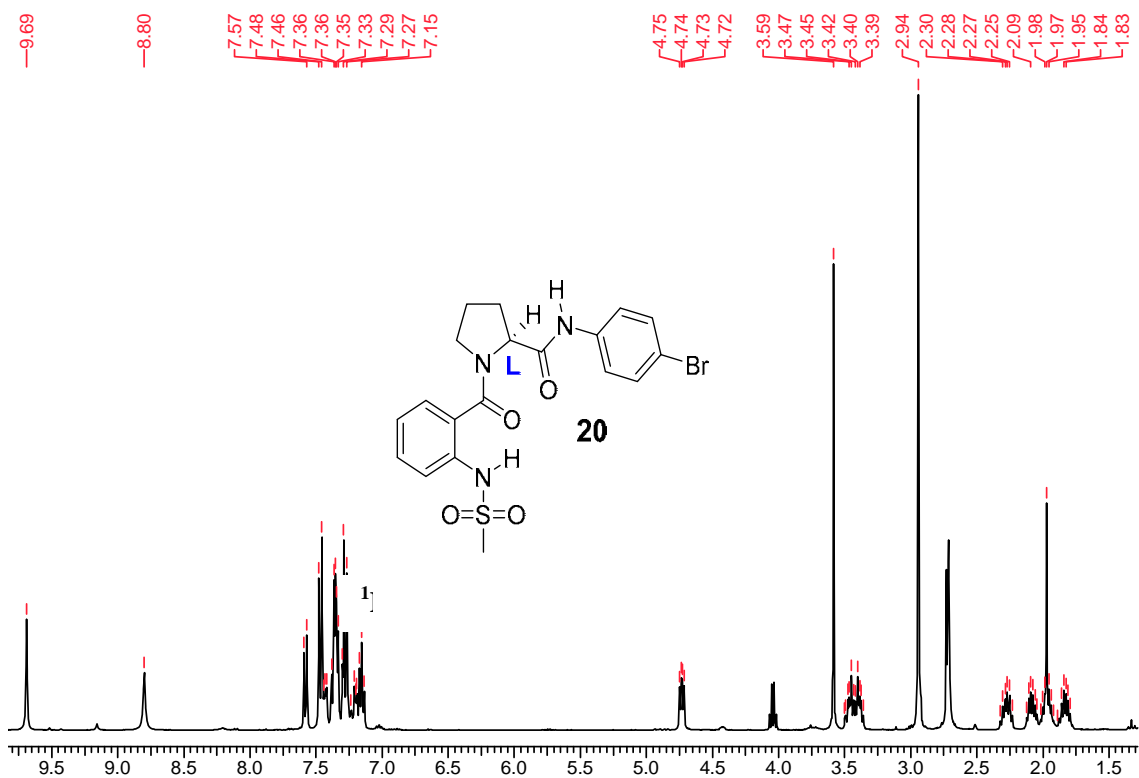
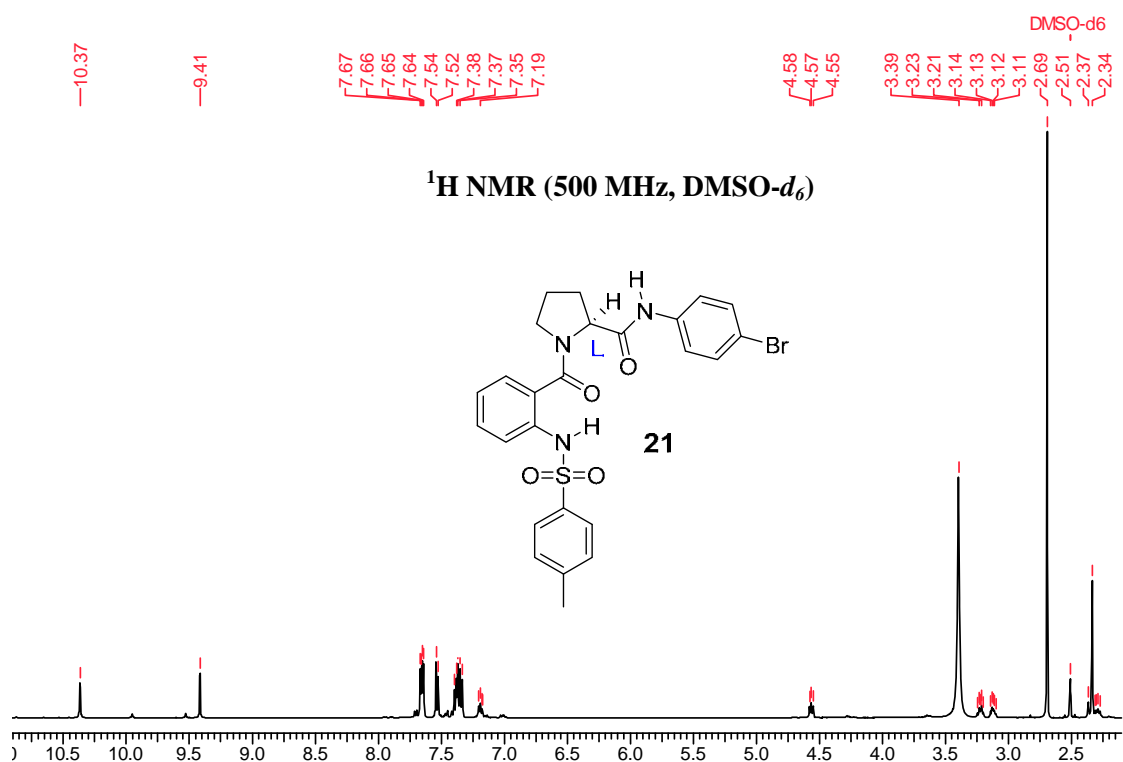


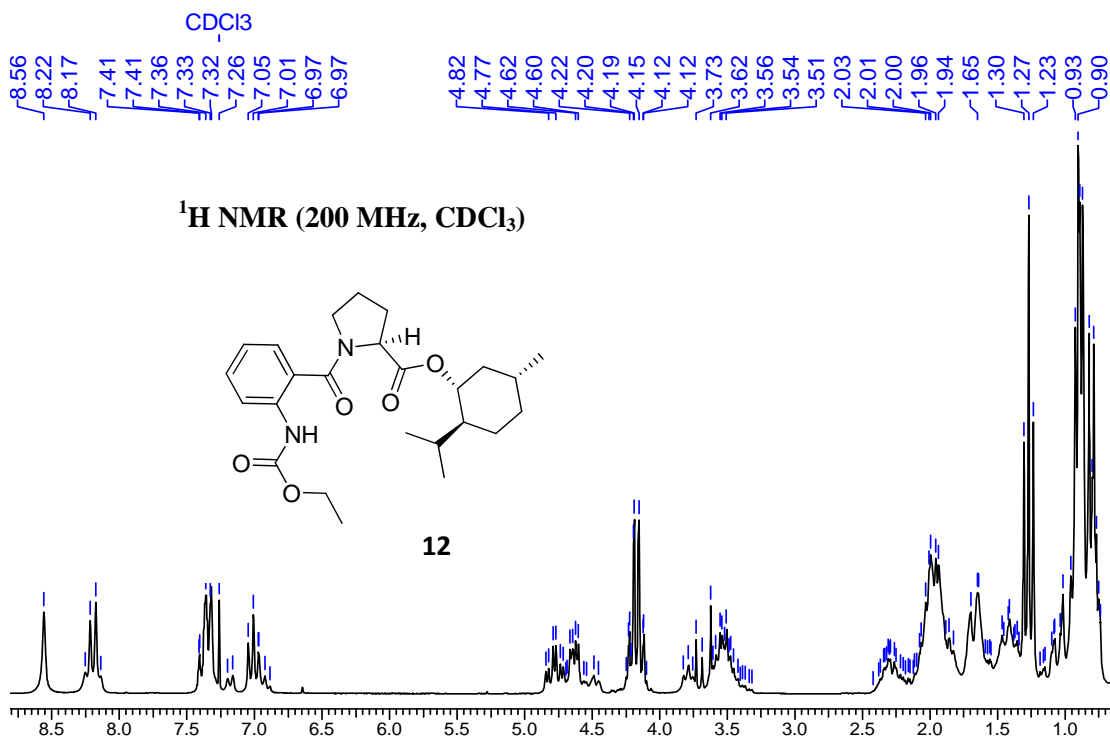
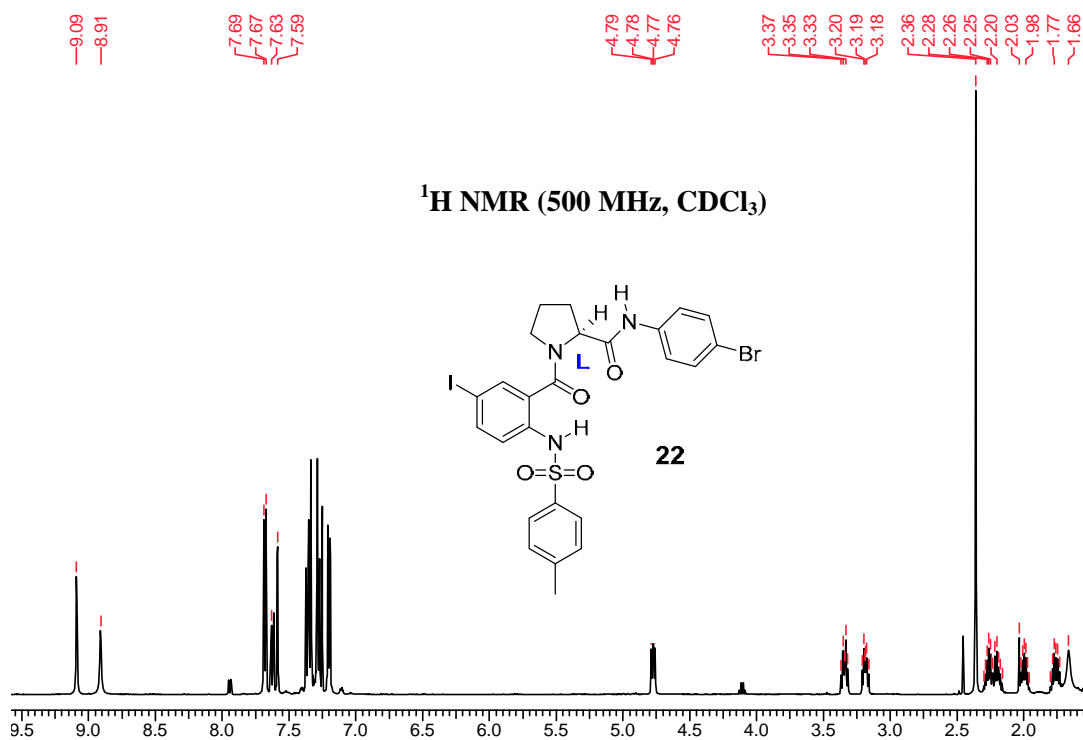






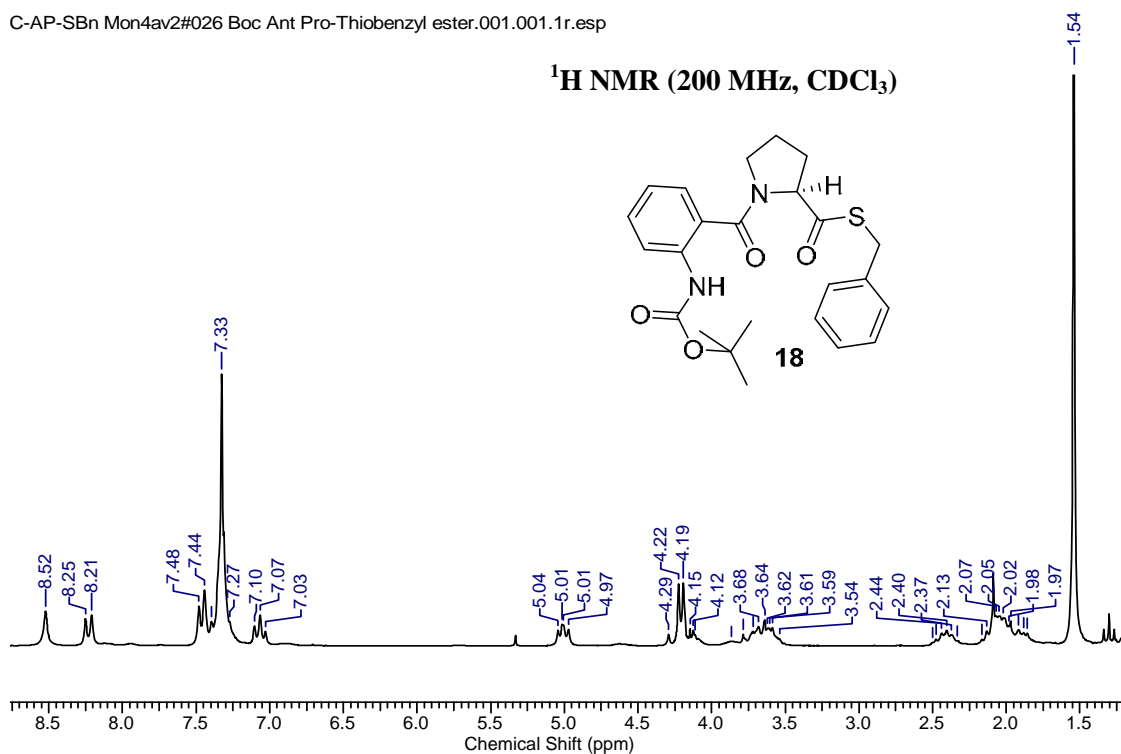






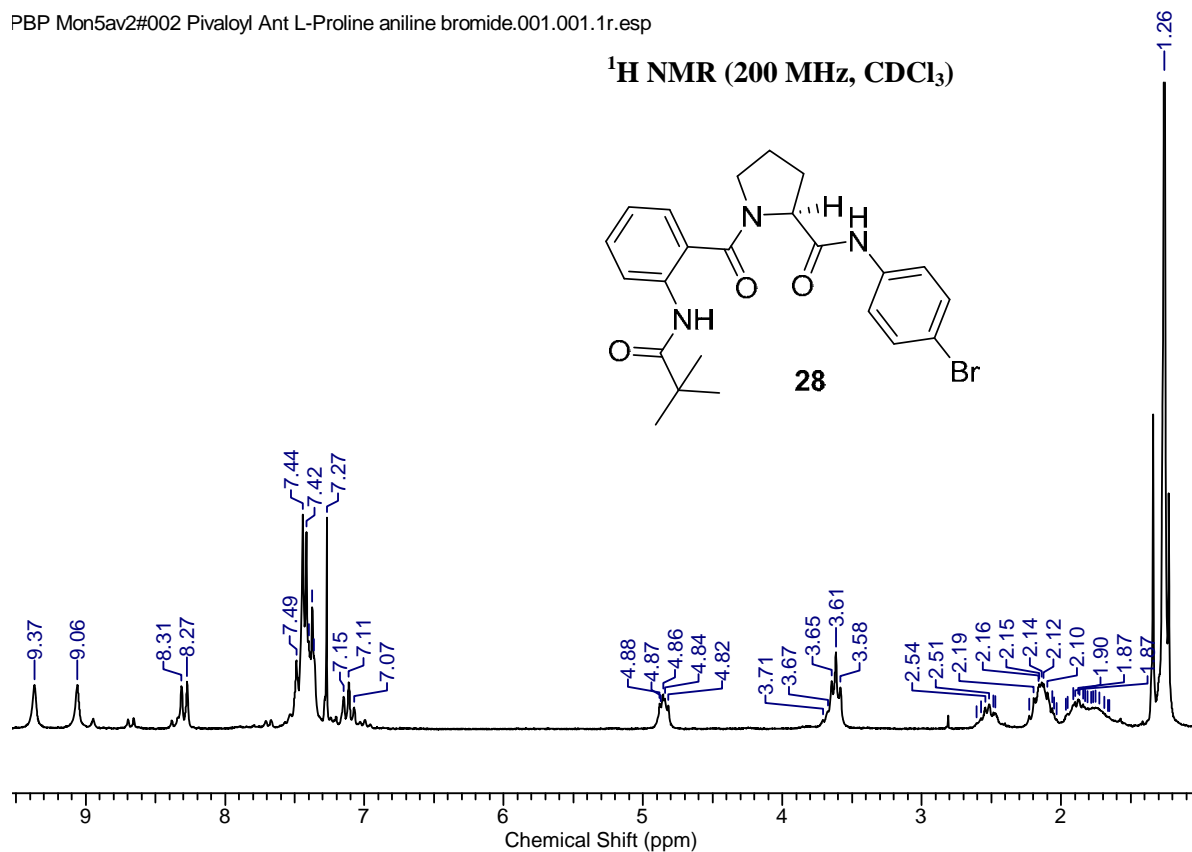
C-AP-SBn Mon4av2#026 Boc Ant Pro-Thiobenzyl ester.001.001.1r.esp

<sup>1</sup>H NMR (200 MHz, CDCl<sub>3</sub>)

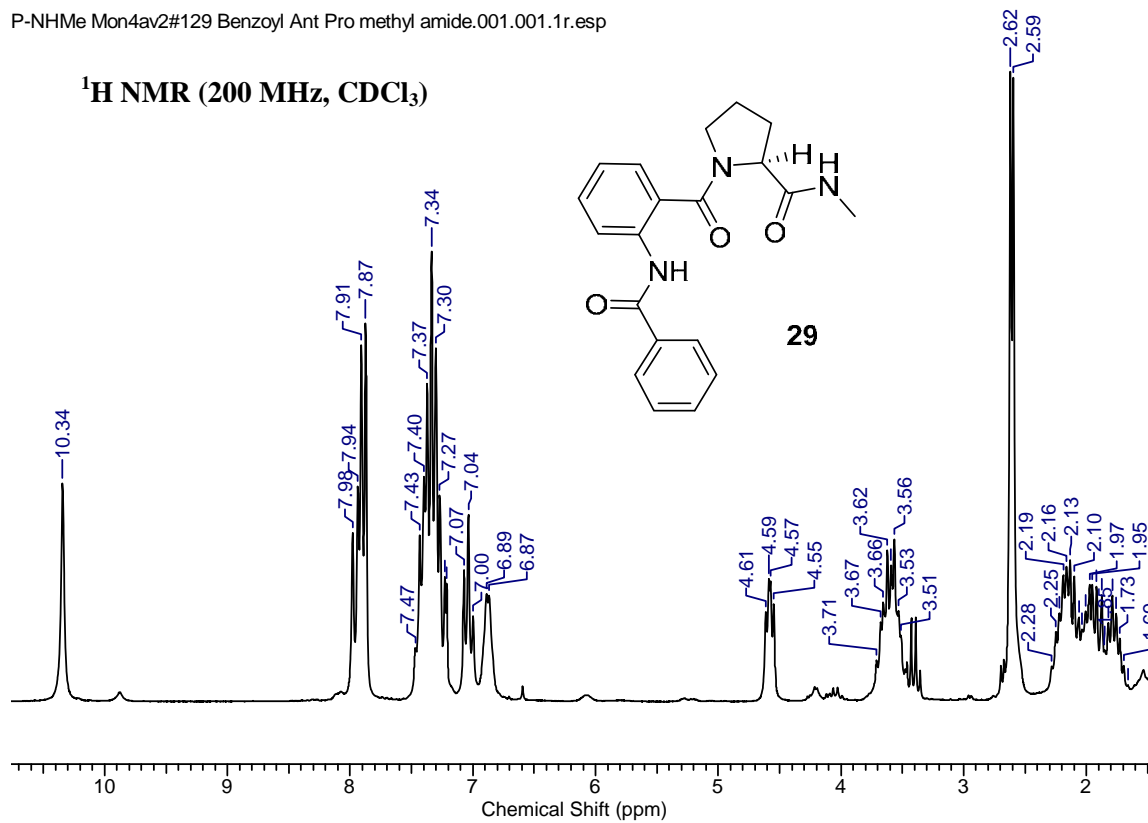


PBP Mon5av2#002 Pivaloyl Ant L-Proline aniline bromide.001.001.1r.esp

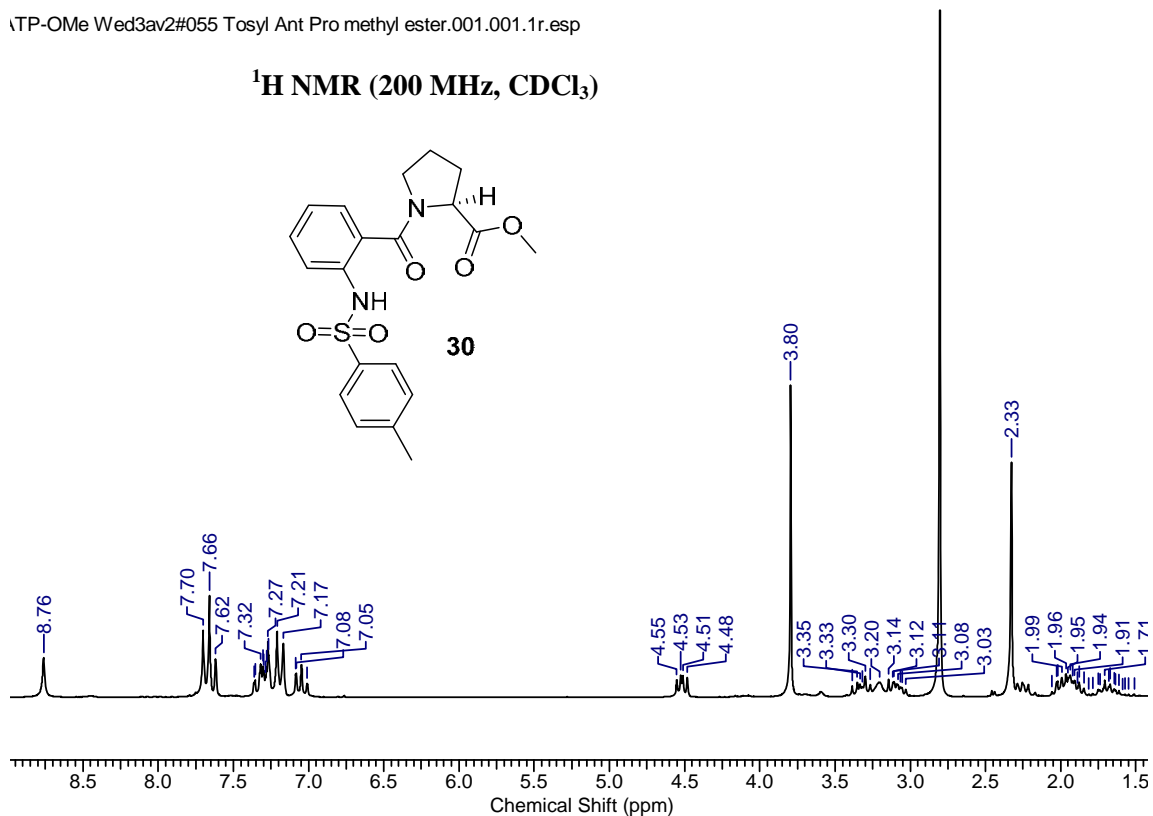
<sup>1</sup>H NMR (200 MHz, CDCl<sub>3</sub>)



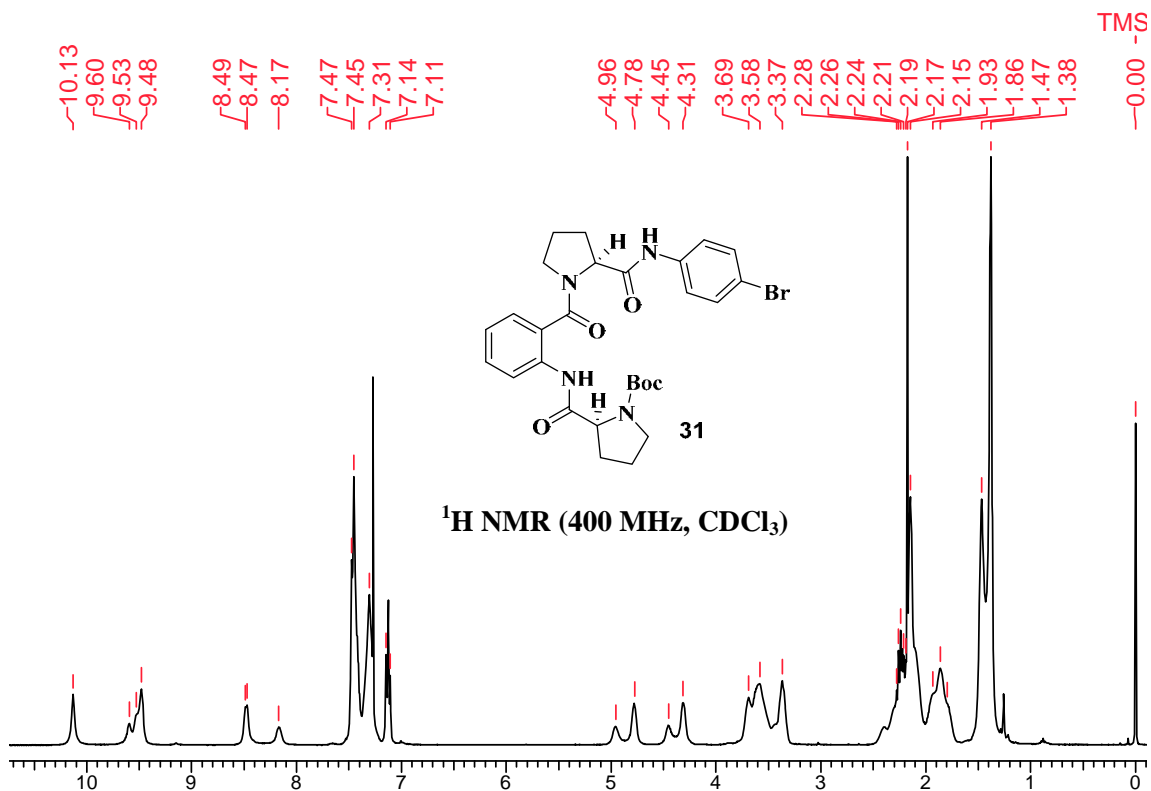
P-NHMe Mon4av2#129 Benzoyl Ant Pro methyl amide.001.001.1r.esp

 $^1\text{H NMR}$  (200 MHz,  $\text{CDCl}_3$ )

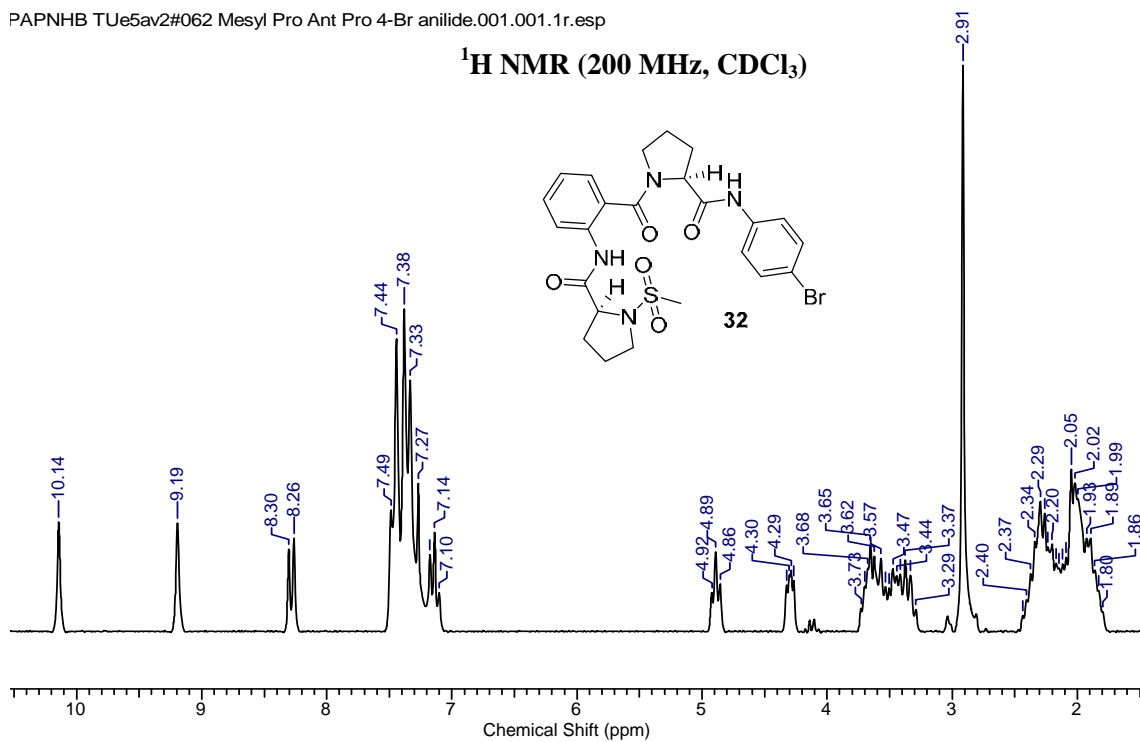
\TP-OMe Wed3av2#055 Tosyl Ant Pro methyl ester.001.001.1r.esp

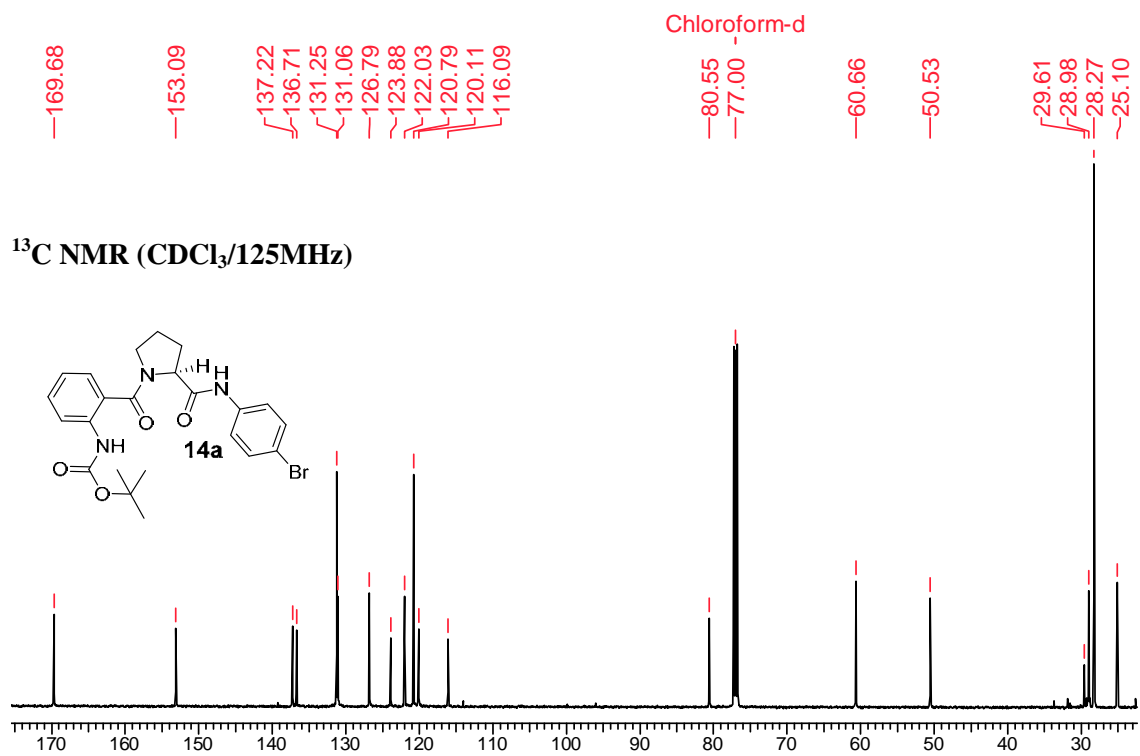
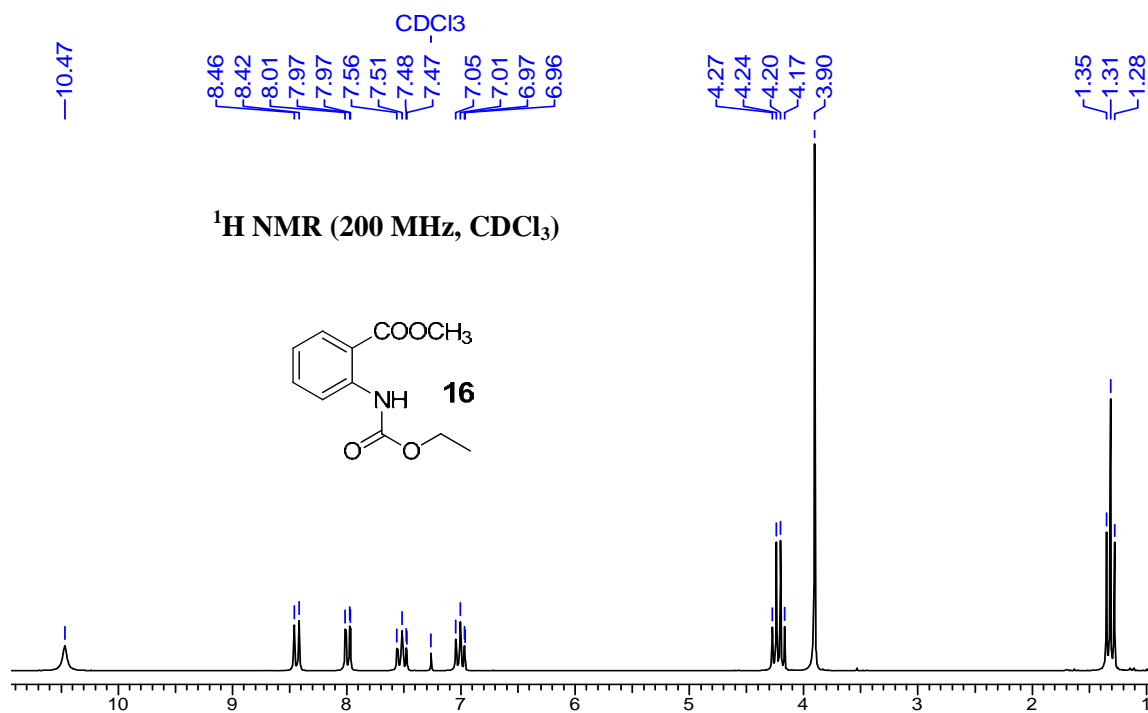
 $^1\text{H NMR}$  (200 MHz,  $\text{CDCl}_3$ )

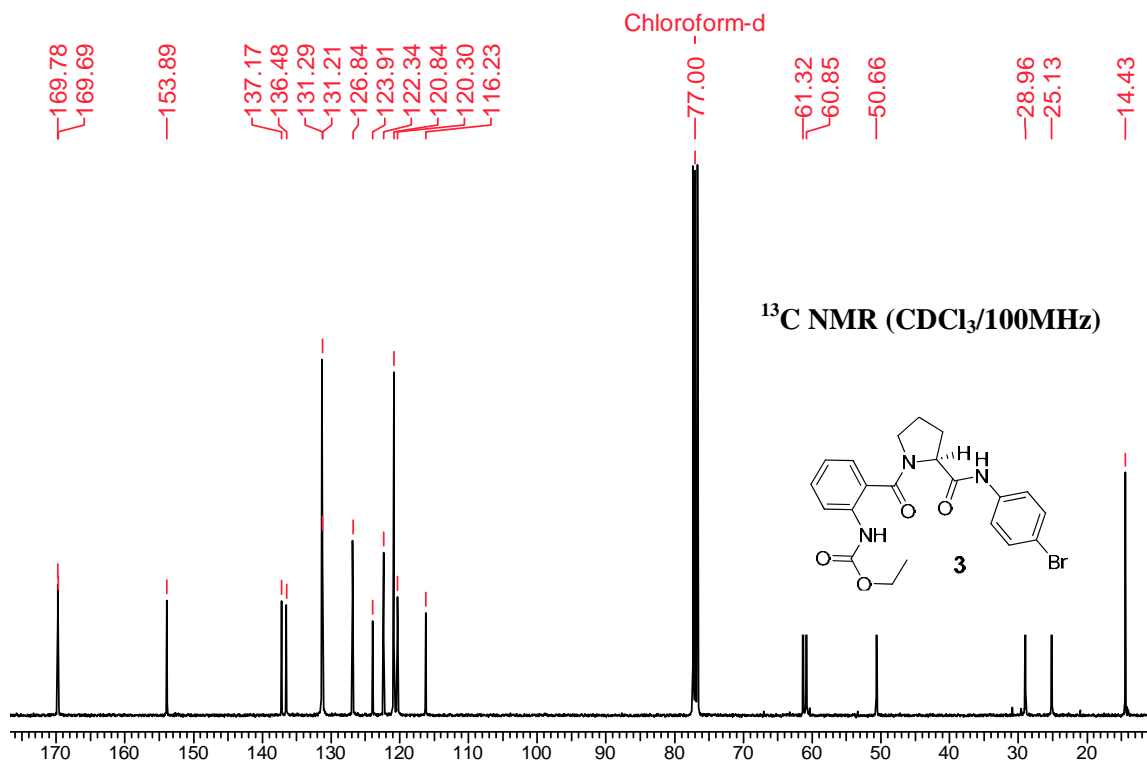
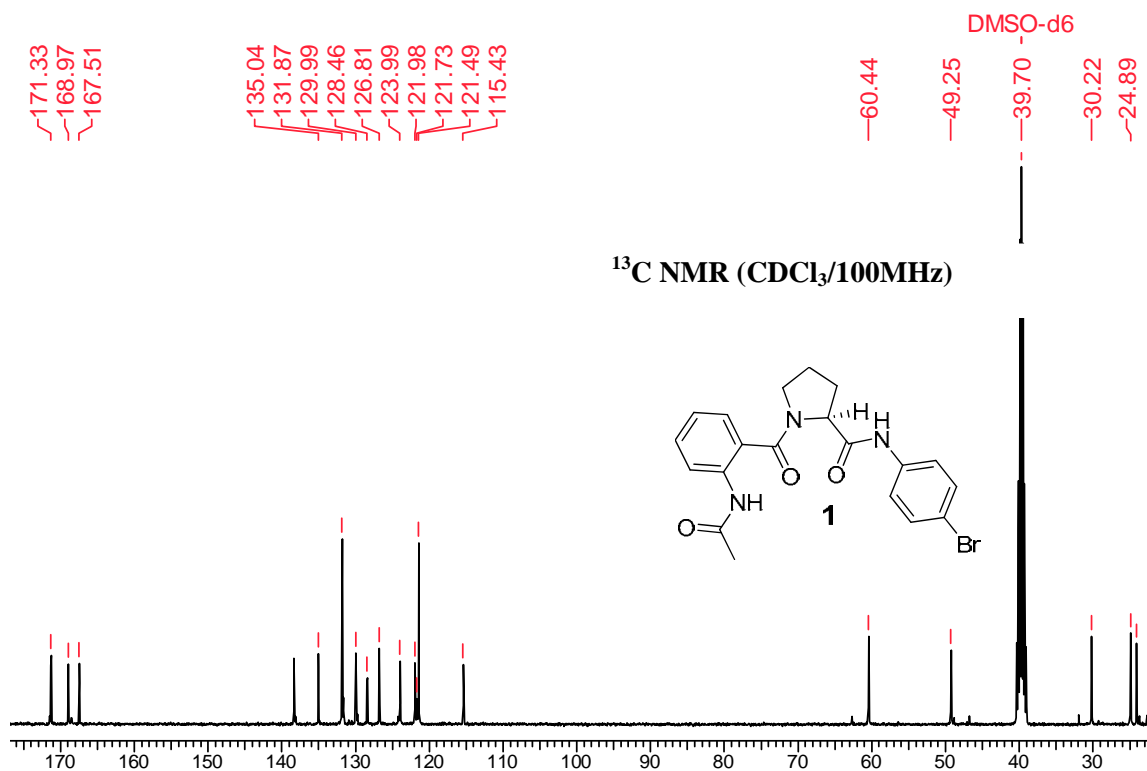


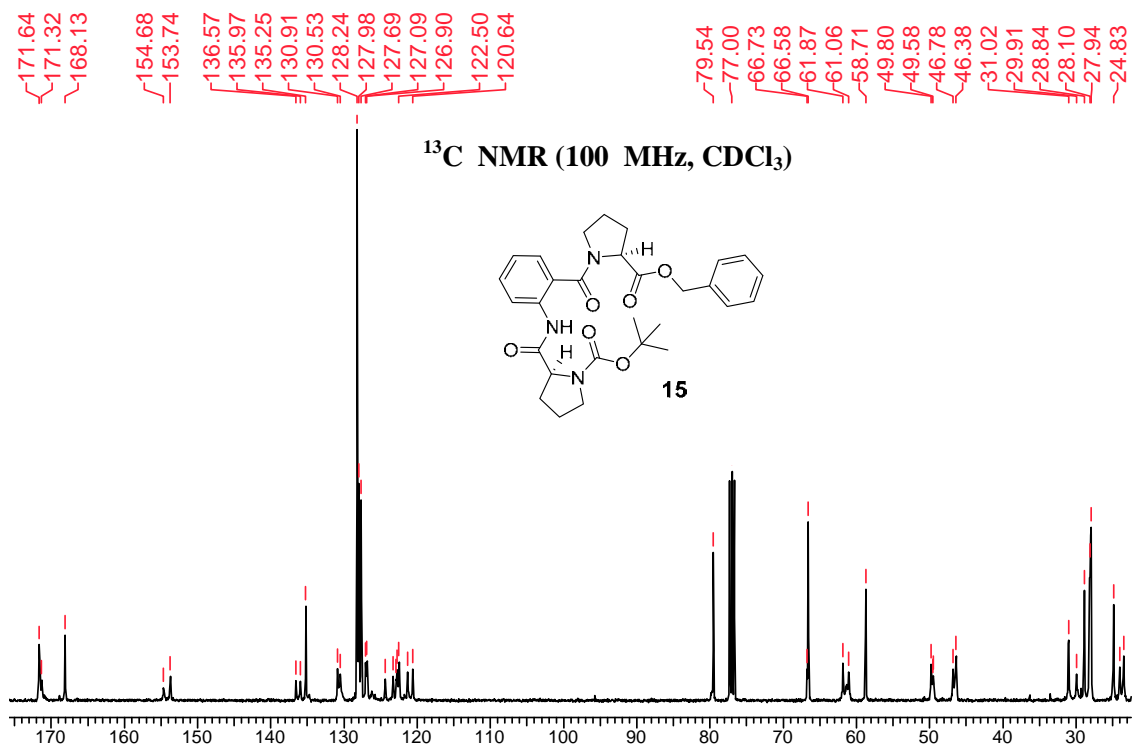
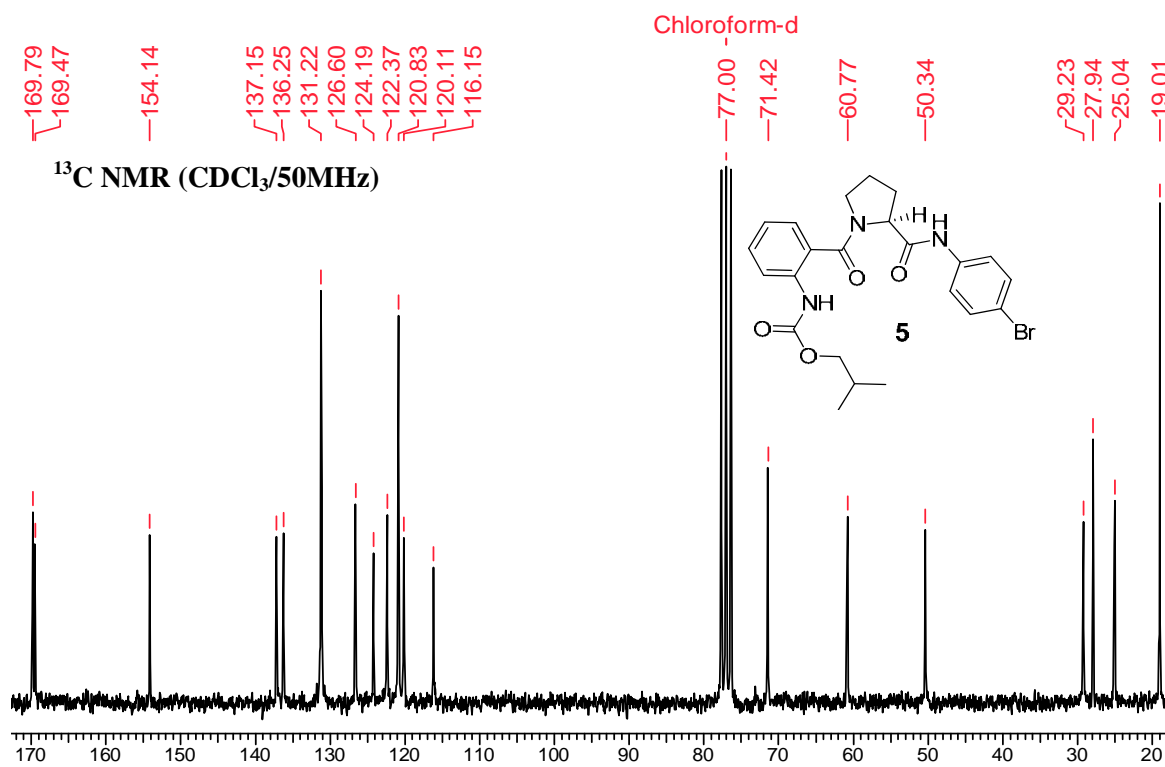


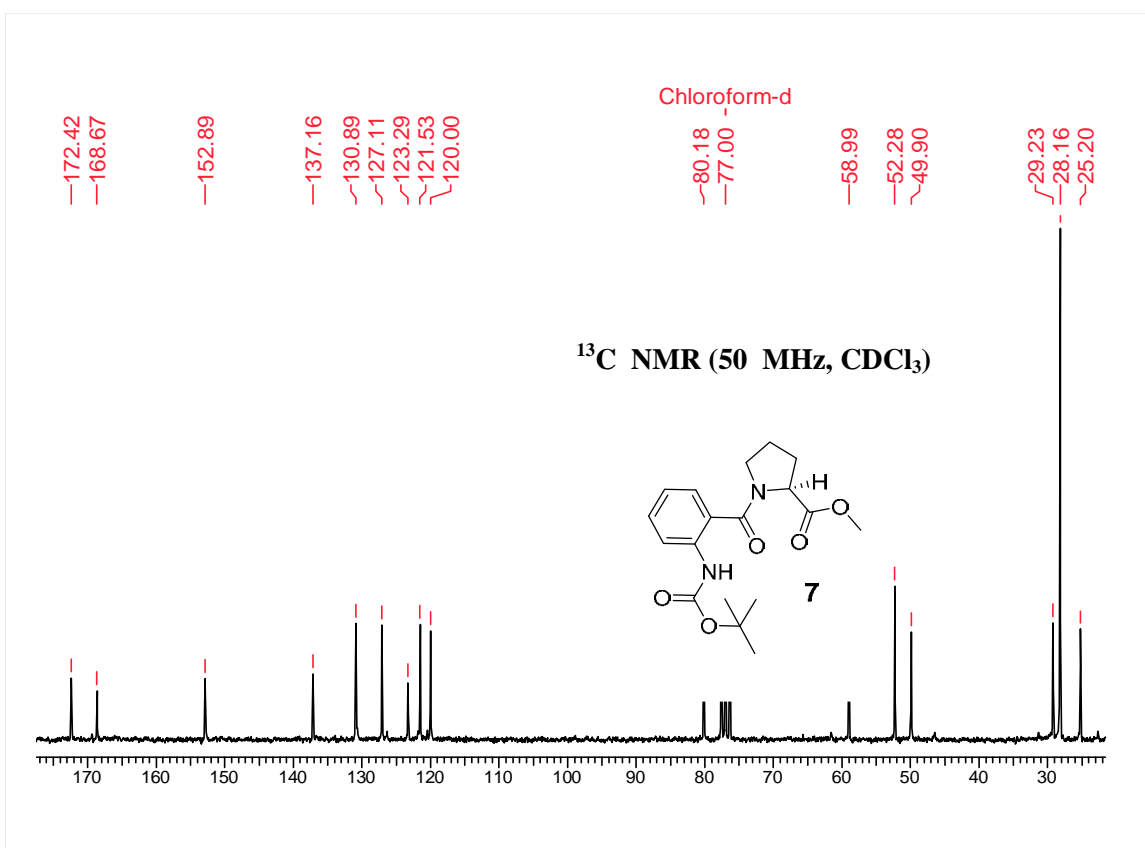
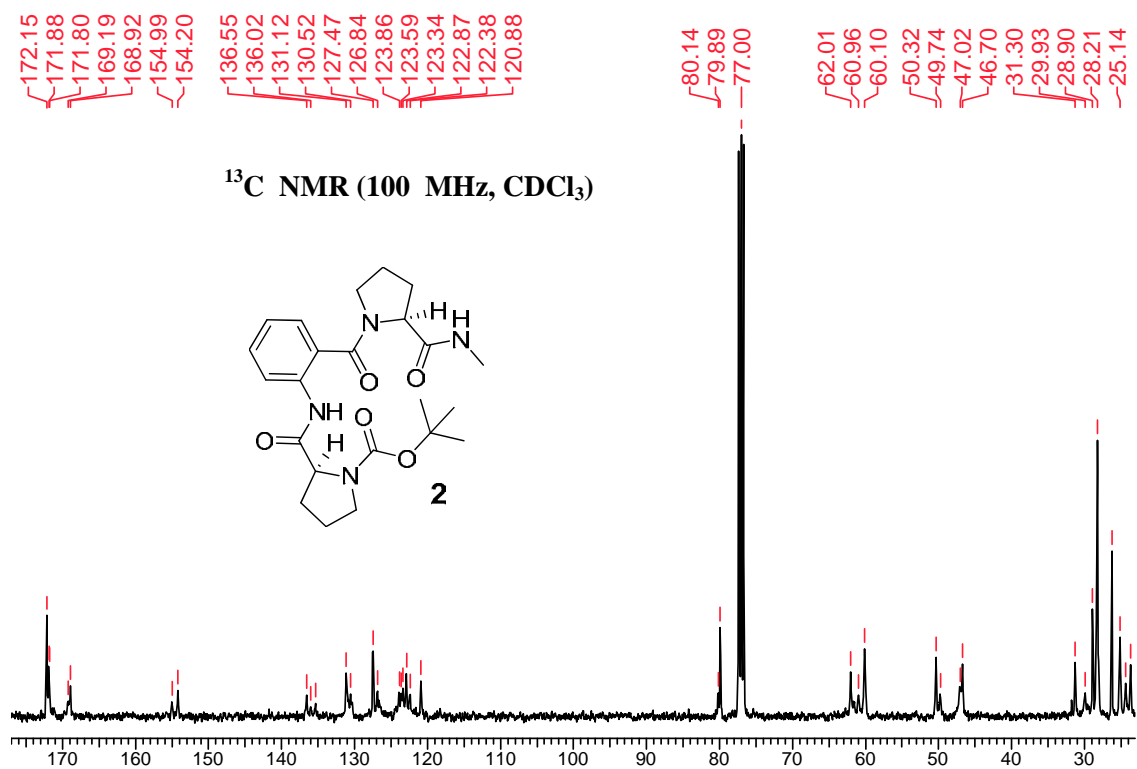
PAPNHB TUe5av2#062 Mesyl Pro Ant Pro 4-Br anilide.001.001.1r.esp

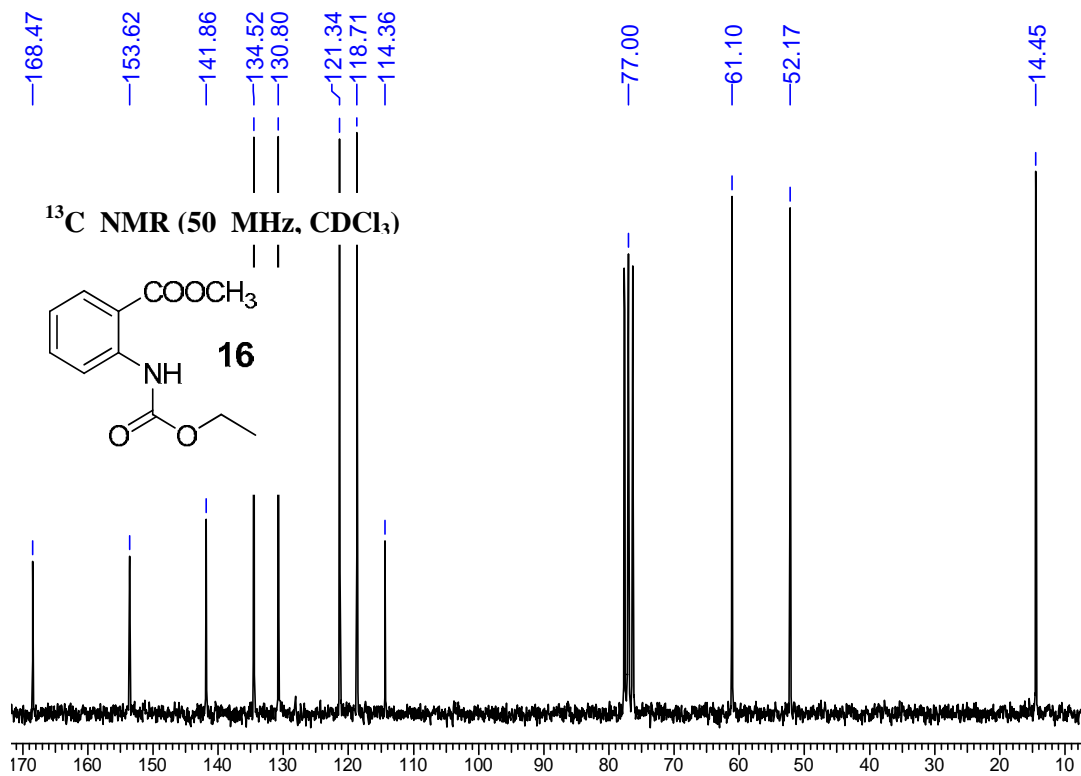
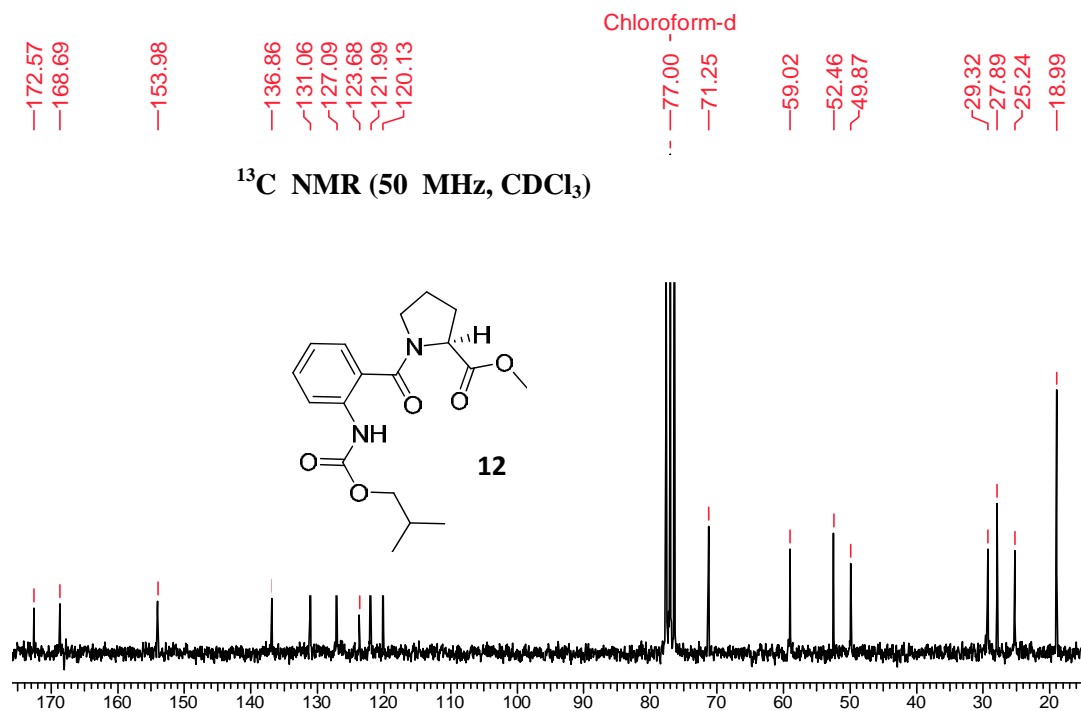


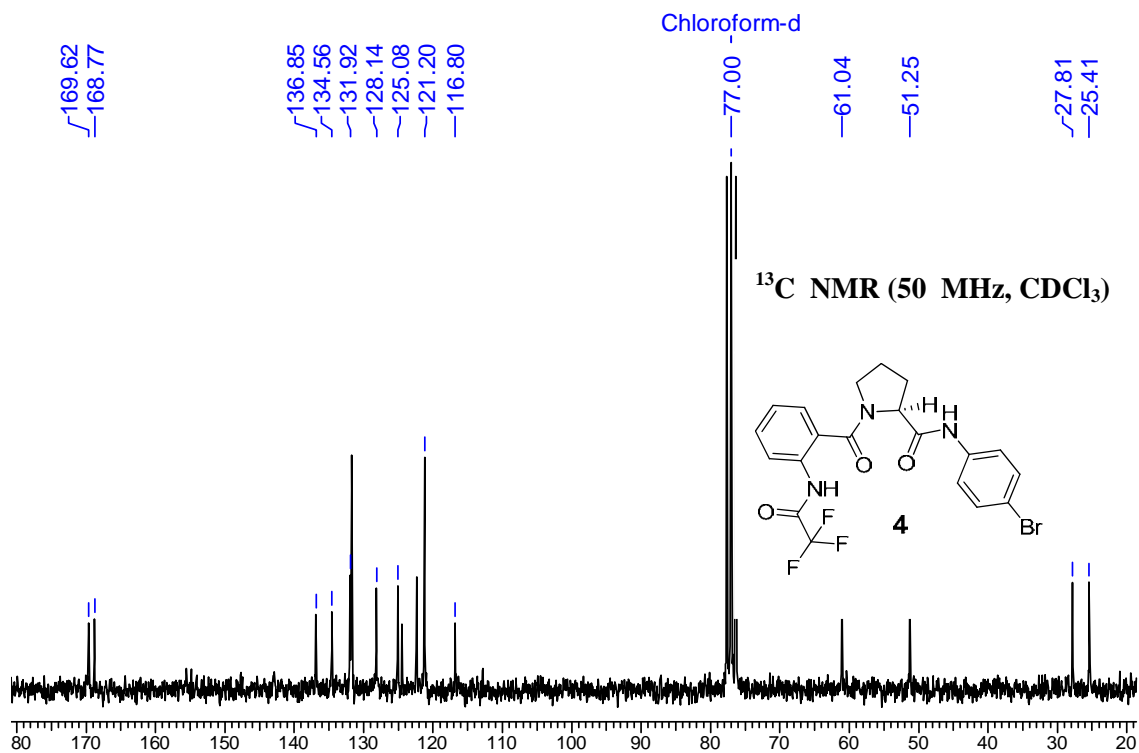
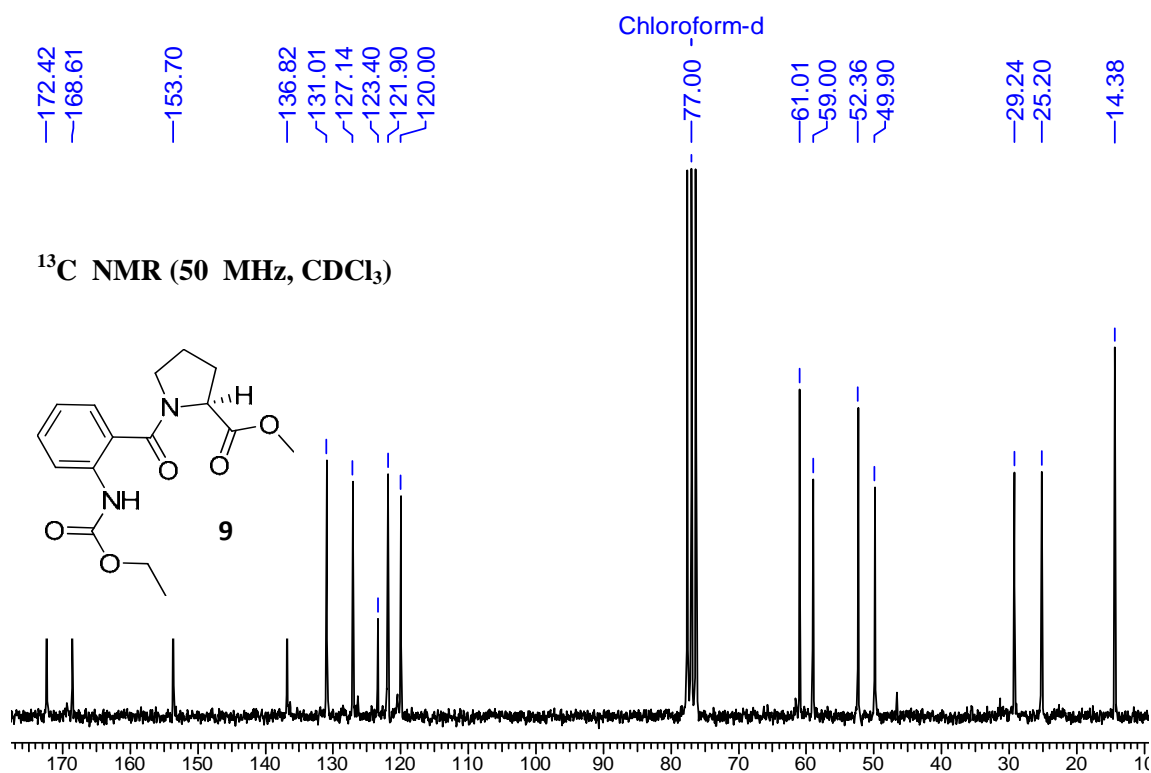


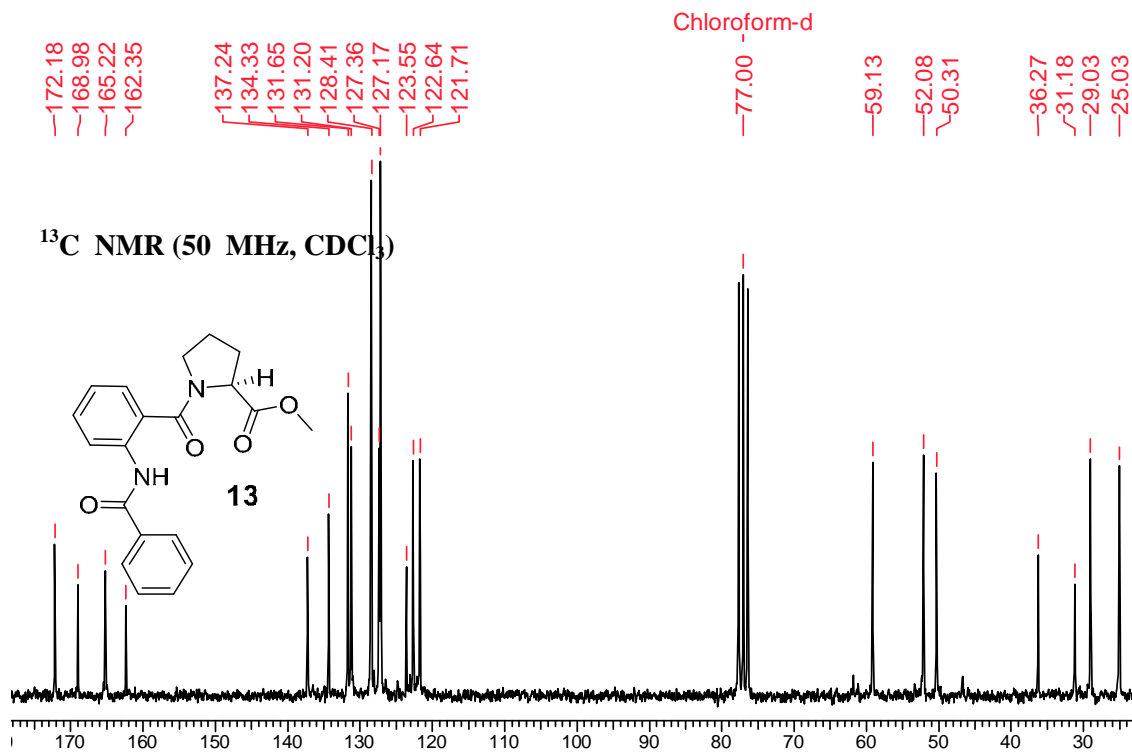
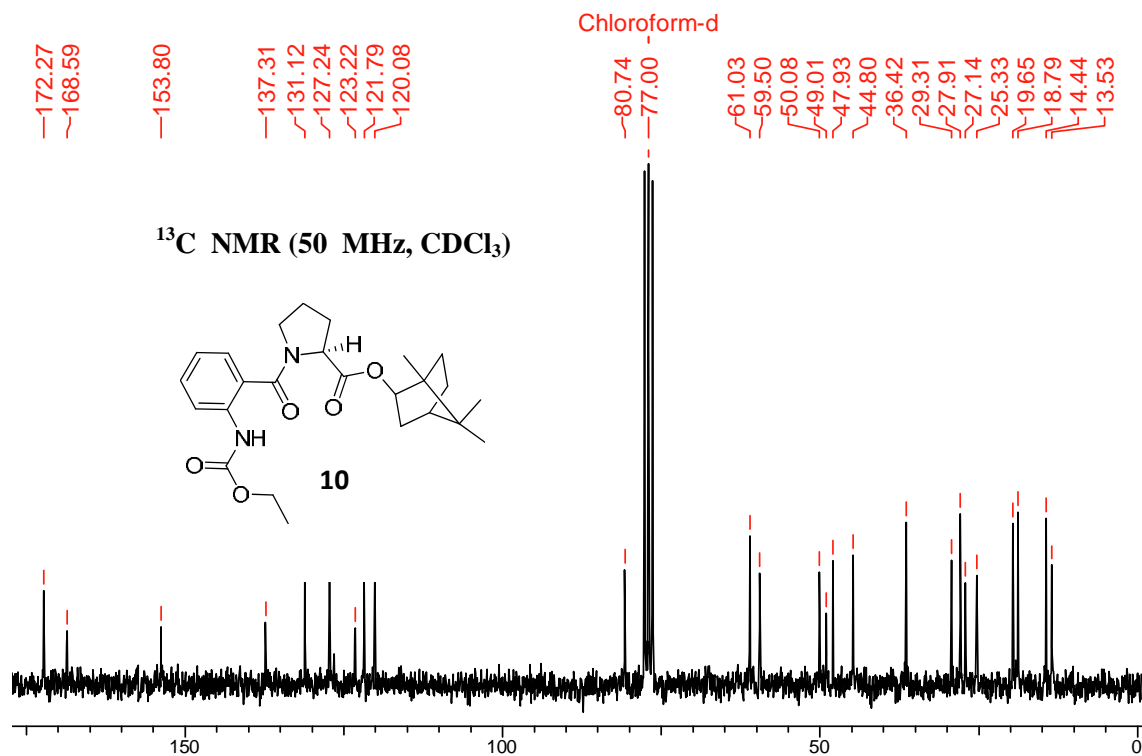




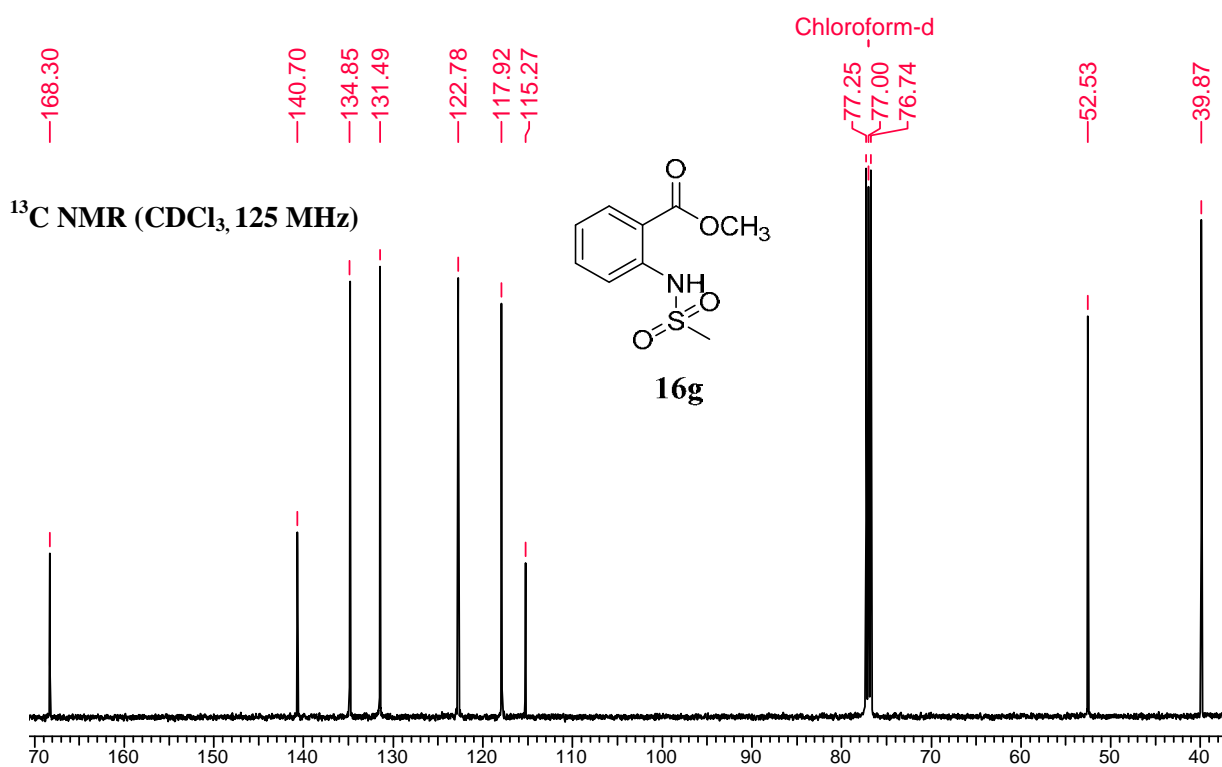
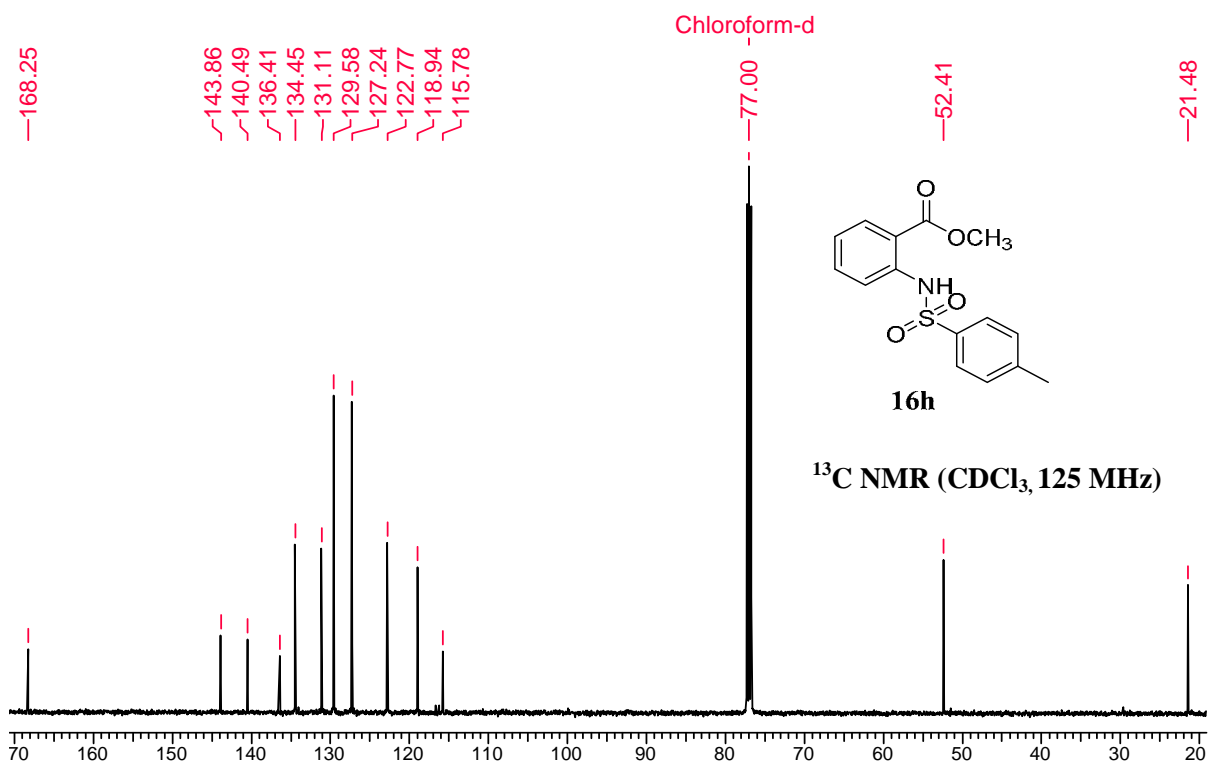


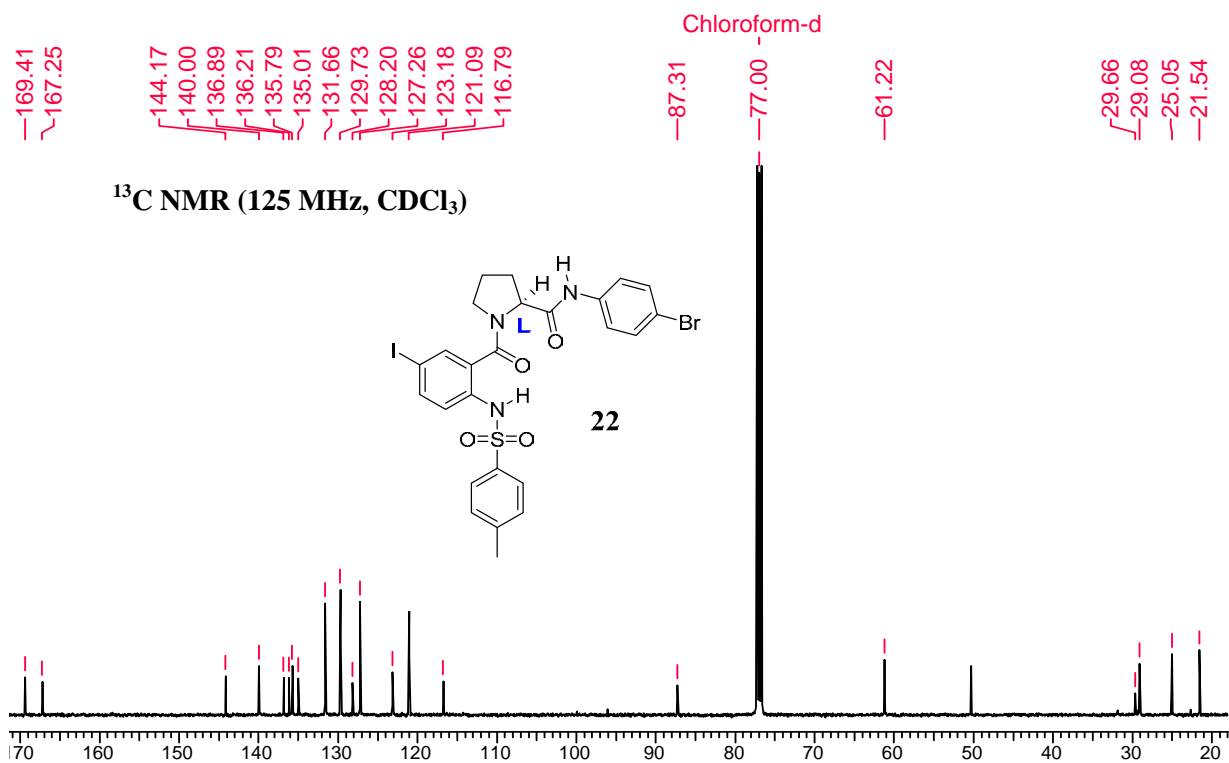
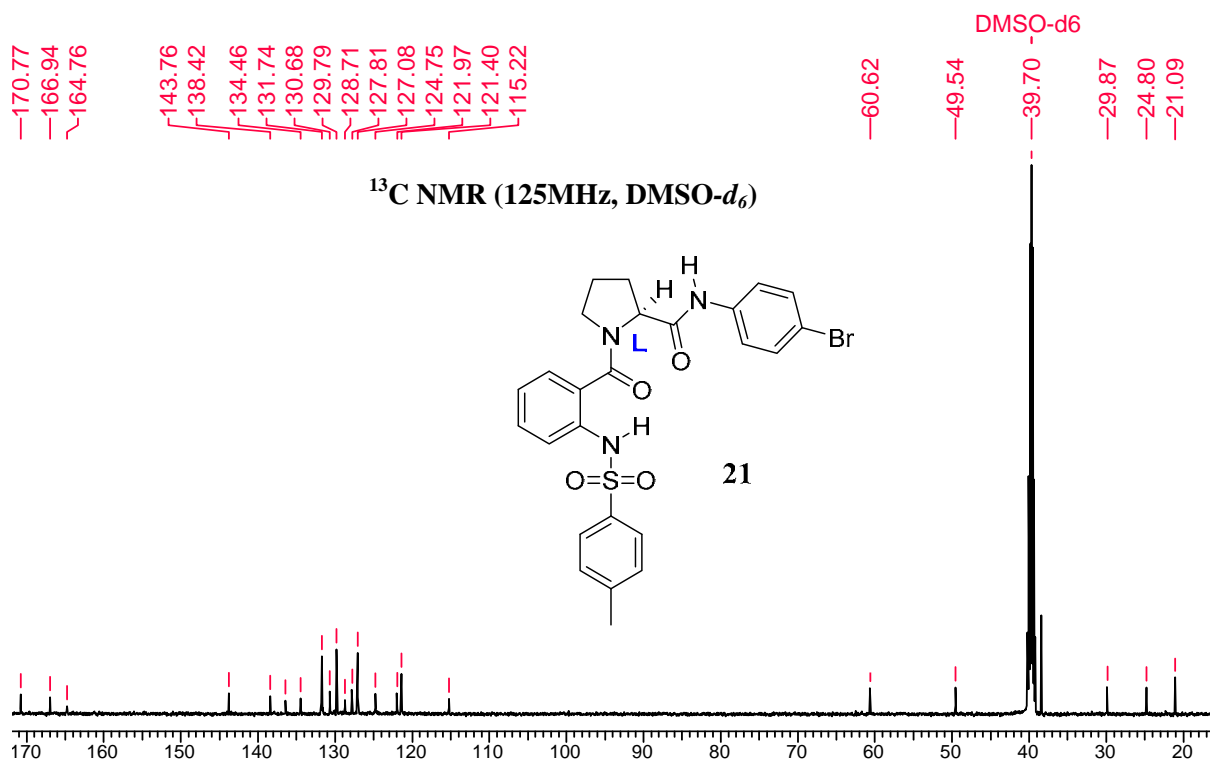


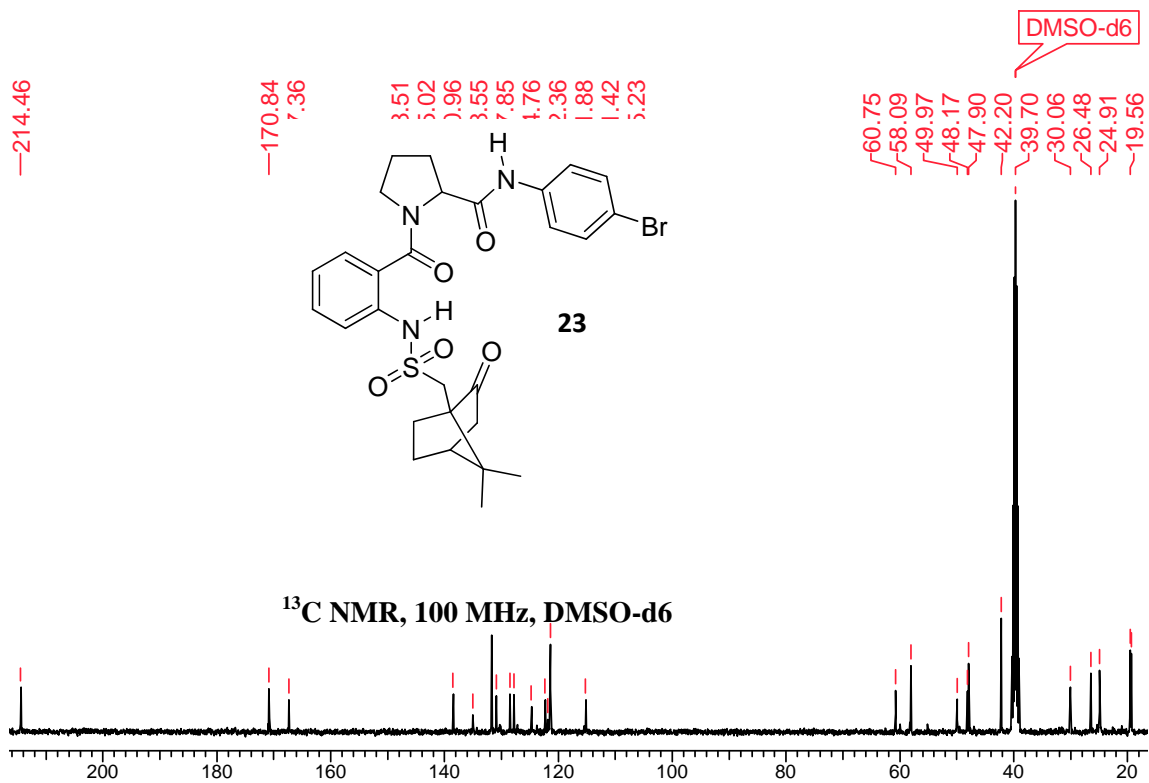
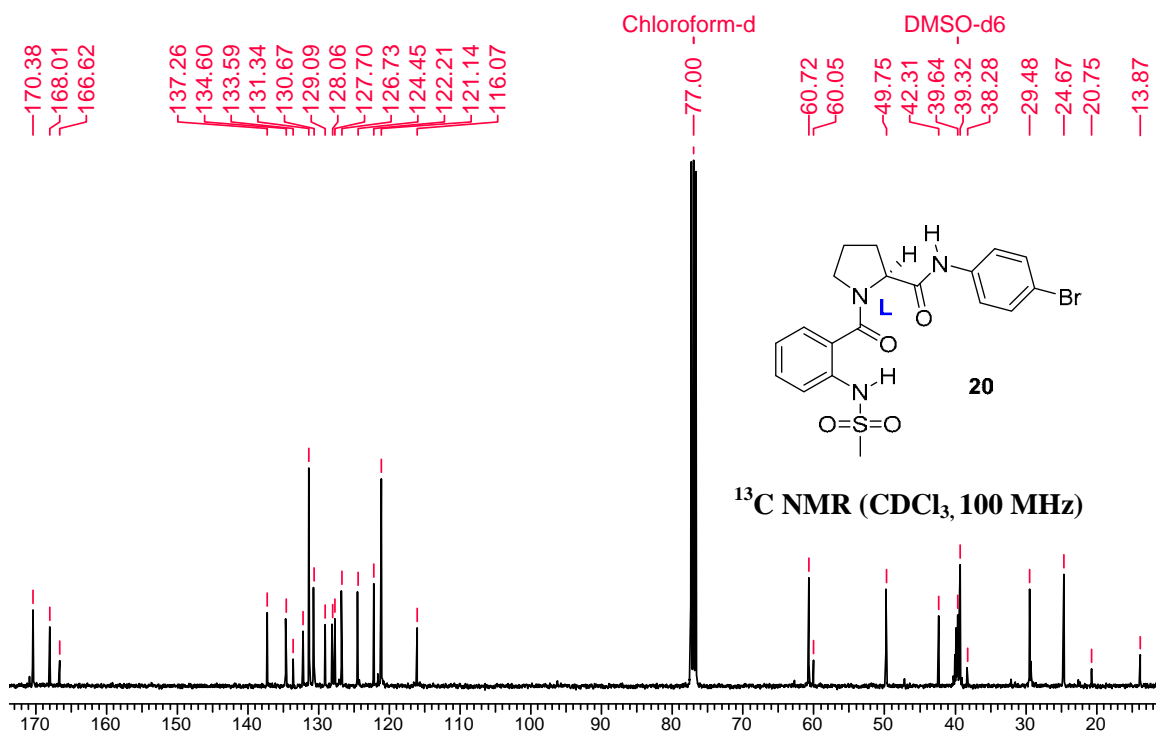


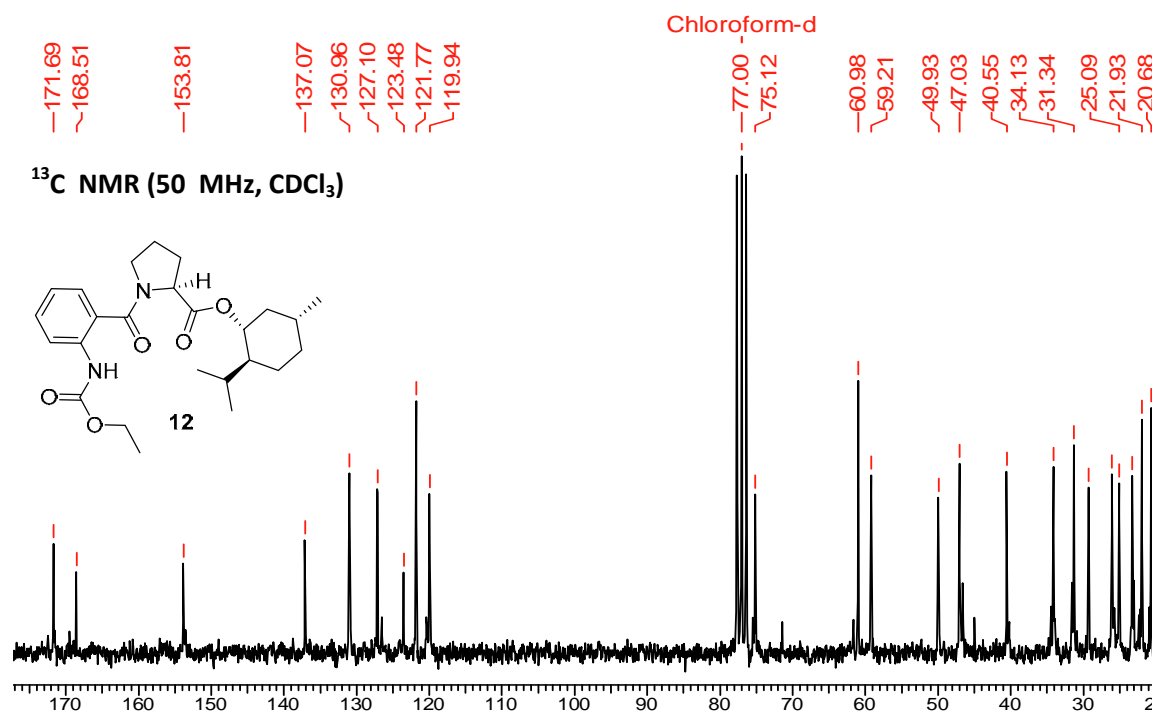




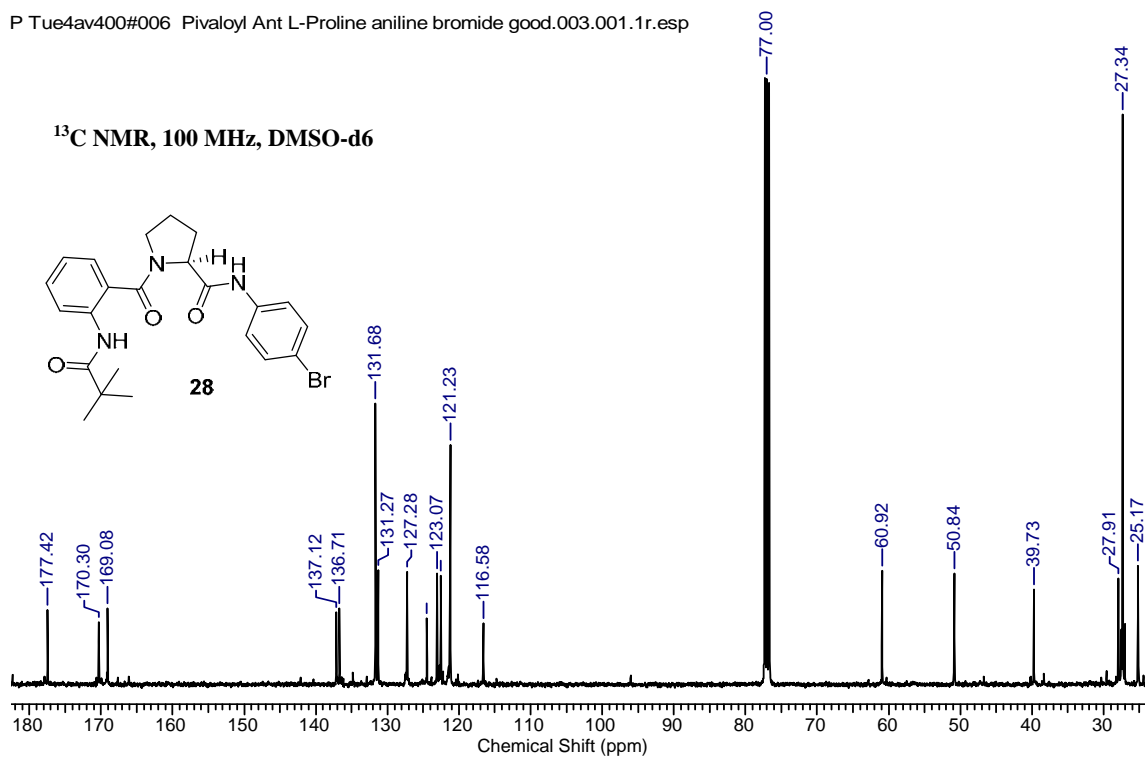




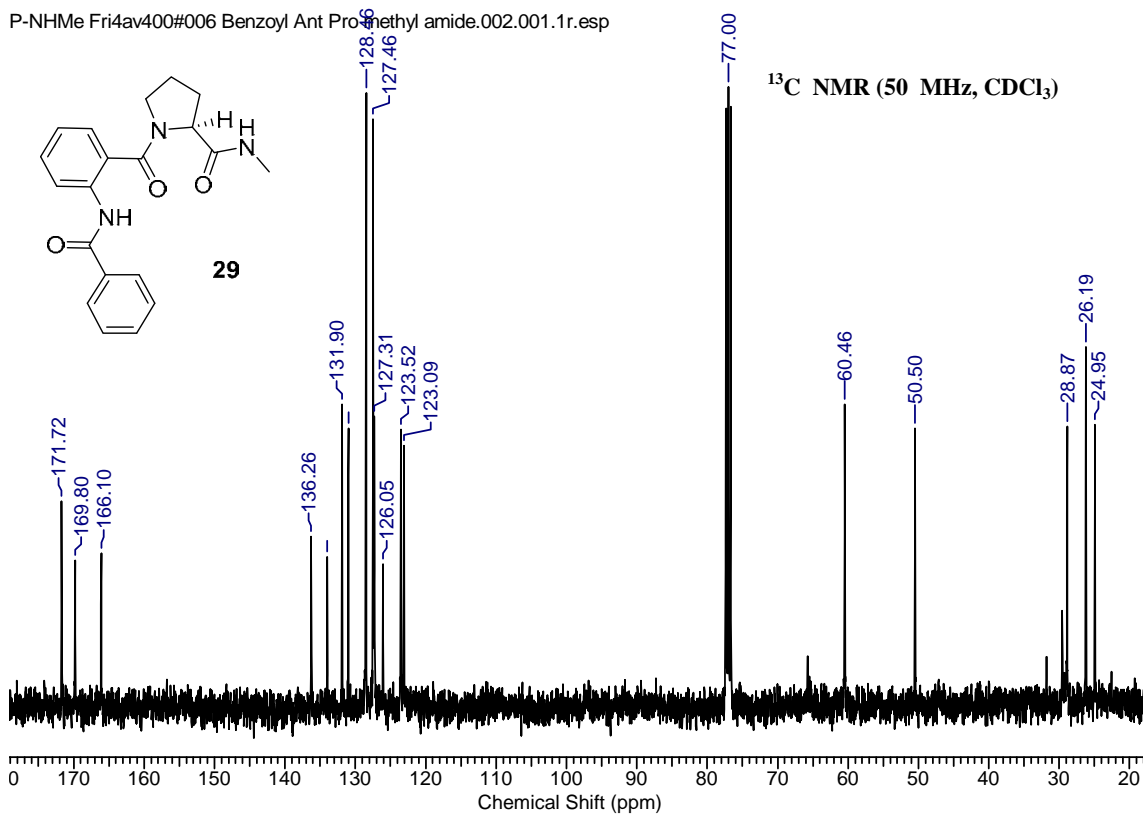




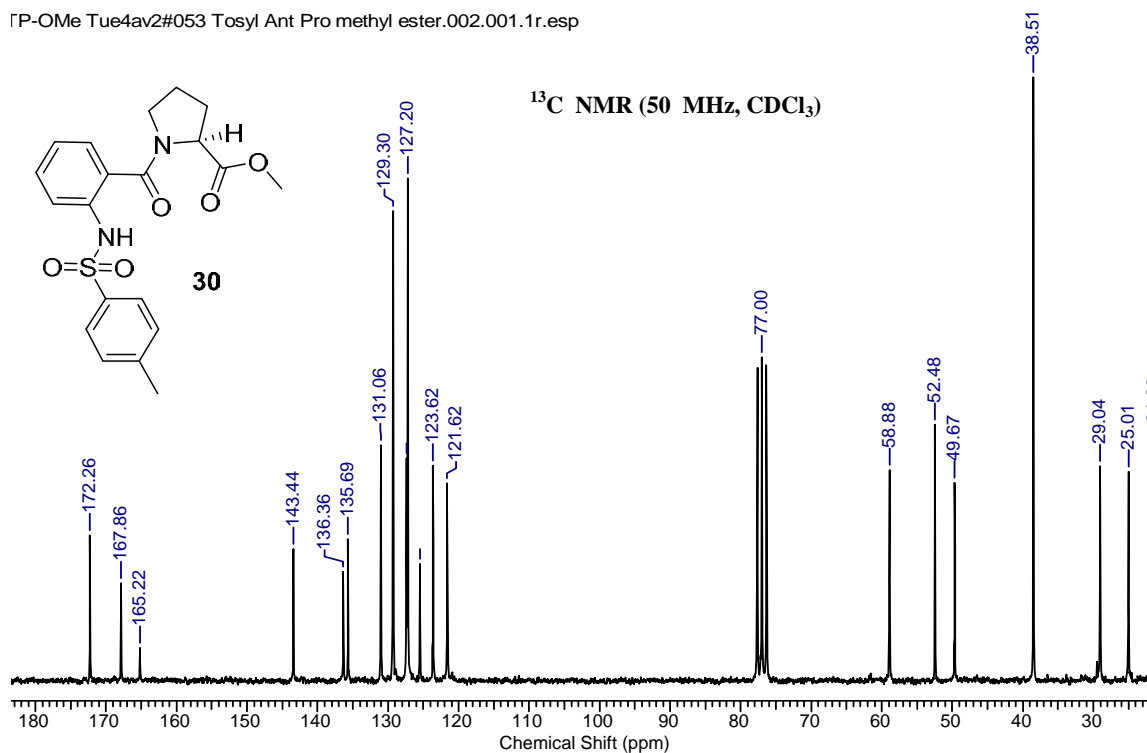
P Tue4av400#006 Pivaloyl Ant L-Proline aniline bromide good.003.001.1r.esp

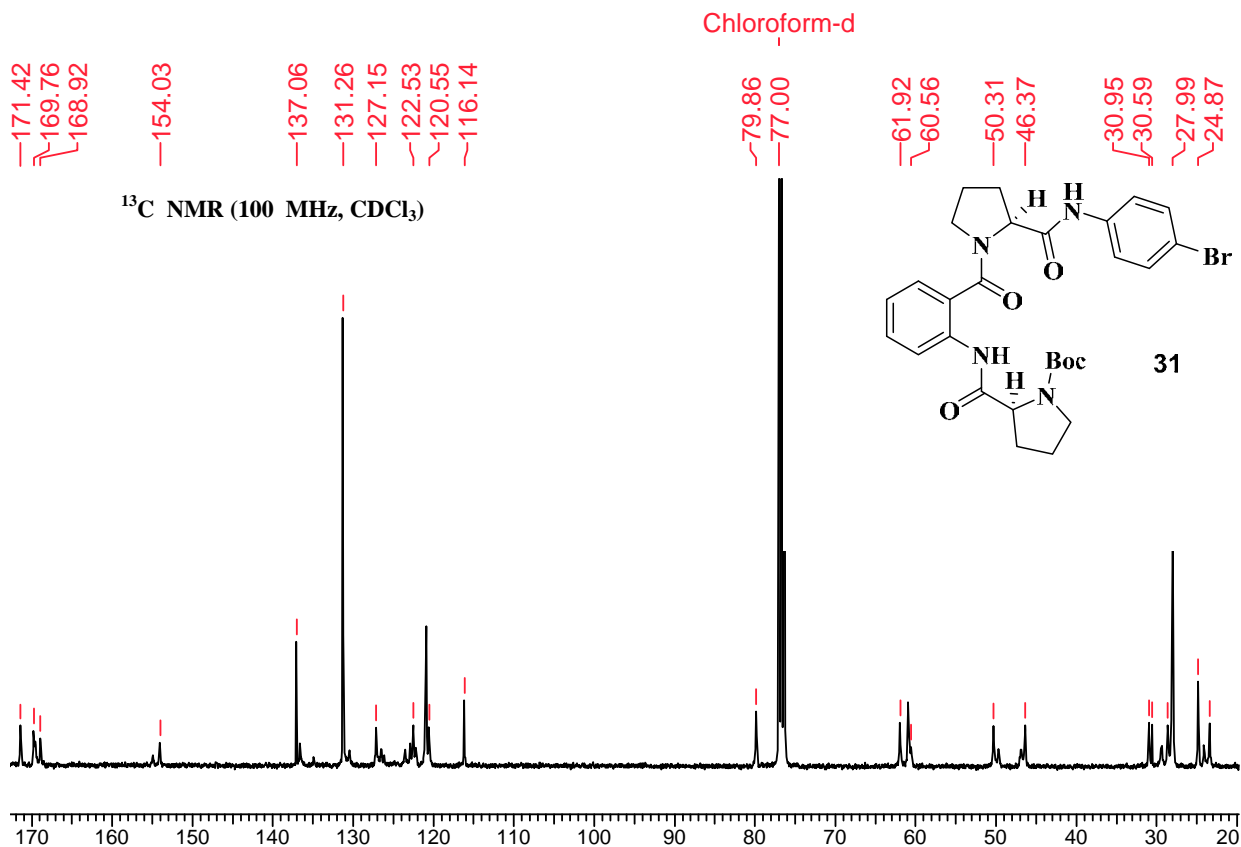


P-NHMe Fri4av400#006 Benzoyl Ant Pro methyl amide.002.001.1r.esp

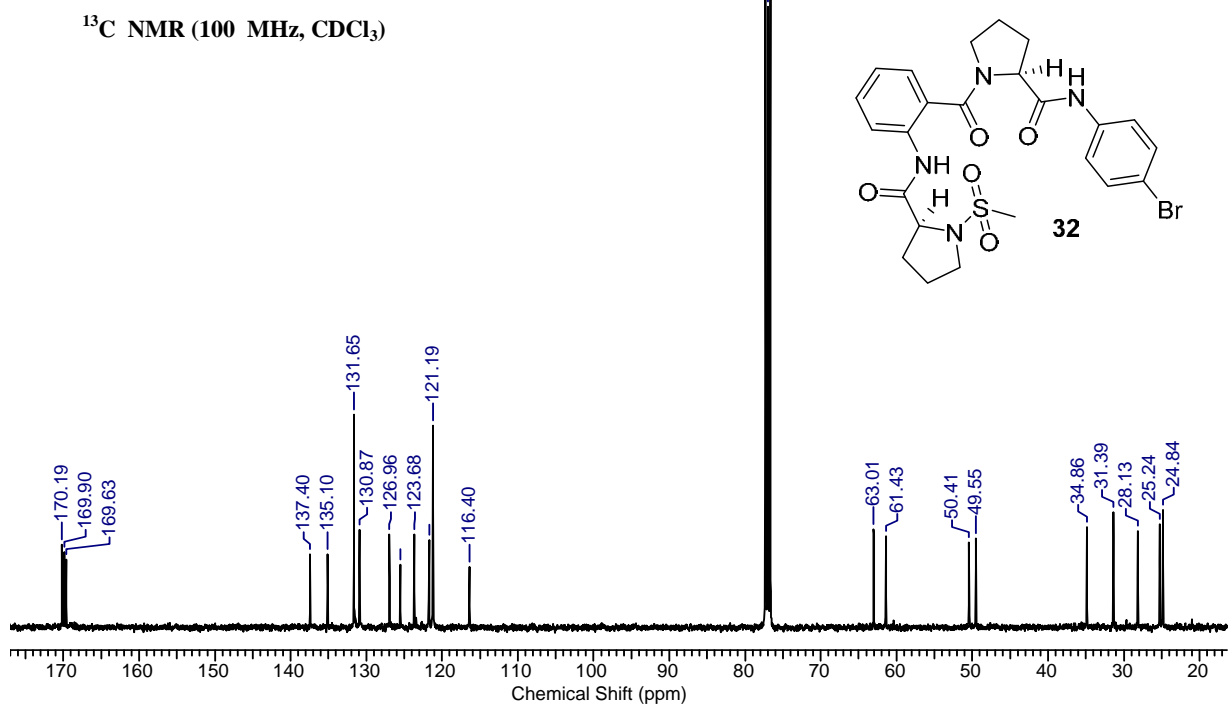


ΓP-OMe Tue4av2#053 Tosyl Ant Pro methyl ester.002.001.1r.esp





u1ECX400#012\_CARBO-3.jdf



## 1.25 References

- (1) Arunan, E.; Desiraju, G. R.; Klein, R. A.; Sadlej, J.; Scheiner, S.; Alkorta, I.; Clary, D. C.; Crabtree, R. H.; Dannenberg, J. J.; Hobza, P.; Kjaergaard, H. G.; Legon, A. C.; Mennucci, B.; Nesbitt, D. J. *Pure Appl. Chem.* **2011**, *83*, 1619.
- (2) Emsley, J. *Acc. Chem. Res.* **1980**, *9*, 91.
- (3) Etter, M. C. *Acc. Chem. Res.* **1990**, *23*, 120.
- (4) Chou, P. Y.; Fasman, G. D. *Adv. Enzymol.* **1978**, *47*, 45.
- (5) Baker, E. N.; Hubbard, R. E. *Prog. Biophys. Mol. Biol.* **1984**, *44*, 97
- (6) Presta, L. G.; Rose, G. D. *Science* **1988**, *240*, 1632.
- (7) Rose, G. D.; Fleming, P. J.; Banavar, J. R.; Maritan, A. *PNAS* **2006**, *103*, 16623.
- (8) Wilmot, C. M.; Thornton, J. M. *J. Mol. Biol.* **1988**, *203*, 221.
- (9) Vasudev, P. G.; Chatterjee, S.; Shamala, N.; Balaram, P. *Chem. Rev.* **2010**, *111*, 657.
- (10) Chatterjee, S.; Roy, R. S.; Balaram, P. *J. R. Soc. Interface* **2007**, *4*, 587.
- (11) Chou, K. C. *Anal. Biochem.* **2000**, *286*, 1.
- (12) Baruah, P. K.; Sreedevi, N. K.; Gonnade, R.; Ravindranathan, S.; Damodaran, K.; Hofmann, H.-J.; Sanjayan, G. J. *J. Org. Chem.* **2006**, *72*, 636.
- (13) Frishman, D.; Argos, P. *Proteins* **1995**, *23*, 566.
- (14) Milner-White, E. J. *J. Mol. Biol.* **1990**, *216*, 386.
- (15) Rose, G. D.; Gierasch, L. M.; Smith, J. A. *Adv. Protein Chem.* **1985**, *37*, 1.
- (16) Raghothama, S. R.; Awasthi, S. K.; Balaram, P. *J. Chem. Soc., Perkin Trans.* **1998**, *2*, 137.
- (17) Blank, J. T.; Guerin, D. J.; Miller, S. J. *Org. Lett.* **2000**, *2*, 1247.
- (18) Wiesner, M.; Neuburger, M.; Wennemers, H. *Chem. -Eur. J.* **2009**, *15*, 10103.
- (19) Wiesner, M.; Revell, J. D.; Wennemers, H. *Angew. Chem., Int. Ed.* **2008**, *47*, 1871.
- (20) Arakawa, Y.; Wiesner, M.; Wennemers, H. *Adv. Synth. Catal.* **2011**, *353*, 1201.
- (21) Blakeney, J. S.; Reid, R. C.; Le, G. T.; Fairlie, D. P. *Chem. Rev.* **2007**, *107*, 2960.
- (22) Lohse, M.; Benovic, J.; Codina, J.; Caron, M.; Lefkowitz, R. *Science* **1990**, *248*, 1547.
- (23) Cherezov, V.; Rosenbaum, D. M.; Hanson, M. A.; Rasmussen, S. G. F.; Thian, F. S.; Kobilka, T. S.; Choi, H.-J.; Kuhn, P.; Weis, W. I.; Kobilka, B. K.; Stevens, R. C. *Science* **2007**, *318*, 1258.
- (24) Rosenbaum, D. M.; Zhang, C.; Lyons, J. A.; Holl, R.; Aragao, D.; Arlow, D. H.; Rasmussen, S. G. F.; Choi, H.-J.; DeVree, B. T.; Sunahara, R. K.; Chae, P. S.; Gellman,

- S. H.; Dror, R. O.; Shaw, D. E.; Weis, W. I.; Caffrey, M.; Gmeiner, P.; Kobilka, B. K. *Nature* **2011**, *469*, 236.
- (25) Rosenbaum, D. M.; Cherezov, V.; Hanson, M. A.; Rasmussen, S. G. F.; Thian, F. S.; Kobilka, T. S.; Choi, H.-J.; Yao, X.-J.; Weis, W. I.; Stevens, R. C.; Kobilka, B. K. *Science* **2007**, *318*, 1266.
- (26) Rasmussen, S. G. F.; Choi, H.-J.; Rosenbaum, D. M.; Kobilka, T. S.; Thian, F. S.; Edwards, P. C.; Burghammer, M.; Ratnala, V. R. P.; Sanishvili, R.; Fischetti, R. F.; Schertler, G. F. X.; Weis, W. I.; Kobilka, B. K. *Nature* **2007**, *450*, 383.
- (27) D.V.Nataraj; Srinivasan, N.; Sowdhamini, R.; C.Ramakrishnan *Curr. Sci.* **1995**, *69*, 434.
- (28) Pavone, V.; Geata, G.; Lombardi, A.; Natri, F.; Maglio, O.; Isernia, C.; Saviano, M. *Biopolymers* **1996**, *38*, 705.
- (29) Cavacini, L. A.; Stanfield, R. L.; Burton, D. R.; A.Wilson, I. *J. Mol. Biol.* **2008**, *375*, 969.
- (30) Hahin, R.; Chen, Z.; Wang, D.; Reddy, G.; Mao, L. *Cell Biochem. Biophys.* **2002**, *37*, 169.
- (31) Hellgren, M.; Kaiser, C.; Haij, S. d.; Norberg, A.; Hoog, J.-O. *Cell. Mol. Life Sci.* **2007**, *64*, 3129.
- (32) Choudhary, A.; Raines, R. T. *ChemBioChem* **2011**, *12*, 1801.
- (33) Emsley, J. *Chem. Soc. Rev.* **1980**, *9*, 91.
- (34) Markovitch, O.; Agmon, N. *J. Phys. Chem. A* **2007**, *111*, 2253.
- (35) Choudhary, A.; Gandla, D.; Krow, G. R.; Raines, R. T. *J. Am. Chem. Soc.* **2009**, *131*, 7244.
- (36) Culik, R. M.; Jo, H.; DeGrado, W. F.; Gai, F. *J. Am. Chem. Soc.* **2012**, *134*, 8026.
- (37) Janssen, M. J.; Sandstrom, J. *Tetrahedron* **1964**, *20*, 2339.
- (38) Shin, I.; Ting, A. Y.; Schultz, P. G. *J. Am. Chem. Soc.* **1997**, *119*, 12667.
- (39) Scheike, J. A.; Baldauf, C.; Spengler, J.; Albericio, F.; Pisabarro, M. T.; Koks, B. *Angew. Chem., Int. Ed.* **2007**, *46*, 7766.
- (40) Yang, X.; Wang, M.; Fitzgerald, M. C. *Bioorg. Chem.* **2004**, *32*, 438.
- (41) Deechongkit, S.; Nguyen, H.; Powers, E. T.; Dawson, P. E.; Gruebele, M.; Kelly, J. W. *Nature* **2004**, *430*, 101.
- (42) Deechongkit, S.; Dawson, P. E.; Kelly, J. W. *J. Am. Chem. Soc.* **2004**, *126*, 16762.
- (43) Koh, J. T.; Cornish, V. W.; Schultz, P. G. *Biochemistry* **1997**, *36*, 11314.
- (44) Beligere, G. S.; Dawson, P. E. *J. Am. Chem. Soc.* **2000**, *122*, 12079.



- (45) Blankenship, J. W.; Balambika, R.; Dawson, P. E. *Biochemistry* **2002**, *41*, 15676.
- (46) Chapman, E.; Thorson, J. S.; Schultz, P. G. *J. Am. Chem. Soc.* **1997**, *119*, 7151.
- (47) Wales, T. E.; Fitzgerald, M. C. *J. Am. Chem. Soc.* **2001**, *123*, 7709.
- (48) Silinski, P.; Fitzgerald, M. C. *Biochemistry* **2003**, *42*, 6620.
- (49) Eildal, J. N. N.; Hultqvist, G.; Balle, T.; Stuhr-Hansen, N.; Padrah, S.; Gianni, S.; Strømgaard, K.; Jemth, P. *J. Am. Chem. Soc.* **2013**, *135*, 12998.
- (50) Aravinda, S.; Shamala, N.; Rajkishore, R.; Gopi, H. N.; Balaram, P. *Angew. Chem., Int. Ed.* **2002**, *41*, 3863.
- (51) Aravinda, S.; Harini, V. V.; Shamala, N.; Das, C.; Balaram, P. *Biochemistry* **2004**, *43*, 1832.
- (52) Harini, V. V.; Aravinda, S.; Rai, R.; Shamala, N.; Balaram, P. *Chem. Eur. -J.* **2005**, *11*, 3609.
- (53) Rai, R.; Vasudev, P. G.; Ananda, K.; Raghothama, S.; Shamala, N.; Karle, I. L.; Balaram, P. *Chem. Eur. -J.* **2007**, *13*, 5917.
- (54) Das, C.; Naganagowda, G. A.; Karle, I. L.; Balaram, P. *Biopolymers* **2001**, *58*, 335.
- (55) Nesloney, C. L.; Kelly, J. W. *J. Am. Chem. Soc.* **1996**, *118*, 5836.
- (56) Banerjee, A.; Raghothama, S.; Balaram, P. *J. Chem. Soc., Perkin Trans.* **1997**, *2*, 2087.
- (57) Haque, T. S.; Little, J. C.; Gellman, S. H. *J. Am. Chem. Soc.* **1996**, *118*, 6975.
- (58) Chatterjee, B.; Saha, I.; Raghothama, S.; Aravinda, S.; Rai, R.; Shamala, N.; Balaram, P. *Chem. Eur. J.* **2008**, *14*, 6192.
- (59) Chatterjee, S.; Vasudev, P. G.; Ananda, K.; Raghothama, S.; Shamala, N.; Balaram, P. *J. Org. Chem.* **2008**, *73*, 6595.
- (60) Yoder, G.; Polese, A.; Silva, R. A. G. D.; Formaggio, F.; Crisma, M.; Broxterman, Q. B.; Kamphuis, J.; Toniolo, C.; Keiderling, T. A. *J. Am. Chem. Soc.* **1997**, *119*, 10278.
- (61) Prabhakaran, P.; Kale, S. S.; Puranik, V. G.; Rajamohanam, P. R.; Chetina, O.; Howard, J. A. K.; Hofmann, H.-J.; Sanjayan, G. J. *J. Am. Chem. Soc.* **2008**, *130*, 17743.
- (62) Etter, M. C.; Lipkowska, Z. U.; Decoret, C.; Royer, J.; Bayard, F.; Vicens, J. *Mol. Cryst. Liq. Cryst. Inc. NonLin. Opt.* **1988**, *161*, 43.
- (63) Thilagavathy, R.; Kavitha, H. P.; Arulmozhi, R.; Vennila, J. P.; Manivannan, V. *Acta Cryst.* **2009**, *E65*, o127.
- (64) Li, X.; Huo, X.; Li, J.; She, X.; Pan, X. *Chin. J. Org. Chem.* **2009**, *27*, 1379.
- (65) Ramesh, V. V. E.; Priya, G.; Kotmale, A. S.; Gonnade, R. G.; Rajamohanam, P. R.; Sanjayan, G. J. *Chem. Commun.* **2012**, *48*, 11205.

- (66) Venkadachalapathy, Y. V.; Balaram, P. *Biopolymers* **1981**, *20*, 1137.
- (67) Raj, P. A.; Balaram, P. *Biopolymers* **1985**, *24*.
- (68) Chatterjee, B.; Saha, I.; Raghothama, S.; Aravinda, S.; Rai, R.; Shamala, N.; Balaram, P. *Chem.-Eur. J.* **2008**, *14*, 6192.
- (69) Abboud, J.-L. M.; Mo, O.; Paz, J. L. G. d.; Yanez, M.; Esseffar, M.; Bouab, W.; El-Mouhtadi, M.; Mokhlisse, R.; Ballesteros, E.; Herreros, M.; Homan, H.; Lopez-Mardomingo, C.; Notarios, R. *J. Am. Chem. Soc.* **1993**, *115*, 12468.
- (70) Janssen, M. J.; Sandstrom, J. *Tetrahedron* **1964**, *20*, 2339.
- (71) Gennari, C.; Salom, B.; Potenza, D.; Williams, A. *Angew. Chem., Int. Ed.* **1994**, *33*, 2067.
- (72) Gennari, C.; Salom, B.; Potenza, D.; Longari, C.; Fioravanzo, E.; Carugo, O.; Sardone, N. *Chem.-Eur. J.* **1996**, *2*, 644.
- (73) Liskamp, R. M. J.; Kruijtzter, J. A. W. *Mol. Diversity* **2004**, *8*, 79.
- (74) Langenhan, J. M.; Fisk, J. D.; Gellman, S. H. *Org. Lett.* **2001**, *3*, 2559.
- (75) Liskamp, R. M. J.; Rijkers, D. T. S.; Kruijtzter, J. A. W.; Kemmink, J. *ChemBioChem* **2011**, *12*, 1626.
- (76) Turcotte, S.; Gervais, S. H. B.; Lubell, W. D. *Org. Lett.* **2012**, *14*, 1318.
- (77) Baldauf, C.; Gunther, R.; Hofmann, H.-J. *THEOCHEM* **2004**, *675*, 19.
- (78) Kelly, S. M.; Price, N. C. *Curr. Protein Pept. Sc.* **2000**, *1*, 349.
- (79) Pomerantz, W. C.; Grygiel, T. L. R.; Lai, J. R.; Gellman, S. H. *Org. Lett.* **2008**, *10*, 1799.
- (80) G. P. Manfio; E. Atalan; J. Z. – Czerwinska; M. Mordarski; C. Rodriguez; Collins, M. D.; Goodfellow, M. *Antonie van Leeuwenhoek* **2003**, *83*, 245.

*Chapter 2*

Orthanilic Acid-Mediated Pseudo  $\beta$ -turn  
Motifs

## Robust Reverse Turn comprising Orthanilic Acid (<sup>s</sup>Ant) and Proline (Pro), featuring C-9 H-bonding.

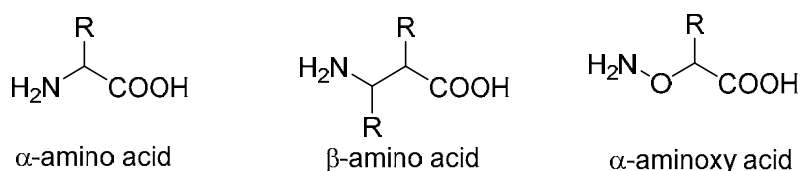
**2.1 Folding in peptides:** Protein folding is the physical process by which a polypeptide folds into its characteristic and functional three-dimensional structure from its random coil structure. Folding of peptides are facilitated by various non covalent interactions like hydrogen bonding, hydrophobic interactions, van der Waals interactions, halogen-bonding and covalent interactions, like disulfide bond formation, metal cluster formation etc. Temperature, solvent medium, concentration of salt present in the environment, presence of molecular chaperones *etc.* can influence the folding of peptides. Denaturation is a process by which proteins or peptides lose their tertiary and secondary structures with the aid of external stimuli. The egg white protein (albumin) is an example where an irreversible denaturation is caused by the high rise of temperature during cooking process and consequent loss of solubility. Application of external stress, chemicals like acid or base, presence of concentrated inorganic salts, organic solvents (e.g., alcohol or chloroform) can cause the denaturation of proteins. Most biological substrates lose their biological function when denatured. For example, enzymes lose their activity, because of the inability of substrates to reach the active site and stabilize substrates' transition states. In very few cases, denaturation is reversible *i.e.* the proteins can regain their native state when the denaturing influence is removed and is called renaturation.<sup>1</sup> Covalent forces like disulfide bonds often rigidify the peptide structures in cysteine containing proteins.<sup>2-4</sup> It also creates a considerable degree of hydrophobicity in the backbone and resists proteolysis. Hair and feathers (of birds) are made up of keratin which is composed of a large number of disulfide bonds that resists water. Hence, eye lashes protect eyes from dust, sweat and rain. Hydrophobic and hydrogen bonding interactions are the two major factors influencing the folding of peptides.<sup>5</sup> All these covalent and van der Waals forces get disturbed on denaturation.

**2.2 Role of hydrogen bonding in peptide folding:** Hydrogen bond is a non-covalent interaction in which the electron density of a hydrogen atom is shared with two electro negative atoms *i.e.* a donor and an acceptor. As discussed in chapter 1, hydrogen bonding explains the dimerization of carboxylic acids in its vapor state, crystal formation of ice, self assembly and consequent insolubility of cellulose, double helical structure of DNA and folded structure of proteins. In proteins, hydrogen bonds are formed between the amide 'NH' and carbonyl 'O' where 'H' is the donor atom and 'O' is the acceptor atom.

Although the energy of the hydrogen bond (~12 kJ/mol) is fairly weak when compared to covalent interactions, they are in large amount, and together contribute a significant amount of energy and stability to the protein conformation. A protein intrinsically folds into a highly complex three dimensional structure utilizing *intra*-molecular hydrogen-bonding, while at the surface it interacts with water or other proteins through *inter*-molecular hydrogen bonding. The *intra*-molecular hydrogen bonding facilitates proteins to adopt a particular shape and to get enveloped or stabilized by hydrophobic interactions of amino acid side chains. The secondary structures of proteins like  $\alpha$ -helix,  $\beta$ -sheets, turns *etc.* are stabilized by intra-molecular H-bonding.<sup>6</sup>

**2.3 Significance of backbone modification in peptides:** Enormous research has been under taken for the past decades to understand the role of back bone modifications in peptide folding and stabilization. Varying the amino acid chains, swapping of hydrogen bonding codes like NH and CO, modification of amide bonds, modifications in amino acid back bone *etc.* have been carried out to study their significance in the peptide folding. These practices have led to the development of a wide variety foldamer motifs like aminoxyacids,<sup>7-8</sup> peptoids,<sup>9-10</sup> sugar aminoacids,<sup>11-13</sup> dehydro aminoacids,<sup>14</sup> cyclic<sup>15-18</sup> and bicyclic aminoacids<sup>19-20</sup> *etc.* The isosteric replacement involving the swapping of a carboxamide with a sulfonamide bond is of significance because of the fact that both of them have entirely different conformational and geometrical preferences. Various structural motifs have been discussed in brief in subsequent sections.

**$\alpha$ -aminoxyacids:**  $\alpha$ -aminoxy acids are analogs of  $\beta$ -amino acids in which the  $\beta$ -carbon atom in the  $\beta$ -amino acid backbone is replaced with an oxygen atom. Dan Yang and coworkers initially reported a novel turn structure in the peptides containing  $\alpha$ -aminoxyacetic acids with rigid eight-membered-ring hydrogen bonded structure called  $\alpha$  N-O turn.<sup>7-8</sup>



Oligomers of  $\alpha$ -aminoxy acids form helix featuring 8-membered hydrogen bonding.<sup>21-22</sup> Hybrid peptides featuring  $\alpha$ -amino acids and  $\alpha$ -aminoxy acids feature a  $\gamma$ -turn in addition to the 8-membered hydrogen bonding observed in  $\alpha$ -aminoxy acid

helix.<sup>23</sup> Recently, aminoxy acids also have been used to develop cell-penetrating peptides.<sup>24</sup>

**Peptoids:** Peptoids are poly-N-substituted glycines. They are a class of peptidomimetics, whose side chains are attached to the nitrogen atom of the peptide backbone than to the  $\alpha$ -carbons. These are structural motifs, which are bio-inspired polymers having pharmaceutical applications.<sup>24-25</sup> Peptoids are versatile tools to probe biological processes and are promising as therapeutic agents.<sup>9</sup> Krishenbaum *et al.* used the property of atropisomerism in peptoid backbone to rigidify the backbone.<sup>26</sup> A new peptoid ribbon secondary structure arose from a primary sequence comprising of a regular alternating sequence of N-(S)-1-(1-naphthyl)ethyl (Ns1npe) and N-aryl peptoid monomers to enforce an alternating pattern of *cis* and *trans* main-chain amides as demonstrated by Blackwell *et al.*<sup>27</sup> Amphiphilic cyclic peptoids are shown to exhibit antimicrobial activity by disrupting *Staphylococcus aureus* cell membranes.<sup>28</sup> Cyclic peptoids are another important class of peptoids with back bone modifications reported from Taillefumier *et al.*, recently.<sup>29-30</sup> A class of fluorescent water-soluble peptoids that include strongly helix-promoting (S)-N-1-(naphthylethyl)glycine residues, have been also reported from Fuller and coworkers.<sup>31</sup>

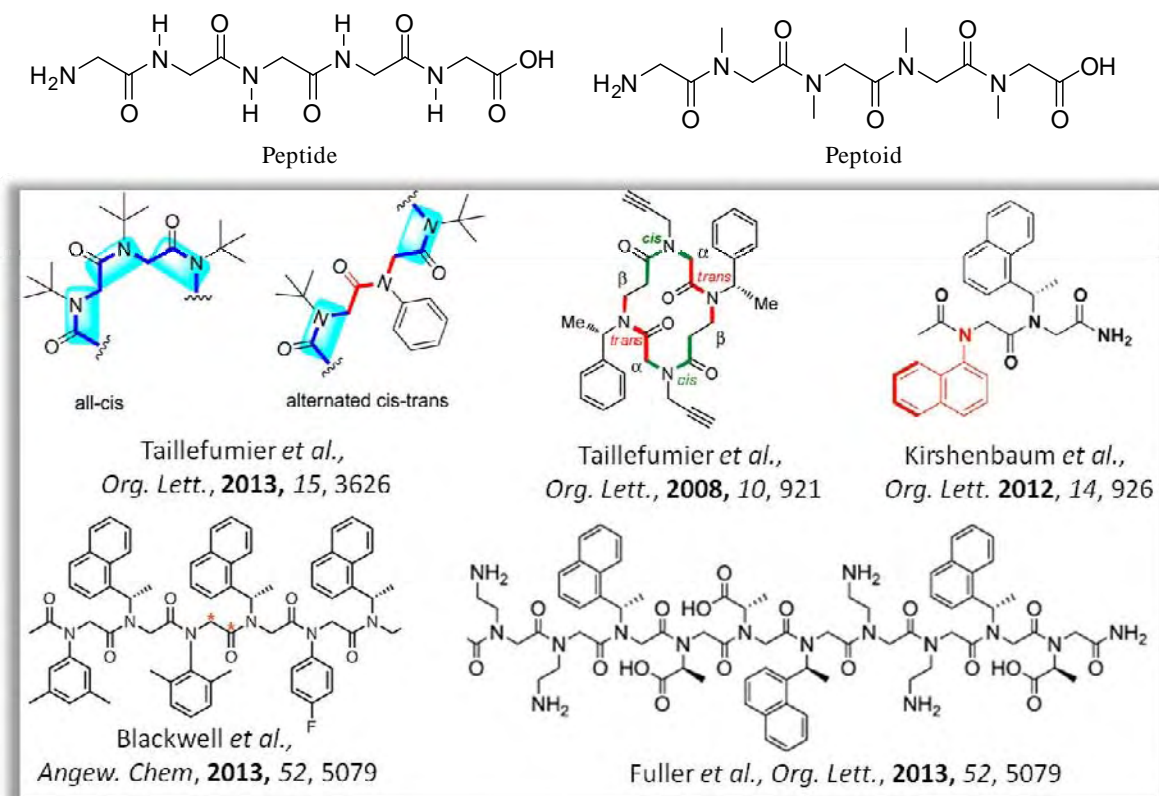
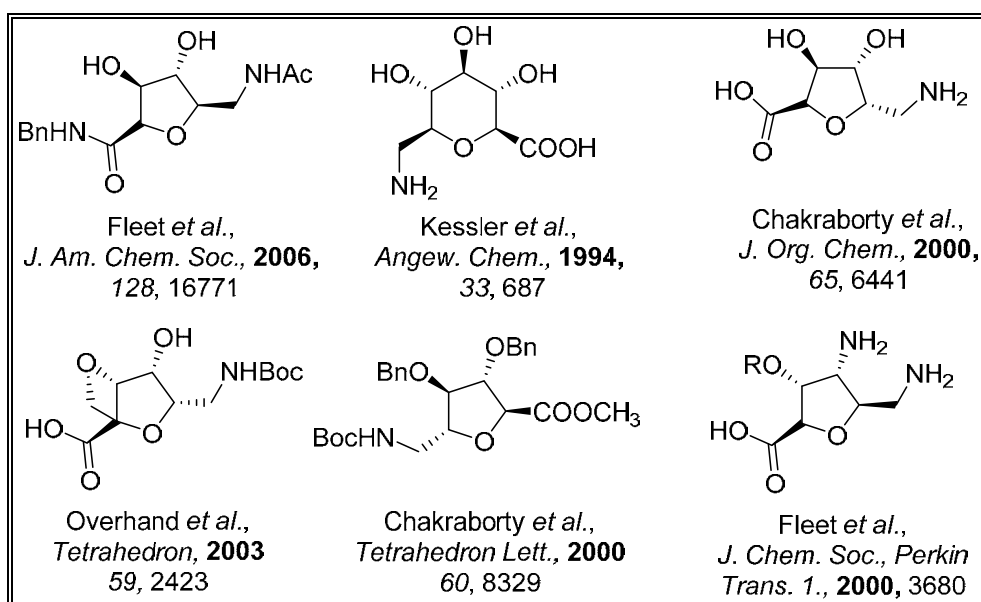


Fig. 2.1: Peptide and peptoids.

**Sugar-based aminoacids:** Sugar-based amino acids (SAAs) are carbohydrate derivatives bearing both amino and carboxylic acid functionalities. SAAs are very versatile conformationally biased building blocks, acquiescent to serve as glyco- or peptidomimetics.<sup>32</sup> The stereochemical arrangement of the substituents of the sugar ring, its ring-size as well as the presence of additional functional groups provides a surfeit of possible arrangements.<sup>33-34</sup> Infact, sugar-modified foldamers are considered as some of the conformationally defined and biologically distinct glycopeptide mimics.<sup>35</sup> Kessler's and Fleet's group pioneered in developing diverse classes of sugar based amino acids and peptides.<sup>36-39</sup> A variety of sugar based amino acids have also been developed from Taillefumier,<sup>40</sup> Kunwar,<sup>41-42</sup> Chakraborty,<sup>42-43</sup> Sharma<sup>41-42</sup> *et al. etc.* Some conformationally restricted sugar amino acids were also developed by Overhand *et al.*<sup>44</sup>



**Fig. 2.2:** A few examples of sugar-based amino acids.

**Cyclic, dehydro and bicyclic amino acids:** Various research groups developed diverse classes of amino acids with enormous structural and backbone modifications, whose secondary structure formation and folding propensities have been well investigated. This led to the development of a class of constrained cyclic  $\beta$ -amino acids like 2-amino cyclopentane carboxylic acid (ACPC),<sup>45</sup> 2-amino pyrrolidine-3-carboxylic acid (APC),<sup>45</sup> 2-amino cyclopropanecarboxylic acid,<sup>46</sup> 2-amino cyclobutanecarboxylic acid (ACBC),<sup>47</sup> 2-amino cyclohexanecarboxylic acid (ACHC)<sup>48</sup>, *etc.* Efforts to further rigidify the backbone or ring led to dehydro amino acids<sup>49</sup> and bicyclic amino acids.<sup>50-51</sup> Besides monocyclic  $\beta$ -amino acid building blocks, bulky and strained bridged bicyclic side-chains

have been incorporated in monoterpene-derived apopinane skeleton (2-amino-6,6-dimethyl-bicyclo[3.1.1]-heptane-3-carboxylic acid; ABHC).<sup>52</sup>

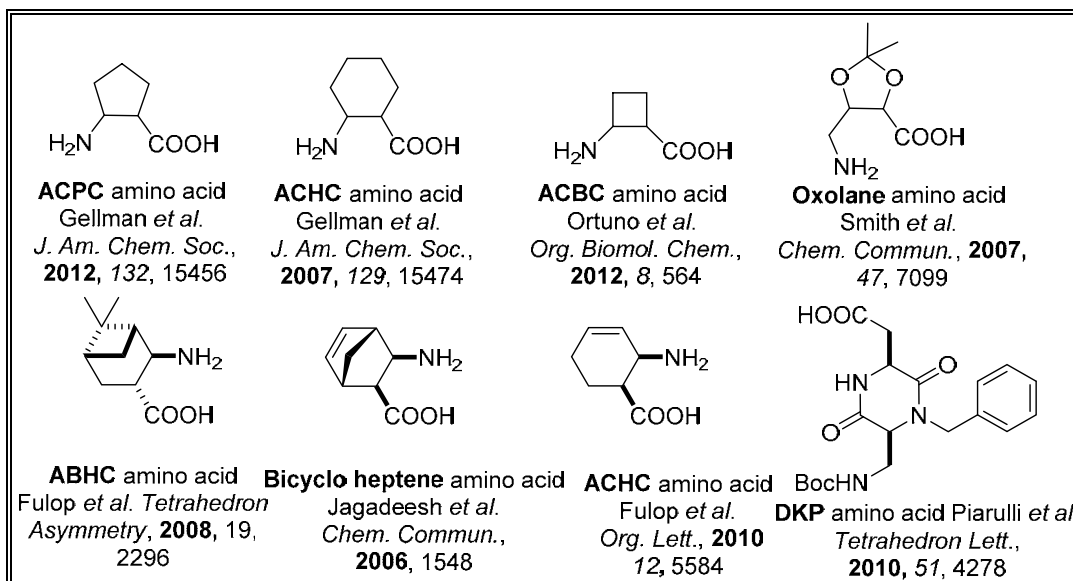


**Fig. 2.3:** Representative examples of cyclic amino acids.

**2.4: Amino acids and secondary structure propensities:** The secondary structures of proteins can be predicted by the side chains of amino acid residues present in the structure. Amino acids like glutamine (Gln), methionine (Met), alanine (Ala) are often associated with  $\alpha$ -helix, while isoleucine (Ile), valine (Val), tyrosine (Tyr), phenyl alanine (Phe), leucine (Leu), tryptophan (Trp) are found in the strands of the  $\beta$ -sheets.

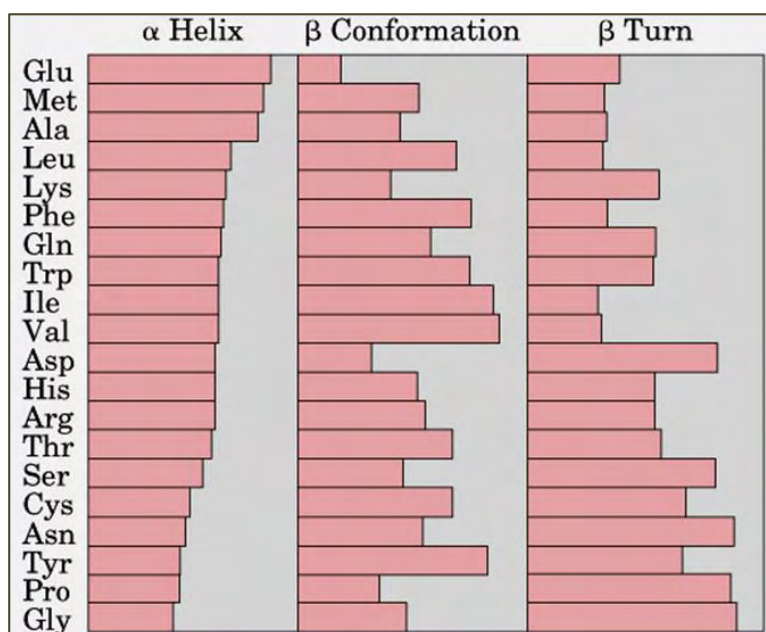


**Fig. 2.4:** Graph showing the turn propensities of amino acids.



Proline (Pro), glycine (Gly) and aspartic acid (Asp) compose turn region of the secondary structure. The folding propensities of peptides containing each amino acid are represented in the graph (fig. 2.4, *vide supra*). The preferential occurrence of amino acids as of part of various secondary structures depends on the side chain, dihedral angles  $\phi$  and  $\psi$ , presence of aromatic interactions, presence of disulfide bonds, electrostatic interactions, *etc.*

## 2.5 Torsion angles of peptide bond

A peptide bond is planar with fixed *hybridization*. The rotation around the bonds connected to the  $\alpha$ -carbon is permitted. Peptide bonds in proteins are represented by the dihedral angles  $\phi$ ,  $\psi$ ,  $\omega$ ,  $\theta$ , *etc.*, which greatly determine the folding of peptides<sup>53-55</sup> (fig. 2.5).

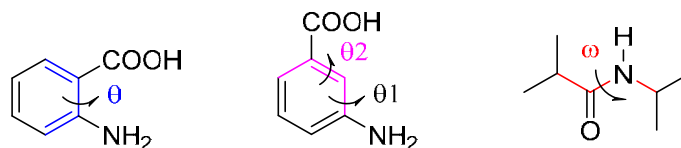
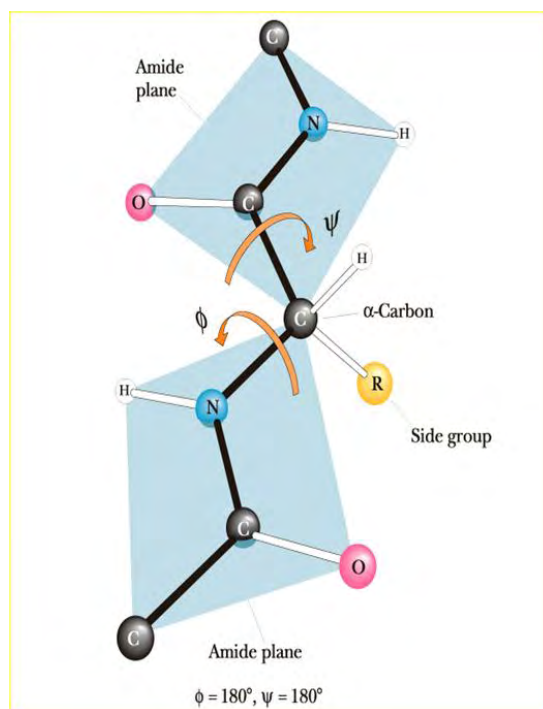


**Fig. 2.5:** Figure showing the representations of  $\phi$ ,  $\psi$ ,  $\omega$ , and  $\theta$  angles in amino acids.

The dihedral angles are defined as follows. Dihedral angle  $\psi$  (*psi*) corresponds to the angle between  $\alpha$ -carbon and carbonyl carbon. It is  $0^\circ$ , when the amide plane containing the carbonyl bisects the  $\alpha$ -carbon in a *cis* conformation.

Dihedral angle  $\phi$  (*phi*) corresponds to the angle through the  $\alpha$ -carbon and the amide nitrogen. It is  $0^\circ$  when the amide plane containing the nitrogen bisects the  $\alpha$ -carbon in a *cis* conformation.

Dihedral angle  $\theta$  (*theta*) is seen in amino acids other than  $\alpha$ -amino acids. It corresponds to the angle through the carbon-carbon bonds between amide carbonyl and amide NH. It is close to  $0^\circ$  in aromatic amino acids.

Dihedral angle  $\omega$  (*omega*) is the angle through amide bonds and is  $\sim 180^\circ$  for carboxamides. On the other hand, ' $\omega$ ' is reduced to  $\sim 90^\circ$  in sulfonamides

Extensive research based on unnatural amino acids which induce twist (folding) in the conformation, were carried out to understand the folding of peptides.<sup>56-58</sup> The most widely used one is the  $\alpha$ -aminoisobutyric acid (Aib) - a highly constrained  $\alpha$ -amino acid,<sup>59-60</sup> which is the homologue of  $\alpha$ -alanine. Use of unnatural amino acids with unique dihedral angle preferences can induce folding in peptides. Another fine case is gabapentin (2-[1-(aminomethyl)cyclohexyl]acetic acid). Though it is a pharmaceutical drug, specifically a GABA analog, which is used to treat epilepsy and to relieve neuropathic pain, it has been used well in peptidomimetics.<sup>61</sup> There are examples in which unnatural turn moieties in aromatic templates along with flexible chains facilitate lamellar sheet formation in peptides.<sup>62</sup> In another case, an organo-metallic amino acid like 1'-aminoferrocene-1-carboxylic acid was used as a turn inducer to derive  $\beta$ -sheets.<sup>63</sup> Taking advantage of the inherent rigidity of aromatic frameworks, peptide scientists have used them to develop turn units to form several  $\beta$ -sheet structures.<sup>64-65</sup> Smith *et al.* showed that a non-peptidomimetic reverse turn resulted in a hairpin conformation which eventually stabilizes sheet structures in both solid and solution state.<sup>46,66</sup> The concept and utility of conformationally rigid two-dimensional aromatic amino acids is also blooming that it offers conformational ordering in foldamer design and creates intriguing structural architects.<sup>67-69</sup> An effort to compare the conformational propensities of carboxamide and sulfonamide led to the utilization of 2-amino benzene sulfonic acid ( $^S$ Ant) as a sulfonyl analogue of  $\beta$ -amino acid anthranilic acid.<sup>70</sup>

**2.6 Sulfonamides:** Sulfonamides represent a potent class of compounds immensely renowned for their diverse bio-active properties such as antibacterial, antitumor, diuretic, hypoglycemic, antithyroid and protease inhibitor activities. Consequently, the idea of

using sulfonamides as connecting elements for synthetic peptides has fascinated various research groups.<sup>71-78</sup>

## 2.7 Sulfonamides: A potent bioactive compound.

Sulfonamides, sometimes called sulfa drugs, are medicines that prevent the growth of bacteria in the body. Sulfonamides are used to treat many kinds of infections caused by bacteria and certain other microorganisms and many other diseases.<sup>71,79-85</sup> Physicians may prescribe these drugs to treat urinary tract infections, ear infections, frequent or long lasting bronchitis, bacterial meningitis, certain eye infections, *Pneumocystis carinii* pneumonia, traveler's diarrhea and a number of other kinds of infections. Sulfisoxazole (gantrisin) is used to treat urinary tract infections. In combination with erythromycin, sulfisoxazole may be used to treat ear infections in children. Trimethoprim/sulfamethoxazole (bactrim, septrin) is a combination of two sulfonamides used together. This combination is found to be more effective than giving either drug alone in a larger dose. The combination is commonly used to treat urinary tract infections and other infections that cannot be treated with antibiotics. The most common use for sulfonamides is in adults in the treatment of urinary tract infections. Sulfonamides may interact with a large number of other medicines. When interaction occurs, the effects of one or both of the drugs may change or the risk of side effects may be greater.

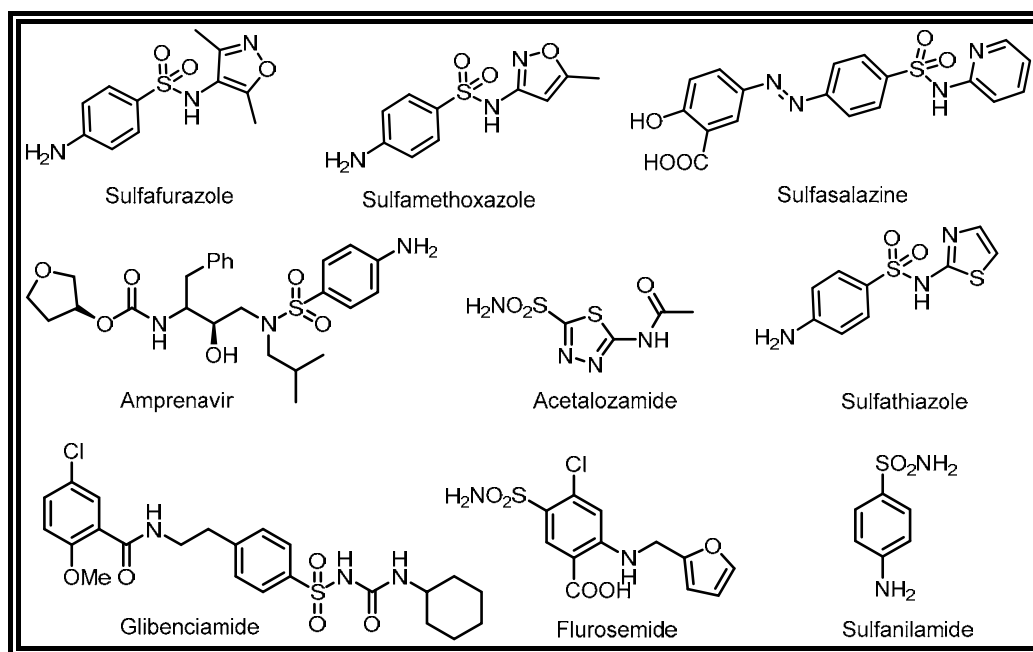
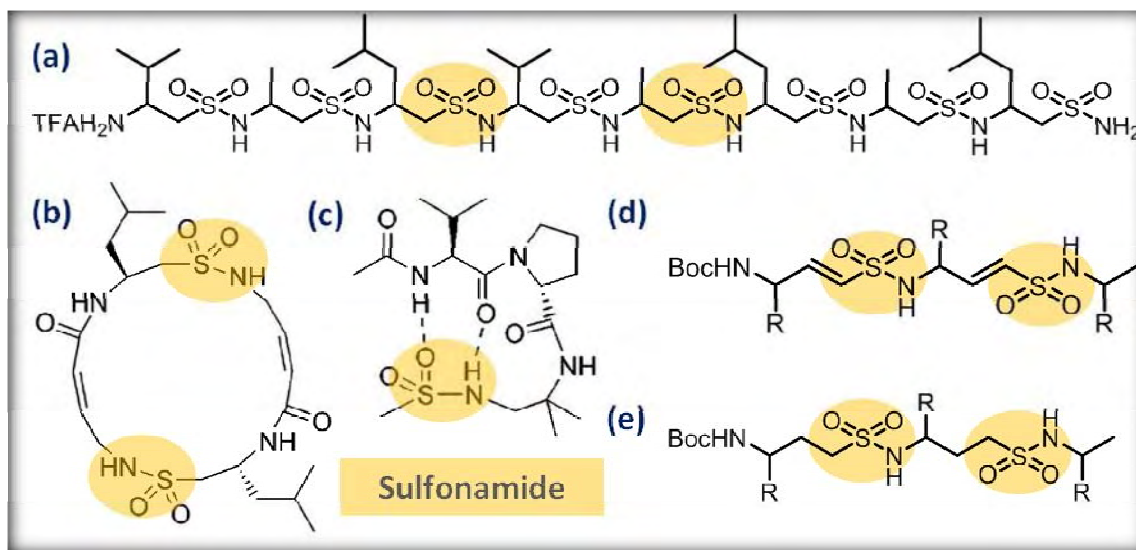


Fig. 2.6: A few sulfonamide based drugs

## 2.8 Sulfonamides: A connecting element for foldamers or synthetic peptides.

Earlier efforts to introduce the sulfonamide bond as foldamer linkers were realized by Gennari and Liskamp *et al.*<sup>72-73,75-76</sup> Efforts to mimic the amide bond with sulfonamide bonds led to the development of *pseudo* peptide foldamers containing vinylogous sulfonamide peptides (fig. 2.7d). Liskamp's group used peptide transformation by sulfonamide bond formation, leading to peptide-peptidosulfonamide hybrids and oligopeptide sulfonamides. Similar strategy was used for the development of  $\beta$ -ethylamino sulfonamide foldamers (fig. 2.7a) and cyclic-peptidosulfonamides (fig. 2.7b).<sup>86-87</sup> Gellman *et al.* showed the hydrogen bonding complementarities between a single secondary sulfonamide group and an  $\alpha$ -amino acid residue, which can be used for the development of sulfonamide strand mimics, using a hairpin folding motif (fig. 2.7c).<sup>74</sup> A CO and NH in an amide bond never exist in a *cis* position and as a result the amide NH and CO never participate in hydrogen bonding simultaneously. Gellman *et al.* illustrated that, in a sulfonamide bond, the *cis* disposition of SO and NH can result in its involvement of two hydrogen bonding simultaneously.<sup>74</sup>



**Fig. 2.7:** Sulfonamide based foldamers or synthetic peptide mimics - Liskamp *et al.* (a, b)<sup>72-73</sup>; Gellman *et al.* (c)<sup>74</sup> and Gennari *et al.* (d, e)<sup>75-76</sup>.

## 2.9 Sulfonamides vs. carboxamides in peptide folding - the utilization of the geometrical preferences of sulfonamide bond: Present study

A sulfonamide bond is one of the isosteric replacements of a carboxamide. The superior stability of a sulfonamide bond towards hydrolysis makes it a better isostere for a carboxamide against proteolysis. The presence of an additional acceptor oxygen atom

attached to a sulfur atom increases the hydrogen bonding preference of a sulfonamide. The sulfonamide NH is relatively more acidic and thus is a strong hydrogen bond donor than a carboxamide. The exceptionality of a sulfonamide bond showing a major twist occur from the reduction of the dihedral angle ' $\omega$ ' from  $\sim 180^\circ$  (carboxamide) to  $\sim 90^\circ$  (sulfonamide;  $\pm 20$ ) explaining why sulfonamide has a twisted conformation (non-planar) while an amide bond is planar. The present study attempts to examine the outcome of the amide modification to sulfonamide around Ant-Pro turn unit, considering the significant differences between the sulfonamides and carboxamides.<sup>72-76</sup>

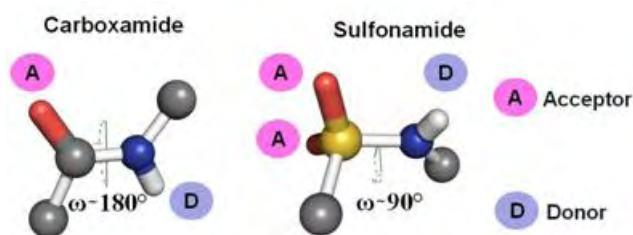


**Fig. 2.8:** Geometrical differences between a carboxamide bond (left) and a sulfonamide bond (right).

### 2.10 Objective of present work: Investigating the robustness of <sup>S</sup>Ant-Pro C<sub>9</sub> turn

The two-residue Ant-Pro motif adopts a robust *pseudo*  $\beta$ -turn conformation featuring a strong 9-membered-ring hydrogen bonding, formed in the forward direction of the sequence 1 $\rightarrow$ 2.<sup>88-89</sup> The steric clash between the rings, anthranilic acid (Ant) and proline (Pro) coerces them to adopt an anti-periplanar arrangement, breaking the 6-membered hydrogen bond of Ant and leading to the formation of a closed 9-membered hydrogen bonded network. Considering the substantial geometrical, hydrogen bonding and conformational differences of carboxamides and sulfonamides, as noted earlier, the robustness of the turn is tested by the introduction of sulfonamides at the folding core of Ant-Pro reverse turn unit (fig. 2.9). As there is a significant difference in the dihedral angle preferences for carboxamide and sulfonamide, we anticipate a dissimilar conformational feature. Due to the  $sp^3$  hybrid nature of the sulfonamide bond, Ant and Pro rings may be positioned in an anti-periplanar direction before it faces the steric clash. Hence, the objective here is to investigate the structural preferences adopted by the dipeptide motif when the Ant-carboxamide is replaced with Ant-sulfonamide.

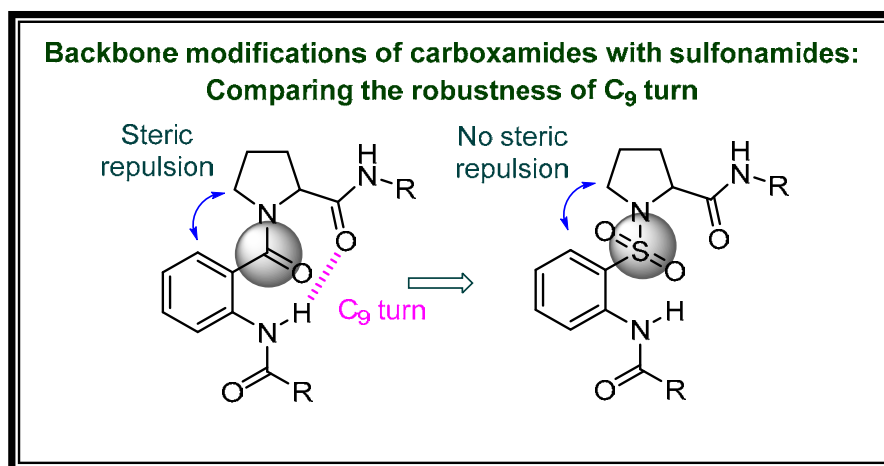
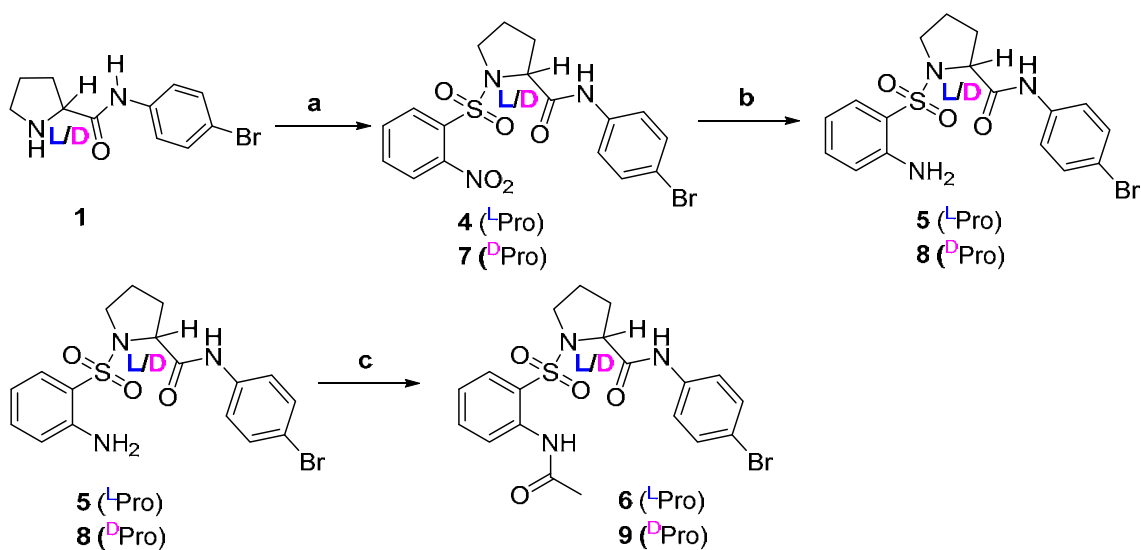


**Fig. 2.9:** Amide to sulfonamide modification at the folding core of Ant-Pro reverse motif.

## 2.11 Synthesis

In order to understand clearly the effect of swapping carboxamides with sulfonamides, the central carboxamide bond of Ant-Pro was modified with sulfonamide bond. H-<sup>L/D</sup>Pro *p*-Br anilide was sulfonylated with 2-nitrobenzene sulfonyl chloride that yielded **4** and **7**, which were subjected to nitro reduction<sup>90</sup> using zinc (pretreated with HCl and thoroughly washed with water and ether prior to use) and ammonium formate in methanol to yield the free amines **5** and **8**, respectively, which on subsequent acetylation at N-terminal afforded compounds **6** and **9**, respectively.

**Scheme 2.1:** Synthesis of <sup>S</sup>Ant-Pro di-peptide units



*Reagents and Conditions:* (a) 2-nitro benzene sulfonyl chloride, Et<sub>3</sub>N, DCM, rt, 3h; (b) Zn, HCOONH<sub>4</sub>, MeOH, rt, 3h; (c) CH<sub>3</sub>COBr, Et<sub>3</sub>N, DCM, rt, 12h.

## 2.12 Conformational analyses

Conformational analyses were performed using single crystal X-ray diffraction studies of compounds **6** and **9** and the solution state conformation of **6** was determined using 2D NOESY studies.

**2.12.1 Single crystal X-ray diffraction studies:** Solid-state studies were performed using single crystal X-ray analysis that revealed the presence of C-9 turn in the turn units **6** and **9**. A closer examinations of the crystal structures showed the presence of a large value of ' $\omega$ ' = 163° for a sulphonamide bond around the folding core - a conformation similar to those observed for a carboxamide bond of Ant-Pro unit.

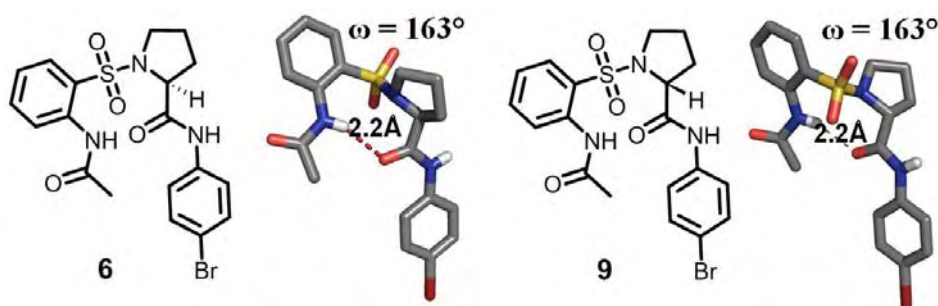


**Fig. 210:** Molecular structures and crystal structures of compounds **6** and **9** showing C-9 H-bonding.

**2.12.2 Solution state 2D NOESY NMR studies:** The three dimensional conformation of compound **6** in solution state was analysed and confirmed using 2D NOESY studies.

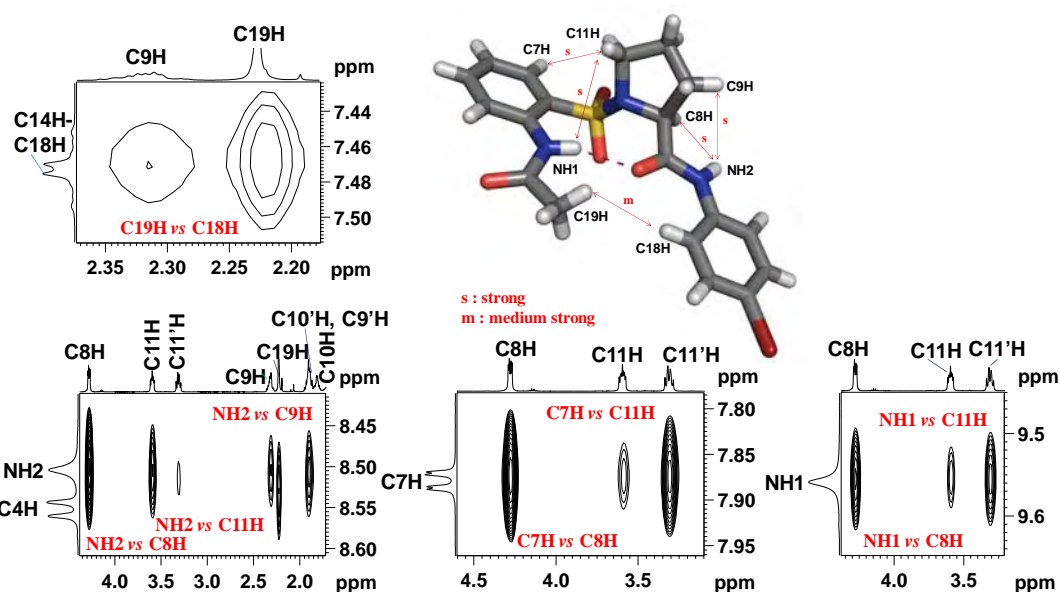


**Fig. 211:** 2D NOESY extracts of molecule **6** showing C-9 H-bonding (500MHz, CDCl<sub>3</sub>).

The characteristic nOes like C19H vs. C18H, NH1 vs. C11H, C7H vs. C11H supported the three dimensional conformation of the dipeptide unit featuring <sup>S</sup>Ant-Pro reverse turn unit. A similar C-9 turn like conformation was observed for its exact configurational isomer **9** featuring a <sup>S</sup>Ant-<sup>D</sup>Pro reverse turn unit.

**2.12.3 DMSO-*d*<sub>6</sub> titration studies of **6**:** DMSO-*d*<sub>6</sub> titration studies of compound **6** were done at two different concentrations (10mM and 2mM). In both cases, NH1 which involved in intra-molecular hydrogen bonding (C<sub>9</sub> hydrogen bonding) showed negligible shift ( $\Delta\delta$  NH: <0.18 ppm), while NH2 which is not involved in *intra*-molecular hydrogen bonding (C<sub>9</sub> hydrogen-bonding) showed considerable shift of 1.09 ppm. Note that NH1 revealed closely similar graph (fig 2.12) at both concentrations, indicating the high stability of *intra*-molecular hydrogen bonding (C<sub>9</sub>) in **6**.

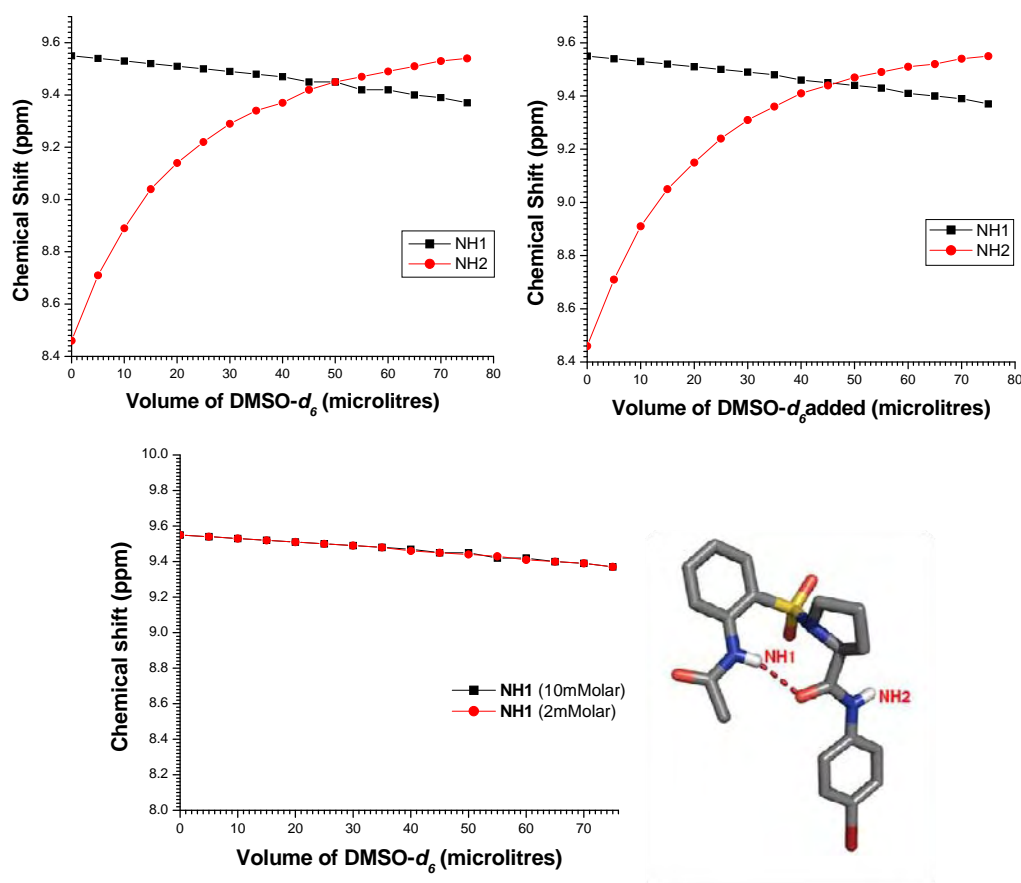


**Fig. 2.12:** Solution-state NMR experiments of compound **6** - DMSO-*d*<sub>6</sub> titration studies (400MHz, CDCl<sub>3</sub>) at 10 mM solution and 2 mM solution and combined graph of NH1 at 10 mM & 2 mM, showing the dilution effect.

**2.12.4 MeOD exchange studies of **6**:** Due to the poor solubility of compound **6** in methanol, the deuterium exchange of the amide protons (NH/D) was carried out at 400



MHz by dissolving the compound in  $\text{CDCl}_3$  (0.5 ml, 10 mM) and methanol- $d_4$  (0.1mL). The experiment was initiated immediately using the following parameters: number of scans = 16, relaxation delay = 1 sec, flip angle =  $30^\circ$ , spectral width = 8223. The  $^1\text{H}$  NMR spectra were recorded at every 1-2 min for 32 minutes and then at intervals of 5 minutes up to 1 hour and finally up to 67 hours at 296K. A stacked plot using Bruker Topspin 3.0.b.8 software at different time intervals was plotted (fig. 2.13).

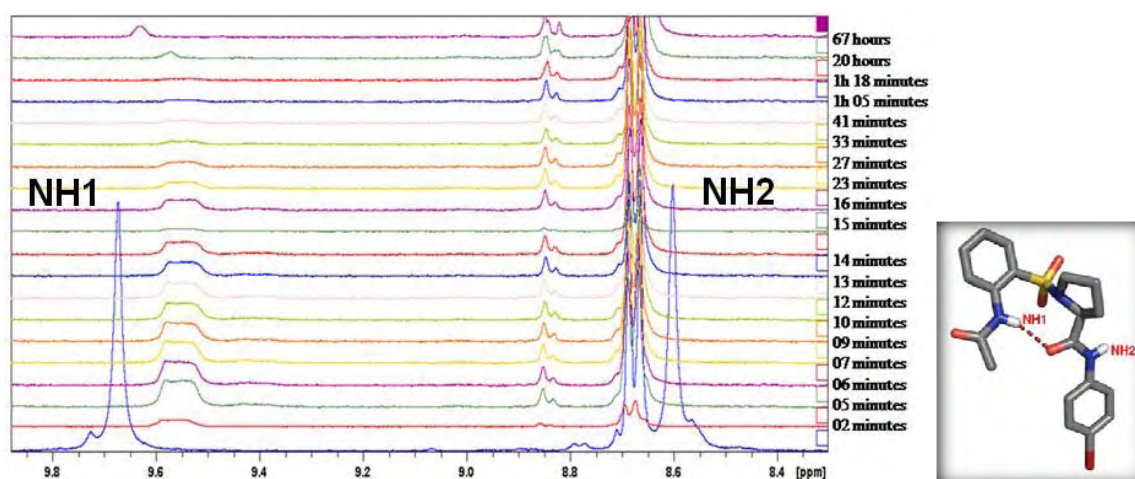


**Fig. 2.13:** MeOD exchange studies in  $\text{CDCl}_3$  (500MHz,  $\text{CDCl}_3$ ).

The major inferences of MeOD exchange studies include; (a) Within 2 minutes after addition of  $\text{MeOH-}d_4$ , the NH (8.6ppm) which was participating in intermolecular hydrogen bonding vanished quickly, (b) The NH (9.65ppm) which was involved in intramolecular C (9) hydrogen-bond persisted even after 67 hours. The small upfield shift was observed presumably due to the prevention of aggregation.

### 2.13 The unusual conformational similarity of sulfonamides and carboxamides: Consequence of the robustness of $^{\text{S}}\text{Ant-Pro}$ *inter-residual* C<sub>9</sub> hydrogen-bond

As discussed earlier, the sulfonamides in general show substantial geometrical and conformational preferences which are distinctly different from that of carboxamides. Surprisingly, an unusual conformational similarity was seen on swapping of Ant-Pro carboxamide with sulfonamide. A recent statistical survey on sulfonamide conformations showed that among 941 structures, there are only two examples of the torsion angle ' $\omega$ ' larger than  $140^\circ$ .<sup>91</sup> Extensive structural investigations over  $^{\text{S}}\text{Ant-Pro}$  systems showed that the unusual conformational similarity was attained in order to compromise for the

persistence of C-9 hydrogen bonding, which is discussed in detail in the following section.

## 2.14 Conformational investigations

The conformational investigations of compounds **13** (carboxamide) and **6** (sulfonamide) were carried out using single crystal X-ray diffraction. Solution state NMR studies of **6** was carried out to support the three dimensional structure of **6**. The strength of C-9 bond in the sulfonamide analogue was evaluated using DMSO-*d*<sub>6</sub> titration studies, dilution studies in CDCl<sub>3</sub> in presence of DMSO-*d*<sub>6</sub> and methanol-*d*<sub>4</sub> exchange of NHs.

**2.14.1 Solid state structural investigations:** The two-residue Ant-Pro motif (anthranilic acid-proline) adopted a robust *pseudo*  $\beta$ -turn conformation featuring a strong 9-membered-ring hydrogen bonding, formed in the forward direction of the sequence 1→2. Since sulfonamides themselves have twisted conformation, the effect of swapping the central carboxamide group in Ant-Pro dipeptide, **13** with a sulfonamide group, as in compound **6**, was investigated.

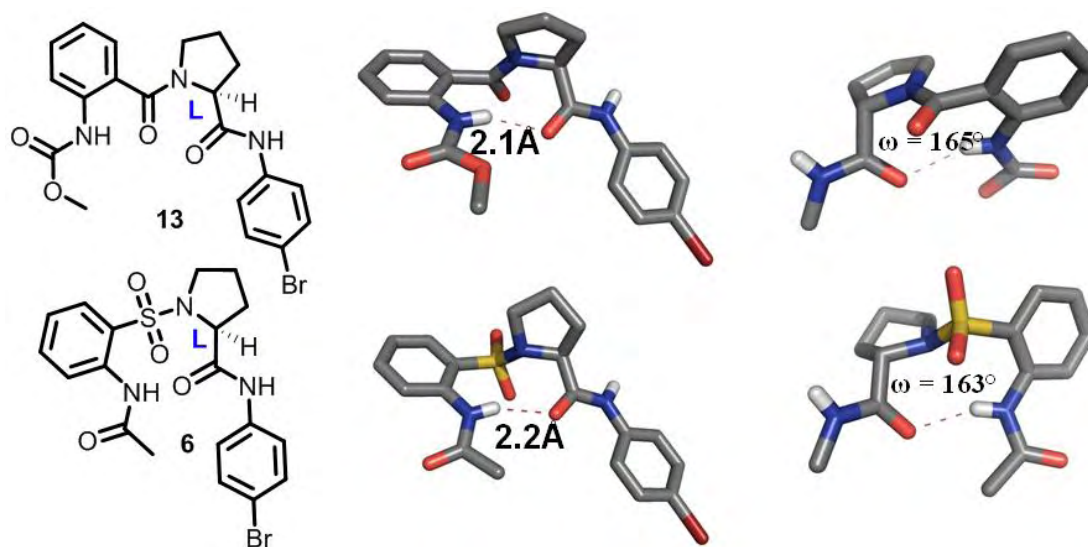


**Fig. 2.14:** Molecular structures (left), corresponding crystal structures (middle) of **13** and **6** dipeptide units and their expanded H-bonded site (right) showing high degree of conformational resemblance.

Considering the substantial geometrical and hydrogen-bonding differences of carboxamides and sulfonamides, a significant difference in their conformational feature was anticipated. The results of the crystallographic analysis on **6** and the carboxamide analogue of **6** indicated that a similar conformational feature was displayed by both peptide units. The sulfonamide in **6** and **9** featured a highly deviated ' $\omega$ ' ( $163^\circ$ ), which is

comparable to the ' $\omega$ ' of carboxamide ( $\sim 165^\circ$ ). This striking conformational similarity is due to the very strong *intra*-molecular hydrogen bonding that connects the N- and C-termini of the folded structure, which restrained the sulfonamide from attaining its preferred ' $\omega$ ' value ( $\sim 90^\circ$ ).

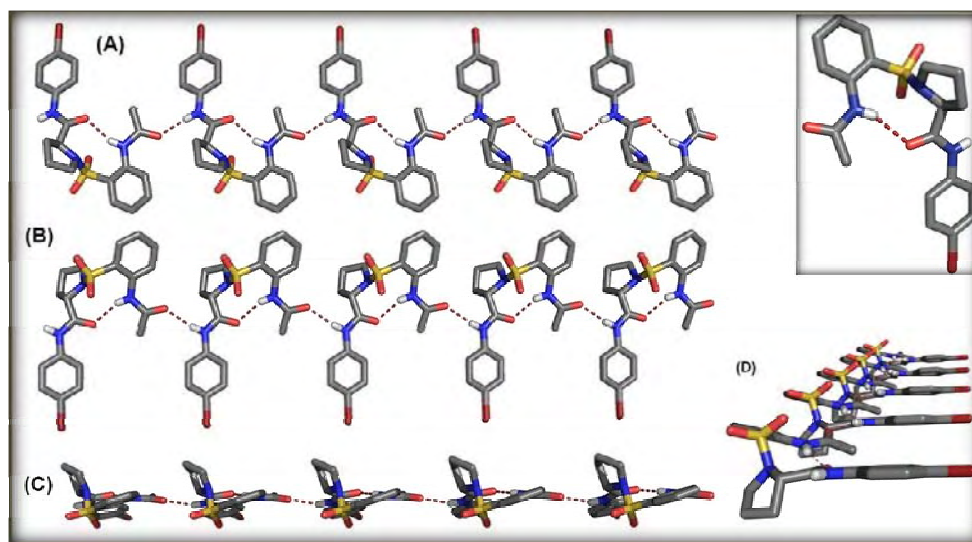


**Fig. 2.15:** Molecular crystal packing (different views) observed for compound **6** (A-D).

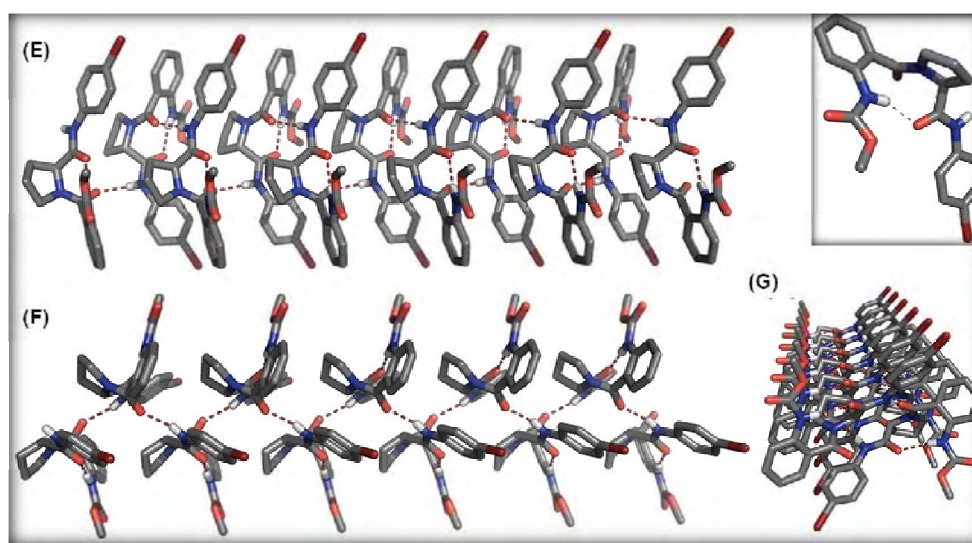


**Fig. 2.16:** Molecular crystal packing (different views) observed for compound **13** (E-G).

Compound **13** (carboxamide) displayed a highly close-packed arrangement of molecules in crystals (fig. 2.15), mediated by *intra*-molecular 9-membered hydrogen bonding ( $2.098 \text{ \AA}$ ) and *inter*-molecular hydrogen bonding ( $2.006 \text{ \AA}$ ) between the CO of Ant ring and 4-Br aniline. On the other hand compound **6** (sulfonamide) showed a linear array (fig. 2.15A-D) of molecules, self-assembled by *intra*-molecular 9-membered ( $2.224$

Å) hydrogen bonding and *intra*-molecular hydrogen bonding (2.197 Å) between the acetyl CO of one molecule and 4-bromo anilide 'NH'. This confirmed that the similar conformational feature was not due to molecular crystal packing.

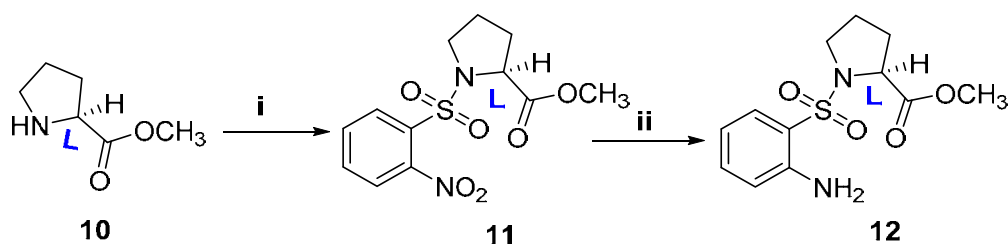
**2.14.2 Solution state IR dilution studies:** IR dilution studies of **13** and **6** at concentrations from 10 mM solutions to 0.625 mM solutions were recorded in CDCl<sub>3</sub> and the IR stacked plots were obtained (see experimental section, page 191-192, figure 9-12, for details). The sample concentrations in CDCl<sub>3</sub> were prepared separately and 25 µl of each sample was used to record spectra using NaCl crystal. Both compounds showed negligible shift in IR NH values. Compound **13** and **6** showed IR absorption peaks at 3445 and 3444 cm<sup>-1</sup> respectively. Compound **13** showed a difference of 6 cm<sup>-1</sup> in frequency from 3445cm<sup>-1</sup>, while the intensity decreased with dilution. Compound **6** showed an almost negligible shift from 3444 cm<sup>-1</sup>. These comparisons showed a significant strength as well as similarity in the *intra*-molecular nine-membered H-bonding observed in **13** and **6**. This observation was also seen in the IR absorption values of CO. In **13**, CO showed a negligible shift of 1 cm<sup>-1</sup> between the 1640 and 1641 cm<sup>-1</sup>, and compound **6** showed a shift of 4 cm<sup>-1</sup> from 1641 to 1645 cm<sup>-1</sup>, upon dilution.

### 2.15 Role of *intra*-residual hydrogen-bonding in stabilizing the <sup>S</sup>Ant-Pro turn formation.

The similar conformational feature displayed by Ant-Pro carboxamides and sulfonamides, maintaining the 9-membered-ring hydrogen bonding intact, are startling considering the fact that sulfonamides and carboxamides are well-documented to display substantially different hydrogen bonding preferences and conformational characteristics. To understand clearly the role of *intra*-residual H-bonding (C-9 H-bonding), the ester analogue **12** of **6** was synthesized, expecting the absence of C-9 H-bonding as observed in amide **6**. As anticipated, the C-terminal ester analogue **12** failed to form the closed 9-membered ring hydrogen bonding, owing to the reduced hydrogen-bonding potential of its ester carbonyl.<sup>92-96</sup>

### 2.16 Synthesis

H<sup>L</sup>-Pro-OMe was sulfonylated with 2-nitrobenzene sulfonyl chloride yielding **11**, which was subjected to nitro reduction using zinc and ammonium formate to yield the free amine ester **12**.

**Scheme 2.2:** Synthesis of <sup>S</sup>Ant-Pro amino-ester

*Reagents and Conditions:* (i) 2-nitro benzene sulfonyl chloride, Et<sub>3</sub>N, DCM, rt, 3h; (ii) Zn, HCOONH<sub>4</sub>, MeOH, rt, 3h; (iii) Ac<sub>2</sub>O, Et<sub>3</sub>N, DCM, rt, 12h.

**2.17 Conformational investigations in solid state:** The amino ester **12** although possessing a Pro residue, did not adopt the unusually large ‘ $\omega$ ’ as **6** (fig. 2.15). This is presumably because of the fact that compound **12** does not have the opportunity to form the 9-membered hydrogen bonding, owing to the reduced hydrogen bonding potential of the ester carbonyl, as noted earlier. Thus, in the absence of the 9-membered ring hydrogen bonding, the sulfonamide in **12** exploited its freedom to adopt the usually observed value for  $\omega \sim 90^\circ$ . Also, the hydrogen bonding interaction played a crucial role in coercing **6** to adopt the unusually large ‘ $\omega$ ’ (163°) as clearly understood by the following analysis by single crystal X-ray diffraction studies of compounds.

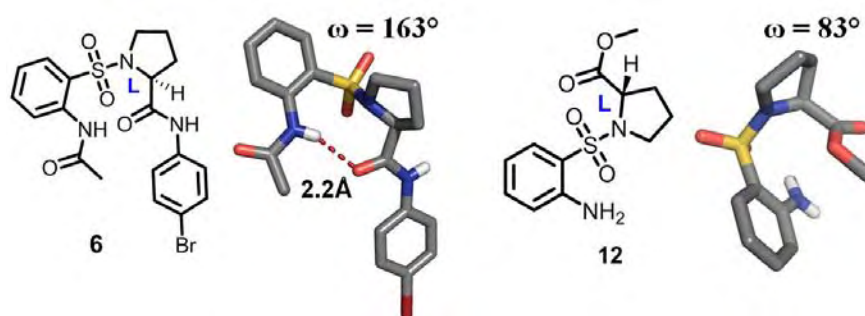


**Fig. 2.17:** Molecular structures (left) and corresponding crystal structures (right) of compounds **6** and **12**. Note that the C-terminal ester analogue fails to form C-9 H-bonding

### 2.18 Stability of methyl ((2-aminophenyl)sulfonyl)prolinate: Formation of thiadiazepinones

An intriguing geometrical preference was exerted by the sulfonamide in the cyclization tendency of the amino esters **12** and **14**. Whereas, the amino ester **14** cannot be isolated owing to its high tendency for cyclization leading to the formation of diazepine **15**, its corresponding sulfonamide analog **12** was found to be surprisingly stable and isolable. However, compound **16** (i.e. (S)-1,2,3,11a-tetrahydrobenzo[f]pyrrolo[1,2-

b)[1,2,5]thiadiazepin-11(10H)-one 5,5-dioxide) was obtained in our case during peptide coupling as a side reaction (fig. 2.17). The synthetic obscurity in the spontaneous cyclization of Ant-Pro esters leading to the formation of 2,3-dihydro-1H-benzo[e]pyrrolo[1,2-a][1,4]diazepine-5,11(10H,11aH)-dione<sup>97-101</sup> (compound **16**) usually occurs due to the closer positioning of the amino and ester termini of the building block, due to which it leads to the failure of reverse sequence approach for synthesis in Ant Pro oligomers. The <sup>S</sup>Ant-Pro unit seems to have an additional advantage in this regard.

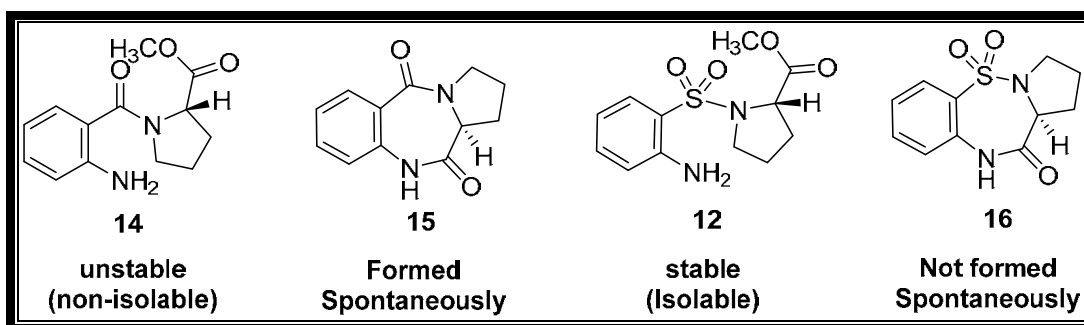


**Fig. 2.18:** Comparison of the stability of NH<sub>2</sub>-Ant-Pro ester (compound **14**) with its side product diazepinone (compound **15**) and NH<sub>2</sub>-<sup>S</sup>Ant-Pro ester (compound **12**) with the side product thiodiazepinone derivative (compound **16**)

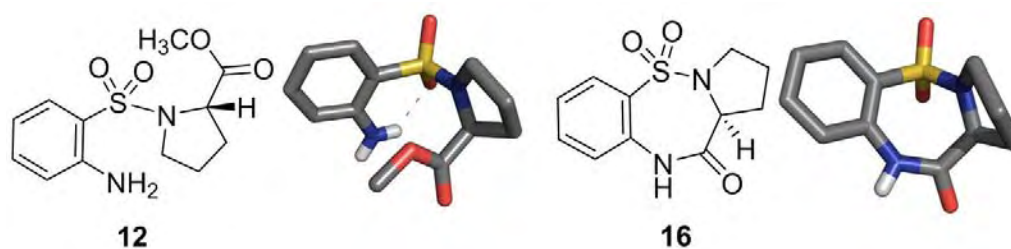


**Fig. 2.19:** Molecular structures and crystal structures of <sup>S</sup>Ant-Pro amine (compound **12**) and its cyclised product (compound **16**).

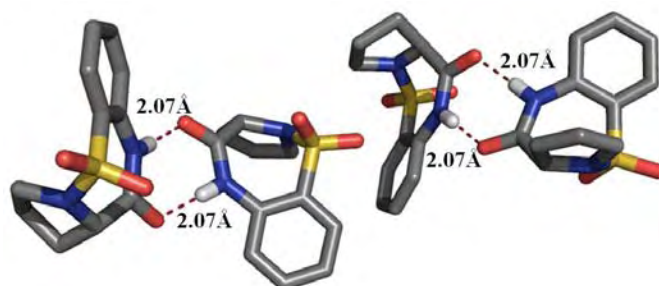


**Fig. 2.20:** Crystal structures showing the dimer formation of compound **16**, by hydrogen bonding. *Note:* compound **16** exists in two conformations in crystals.

Compound **16** existed as two (dimer) conformations in the solid state. The molecules in the dimers were seen connected by self-assembling primary amide intermolecular H-bonding interactions<sup>102-103</sup> ( $d(\text{NH}\cdots\text{O}) = 2.07\text{\AA}$ ). Considering the bioactive potential of benzo-diazepinones<sup>97</sup>, compound **16**, a sulfonamide derivative, benzo-thia-diazepines are anticipated to act as a potent bioactive compounds.<sup>97</sup>

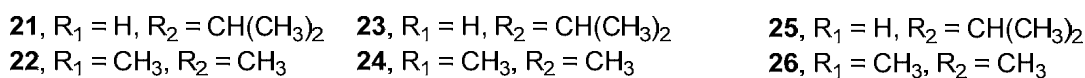
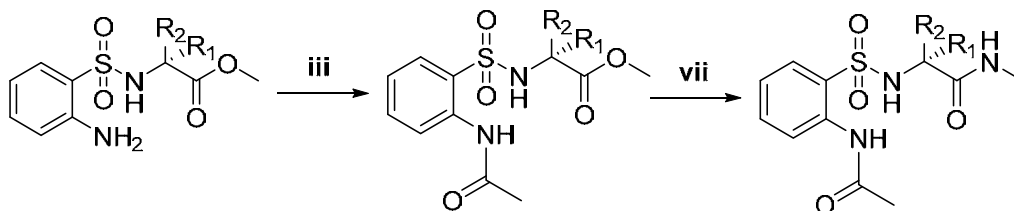
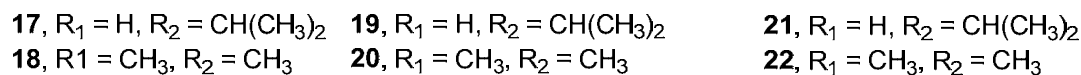
## Reverse Turn Formation in <sup>S</sup>Ant-AA Residues: Role of Sulfonamide in Inducing Folding

### 2.19 Objective of the work: Role of <sup>S</sup>Ant in <sup>S</sup>Ant-Pro C-9 turn formation

Reverse turn motifs featuring orthanilic acid (<sup>S</sup>Ant) and proline showed a nine membered hydrogen bonding in the forward direction of the turn. The surprising conformational similarity observed in carboxamides and sulfonamides prompted us to compare the role of proline<sup>104</sup> residue in the stability of the 9-membered hydrogen bonded ring. Proline, apart from other natural  $\alpha$ -aminoacids, induces interesting conformational features in peptides because of its unique dihedral angle preferences owing to its cyclic constraints. In order to investigate the role of <sup>S</sup>Ant, the features of proline which contribute for folding were analyzed and removed in <sup>S</sup>Ant-Pro turn motif. The cyclic constraints of proline were detached by replacing it with open chain amino acids like valine (a sheet inducer) and Aib ( $\alpha$ -aminoisobutyric acid - turn inducer). Aib, being constraint at C $_{\alpha}$  position with unique dihedral angles  $\phi = 60^{\circ}$  and  $\psi = 30^{\circ}$ , is considerably conformationally restricted to act as a sheet breaker.<sup>59,105-106</sup> The part of N-alkyl constraint of proline was evaluated by N-methylation of open chain amino acid derivatives - a strategy which induces turn in peptides.<sup>107-108</sup>

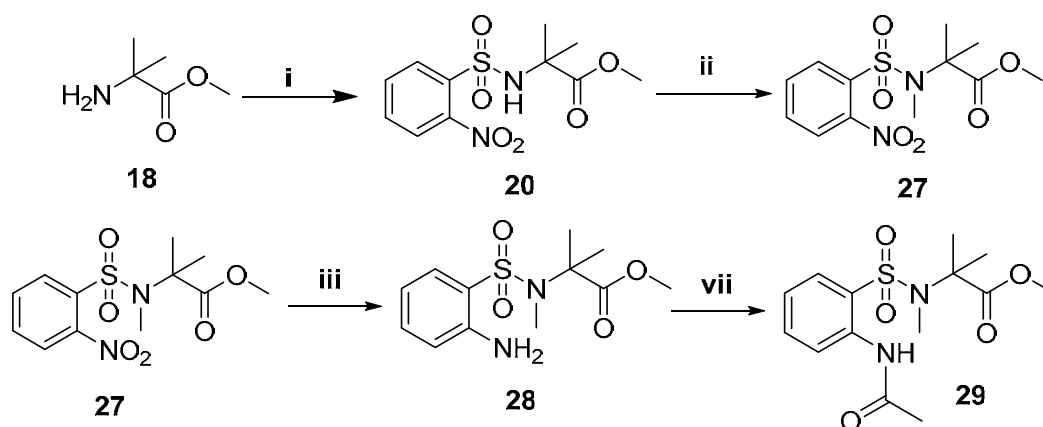
### 2.20 Synthesis

In order to understand the role of proline in 9-membered hydrogen bond formation, proline in the dipeptide unit was replaced by open chain amino acid analogues <sup>L</sup>Val and Aib. The methyl esters of L-valine and Aib were sulfonylated with 2-nitrobenzenesulfonyl chloride yielding **19** and **20**, respectively, which were subjected to nitro reduction, using zinc and ammonium formate in methanol, to yield the free amine ester **21** and **22**, respectively. Upon acetylation, using acetylchloride in presence of Et<sub>3</sub>N in DCM, and subsequent amidation, using methylamide, **25** and **26**, respectively were obtained.

**Scheme 2.3:** Synthesis of <sup>s</sup>Ant-AAs dipeptide units


**Reagents and Conditions:** (i) 2-nitrobenzenesulfonyl chloride, Et<sub>3</sub>N, DCM, rt, 3h; (ii) Zn, HCOONH<sub>4</sub>, MeOH, rt, 3h; (iii) CH<sub>3</sub>COCl, Et<sub>3</sub>N, DCM, rt, 12h.

Further, the role/effect of the N-methyl constraint of proline was examined by the use of N-methyl open chain amino acid N-*Me*-Aib. Compound **20** was methylated using methyl iodide in presence of silver oxide in DMF to form **27**. Compound **27** was then subjected to nitro reduction, followed by acetylation yielding **29**.

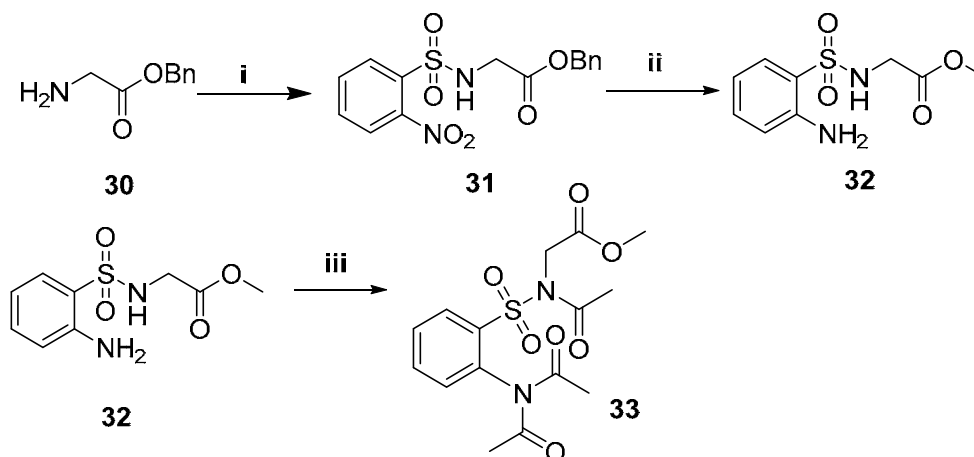
**Scheme 2.4:** Synthesis of <sup>s</sup>Ant-N-alkyl-AA dipeptide units


**Reagents and Conditions:** (i) 2-nitrobenzenesulfonyl chloride, Et<sub>3</sub>N, DCM, rt, 3h; (ii) Ag<sub>2</sub>O, CH<sub>3</sub>I, DMF, rt, 12h; (iii) Zn, HCOONH<sub>4</sub>, MeOH, rt, 3h; (vii) CH<sub>3</sub>COCl, Et<sub>3</sub>N, DCM, rt, 12h.



Glycine benzyl ester was sulfonylated by 2-nitrobenzenesulfonyl chloride to obtain **31**, which upon treating with Zn and HCOONH<sub>4</sub> underwent simultaneous nitro reduction and benzyl to methyl *trans*-esterification yielding **32**. Compound **32** was then subjected to acetylation using excess Ac<sub>2</sub>O in presence of Et<sub>3</sub>N in DCM to yield completely acetylated product **33**.

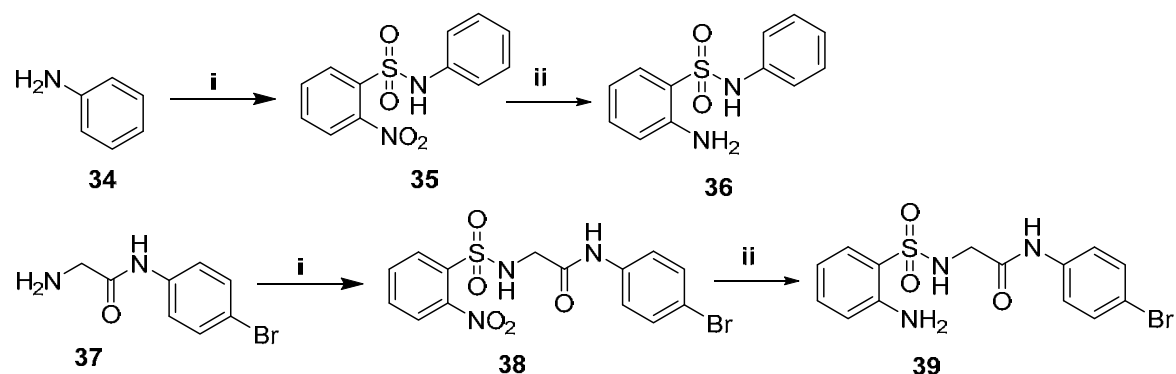
**Scheme 2.5:** Synthesis of **33**



*Reagents and Conditions:* (i) 2-nitrobenzenesulfonyl chloride, Et<sub>3</sub>N, DCM, rt, 3h; (ii) Zn, HCOONH<sub>4</sub>, MeOH, rt, 3h; (iii) (CH<sub>3</sub>CO)<sub>2</sub>O, Et<sub>3</sub>N, DCM, rt, 12h.

It has been noted that N-acetylation of primary amides generally requires special reaction conditions. Compounds **36** and **39** were obtained by following the corresponding procedures (scheme 2.5)

**Scheme 2.6:** Synthesis of NH<sub>2</sub>-<sup>S</sup>Ant-R



*Reagents and Conditions:* (i) 2-nitrobenzenesulfonyl chloride, Et<sub>3</sub>N, DCM, rt, 3h; (ii) Zn, HCOONH<sub>4</sub>, MeOH, rt, 3h.

### 2.21 <sup>S</sup>Ant-NMe-Aib featuring C-9 Turn: Conformational investigations in solid state

In order to confirm the role of proline in <sup>S</sup>Ant-Pro C-9 turn formation, proline in the turn unit was replaced with N-methyl-Aib. The dipeptide unit, *i.e.* the <sup>S</sup>Ant-NMe Aib turn system, featured nine-membered hydrogen bonding as similar to that observed for <sup>S</sup>Ant-Pro turn. The turn formation also confirmed the possibility of cyclic and N-methyl constraints of proline which are responsible for the <sup>S</sup>Ant-Pro turn formation. It was also noted that, the necessity of large value of 'ω' (ω = 155° for sulfonamide bond) can also be explained as a requirement for turn formation in <sup>S</sup>Ant-AA dipeptide units. As the N-methylation represents a general strategy used for inducing turn in peptides,<sup>108</sup> the versatility of proline in inducing the turn can be once again understood.

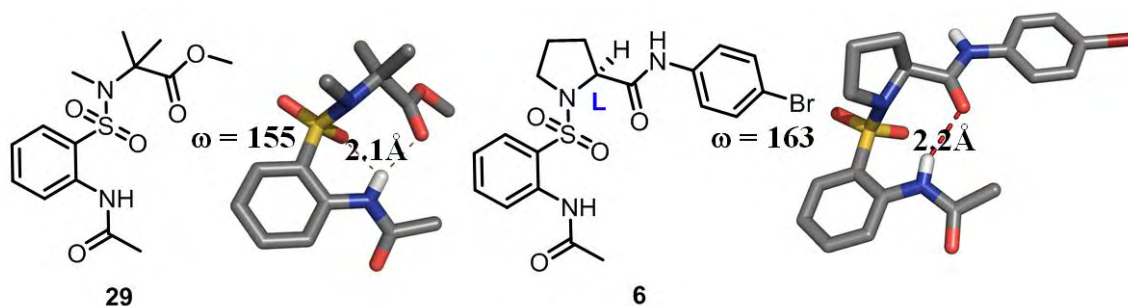


**Fig. 2.21:** Molecular structures and crystal structures of <sup>S</sup>Ant-NMe-Aib (**29**) and <sup>S</sup>Ant-Pro (**6**) turn motifs.

As <sup>S</sup>Ant-NMe Aib turn system showed a 9-membered hydrogen bonding upon using N-methylated amino acid Aib, the role of N-methylation was assessed by removing the N-methylation and exposing the NH of Aib for turn formation as in <sup>S</sup>Ant-Aib dipeptide analogues. Analogues featuring <sup>S</sup>Ant-AA turn systems *viz.* <sup>S</sup>Ant-Aib and <sup>S</sup>Ant-Val were synthesized. Crystallographic investigations of analogues **23**, **24**, **25** and **26** clearly revealed the absence of 9-membered hydrogen bonded ring observed in the N-methyl system **29**, thereby suggesting that the N-alkyl constraint of proline was also crucial in the stability of <sup>S</sup>Ant-Pro nine-membered hydrogen bonded ring. The turn system now carries the *intra*-residual C-6 hydrogen-bonding of <sup>S</sup>Ant. Even though there is absence of *inter*-residual C-9 hydrogen-bonding, these analogues show folding at the sulfonamide bond.

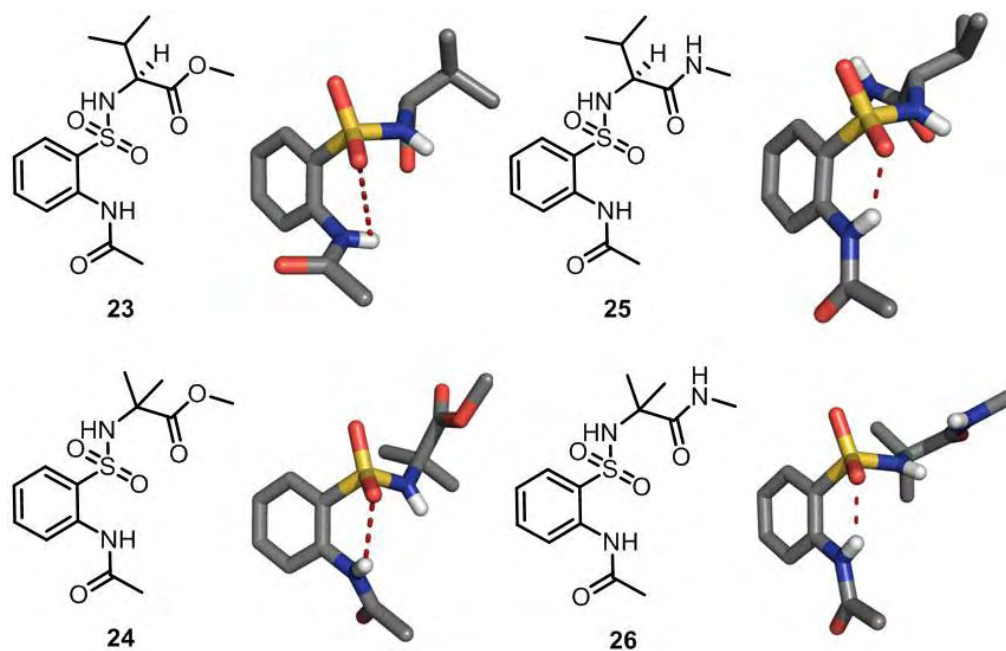


**Fig. 2.22:** Molecular structures and corresponding crystal structures of  $^5\text{Ant-AA}$  dipeptide units showing folding at the  $^5\text{Ant}$  unit.

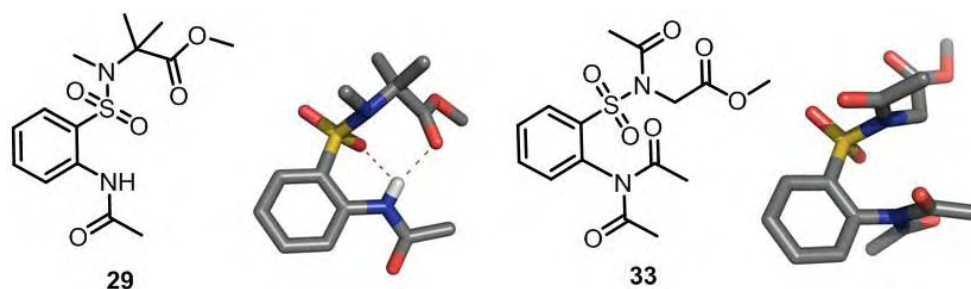


**Fig. 2.22:** Molecular structures and corresponding crystal structures of  $^5\text{Ant-NR-AA}$  dipeptide units showing folding at the  $^5\text{Ant}$  unit.

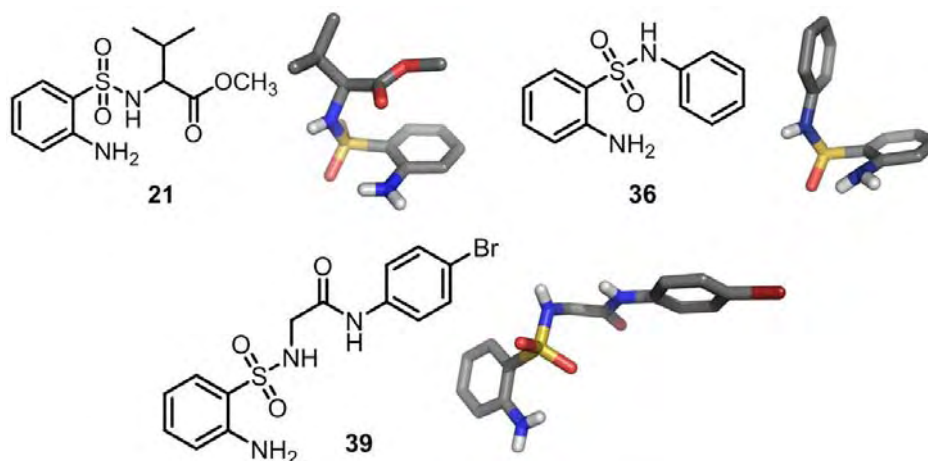


**Fig. 2.23:** Molecular structures and crystal structures of orthanilamides showing folding at sulfonamide bond.

A dipeptide analogue, devoid of all the NHs, was synthesized to determine the role of sulfonamide in folding due to orthanilic acid. The dipeptide analogue **33**, even in the absence of hydrogen bonding, showed folding (twist) at the sulphonamide bond. The solid state studies, involving hydrogen bonding parameters and torsion angle analysis of the crystal structures, also showed the role of sulfonamide in inducing folding in the conformation. In the absence of the 9-membered ring hydrogen bonding, the orthanilamides featured 6-membered-ring hydrogen bonding as seen in the sulfonamide derivatives **21**, **36** and **39**.

## 2.22 Crystallization tendency of sulfonamides

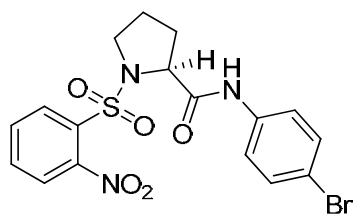
As noted earlier, sulfonamides have higher tendency for crystal formation and the crystals formed are of high quality having R-factor sometimes called residual factor or reliability factor or the R-value or  $R_{\text{work}}$ . This may be due to the presence of heavy atom sulfur and the presence of additional acceptor oxygen of  $\text{SO}_2$  group which can form more than one hydrogen bonding interaction.

## 2.23 Conclusions

The present study described a 9-membered *pseudo  $\beta$ -turn* formation in reverse turns featuring orthanilic acid and proline. It also explained the unusual structural and conformational similarity revealed by the two peptides featuring a carboxamide (Ant-Pro turn) and a sulfonamide ( $^{\text{S}}$ Ant-Pro) at the folding core. This is unusual given the fact that these groups have strikingly different hydrogen bonding and geometrical preferences. The unusual similarity could be attributed presumably to the strong *intra*-molecular 9-membered ring hydrogen bonding that forces the backbone to fold. The chapter also described the stability of amino  $^{\text{S}}$ Ant-Pro ester, when compared to its close analog amino Ant-Pro ester, which spontaneously formed diazepinones. But the thia-diazepinone formation was not found to be spontaneous owing to the geometrical differences created by the sulfonamide bond. The absence of 9-membered hydrogen bonding networks, which featured in  $^{\text{S}}$ Ant-Pro reverse turns, in the analogues  $^{\text{S}}$ Ant-AA dipeptide residues confirmed the role of proline in the turn formation. On the other hand, the N-methylation of the  $\alpha$ -amino acid residues induced the C-9 turn formation justifying the effect of N-methylation. It also explained the role of  $^{\text{S}}$ Ant (sulfonamides) in turn formation.

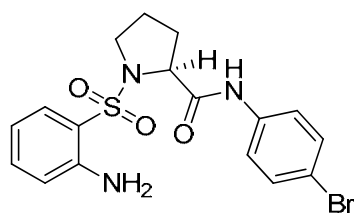
## 2.24 Experimental procedures

### (S)-N-(4-bromophenyl)-1-(2-nitrophenylsulfonyl)pyrrolidine-2-carboxamide **4**



To a solution of compound H-<sup>L</sup>Pro *p*-Br anilide (1.35g, 5.02mmols) in DCM (20mL), Et<sub>3</sub>N (2mL, 1.5g, 15mmols) was added, followed by 2-nitrobenzenesulfonyl chloride (0.926g, 4.18mmols) and 25% wt. of DMAP (0.030g). After 12 hours, the reaction mixture was diluted with DCM (5mL) and the organic layer was washed with saturated solutions of sodium bicarbonate (10mL), potassium bisulphate (10mL), water (10mL) and saturated NaCl solution (10mL). The organic layer was dried over anhydrous Na<sub>2</sub>SO<sub>4</sub> solution and evaporated under reduced pressure to obtain the crude product which was purified by column chromatography, (50:50 pet. ether/ethyl acetate, R<sub>f</sub>: 0.5) to afford **4** as a colorless viscous liquid (1.76g, 93%) [ $\alpha$ ]<sub>D</sub><sup>28</sup>: -121° (*c* = 0.1, CHCl<sub>3</sub>); IR (CHCl<sub>3</sub>,  $\nu$  (cm<sup>-1</sup>): 3019, 1691, 1625, 1591, 1546, 1370, 1215; <sup>1</sup>H NMR (CDCl<sub>3</sub>/400MHz): 8.70 (s, 1H), 8.03-8.06 (m, 1H), 7.64-7.69 (m, 2H), 7.57-7.59 (m, 1H), 7.30-7.35 (m, 4H), 4.52-4.55 (dd, *J*=8.51, *J*=2.55, 1H), 3.54-3.66 (m, 2H), 2.27-2.34 (m, 1H), 2.08-2.18 (m, 1H), 1.88-2.03 (m, 2H); <sup>13</sup>C NMR (CDCl<sub>3</sub>, 105MHz):  $\delta$  ppm 169.0, 165.4, 148.0, 136.3, 134.4, 132.0, 131.6, 131.1, 130.5, 124.0, 121.2, 116.9, 62.5, 49.5, 38.5, 30.8, 24.4; LC-MS: 475.97 (M+Na)<sup>+</sup>; Elemental analysis calculated for C<sub>17</sub>H<sub>16</sub>BrN<sub>3</sub>O<sub>5</sub>S: C, 44.94; H, 3.55; N, 9.25; Found: C, 44.33; H, 3.97; N, 8.84.

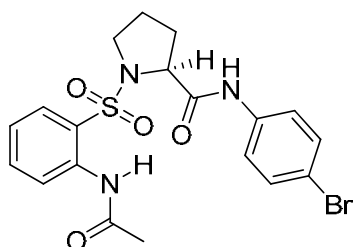
### (S)-1-(2-aminophenylsulfonyl)-N-(4-bromophenyl)pyrrolidine-2-carboxamide **5**



To a solution of compound **4** (2g, 4.4moles) in MeOH (10mL), anhydrous HCOONH<sub>4</sub> (2.77, 44.02) and activated Zn (2.87, 44.02, pre-treated with HCl and thoroughly washed with water and ether prior to use) were added and stirred at room temperature for 3 hours. The reaction mixture was then filtered through Celite and the filtrate was evaporated under reduced pressure. The residue obtained was dissolved in DCM (10mL) and purified by column chromatography, (65:35 pet. ether/ethyl acetate, R<sub>f</sub>: 0.5) to afford **5** as a colorless viscous liquid (1.8, 97%). [ $\alpha$ ]<sub>D</sub><sup>27</sup>: -130° (*c* = 0.1, CHCl<sub>3</sub>); IR (CHCl<sub>3</sub>,  $\nu$  (cm<sup>-1</sup>): 3384, 3019, 1686, 1591, 1520, 1340, 1306, 1215; <sup>1</sup>H NMR (CDCl<sub>3</sub>/400MHz):  $\delta$  ppm 8.84

(s, 1H), 7.66-7.69 (m, 1H), 7.38-7.46 (m, 4H), 7.29-7.33 (m, 1H), 6.72-6.90 (m, 2H), 5.16 (s, 2H) 4.42-4.45 (dd,  $J=8.98$ ,  $J=2.94$ , 1H), 3.44-3.54 (m, 2H), 2.28-2.34 (m, 1H), 1.91-2.03 (m, 1H), 1.72-1.86 (m, 2H);  $^{13}\text{C}$  NMR ( $\text{CDCl}_3$ , 100MHz):  $\delta$  ppm 169.4, 146.2, 136.4, 135.1, 131.7, 130.3, 121.3, 118.0, 117.0, 62.1, 49.6, 30.4, 24.5; LC-MS: 445.99 ( $\text{M}+\text{Na}$ ) $^+$ ; Elemental analysis calculated for  $\text{C}_{17}\text{H}_{18}\text{BrN}_3\text{O}_3\text{S}$ : C, 48.12; H, 4.28; N, 9.90; Found: C, 47.94; H, 4.76; N, 9.23.

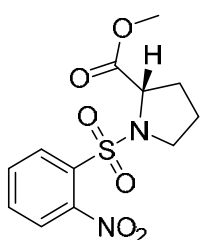
### (S)-1-(2-acetamidophenylsulfonyl)-N-(4-bromophenyl)pyrrolidine-2-carboxamide 6



To a solution of compound **5** (0.4g, 9.42mmoles) in DCM (10mL),  $\text{Et}_3\text{N}$  (0.4mL, 2.86g, 28.28mmoles) was added followed by acetyl chloride (0.11mL, 0.1739g, 14.28mmoles). After 3 hours, the reaction mixture was diluted with DCM (5mL) and the organic layer was washed with saturated solutions of sodium bicarbonate

(5mL), potassium bisulphate (5mL), water (5mL) and NaCl (5mL). The organic layer was dried over anhydrous  $\text{Na}_2\text{SO}_4$  solution and evaporated under reduced pressure to obtain the crude product which was purified by column chromatography, (30:70 pet. ether/ethyl acetate,  $R_f$ : 0.5) to afford **6** as a white crystalline solid (0.35, 80%). mp: 198-200°C;  $[\alpha]_{\text{D}}^{28}$ : -129° ( $c = 0.1$ ,  $\text{CHCl}_3$ ); IR ( $\text{CHCl}_3$ ,  $\nu$  ( $\text{cm}^{-1}$ ): 3020, 1699, 1589, 1521, 1427, 1338, 1217;  $^1\text{H}$  NMR ( $\text{CDCl}_3$ /200MHz):  $\delta$  ppm 9.54 (s, 1H), 8.51-8.55 (m, 1H), 8.48 (s, 1H), 7.83-7.88 (dd,  $J=8.09\text{Hz}$ ,  $J=1.52\text{Hz}$ , 1H), 7.58-7.67 (m, 1H), 7.39-7.50 (m, 4H), 7.20-7.28 (m, 1H), 4.22-4.28 (m, 1H), 3.53-3.63 (m, 1H), 3.22-3.34 (m, 1H), 2.26-2.36 (m, 1H), 2.20 (s, 3H) 1.78-1.98 (m, 3H);  $^{13}\text{C}$  NMR ( $\text{CDCl}_3$ ,125MHz):  $\delta$  ppm 170.5, 169.0, 138.1, 136.7, 134.6, 131.8, 129.9, 124.7, 124.4, 121.6, 115.6, 60.9, 49.1, 39.7, 31.7, 24.8, 24.4; ESI-MS: 490.1619 ( $\text{M}+\text{Na}$ ) $^+$ ; Elemental analysis calculated for  $\text{C}_{19}\text{H}_{20}\text{BrN}_3\text{O}_4\text{S}$ : C, 48.93; H, 4.32; N, 9.01; Found: C, 48.14; H, 4.85; N, 8.76.

### (S)-methyl 1-(2-nitrophenylsulfonyl)pyrrolidine-2-carboxylate 11



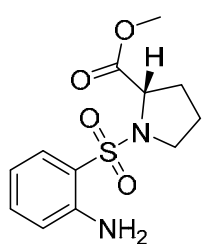
Compound **11** was synthesized following the procedure for **4**

Purified by column chromatography, (40:60 ethyl acetate/pet. ether,  $R_f$ : 0.5) white crystalline solid (67%). mp: 86-88°C;  $[\alpha]_{\text{D}}^{28}$ : -92° ( $c = 0.1$ ,  $\text{CHCl}_3$ ); IR ( $\text{CHCl}_3$ ,  $\nu$  ( $\text{cm}^{-1}$ ): 3020, 1743, 1616, 1523, 1483,

1338, 1215;  $^1\text{H}$  NMR ( $\text{CDCl}_3/200\text{MHz}$ ):  $\delta$  ppm 8.05-8.14 (m, 1H), 7.58-1.74 (m, 3H), 4.55-4.61 (m, 1H), 3.65 (s, 3H), 3.47-3.64 (m, 2H), 2.21-2.35 (m, 1H), 1.88-2.16 (m, 3H);  $^{13}\text{C}$  NMR ( $\text{CDCl}_3$ , 50 MHz):  $\delta$  ppm 172.2, 147.9, 133.5, 132.7, 131.6, 130.9, 123.9, 60.8, 52.3, 48.4, 30.8, 24.4; LC-MS: 337.02 ( $\text{M}+\text{Na}$ ) $^+$ ; Elemental analysis calculated for  $\text{C}_{12}\text{H}_{14}\text{N}_2\text{O}_6\text{S}$ : C, 45.85; H, 4.49; N, 8.91; Found: C, 45.25; H, 4.92; N, 8.34.

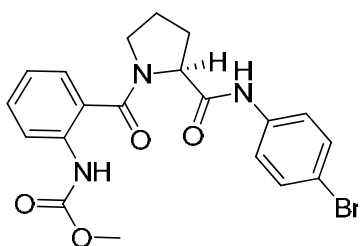
### (S)-methyl 1-((2-aminophenyl)sulfonyl)pyrrolidine-2-carboxylate **12**

Compound **12** was synthesized following the procedure for **5**



Purified by column chromatography, (35:75 ethyl acetate/pet. ether,  $R_f$ : 0.5), white solid (97%), crystallized from methanol. mp: 118-119°C;  $[\alpha]_{\text{D}}^{27}$ :  $-88^\circ$  ( $c = 0.1$ ,  $\text{CHCl}_3$ ); IR ( $\text{CHCl}_3$ ,  $\nu$  ( $\text{cm}^{-1}$ ): 3022, 2890, 1751, 1590, 1546, 1371, 1216;  $^1\text{H}$  NMR ( $\text{CDCl}_3/200\text{MHz}$ ):  $\delta$  ppm 7.67-7.72 (m, 1H), 7.26-7.34 (m, 1H), 6.69-6.76 (m, 2H), 5.27 (s, 2H), 4.48-4.54 (m, 1H), 3.72 (s, 3H) 3.34-3.42 (m, 2H), 1.75-2.28 (m, 4H);  $^{13}\text{C}$  NMR ( $\text{CDCl}_3$ , 100MHz):  $\delta$  ppm 172.9, 146.3, 134.3, 130.2, 118.8, 117.4, 116.6, 59.4, 52.3, 48.4, 30.8, 24.7; LC-MS: 307.04 ( $\text{M}+\text{Na}$ ) $^+$ ; Elemental analysis calculated for  $\text{C}_{12}\text{H}_{16}\text{N}_2\text{O}_4\text{S}$ : C, 50.69; H, 5.67; N, 9.85; Found: C, 50.23; H, 5.15; N, 9.27.

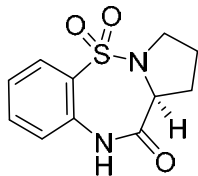
### (S)-Methyl 2-(2-(4-bromophenylcarbamoyl)pyrrolidine-1-carbonyl)phenylcarbamate, **13**



Compound **13**, obtained by following the procedure used for preparation of **1** (*vide supra*), except using methyl chloroformate as the acylating agent, was purified by column chromatography, (30:70 pet. ether/ethyl acetate,  $R_f$ : 0.5) to afford **1** as a white solid (0.076g, 64%) which was later crystallized from a solution of methanol and dichloromethane. mp: 216-220°C;  $[\alpha]_{\text{D}}^{27}$ :  $-23^\circ$  ( $c = 0.1$ ,  $\text{CHCl}_3$ ); IR ( $\text{CHCl}_3$ ,  $\nu$  ( $\text{cm}^{-1}$ ): 3020, 1732, 1686, 1616, 1541, 1427, 1398, 1302, 1215;  $^1\text{H}$  NMR ( $\text{CDCl}_3/200\text{MHz}$ ):  $\delta$  ppm 9.50 (s, 1H), 8.67(s, 1H), 8.25-8.21 (d,  $J=8.26\text{Hz}$ , 1H), 7.38-7.56 (m, 2H), 7.23-7.31 (m, 4H), 7.08-7.18 (m, 2H), 4.96-5.03 (t,  $J=6.69$ , 1H), 3.80 (s, 3H), 3.43-3.71 (m, 2H), 2.27-2.37 (m, 2H), 2.05-2.20 (m, 1H), 1.83-2.00 (m, 1H);  $^{13}\text{C}$  NMR ( $\text{CDCl}_3$ , 50MHz):  $\delta$  ppm 169.7, 169.6 154.1, 137.1, 136.4, 131.3, 127.0, 126.8, 123.7, 122.4, 120.9, 120.4, 116.3, 60.9, 52.4, 50.7, 28.6, 25.2; LC-MS: 470.08 ( $\text{M}+\text{Na}$ ) $^+$ ;

Elemental analysis calculated for  $C_{20}H_{20}BrN_3O_4$ : C, 53.82; H, 4.52; N, 9.42; Found: C, 52.22; H, 5.01; N, 8.79.

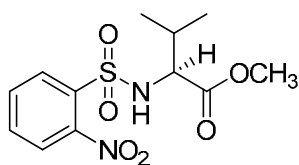
**(S)-1,2,3,11a-tetrahydrobenzo[f]pyrrolo[1,2-b][1,2,5]thiadiazepin-11(10H)-one 5,5-dioxide) 16**



White solid, crystallized from methanol (30:70 pet. ether/ethyl acetate,  $R_f$ : 0.5), mp: 187-189°C; IR ( $CHCl_3$ ,  $\nu$  ( $cm^{-1}$ ): 3022, 1710, 1659, 1588, 1472, 1438, 1332, 1216;  $^1H$  NMR ( $CDCl_3/200MHz$ ):  $\delta$  ppm 8.93 (s, 1H), 7.89-7.93 (m, 1H), 7.48-7.57 (m, 1H), 7.12-7.25 (m, 2H), 4.61-4.68 (m, 1H), 3.45-3.56 (m, 1H), 2.96-3.08 (m, 1H), 2.41-2.58 (m, 1H), 2.11-2.30 (m, 1H), 1.75-2.07 (m, 2H);  $^{13}C$  NMR ( $CDCl_3$ , 100MHz):  $\delta$  ppm 174.8, 134.4, 134.0, 129.3, 129.0, 123.7, 121.5, 63.6, 48.4, 32.4, 24.5; LC-MS: 277.05 ( $M+Na$ )<sup>+</sup>, 293.03 ( $M+K$ )<sup>+</sup>; Elemental analysis calculated for  $C_{11}H_{12}N_2O_3S$ : C, 52.37; H, 4.79; N, 11.10; Found: C, 51.83; H, 5.25; N, 11.46.

**(S)-methyl 3-methyl-2-(2-nitrophenylsulfonamido)butanoate 19**

Compound **19** was synthesized following the procedure for **4**



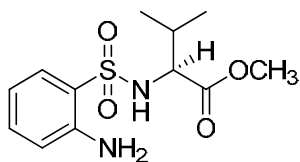
Purified by column chromatography, (70:30 pet. ether/ethyl acetate,  $R_f$ : 0.5), colorless high viscous liquid (77%).  $[\alpha]_D^{28}$ : -46° ( $c = 0.1$ ,  $CHCl_3$ ); IR ( $CHCl_3$ ,  $\nu$  ( $cm^{-1}$ ): 3021, 1740, 1542, 1426, 1361, 1216;  $^1H$  NMR ( $CDCl_3/500MHz$ ):  $\delta$  ppm 8.02-8.05 (m, 1H), 7.89-1.92 (m, 1H), 7.70-7.75 (m, 2H), 6.03-6.05 (d,  $J=9.93Hz$ , 1H), 3.98-4.01 (m, 1H), 3.42 (s, 3H), 2.11-2.19 (m, 1H), 0.99-1.00 (d,  $J=6.69$ , 3H), 0.92-0.93 (d,  $J=6.69$ , 1H);  $^{13}C$  NMR ( $CDCl_3, 125MHz$ ):  $\delta$  ppm 172.0, 147.6, 134.0, 133.6, 132.8, 130.3, 125.5, 62.1, 52.0, 31.4, 18.8, 17.4; LC-MS: 339.04 ( $M+Na$ )<sup>+</sup>; Elemental analysis calculated for  $C_{12}H_{16}N_2O_6S$ : C, 45.56; H, 5.10; N, 8.86; Found: C, 45.82; H, 4.70; N, 8.14.

**(S)-methyl 2-(2-aminophenylsulfonamido)-3-methylbutanoate 21**

Compound **21** was synthesized following the procedure for **5**

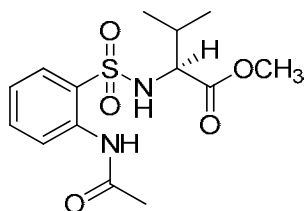
Purified by column chromatography, (65:35 pet. ether/ethyl acetate,  $R_f$ : 0.5), white crystalline solid (95%). mp: 96-98°C;  $[\alpha]_D^{27}$ : -49° ( $c = 0.1$ ,  $CHCl_3$ ); IR ( $CHCl_3$ ,  $\nu$  ( $cm^{-1}$ ):





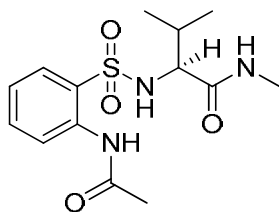
3020, 1738, 1618, 1618, 1482, 1425, 1341, 1215;  $^1\text{H}$  NMR ( $\text{CDCl}_3/400\text{MHz}$ ): 7.62-7.64 (d,  $J=7.86\text{Hz}$ , 1H), 7.27-7.31 (m, 1H), 6.73-6.76 (m, 2H), 5.50-5.52 (m, 1H), 4.98 (s, 2H), 3.66-3.69 (m, 1H), 3.43 (s, 3H), 1.95-2.02 (m, 1H), 0.91-0.93 (d,  $J=6.68$ , 3H), (d,  $J=6.82$ , 3H);  $^{13}\text{C}$  NMR ( $\text{CDCl}_3, 125\text{MHz}$ ):  $\delta$  ppm 171.5, 145.4, 134.1, 129.4, 120.9, 117.4, 117.3, 60.9, 52.1, 31.4, 18.7, 17.4; LC-MS: 309.07 ( $\text{M}+\text{Na}$ ) $^+$ ; Elemental analysis calculated for  $\text{C}_{12}\text{H}_{18}\text{N}_2\text{O}_4\text{S}$ : C, 50.33; H, 6.34; N, 9.78; Found: C, 50.87; H, 6.76; N, 9.29.

### **(S)-Methyl 2-(2-acetamidophenylsulfonamido)-3-methylbutanoate 23**



Compound **23** was prepared following the general procedure for **6**, except that acetic anhydride was used as the acetylating agent. Purification by column chromatography (65:35 pet. ether/ethyl acetate,  $R_f$ : 0.5) afforded **23** as a white crystalline solid (92%), crystallized from a solution of chloroform and methanol. mp: 122-124°C;  $[\alpha]_D^{27}$ :  $-20^\circ$  ( $c = 0.1$ ,  $\text{CHCl}_3$ ); IR ( $\text{CHCl}_3$ ,  $\nu$  ( $\text{cm}^{-1}$ ): 3020, 1740, 1702, 1587, 1527, 1468, 1337, 1216;  $^1\text{H}$  NMR ( $\text{CDCl}_3/200\text{MHz}$ ):  $\delta$  ppm 9.19 (s, 1H), 8.38-8.42 (d,  $J=8.22\text{Hz}$ , 1H), 7.78-7.83 (dd,  $J=8.02\text{Hz}$ ,  $J=1.51\text{Hz}$ , 1H), 7.48-7.57 (m, 1H), 7.11-7.19 (m, 1H), 5.62-5.67 (d,  $J=9.92\text{Hz}$ , 1H), 3.55-3.65 (m, 1H), 3.45 (s, 3H), 2.22 (s, 3H), 1.89-2.06 (m, 1H), 0.80-0.87 (m, 6H);  $^{13}\text{C}$  NMR ( $\text{CDCl}_3$ , 100MHz):  $\delta$  ppm 171.2, 168.5, 136.2, 134.2, 129.2, 126.1, 123.4, 122.6, 61.0, 52.4, 31.3, 25.0, 18.7, 17.3; LC-MS: 351.06 ( $\text{M}+\text{Na}$ ) $^+$ ; Elemental analysis calculated for  $\text{C}_{21}\text{H}_{22}\text{BrN}_3\text{O}_4$ : C, 54.79; H, 4.82; N, 9.13; Found: C, 58.16; H, 4.38; N, 8.92.

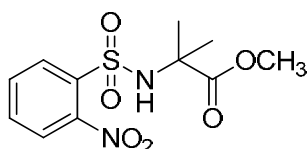
### **(S)-2-(2-acetamidophenylsulfonamido)-N,3-dimethylbutanamide 25**



Compound **23** was amidated using saturated methanolic methylamine (5mL). After 12 hours, the reaction mixture was evaporated under reduced pressure to obtain crude product which was purified by column chromatography, (05:95 methanol/ethyl acetate,  $R_f$ : 0.5) to afford **25** as a white crystalline solid (95%), crystallized from a solution of chloroform and methanol. mp: 172-174°C;  $[\alpha]_D^{27}$ :  $-4^\circ$  ( $c = 0.1$ ,  $\text{CHCl}_3$ ); IR ( $\text{CHCl}_3$ ,  $\nu$  ( $\text{cm}^{-1}$ ): 3020, 1678, 1586, 1435, 1332, 1216;  $^1\text{H}$  NMR ( $\text{CDCl}_3/200\text{MHz}$ ):  $\delta$  ppm 9.13 (s, 1H), 8.21-8.25 (d,  $J=8.07\text{Hz}$ ,

1H), 7.80-7.85 (m, 1H), 7.50-7.58 (m, 1H), 7.16-7.23 (m, 1H), 6.09-6.25 (m, 2H), 3.31-3.38 (m, 1H), 2.54-2.57 (d,  $J=4.81$ , 3H), 2.22 (s, 3H), 1.88-2.01 (m, 1H), 0.76-0.83 (m, 6H);  $^{13}\text{C}$  NMR ( $\text{CDCl}_3$ , 50MHz):  $\delta$  ppm 170.8, 169.5, 149.6, 135.8, 134.1, 129.3, 124.2, 123.8, 116.0, 62.4, 31.1, 26.2, 24.8, 18.9; LC-MS: 350.22 ( $\text{M}+\text{Na}$ ) $^+$ ; Elemental analysis calculated for  $\text{C}_{14}\text{H}_{21}\text{N}_3\text{O}_4\text{S}$ : C, 51.36; H, 6.47; N, 12.83; Found: C, 50.85; H, 6.86; N, 12.21.

### Methyl 2-methyl-2-(2-nitrophenylsulfonamido)propanoate 20

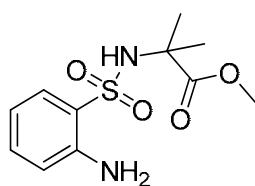


Compound **20** was synthesized following the procedure for **4**

Purified by column chromatography, (60:40 pet. ether/ethyl acetate,  $R_f$ : 0.5), white crystalline solid (57%). mp: 108-112°C; IR ( $\text{CHCl}_3$ ,  $\nu$  ( $\text{cm}^{-1}$ ): 3020, 1740, 1542, 1215;  $^1\text{H}$  NMR ( $\text{CDCl}_3$ /200MHz): 8.04-8.15 (m, 1H), 7.83-7.94 (m, 1H), 7.66-7.79 (m, 2H), 6.16 (s, 1H), 3.63 (s, 3H), 1.56 (s, 6H);  $^{13}\text{C}$  NMR ( $\text{CDCl}_3$ , 50MHz):  $\delta$  ppm 173.6, 147.4, 136.0, 133.3, 132.9, 130.0, 125.2, 60.0, 52.8, 26.2; LC-MS: 347.01 ( $\text{M}+\text{Na}$ ) $^+$ ; Elemental analysis calculated for  $\text{C}_{11}\text{H}_{14}\text{N}_2\text{O}_6\text{S}$ : C, 43.70; H, 4.67; N, 9.27; Found: C, 43.24; H, 4.92; N, 8.96.

### Methyl 2-methyl-2-(2-nitrophenylsulfonamido)propanoate 22

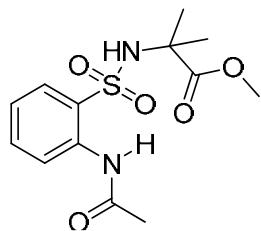
Compound **22** was synthesized following the procedure for **5**



Purified by column chromatography, (50:50 pet. ether/ethyl acetate,  $R_f$ : 0.5), white crystalline solid (97%). mp: 123-129°C; IR ( $\text{CHCl}_3$ ,  $\nu$  ( $\text{cm}^{-1}$ ): 3020, 1732, 1620, 1522, 1436, 1216;  $^1\text{H}$  NMR ( $\text{CDCl}_3$ /200MHz):  $\delta$  ppm 7.66-7.70 (d,  $J=7.89\text{Hz}$ , 1H), 7.30-7.34 (d,  $J=6.36\text{Hz}$ , 1H), 6.79-6.82 (m, 2H), 5.85 (s, 1H), 4.94 (s, 2H), 3.60 (s, 3H), 1.42 (s, 6H);  $^{13}\text{C}$  NMR ( $\text{CDCl}_3$ , 50 MHz):  $\delta$  ppm 174.3, 133.9, 129.2, 118.2, 58.8, 52.8, 25.5; LC-MS: 295.04 ( $\text{M}+\text{Na}$ ) $^+$ ; Elemental analysis calculated for  $\text{C}_{11}\text{H}_{16}\text{N}_2\text{O}_4\text{S}$ : C, 48.52; H, 5.92; N, 10.29; Found: C, 48.87; H, 5.25; N, 9.92.

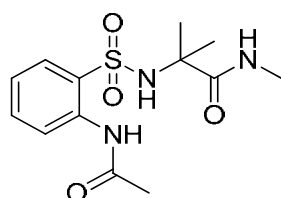
### Methyl 2-(2-acetamidophenylsulfonamido) acetate 24

Compound **24** was prepared following the general procedure for **6**, except that acetic anhydride was used as the acetylating agent. Purified by column chromatography, (60:40



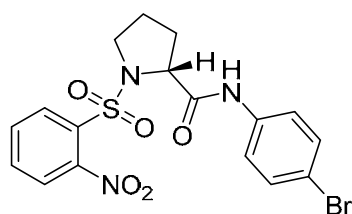
pet. ether/ethyl acetate,  $R_f$ : 0.5) to furnish **24** as a white solid (96%), crystallized from methanol. mp: 158-160°C; IR ( $\text{CHCl}_3$ ,  $\nu$  ( $\text{cm}^{-1}$ ): 3020, 1711, 1652, 1585, 1469, 1438, 1343, 1216;  $^1\text{H}$  NMR ( $\text{CDCl}_3/200\text{MHz}$ ):  $\delta$  ppm 9.05 (s, 1H), 8.30-8.35 (d,  $J=8.25\text{Hz}$ , 1H), 7.85-7.89 (m, 1H), 7.50-7.59 (m, 1H), 7.15-7.22 (m, 1H), 5.80-5.87 (m, 1H), 3.65 (s, 3H), 2.25 (s, 3H), 1.42 (s, 6H);  $^{13}\text{C}$  NMR ( $\text{CDCl}_3$ , 50MHz):  $\delta$  ppm 174.3, 168.8, 135.8, 133.9, 128.9, 123.8, 123.6, 59.2, 53.0, 25.5, 24.9; LC-MS: 337.07 ( $\text{M}+\text{Na}$ ) $^+$ ; Elemental analysis calculated for  $\text{C}_{13}\text{H}_{18}\text{N}_2\text{O}_5\text{S}$ : C, 49.67; H, 5.77; N, 8.91; Found: C, 49.83; H, 5.25; N, 8.46.

### Methyl 2-(2-acetamidophenylsulfonamido)-2-methylpropanoate **26**



Compound **26** was prepared following the procedure for **25**. Purified by column chromatography, (05:95 methanol/ethyl acetate,  $R_f$ : 0.5), to furnish **26** as a white crystalline solid (94%), crystallized from a solution of chloroform and methanol. mp: 157-161°C; IR ( $\text{CHCl}_3$ ,  $\nu$  ( $\text{cm}^{-1}$ ): 3019, 1670, 1586, 1528, 1437, 1329, 1323, 1216;  $^1\text{H}$  NMR ( $\text{CDCl}_3/200\text{MHz}$ ):  $\delta$  ppm 9.04 (s, 1H), 8.19-8.23 (d,  $J=7.93\text{Hz}$ , 1H), 7.84-7.88 (m, 1H), 7.49-7.57 (m, 1H), 7.16-7.24, 6.91 (s, 1H), 6.63-6.65 (m, 1H), 2.68-2.71 (d,  $J=4.63$ , 3H), 2.20 (s, 3H), 1.35 (s, 6H);  $^{13}\text{C}$  NMR ( $\text{CDCl}_3$ , 50MHz):  $\delta$  ppm 174.6, 169.4, 135.4, 133.7, 130.7, 128.6, 124.2, 59.71, 26.6, 25.6, 24.7; LC-MS: 336.09 ( $\text{M}+\text{Na}$ ) $^+$ ; Elemental analysis calculated for  $\text{C}_{13}\text{H}_{19}\text{N}_3\text{O}_4\text{S}$ : C, 49.83; H, 6.11; N, 13.41; Found: C, 49.17; H, 6.85; N, 13.93.

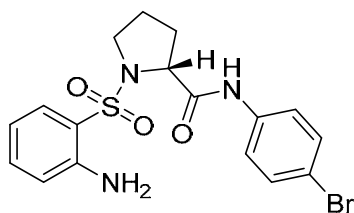
### (R)-N-(4-bromophenyl)-1-(2-nitrophenylsulfonyl)pyrrolidine-2-carboxamide **7**



To a solution of compound  $\text{H-DPro } p\text{-Br anilide}$  (1.35g, 5.016mmoles) in DCM (20mL),  $\text{Et}_3\text{N}$  (2mL, 1.5g, 15mmoles) was added, followed by 2-nitrobenzene sulfonyl chloride (0.926g, 4.18mmoles) and 25% wt. of DMAP (0.030g). After 12 hours, the reaction mixture was diluted with DCM (5mL) and the organic layer was washed with saturated solutions of sodium bicarbonate (10mL), potassium bisulphate (10mL), water (10mL) and saturated NaCl solution (10mL). The organic layer was dried over anhydrous  $\text{Na}_2\text{SO}_4$  solution and evaporated under reduced pressure to obtain the crude product which was purified by

column chromatography, (50:50 pet. ether/ethyl acetate,  $R_f$ : 0.5) to afford **7** as a white solid (1.8g, 94%). mp: 68-72°C;  $[\alpha]_D^{28}$ : +127° ( $c = 0.1$ ,  $\text{CHCl}_3$ ); IR ( $\text{CHCl}_3$ ,  $\nu$  ( $\text{cm}^{-1}$ ): 3356, 3019, 1691, 1653, 1591, 1546, 1370, 1215;  $^1\text{H}$  NMR ( $\text{CDCl}_3/200\text{MHz}$ ): 8.52 (s, 1H), 8.03-8.12 (m, 1H), 7.66-7.75 (m, 2H), 7.59-7.64 (m, 1H), 7.30-7.40 (m, 4H), 4.52-4.55 (m, 1H), 3.62-3.71 (m, 2H), 2.34-2.46 (m, 1H), 2.11-2.26 (m, 1H), 1.92-2.07 (m, 2H);  $^{13}\text{C}$  NMR ( $\text{CDCl}_3, 50\text{MHz}$ ):  $\delta$  ppm 168.8, 148.1, 136.2, 134.5, 132.0, 131.8, 131.3, 130.5, 124.2, 121.2, 117.1, 62.6, 49.6, 30.8, 24.5; MALDI-TOF-MS: 454.0768 ( $\text{M}+\text{H}$ )<sup>+</sup>, 476.0637 ( $\text{M}+\text{Na}$ )<sup>+</sup>, 492.0313 ( $\text{M}+\text{K}$ )<sup>+</sup>; Elemental analysis calculated for  $\text{C}_{17}\text{H}_{16}\text{BrN}_3\text{O}_5\text{S}$ : C, 44.94; H, 3.55; N, 9.25; Found: C, 44.28; H, 4.02; N, 8.66.

### (R)-1-(2-aminophenylsulfonyl)-N-(4-bromophenyl)pyrrolidine-2-carboxamide **8**

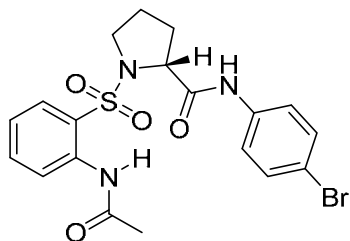


To a solution of compound **7** (2g, 4.40mmols) in MeOH (10mL), anhydrous  $\text{HCOONH}_4$  (2.77, 44.02mmols) and activated Zn (2.87, 44.02mmols), pre-treated with HCl and thoroughly washed with water and ether prior to use) were added and stirred at room temperature for 3 hours.

The reaction mixture was then filtered through Celite and the filtrate was evaporated under reduced pressure. The residue obtained was dissolved in DCM (10mL) and purified by column chromatography, (65:35 pet. ether/ethyl acetate,  $R_f$ : 0.5) to afford **8** as a colorless viscous liquid (1.7, 96%). mp: 60-63°C;  $[\alpha]_D^{27}$ : +129° ( $c = 0.1$ ,  $\text{CHCl}_3$ ); IR ( $\text{CHCl}_3$ ,  $\nu$  ( $\text{cm}^{-1}$ ): 3486, 3384, 3019, 1687, 1590, 1519, 1341, 1306, 1215;  $^1\text{H}$  NMR ( $\text{CDCl}_3/200\text{MHz}$ ):  $\delta$  ppm 8.845 (s, 1H), 7.67-7.72 (m, 1H), 7.43-7.45 (m, 4H), 7.29-7.49 (m, 1H), 6.72-6.85 (m, 2H), 5.15 (s, 2H) 4.42-4.47 (m, 1H), 3.48-3.55 (m, 2H), 2.29-2.37 (m, 1H), 1.73-2.01 (m, 3H);  $^{13}\text{C}$  NMR ( $\text{CDCl}_3$ , 50MHz):  $\delta$  ppm 169.4, 146.2, 136.4, 135.1, 131.7, 130.3, 121.3, 118.2, 118.0, 117.0, 62.1, 49.6, 30.4, 24.5; MALDI-TOF-MS: 424.0486 ( $\text{M}+\text{H}$ )<sup>+</sup>, 446.0358 ( $\text{M}+\text{Na}$ )<sup>+</sup>, 462.0073 ( $\text{M}+\text{K}$ )<sup>+</sup>; Elemental analysis calculated for  $\text{C}_{17}\text{H}_{18}\text{BrN}_3\text{O}_3\text{S}$ : C, 48.12; H, 4.28; N, 9.90; Found: C, 47.75; H, 4.52; N, 9.68.

### (R)-1-(2-acetamidophenylsulfonyl)-N-(4-bromophenyl)pyrrolidine-2-carboxamide **9**

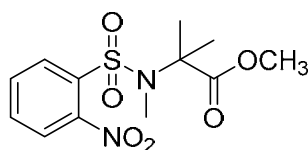
To a solution of compound **8** (0.4g, 9.427mmols) in DCM (10mL),  $\text{Et}_3\text{N}$  (0.4mL, 2.86g, 28.28mmols) was added followed by acetyl chloride (0.11mL, 0.1739g, 14.28mmols). After 3 hours, the reaction mixture was diluted with DCM (5mL) and the organic layer was washed with saturated solutions of sodium bicarbonate (5mL), potassium bisulfate



(5mL), water (5mL) and NaCl (5mL). The organic layer was dried over anhydrous  $\text{Na}_2\text{SO}_4$  solution and evaporated under reduced pressure to obtain the crude product which was purified by column chromatography, (30:70 pet. ether/ethyl acetate,  $R_f$ : 0.5) to afford **9** as a white crystalline solid (0.37, 81%). mp: 202-205°C;

$[\alpha]_D^{28}$ : +132.9° ( $c = 0.1$ ,  $\text{CHCl}_3$ ); IR ( $\text{CHCl}_3$ ,  $\nu$  ( $\text{cm}^{-1}$ ): 3390, 3019, 1698, 1588, 1427, 1338, 1217;  $^1\text{H}$  NMR ( $\text{CDCl}_3/200\text{MHz}$ ):  $\delta$  ppm 9.54 (s, 1H), 8.54 (s, 1H), 8.51 (s, 1H), 7.84-7.89 (m, 1H), 7.59-7.67 (m, 1H), 7.4-7.49 (m, 4H), 7.21-7.28 (m, 1H), 4.24-4.34 (m, 1H), 3.52-3.61 (m, 1H), 3.22-3.35 (m, 1H), 2.21 (s, 3H) 1.75-2.00 (m, 4H);  $^{13}\text{C}$  NMR ( $\text{CDCl}_3$ , 50MHz):  $\delta$  ppm 168.8, 137.0, 136.2, 135.1, 131.9, 129.9, 124.7, 124.4, 123.3, 123.2, 121.4, 117.3, 62.5, 49.9, 30.5, 25.0, 24.5; MALDI-TOF-MS: 446.1022 ( $\text{M}+\text{H}$ )<sup>+</sup>, 488.0991, 504.0633 ( $\text{M}+\text{K}$ )<sup>+</sup>; Elemental analysis calculated for  $\text{C}_{19}\text{H}_{20}\text{BrN}_3\text{O}_4\text{S}$ : C, 48.93; H, 4.32; N, 9.01; Found: C, 48.35; H, 4.56; N, 8.86.

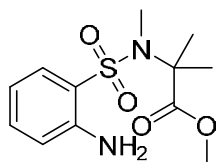
### Methyl 2-methyl-2-((N-methyl-2-nitrophenyl)sulfonamido)propanoate 27



To a solution of compound **20** (0.5g, 1.65 mmols) in DMF (5mL),  $\text{Ag}_2\text{O}$  (0.7676g, 3.3112mmols) was added followed by methyl iodide (0.2mL, 0.470g, 3.3112mmols). After 3 hours, the reaction mixture was diluted with ethyl acetate (5mL) and the organic layer was washed with water (5mL) and brine (5mL). The organic layer was dried over anhydrous  $\text{Na}_2\text{SO}_4$  solution and evaporated under reduced pressure to obtain the crude product which was purified by column chromatography, (30:70 pet. ether/ethyl acetate,  $R_f$ : 0.5) to afford **9** as a white crystalline solid (0.42, 80%). mp: 101-103°C; IR ( $\text{CHCl}_3$ ,  $\nu$  ( $\text{cm}^{-1}$ ): 3404, 3021, 1740, 1546, 1437, 1372, 1216;  $^1\text{H}$  NMR ( $\text{CDCl}_3/200\text{MHz}$ ): 8.19-8.24 (m, 1H), 7.63-7.73 (m, 3H), 3.72 (s, 3H), 2.93 (s, 3H), 1.56 (s, 6H);  $^{13}\text{C}$  NMR ( $\text{CDCl}_3$ , 50MHz):  $\delta$  ppm 170.4, 147.7, 133.5, 132.3, 131.4, 130.7, 123.8, 64.7, 51.5, 30.6, 27.8; MALDI-TOF-MS: 317.1046 ( $\text{M}+\text{H}$ )<sup>+</sup>, 339.1021 ( $\text{M}+\text{Na}$ )<sup>+</sup>, 355.0847 ( $\text{M}+\text{K}$ )<sup>+</sup>; Elemental analysis calculated for  $\text{C}_{12}\text{H}_{16}\text{N}_2\text{O}_6\text{S}$ : C, 45.56; H, 5.10; N, 8.86; Found: C, 46.29; H, 4.92; N, 8.96.

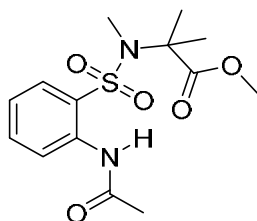
### Methyl 2-((2-amino-N-methylphenyl)sulfonamido)-2-methylpropanoate 28

Compound **28** was synthesized following the procedure for **5**



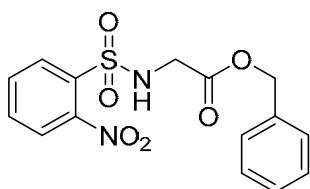
Purified by column chromatography, (70:30 pet. ether/ethyl acetate,  $R_f$ : 0.5), white crystalline solid (97%). mp: 114-116°C; IR ( $\text{CHCl}_3$ ,  $\nu$  ( $\text{cm}^{-1}$ ): 3486, 3380, 3235, 3020, 1735, 1637, 1485, 1454, 1216;  $^1\text{H}$  NMR ( $\text{CDCl}_3$ /200MHz):  $\delta$  ppm 7.73-7.77 (m, 1H), 7.25-7.33 (m, 1H), 6.65-6.74 (m, 2H), 5.30 (s, 2H), 3.82 (s, 3H), 2.63 (s, 3H) 1.56 (s, 6H);  $^{13}\text{C}$  NMR ( $\text{CDCl}_3$ , 50 MHz):  $\delta$  ppm 157.7, 146.4, 134.5, 131.2, 118.1, 117.4, 116.3, 62.3, 52.7, 30.2, 24.1; LC-MS: 308.86 ( $\text{M}+\text{Na}^+$ ); Elemental analysis calculated for  $\text{C}_{12}\text{H}_{18}\text{N}_2\text{O}_4\text{S}$ : C, 50.33; H, 6.34; N, 9.78; Found: C, 49.87; H, 5.95; N, 9.92.

### Methyl 2-((2-acetamido-N-methylphenyl)sulfonamido)-2-methylpropanoate **29**



Compound **29** was prepared following the general procedure for **6**, except that acetyl chloride was used as the acetylating agent. Purified by column chromatography, (70:30 pet. ether/ethyl acetate,  $R_f$ : 0.5) to furnish **29** as a white solid (96%), crystallized from methanol. mp: 92-94°C; IR ( $\text{CHCl}_3$ ,  $\nu$  ( $\text{cm}^{-1}$ ): 3334, 3019, 1737, 1699, 1583, 1529, 1468, 1436, 1322, 1216;  $^1\text{H}$  NMR ( $\text{CDCl}_3$ /200MHz):  $\delta$  ppm 9.55 (s, 1H), 8.56-8.61 (d,  $J=8.34\text{Hz}$ , 1H), 7.95-7.99 (dd,  $J=8.02\text{Hz}$ ,  $J=1.45\text{Hz}$ , 1H), 7.52-7.61 (m, 1H), 7.13-7.21 (m, 1H), 3.83 (s, 3H), 2.62 (s, 3H), 2.33 (s, 3H), 1.56 (s, 6H);  $^{13}\text{C}$  NMR ( $\text{CDCl}_3$ , 50MHz):  $\delta$  ppm 175.6, 169.6, 137.3, 134.5, 130.8, 124.6, 122.9, 62.9, 53.0, 30.5, 24.8, 24.1; LC-MS: 339.06 ( $\text{M}+\text{Na}^+$ ); Elemental analysis calculated for  $\text{C}_{14}\text{H}_{20}\text{N}_2\text{O}_5\text{S}$ : C, 51.21; H, 6.14; N, 8.53; Found: C, 50.83; H, 5.82; N, 8.26.

### Methyl ((2-nitrophenyl)sulfonyl)glycinate **31**

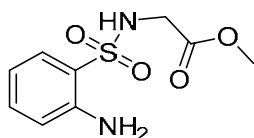


Compound **31** was synthesized following the procedure for **4**. Purified by column chromatography, (70:30 pet. ether/ethyl acetate,  $R_f$ : 0.5), viscous liquid (57%). IR ( $\text{CHCl}_3$ ,  $\nu$  ( $\text{cm}^{-1}$ ): 3360, 3022, 1747, 1668, 1595, 1539, 1416, 1217;  $^1\text{H}$  NMR ( $\text{CDCl}_3$ /200MHz): 7.99-8.08 (m, 1H), 7.79-7.89 (m, 1H), 7.61-7.74 (m, 2H), 7.31-7.36 (m, 3H), 7.20-7.25 (m, 2H), 6.13 (s, 1H), 5.02 (s, 2H), 4.06 (s, 2H);  $^{13}\text{C}$  NMR ( $\text{CDCl}_3$ , 125MHz):  $\delta$  ppm 168.4, 147.5, 134.6, 133.7, 133.6, 132.8, 130.4, 128.5, 128.3, 125.5, 67.4, 44.9; LC-MS: 372.87

(M+Na)<sup>+</sup>; Elemental analysis calculated for C<sub>15</sub>H<sub>14</sub>N<sub>2</sub>O<sub>6</sub>S: C, 51.43; H, 4.03; N, 8.00; Found: C, 53.24; H, 4.22; N, 8.16.

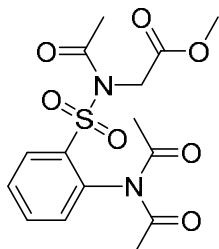
### Methyl ((2-aminophenyl)sulfonyl)glycinate **32**

Compound **32** was synthesized following the procedure for **5**



Purified by column chromatography, (75:25 pet. ether/ethyl acetate, R<sub>f</sub>: 0.5), white crystalline solid (92%). mp: 64-67°C; IR (CHCl<sub>3</sub>, ν (cm<sup>-1</sup>): 3482, 3380, 3021, 1747, 1619, 1571, 1483, 1455, 1337; <sup>1</sup>H NMR (CDCl<sub>3</sub>/200MHz): δ ppm 7.63-7.68 (dd, *J*=8.21Hz, *J*=1.65Hz, 1H), 7.27-7.36 (m, 1H), 6.73-6.80 (m, 2H), 5.64-5.69 (t, *J*=5.56Hz, 1H), 4.76 (s, 2H), 3.72-3.75 (d, *J*=5.68Hz, 2H), 3.61 (s, 3H); <sup>13</sup>C NMR (CDCl<sub>3</sub>, 50 MHz): δ ppm 169.2, 145.4, 134.3, 129.4, 120.2, 117.7, 117.4, 52.4, 43.9; MALDI-TOF-MS: 245.0726 (M+H)<sup>+</sup>, 294.1156 (M+K)<sup>+</sup>; Elemental analysis calculated for C<sub>9</sub>H<sub>12</sub>N<sub>2</sub>O<sub>4</sub>S: C, 44.25; H, 4.95; N, 11.47; Found: C, 44.87; H, 5.04; N, 11.92.

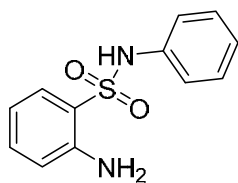
### Methyl N-acetyl-N-((2-(N-acetylacetamido)phenyl)sulfonyl)glycinate **33**



Compound **33** was prepared following the general procedure for **6**, except that excess acetic anhydride 5ml was used as the acetylating agent (10 equivalents). Purified by column chromatography, (65:35 pet. ether/ethyl acetate, R<sub>f</sub>: 0.5) to furnish **24** as a white solid (96%), crystallized from methanol. mp: 128-129°C; IR (CHCl<sub>3</sub>, ν (cm<sup>-1</sup>): 3380, 3019, 1752, 1718, 1588, 1527, 1474, 1438, 1364, 1216; <sup>1</sup>H NMR (CDCl<sub>3</sub>/200MHz): δ ppm 8.30-8.34 (d, *J*=7.71Hz, 1H), 7.58-7.87 (m, 2H), 7.31-7.35 (d, *J*=7.58Hz, 1H), 4.41 (s, 2H), 3.77 (m, 3H), 2.31 (s, 6H), 2.22 (s, 3H); <sup>13</sup>C NMR (DMSO-*d*<sub>6</sub>, 50MHz): δ ppm 172.3, 169.6, 168.4, 137.3, 136.0, 135.9, 132.7, 131.1, 130.1, 52.6, 46.8, 26.5, 23.6; MALDI-TOF-MS: 393.1343 (M+Na)<sup>+</sup>, 409.1205 (M+K)<sup>+</sup>; Elemental analysis calculated for C<sub>15</sub>H<sub>18</sub>N<sub>2</sub>O<sub>7</sub>S: C, 48.64; H, 4.90; N, 7.56; Found: C, 49.13; H, 5.02; N, 7.26.

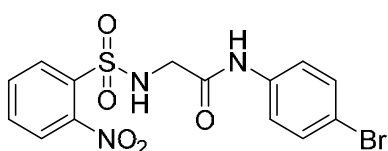
### 2-Amino-N-phenylbenzenesulfonamide **36**

Compound **36** was synthesized from **35** following the procedure for **5**



Purified by column chromatography, (75:25 pet. ether/ethyl acetate,  $R_f$ : 0.5), white crystalline solid (97%). mp: 112-116°C; IR ( $\text{CHCl}_3$ ,  $\nu$  ( $\text{cm}^{-1}$ ): 3459, 3371, 3021, 1619, 1482, 1381, 1219;  $^1\text{H}$  NMR ( $\text{CDCl}_3/200\text{MHz}$ ):  $\delta$  ppm 7.47-7.52 (dd,  $J=7.96\text{Hz}$ ,  $J=1.52\text{Hz}$ , 1H), 7.02-7.29 (m, 7H), 6.61-6.74 (m, 2H), 4.89 (s, 2H);  $^{13}\text{C}$  NMR ( $\text{CDCl}_3$ , 50 MHz):  $\delta$  ppm 144.9, 136.2, 134.4, 129.9, 129.0, 125.7, 122.5, 120.7, 117.8, 117.6; MALDI-TOF-MS: 249.1779 ( $\text{M}+\text{H}$ ) $^+$ , 271.0966 ( $\text{M}+\text{Na}$ ) $^+$ , 287.2115 ( $\text{M}+\text{K}$ ) $^+$ ; Elemental analysis calculated for  $\text{C}_{12}\text{H}_{12}\text{N}_2\text{O}_2\text{S}$ : C, 58.05; H, 4.87; N, 11.28; Found: C, 58.87; H, 4.65; N, 11.32.

### N-(4-bromophenyl)-2-((2-nitrophenyl)sulfonamido)acetamide **38**

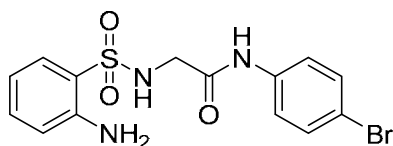


Compound **38** was synthesized following the procedure for **4**

Purified by column chromatography, (70:30 pet. ether/ethyl acetate,  $R_f$ : 0.5), viscous liquid (57%). ( $\text{CHCl}_3$ ,  $\nu$  ( $\text{cm}^{-1}$ ): 3360, 3022, 1688, 1542, 1215;  $^1\text{H}$  NMR ( $\text{DMSO}-d_6/400\text{MHz}$ ): 10.15 (s, 1H), 8.39-8.41 (t,  $J=5.14\text{Hz}$ , 1H), 8.05-8.08 (m, 1H), 7.95-7.97 (m, 1H), 7.82-7.85 (m, 2H), 7.45 (s, 4H), 3.87-3.88 (d,  $J=5.27\text{Hz}$ , 2H), 1.56 (s, 6H);  $^{13}\text{C}$  NMR ( $\text{DMSO}-d_6$ , 100MHz):  $\delta$  ppm 166.4, 147.4, 137.9, 134.0, 133.2, 132.6, 131.6, 129.7, 124.4, 121.1, 115.1, 45.9; MALDI-TOF-MS: 437.9852 ( $\text{M}+\text{Na}$ ) $^+$ , 451.9622 ( $\text{M}+\text{K}$ ) $^+$ ; Elemental analysis calculated for  $\text{C}_{14}\text{H}_{12}\text{BrN}_3\text{O}_5\text{S}$ : C, 40.59; H, 2.92; N, 10.14; Found: C, 40.24; H, 2.79; N, 10.96.

### 2-((2-Aminophenyl)sulfonamido)-N-(4-bromophenyl)acetamide **39**

Compound **39** was synthesized following the procedure for **5**



Purified by column chromatography, (75:25 pet. ether/ethyl acetate,  $R_f$ : 0.5), white crystalline solid (97%). mp: 164-168°C; IR ( $\text{CHCl}_3$ ,  $\nu$  ( $\text{cm}^{-1}$ ): 3469, 3379, 3019, 1655, 1600, 1523, 1480, 1423, 1216;  $^1\text{H}$  NMR ( $\text{DMSO}-d_6/500\text{MHz}$ ):  $\delta$  ppm 10.01 (s, 1H), 7.93-7.96 (t,  $J=5.95\text{Hz}$ , 1H), 7.45-7.52 (m, 4H), 7.22-7.25 (m, 1H), 6.79-6.80 (d,  $J=8.24\text{Hz}$ , 1H), 6.57-6.61 (m, 1H), 5.98 (s, 2H), 3.61-3.62 (d,  $J=5.80\text{Hz}$ , 2H);  $^{13}\text{C}$  NMR ( $\text{CDCl}_3$ , 50 MHz):  $\delta$  ppm 166.6, 146.4, 137.9, 133.7, 131.6, 129.1, 121.2, 119.4, 117.0, 115.1, 45.4; MALDI-TOF-MS: 406.0224



(M+Na)<sup>+</sup>, 421.9926 (M+K)<sup>+</sup>; Elemental analysis calculated for C<sub>14</sub>H<sub>14</sub>BrN<sub>3</sub>O<sub>3</sub>S: C, 43.76; H, 3.67; N, 10.94; Found: C, 43.87; H, 3.25; N, 10.82.

### 2.25 Single Crystal X-ray Crystallographic Data.

Crystal Data for the compounds were collected at  $T = 293$  K, on SMART APEX CCD Single crystal X-ray diffractometer using Mo KR radiation ( $\lambda$ ) 0.7107 Å. The structures were solved by direct methods using SHELXTL. All the data were corrected for Lorentz polarization and absorption effects. SHELX-97 (ShelxTL) was used for structure solution and full matrix least-squares refinement on  $F^2$ . Hydrogen atoms were included in the refinement in the riding mode. The refinements were carried out using SHELXL-97. For reference, see: G. M. Sheldrick, SHELX-97 program for crystal structure solution and refinement, University of Gottingen, Germany, 1997.

**Compound 6:** Single crystals of **6** were grown by slow evaporation of the solution mixture of methanol and dichloromethane. Colorless needle crystal of size 0.55 x 0.15 x 0.12 mm<sup>3</sup>, was used for data collection, temperature = 273K, wave length = 0.71073 Å, quadrant data acquisition, Total scans = 4, F(000) = 952,  $\theta$  range = 2.31° to 25.00°, completeness to  $\theta$  of 24.99° is 99.9 %, goodness-of-fit on  $F^2 = 1.018$ , C<sub>19</sub>H<sub>20</sub>BrN<sub>3</sub>O<sub>4</sub>S, M = 466.35. Crystals belong to Orthorhombic, space group P212121, a = 9.3380(6) , b = 13.9088(9), c = 15.438(1) Å, V = 2005.1(2) Å<sup>3</sup>, Z = 4, Dc = 1.545 g/cc,  $\mu$  (Mo-K $\alpha$ ) = 2.185 mm<sup>-1</sup>, 10047 reflections collected, 3513 unique [ $I > 2\sigma(I)$ ], R value 0.0352, wR2 = 0.0950, largest diff. peak and hole 0.605 and -0.202 e. Å<sup>-3</sup>, absolute structure parameter = 0.008(7).

**Compound 9:** Single crystals of **9** were obtained from the solution mixture of CHCl<sub>3</sub> and methanol. Colorless needle type crystal of approximate size 0.45 x 0.23 x 0.19 mm<sup>3</sup>, was used for data collection, Temperature = 296(2) K, Wave length = 0.71073 Å, Quadrant data acquisition, Total scans = 4, F(000) = 952,  $\theta$  range = 2.56° to 28.31°, Goodness-of-fit on  $F^2 = 0.988$ , C<sub>19</sub>H<sub>20</sub>BrN<sub>3</sub>O<sub>4</sub>S, M = 466.35. Crystals belong to Orthorhombic, space group P212121, a = 9.2942(10) Å, b = 13.9119(13) Å, c = 15.3096(17) Å,  $\alpha = \beta = \gamma = 90^\circ$ , V = 1979.5 (4) Å<sup>3</sup>, Z = 4, Dc = 1.565 g/cc,  $\mu$  (Mo-K $\alpha$ ) = 0.71073 mm<sup>-1</sup>, total reflections = 4865, 3065 unique reflections, R value 0.0432, wR2 = 0.0926.

**Compound 12:** Single crystals of **12** were grown by slow evaporation of the solution of methanol. Colorless rectangular type crystal of approximate size 0.27 x 0.19 x 0.12 mm<sup>3</sup>,

was used for data collection, temperature = 90(2) K, wave length = 0.71073 Å, quadrant data acquisition, total scans = 4, F(000) = 600,  $\theta$  range = 2.28 to 25.00°, completeness to  $\theta$  of 25.00° is 100.0 %, goodness-of-fit on F2 = 1.094, C<sub>12</sub>H<sub>16</sub>N<sub>2</sub>O<sub>4</sub>S, M = 284.33. Crystals belong to orthorhombic, space group P212121, a = 7.6518(4) Å, b = 11.1273(6) Å, c = 14.9119(9) Å, V = 1269.66(12) Å<sup>3</sup>, Z = 4, D<sub>c</sub> = 1.487 g/cc,  $\mu$  (Mo-K $\alpha$ ) = 0.268 mm<sup>-1</sup>, 10339 reflections collected, 2224 unique [I>2s(I)], R value 0.0253, wR2 = 0.0672, largest diff. peak and hole 0.295 and -0.199e. Å<sup>-3</sup>, absolute structure parameter = -0.05(6).

**Compound 16:** Single crystals of **16** were grown by slow evaporation of the solution of methanol. Colorless block crystal of approximate size 0.56 x 0.43 x 0.41 mm<sup>3</sup>, was used for data collection, temperature = 297(2) K, wave length = 0.71073 Å, quadrant data acquisition, F(000) = 1056,  $\theta$  range = 1.73 to 28.59°, completeness to  $\theta$  is 98 %, goodness-of-fit on F2 = 1.094, C<sub>11</sub>H<sub>12</sub>N<sub>2</sub>O<sub>3</sub>S, M = 252.29. Crystals belong to orthorhombic, space group P212121, a = 7.715(7) Å, b = 15.536(13) Å, c = 19.077(17) Å, V = 2287(3) Å<sup>3</sup>,  $\alpha = \beta = \gamma = 90^\circ$  Z = 8, D<sub>c</sub> = 1.466 g/cc,  $\mu$  (Mo-K $\alpha$ ) = 0.281 mm<sup>-1</sup>, 5747 total reflections, 4052 unique [I>2s(I)], R value 0.0504, wR2 = 0.1308.

**Compound 23:** Single crystals of **23** were grown by slow evaporation of the solution mixture of methanol and dichloromethane. Colorless plate crystal of size 0.24 x 0.20 x 0.05 mm<sup>3</sup>, was used for data collection, temperature = 90.2K, wave length = 0.71073 Å, quadrant data acquisition, Total scans = 4, F(000) = 1392,  $\theta$  range = 2.55° to 24.99°, completeness to  $\theta$  of 24.99 ° is 100.0 %, goodness-of-fit on F2 = 1.045, C<sub>14</sub>H<sub>20</sub>N<sub>2</sub>O<sub>5</sub>S, M = 328.38. Crystals belong to monoclinic, space group C2, a = 15.395(4) Å, b = 8.2539(4) Å, c = 15.438(1) Å, V = 3368.2(9) Å<sup>3</sup>, Z = 8, D<sub>c</sub> = 1.295 g/cc,  $\mu$  (Mo-K $\alpha$ ) = 0.215 mm<sup>-1</sup>, 18875 reflections collected, 5941 unique [I>2s(I)], R value 0.0312, wR2 = 0.0845, largest diff. peak and hole 0.282 and -0.177 e. Å<sup>-3</sup>, absolute structure parameter = 0.02(5).

**Compound 24:** Single crystals of **24** were grown by slow evaporation of the solution of methanol. Colorless cubic crystal of approximate size 0.45 x 0.12 x 0.07 mm<sup>3</sup>, was used for data collection, temperature = 296(2) K, wave length = 0.71073 Å, quadrant data acquisition, total scans = 4, F(000) = 664,  $\theta$  range = 2.81 to 28.39°, completeness to  $\theta$  of 28.39° is 99.6 %, Goodness-of-fit on F2 = 1.069, C<sub>13</sub>H<sub>18</sub>N<sub>2</sub>O<sub>5</sub>S, M = 314.35. Crystals belong to monoclinic, space group P21/c, a = 12.8333(2) Å, b = 8.3635(1) Å, c =

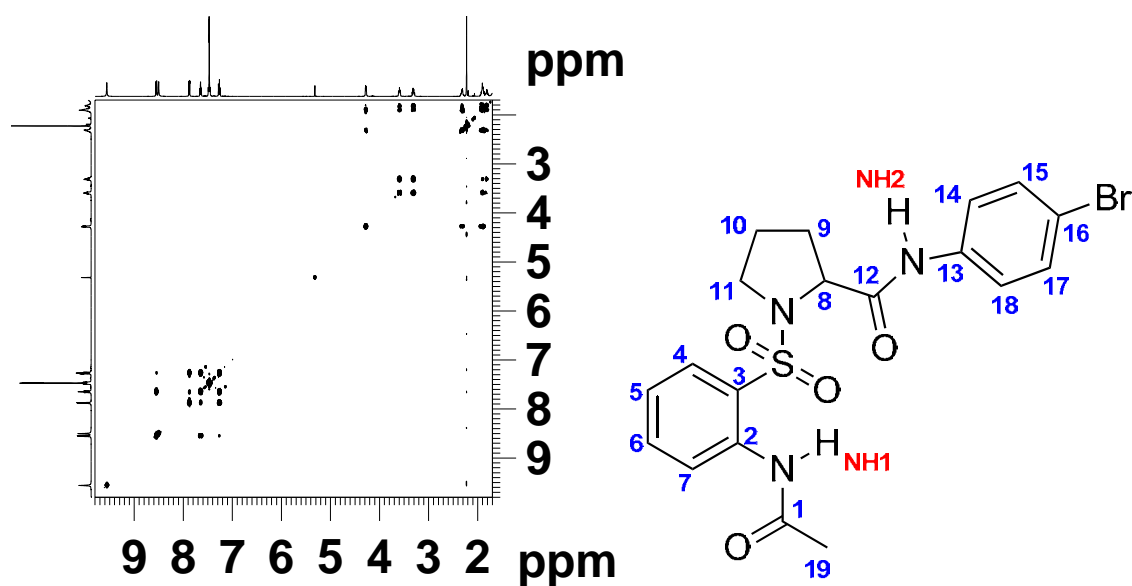
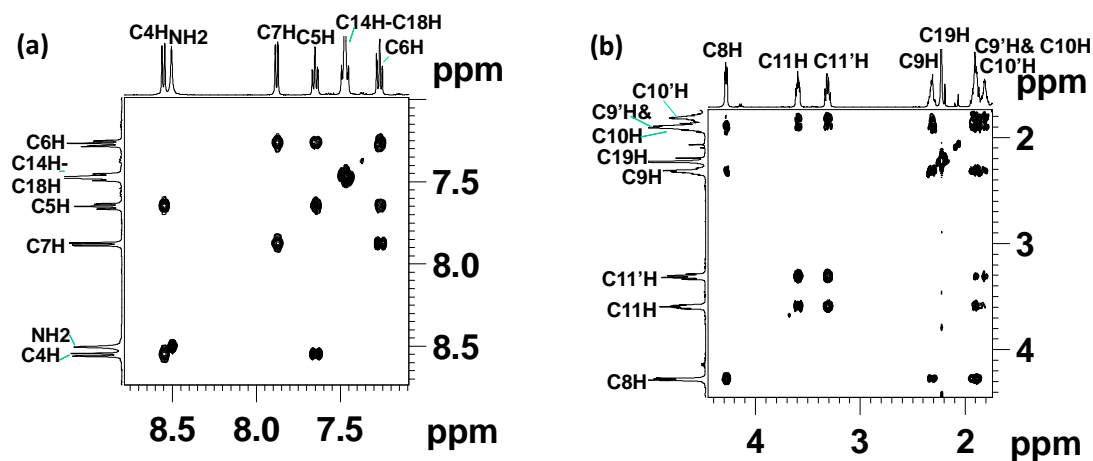
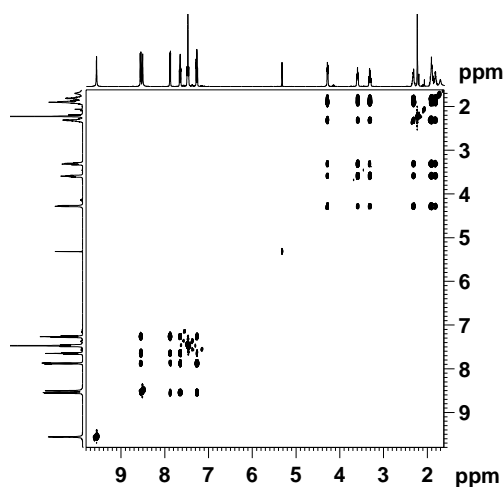
15.0888(2) Å,  $V = 1556.60(4) \text{ \AA}^3$ ,  $Z = 4$ ,  $D_c = 1.341 \text{ g/cc}$ ,  $\mu (\text{Mo-K}\alpha) = 0.230 \text{ mm}^{-1}$ , 13960 reflections collected, 3888 unique [ $I > 2s(I)$ ],  $R$  value 0.0380,  $wR2 = 0.1120$ , largest diff. peak and hole 0.376 and  $-0.344 \text{ e. \AA}^{-3}$ , absolute structure parameter = 0.07(8).

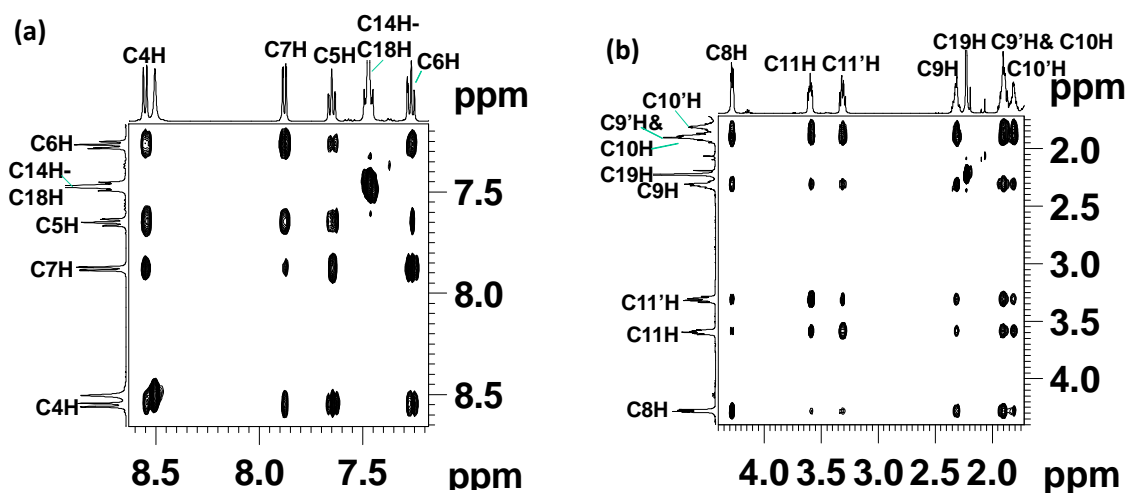
**Compound 25:** Single crystals of **25** were grown by slow evaporation of the solution mixture of chloroform and methanol. Colorless plate type crystal of approximate size  $0.17 \times 0.10 \times 0.05 \text{ mm}^3$ , was used for data collection, temperature = 100.2K, wave length = 0.71073 Å, quadrant data acquisition, total scans = 4,  $F(000) = 348$ ,  $\theta$  range =  $2.37^\circ$  to  $24.98^\circ$ , completeness to  $\theta$  of  $24.98^\circ$  is 99.9 %, goodness-of-fit on  $F2 = 1.033$ ,  $C_{14}H_{20}N_2O_5S$ ,  $M = 328.38$ . Crystals belong to monoclinic, space group P21,  $a = 4.9219(1) \text{ \AA}$ ,  $b = 10.1580(3) \text{ \AA}$ ,  $c = 16.0223(5) \text{ \AA}$ ,  $V = 3368.2(9) \text{ \AA}^3$ ,  $Z = 2$ ,  $D_c = 1.357 \text{ g/cc}$ ,  $\mu (\text{Mo-K}\alpha) = 0.223 \text{ mm}^{-1}$ , 3554 reflections collected, 2463 unique [ $I > 2s(I)$ ],  $R$  value 0.0345,  $wR2 = 0.0821$ , largest diff. peak and hole 0.345 and  $-0.351 \text{ e. \AA}^{-3}$ , absolute structure parameter = 0.07(8).

**Compound 26:** Single crystals of **26** were grown by slow evaporation of the solution mixture of chloroform and methanol. Colorless needle type crystal of approximate size  $0.45 \times 0.12 \times 0.07 \text{ mm}^3$ , was used for data collection, temperature = 90(2) K, wave length = 0.71073 Å, quadrant data acquisition, total scans = 4,  $F(000) = 2656$ ,  $\theta$  range =  $1.54$  to  $25.00^\circ$ , completeness to  $q$  of  $25.00^\circ$  is 99.8 %, goodness-of-fit on  $F2 = 1.175$ ,  $C_{13}H_{19}N_3O_4S$ ,  $M = 313.37$ . Crystals belong to monoclinic, space group C2/c,  $a = 34.8270(8) \text{ \AA}$ ,  $b = 8.3408(4) \text{ \AA}$ ,  $c = 26.8610(9) \text{ \AA}$ ,  $V = 6036.5(4) \text{ \AA}^3$ ,  $Z = 16$ ,  $D_c = 1.379 \text{ g/cc}$ ,  $\mu (\text{Mo-K}\alpha) = 0.234 \text{ mm}^{-1}$ , 14623 reflections collected, 5300 unique [ $I > 2s(I)$ ],  $R$  value 0.0563,  $wR2 = 0.1164$ , largest diff. peak and hole 0.626 and  $-0.879 \text{ e. \AA}^{-3}$ .

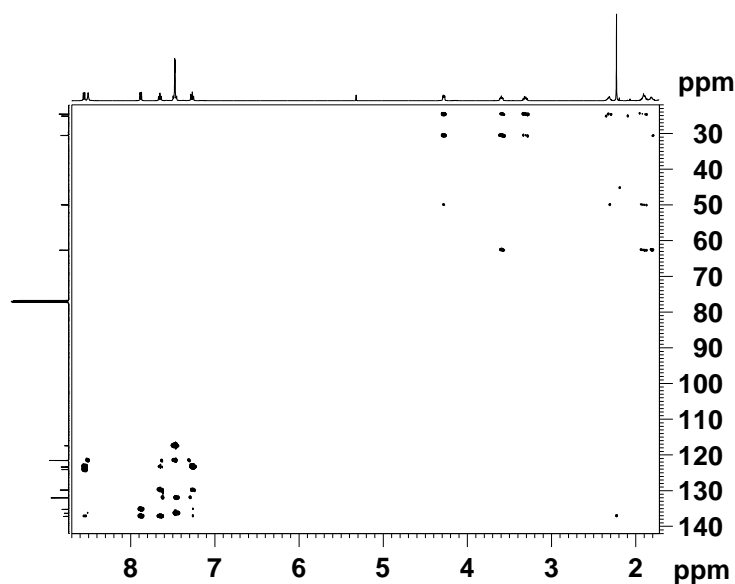
**Compound 29:** Single crystals of **29** were grown by slow evaporation of the solution of methanol. Colorless block crystal of approximate size  $0.66 \times 0.27 \times 0.14 \text{ mm}^3$ , was used for data collection, Temperature = 297(2) K, Wave length = 0.227 Å, Quadrant data acquisition,  $F(000) = 348$ ,  $\theta$  range =  $2.69$  to  $28^\circ$ , completeness to  $\theta$  of  $28^\circ$  is 99.3 %, Goodness-of-fit on  $F2 = 1.059$ ,  $C_{14}H_{20}N_2O_5S$ ,  $M = 328.38$ . Crystals belong to Triclinic, space group P1,  $a = 7.1146(3) \text{ \AA}$ ,  $b = 8.0387(3) \text{ \AA}$ ,  $c = 15.0865(6) \text{ \AA}$ ,  $\alpha = 90.323(2)$ ,  $\beta = 100.054(2)$ ,  $\gamma = 109.252(2)$ ,  $V = 800.21(6) \text{ \AA}^3$ ,  $Z = 2$ ,  $D_c = 1.363 \text{ g/cc}$ ,  $\mu (\text{Mo-K}\alpha) = 0.227 \text{ mm}^{-1}$ , 3852 reflections collected, 3360 unique [ $I > 2s(I)$ ],  $R$  value 0.0386,  $wR2 = 0.1169$ .

## 2.26 Spectra of compounds.

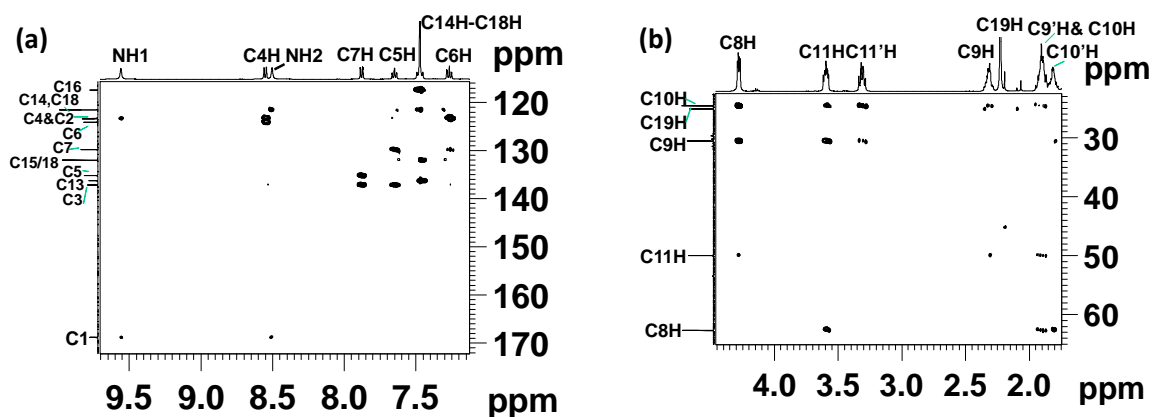

 Figure 1: COSY spectra of **6** (500MHz, CDCl<sub>3</sub>)

 Figure 2: Partial COSY spectra of **6** (500MHz, CDCl<sub>3</sub>): aromatic (a) and aliphatic (b) regions.

 Figure 3: TOCSY spectrum of **6** (500MHz, CDCl<sub>3</sub>)



**Figure 4:** Partial TOCSY spectra of **6** (500MHz,  $\text{CDCl}_3$ ): aromatic (a) & aliphatic (b) regions.



**Figure 5:** HMBC spectrum of **6** (500MHz,  $\text{CDCl}_3$ )



**Figure 6:** Partial HMBC spectrum of **6** (500MHz,  $\text{CDCl}_3$ ): aromatic (a) and aliphatic regions (b).

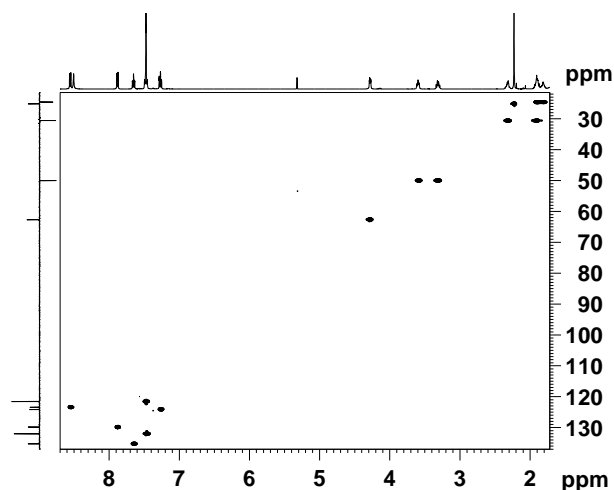


**Figure 7:** HSQC spectrum of **6** (500MHz,  $\text{CDCl}_3$ )

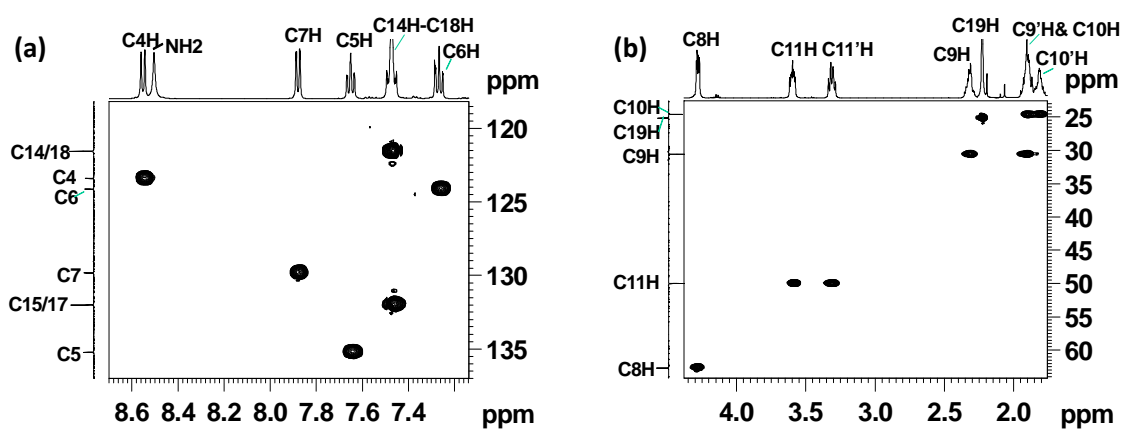


**Figure 8:** Partial HSQC spectrum of **6** (500MHz,  $\text{CDCl}_3$ ): aromatic (a) & aliphatic regions (b).

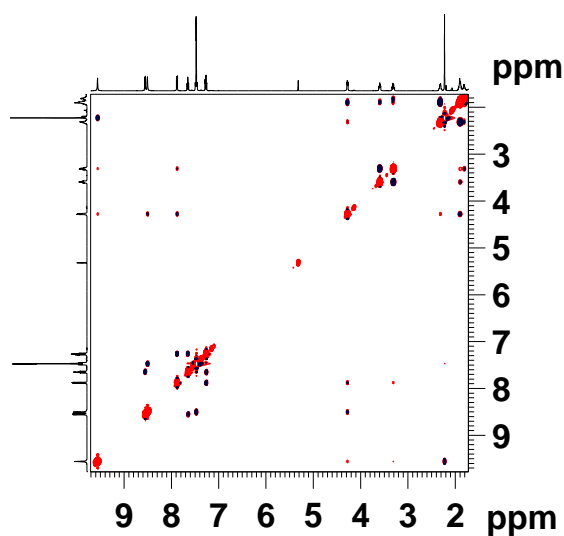


**Figure 9:** 2D NOESY spectra of N-terminal sulfonamide **6** (500MHz,  $\text{CDCl}_3$ ).

**Table 1:** NMR DMSO-*d*<sub>6</sub> titration studies of **6** (10mM, 400MHz, CDCl<sub>3</sub>).

No:	V <sub>DMSO-<i>d</i><sub>6</sub></sub> (in μ lit)	δNH2	δNH1
1	0	9.55	8.46
2	5	9.54	8.71
3	10	9.53	8.89
4	15	9.52	9.04
5	20	9.51	9.14
6	25	9.5	9.22
7	30	9.49	9.29
8	35	9.48	9.34
9	40	9.47	9.37
10	45	9.45	9.42
11	50	9.45	9.45
12	55	9.42	9.47
13	60	9.42	9.49
14	65	9.4	9.51
15	70	9.39	9.53
16	75	9.37	9.54

**Table 2:** NMR DMSO-*d*<sub>6</sub> titration studies of **6** (2mM, 400MHz, CDCl<sub>3</sub>).

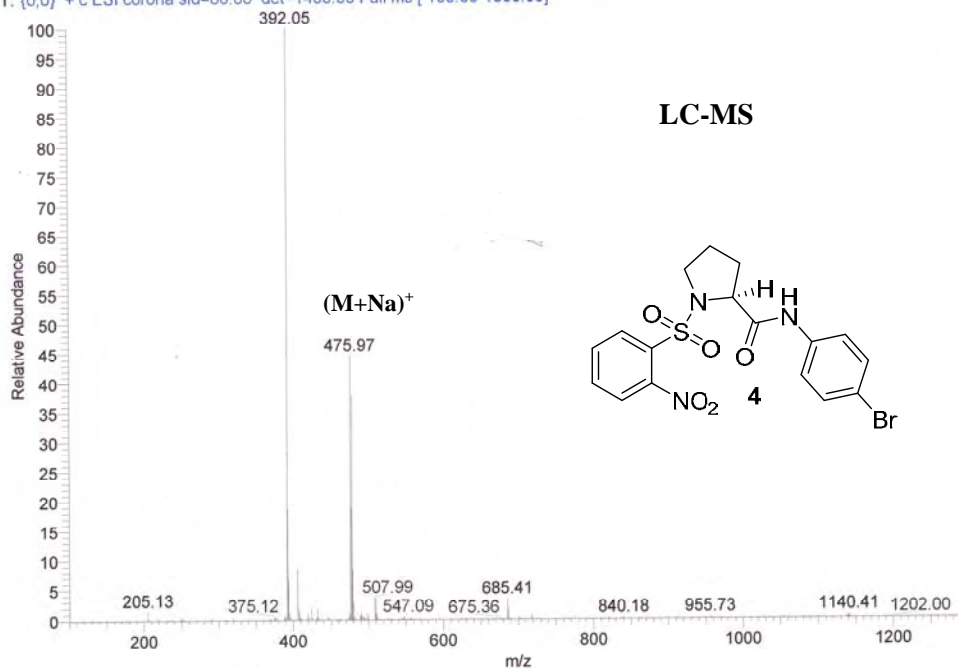
No:	V <sub>DMSO-<i>d</i><sub>6</sub></sub> (in μ lit)	δNH2	δNH1
1	0	9.55	8.46
2	5	9.54	8.71
3	10	9.53	8.91
4	15	9.52	9.05
5	20	9.51	9.15
6	25	9.5	9.24
7	30	9.49	9.31
8	35	9.48	9.36
9	40	9.46	9.41
10	45	9.45	9.44
11	50	9.44	9.47
12	55	9.43	9.49
13	60	9.41	9.51
14	65	9.4	9.52
15	70	9.39	9.54
16	75	9.37	9.55



F:\DATA\FEB-12\GJS\INO2-SBP

2/23/2012 4:04:49 PM

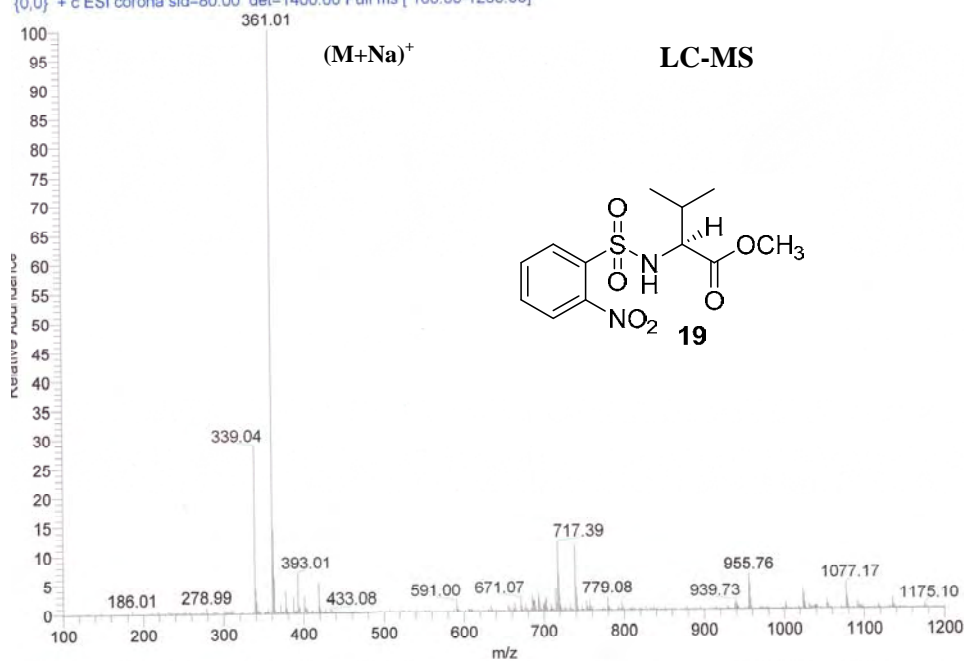
NO2-SBP #8-25 RT: 0.12-0.42 AV: 18 SB: 16 0.02-0.09, 0.58-0.75 NL: 1.28E7  
T: {0,0} + c ESI corona sid=80.00 det=1400.00 Full ms [ 100.00-1300.00]

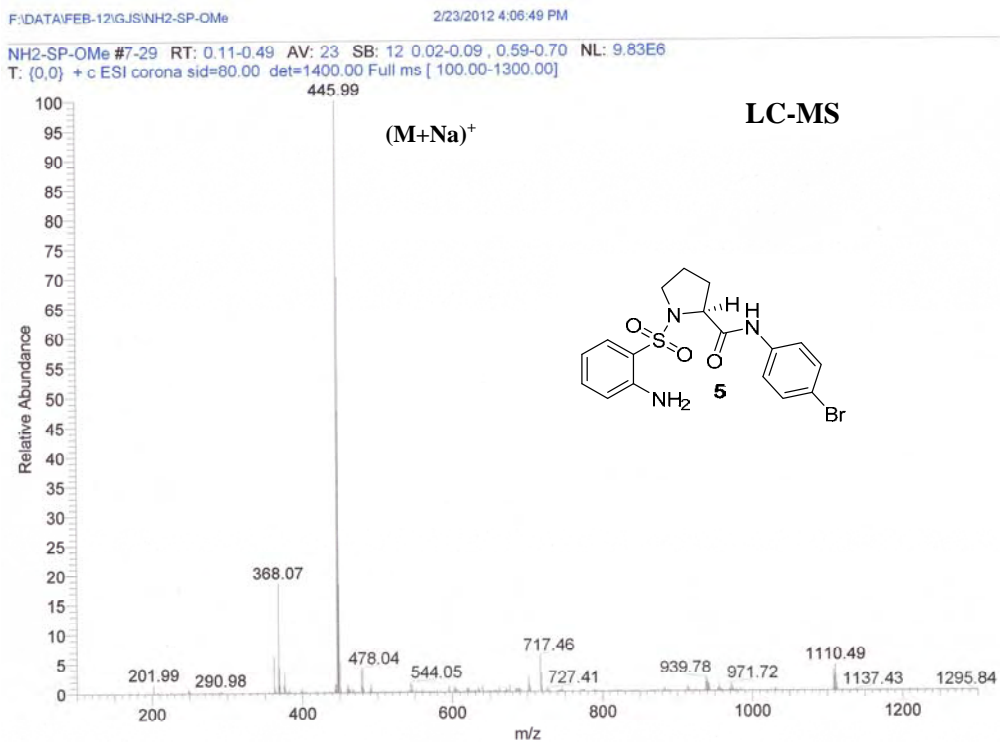
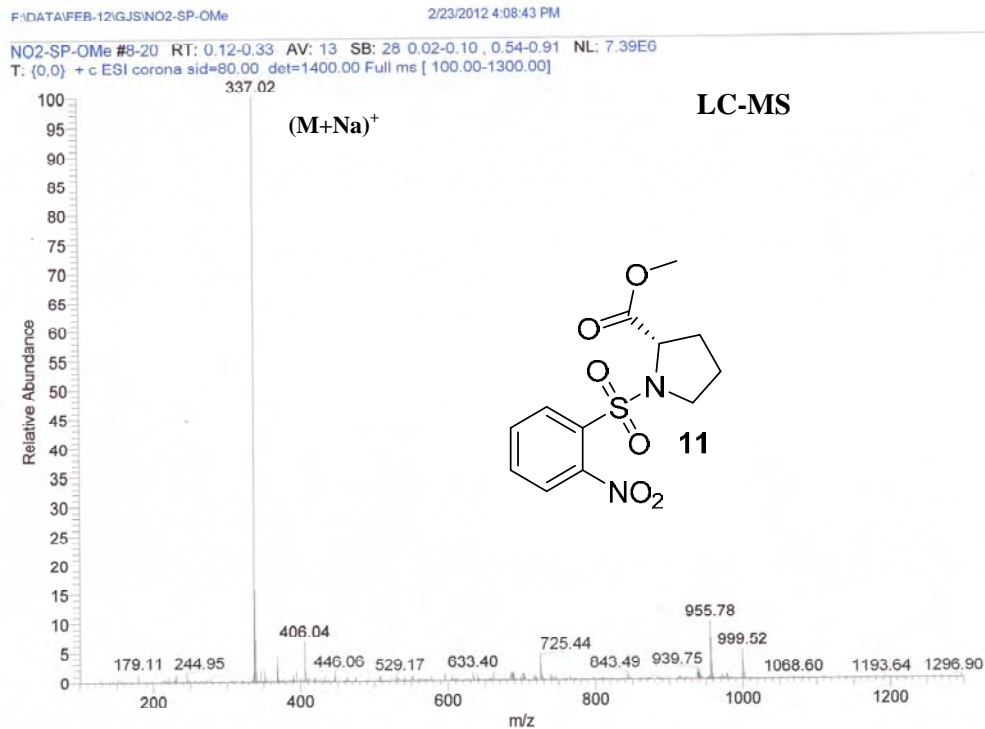


DATA\...GJS\INO2-SV-OMe\_120229153439

2/29/2012 3:34:39 PM

12-SV-OMe\_120229153439 #7-30 RT: 0.10-0.50 AV: 24 SB: 23 0.02-0.12, 0.61-0.87 NL: 4.84E6  
{0,0} + c ESI corona sid=80.00 det=1400.00 Full ms [ 100.00-1200.00]

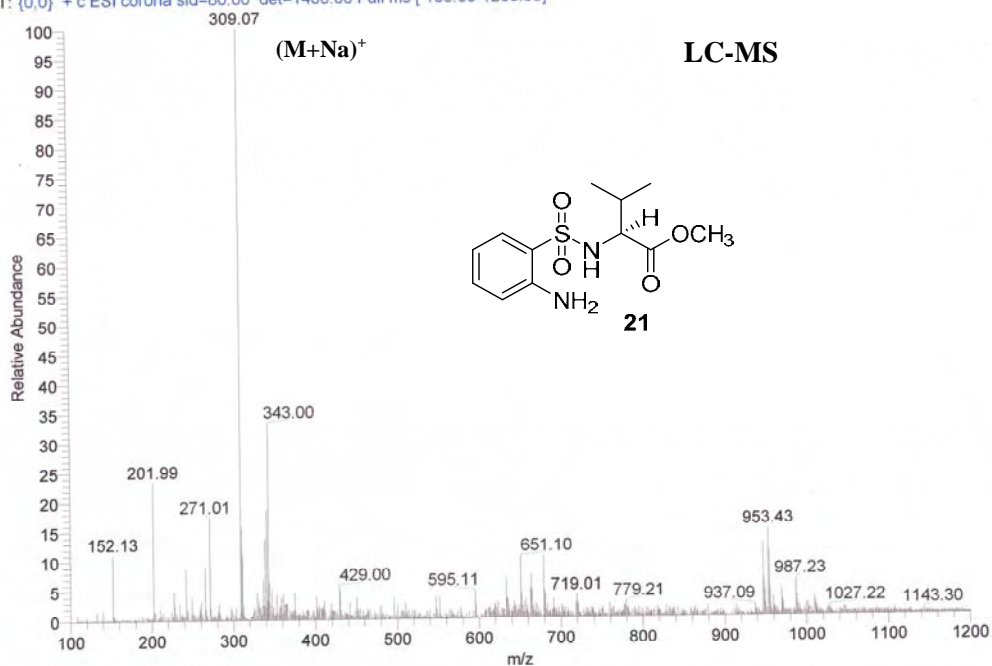




F:\DATA\FEB-12\GJS\NH2-SV-OMe

2/27/2012 3:07:08 PM

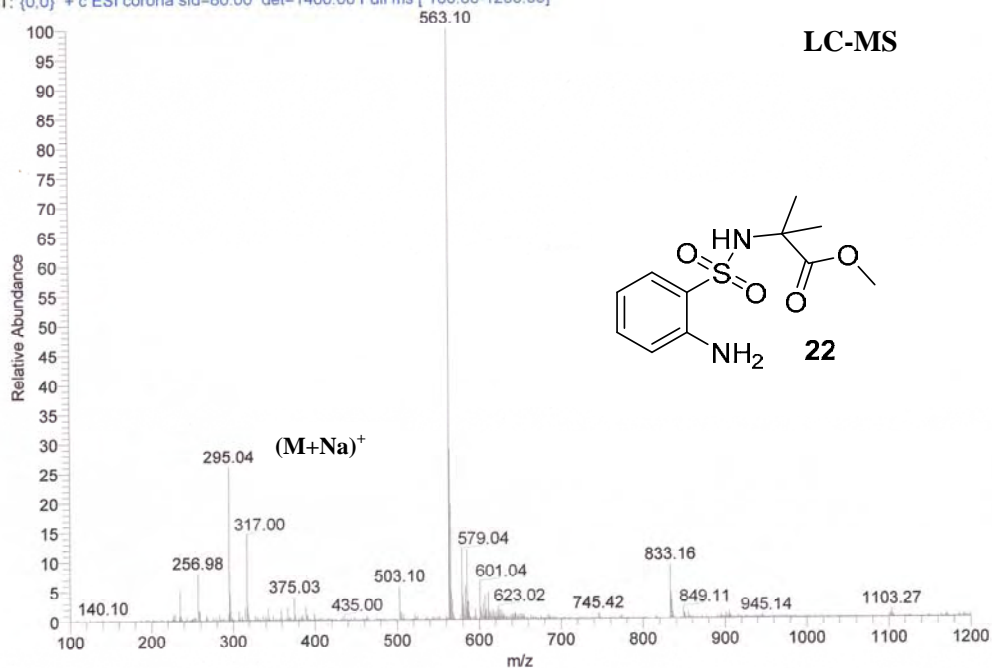
NH2-SV-OMe #7-34 RT: 0.10-0.57 AV: 28 SB: 28 0.00-0.12, 0.80-1.13 NL: 1.28E6  
T: (0,0) + c ESI corona sid=80.00 det=1400.00 Full ms [ 100.00-1200.00]

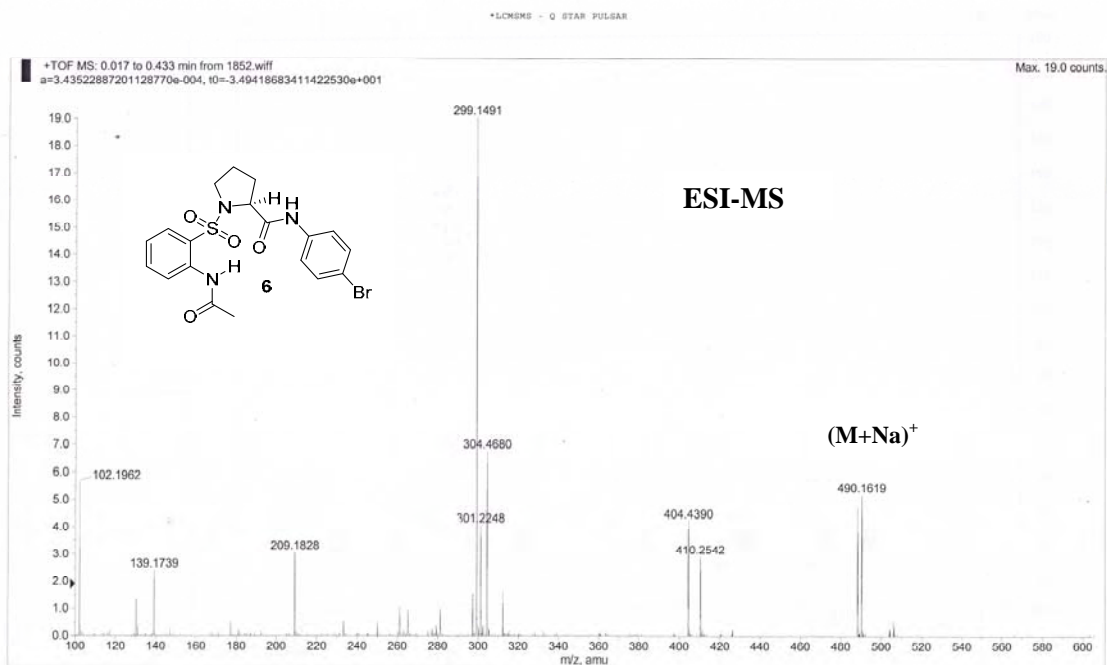
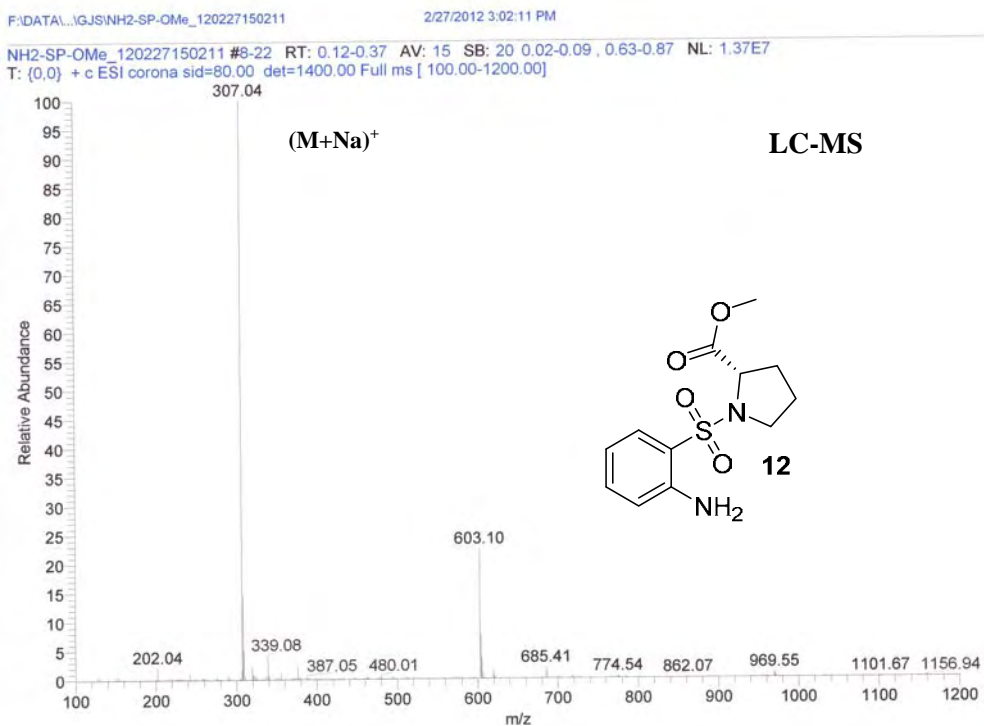


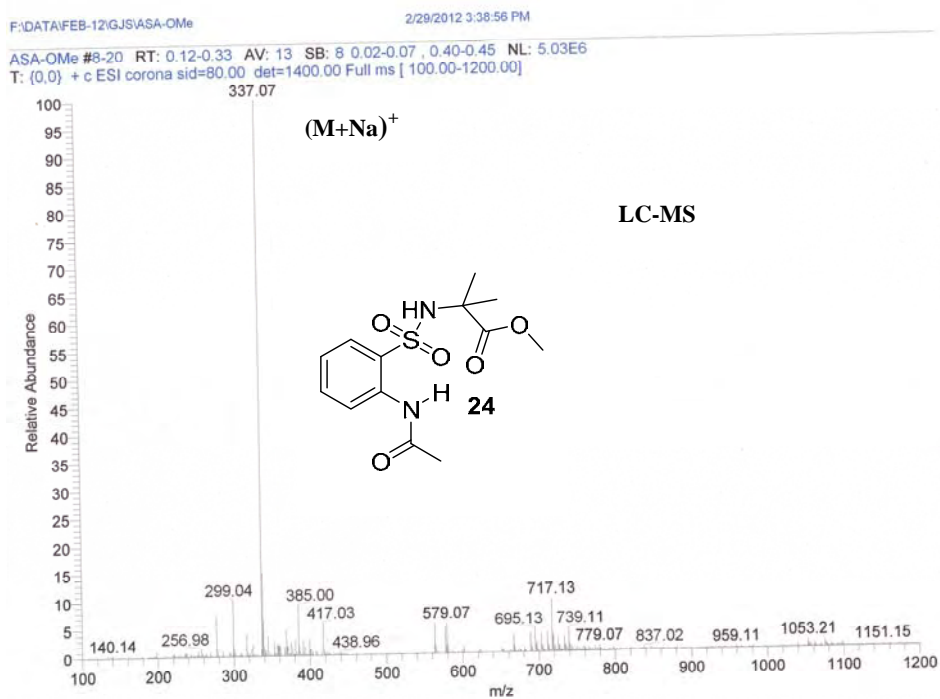
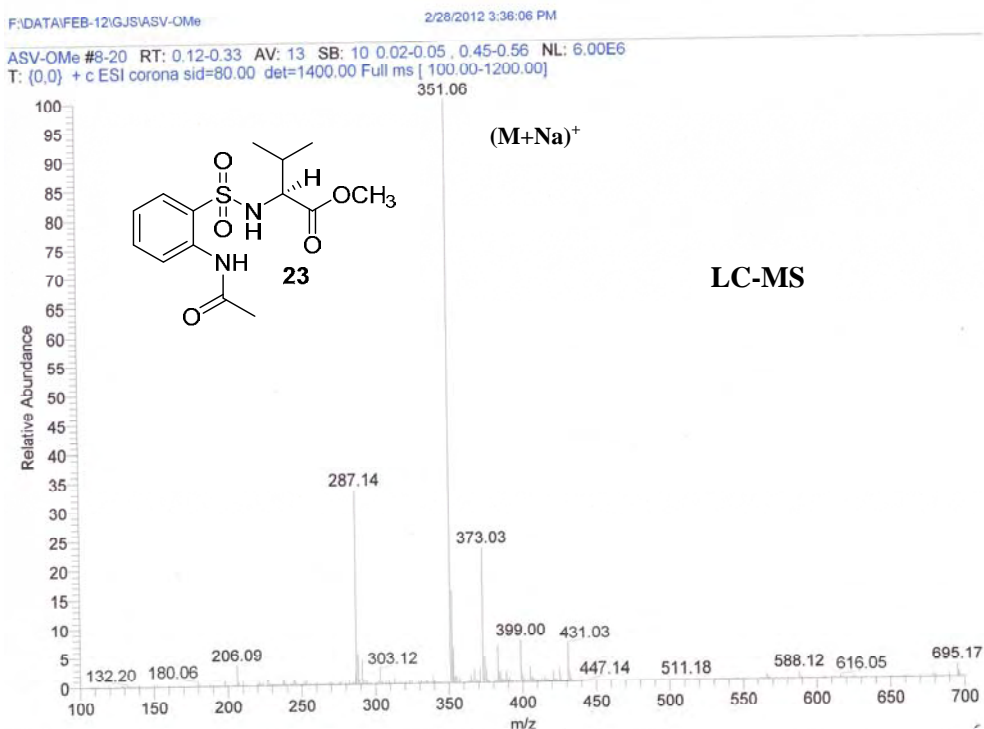
F:\DATA\FEB-12\GJS\NH2-SA-OMe

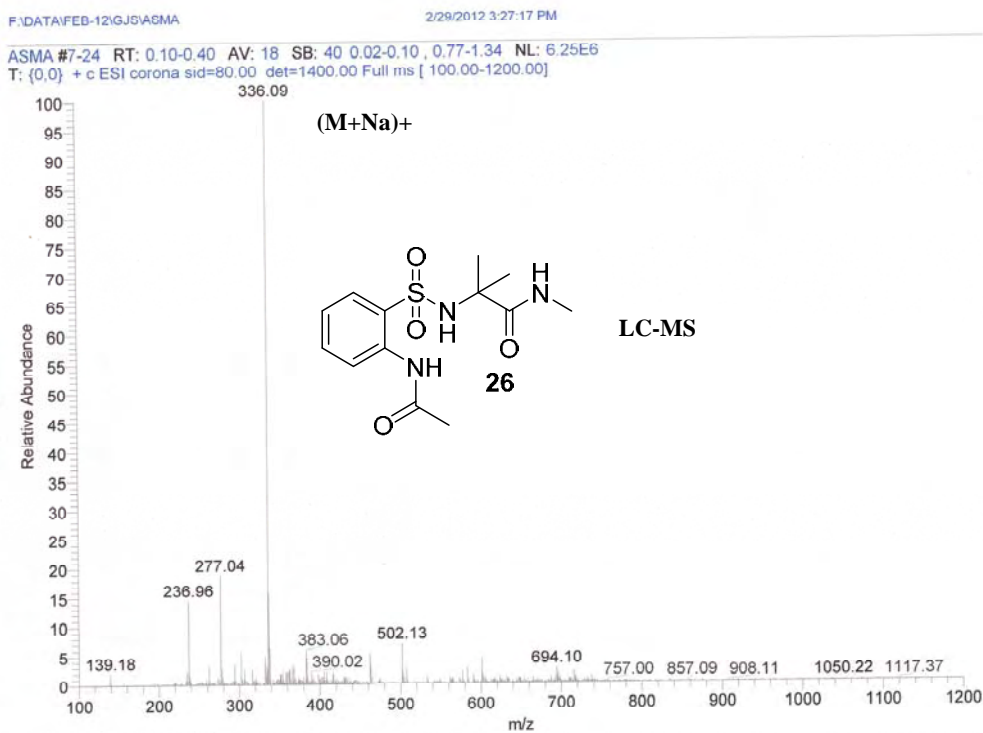
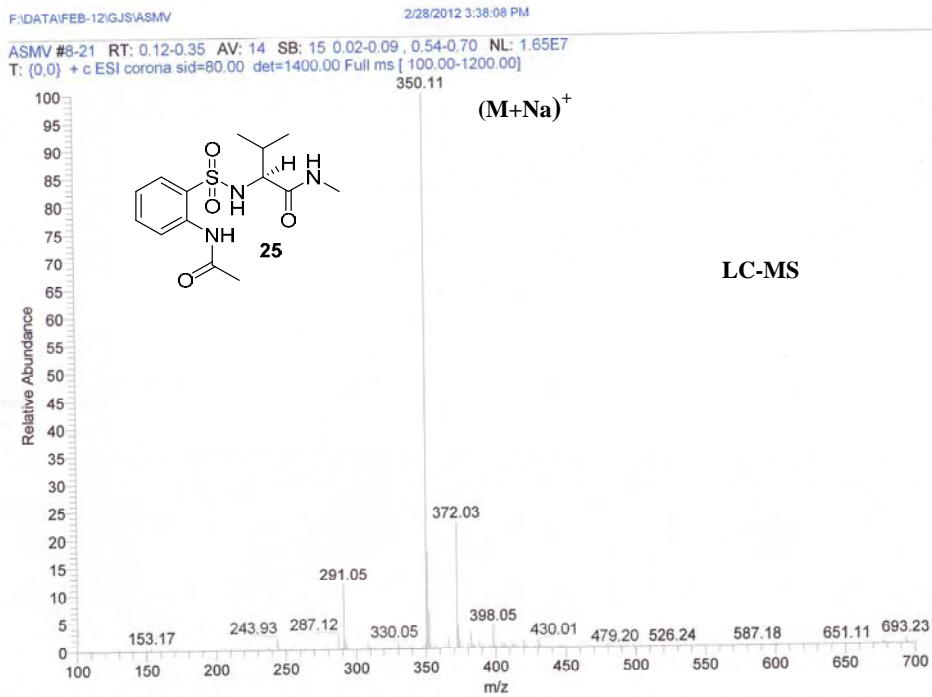
2/29/2012 3:36:33 PM

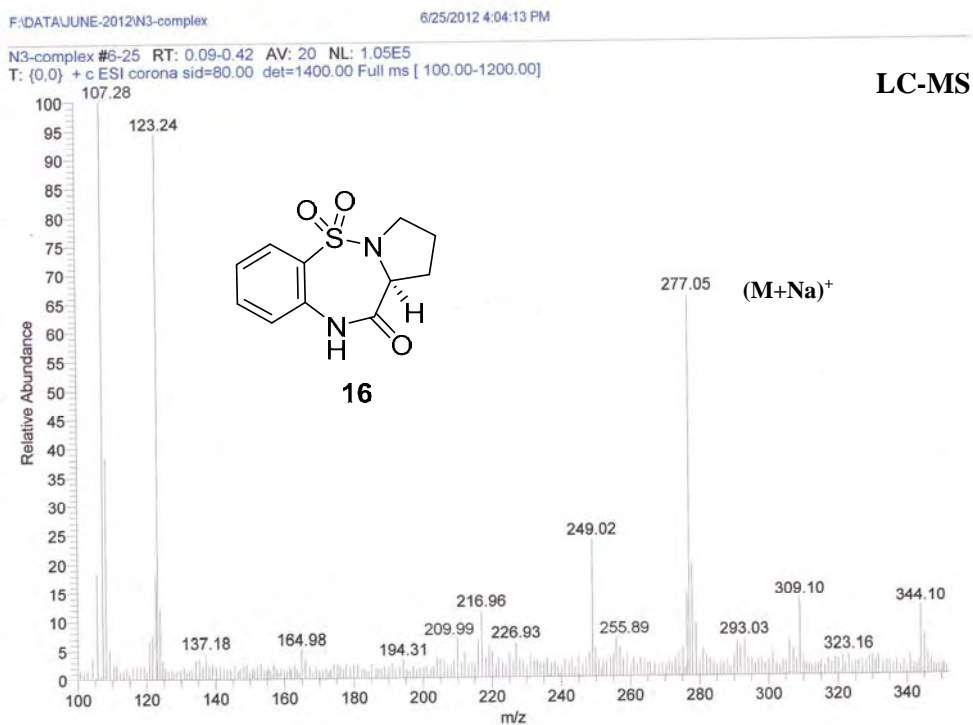
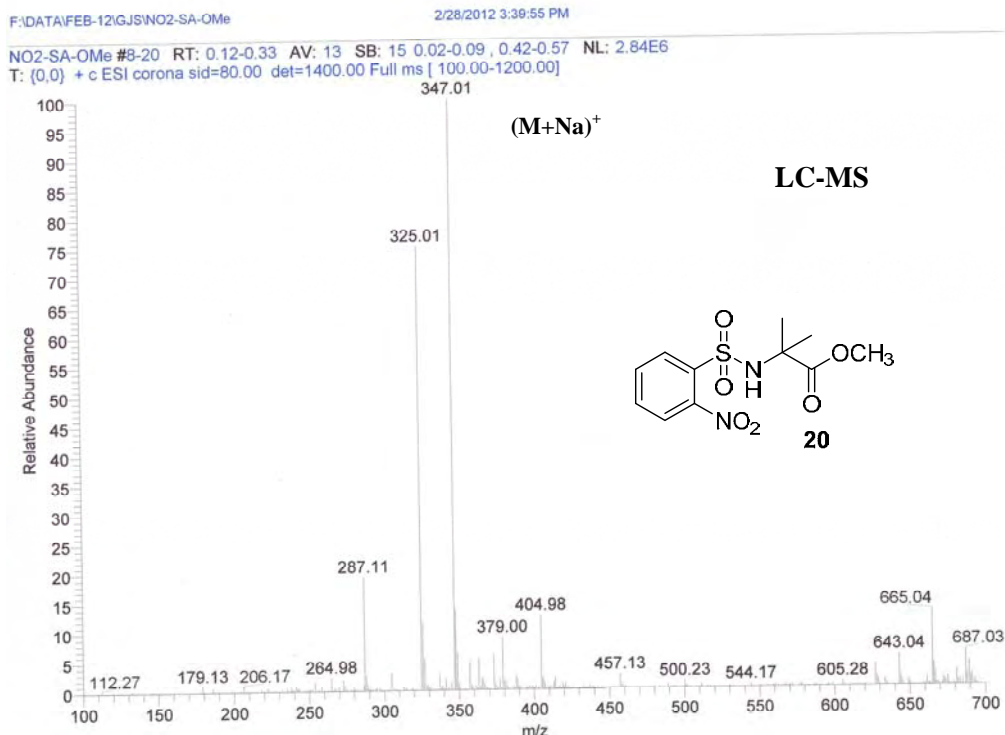
NH2-SA-OMe #8-20 RT: 0.12-0.33 AV: 13 SB: 23 0.02-0.09, 0.52-0.82 NL: 7.16E6  
T: (0,0) + c ESI corona sid=80.00 det=1400.00 Full ms [ 100.00-1200.00]

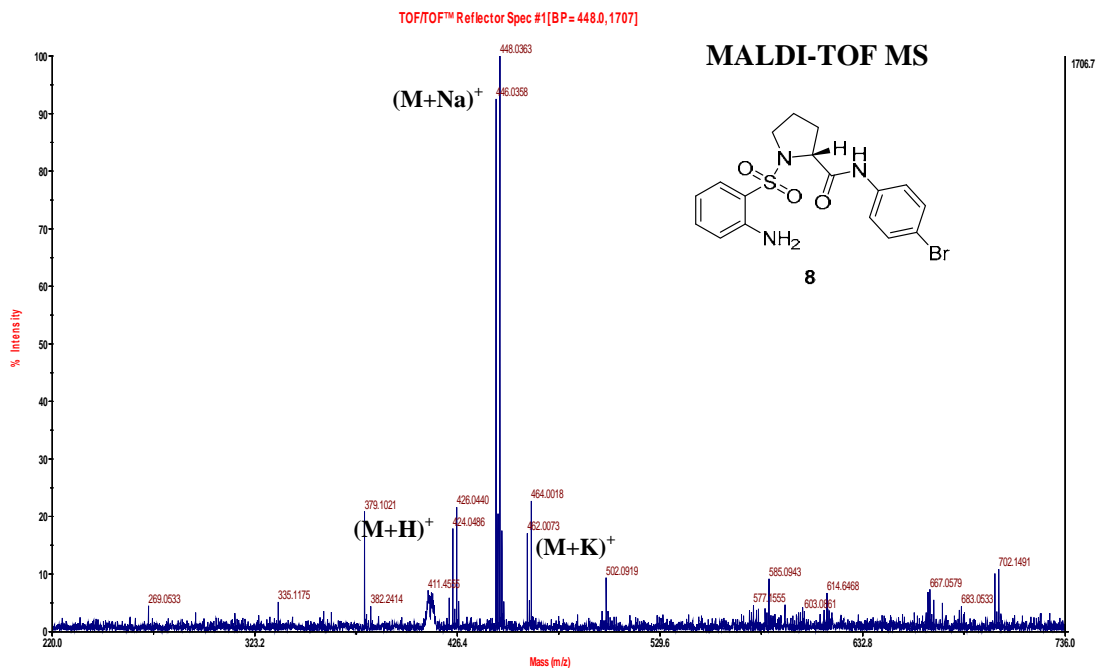
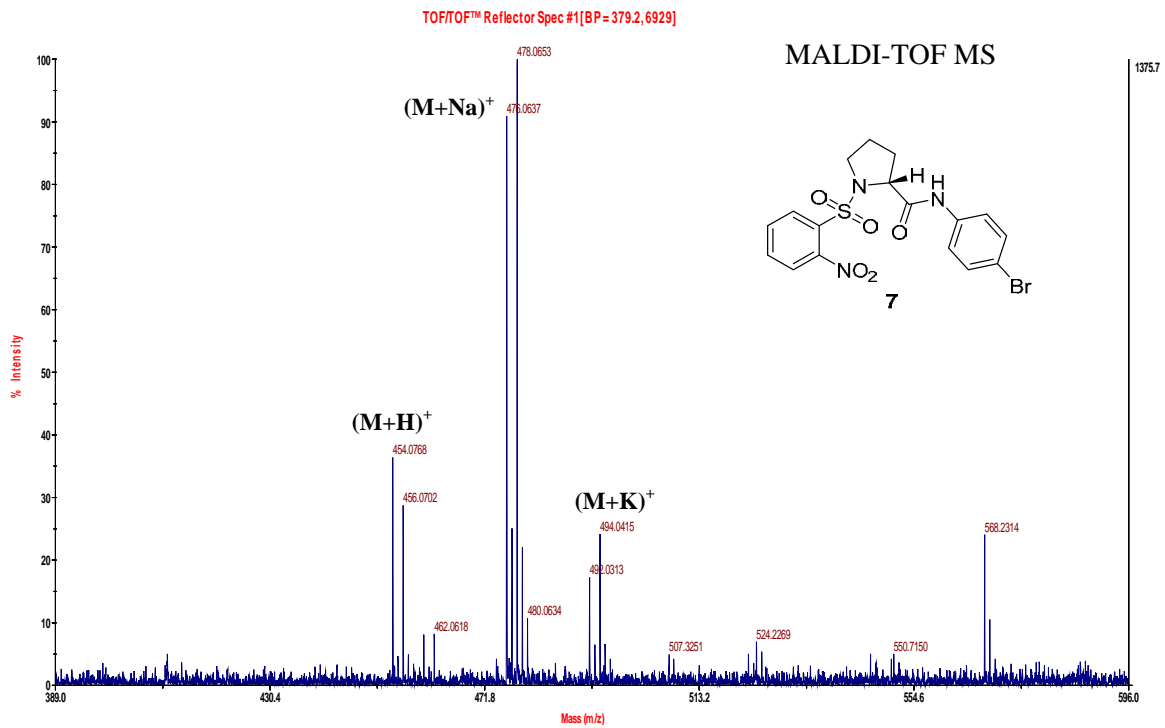




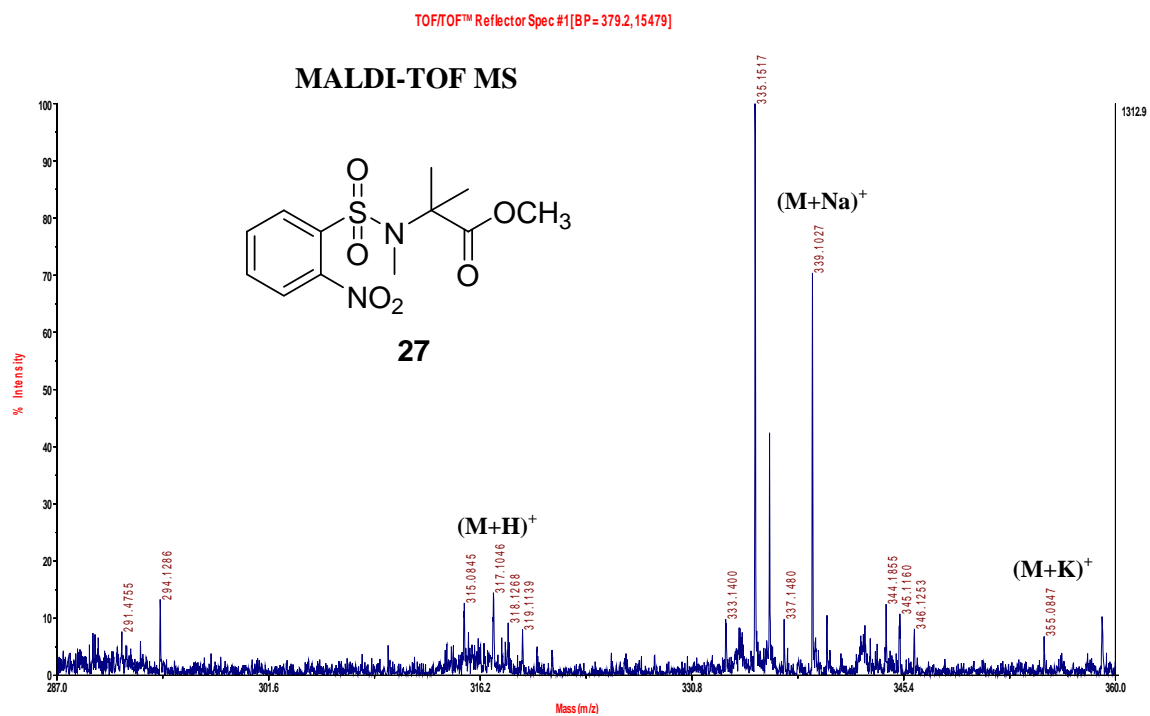
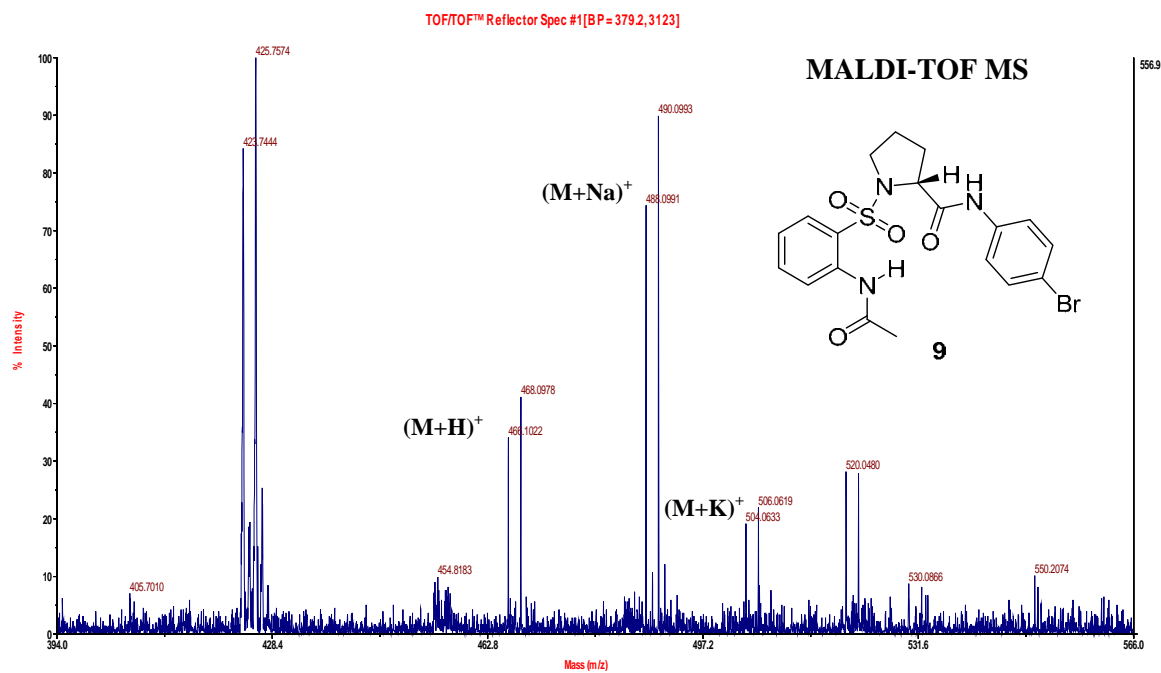


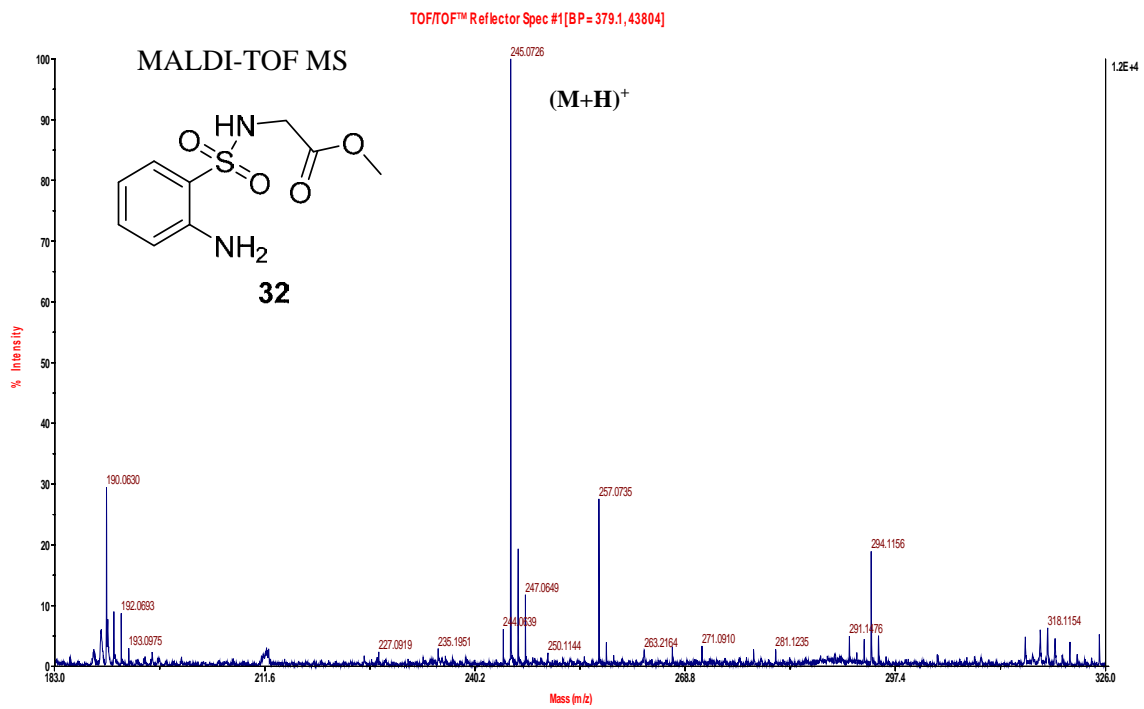
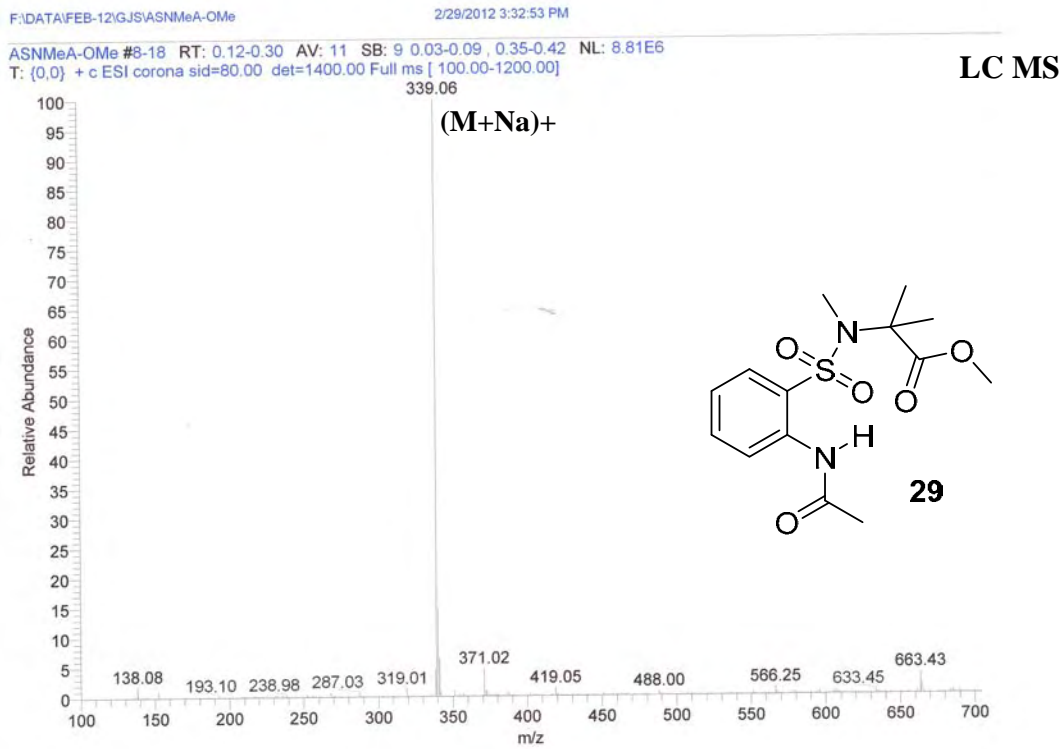


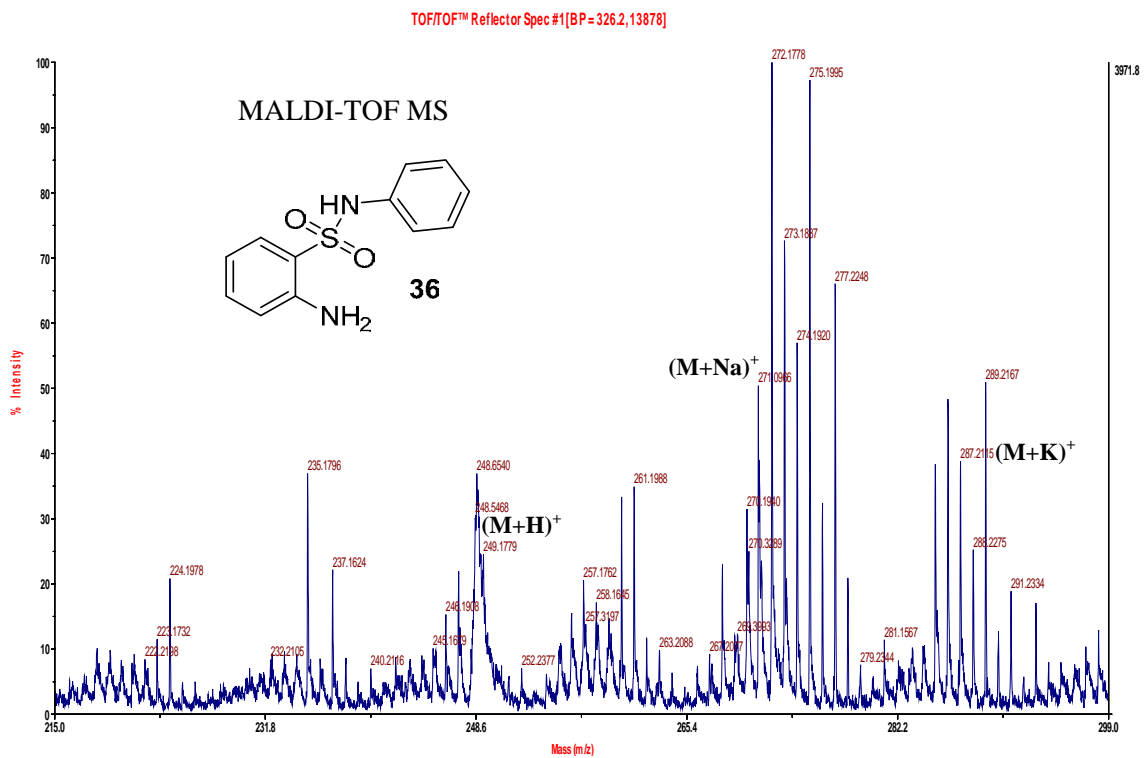
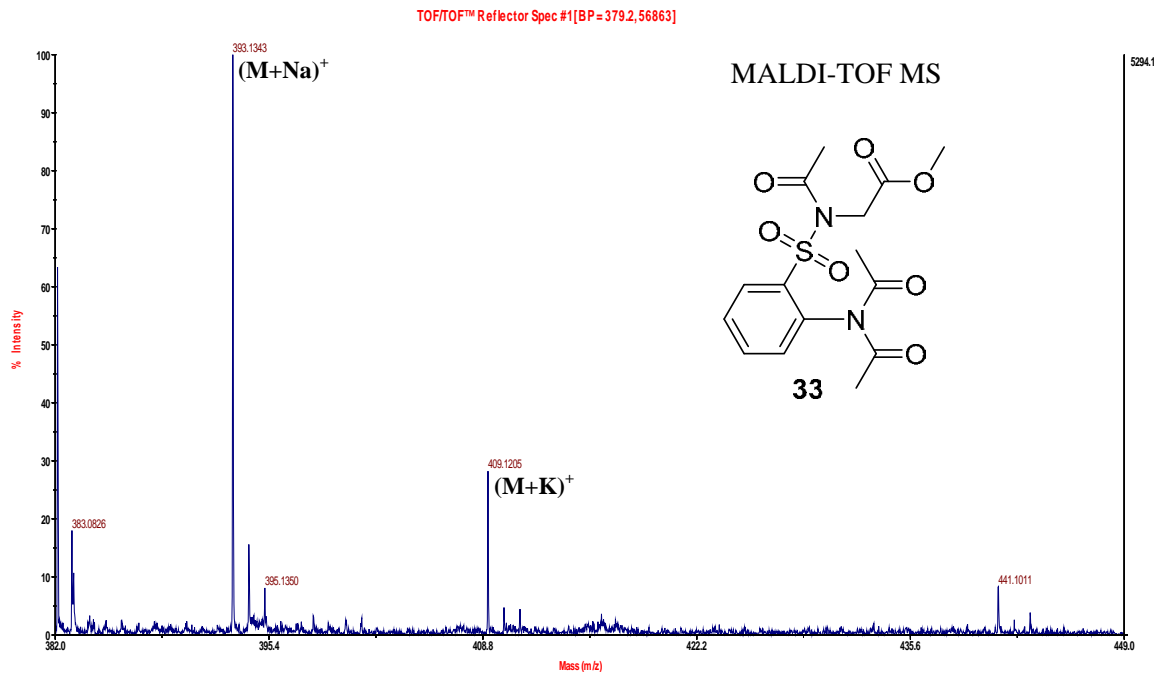


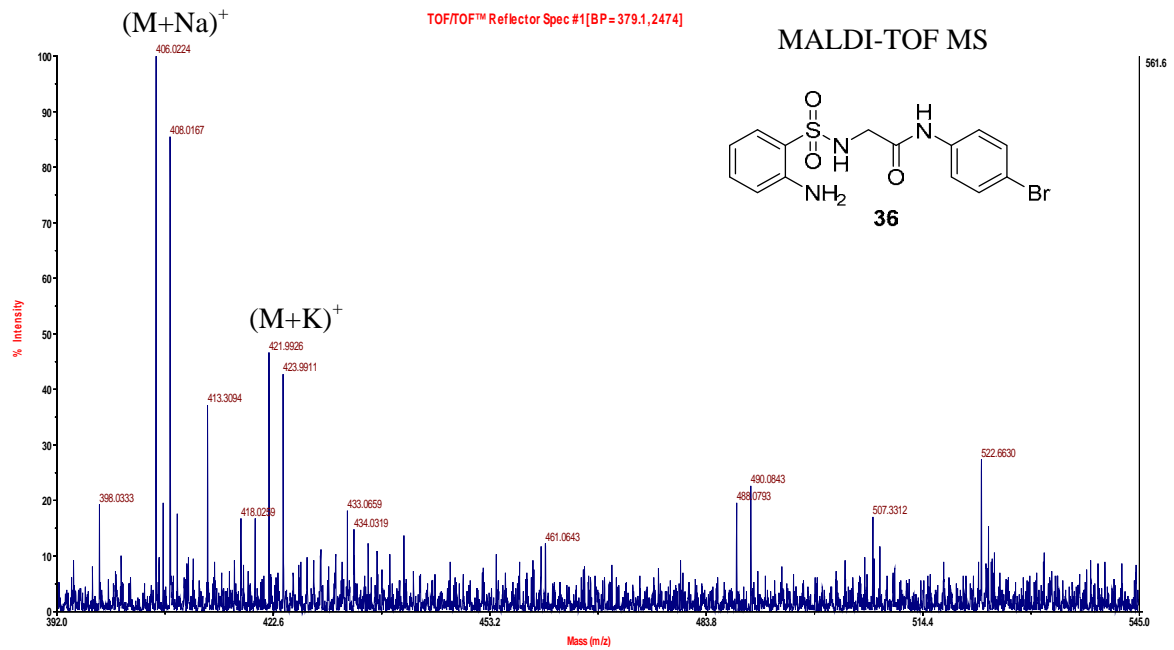
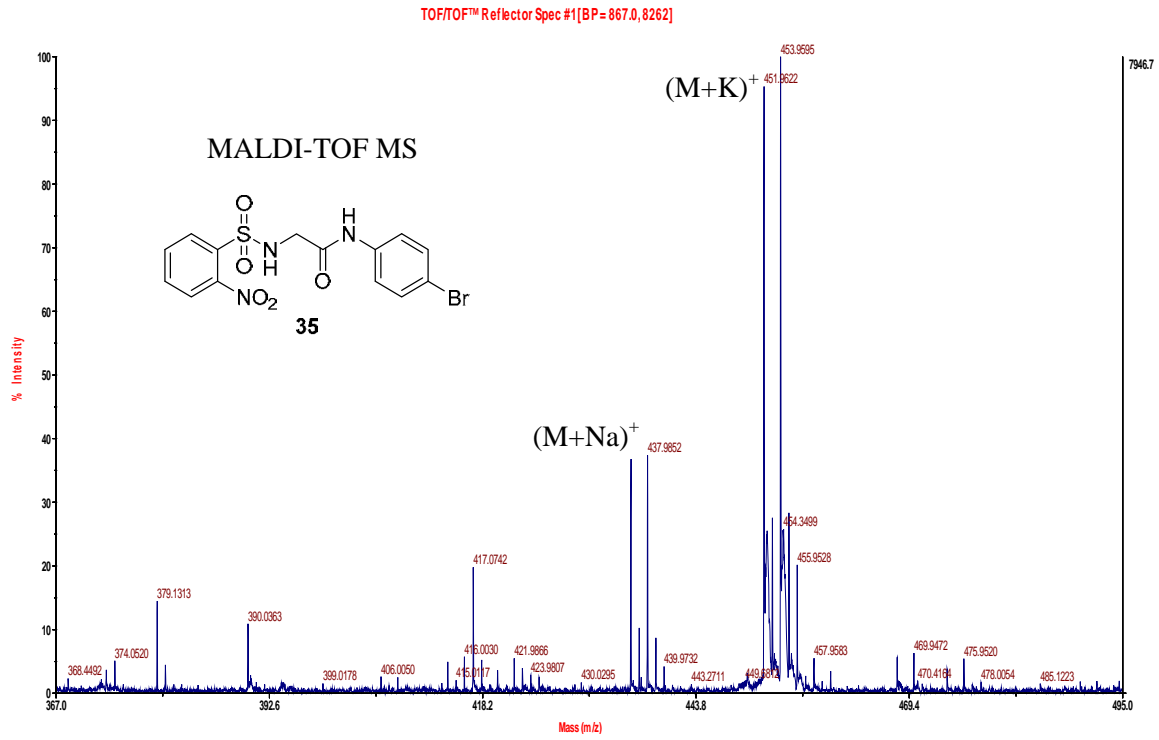


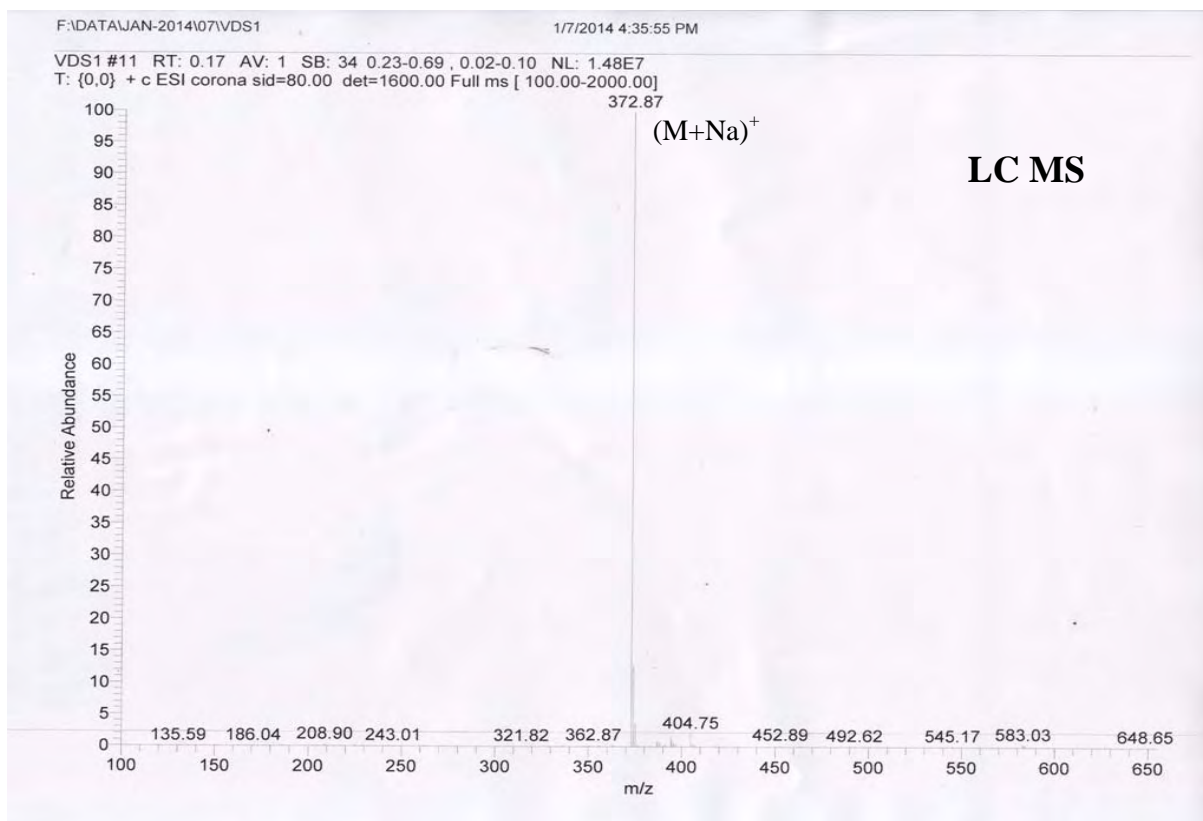
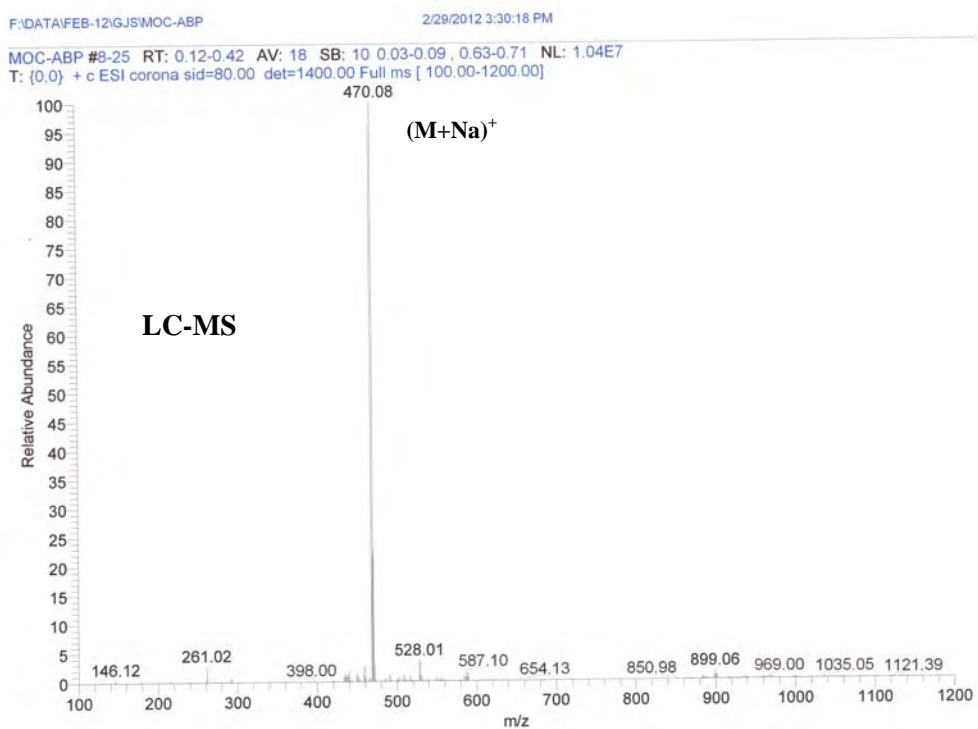


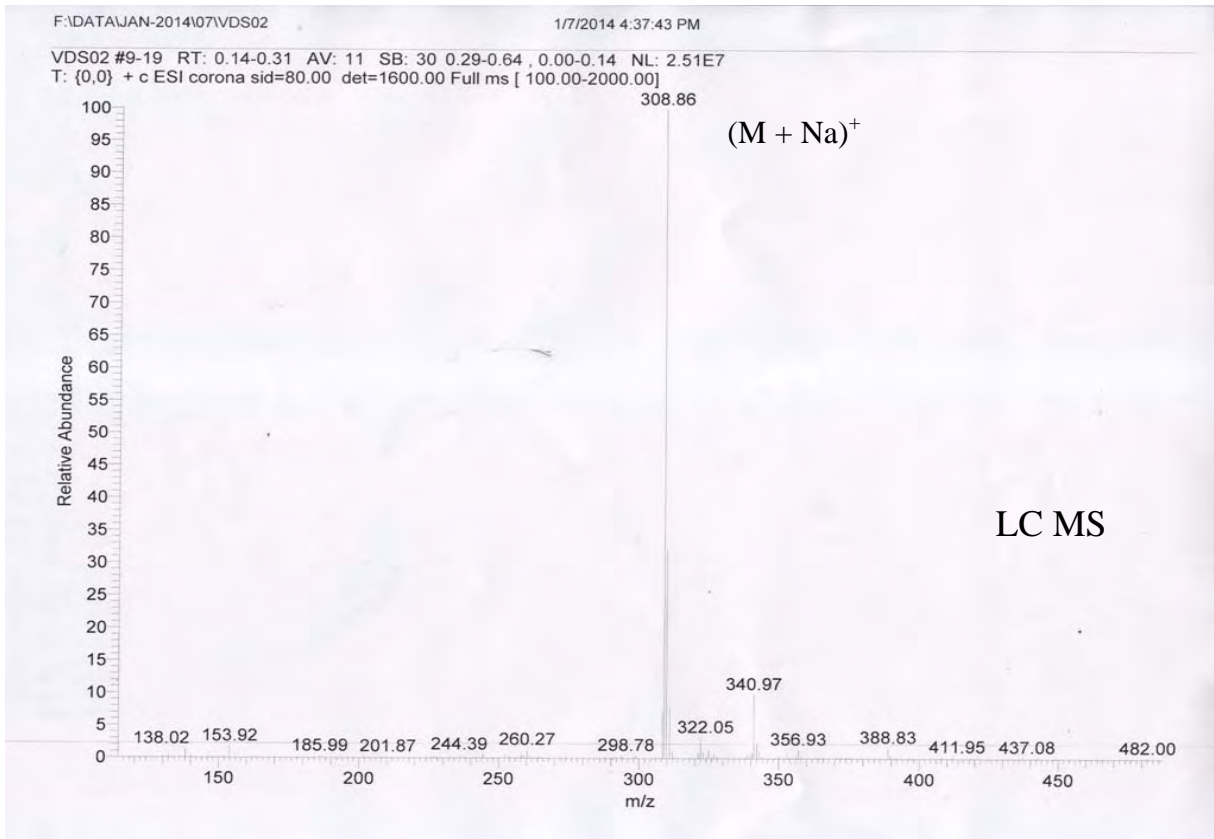


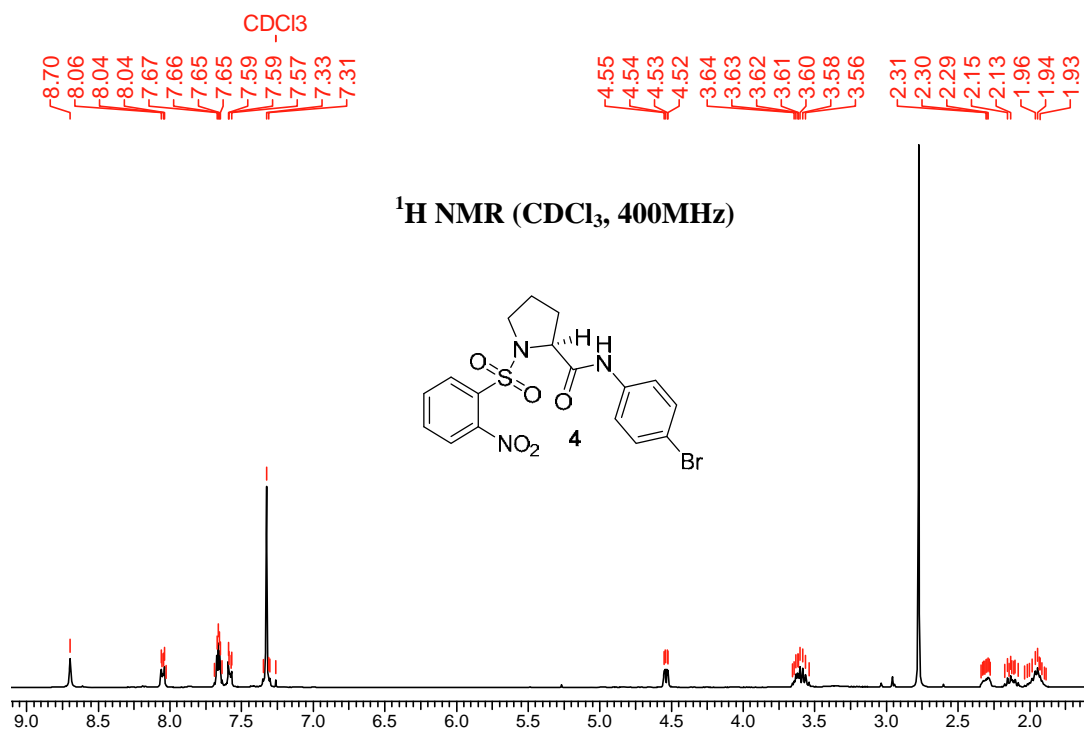
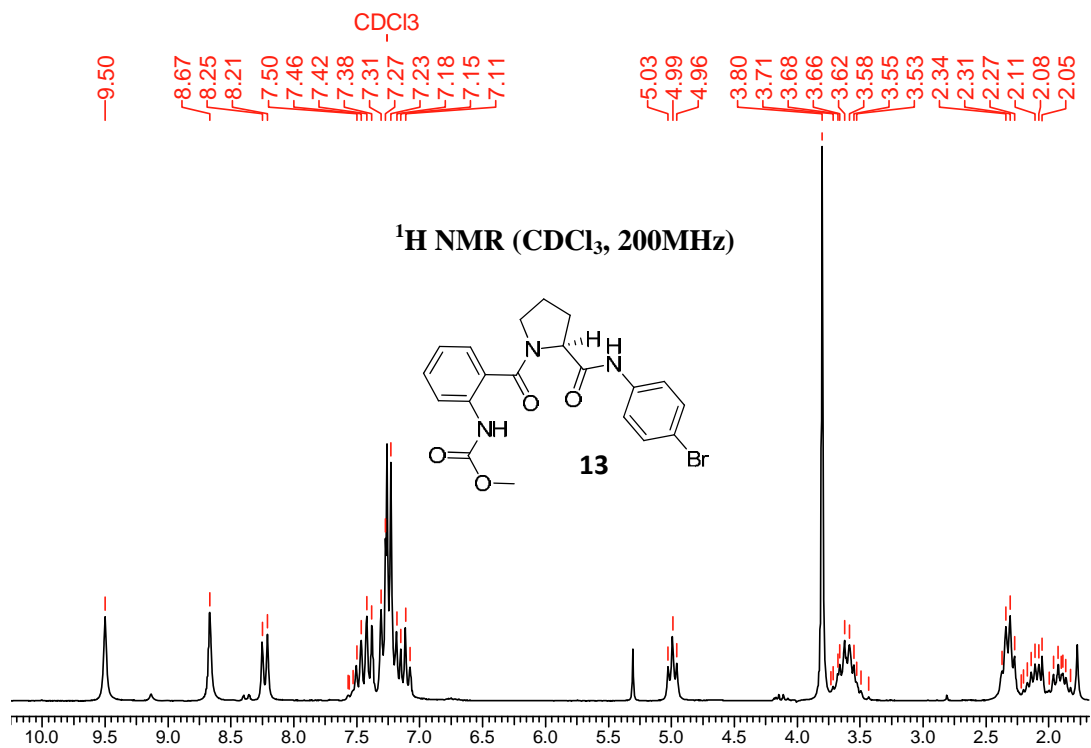


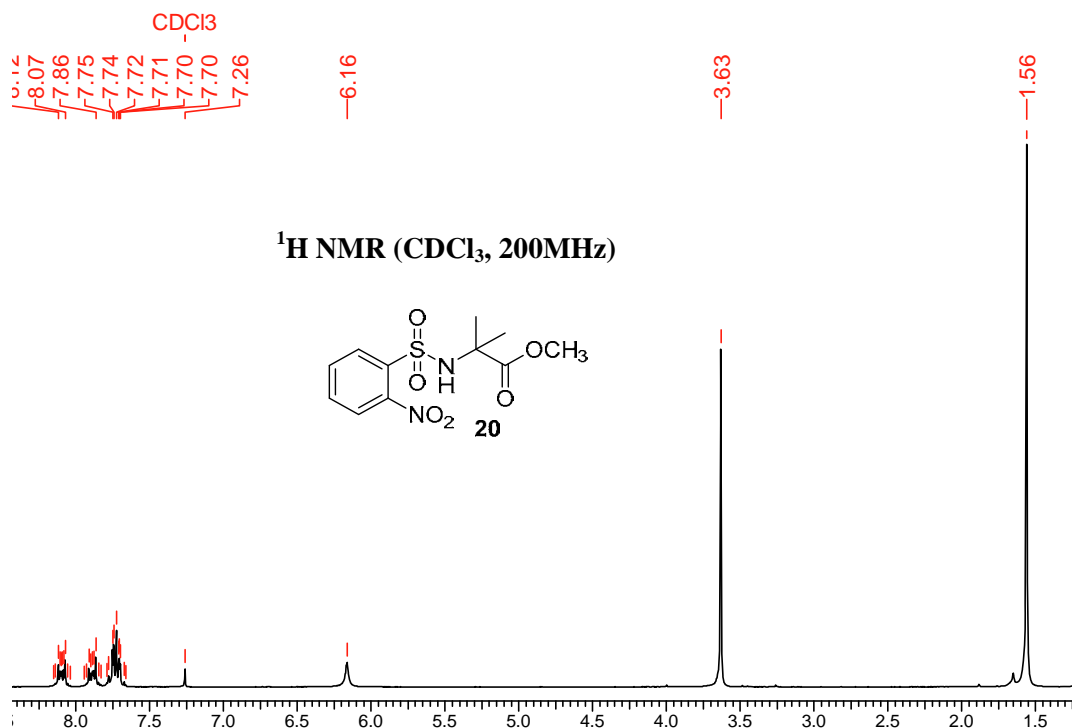
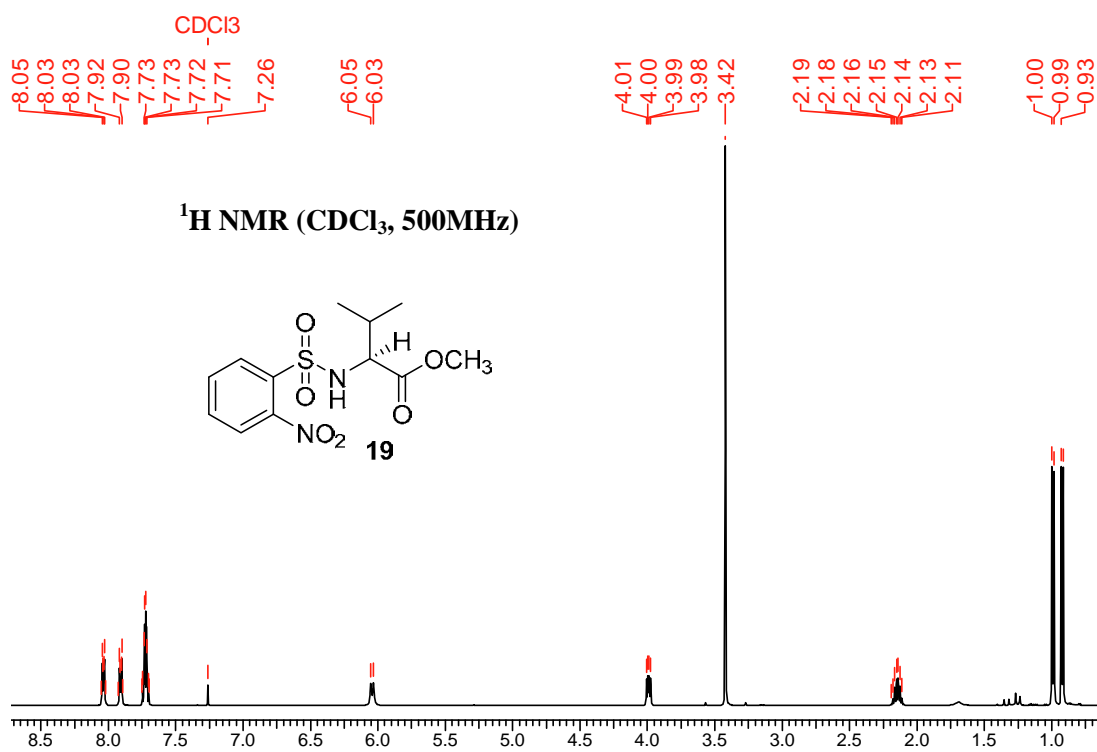




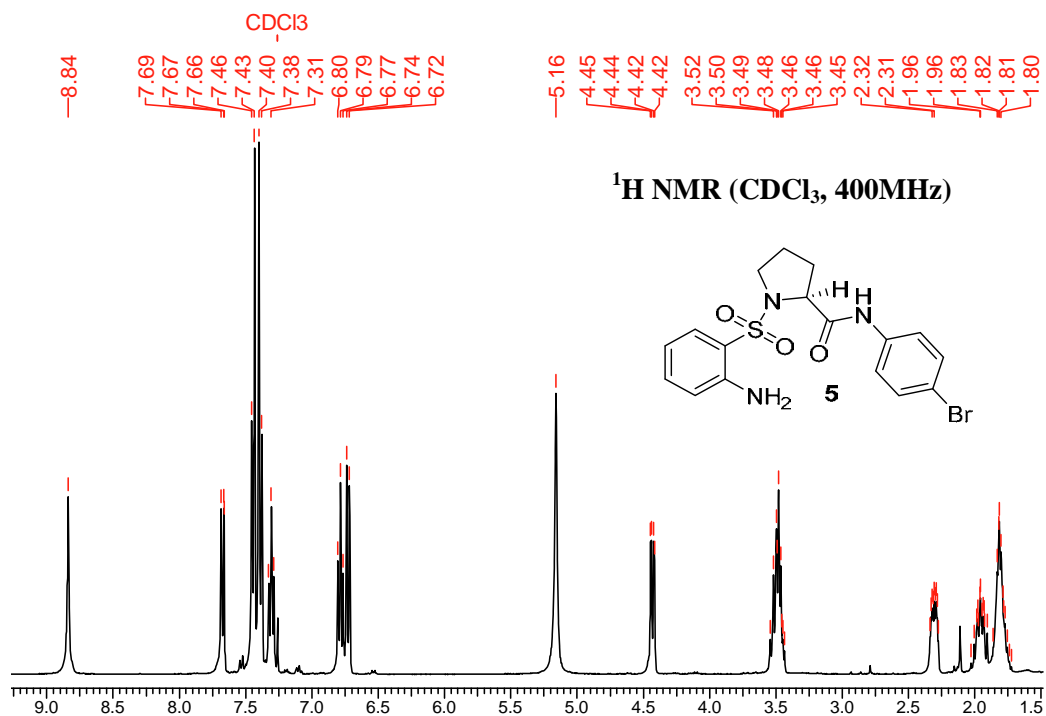
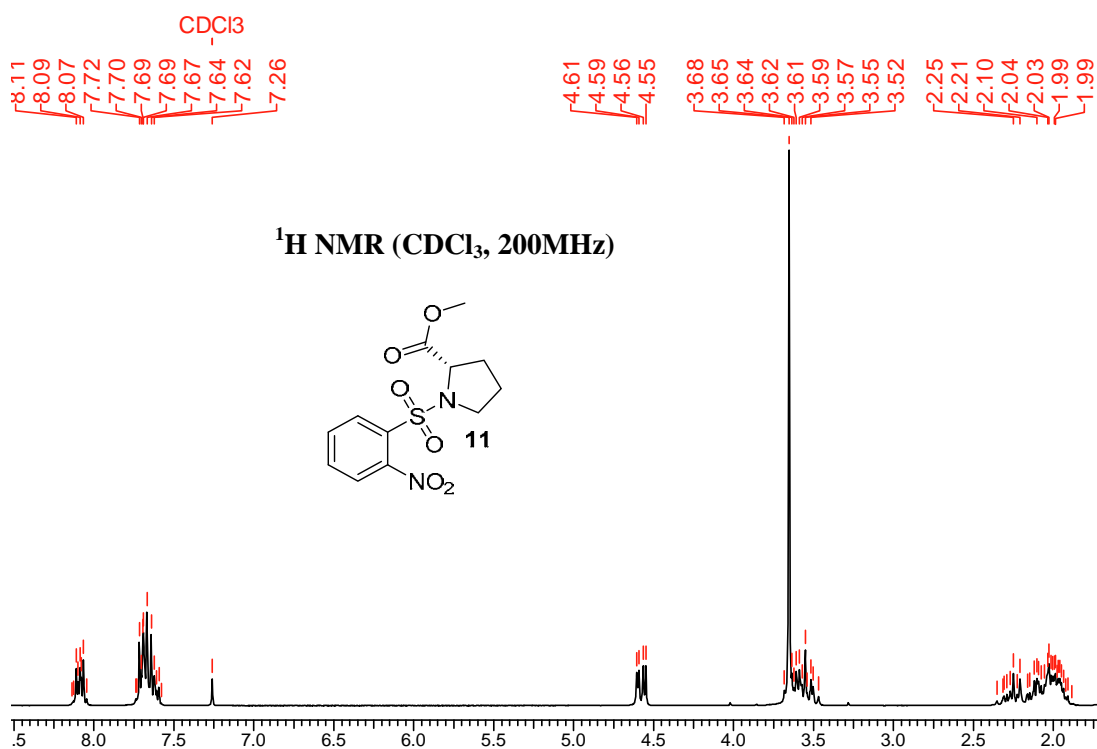


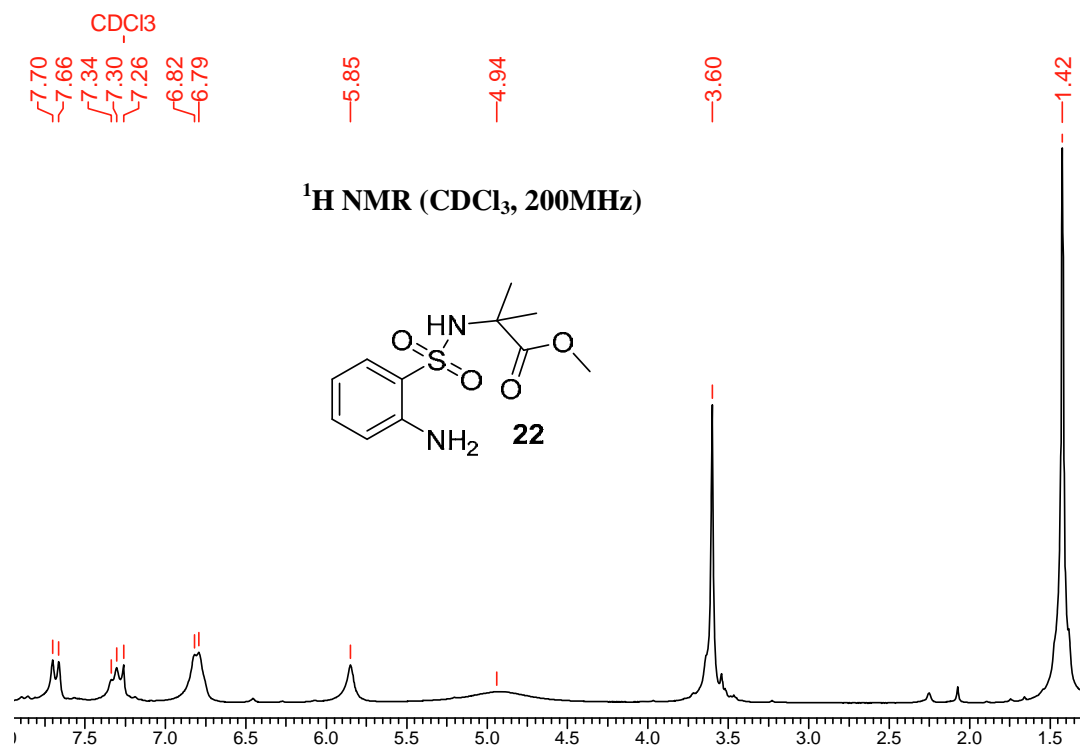
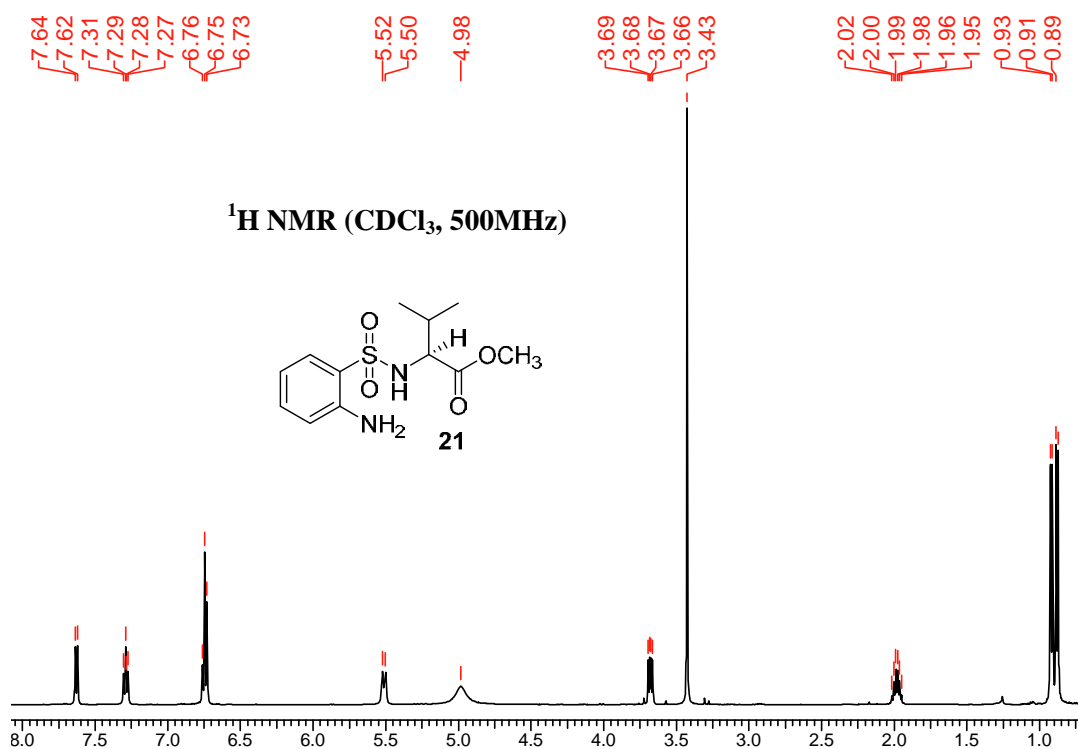


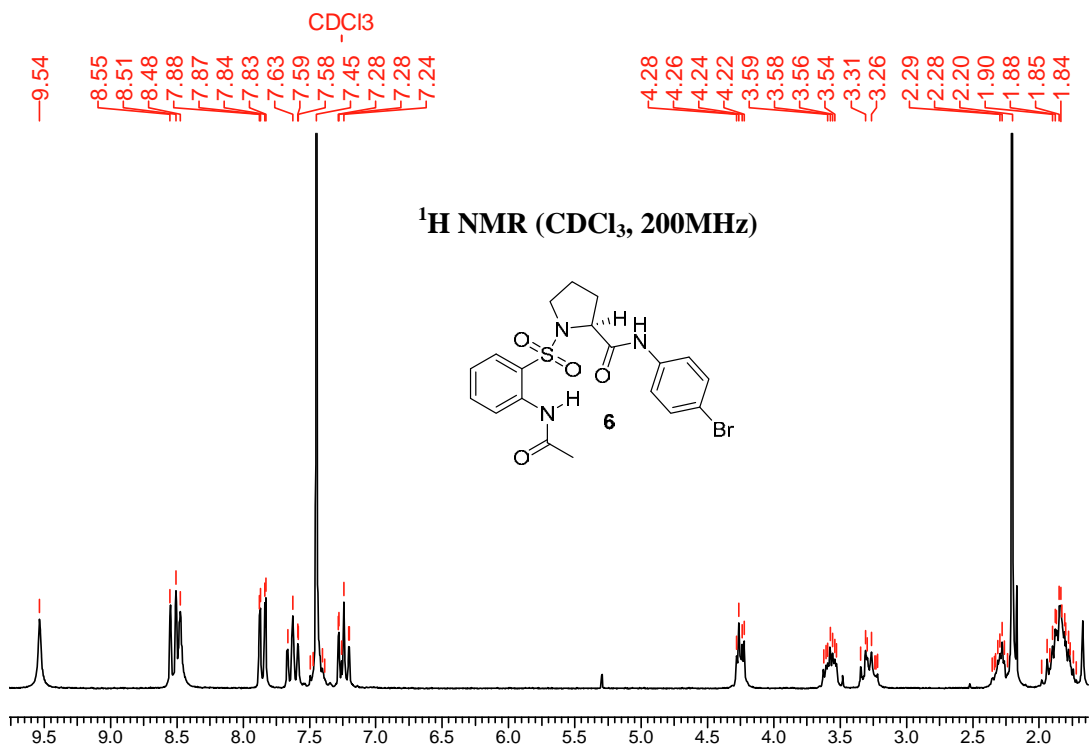
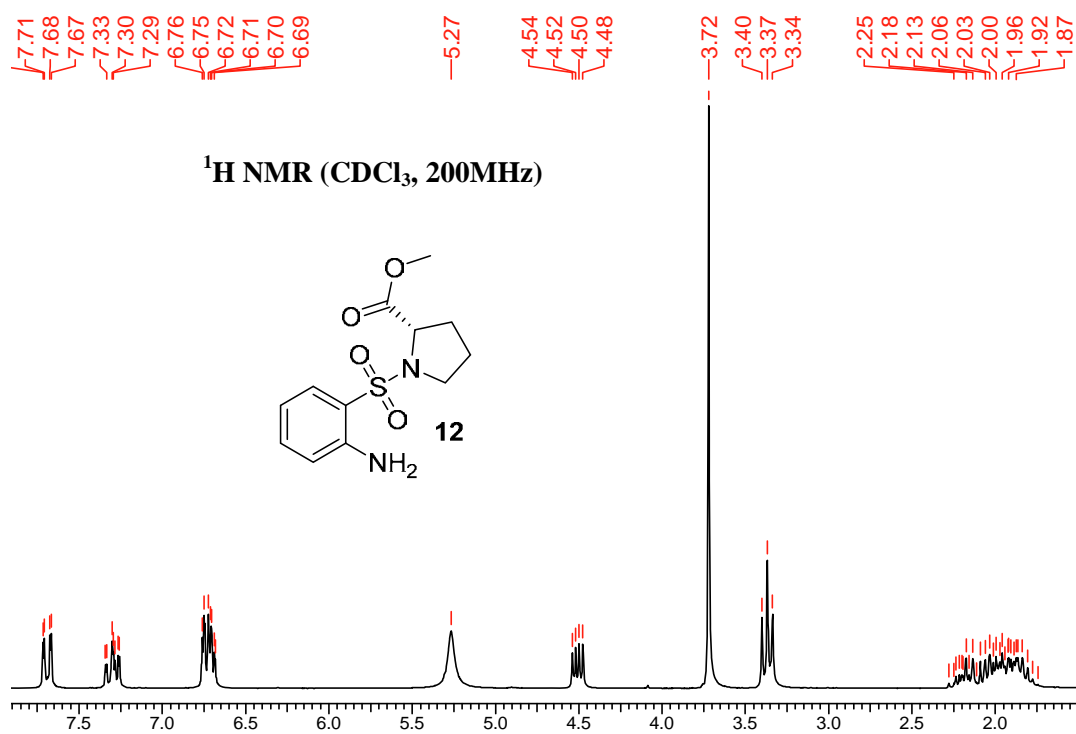


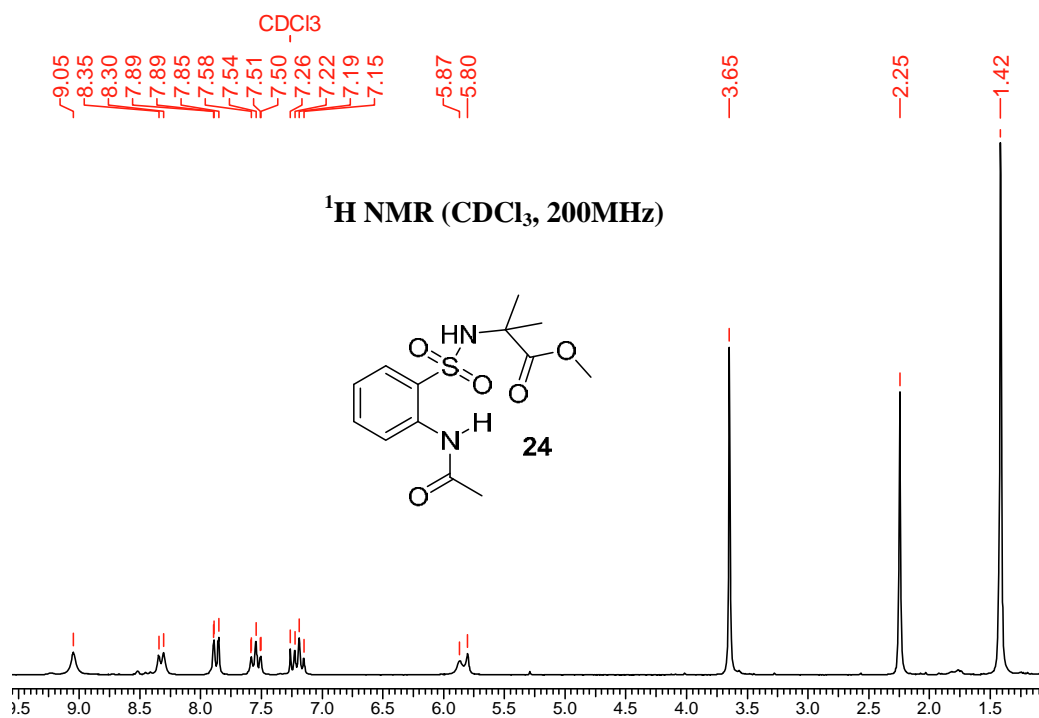
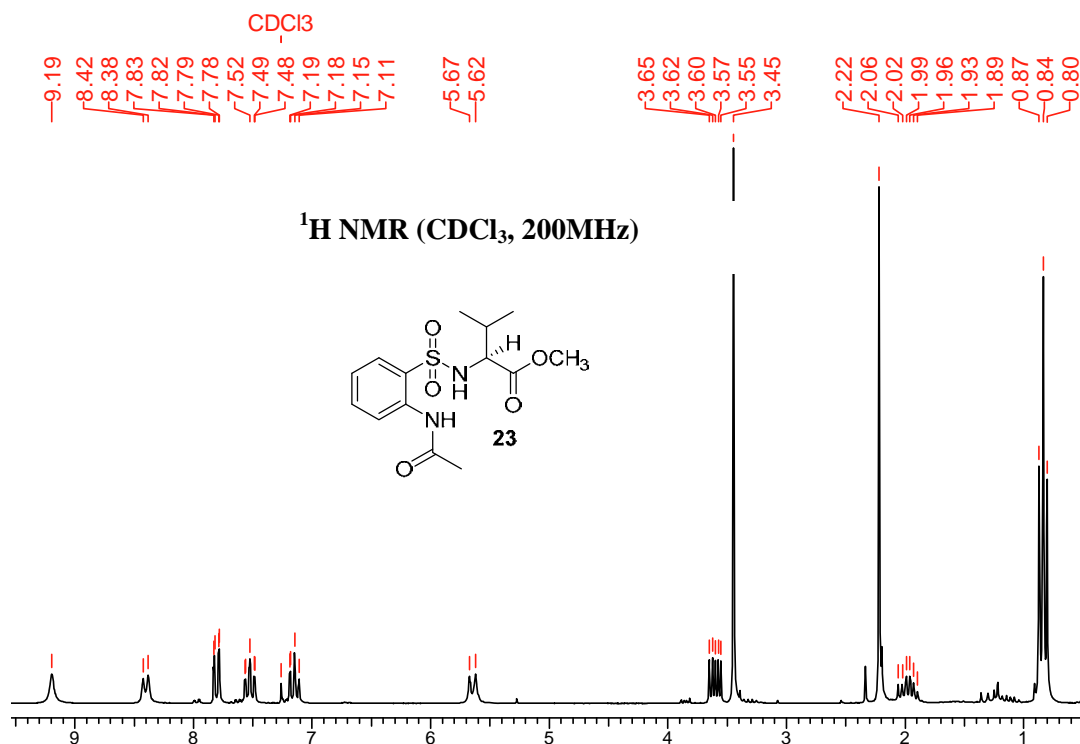


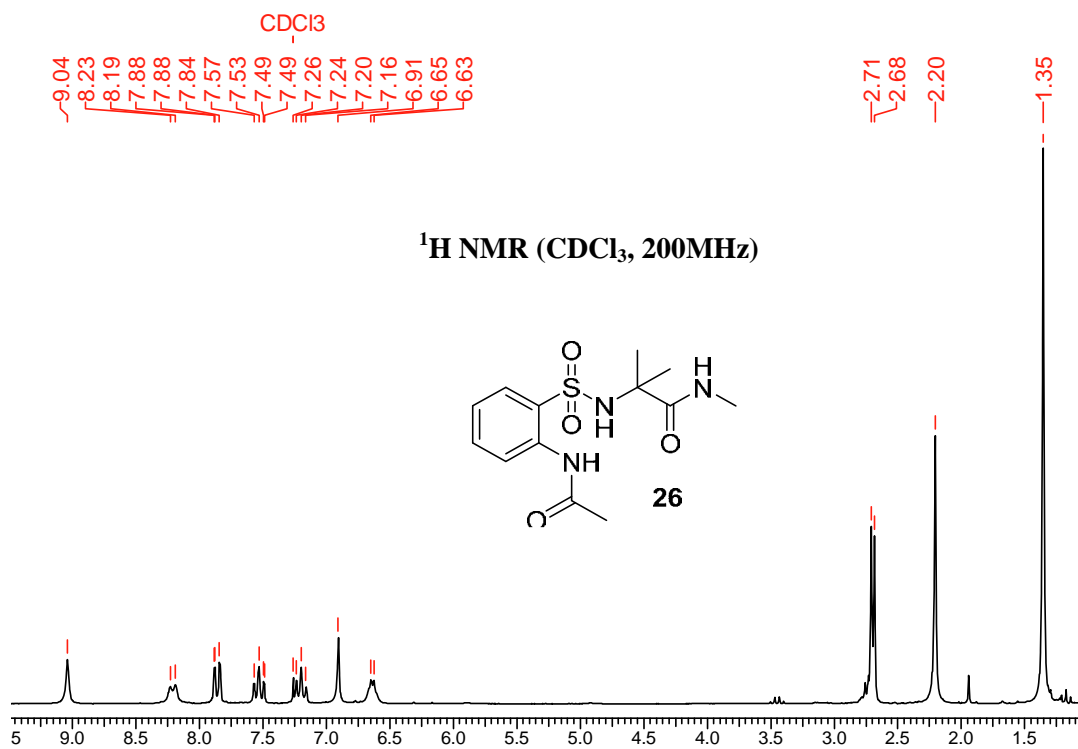
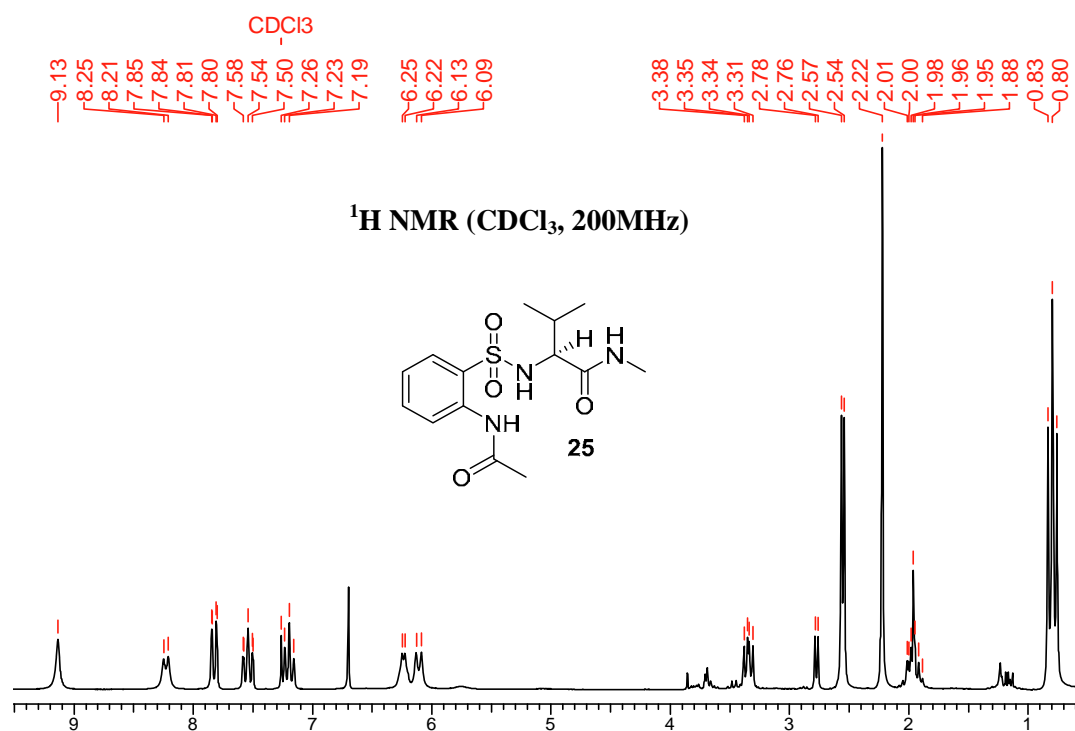






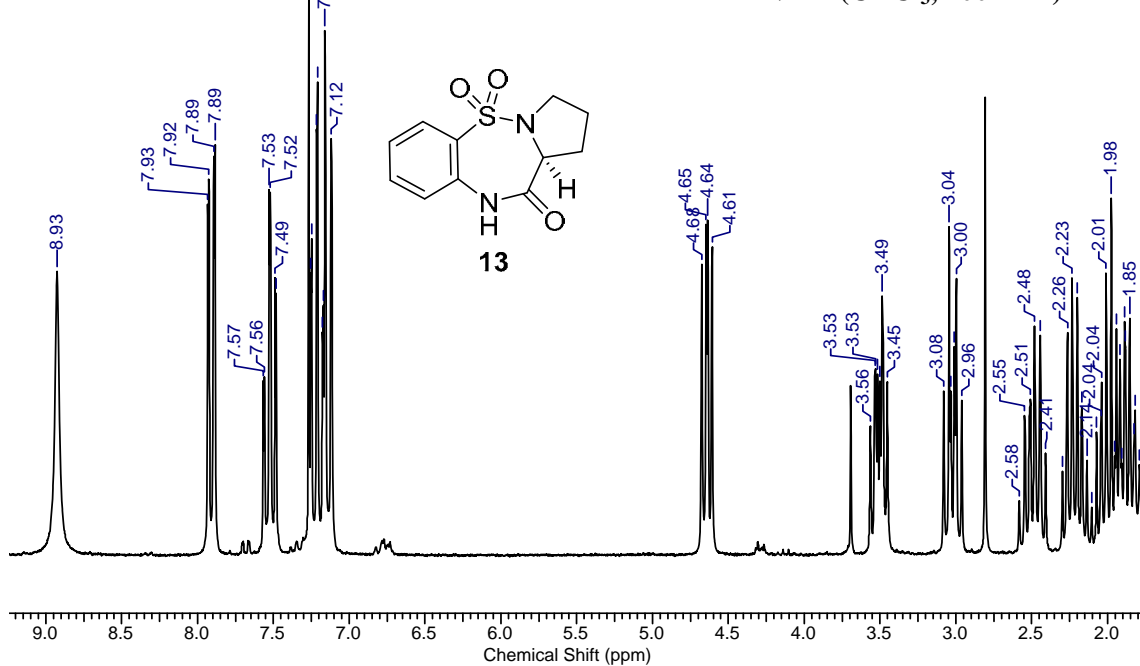






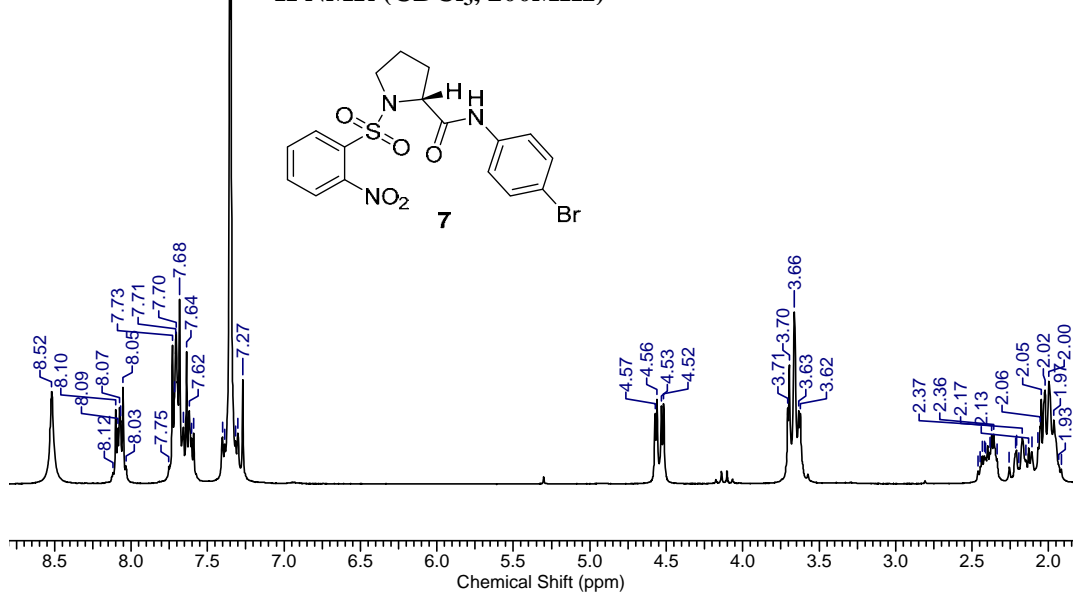
hiadiazepinone Mon3av2#077.001.001.1r.esp

<sup>1</sup>H NMR (CDCl<sub>3</sub>, 200MHz)

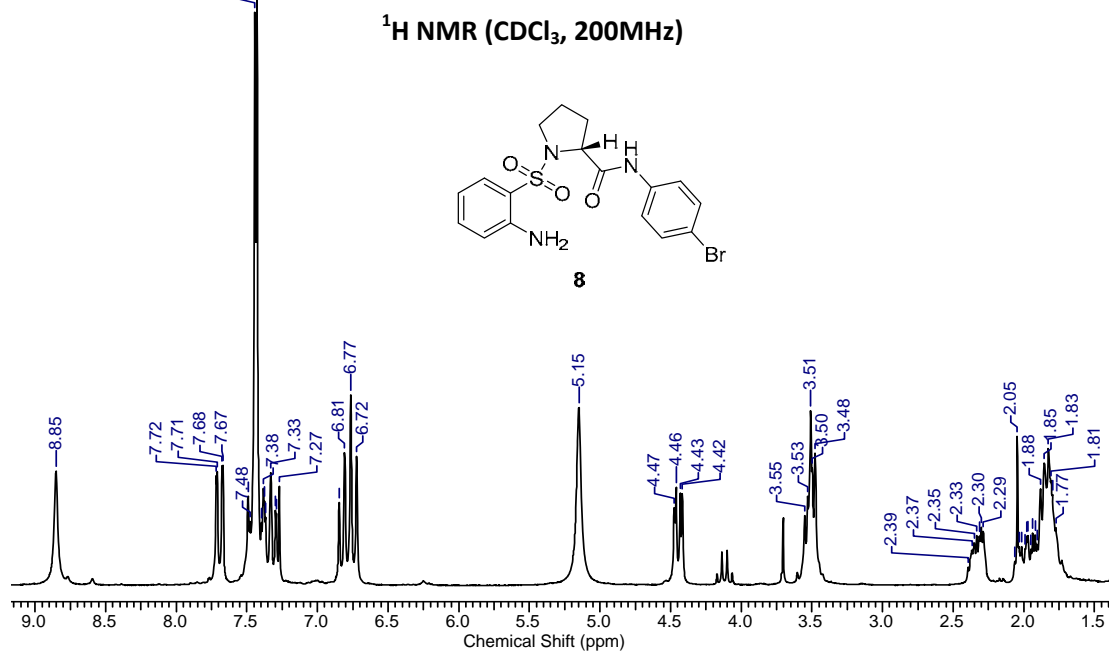


NO2-S-D-Pro-NHB Mon5av2#014 2-nitro benzenesulfonyl D-Pro 4-Br anilide.001.001.1r.esp

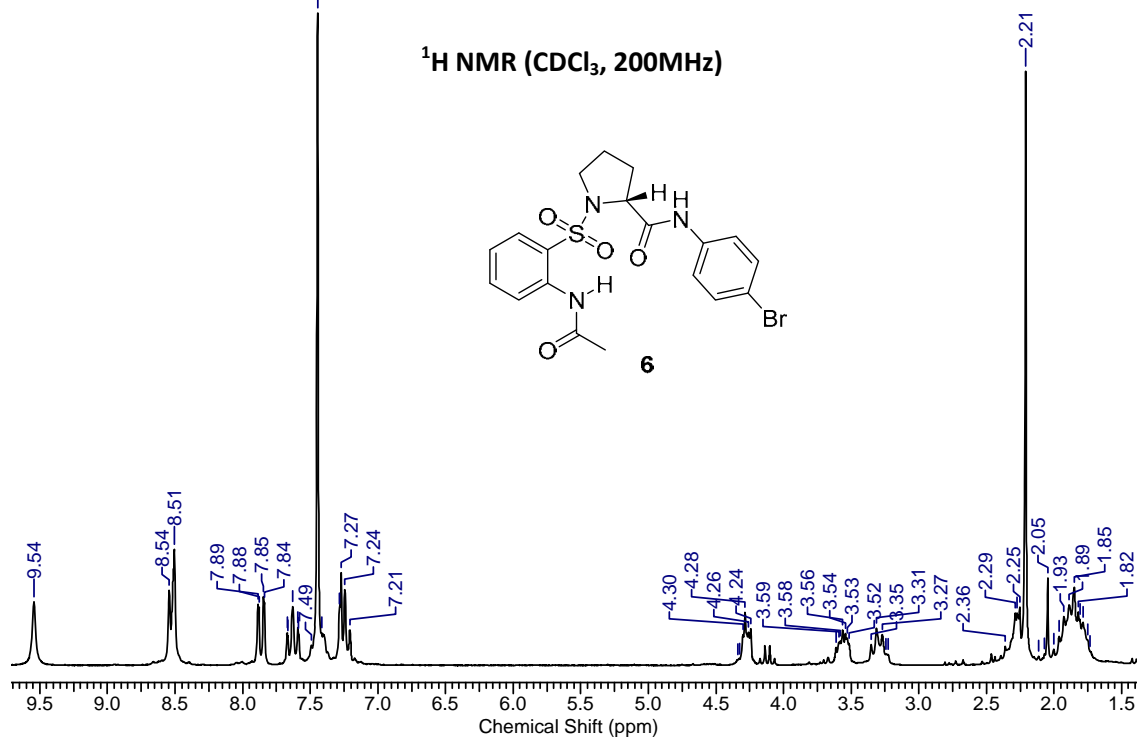
<sup>1</sup>H NMR (CDCl<sub>3</sub>, 200MHz)



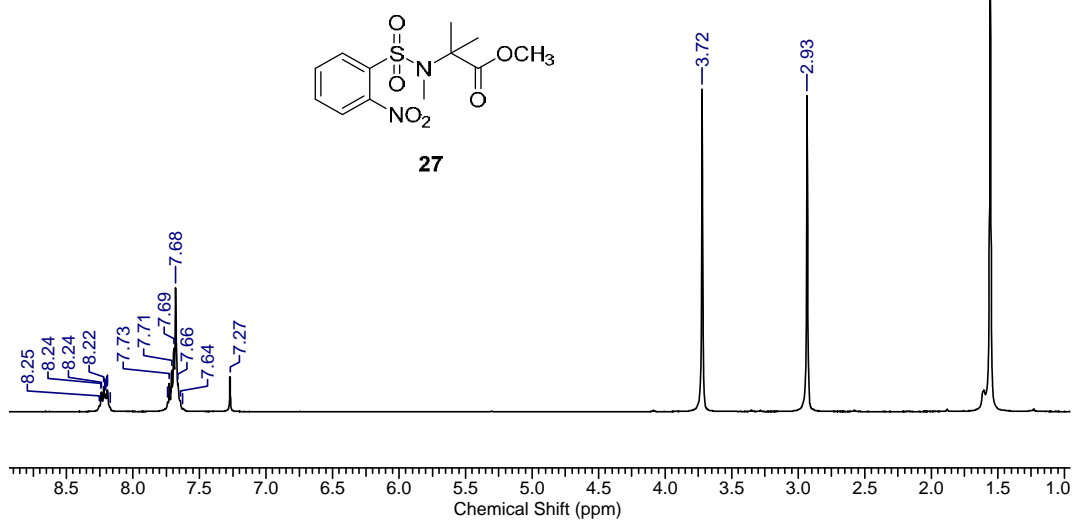
l2-S-D-Pro-NHB MOn5av2#006 2-amino benzenesulfonyl D-proline 4-br anilide.001.001.1r.esp



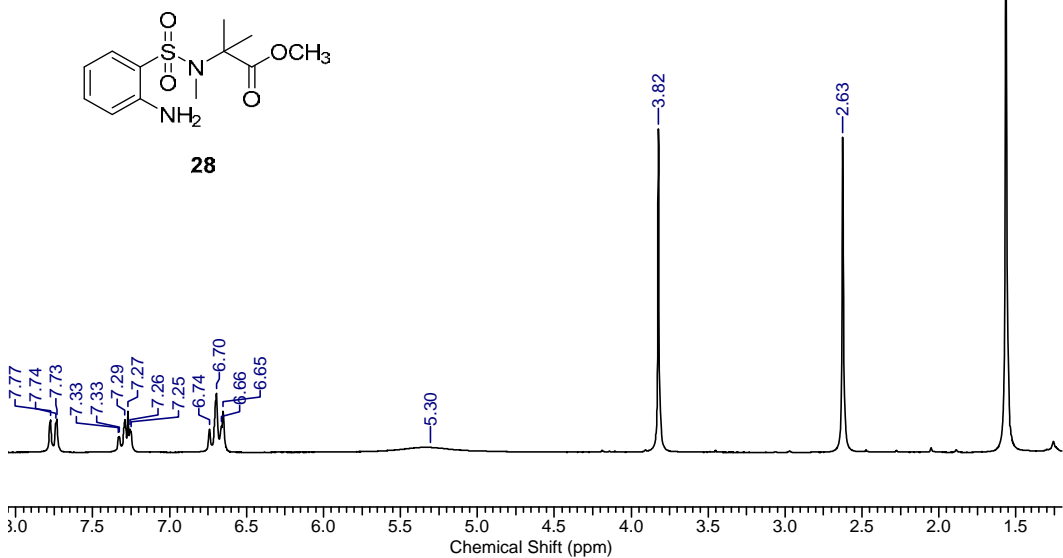
5DBP Mon2av2#006 Acetyl S-Ant D-Pro 4-Br anilide.001.001.1r.esp



VO2-S-(NMe)AIB-OMe Thu3av2#044 2-nitro benzene sulfonyl N-methyl AIB methyl ester.001.001.1r.esp

 $^1\text{H}$  NMR (CDCl<sub>3</sub>, 200MHz)

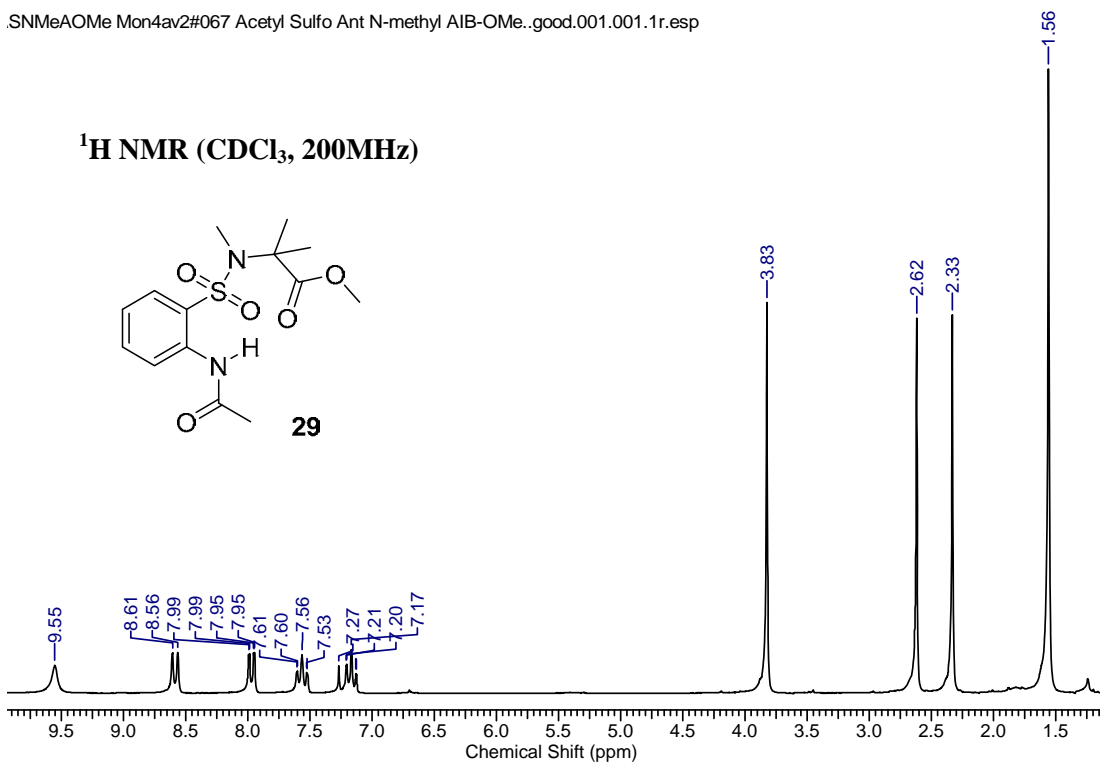
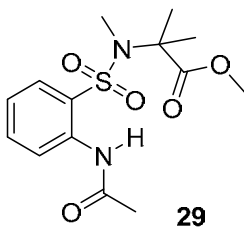
NH2-S-(NMe)A-OMe Fri3av2#019 2-Amino benzene sulfonyl N-methyl AIB-OMe.001.001.1r.esp

 $^1\text{H}$  NMR (CDCl<sub>3</sub>, 200MHz)



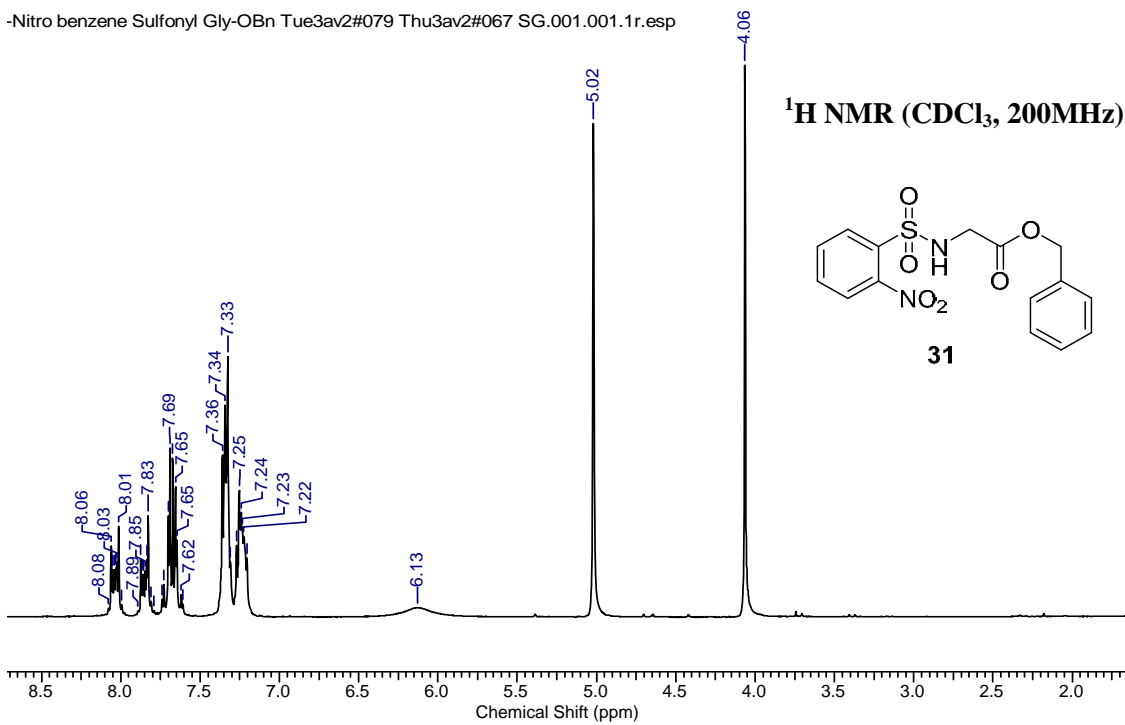
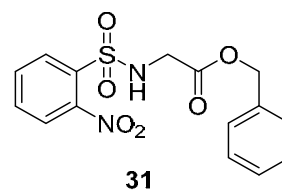
SNMeAOMe Mon4av2#067 Acetyl Sulfo Ant N-methyl AIB-OMe..good.001.001.1r.esp

<sup>1</sup>H NMR (CDCl<sub>3</sub>, 200MHz)



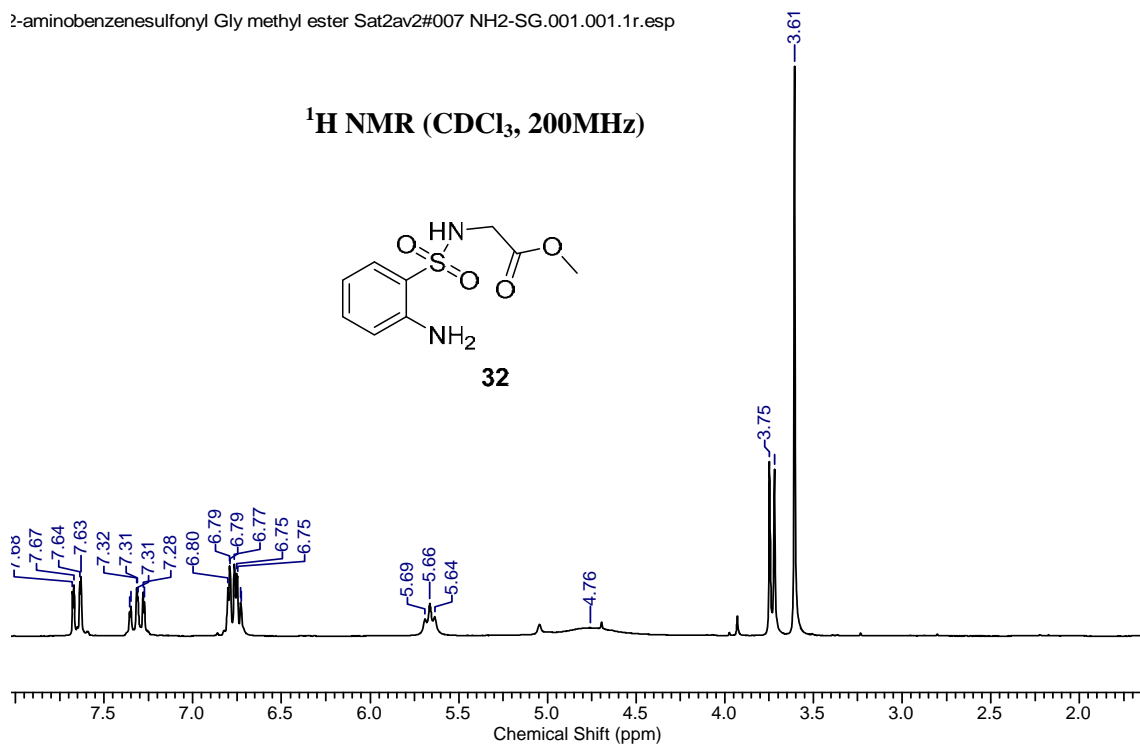
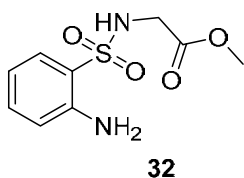
-Nitro benzene Sulfonyl Gly-OBn Tue3av2#079 Thu3av2#067 SG.001.001.1r.esp

<sup>1</sup>H NMR (CDCl<sub>3</sub>, 200MHz)



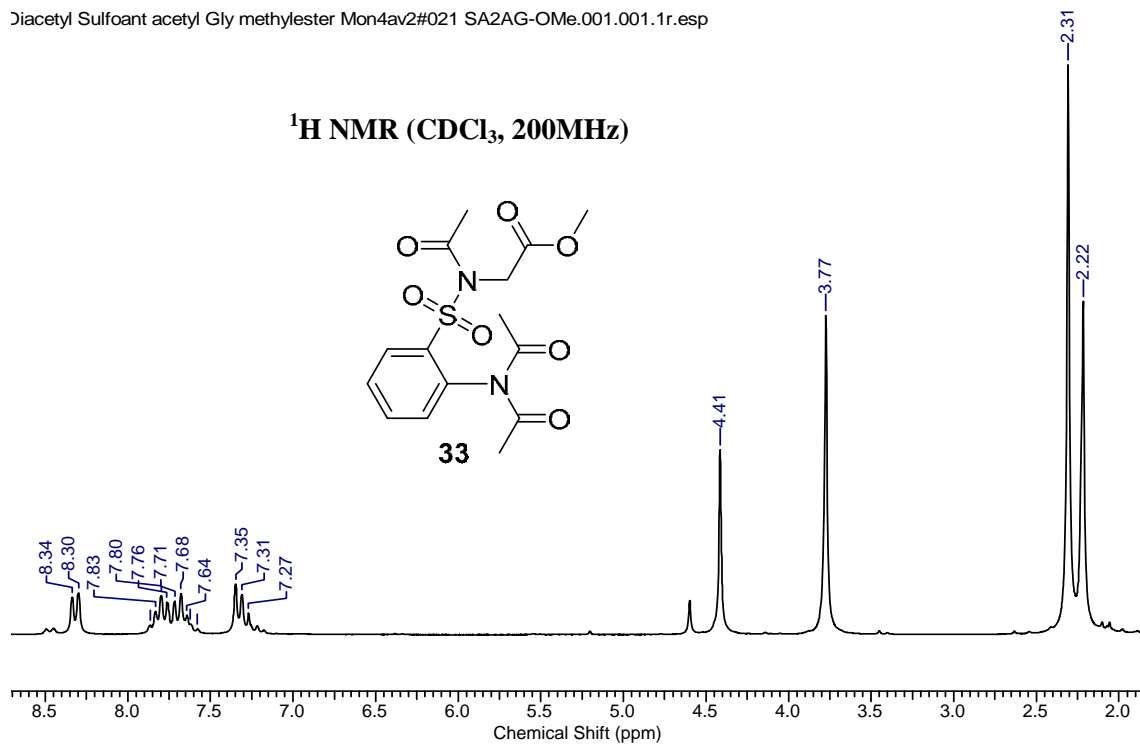
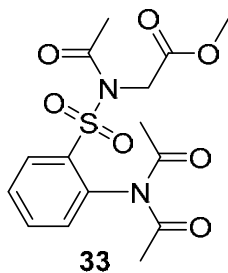
2-aminobenzenesulfonyl Gly methyl ester Sat2av2#007 NH2-SG.001.001.1r.esp

<sup>1</sup>H NMR (CDCl<sub>3</sub>, 200MHz)



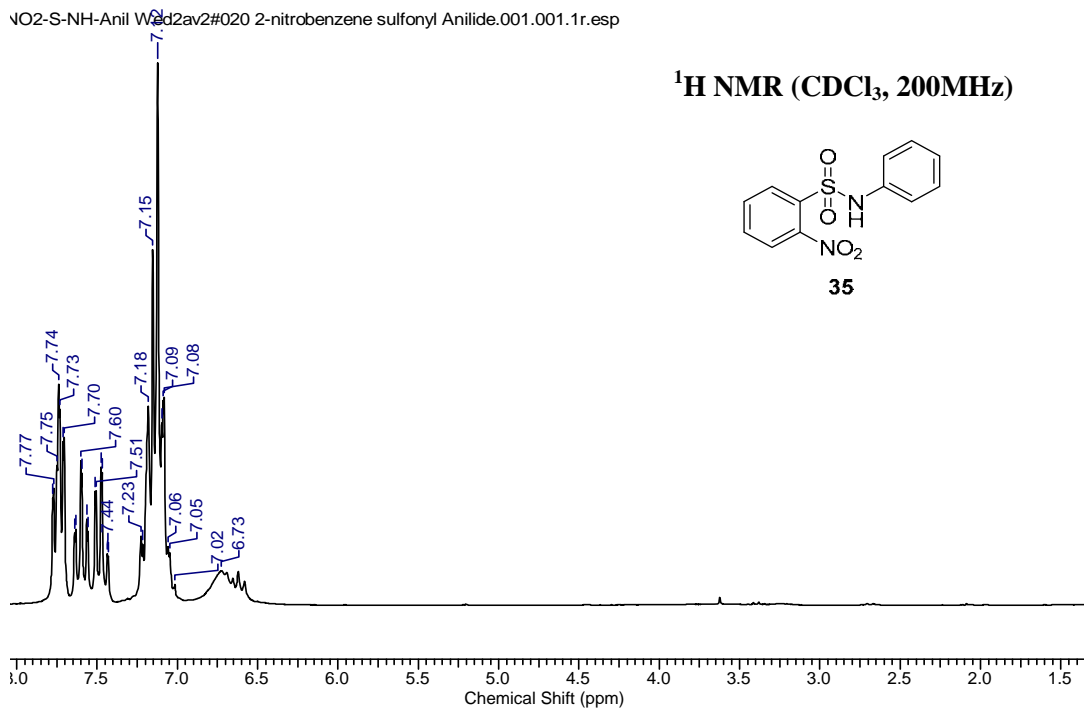
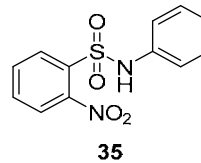
Diacetyl Sulfoant acetyl Gly methylester Mon4av2#021 SA2AG-OMe.001.001.1r.esp

<sup>1</sup>H NMR (CDCl<sub>3</sub>, 200MHz)



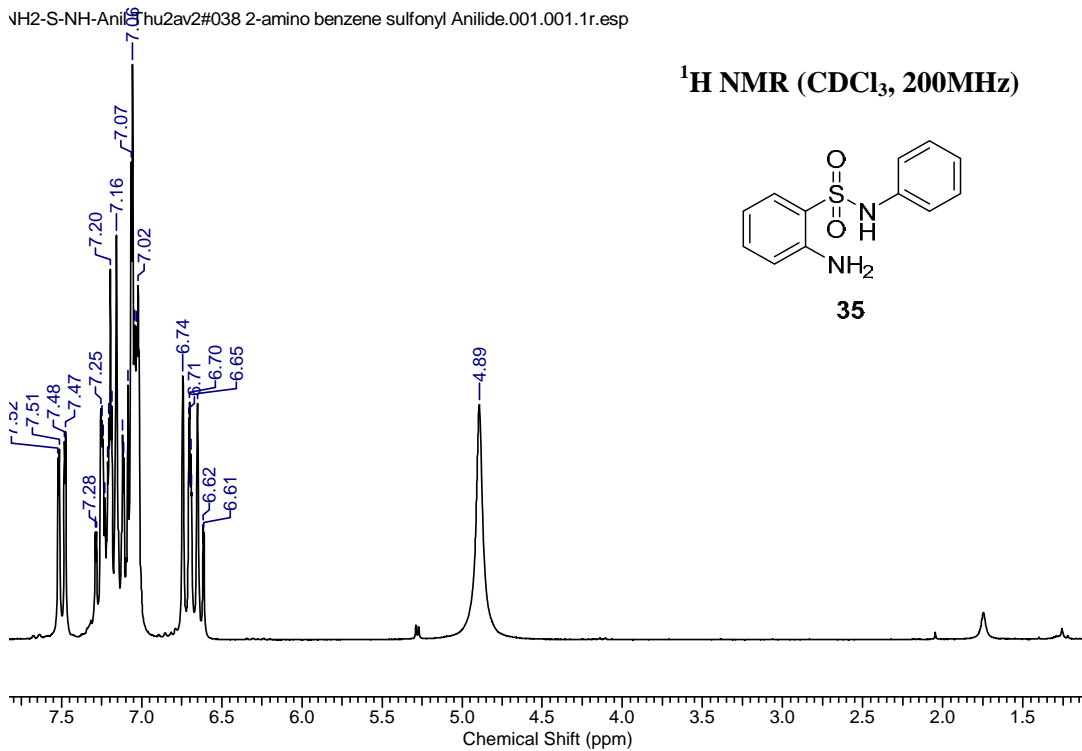
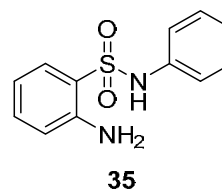
NO2-S-NH-Anil Wed2av2#020 2-nitrobenzene sulfonyl Anilide.001.001.1r.esp

<sup>1</sup>H NMR (CDCl<sub>3</sub>, 200MHz)

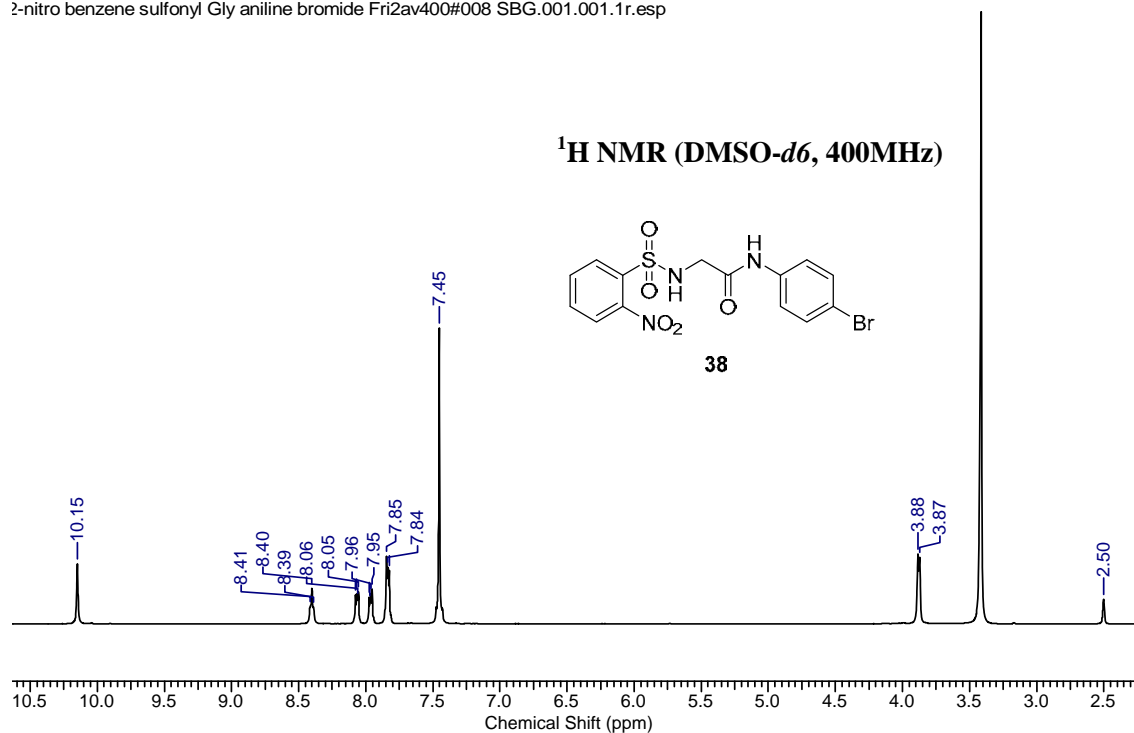


NH2-S-NH-Anil hu2av2#038 2-amino benzene sulfonyl Anilide.001.001.1r.esp

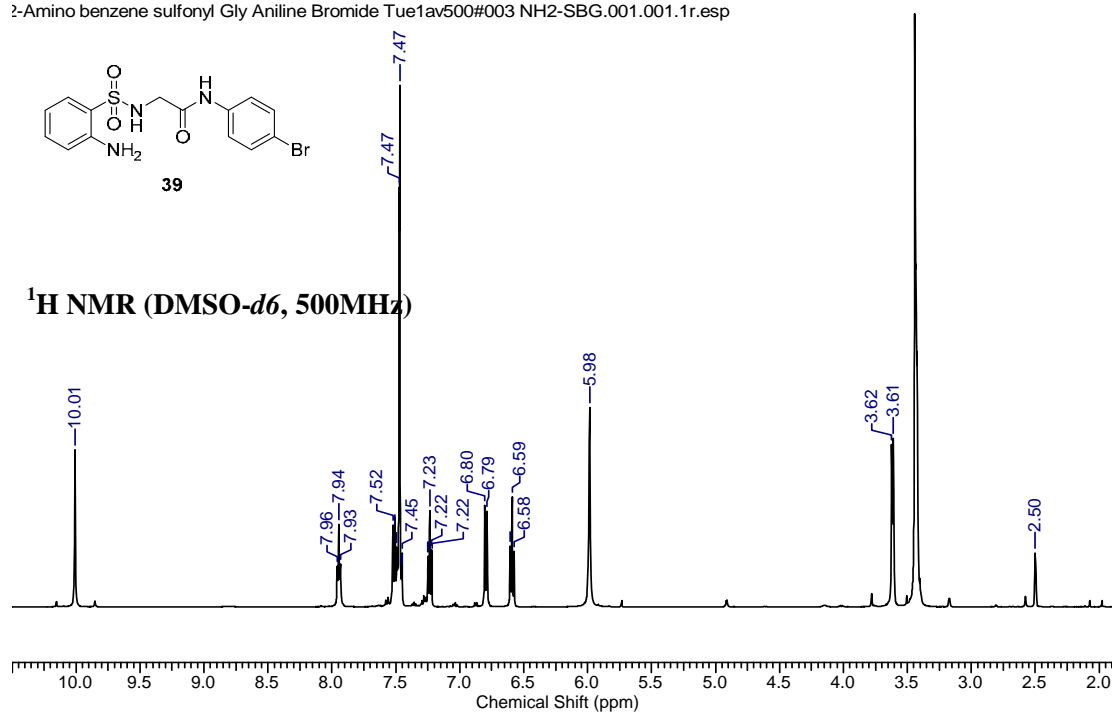
<sup>1</sup>H NMR (CDCl<sub>3</sub>, 200MHz)

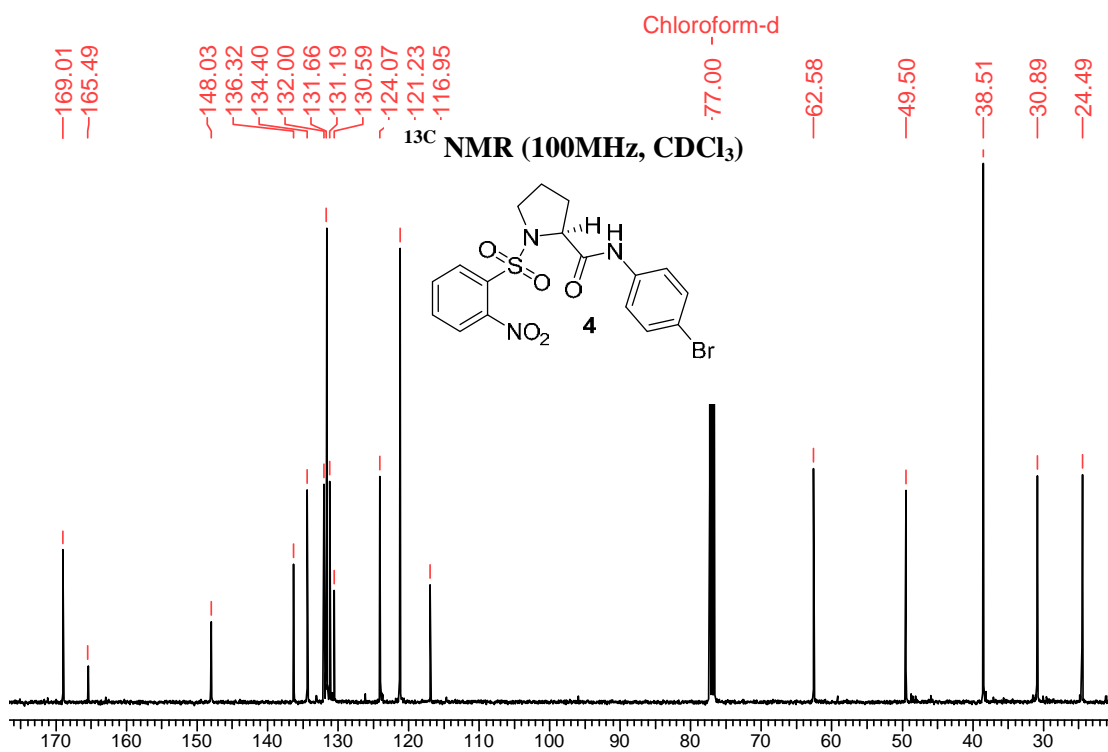
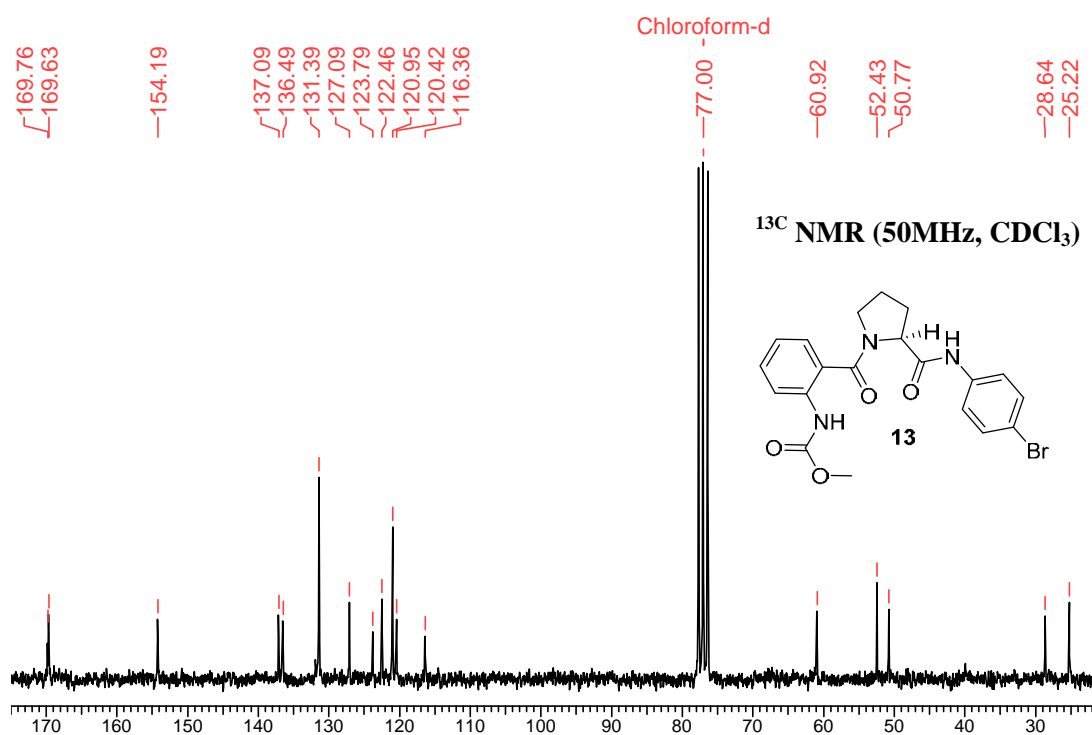


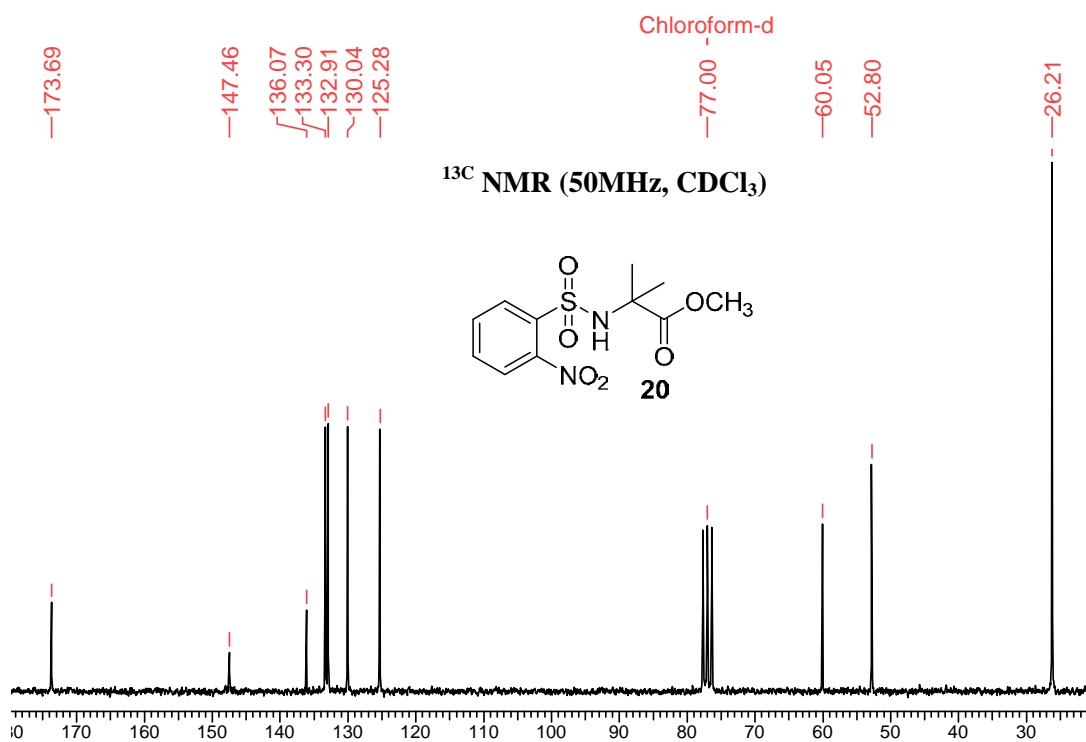
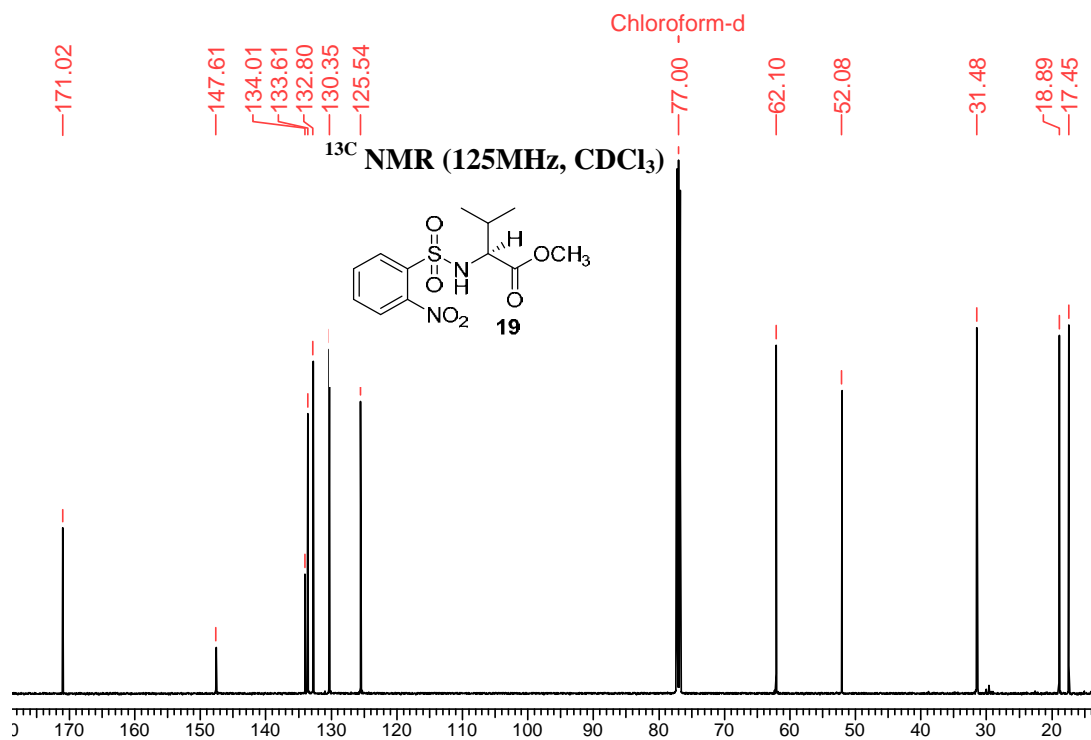
2-nitro benzene sulfonyl Gly aniline bromide Fri2av400#008 SBG.001.001.1r.esp

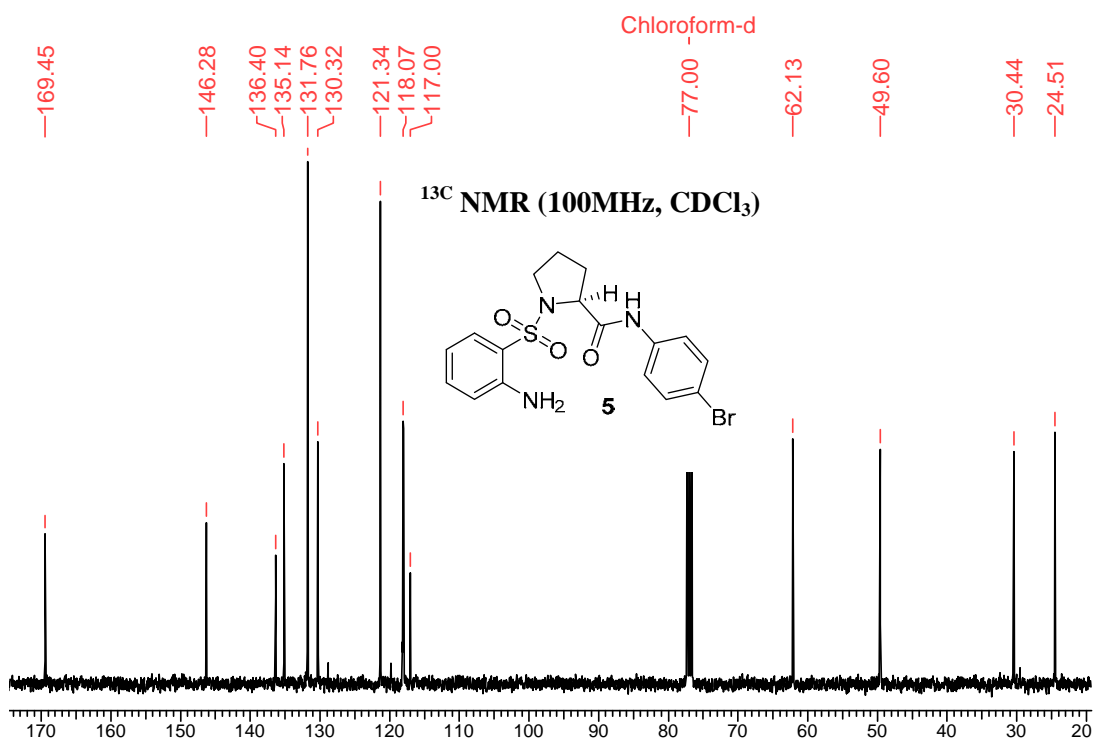
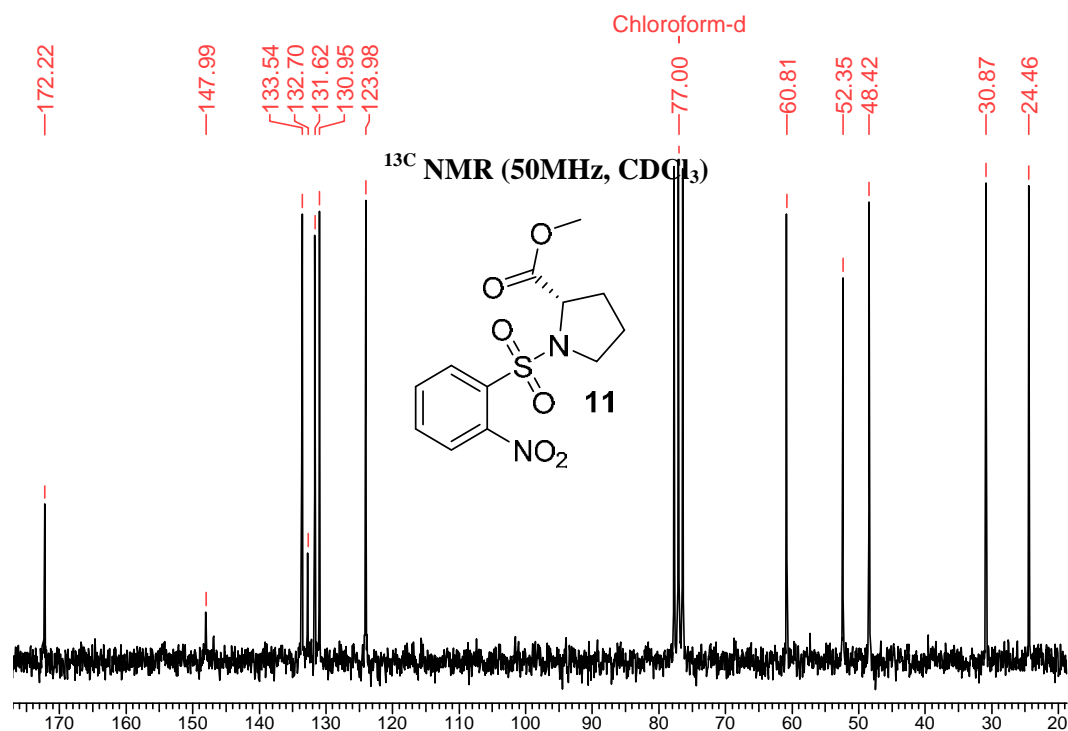


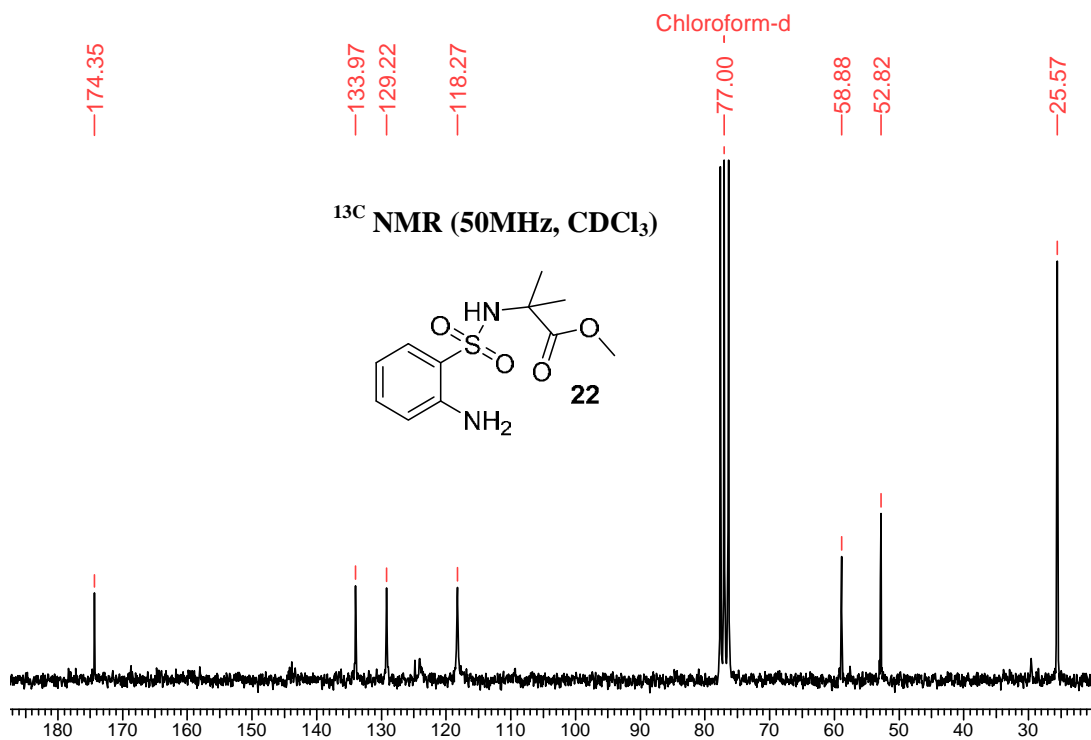
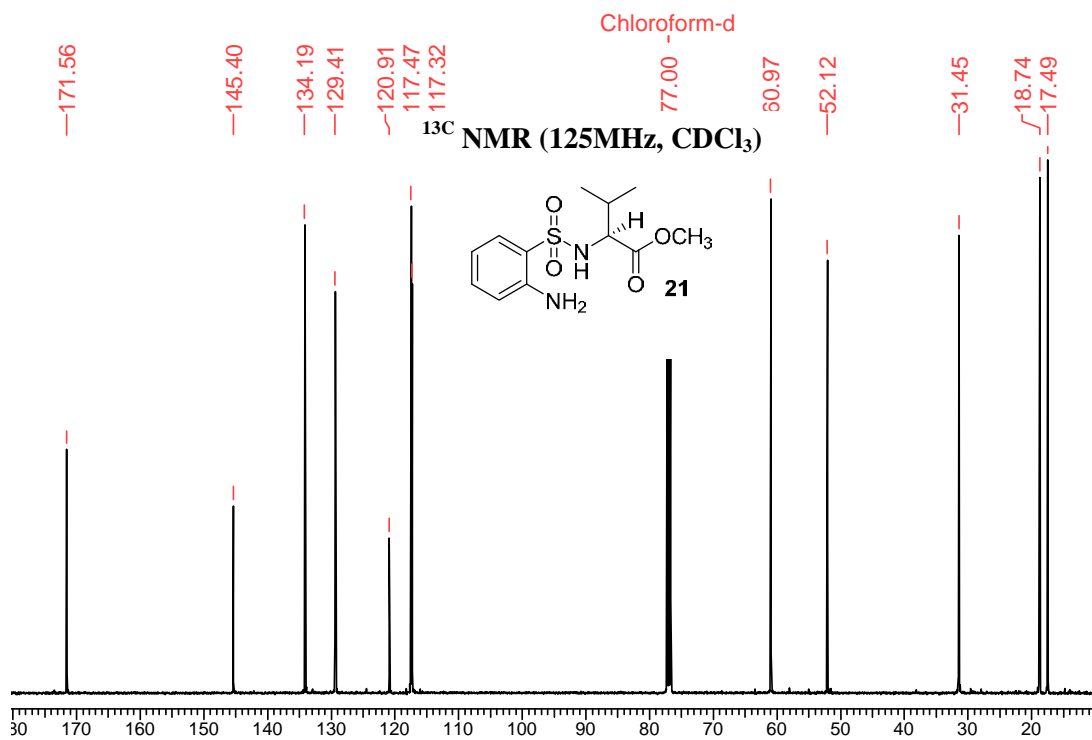
2-Amino benzene sulfonyl Gly Aniline Bromide Tue1av500#003 NH2-SBG.001.001.1r.esp



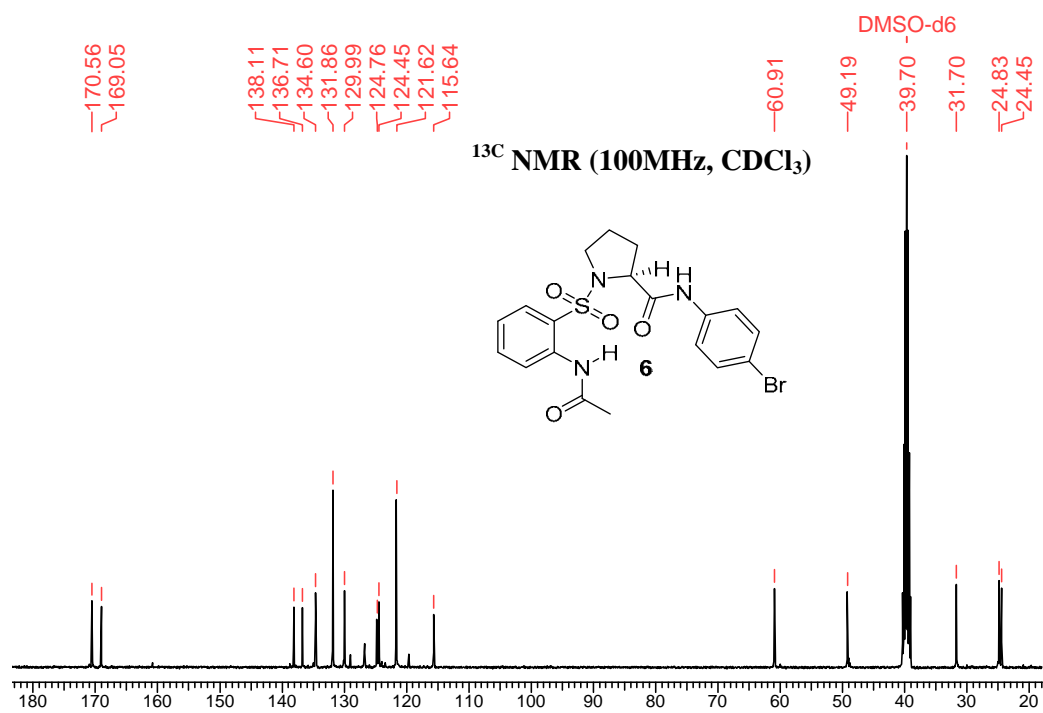
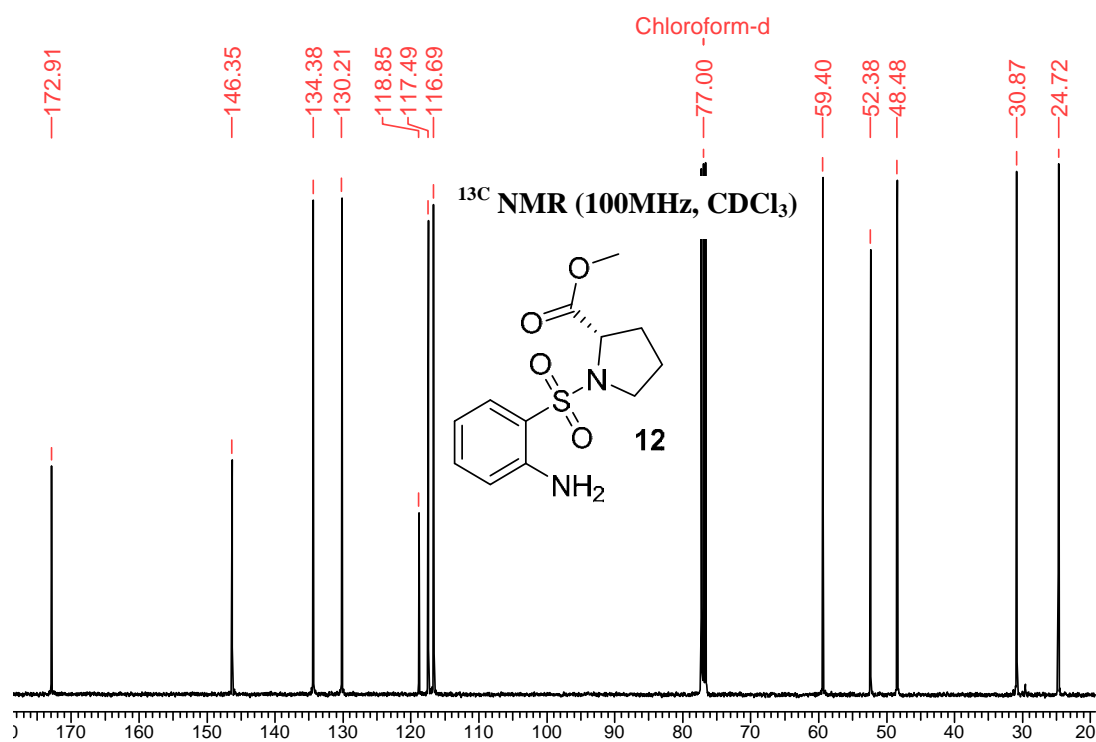


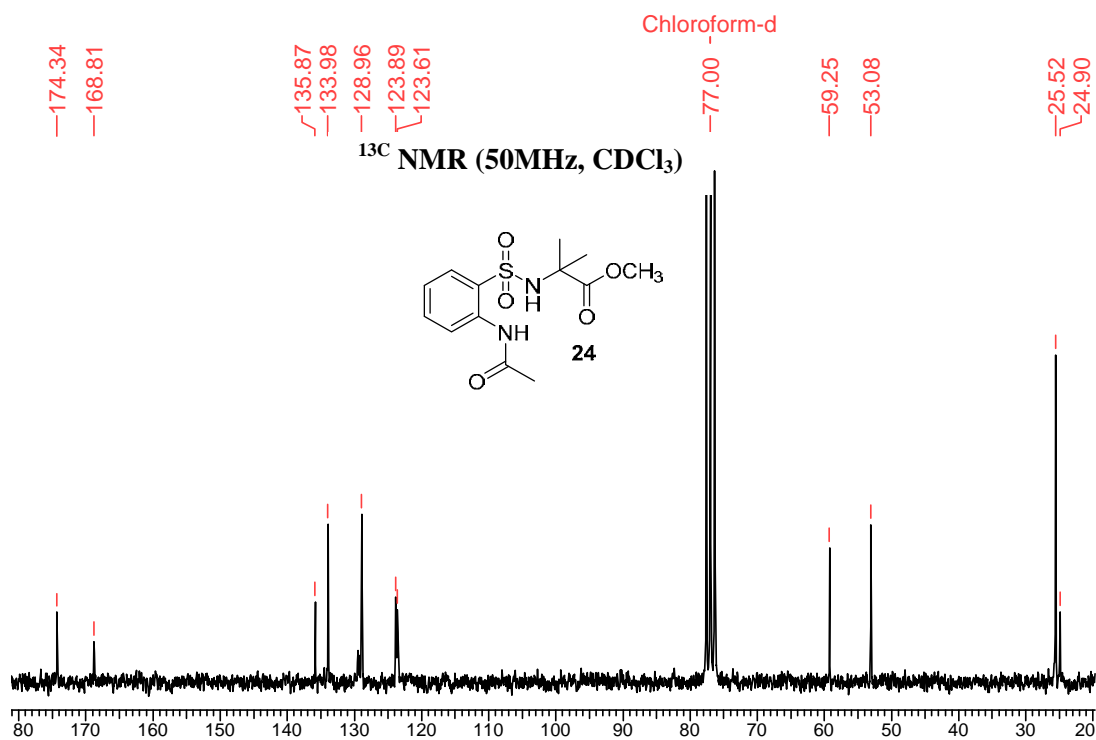
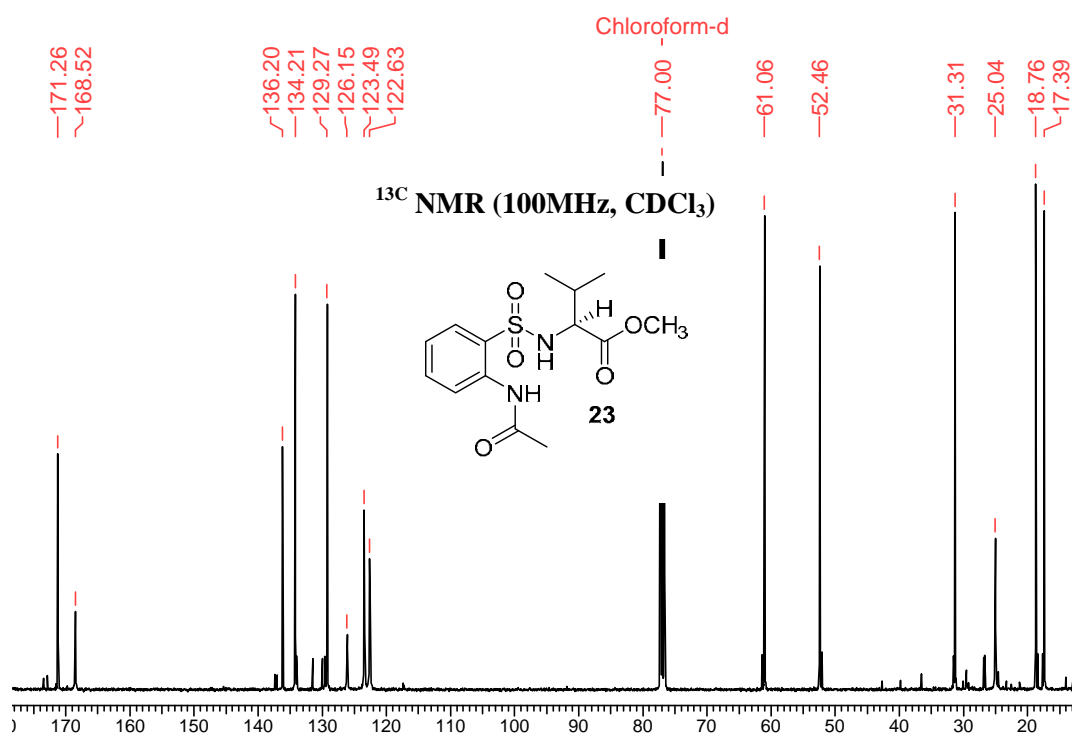


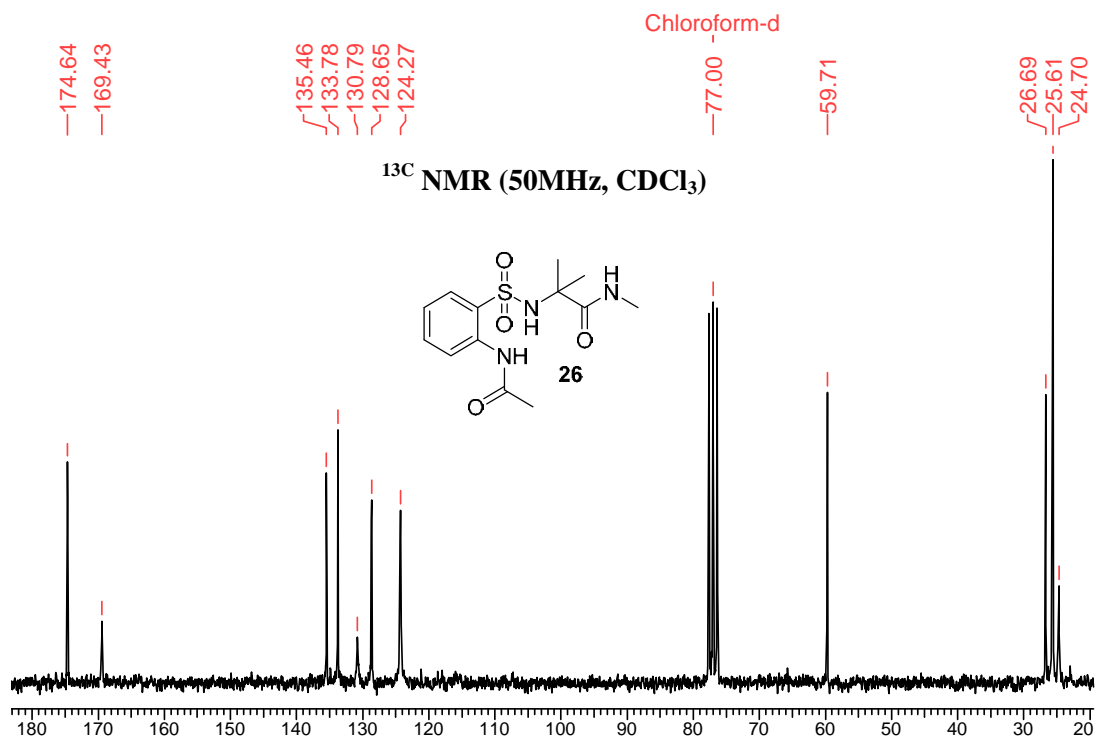
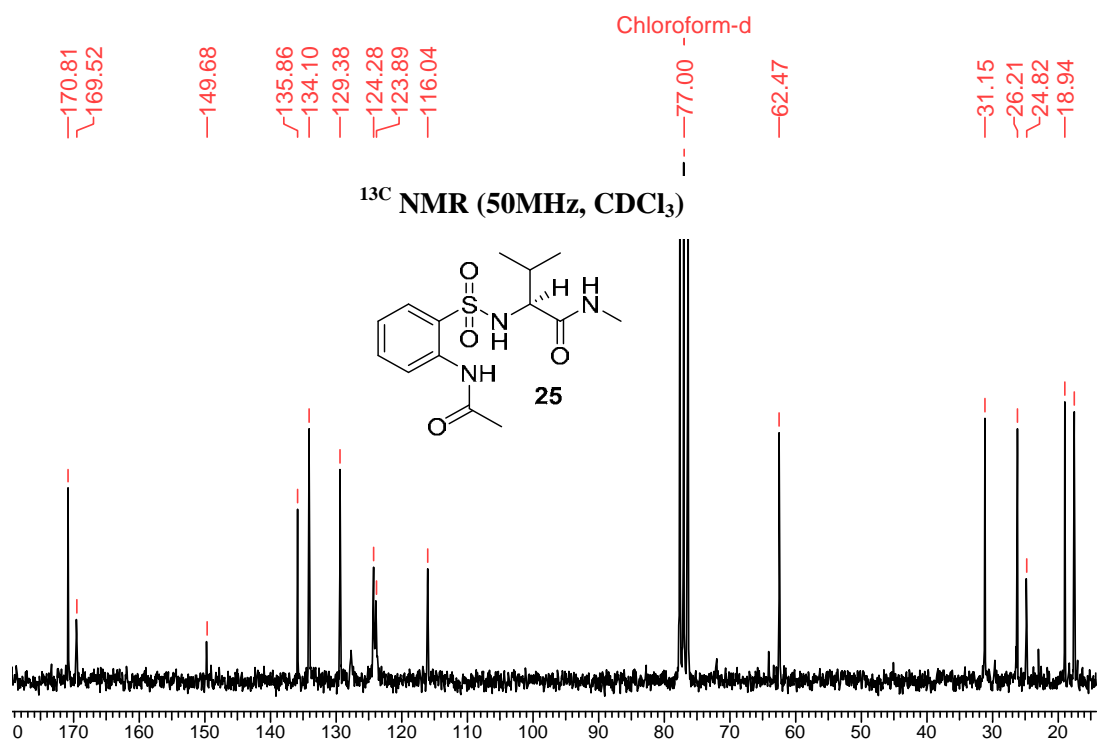






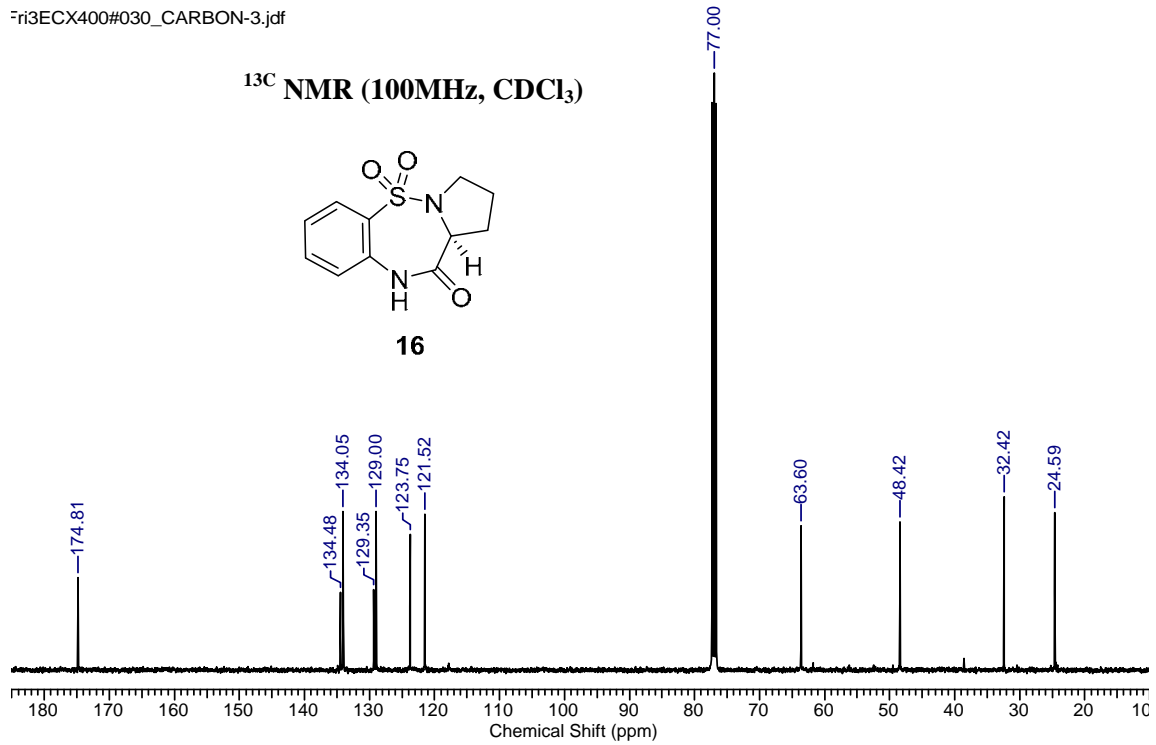
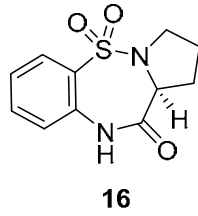




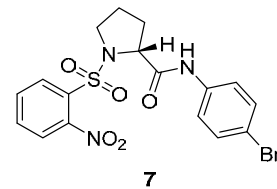


Fri3ECX400#030\_CARBON-3.jdf

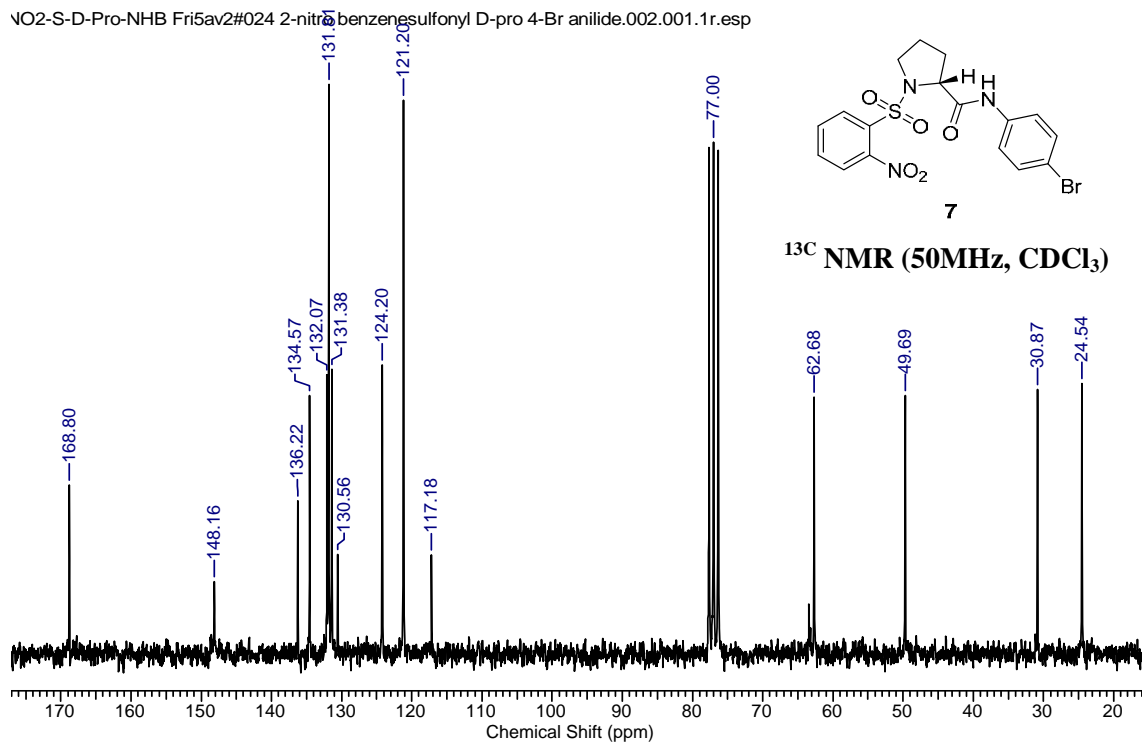
<sup>13</sup>C NMR (100MHz, CDCl<sub>3</sub>)



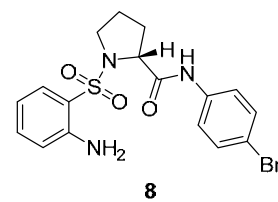
VO2-S-D-Pro-NHB Fri5av2#024 2-nitrobenzenesulfonyl D-pro 4-Br anilide.002.001.1r.esp



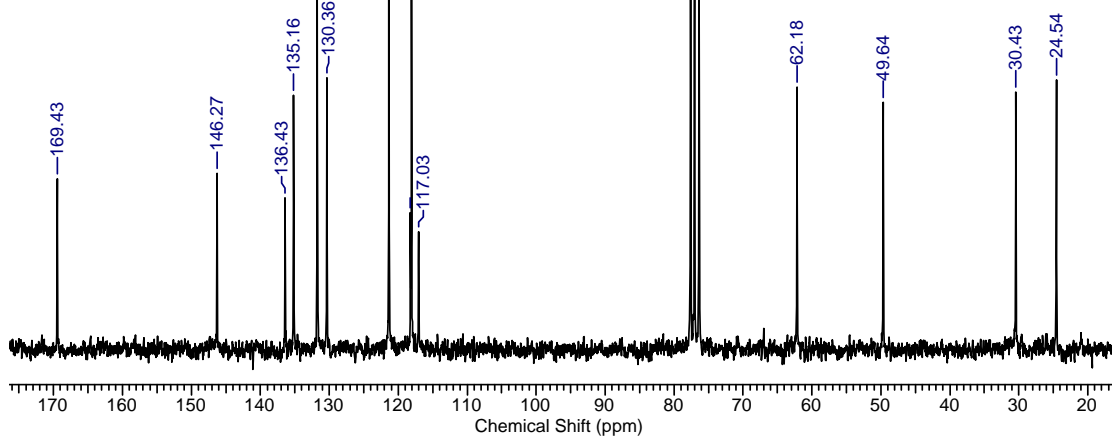
<sup>13</sup>C NMR (50MHz, CDCl<sub>3</sub>)



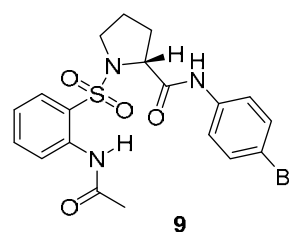
NH2-S-D-Pro-NHB Fri5av2#066 2-amino benzenesulfonyl D-Pro 4-Br anilide.002.001.1r.esp



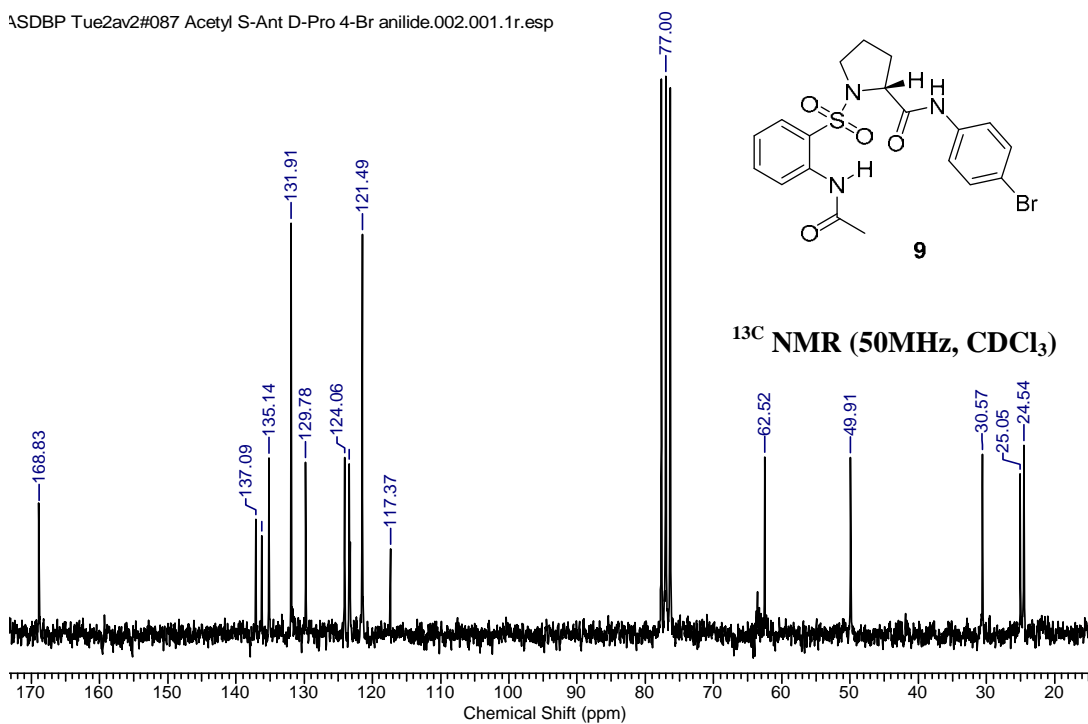
<sup>13</sup>C NMR (50MHz, CDCl<sub>3</sub>)

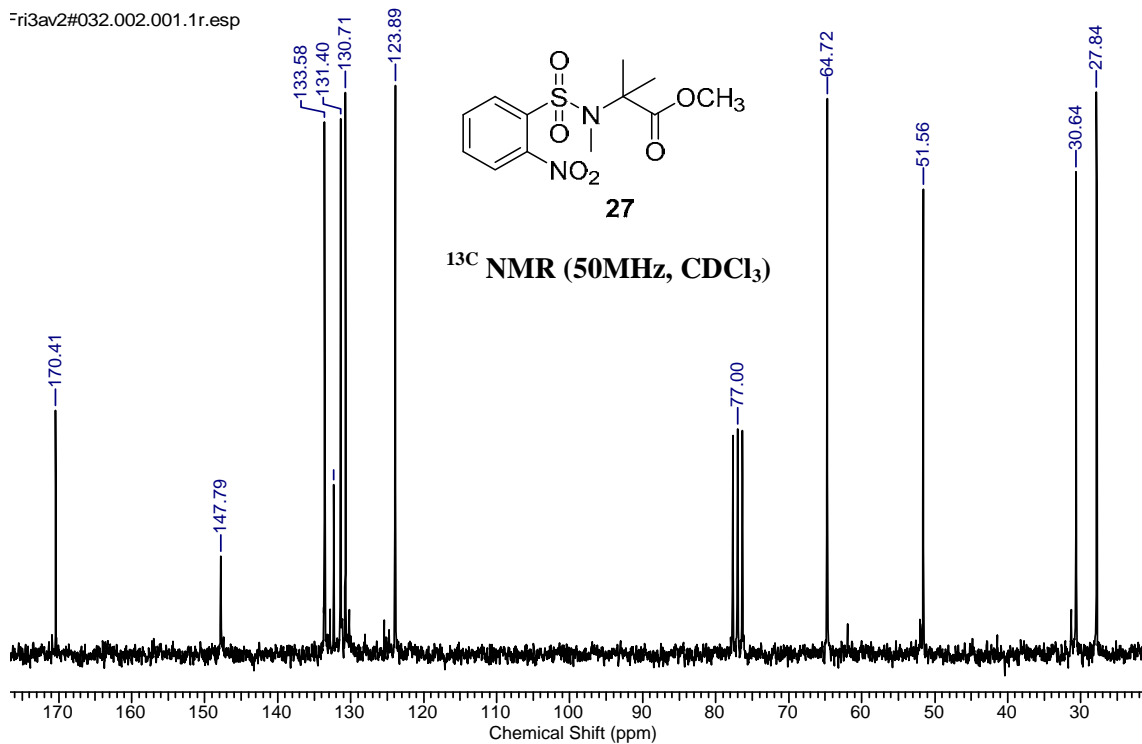


\SDBP Tue2av2#087 Acetyl S-Ant D-Pro 4-Br anilide.002.001.1r.esp

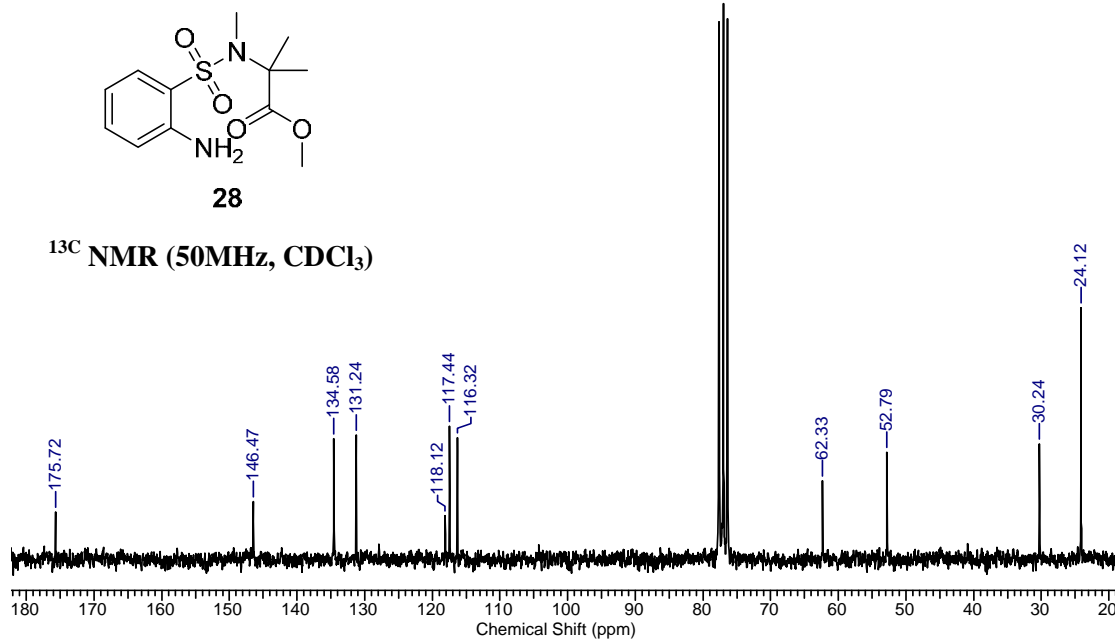


<sup>13</sup>C NMR (50MHz, CDCl<sub>3</sub>)

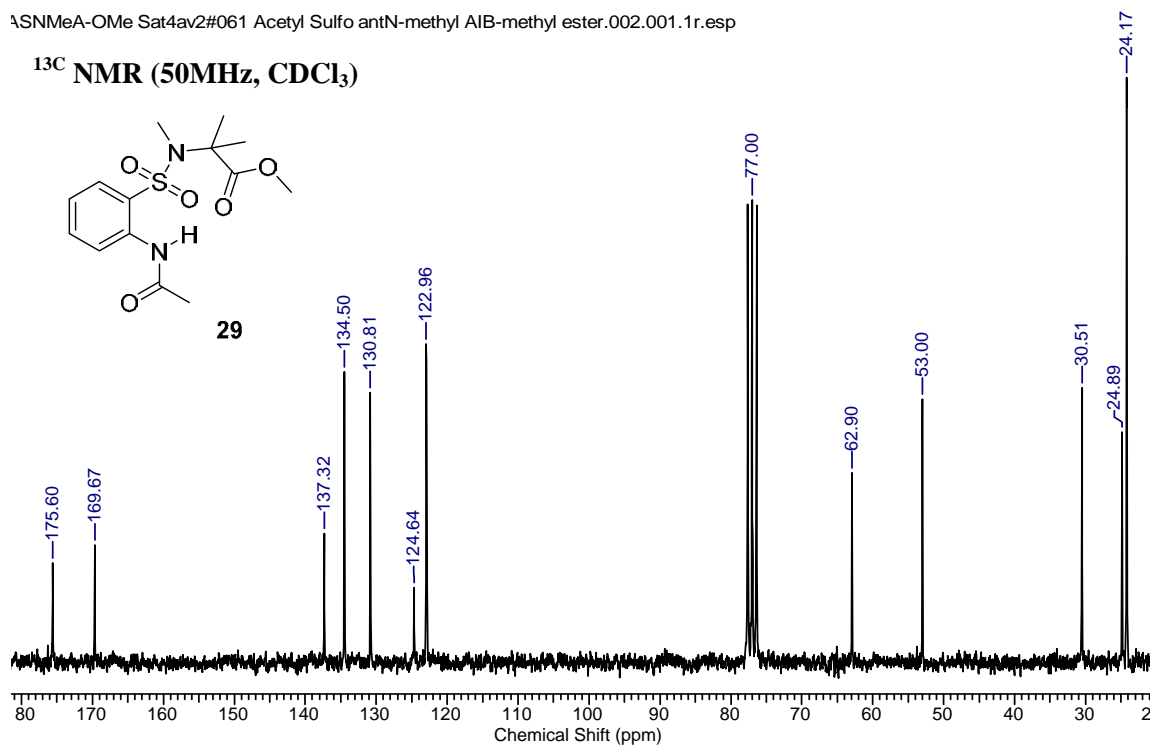




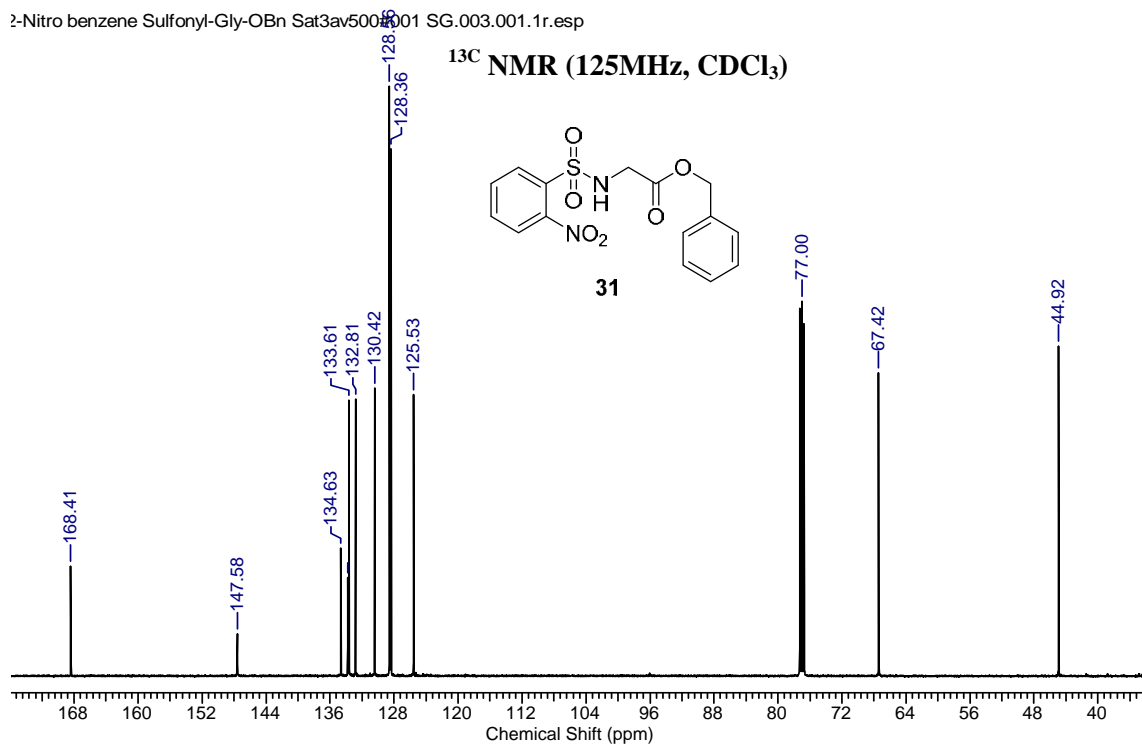
NH2-S-NMe-A-OMe Sat1av2#041 2-amino benzene sulfonyl N-methyl AIB methyl ester. 002.001.1r.esp



ASNMeA-OMe Sat4av2#061 Acetyl Sulfo antN-methyl AIB-methyl ester.002.001.1r.esp

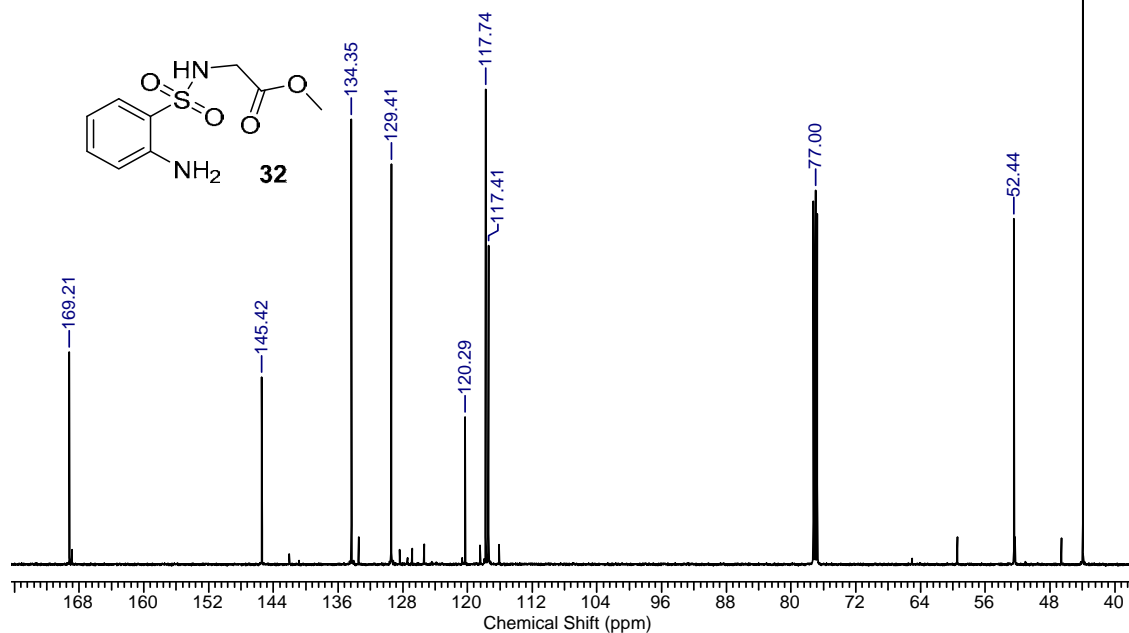
 $^{13}\text{C}$  NMR (50MHz,  $\text{CDCl}_3$ )

2-Nitro benzene Sulfonyl-Gly-OBn Sat3av500#001 SG.003.001.1r.esp

 $^{13}\text{C}$  NMR (125MHz,  $\text{CDCl}_3$ )

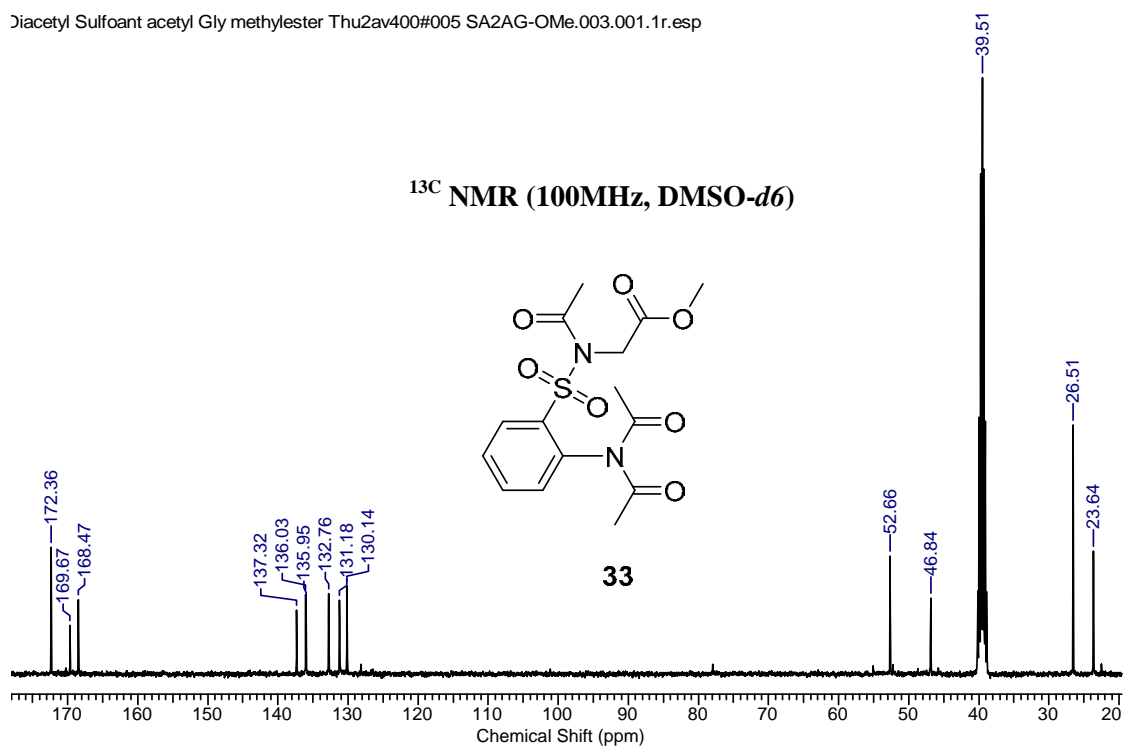
2-Aminobenzenesulfonyl Gly Methyl ester Tue3av500#002 NH2-SG.003.001.1r.esp

<sup>13</sup>C NMR (125MHz, CDCl<sub>3</sub>)



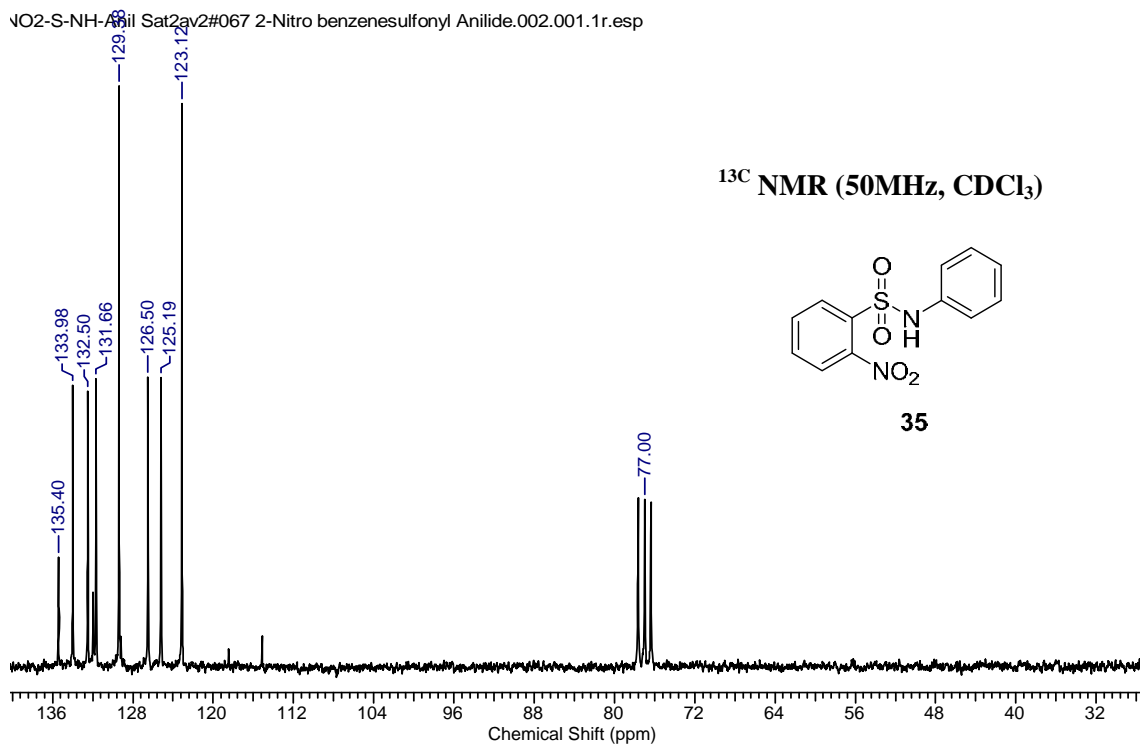
Diacetyl Sulfoant acetyl Gly methylester Thu2av400#005 SA2AG-OMe.003.001.1r.esp

<sup>13</sup>C NMR (100MHz, DMSO-d<sub>6</sub>)

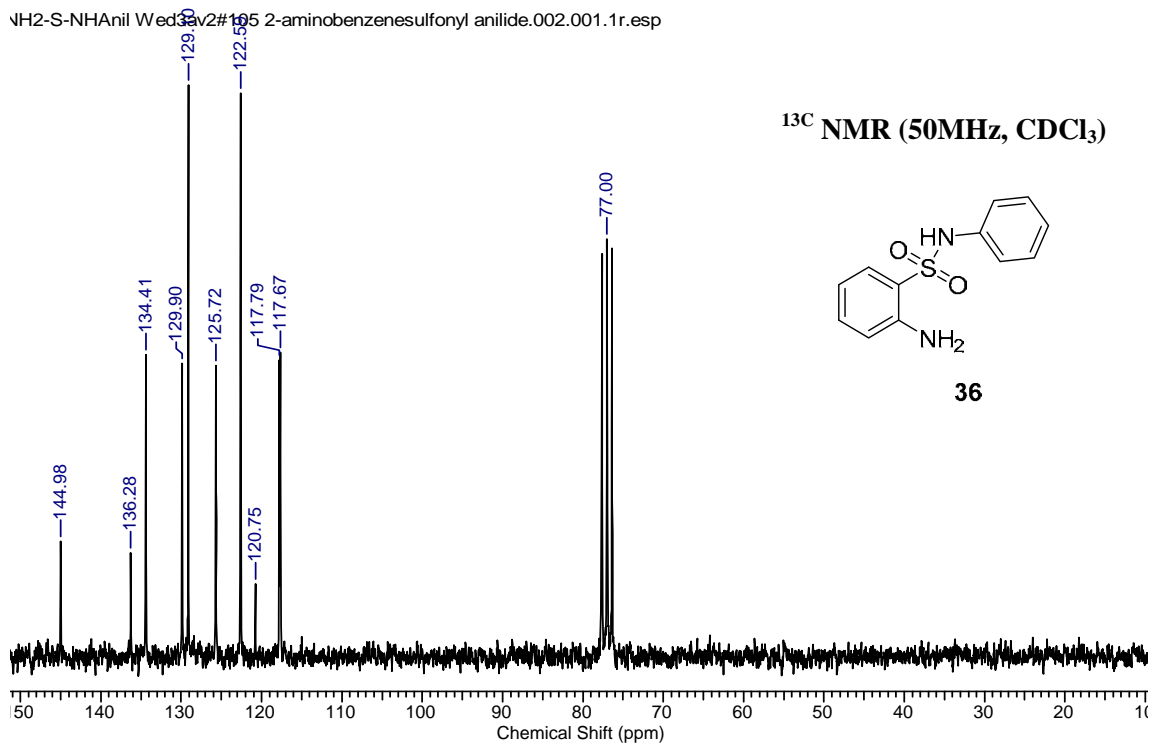




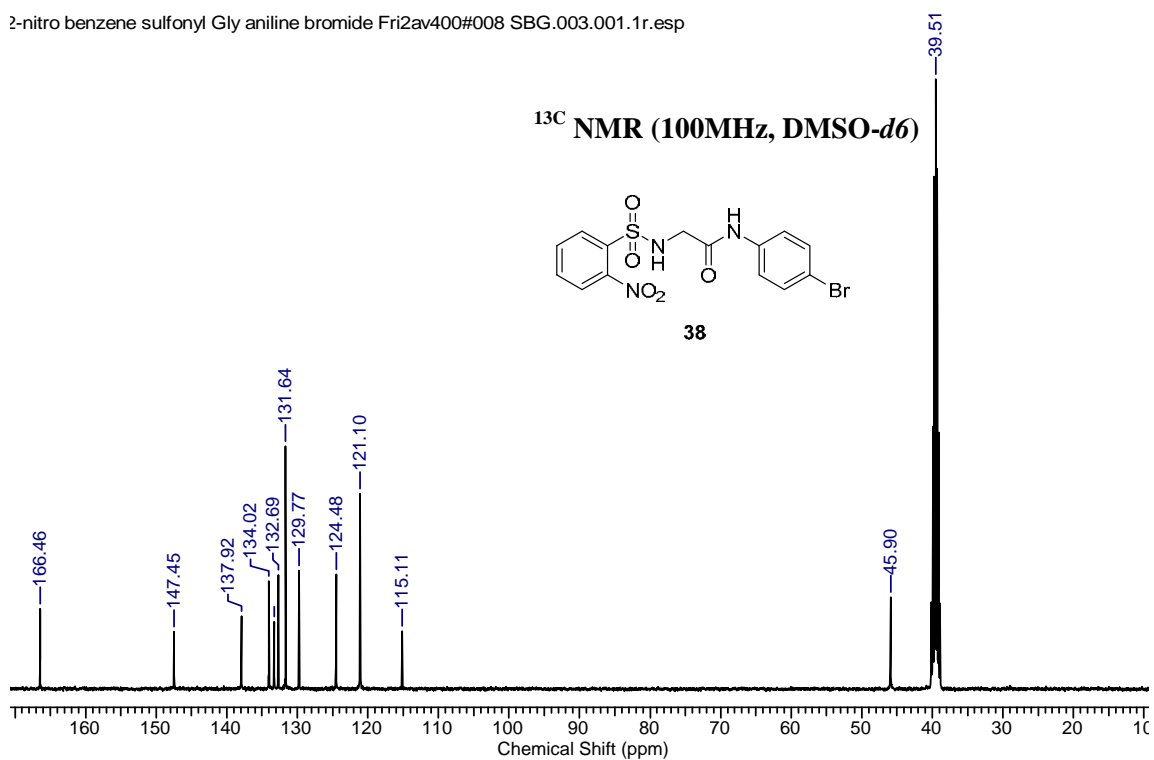
VO2-S-NH-Anil Sat2av2#067 2-Nitro benzenesulfonyl Anilide.002.001.1r.esp



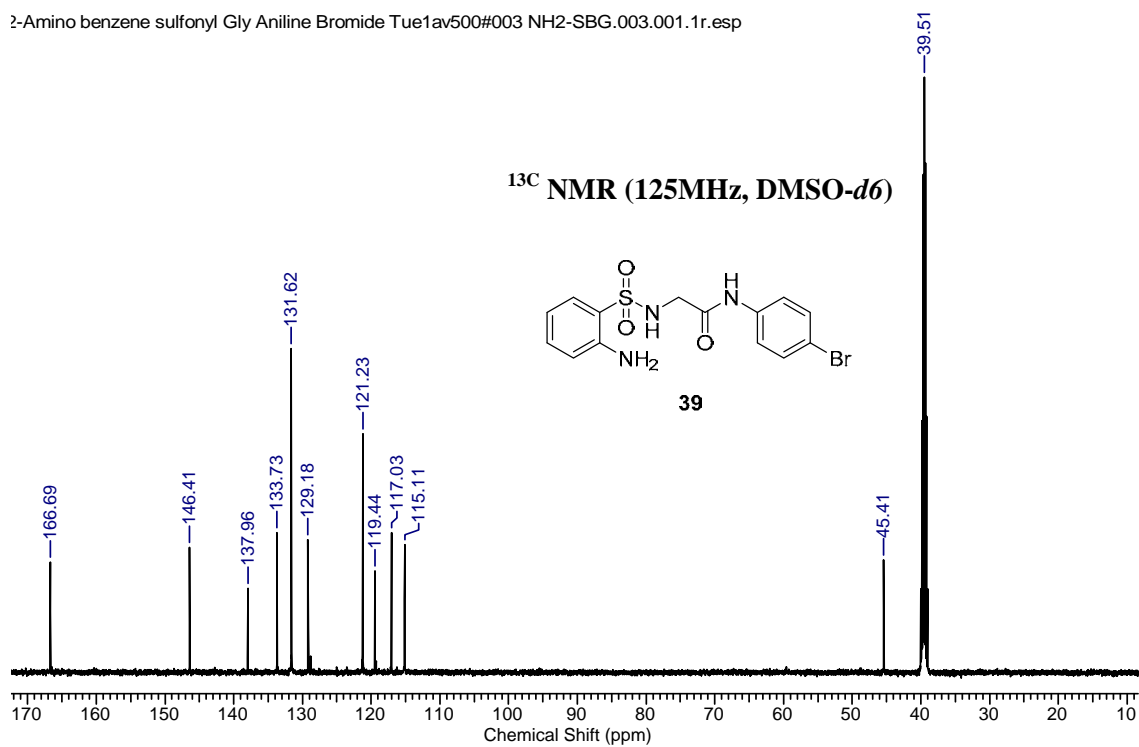
NH2-S-NHAnil Wed3av2#165 2-aminobenzenesulfonyl anilide.002.001.1r.esp



2-nitro benzene sulfonyl Gly aniline bromide Fri2av400#008 SBG.003.001.1r.esp



2-Amino benzene sulfonyl Gly Aniline Bromide Tue1av500#003 NH2-SBG.003.001.1r.esp



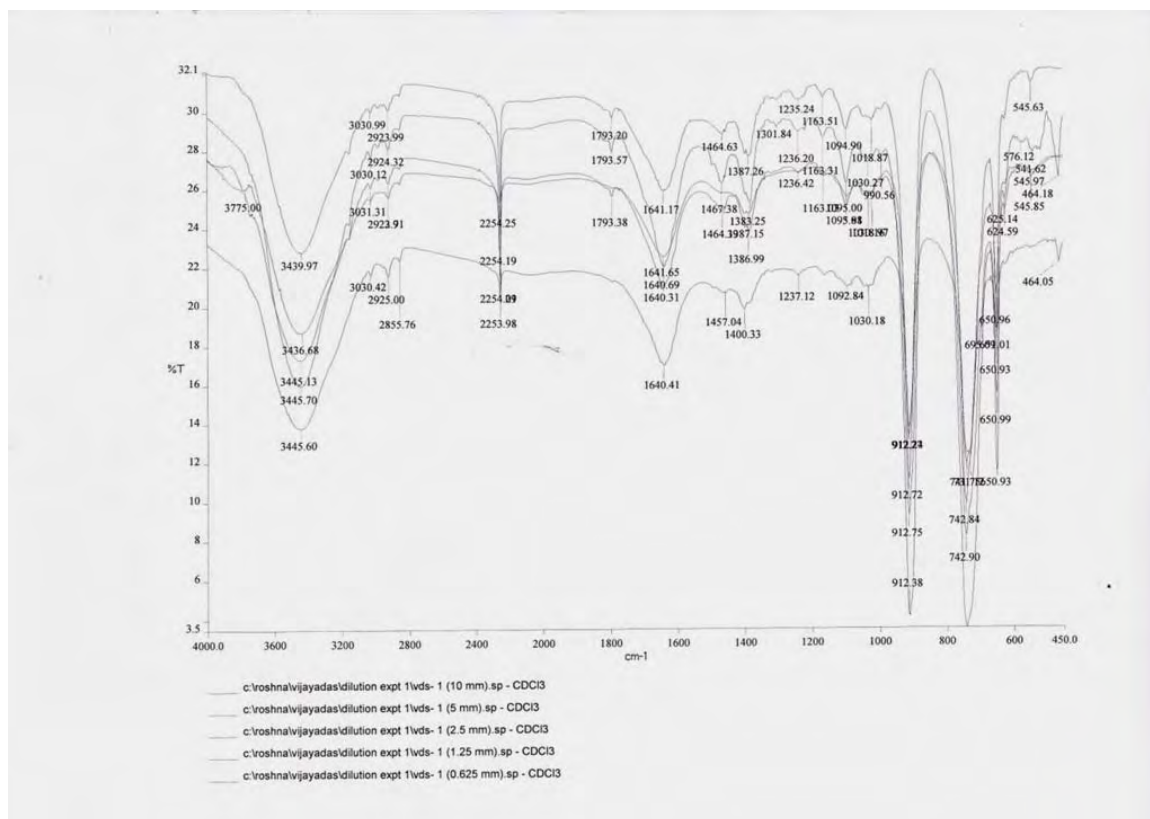


Figure 9: Stacked plot representing the IR absorption of compound 13 at various concentrations

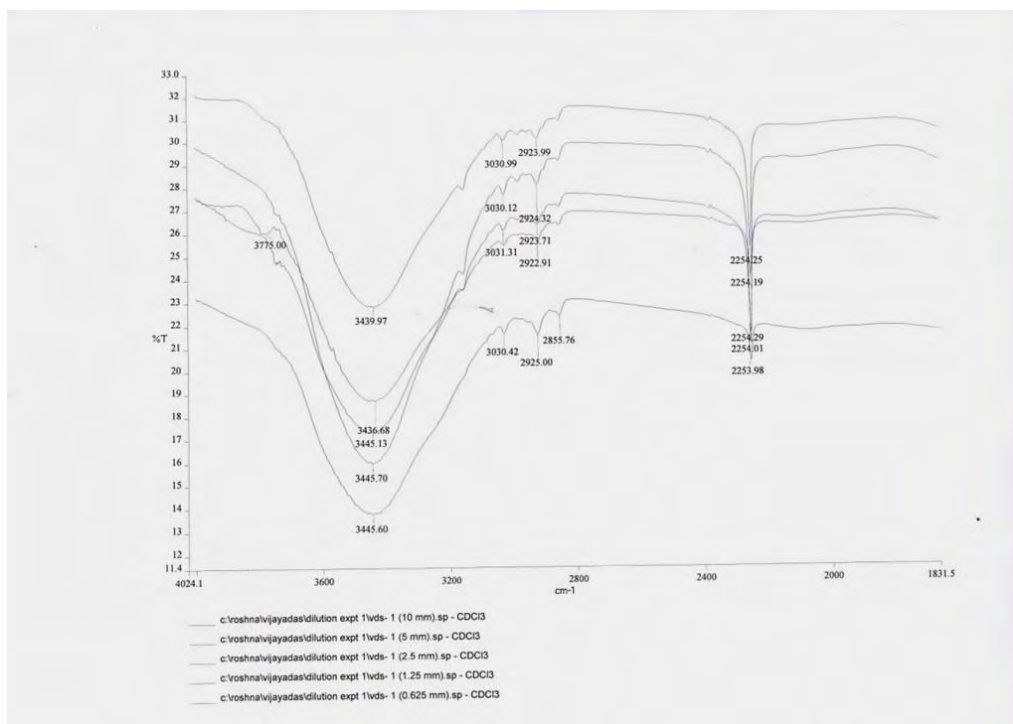


Figure 10: Stacked plot representing the expanded IR absorption at the region of ‘NH’ of compound 13 at various concentrations

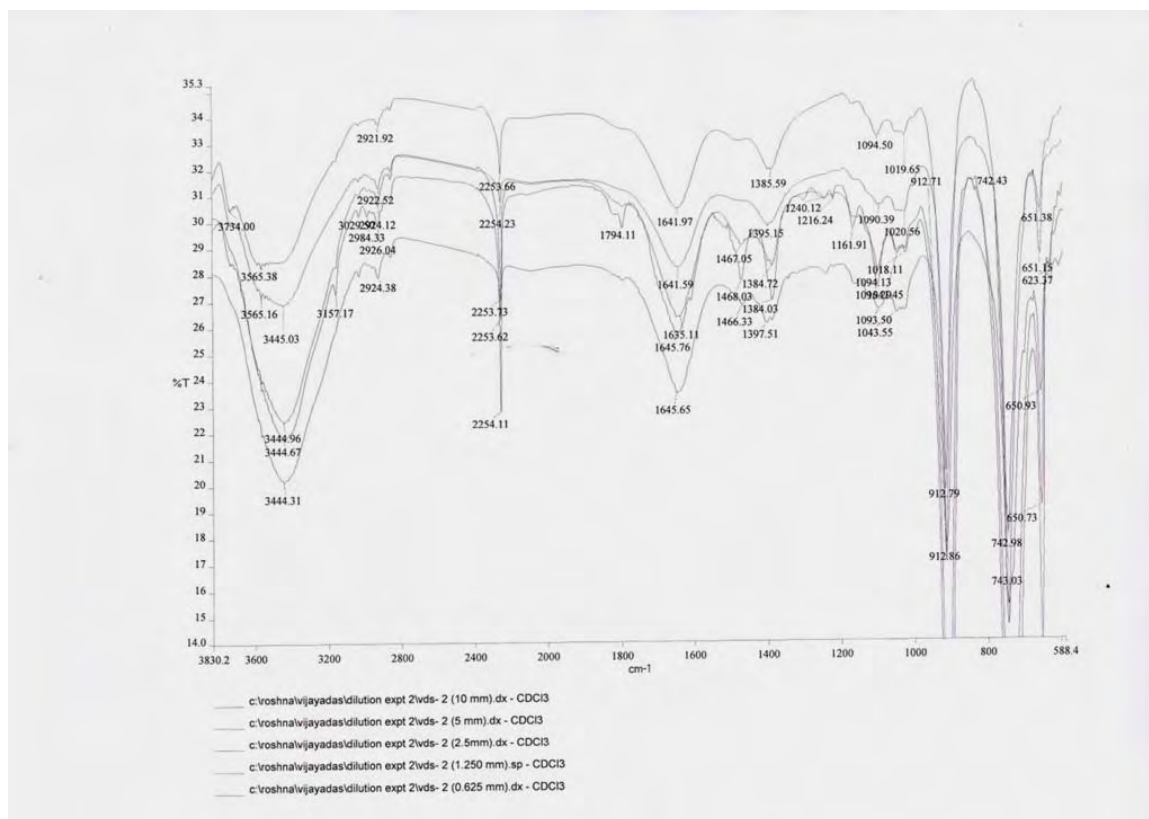


Figure 11: Stacked plot representing the IR absorption of Compound 6 at various concentrations

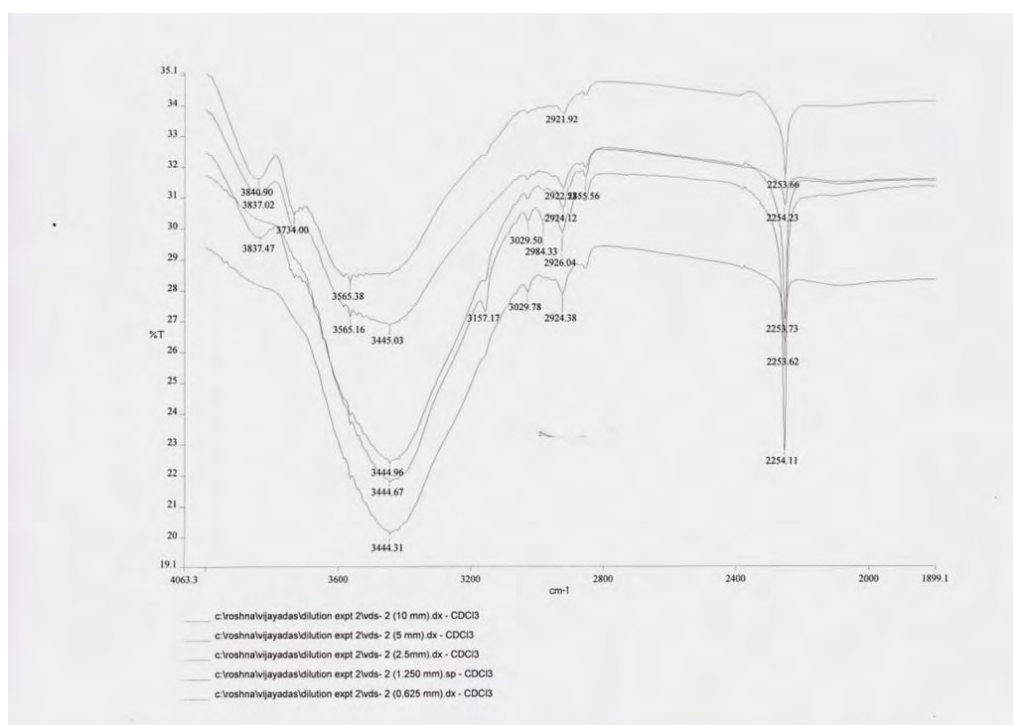


Figure 12: Stacked plot representing the expanded IR absorption at the region of 'NH' of compound 6 at various concentrations

## 2.27 References

- (1) Anfinsen, C. B. *Science* **1973**, *181*, 223.
- (2) Uma, K.; Kishore, R.; Balaram, P. *Biopolymers* **1993**, *33*, 865.
- (3) Karle, I. L.; Kishore, R.; Raghobama, S.; Balaram, P. *J. Am. Chem. Soc.* **1988**, *110*, 1958.
- (4) Cheng, R. P.; DeGrado, W. F. *J. Am. Chem. Soc.* **2002**, *124*, 11564.
- (5) Rose, G. D.; Fleming, P. J.; Banavar, J. R.; Maritan, A. *PNAS* **2006**, *103*, 16623.
- (6) Bordo, D.; Argos, P. *J. Mol. Biol.* **1994**, *243*, 504.
- (7) Li, X.; Wu, Y.-D.; Yang, D. *Acc. Chem. Res.* **2008**, *41*, 1428.
- (8) Li, X.; Yang, D. *Chem. Commun.* **2006**, 3367.
- (9) Fowler, S. A.; Blackwell, H. E. *Org. Biomol. Chem.* **2009**, *7*, 1508.
- (10) Olsen, C. A. *ChemBioChem* **2010**, *11*, 152.
- (11) Gruner, S. A. W.; Locardi, E.; Lohof, E.; Kessler, H. *Chem. Rev.* **2002**, *102*, 491.
- (12) Nash, R. J.; Kato, A.; Yu, C.-Y.; Fleet, G. W. J. *Future Med. Chem.* **2011**, *3*, 1513.
- (13) Hirschmann, R. F.; Nicolaou, K. C.; Angeles, A. R.; Chen, J. S.; Smith, A. B. *Acc. Chem. Res.* **2009**, *42*, 1511.
- (14) Mitra, S. N.; Dey, S.; Karthikeyan, S.; Singh, T. P. *Biopolymers* **1997**, *41*, 97.
- (15) Cheng, R. P.; Gellman, S. H.; DeGrado, W. F. *Chem. Rev.* **2001**, *101*, 3219.
- (16) Horne, W. S.; Gellman, S. H. *Acc. Chem. Res.* **2008**, *41*, 1399.
- (17) Torres, E.; Gorrea, E.; Burusco, K. K.; Da Silva, E.; Nolis, P.; Rua, F.; Boussert, S.; Diez-Perez, I.; Dannenberg, S.; Izquierdo, S.; Giralt, E.; Jaime, C.; Branchadell, V.; Ortuno, R. M. *Org. Biomol. Chem.* **2010**, *8*, 564.
- (18) Khurram, M.; Qureshi, N.; Smith, M. D. *Chem. Commun.* **2006**, 5006.
- (19) Hanessian, S.; Auzzas, L. *Acc. Chem. Res.* **2008**, *41*, 1241.
- (20) Martinek, T. A.; Fulop, F. *Chem. Soc. Rev.* **2012**, *41*, 687.
- (21) Yang, D.; Qu, J.; Li, B.; Ng, F.-F.; Wang, X.-C.; Cheung, K.-K.; Wang, D.-P.; Wu, Y.-D. *J. Am. Chem. Soc.* **1999**, *121*, 589.
- (22) Yang, D.; Li, B.; Ng, F.-F.; Yan, Y.-L.; Qu, J.; Wu, Y.-D. *J. Org. Chem.* **2001**, *66*, 7303.
- (23) Yang, D.; Li, W.; Qu, J.; Luo, S.-W.; Wu, Y.-D. *J. Am. Chem. Soc.* **2003**, *125*, 13018.
- (24) Ma, Y.; Yang, D.; Ma, Y.; Zhang, Y.-H. *ChemBioChem* **2012**, *13*, 73.

- (25) Udugamasooriya, D. G.; Dineen, S. P.; Brekken, R. A.; Kodadek, T. *J. Am. Chem. Soc.* **2008**, *130*, 5744.
- (26) Paul, B.; Butterfoss, G. L.; Boswell, M. G.; Huang, M. L.; Bonneau, R.; Wolf, C.; Kirshenbaum, K. *Org. Lett.* **2012**, *14*, 926.
- (27) Crapster, J. A.; Guzei, I. A.; Blackwell, H. E. *Angew. Chem., Int. Ed.* **2013**, *52*, 5079.
- (28) Huang, M. L.; Benson, M. A.; Shin, S. B. Y.; Torres, V. J.; Kirshenbaum, K. *Eur. J. Org. Chem.* **2013**, *2013*, 3560.
- (29) Roy, O.; Faure, S.; Thery, V.; Didierjean, C.; Taillefumier, C. *Org. Lett.* **2008**, *10*, 921.
- (30) Caumes, C.; Fernandes, C.; Roy, O.; Hjelmgaard, T.; Wenger, E.; Didierjean, C.; Taillefumier, C.; Faure, S. *Org. Lett.* **2013**, *15*, 3626.
- (31) Fuller, A. A.; Yurash, B. A.; Schaumann, E. N.; Seidl, F. J. *Organic Letters* **2013**, *15*, 5118.
- (32) Gruner, S. A. W.; Locardi, E.; Lohof, E.; Kessler, H. *Chem. Rev.* **2002**, *102*, 491.
- (33) Risseuw, M. D. P.; Overhand, M.; Fleet, G. W. J.; Simone, M. I. *Tetrahedron: Asymmetry* **2007**, *18*, 2001.
- (34) Chakraborty, T.; Srinivasu, P.; Tapadar, S.; Mohan, B. *Glycoconj J* **2005**, *22*, 83.
- (35) Siriwardena, A.; Pulukuri, K. K.; Kandiyal, P. S.; Roy, S.; Bande, O.; Ghosh, S.; Garcia Fernández, J. M.; Ariel Martin, F.; Ghigo, J.-M.; Beloin, C.; Ito, K.; Woods, R. J.; Ampapathi, R. S.; Chakraborty, T. K. *Angew. Chem., Int. Ed.* **2013**, *52*, 10221.
- (36) Krulle, T. M.; Davis, B.; Ardron, H.; Long, D. D.; Hindle, N. A.; Smith, C.; Brown, D.; Lane, A. L.; Watkin, D. J.; Marquess, D. G.; Fleet, G. W. J. *Chem. Commun.* **1996**, 1271.
- (37) Glawar, A. F. G.; Jenkinson, S. F.; Newberry, S. J.; Thompson, A. L.; Nakagawa, S.; Yoshihara, A.; Akimitsu, K.; Izumori, K.; Butters, T. D.; Kato, A.; Fleet, G. W. J. *Org. Biomol Chem.* **2013**, *11*, 6886.
- (38) Jenkinson, S. F.; Best, D.; Saville, A. W.; Mui, J.; Martínez, R. F.; Nakagawa, S.; Kunimatsu, T.; Alonzi, D. S.; Butters, T. D.; Norez, C.; Becq, F.; Blériot, Y.; Wilson, F. X.; Weymouth-Wilson, A. C.; Kato, A.; Fleet, G. W. J. *J. Org. Chem.* **2013**, *78*, 7380.
- (39) von Roedern, E. G.; Kessler, H. *Angew. Chem., Int. Ed. Eng.* **1994**, *33*, 687.
- (40) Taillefumier, C.; Lakhrissi, Y.; Lakhrissi, M.; Chapleur, Y. *Tetrahedron: Asymmetry* **2002**, *13*, 1707.

- (41) Sharma, G. V. M.; Reddy, K. R.; Krishna, P. R.; Sankar, A. R.; Narsimulu, K.; Kumar, S. K.; Jayaprakash, P.; Jagannadh, B.; Kunwar, A. C. *J. Am. Chem. Soc.* **2003**, *125*, 13670.
- (42) Sharma, G. V. M.; Jadhav, V. B.; Ramakrishna, K. V. S.; Jayaprakash, P.; Narsimulu, K.; Subash, V.; Kunwar, A. C. *J. Am. Chem. Soc.* **2006**, *128*, 14657.
- (43) Gajula, P. K.; Asthana, J.; Panda, D.; Chakraborty, T. K. *J. Med. Chem.* **2013**, *56*, 2235.
- (44) van Well, R. M.; Meijer, M. E. A.; Overkleeft, H. S.; van Boom, J. H.; van der Marel, G. A.; Overhand, M. *Tetrahedron* **2003**, *59*, 2423.
- (45) Horne, W. S.; Gellman, S. H. *Acc. Chem. Res.* **2008**, *41*, 1399.
- (46) Jones, C. R.; Qureshi, M. K. N.; Truscott, F. R.; Hsu, S.-T. D.; Morrison, A. J.; Smith, M. D. *Angew. Chem., Int. Ed.* **2008**, *47*, 7099.
- (47) Torres, E.; Gorrea, E.; Burusco, K. K.; Da Silva, E.; Nolis, P.; Rua, F.; Boussert, S.; Diez-Perez, I.; Dannenberg, S.; Izquierdo, S.; Giralt, E.; Jaime, C.; Branchadell, V.; Ortuno, R. M. *Org. Biomol. Chem.* **2010**, *8*, 564.
- (48) Cheng, R. P.; Gellman, S. H.; DeGrado, W. F. *Chem. Rev.* **2001**, *101*, 3219.
- (49) Mitra, S. N.; Dey, S.; Karthikeyan, S.; Singh, T. P. *Biopolymers* **1997**, *41*, 97.
- (50) Martinek, T. A.; Fulop, F. *Chem. Soc. Rev.* **2012**, *41*, 687.
- (51) Hanessian, S.; Auzzas, L. *Acc. Chem. Res.* **2008**, *41*, 1241.
- (52) Szakonyi, Z.; Martinek, T. A.; Sillanpää, R.; Fülöp, F. *Tetrahedron: Asymmetry* **2008**, *19*, 2296.
- (53) Ramachandran, G. N.; Ramakrishnan, C.; Sasisekharan, V. *J. Mol. Biol.* **1963**, *7*, 95.
- (54) Ramachandran, G. N.; Sasisekharan, V. *Adv. Protein Chem.* **1968**, *23*, 283.
- (55) Ramakrishnan, C.; Ramachandran, G. N. *Biophys. J.* **1965**, *5*, 909.
- (56) Vasudev, P. G.; Chatterjee, S.; Shamala, N.; Balaram, P. *Acc. Chem. Res.* **2009**, *42*, 1628.
- (57) Venkatraman, J.; Shankaramma, S. C.; Balaram, P. *Chem. Rev.* **2001**, *101*, 3131.
- (58) Chatterjee, S.; Roy, R. S.; Balaram, P. *J. R. Soc. Interface* **2007**, *4*, 587.
- (59) Toniolo, C.; Crisma, M.; Formaggio, F.; Peggion, C. *Biopolymers* **2002**, *60*, 396.
- (60) Antonello, S.; Formaggio, F.; Moretto, A.; Toniolo, C.; Maran, F. *J. Am. Chem. Soc.* **2003**, *125*, 2874.

- (61) Vasudev, P. G.; Chatterjee, S.; Shamala, N.; Balaram, P. *Acc. Chem. Res.* **2009**, *42*, 1628.
- (62) Gobbo, C.; Li, M.; Mali, K. S.; van Esch, J. H.; De Feyter, S. *ACS Nano* **2012**, *6*, 10684.
- (63) Barišić, L.; Čakić, M.; Mahmoud, K. A.; Liu, Y.-n.; Kraatz, H.-B.; Pritzkow, H.; Kirin, S. I.; Metzler-Nolte, N.; Rapić, V. *Chem. –Eur J.* **2006**, *12*, 4965.
- (64) Atkinson, R. C. J.; Gibson, V. C.; Long, N. J. *Chem. Soc. Rev.* **2004**, *33*, 313.
- (65) Stigers, K. D.; Soth, M. J.; Nowick, J. S. *Curr. Opin. Chem. Biol.* **1999**, *3*, 714.
- (66) Jones, C. R.; Baruah, P. K.; Thompson, A. L.; Scheiner, S.; Smith, M. D. *J. Am. Chem. Soc.* **2012**, *134*, 12064.
- (67) Thoß, M.; Seidel, R. W.; Feigel, M. *Tetrahedron* **2010**, *66*, 8503.
- (68) Ramesh, V. V. E.; Roy, A.; Vijayadas, K. N.; Kendhale, A. M.; Prabhakaran, P.; Gonnade, R.; Puranik, V. G.; Sanjayan, G. J. *Org. Biomol. Chem.* **2011**, *9*, 367.
- (69) Kendhale, A. M.; Gonnade, R.; Rajamohanan, P. R.; Hofmann, H.-J.; Sanjayan, G. J. *Chem. Commun.* **2008**, 2541.
- (70) Kale, S. S.; Priya, G.; Kotmale, A. S.; Gawade, R. L.; Puranik, V. G.; Rajamohanan, P. R.; Sanjayan, G. J. *Chem. Commun.* **2013**, *49*, 2222.
- (71) Supuran, C. T.; Casini, A.; Scozzafava, A. *Med. Res. Rev.* **2003**, *23*, 535.
- (72) Liskamp, R. M. J.; Rijkers, D. T. S.; Kruijtzter, J. A. W.; Kemmink, J. *ChemBioChem* **2011**, *12*, 1626.
- (73) Liskamp, R. M. J.; Kruijtzter, J. A. W. *Mol. Diversity* **2004**, *8*, 79.
- (74) Langenhan, J. M.; Fisk, J. D.; Gellman, S. H. *Org. Lett.* **2001**, *3*, 2559.
- (75) Gennari, C.; Salom, B.; Potenza, D.; Longari, C.; Fioravanzo, E.; Carugo, O.; Sardone, N. *Chem.-Eur. J.* **1996**, *2*, 644.
- (76) Gennari, C.; Salom, B.; Potenza, D.; Williams, A. *Angew. Chem., Int. Ed.* **1994**, *33*, 2067.
- (77) Baldauf, C.; Gunther, R.; Hofmann, H.-J. *THEOCHEM* **2004**, *675*, 19.
- (78) Turcotte, S.; Gervais, S. H. B.; Lubell, W. D. *Org. Lett.* **2012**, *14*, 1318.
- (79) Yokoi, A.; Kuromitsu, J.; Kawai, T.; Nagasu, T.; Sugi, N. H.; Yoshimatsu, K.; Yoshino, H.; Owa, T. *Molecular Cancer Therapeutics* **2002**, *1*, 275.
- (80) Liou, J.-P.; Hsu, K.-S.; Kuo, C.-C.; Chang, C.-Y.; Chang, J.-Y. *JPET* **2007**, *323*, 398.
- (81) Hung, A. W.; Silvestre, H. L.; Wen, S.; Ciulli, A.; Blundell, T. L.; Abell, C. *Angew. Chem., Int. Ed.* **2009**, *48*, 8452.



- (82) Cohen, E.; Klarberg, B.; Jr., J. R. V. *J. Am. Chem. Soc.* **1960**, *82*, 2731.
- (83) Tsai, H. J.; Chou, S.-Y.; Chuang, S.-H.; Chen, C.-C.; Hsu, F.-L. *Drug Development Research* **2008**, *69*, 514.
- (84) Ye, X. M.; Konradi, A. W.; Smith, J.; Xu, Y.-Z.; Dressen, D.; Garofalo, A. W.; Marugg, J.; Sham, H. L.; Truong, A. P.; Jagodzinski, J.; Pleiss, M.; Zhang, H.; Goldbach, E.; Sauer, J.-M.; Brigham, E.; Bova, M.; Basi, G. S. *Bioorg. Med. Chem. Lett.* **2010**, *20*, 2195.
- (85) Gopalsamy, A.; Chopra, R.; Lim, K.; Ciszewski, G.; Shi, M.; Curran, K. J.; Sukits, S. F.; Svenson, K.; Bard, J.; Ellingboe, J. W.; Agarwal, A.; Krishnamurthy, G.; Howe, A. Y. M.; Orłowski, M.; Feld, B.; O'Connell, J.; Mansour, T. S. *J. Med. Chem.* **2006**, *49*, 3052.
- (86) Ameijde, J. v.; Liskamp, R. M. J. *Tetrahedron Lett.* **2000**, *41*, 1103.
- (87) Brouwer, A. J.; Liskamp, R. M. J. *J. Org. Chem.* **2004**, *69*, 3662.
- (88) Prabhakaran, P.; Kale, S. S.; Puranik, V. G.; Rajamohanam, P. R.; Chetina, O.; Howard, J. A. K.; Hofmann, H.-J.; Sanjayan, G. J. *J. Am. Chem. Soc.* **2008**, *130*, 17743.
- (89) Thorat, V. H.; Ingole, T. S.; Vijayadas, K. N.; Nair, R. V.; Kale, S. S.; Ramesh, V. V. E.; Davis, H. C.; Prabhakaran, P.; Gonnade, R. G.; Gawade, R. L.; Puranik, V. G.; Rajamohanam, P. R.; Sanjayan, G. J. *Eur. J. Org. Chem.* **2013**, 3529.
- (90) Gowda, D.; Mahesh, B.; Shankare, G. *Ind. J. Chem. Sect. B* **2001**, *40*, 75.
- (91) Parkin, A.; Collins, A.; Gilmore, C. J.; Wilson, C. C. *Acta Crystallogr., Sect. B* **2008**, *64*, 66.
- (92) Beligere, G. S.; Dawson, P. E. *J. Am. Chem. Soc.* **2000**, *122*, 12079.
- (93) Blankenship, J. W.; Balambika, R.; Dawson, P. E. *Biochemistry* **2002**, *41*, 15676.
- (94) Chapman, E.; Thorson, J. S.; Schultz, P. G. *J. Am. Chem. Soc.* **1997**, *119*, 7151.
- (95) Deechongkit, S.; Nguyen, H.; Powers, E. T.; Dawson, P. E.; Gruebele, M.; Kelly, J. W. *Nature* **2004**, *430*, 101.
- (96) Deechongkit, S.; Dawson, P. E.; Kelly, J. W. *J. Am. Chem. Soc.* **2004**, *126*, 16762.
- (97) Fantò, N.; Gallo, G.; Ciacci, A.; Semproni, M.; Vignola, D.; Quaglia, M.; Bombardi, V.; Mastroianni, D.; Zibella, M. P.; Basile, G.; Sassano, M.; Ruggiero, V.; Santis, R. D.; Carminati, P. *J. Med. Chem.* **2008**, *51*, 1189.
- (98) Feigel, M.; Lugert, G.; Manero, J.; Bremer, M. Z. *Naturforsch.* **1990**, *45b*, 258.
- (99) Neidle, S.; Webster, G. D.; Jones, J. B.; Thurston, D. E. *Acta. Crystallogr., Sect. C* **1991**, *47*, 2678.

- (100) Moroder, L.; Lutz, J.; Grams, F.; Rudolph-Boehner, S.; Oesapay, G.; Goodman, M.; Kolbeck, W. *Biopolymers* **1996**, *38*, 295.
- (101) Clark, R. L.; Carter, K. C.; Mullen, A. B.; Coxon, G. D.; Owusu-Dapaah, G.; McFarlane, E.; Thi, M. D. D.; Grant, M. H.; Tettey, J. N. A.; Mackay, S. P. *Bioorg. Med. Chem. Lett.* **2007**, *17*, 624.
- (102) Leiserowitz, L.; Schmidt, G. M. J. *J. Chem. Soc. A* **1969**, 2372.
- (103) Seo, M.; Park, J.; Kim, S. Y. *Org. Biomol. Chem.* **2012**, *10*, 5332.
- (104) Wilmot, C. M.; Thornton, J. M. *J. Mol. Biol.* **1988**, *203*, 221.
- (105) Prasad, B. V. V.; Balaram, P. *CRC Crit. Rev. Biochem.* **1984**, *16*, 307.
- (106) Prasad, B. V. V.; Sasisekharan, V. *Macromolecules* **1979**, *12*, 1107.
- (107) Moretto, A.; Crisma, M.; Kaptein, B.; Broxterman, Q. B.; Toniolo, C. *Biopolymers* **2006**, *84*, 553.
- (108) Chatterjee, J.; Gilon, C.; Hoffman, A.; Kessler, H. *Acc. Chem. Res.* **2008**, *41*, 1331.

## *Chapter 3*

# Studies Regarding the Role of Ant-Sulfonamide (<sup>s</sup>Ant) as Turn Inducer in Peptides

## Part A: Multifaceted Folding in Orphanic acid (<sup>s</sup>Ant)-Based Reverse Turn Motifs.

### 3.1 Non-covalent interactions and drug target receptors

Non-covalent forces such as hydrogen bonding, halogen bonding, hydrophobic interactions, hydrophilic interactions, dipole-dipole interactions *etc.*, are the ones which perform the task of binding drug to receptors.<sup>1-3</sup> Among which, hydrogen bonding interactions have significant role in rigidifying the conformation of peptide drugs, as the reverse-turn regions are targeted areas for most of the receptors, particularly G-Protein coupled Receptors (GPCRs).<sup>4-8</sup> G protein coupled receptors (GPCRs) are also called seven-trans-membrane domain receptors, 7TM receptors, heptahelical receptors, serpentine receptor, and G protein-linked receptors (GPLR). They constitute a large protein family of receptors that sense molecules outside the cell and activate inside signal transduction pathways and responses. They are called also trans-membrane receptors because they pass through the cell membrane and as they pass through the cell membrane 7 times, they are called seven-trans-membrane receptors.<sup>9</sup> Conformational changes play a crucial role in the function of GPCRs as the receptor molecule exists in a conformational equilibrium between active and inactive biophysical states, although the signal transduction through the membrane by the receptor is not completely understood.<sup>10-14</sup>

### 3.2 Reverse turns - The targeted areas for drug receptors

Mimicking elements of secondary structures in proteins (helices, turns, strands or sheets) or grafting bioactive peptides onto stable scaffolds is one of the promising areas in the development of peptide drugs. The approach which involves mimicking the secondary structural motifs in small, carefully designed, peptides to replicate their protein-like biological activities is based on the fact that many protein–protein interactions involve recognition of key elements of secondary structure. On the other hand, small protein scaffolds in nature are mostly stable and acquiescent to sequence insertions, or embedding of bioactive peptides. For example, scaffolds including knottins<sup>15-16</sup> and cyclotides<sup>17</sup> from plants, lasso peptides from bacteria<sup>18</sup> and a variety of animal toxins, conotoxins<sup>19-20</sup> from marine cone snail venoms *etc.* are relatively stable due to the presence of disulfide bonds. These approaches offer the prospects of utilizing protein–protein interactions through conformational constraints to reduce peptide flexibility. This may either allow reduced exposure to their solvation by water by hydrogen bonding or

covering hydrogen bonding entities atoms within a peptide. Since turns or loops form >30% of protein structure, peptide drugs are developed mimicking turns, especially  $\beta$ -turns.

### 3.3 Peptidomimetics - Tool for drug development

$\beta$ -Turns form a large number of protein-protein interactions in peptides.  $\beta$ -Turn mimetics have been designed for the inhibition of specific protein-protein interactions from carbohydrate scaffolds. A mimetic for the cyclic peptide somatostatin has been synthesized using a  $\alpha$ -D-glucose scaffold by Hirschmann *et al.*<sup>21-22</sup> Smith and Hirschmann designed a pyrrolinone-based scaffold that mimicked peptide  $\beta$ -sheet backbone including hydrogen bonding donors, acceptors, and side chains and were incorporated into peptide residues.<sup>23-24</sup> The peptidomimetic structure was shown to have an affinity similar to that of the original peptide sequence for the MHC class II molecule.<sup>25</sup> Pyrrolidinone-based peptidomimetics, in which the peptide bond is forced to adopt either a *cis* or *trans* geometry, have also been prepared from readily available amino acids.<sup>26</sup> Carbohydrate-derived conformationally restricted bicyclic dipeptides characterized by a constrained  $\beta$ -lactam ring fused with a pyrrolidine ring carrying a hydroxyethylamine isostere (HEA)<sup>27-33</sup> on the backbone offers the possibility of developing foldamers with interesting structural architectures, clearly different from those classically observed.<sup>32-34</sup> Naturally occurring constrained  $\alpha$ -amino acid proline (Pro), with constrained  $\phi$  and  $\psi$  angles, is known to induce a helical conformation, described as polyproline helices, in its *homo* oligomers.<sup>35</sup> It is noteworthy that extensive work with *homo*- and *hetero*-chiral Pro-*Xaa* building blocks has yielded diverse sets of short peptide motifs that can stabilize various peptide secondary structures, as independently demonstrated by the groups of Balaram<sup>36-37</sup> and Gellman.<sup>38-40</sup>

A well-known class of peptidomimetics termed *retro-inverso* peptides was originally developed by the group of the eminent peptide chemist (*late*) Murray Goodman.<sup>41</sup> The remarkable proteolytic stability of such peptidomimetics has a bearing in practical utility and has been carefully exemplified in a number of cases.<sup>42-43</sup> Similarly, the notable feature of the Ant-Pro and <sup>S</sup>Ant-Pro reverse-turn structures is their reversed, hydrogen bonding interaction - an arrangement that offers improved resistance to proteolytic degradation.<sup>44-46</sup>

### 3.4 Multifaceted folding in mesyl-Xaa-<sup>S</sup>Ant-Yaa peptide residues: Present study

The turn induction nature of orthanilic acid (<sup>S</sup>Ant) in  $\alpha$ -peptide residues has led to reverse turn motifs featuring strong C-9 or C-11 *inter-residual* hydrogen bonding networks, in addition to the intra-residual C-6 hydrogen bonding.<sup>46-47</sup> <sup>S</sup>Ant forms C-9 turn with <sup>L</sup>proline between *i*-1 and *i*+2 amino acid residues and hence is called a *pseudo- $\beta$ -turn*.<sup>46</sup> This turn formation is unique as the C-9 hydrogen bonding is avoided, when <sup>L</sup>Pro is replaced with any other  $\alpha$ -amino acid.<sup>46</sup> An 11-membered turn formation is observed when another  $\alpha$ -amino acid is introduced at the N-terminus between *i* and *i*+3 amino acid residues and thus called an extended  $\beta$ -turn.<sup>47</sup> However, when N and C-terminal amino acids are *imino*-acids like <sup>L</sup>Pro, it avoids the opportunity of utilizing an acceptor NH for hydrogen bonding. A sulphonamide modification at the N-terminus facilitates the prospect of using additional donor for hydrogen bonding and hence, it competes for hydrogen bonding. Here a multi-faceted folding is observed for mesyl-Xaa-<sup>S</sup>Ant-Yaa, when one or more of the  $\alpha$ -amino acid is proline.

### 3.5 Objective of the work: Incorporation of <sup>S</sup>Ant in peptide sequences

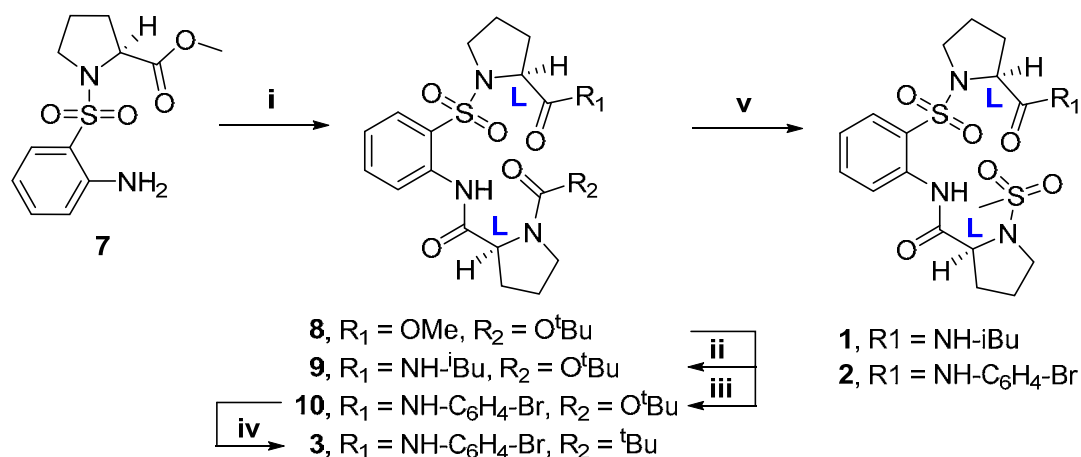
Incorporation of an unnatural  $\beta$ -sulfonic acid like 2-aminobenzene sulfonic acid (<sup>S</sup>Ant) into peptide reverse-turn motifs invokes conformational rigidity and improved proteolytic stability. The presence of sulfonamide bonds, which enter as isosteres of carboxamide bond, induces the twist (folding) in peptide residues due to the lower value of CSNC dihedral angle ' $\omega$ ', when compared to a carboxamide. <sup>S</sup>Ant residue, due to the additional rigidity accomplished upon being an aromatic  $\beta$ -amino sulfonic acid, accounts for the conformational rigidity as well. Another stabilizing factor involves the C-6 intra residual hydrogen bonding of <sup>S</sup>Ant that is observed in orthanilamides. The idea of incorporating <sup>S</sup>Ant involves the design of novel reverse turn motifs with improved folding as well as proteolytic stability.

### 3.6 Synthesis

Compound **7**, being less reactive under normal coupling reaction conditions, was subjected to amide formation with Boc-<sup>L</sup>Pro-OH under mixed anhydride reaction conditions using ethyl chloroformate and triethylamine in THF affording the intermediate **8**, which was further converted to various analogues with modified N- and C-termini. The C-terminus methyl ester was hydrolysed using LiOH.H<sub>2</sub>O and was converted to its

isobutyl amide **9** and 4-Br anilide **10**, respectively, using HBTU and Et<sub>3</sub>N in DCM. Compounds **9** and **10** were then subjected to Boc deprotection using TFA and DCM, followed by mesylation using mesyl chloride and Et<sub>3</sub>N to obtain **1** and **2** respectively (Scheme 3.1). Compound **10** was converted to its pivaloyl derivative using pivaloyl chloride and triethylamine to obtain **3** (Scheme 3.1).

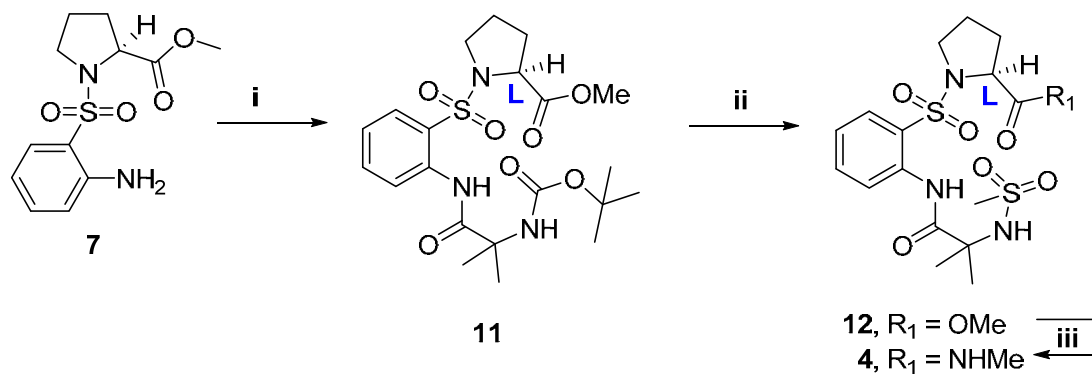
**Scheme 3.1:** Synthesis of Pro-<sup>S</sup>Ant-Pro turn units



*Reagents and conditions:* (i) Boc-<sup>L</sup>Pro-OH, ethyl chloroformate, Et<sub>3</sub>N, THF, 70°C, 48h; (ii) (a) LiOH.H<sub>2</sub>O, MeOH, H<sub>2</sub>O, RT, 3h (b) HBTU, Et<sub>3</sub>N, <sup>i</sup>BuNH<sub>2</sub>, RT, 12h; (iii) (a) iia (b) HBTU, Et<sub>3</sub>N, 4-Br-C<sub>6</sub>H<sub>4</sub>-NH<sub>2</sub>, DCM, RT, 12h; (iv) (a) TFA, DCM, RT, 3h, (b) Piv-Cl, Et<sub>3</sub>N, DCM, RT, 12h; (v) Mesyl-Cl, Et<sub>3</sub>N, DCM, RT, 12h.

Compound **7** was coupled with Boc-Aib-OH using ethyl chloroformate reaction furnishing **11** and compound **11** was subjected to TFA deprotection furnishing the free amine. The free amine was mesylated to obtain **12**, which was then amidated using methylamide solution affording **4** (Scheme 3.2).

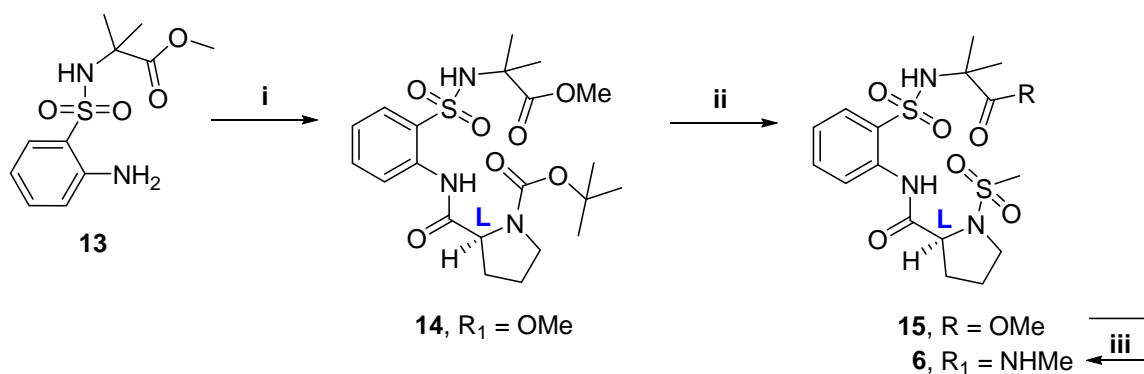
**Scheme 3.2:** Synthesis of mesyl-Aib-<sup>S</sup>Ant-Pro turn units



*Reagents and conditions:* (i) Boc-Aib-OH, ethyl chloroformate, Et<sub>3</sub>N, THF, 70°C, 48h; (ii) (a) TFA, DCM, RT, 3h, (b) Mesyl-Cl, Et<sub>3</sub>N, DCM, RT, 12h; (iii) CH<sub>3</sub>NH<sub>2</sub>, MeOH, 3h.

Compound **13** was subjected to ethyl chloroformate condition to obtain compound **14**, which was then converted to its free amine using TFA and DCM followed by neutralizing with NaHCO<sub>3</sub> solution. The free amine was mesylated to achieve **15** and subsequent amidation using methanolic methylamine forming **5** (Scheme 3.3).

**Scheme 3.3:** Synthesis of Mes-Pro-<sup>S</sup>Ant-Aib turn units



*Reagents and conditions:* (i) Boc-<sup>L</sup>Pro-OH, ethyl chloroformate, Et<sub>3</sub>N, THF, 70°C, 48h; (ii) (a) TFA, DCM, RT, 3h, (b) Mesyl-Cl, Et<sub>3</sub>N, DCM, RT, 12h; (iii) CH<sub>3</sub>NH<sub>2</sub>, MeOH, 3h.

### 3.7 Conformational analysis

Conformational analysis was carried out using solid-state single crystal X-ray analysis and solution-state 2D-NOESY NMR analysis. The *intra*- and *inter*-molecular hydrogen bonding as well as the strength of *intra*-molecular hydrogen bonding were analysed by DMSO-*d*<sub>6</sub> titration and variable temperature experiments in CDCl<sub>3</sub>.

#### 3.7.1 Solid state X-ray and Solution State NMR studies

Incorporation of <sup>S</sup>Ant between Pro residues, which is devoid of a secondary amide NH, have resulted in an unusually folded structure comprising of terminal C-14 hydrogen-bonding networks [d (N-H...O): 2.4Å], formed between the oxygen of SO of the *i*<sup>th</sup> residue and the NH of the (*i* + 4)<sup>th</sup> residue, in the backward direction (5←1), as seen in typical α-turns (5 residue C-13 turn), which can be called as an extended α-turn (5 residue C-14 turn).

Proline, although is a cyclic iminoacid which is devoid of a donor part 'NH' for hydrogen-bonding in the oligomer stage, usually forms stable *homo*- and *hetero*- helices solely due to its unique dihedral angle preferences.<sup>48</sup> The endeavour to surrogate orthonilic acid for proline was apparently due to the twist (folding) in the turn motif, generated at the sulfonamide bonds.



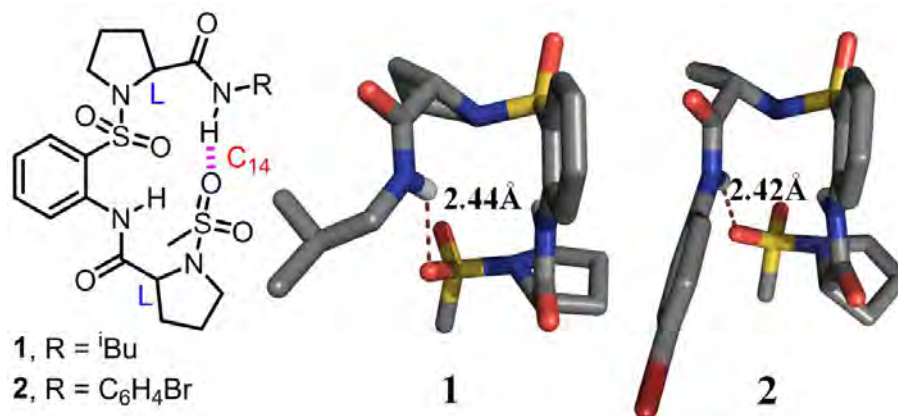


**Fig. 3.1:** Molecular structures and PyMOL rendered crystal structures of Mesyl-Pro-<sup>S</sup>Ant-Pro residues displaying terminal C-14 H-bonding.

The three dimensional structure was supported by solid state single crystal X-ray studies of **1** and **2**, and solution state NMR 2D NOESY studies of **2**. The C-14 hydrogen bonded arrangement of **2** was confirmed by diagnostic NOEs such as NH<sub>2</sub> vs. C1H, C1H vs. C18H, C23H vs. C22H and NH<sub>1</sub> vs. C16H. There are various other NOEs like NH<sub>1</sub> vs. C4H, NH<sub>1</sub> vs. C3H, C21H vs. C23H, NH<sub>1</sub> vs. C23H, NH<sub>1</sub> vs. C2H, NH<sub>2</sub> vs. C13H, NH<sub>2</sub> vs. C14H, NH<sub>1</sub> vs. C16H and C9H vs. C18H also supported the compact dimensional structure of compound **2** (fig 3.2, see page 245 for 2D extracts).

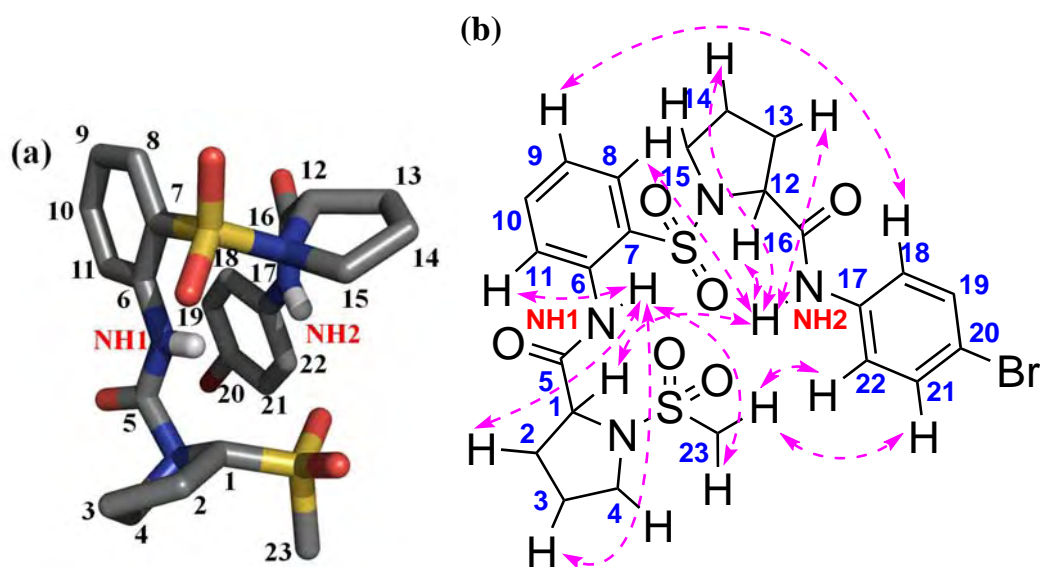


**Fig. 3.2:** PyMOL rendered crystal structures of **2** with numbering (a) and molecular structure with NOE interactions (b).

The sulfonyl group at the N-terminus was seen to play a significant role in the twisted conformation of **1** and **2**. A sulfonamide to carboxamide modification at the N-terminus abolished the C-14 conformation, observed in **1** and **2**, indicating the

significance of a sulfonamide (bond) in inducing folding and thereby altering the hydrogen bonding patterns. The resultant peptide **3** (fig. 3.5) displayed a folded conformation featuring strong inter-residual C-9 hydrogen bonding [d (N-H...O): 2.2Å], observed in <sup>S</sup>Ant-Pro reverse turn units. It was noted that the <sup>S</sup>Ant-Pro, which is devoid of a *pseudo-β*-turn (C-9 turn) in **1** and **2**, showed the CSNC dihedral angle ‘ $\omega$ ’ close to a value of 66° (‘ $\omega$ ’ adopted an unusual value of 152° in the presence of <sup>S</sup>Ant-Pro C-9 turn as that of a typical sulfonamide bond). The solution-state behaviour of **3** was analysed by 2D NOESY studies. The diagnostic NOEs like NH1 vs. C13H, C5H vs. C20H, C20H vs. C25H, C3H vs. C19H, C16H vs. NH1, C9H vs. C15H etc. support the three dimensional conformation of **3** (fig 3.4, see page 246 for 2D extracts).

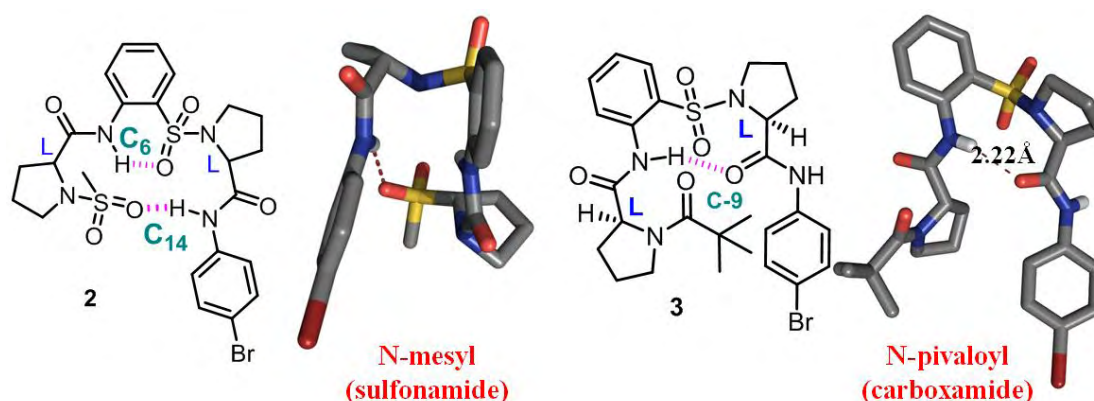


**Fig. 3.3:** Molecular structures and PyMOL-rendered crystal structures of Pro-<sup>S</sup>Ant-Pro residues with N-terminal mesyl (sulphonamide) **2**, featuring C-14 H-bonding and N-terminal pivaloyl (carboxamide) **3**, featuring C-9 H-bonding.

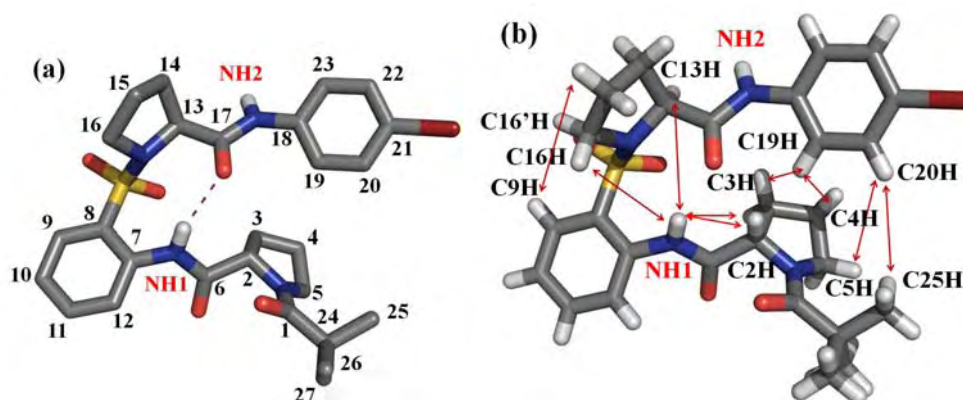


**Fig. 3.4:** PyMOL-rendered crystal structures of **3** with numbering (a) and NOE interactions (b).

Substituent effects resulted in a deleterious effect, when the N- and C-terminal prolines were swapped with constrained  $\alpha$ -aminoacid isobutyric acid (Aib) - an unnatural  $\alpha$ -aminoacid with unique preferences of dihedral angles to induce folding in peptides.

Such a modification also created the involvement of an additional ‘NH’ as a donor atom for hydrogen bonding unlike to that of proline. The substitution of N-terminus Pro with Aib in **4**, abolished the C-9 hydrogen bonding observed in <sup>S</sup>Ant-Pro turn systems and the resultant crystal structure showed the C-6 hydrogen bonding of <sup>S</sup>Ant. The substitution of Pro with Aib at the C-terminus, in **5** (fig. 3.9, C and D), showed the involvement of Aib ‘NH’ in 11-membered hydrogen bonding with proline ‘SO’ in the backward direction (4←1) [d (N-H...O): 2.3Å]. The turn system also featured a weak 7-membered hydrogen bonding between the terminal sulfonyl ‘O’ and <sup>S</sup>Ant ‘NH’, in the backward direction (3←1) [d (N-H...O): 3.0Å], as seen in typical  $\gamma$ -turns (3 residue C-7 turn).

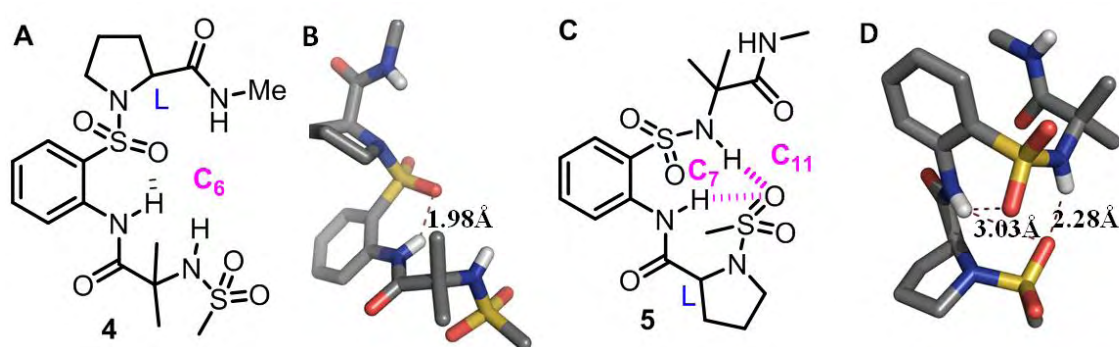


**Fig. 3.5:** Molecular structures and crystal structures of mesyl-*Xaa*-<sup>S</sup>Ant-*Yaa* residues, **4** (with N-terminal Aib) featuring C-6 H-bonding and **5** (N-terminal proline) featuring C-7 and C-11 H-bonding.

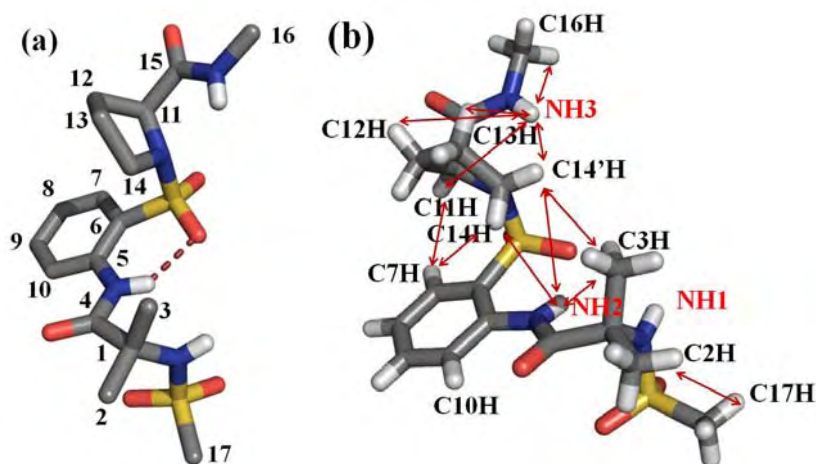


**Fig. 3.6:** PyMOL-rendered crystal structures of **4**; with numbering (a) and NOE interactions (b).

The solid-state behaviors of **4** and **5** were reflected in their solution state 2D NOESY studies. The three dimensional conformation of **4** was evaluated from the characteristic NOEs like C2H vs. C17H, NH2 vs. C3H, C3H vs. C14H, NH2 vs. C14H, C7H vs. C14H, NH3 vs. C12H, NH3 vs. C11H, NH3 vs. C13H and NH3 vs. C16H., (fig

3.6, see page 247 for 2D extracts) representing a conformation similar to that of solid state. The solution-state conformation of **5** was obtained by 2D-NOESY studies which displayed diagnostic NOEs, NH1 vs. C1H, C17H vs. C1H, NH1 vs. C4H, NH1 vs. C2H, NH1 vs. C3H, C11H vs. C2H, C8H vs. C13H, *etc.* NOEs like NH3 vs. C16H, NH3 vs. C13H, and NH2 vs. C14H also supported the solution state conformation (fig 3.7, see page 248 for 2D extracts).

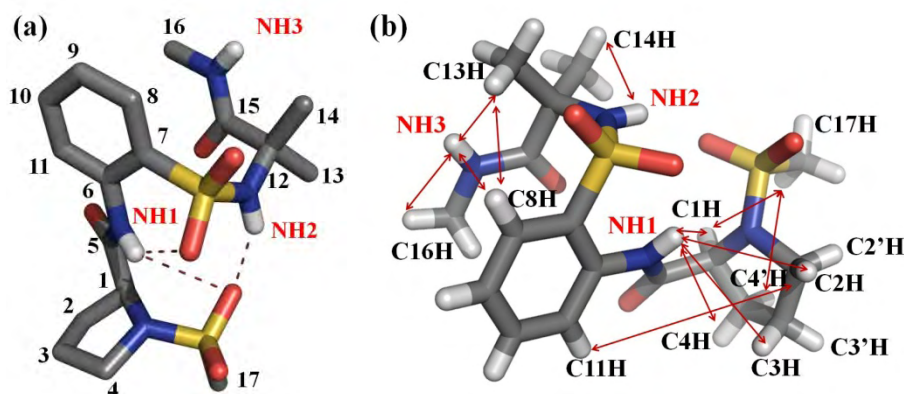


**Fig. 3.7:** PyMOL rendered crystal structures of **5**; with numbering (a) and NOE interactions (b).

### 3.7.2 NMR titration and variable temperature Studies

The diverse hydrogen bonding patterns found in compounds **2-5** were analysed by NMR studies like DMSO- $d_6$  titration and variable temperature studies in  $CDCl_3$ , where NHs which were involved in *intra*-molecular hydrogen bonding interactions undergo negligible shift in their chemical shift values ( $\delta NH_{intra} \leq 0.02\text{ppm}$ ), while those were involved in *inter*-molecular interactions underwent considerable shift.

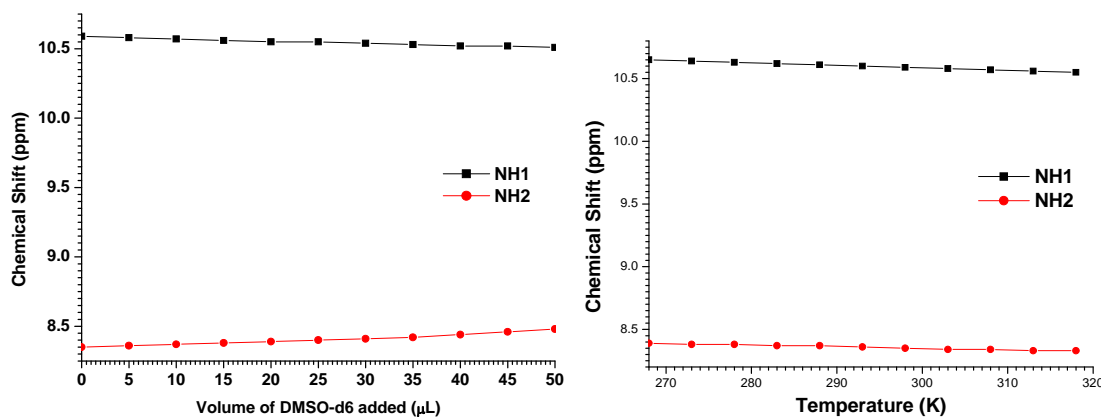


**Fig. 3.8:** Solution-state NMR experiments of compound **2**. DMSO- $d_6$  titration studies at 5 mM concentration (400MHz,  $CDCl_3$ ), and variable temperature NMR studies (400MHz,  $CDCl_3$ ).

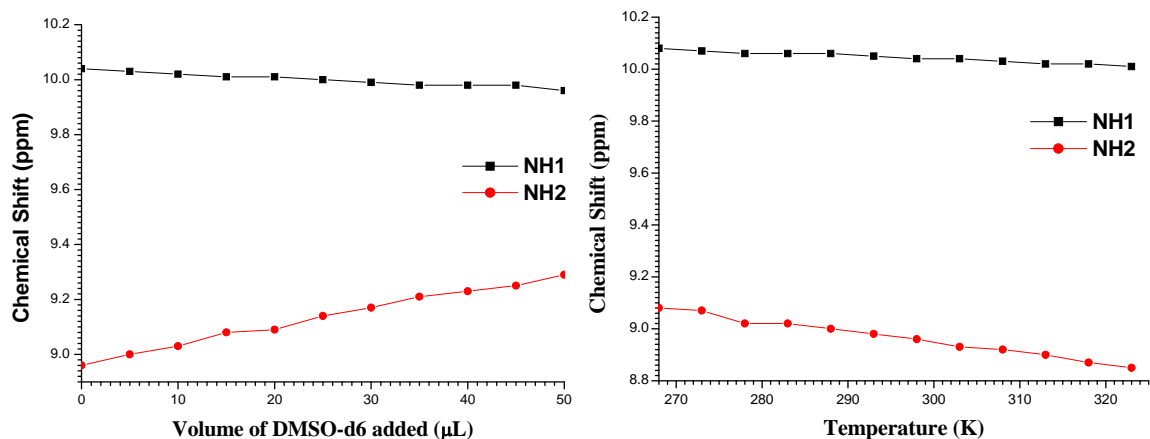


**Fig. 3.9:** Solution-state NMR experiments of compound **3**. DMSO- $d_6$  titration studies at 5 mM concentration (400MHz,  $CDCl_3$ ), and variable temperature studies (400MHz,  $CDCl_3$ ).

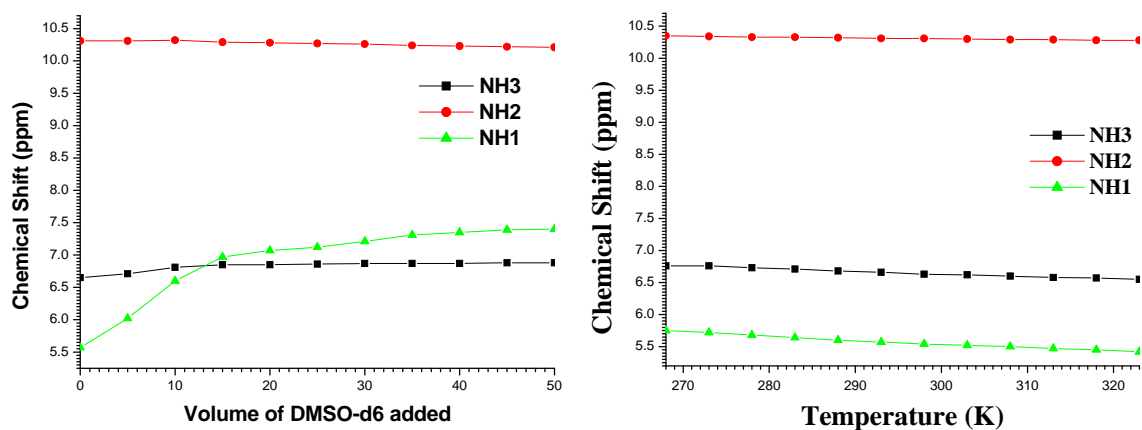


**Fig. 3.10:** Solution-state NMR experiments on compound **4**. DMSO- $d_6$  titration studies at 5 mM solution (400MHz,  $CDCl_3$ ), and variable temperature studies (400MHz,  $CDCl_3$ ).

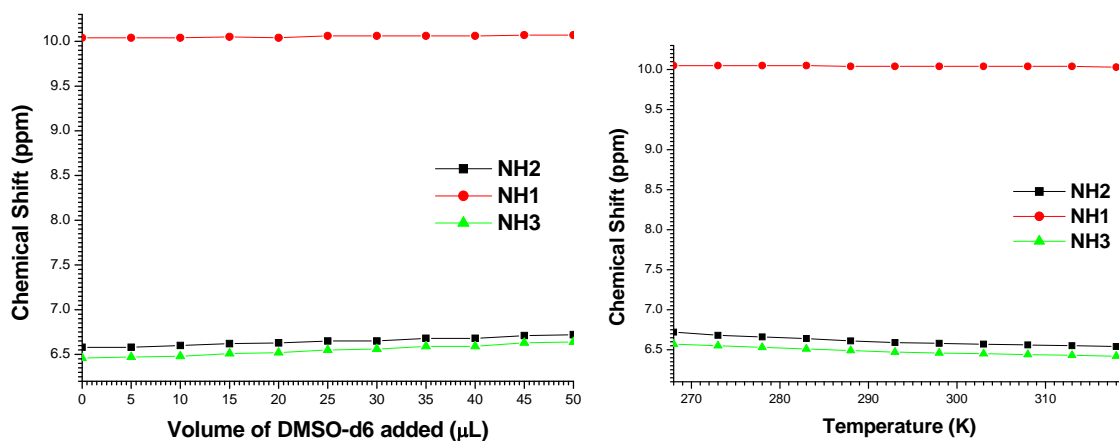


**Fig. 3.11:** Solution-state NMR experiments on compound **5**. DMSO- $d_6$  titration studies at 5 mM solution (400MHz,  $CDCl_3$ ), and variable temperature studies (400MHz,  $CDCl_3$ ).

The NH shifts for compounds **2-5** are charted in table 1.

**Table 1:** NMR DMSO-*d*<sub>6</sub> titration and variable temperature studies of compounds **2-5**.

Compound No.	DMSO- <i>d</i> <sub>6</sub> Titration studies	variable temperature studies	Inferences
<b>2</b>	$\Delta\text{NH1} = 0.08 \text{ ppm}$ $\Delta\text{NH2} = 0.13 \text{ ppm}$	$\Delta\text{NH1} = 0.11 \text{ ppm}$ $\Delta\text{NH2} = 0.07 \text{ ppm}$	NH1 and NH2 are involved in <i>intra</i> -molecular H-bonding interactions
<b>3</b>	$\Delta\text{NH1} = 0.08 \text{ ppm}$ $\Delta\text{NH2} = 0.33 \text{ ppm}$	$\Delta\text{NH1} = 0.07 \text{ ppm}$ $\Delta\text{NH2} = 0.23 \text{ ppm}$	NH1 is involved in <i>intra</i> -molecular H-bonding, while NH2 underwent <i>inter</i> -molecular H-bonding
<b>4</b>	$\Delta\text{NH1} = 0.83 \text{ ppm}$ $\Delta\text{NH2} = 0.10 \text{ ppm}$ $\Delta\text{NH3} = 0.23 \text{ ppm}$	$\Delta\text{NH1} = 0.33 \text{ ppm}$ $\Delta\text{NH2} = 0.07 \text{ ppm}$ $\Delta\text{NH3} = 0.21 \text{ ppm}$	NH1 and NH3 are involved in <i>intra</i> -molecular H-bonding, while NH2 underwent <i>inter</i> -molecular H-bonding
<b>5</b>	$\Delta\text{NH1} = 0.03 \text{ ppm}$ $\Delta\text{NH2} = 0.14 \text{ ppm}$ $\Delta\text{NH3} = 0.18 \text{ ppm}$	$\Delta\text{NH1} = 0.02 \text{ ppm}$ $\Delta\text{NH2} = 0.19 \text{ ppm}$ $\delta\text{NH3} = 0.17 \text{ ppm}$	NH1, NH2 and NH3 are involved in <i>intra</i> -molecular H-bonding interactions

### 3.8 Conclusions

In summary, the three-residue folded peptide structures featuring mesyl-*Xaa*-<sup>S</sup>Ant-*Yaa* exhibited folding patterns with diverse modes of hydrogen bonding patterns unlike that of Pro-<sup>S</sup>Ant-Pro residues. Pro-<sup>S</sup>Ant-Pro tripeptide unit, which adopted a nine-membered hydrogen bonding in <sup>S</sup>Ant-Pro reverse turns, formed C-14 membered hydrogen bonding upon the terminal amide to sulfonamide modification. The analogues formed upon replacing the terminal proline with Aib resulted in significant structural changes in its conformations. The different folding patterns were found to be dependent on the terminal amino acid residues (*i* and *i*+2) and presence of sulfonamide bond between the residues as evidenced from the single crystal analysis and NMR studies. Even though, the folding in **1-5** was characterized by diverse modes of hydrogen bonding patterns, the *intra*-residual C-6 hydrogen bonding of <sup>S</sup>Ant accounts for the conformational restriction in such systems. These hydrogen bonding networks were unusual for the fact that there was a prominence of S-O...H-N hydrogen bonding networks in **1-4** over C-O...H-N C-9 H-bonding between NH of <sup>S</sup>Ant and 'O' of proline carbonyls. The work also illustrates the versatility in the folding behaviour of <sup>S</sup>Ant based foldamers to adopt unique conformational behaviour, aided by C-6 residual hydrogen bonding and amide to sulfonamide modifications.

## Part B: Incorporation of <sup>S</sup>Ant in Aib-Pro $\beta$ -Bends

### 3.9 Incorporation of <sup>S</sup>Ant in Aib-Pro $\beta$ -Bend peptide residues: Present study

The aminoacids, Pro (proline) and Aib ( $\alpha$ -aminoisobutyric acid), often disturb the normal hydrogen bonding patterns found in helices owing to their dihedral constraints, which give rise to  $\beta$ -bend structure featuring C-10 hydrogen bonding in their sequential hybrid peptides.<sup>49-51</sup> <sup>S</sup>Ant, on the other hand, due to the conformational preferences of a sulfonamide bond, induces folding in peptides. As all these three amino acids have unique properties for inducing turn (folding) in peptides, the aim was to substitute one of the amino acids of Aib-Pro  $\beta$ -bend turn motif with <sup>S</sup>Ant. Incorporation of unusual amino acid like <sup>S</sup>Ant in peptide sequences owing to the *intra*-residual C-6 H-bonding and dihedral constraints provide additional stabilization to peptide structures through conformational rigidification.

### 3.10 Objective of the work: Role of conformational restriction on hydrogen bonding

The aminoacids, Aib and Pro, forms a  $\beta$ -bend structure featuring C-10 hydrogen bonding in their sequential hybrid peptides.<sup>49-51</sup> The sequential foldamer motifs featuring Aib-Pro-Adb<sup>51</sup> and Aib-Pro-Ant<sup>52</sup> were designed (fig 3.12) and synthesized to examine the role of conformational restriction upon hydrogen bonding, from our group. In Aib-Pro-Adb foldamer motifs, NH of 3-amino-4,6-dimethoxy benzoic acid (Adb) restricted by 5-membered hydrogen bonding with the nearby methoxy oxygens was involved in C-10 hydrogen bonding (periodic  $\beta$ -turn) with CO of Aib.<sup>51</sup> On the other hand, Aib-Pro-Ant repeating units, where the NH was restricted by C-6 hydrogen bonding of 2-aminobenzoic acid (Ant), failed to form the anticipated  $\beta$ -turn structure.<sup>52</sup>

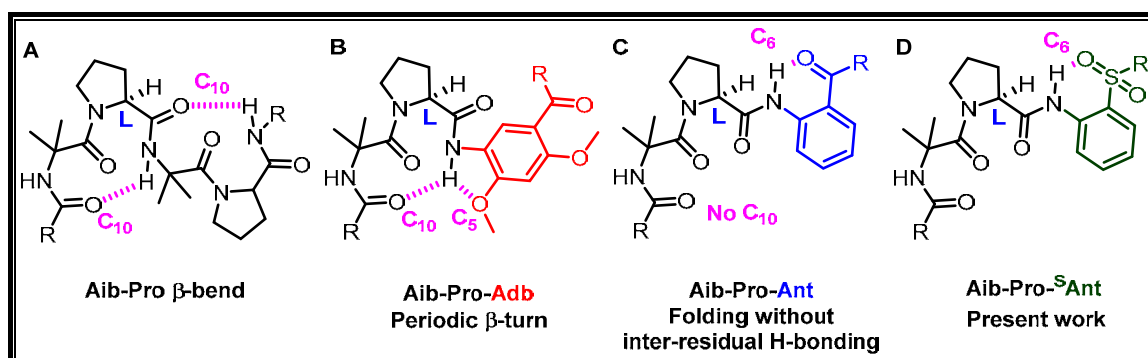


**Fig. 3.12:** Representative structures of Aib-Pro  $\beta$ -bend structure (A), Aib-Pro-Adb featuring periodic  $\beta$ -turn (B),<sup>51</sup> Aib-Pro-Ant featuring intra-residual C-6 H-bonding (C)<sup>52</sup> and the present work - Aib-Pro-<sup>S</sup>Ant turn motifs (D).

Thus, the objective was to replace Ant in Aib-Pro-Ant repeating units with its sulfonamide analogue  $^S$ Ant (2-aminobenzenesulfonic acid), as Aib-Pro- $^S$ Ant, which possibly would allow a folding at the sulfonamide bond even though the NH will be conformationally restricted due to C-6 hydrogen bonding.

### 3.11 Hybrid systems having multiple folds: Design strategy

In an effort to understand the role of conformational restriction and folding ability of  $^S$ Ant, peptide motifs featuring Piv-Aib- $^L$ Pro- $^S$ Ant-NH $^i$ Bu (**21**, fig. 3.13) and Boc-Aib- $^L$ Pro- $^S$ Ant- $^L$ Pro-NHR unit (**22-24**, fig. 3.17) were synthesized.

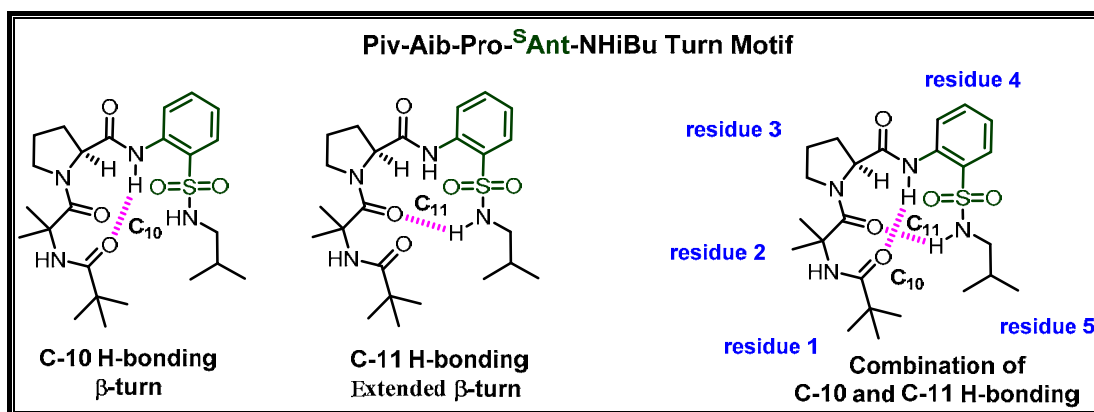


**Fig. 3.13:** Piv-Aib-Pro- $^S$ Ant-NH $^i$ Bu turns featuring plausible C-10 and C-11 hydrogen-bonding.

The turn system **21** (fig. 3.13) may exist as a combination of a  $\beta$ -turn (Aib-Pro C<sub>10</sub> - between ' $i$ ' and ' $(i+3)$ ' amino acid residues) and an extended  $\beta$ -turn (Pro- $^S$ Ant-NHR C<sub>11</sub> - between ' $i$ ' and ' $(i+3)$ ' amino acid residues)<sup>47,52</sup>.

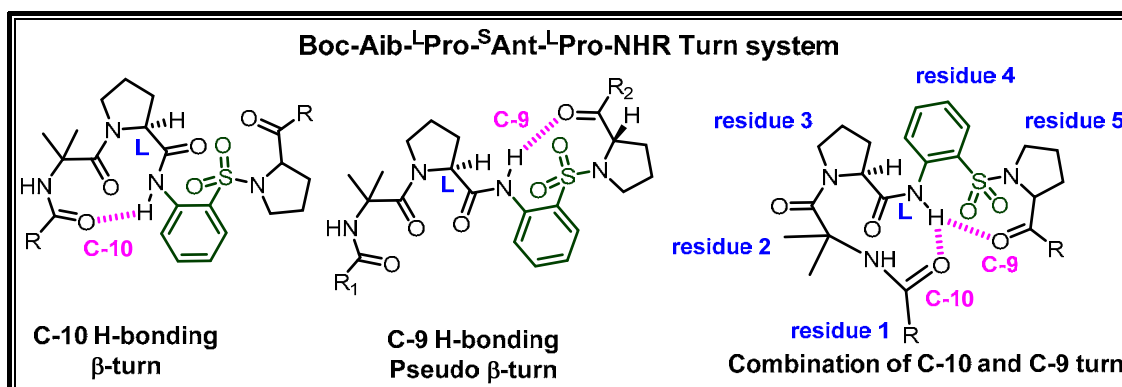


**Fig. 3.14:** R-Aib-Pro- $^S$ Ant-Pro-NHR turns featuring plausible C-10 and C-9 hydrogen bonding.

The second system in which the  $^S$ Ant is now linked to an imino acid proline that is devoid of an acceptor NH to form C<sub>11</sub> hydrogen bonding pattern as observed in former

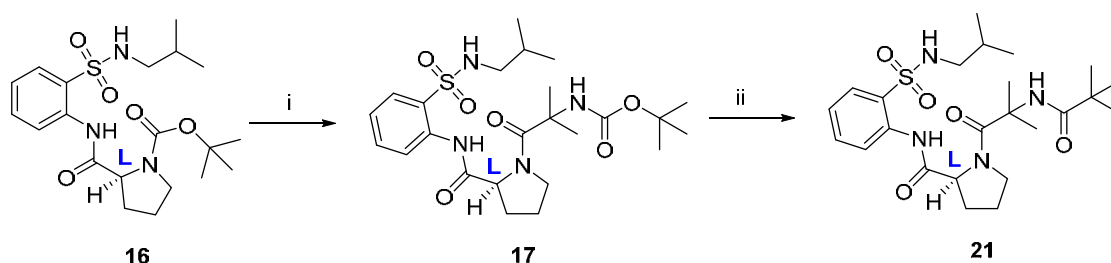


turn systems. Here, the <sup>S</sup>Ant 'NH' will be under competition for two of the hydrogen bonding networks  $\beta$ -turn (Aib-Pro C<sub>10</sub> - between '*i*' and '*(i+3)*' amino acid residues)<sup>49</sup> and a *pseudo*  $\beta$ -turn (<sup>S</sup>Ant-Pro C<sub>9</sub> - between '*(i-1)*' and '*(i+2)*' amino acid residues)<sup>46</sup>.

### 3.12 Synthesis

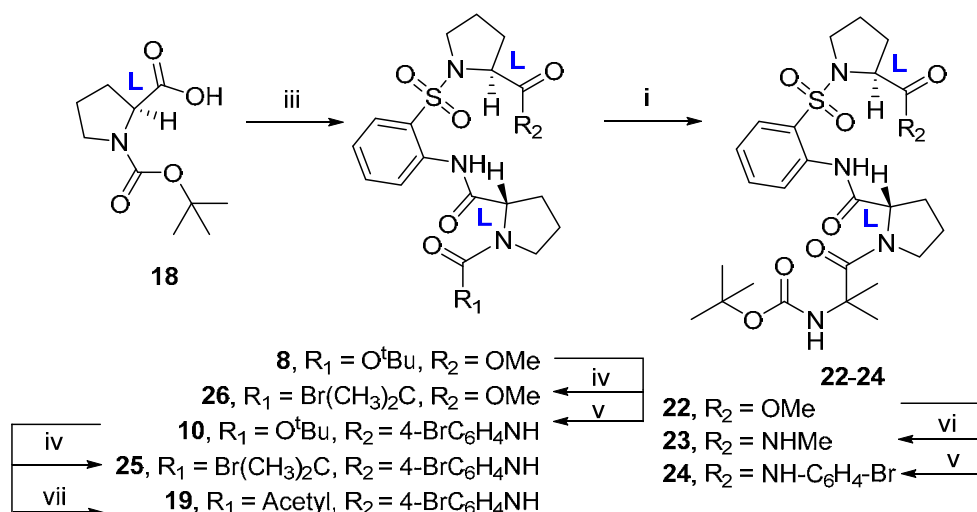
Compound **16** was subjected to 'Boc deprotection using TFA and DCM obtaining the free amine, which was coupled with Boc-Aib-OH using HBTU and Et<sub>3</sub>N in chloroform that furnished compound **17**. Compound **17** was again subjected to 'Boc deprotection and acylation using pivaloyl chloride affording compound **21** (scheme 3.4).

**Scheme 3.4:** Synthesis of Aib-Pro-<sup>S</sup>Ant-NH<sup>t</sup>Bu turns



*Reagents and conditions:* (i) (a) TFA, DCM, RT, 2h, (b) Boc-Aib-OH, HBTU, Et<sub>3</sub>N, CHCl<sub>3</sub>, RT, 12h; (ii) (a) TFA, DCM, RT, 2h, (b) Piv-Cl, Et<sub>3</sub>N, CHCl<sub>3</sub>, RT, 12h;

**Scheme 3.5:** Synthesis of Aib-Pro-<sup>S</sup>Ant-Pro turns



*Reagents and conditions:* (i) (a) TFA, DCM, RT, 2h, (b) Boc-Aib-OH, HBTU, Et<sub>3</sub>N, CHCl<sub>3</sub>, RT, 12h; (ii) (a) TFA, DCM, RT, 2h, (b) Piv-Cl, Et<sub>3</sub>N, CHCl<sub>3</sub>, RT, 12h; (iii) (a) Et<sub>3</sub>N, C<sub>2</sub>H<sub>5</sub>OCOC<sub>2</sub>H<sub>5</sub>, 12<sup>1</sup>, THF, reflux, 48h; (iv) (a) TFA, DCM, RT, 2h, (b) 2-bromo-2-methyl propionyl bromide, Et<sub>3</sub>N, CHCl<sub>3</sub>, RT, 12h; (v) (a) LiOH.H<sub>2</sub>O, MeOH, H<sub>2</sub>O, (b) 4-Br aniline, HBTU, Et<sub>3</sub>N, CHCl<sub>3</sub>, RT, 12h; (vi) methanolic CH<sub>3</sub>NH<sub>2</sub>, RT, 3h; (vii) Acetyl-Cl, Et<sub>3</sub>N, CHCl<sub>3</sub>, RT, 12h;.

Compounds **8** and **10** acted as common intermediates for the preparation of different analogues. Compounds **8** and **10** were subjected to <sup>t</sup>Boc deprotection and acylated with 2-Br isopropionyl bromide to gain **25** and **26**, respectively (scheme 3.5). The free amine of compound **10** was also acylated using acetyl chloride yielding **19**. Compound **10** was subjected to <sup>t</sup>Boc deprotection and coupling with Boc-Aib-OH to obtain **22**, which was converted into its methylamide derivative **23** using methanolic methylamine (scheme 3.5). Compound **22** was then subjected to saponification reaction and coupling with *p*-Br aniline affording compound **24** (scheme 3.5).

### 3.13 Conformational analyses

Conformational analyses were carried out using solid-state single crystal X-ray analysis and solution state 2D NOESY NMR analysis. The *intra* and *inter*-molecular hydrogen bonding, as well as, the strength of *intra*-molecular hydrogen bonding were analysed by DMSO-*d*<sub>6</sub> titration and variable temperature experiments in CDCl<sub>3</sub>.

#### 3.13.1 Single crystal X-ray analysis

In order to understand the role of conformational restriction and folding ability of <sup>S</sup>Ant, peptides featuring Piv-Aib-<sup>L</sup>Pro-<sup>S</sup>Ant-NH<sup>i</sup>Bu (**21**, fig. 3.15) and Boc-Aib-<sup>L</sup>Pro-<sup>S</sup>Ant-<sup>L</sup>Pro-NHR unit (**22-24**, fig. 3.15), were synthesized.

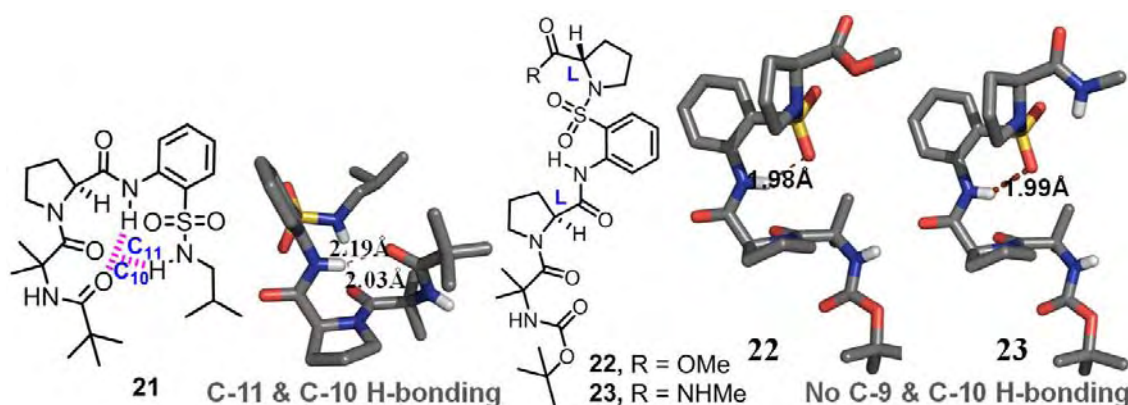


**Fig. 3.15:** Molecular structures (left) and crystal structures (right) of **21** showing a concurrent display of C-10 hydrogen bonding between Aib and Pro and C-11 hydrogen bonding between Pro-<sup>S</sup>Ant-Pro while **22** and **23** featured only C-6 hydrogen bonding. *Note:* The compound **21** is devoid of C-6 hydrogen bonding, while **22** and **23** were devoid of both <sup>S</sup>Ant-Pro C-9 and Aib-Pro C-10 H-bonding.

The turn system **21** (Fig. 3.15) that features Aib-Pro C-10 hydrogen bonding ( $\beta$ -bend structure) and Pro-<sup>S</sup>Ant-NH<sup>i</sup>Bu C-11 hydrogen bonding, run mutually to stabilize

the turn structures, wherein each carbonyl satisfies an ‘NH’ for hydrogen bonding. It was noted that the <sup>S</sup>Ant ‘NH’, which is not involved in C-6 intra-residual hydrogen bonding, aligned to form the C-10 hydrogen bonding.

On the other hand, the turn systems **22** & **23** (fig. 3.15) that would have featured a combination of a  $\beta$ -turn (Aib-Pro C<sub>10</sub> - between ‘*i*’ and ‘(*i*+3)’ amino acid residues) and a *pseudo*  $\beta$ -turn (<sup>S</sup>Ant-Pro C<sub>9</sub> - between ‘(*i*-1)’ and ‘(*i*+2)’ amino acid residues), failed to form either of the hydrogen bonding networks, probably due to the conformational restriction offered by C-6 hydrogen bonding of <sup>S</sup>Ant. These systems have <sup>S</sup>Ant now linked to an imino acid proline, which is devoid of acceptor NH to form C-11 hydrogen bonding as observed in former turn systems. Here, the <sup>S</sup>Ant ‘NH’, which would be facing competition for two of the hydrogen bonding networks, surprisingly, failed to form any of these hydrogen bonds in **22-23** and showed only C-9 hydrogen bonding in **24**.

In order to understand the difference in conformational features observed between compounds **22** and **24**, their analogues **25** and **26** were synthesized. The peptide **25** (fig. 3.2), apart from **22** and **23**, showed a conformation similar to **24** (fig. 3.2), as observed in <sup>S</sup>Ant-Pro reverse turns, presumably due to the additional stabilization that arose from the intermolecular aromatic interactions between <sup>S</sup>Ant and 4-Br-anilide rings, and intramolecular C-H $\cdots$  $\pi$  interactions between Prolyl CH and 4-Br-anilide. This is again confirmed by the analogue **26**, which is devoid of an aromatic residue at C-terminus, featuring a conformation similar to that of **22** and **23**. The rigid three dimensional structure of **22**, **23** and **26** (fig. 3.2), devoid of C-9 hydrogen bonding, are due to the conformational restriction offered by *intra*-residual C-6 hydrogen bonding of <sup>S</sup>Ant, in addition to the presence of rigid amino acid residues.

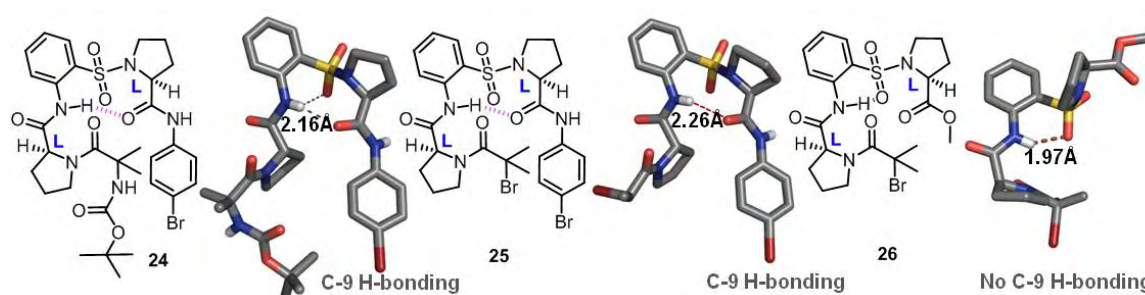


**Fig. 3.16:** Molecular structure and crystal structures of compounds **24**, **25** and **26**. Compounds **24** and **25** (with terminal aromatic residue) featured C-9 hydrogen bonding, whilst **26** (without terminal aromatic residue) showed absence of C-9 hydrogen bonding.

### 3.13.2 Solution-state NMR analysis

The conformational changes observed in solid state by compounds **21-26** is reflected in their solution-state. The NOE interactions, mainly NH3 vs. C4H, NH1 vs. C3H, NH3 vs. NH2 and C20H vs. C22H (fig. 3.17) accounted for the solution-state conformation of **21**, similar to that observed for solid-state (fig 3.17, see page 249 for 2D extracts). The other NOEs which supported the solution-state conformation include NH2 vs. C6H, C8H vs. C16H, NH1 vs. C9H, C20H vs. C4H, C19H vs. NH3 and NH1 vs. C24H. (fig. 3.17).

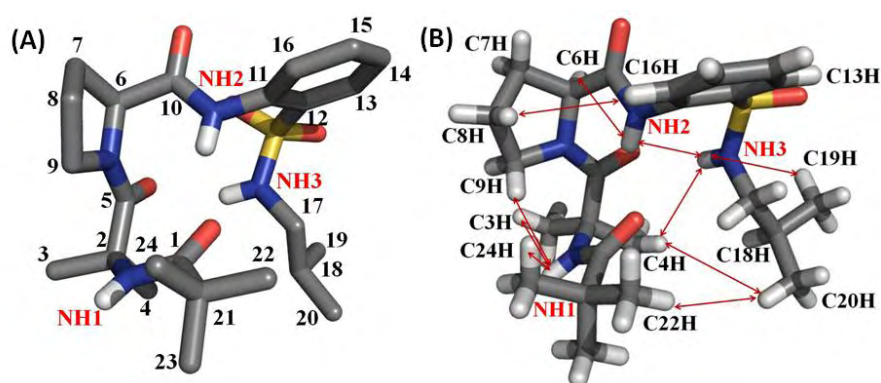


**Fig. 3.17:** PyMOL-rendered crystal structures of **21**; with numbering (A) and NOE interactions (B).

The solution-state study of **22** was also supported from its conformational features observed in its solid-state (fig 3.18, see page 250 for 2D extracts). The NOE interactions which supported the three dimensional conformation of **22** included C4H vs. C22H, C4H vs. NH2, C9H vs. NH2, C6H vs. NH2, NH2 vs. C20H and C20H vs. C13H, indicating fraying.

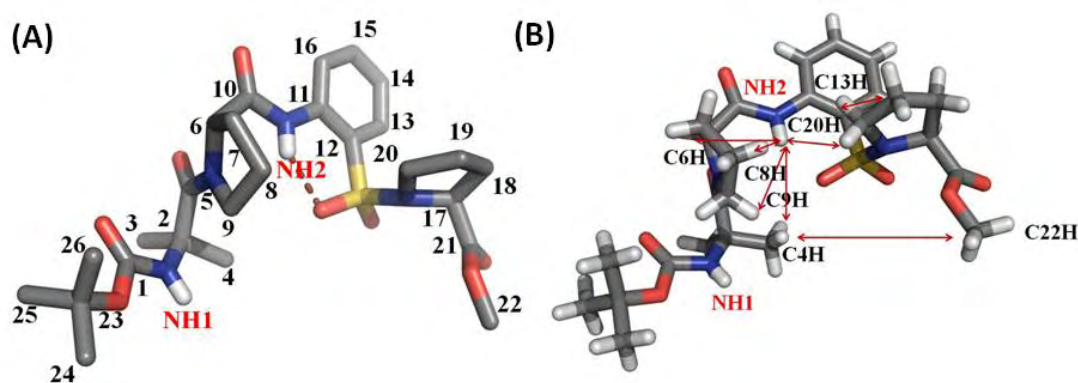


**Fig. 3.18:** PyMOL-rendered crystal structures of **22**; with numbering (A) and NOE interactions (B).

On the other hand, C-9 turn conformation of **24** was confirmed by solution-state studies (fig 3.19, see page 251 for 2D extracts). The NOEs that supported the solution state conformation include C13H vs. C20H, NH3 vs. C20H, NH2 vs. C20H, NH2 vs. C6H, NH3 vs. C27H and C24H vs. C29H. Compound **26**, which is devoid of aromatic residue at C-terminal failed to form C-9 conformation as observed in **22** and **23**. The NOEs which supported the three dimensional conformation of **26** involve C9H vs. C16H, C9H vs. C13H, C16H vs. NH, NH vs. C21H and NH vs. C2H, confirming the role of terminal aromatic residue in turn formation (fig 3.20, see page 252 for 2D extracts).

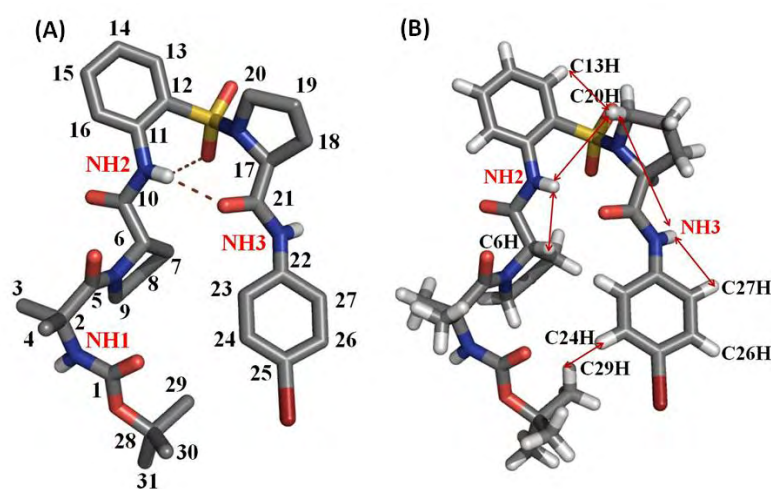


**Fig. 3.19:** PyMOL rendered crystal structures of **24**; with numbering (A) and NOE interactions (B).

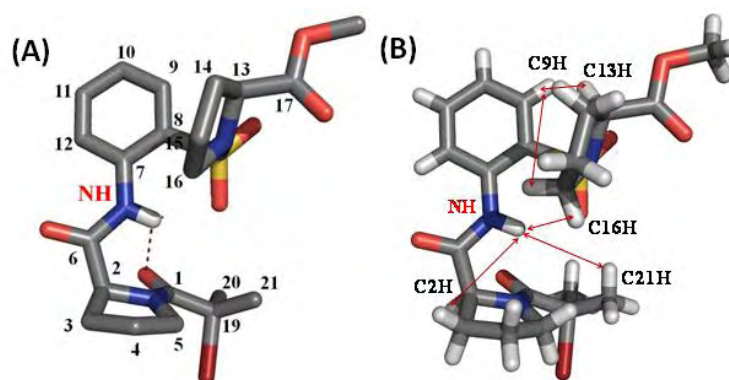


**Fig. 3.20:** PyMOL rendered crystal structures of **26**; with numbering (A) and NOE interactions (B).

### 3.13.3 NMR titration and variable temperature Studies

The diverse hydrogen bonding patterns found in compounds **21-26** were investigated by NMR studies like DMSO- $d_6$  titration and variable temperature studies in CDCl<sub>3</sub>, where the NHs involved in *intra*-molecular hydrogen bonding interactions

undergo negligible shift in their chemical shift values ( $\delta\text{NH}_{\text{intra}} \leq 0.02\text{ppm}$ ), while those involved in *inter*-molecular interactions experience considerable shift.

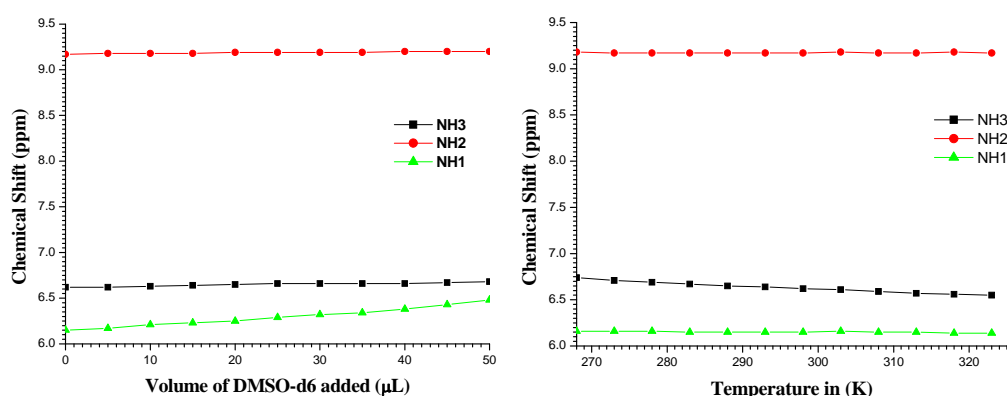


**Fig. 3.21:** Solution-state NMR experiments of compound **21**. DMSO- $d_6$  titration studies at 5 mM solution (400MHz,  $\text{CDCl}_3$ ), and variable temperature studies (400MHz,  $\text{CDCl}_3$ ).

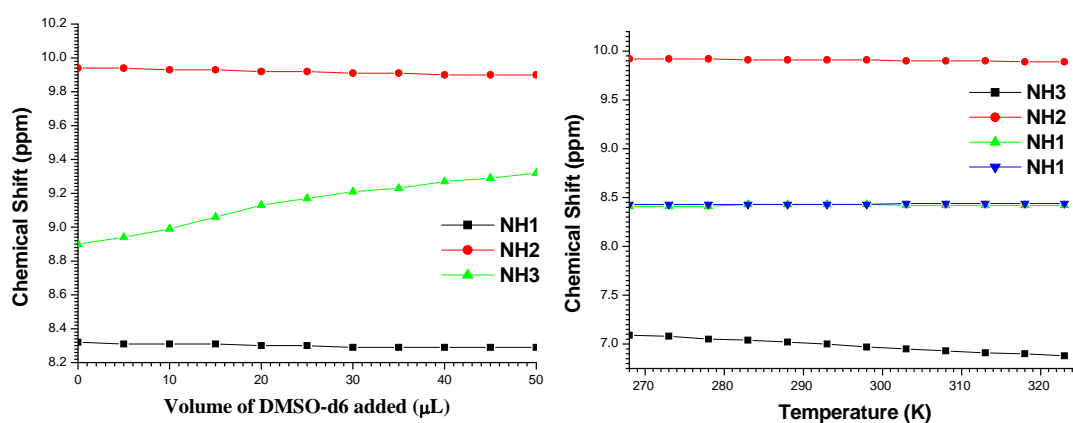


**Fig. 3.22:** Solution-state NMR experiments of compound **23**. DMSO- $d_6$  titration studies at 5 mM solution (400MHz,  $\text{CDCl}_3$ ), and variable temperature studies (400MHz,  $\text{CDCl}_3$ ).

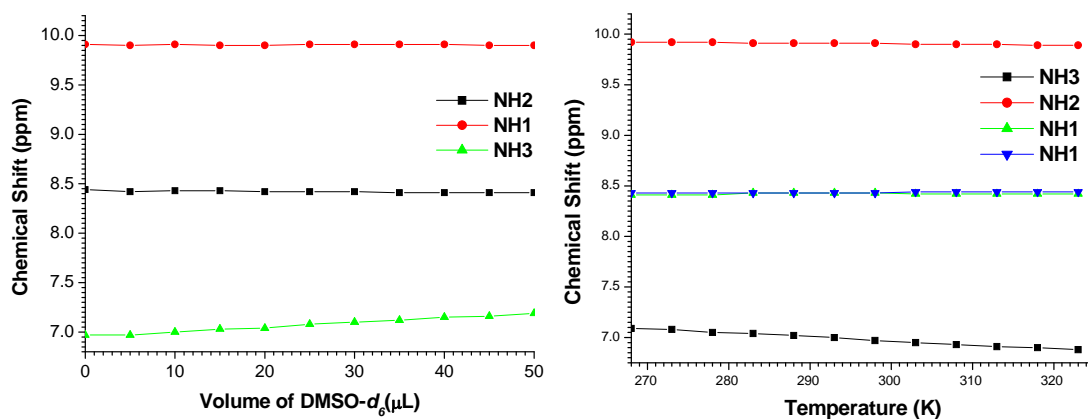


**Fig. 3.23:** Solution-state NMR experiments of compound **24**. DMSO- $d_6$  titration studies at 5 mM solution (400MHz,  $\text{CDCl}_3$ ), and variable temperature studies (400MHz,  $\text{CDCl}_3$ ). *Note:* Broad/Multiple set of signals seen are due to rotamer formation at the N-terminus (N-<sup>1</sup>BOC effect, *Chem. -Eur. J.*, **2008**, *14*, 6192).

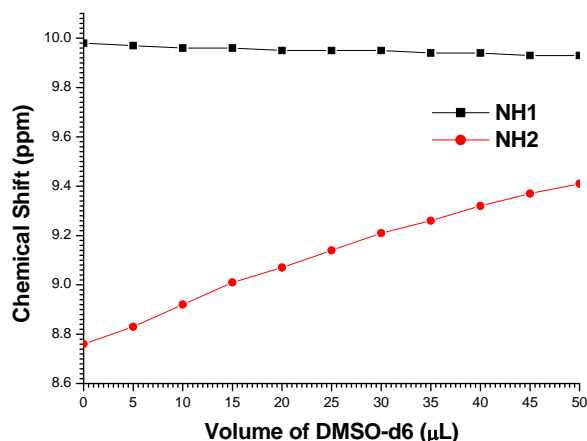


**Fig. 3.24:** DMSO- $d_6$  titration studies of **25** at 5mM solution (400MHz,  $\text{CDCl}_3$ ).

The NH shifts for compounds **21-25** are charted in table 2.

**Table 2:** NMR DMSO- $d_6$  titration and variable temperature studies of compounds **21-25**.

Compound No.	DMSO- $d_6$ Titration studies	variable temperature studies	Inferences
<b>21</b>	$\Delta\text{NH1} = 0.38$ ppm $\Delta\text{NH2} = 0.03$ ppm $\Delta\text{NH3} = 0.06$ ppm	$\Delta\text{NH1} = 0.19$ ppm $\Delta\text{NH2} = 0.01$ ppm $\Delta\text{NH3} = 0.02$ ppm	NH1 are involved in <i>inter</i> -molecular H-bonding, while NH2 and NH3 undergo <i>intra</i> -molecular H-bonding
<b>23</b>	$\Delta\text{NH1} = 0.03$ ppm $\Delta\text{NH2} = 0.01$ ppm $\Delta\text{NH3} = 0.22$ ppm	$\Delta\text{NH1} = 0.03$ ppm $\Delta\text{NH2} = 0.03$ ppm $\Delta\text{NH3} = 0.21$ ppm	NH1 and NH2 are involved in <i>intra</i> -molecular H-bonding, while NH3 bear <i>inter</i> -molecular H-bonding
<b>24</b>	$\Delta\text{NH1} = 0.03$ ppm $\Delta\text{NH2} = 0.04$ ppm $\Delta\text{NH3} = 0.58$ ppm	$\Delta\text{NH1} = 0.06$ ppm $\Delta\text{NH2} = 0.05$ ppm $\Delta\text{NH3} = 0.19$ ppm	NH1 and NH2 are involved in <i>intra</i> -molecular H-bonding, while NH3 experience <i>inter</i> -molecular H-bonding
<b>25</b>	$\Delta\text{NH1} = 0.05$ ppm $\Delta\text{NH2} = 0.65$ ppm	-	NH1 are involved in <i>intra</i> -molecular H-bonding, while NH2 feel <i>inter</i> -molecular H-bonding

The conformational analysis of two peptide systems revealed that one of the turn systems features a combination of C-10 and C-11 hydrogen bonding networks while the other features the absence of C-10 and C-9 hydrogen bonding in **22-23** and only C-9 hydrogen bonding in **24**. It was also noted that the former system shows the absence of C-6 *intra*-residual hydrogen bonding of  $^S\text{Ant}$  which showed in latter. It appears as a fine example in which a  $\beta$ -turn (Aib-Pro C<sub>10</sub> - between 'i' and '(i+3)' amino acid residues) is associated mutually with an extended  $\beta$ -turn (Pro- $^S\text{Ant}$ -NHR C<sub>11</sub> - between 'i' and '(i+3)')

amino acid residues). The latter, that suffers conformational restriction by *intra*-residual C-6 hydrogen bonding of <sup>S</sup>Ant, failed to achieve the co-operative folding (fig 3.25).

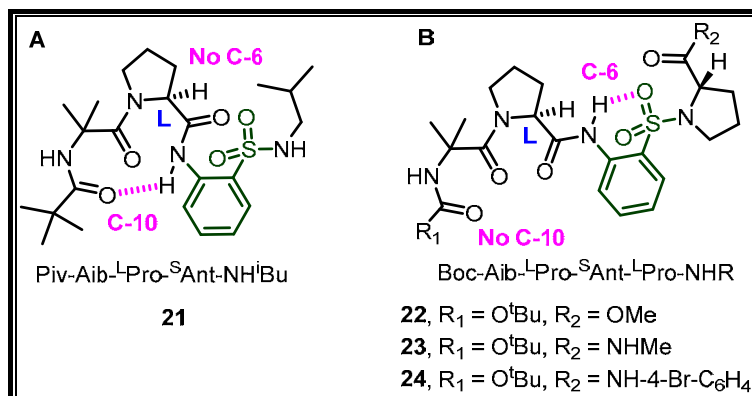


**Fig. 3.25:** Molecular structures of <sup>S</sup>Ant based foldamer motifs featuring Aib-Pro C-10 H-bonding (**21**) and those showing an absence of C-10 hydrogen bonding (**22-24**).

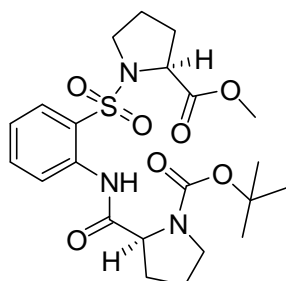
### 3.14 Conclusions

In summary, this section describes orthanilic acid (2-amino benzene sulfonic acid, <sup>S</sup>Ant) based two, structurally related but conformationally dissimilar, hybrid peptide systems having multiple folds. One is having a  $\beta$ -turn (Aib-Pro C<sub>10</sub> - between '*i*' and '*(i+3)*' amino acid residues) which is mutually associated with an extended  $\beta$ -turn (Pro-<sup>S</sup>Ant-NHR C<sub>11</sub> - between '*i*' and '*(i+3)*' amino acid residues) and the other one which failed to form a combination of a  $\beta$ -turn (Aib-Pro C<sub>10</sub> - between '*i*' and '*(i+3)*' amino acid residues) and a *pseudo*  $\beta$ -turn (<sup>S</sup>Ant-Pro C<sub>9</sub> - between '*(i-1)*' and '*(i+2)*' amino acid residues). Structural investigations, including solid state crystal structure and solution-state NMR revealed that the Aib-Pro C-10 hydrogen bonded structure in latter system was seen to be disrupted by the conformational restriction offered by the C-6/ C-9 hydrogen bonding of <sup>S</sup>Ant. The case study is analogous to the instances in peptide systems, which are being subjected to adopt/evade multiple folds. It also provides the opportunity to understand multiple factors affecting the conformation of peptides.



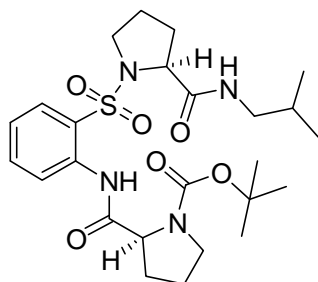
### 3.15 Experimental procedures

#### Tert-butyl(S)-2-((2-(((S)-2-(methoxycarbonyl)pyrrolidin-1-yl)sulfonyl)phenyl)carbamoyl)pyrrolidine-1-carboxylate **8**



To a solution of Boc-<sup>L</sup>Pro-OH (2g, 9.30mmols) in THF (50mL), Et<sub>3</sub>N (2.6mL, 1.88g, 18.61mmols) was added followed by the addition of ethyl chloroformate (1.1mL, 1.288g, 11.944mmols). After 30 minutes, compound **7** in THF (20mL) was added and heated to reflux for 48 hours. The reaction mixture was evaporated under reduced pressure and the residue in DCM (10mL) was washed with saturated solutions of sodium bicarbonate (7mL) followed by potassium bisulphate (7mL) and water (7mL). The washings were extracted with DCM (7mLx3), dried with anhydrous Na<sub>2</sub>SO<sub>4</sub> and evaporated under reduced pressure to obtain the crude residue which was purified by column chromatography, (40:60 pet ether/ethyl acetate, R<sub>f</sub>: 0.5) to afford **8** as a viscous liquid (3.18g, 71%). [α]<sub>D</sub><sup>26</sup>: -232.87° (c = 1, CHCl<sub>3</sub>); IR (CHCl<sub>3</sub>, ν (cm<sup>-1</sup>): 3309, 3018, 1746, 1694, 1584, 1531, 1436, 1247; <sup>1</sup>H NMR (CDCl<sub>3</sub>/200MHz): δ ppm 10.12-9.99<sub>rotamer</sub> (s, 1H), 8.55-8.66 (t, J=10.3, 1H), 7.86 (s, 1H), 7.52-7.59 (t, J=8.14Hz, 1H), 7.15-7.22 (t, J=7.58Hz, 1H), 4.36-4.51 (m, 2H), 3.63 (s, 3H), 3.33-3.49 (m, 4H), 1.37-1.46<sub>rotamer</sub> (s, 9H); <sup>13</sup>C NMR (CDCl<sub>3</sub>, 50MHz): δ ppm 172.1, 136.6, 134.2, 129.5, 125.2, 123.5, 80.2, 60.9, 59.9, 52.4, 48.2, 47.1, 30.8, 28.2, 24.5; MALDI-TOF-MS: 504.1741 (M+Na)<sup>+</sup>, 520.1484 (M+K)<sup>+</sup>; Elemental analysis calculated for C<sub>22</sub>H<sub>31</sub>N<sub>3</sub>O<sub>7</sub>S: C, 54.87; H, 6.49; N, 8.73; Found: C, 59.22; H, 6.01; N, 8.99.

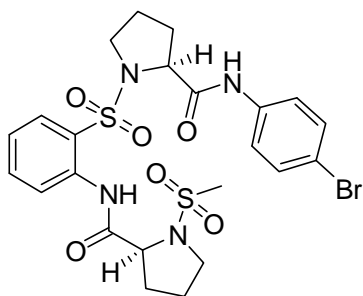
#### Tert-butyl(S)-2-((2-(((S)-2-(isobutylcarbamoyl)pyrrolidin-1-yl)sulfonyl)phenyl)carbamoyl)pyrrolidine-1-carboxylate **9**



Compound **8** (0.5g, 1.038mmol) was subjected to ester hydrolysis using LiOH. H<sub>2</sub>O (0.25g, 10.382mmols) in methanol (5mL) and water (5mL) to obtain the free acid. To a solution of free acid in DCM (10mL), isobutylamine (0.21mL, 0.152g, 2.076mmols), was added followed by HBTU (0.814g, 2.076mmols), and Et<sub>3</sub>N (0.43mL, 0.315g, 3.114mmols). After 12 hours, the reaction mixture was diluted with DCM (5mL) and the organic layer was washed with saturated solutions of sodium bicarbonate (5mL), potassium bisulphate

(5mL) and water (5mL) sequentially. The organic layer was dried over anhydrous  $\text{Na}_2\text{SO}_4$  solution and evaporated under reduced pressure to get crude product which was purified by column chromatography, (30:70 pet. ether/ethyl acetate,  $R_f$ : 0.5) to afford **9** as a white solid (0.476g, 88%). mp: 70-74°C;  $[\alpha]_D^{26}$ : -230.44° ( $c = 0.1$ ,  $\text{CHCl}_3$ ); IR ( $\text{CHCl}_3$ ,  $\nu$  ( $\text{cm}^{-1}$ ): 3317, 3018, 2932, 1689, 1583, 1528, 1398, 1216;  $^1\text{H}$  NMR ( $\text{CDCl}_3/200\text{MHz}$ ):  $\delta$  ppm 10.16-10.28<sub>rotamer</sub> (s, 1H), 8.6-8.75<sub>rotamer</sub> (s, 1H), 7.78-7.82 (s,  $J=7.83\text{Hz}$ , 1H), 7.56-7.64 (t,  $J=7.75\text{Hz}$ , 1H), 7.18-7.25 (t,  $J=7.58\text{Hz}$ , 1H), 6.77-6.83 (m,  $J=5.12\text{Hz}$ , 1H), 4.36 (s, 1H), 4.15-4.19 (m, 1H), 3.49-3.57 (m, 3H), 2.96-3.20 (m, 3H), 2.16-2.18 (m, 2H), 1.66-2.03 (m, 6H), 1.42 (s, 9H), 0.89-0.93 (d,  $J=6.69\text{Hz}$ , 1H);  $^{13}\text{C}$  NMR ( $\text{CDCl}_3$ , 50MHz):  $\delta$  ppm 171.8, 170.5, 134.7, 129.5, 123.9, 80.5, 62.6, 49.2, 46.8, 38.5, 30.3, 28.4, 24.3, 19.9; MALDI-TOF-MS: 545.2320 ( $\text{M}+\text{Na}$ )<sup>+</sup>, 561.2062 ( $\text{M}+\text{K}$ )<sup>+</sup>; Elemental analysis calculated for  $\text{C}_{25}\text{H}_{38}\text{N}_4\text{O}_6\text{S}$ : C, 57.45; H, 7.33; N, 10.72; Found: C, 54.22; H, 7.01; N, 10.59.

**(S)-N-(4-bromophenyl)-1-((2-((S)-1-(methylsulfonyl)pyrrolidine-2-carboxamido)phenyl)sulfonyl)pyrrolidine-2-carboxamide 2**

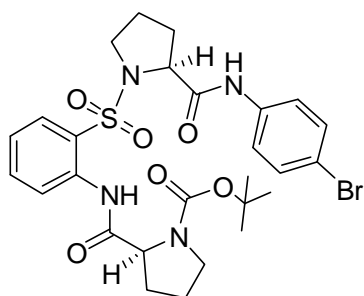


Compound **10** (0.5, 0.81mmol) was subjected to <sup>t</sup>Boc deprotection using TFA (2mL) in DCM (2mL). The reaction mixture was evaporated and the residue was neutralized with  $\text{NaHCO}_3$  solution, followed by extraction using DCM (2mL) and evaporation to yield the free amine.

To a solution of free amine in DCM (5mL),  $\text{Et}_3\text{N}$  (0.34mL, 0.244g, 2.415mmols) was added followed by the addition of mesyl chloride (0.07mL, 0.11g, 0.9662mmols). After 12 hours, reaction mixture was diluted with DCM (2mL) and the organic layer was washed with saturated sodium bicarbonate (2mL), potassium bisulphate (2mL) and water (2mL) sequentially. The organic layer was dried over anhydrous  $\text{Na}_2\text{SO}_4$  solution and evaporated under reduced pressure to get crude product which was purified by column chromatography, (35:65 pet. ether/ethyl acetate,  $R_f$ : 0.5) to afford **2** as a white crystalline solid (0.46, 97%). mp: 190-192°C;  $[\alpha]_D^{27}$ : -248.81° ( $c = 0.1$ ,  $\text{CHCl}_3$ ); IR ( $\text{CHCl}_3$ ,  $\nu$  ( $\text{cm}^{-1}$ ): 3352, 3019, 1692, 1589, 1534, 1341, 1200;  $^1\text{H}$  NMR ( $\text{CDCl}_3/400\text{MHz}$ ):  $\delta$  ppm 10.57 (s, 1H), 8.63-8.65 (d,  $J=7.78$ , 1H), 8.37 (s, 1H), 7.92-7.95 (d,  $J=9.29$ , 1H), 7.51-7.55 (m, 1H), 7.35-7.37 (d,  $J=8.78$ , 2H), 7.26-7.29 (d,  $J=8.78$ , 2H), 7.20-7.24 (m, 1H), 4.26-4.30 (m, 2H), 3.86-3.91 (m, 1H), 3.77-3.81 (m, 1H), 3.52-3.59 (m, 1H), 3.40-3.46 (m, 1H), 2.96-2.98 (s, 3H), 2.28-2.40 (m, 2H), 1.89-2.18 (m, 7H),

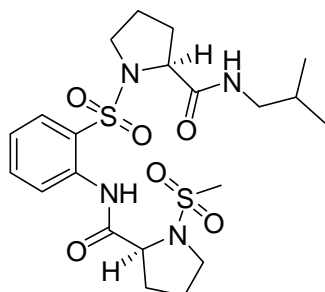
1.72-1.86 (m, 2H);  $^{13}\text{C}$  NMR ( $\text{CDCl}_3$ , 100MHz):  $\delta$  ppm 170.0, 169.1, 136.4, 136.2, 135.3, 131.5, 130.6, 124.0, 121.8, 121.0, 117.0, 63.4, 63.0, 50.1, 48.8, 34.3, 31.8, 31.1, 24.8, 24.7; MALDI-TOF-MS: 621.0372 ( $\text{M}+\text{Na}$ ) $^+$ , 637.0112 ( $\text{M}+\text{K}$ ) $^+$ ; Elemental analysis calculated for  $\text{C}_{23}\text{H}_{27}\text{BrN}_4\text{O}_6\text{S}_2$ : C, 46.08; H, 4.54; N, 9.35; Found: C, 46.64; H, 4.76; N, 9.23.

**Tert-butyl(S)-2-((2-(((S)-2-((4-bromophenyl)carbamoyl)pyrrolidin-1-yl)sulfonyl)phenyl)carbamoyl)pyrrolidine-1-carboxylate 10**



Compound **10** was synthesized following the procedure for **9** using 4-Br aniline as amine. Purified by column chromatography, (35:65 pet. ether/ethyl acetate,  $R_f$ : 0.5) colourless viscous liquid (93%).  $[\alpha]_D^{27}$ :  $-239.31^\circ$  ( $c = 0.1$ ,  $\text{CHCl}_3$ ); IR ( $\text{CHCl}_3$ ,  $\nu$  ( $\text{cm}^{-1}$ ): 3425, 3020, 1682, 1583, 1530, 1370, 1215;  $^1\text{H}$  NMR ( $\text{CDCl}_3/400\text{MHz}$ ): 10.22 (s, 1H), 8.81 (s, 1H), 8.50-8.54 (d,  $J=8.46$ , 1H), 7.82-7.87 (dd,  $J=8.08$ ,  $J=1.26$ , 1H), 7.50-7.58 (t,  $J=7.96$ , 1H), 7.38 (s, 4H), 7.18-7.25 (t,  $J=7.64$ , 1H), 4.29-4.46 (m, 2H), 3.18-3.80 (m, 5H); 2.1-2.32 (m, 3H), 1.79-2.04 (m, 4H), 1.44 (s, 9H);  $^{13}\text{C}$  NMR ( $\text{CDCl}_3, 50\text{MHz}$ ):  $\delta$  ppm 171.3, 169.2, 136.5, 136.2, 134.6, 131.6, 129.5, 124.0, 116.9, 80.7, 62.3, 49.5, 47.3, 31.2, 30.5, 28.3, 24.3; MALDI-TOF-MS: 620.7892 ( $\text{M}$ ) $^+$ , 643.1767 ( $\text{M}+\text{Na}$ ) $^+$ , 659.1454 ( $\text{M}+\text{K}$ ) $^+$ ; Elemental analysis calculated for  $\text{C}_{27}\text{H}_{33}\text{BrN}_4\text{O}_6\text{S}$ : C, 52.18; H, 5.35; N, 9.01; Found: C, 54.33; H, 5.97; N, 8.84.

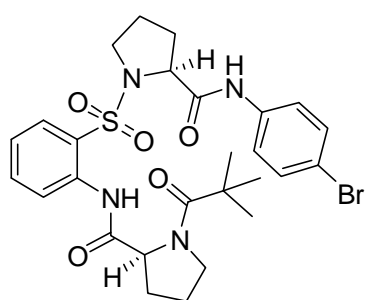
**(S)-N-isobutyl-1-((2-(((S)-1-(methylsulfonyl)pyrrolidine-2-carboxamido)phenyl)sulfonyl)pyrrolidine-2-carboxamide 1**



Compound **1** was synthesized from compound **9**, following the synthetic procedure for compound **2**. Purified by column chromatography, (30:70 pet. ether/ethyl acetate,  $R_f$ : 0.5) to afford **1** as a white crystalline solid (98%). mp: 143-148°C;  $[\alpha]_D^{27}$ :  $-169.19^\circ$  ( $c = 0.1$ ,  $\text{CHCl}_3$ ); IR ( $\text{CHCl}_3$ ,  $\nu$  ( $\text{cm}^{-1}$ ): 3336, 3020, 1699, 1589, 1521, 1427, 1338, 1217;  $^1\text{H}$  NMR ( $\text{CDCl}_3/200\text{MHz}$ ):  $\delta$  ppm 10.47 (s, 1H), 8.69-8.73 (d,  $J=8.46\text{Hz}$ , 1H), 7.88-7.93 (dd,  $J=7.96\text{Hz}$ ,  $J=1.52\text{Hz}$ , 1H), 7.55-7.64 (t,  $J=8.54\text{Hz}$ , 1H), 7.19-7.27 (t,  $J=8.40\text{Hz}$ , 1H), 6.72-6.78 (t,  $J=5.75\text{Hz}$ , 1H), 4.25-4.35 (m, 1H), 4.09-4.15 (m,  $J=8.08\text{Hz}$ ,  $J=3.16\text{Hz}$ , 1H),

3.68-3.81 (m, 1H), 3.38-3.55 (m, 2H), 3.07-3.18 (m, 4H), 2.96 (s, 2H), 2.68-2.98 (m, 2H), 2.23-2.25 (m, 3H), 1.93-2.16 (m, 4H), 1.76-1.93 (m, 2H), 1.56-1.73 (m, 1H), 1.16-1.45 (m, 6H);  $^{13}\text{C}$  NMR ( $\text{CDCl}_3$ , 50MHz):  $\delta$  ppm 170.5, 170.2, 136.5, 135.1, 130.5, 124.0, 123.4, 121.2, 63.3, 62.6, 49.7, 48.5, 46.6, 45.5, 34.8, 31.7, 31.0, 28.2, 24.8, 24.5, 19.9, 8.4; MALDI-TOF-MS: 501.2457 ( $\text{M}+\text{H}$ ) $^+$ , 523.2364 ( $\text{M}+\text{Na}$ ) $^+$ , 539.2071 ( $\text{M}+\text{K}$ ) $^+$ ; Elemental analysis calculated for  $\text{C}_{21}\text{H}_{32}\text{N}_4\text{O}_6\text{S}_2$ : C, 50.38; H, 6.44; N, 11.19; Found: C, 50.14; H, 6.85; N, 11.46.

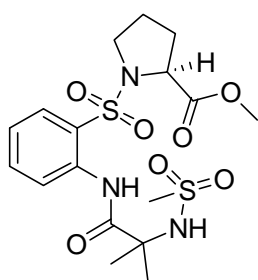
**(S)-N-(4-bromophenyl)-1-((2-((S)-1-pivaloylpyrrolidine-2-carboxamido)phenyl)sulfonyl)pyrrolidine-2-carboxamide 3**



Compound **3** was synthesized from **10**, following the procedure for **9**, using pivaloyl chloride as acylating agent. Purified by column chromatography, (30:70 ethyl acetate/pet. ether,  $R_f$ : 0.5) white crystalline solid (93%). mp: 200-202°C;  $[\alpha]_D^{25}$ : -223.95° ( $c = 0.1$ ,  $\text{CHCl}_3$ ); IR ( $\text{CHCl}_3$ ,  $\nu$  ( $\text{cm}^{-1}$ ): 3331, 3020, 1696, 1598, 1522, 1435,

1338, 1215;  $^1\text{H}$  NMR ( $\text{CDCl}_3/500\text{MHz}$ ):  $\delta$  ppm 10.04 (s, 1H), 8.97 (s, 1H), 8.37-8.38 (d,  $J=7.93\text{Hz}$ , 1H), 7.84-7.86 (d,  $J=6.71\text{Hz}$ , 1H), 7.47-7.50 (t,  $J=7.32\text{Hz}$ , 1H), 7.34-7.40 (m, 4H), 7.17-7.20 (t,  $J=7.32\text{Hz}$ , 1H), 4.54-4.56 (m, 1H), 4.44-4.46 (m, 1H), 3.83-3.86 (t,  $J=7.32\text{Hz}$ , 2H), 3.71-3.76 (m, 1H), 3.54-3.59 (m, 1H), 2.14-2.24 (m, 3H), 2.07-2.11 (m, 1H), 1.96-2.03 (m, 2H), 1.83-1.93 (m, 1H), 1.78-1.83 (m, 1H), 1.28 (s, 9H);  $^{13}\text{C}$  NMR ( $\text{CDCl}_3$ , 125 MHz):  $\delta$  ppm 178.0, 171.3, 169.1, 136.7, 134.6, 131.6, 129.9, 124.0, 122.7, 121.8, 116.9, 64.1, 61.7, 49.6, 48.7, 38.9, 30.6, 28.5, 27.2, 26.0, 24.2; MALDI-TOF-MS: 606.0644 ( $\text{M}+\text{H}$ ) $^+$ , 629.0980 ( $\text{M}+\text{Na}$ ) $^+$ , 645.0698 ( $\text{M}+\text{K}$ ) $^+$ ; Elemental analysis calculated for  $\text{C}_{27}\text{H}_{33}\text{BrN}_4\text{O}_5\text{S}$ : C, 53.55; H, 5.49; N, 9.25; Found: C, 55.25; H, 5.92; N, 9.44.

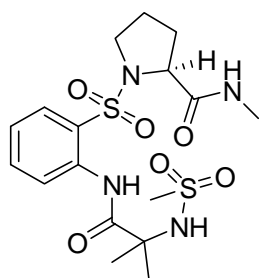
**Methyl((2-(2-methyl-2-(methylsulfonylamido)propanamido)phenyl)sulfonyl)-L-prolinate 12**



Compound **12** was synthesized from **11**, following the procedure for **1**. Purified by column chromatography, (40:60 pet. ether/ethyl acetate,  $R_f$ : 0.5), colorless high viscous liquid (95%).  $[\alpha]_D^{26}$ : -100.61° ( $c = 0.1$ ,  $\text{CHCl}_3$ ); IR ( $\text{CHCl}_3$ ,  $\nu$  ( $\text{cm}^{-1}$ ): 3334, 3020, 1738, 1698, 1586, 1531, 1435, 1328, 1215;  $^1\text{H}$  NMR ( $\text{CDCl}_3/400\text{MHz}$ ):

10.27 (s, 1H), 8.57-8.62 (d,  $J=8.34$ , 1H), 7.55-7.64 (dd,  $J=8.59\text{Hz}$ ,  $J=1.39\text{Hz}$ , 1H), 7.19-7.23 (d,  $J=1.39\text{Hz}$ , 1H), 5.8 (s, 1H), 4.33-4.99 (m, 1H), 3.68 (s, 3H), 3.45-3.55 (m, 1H), 3.29-3.41 (m, 1H), 3.11 (s, 3H), 1.82-2.21 (m, 5H), 1.70-1.73 (d,  $J=5.81\text{Hz}$ , 6H);  $^{13}\text{C}$  NMR ( $\text{CDCl}_3$ , 50MHz):  $\delta$  ppm 173.0, 172.6, 136.7, 134.5, 129.6, 124.8, 123.8, 122.1, 60.5, 60.0, 52.7, 48.7, 44.0, 30.9, 26.0, 25.6, 24.5; MALDI-TOF-MS: 448.2263 ( $\text{M}+\text{H}$ )<sup>+</sup>, 470.1576 ( $\text{M}+\text{Na}$ )<sup>+</sup>, 486.1205 ( $\text{M}+\text{K}$ )<sup>+</sup>; Elemental analysis calculated for  $\text{C}_{17}\text{H}_{25}\text{N}_3\text{O}_7\text{S}_2$ : C, 45.63; H, 5.63; N, 9.39; Found: C, 45.26; H, 5.34; N, 9.57.

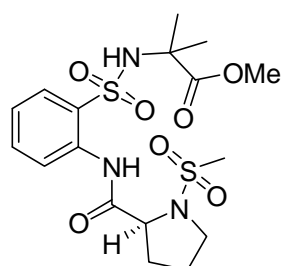
**(S)-N-methyl-1-((2-(2-methyl-2-(methylsulfonamido)propanamido)phenyl)sulfonyl)pyrrolidine-2-carboxamide 4**



Compound **12** (0.2g, 0.45mmol) was amidated using saturated methylamide solution in methanol (5mL). The reaction mixture was evaporated and the residue was purified by column chromatography (05:95 methanol/dichloromethane,  $R_f$ : 0.5) afforded **4** as a white crystalline solid (1.85, 92%), mp: 165-168°C;  $[\alpha]_D^{27}$ : -110.17° ( $c = 0.1$ ,  $\text{CHCl}_3$ ); IR ( $\text{CHCl}_3$ ,  $\nu$  ( $\text{cm}^{-1}$ ): 3335, 3019, 1664, 1585, 1533,

1326, 1216;  $^1\text{H}$  NMR ( $\text{CDCl}_3/400\text{MHz}$ ):  $\delta$  ppm 10.31 (s, 1H), 8.58-8.60 (d,  $J=8.31\text{Hz}$ , 1H), 7.86-7.89 (dd,  $J=8.07\text{Hz}$ ,  $J=1.47\text{Hz}$ , 1H), 7.59-7.63 (t,  $J=8.68\text{Hz}$ , 1H), 7.21-7.26 (t,  $J=8.19\text{Hz}$ , 1H), 6.71 (s, 1H), 5.88 (s, 1H), 4.09-4.12 (dd,  $J=8.80\text{Hz}$ ,  $J=3.67\text{Hz}$ , 1H), 3.65-3.71 (m, 1H), 3.34-3.40 (m, 1H), 3.12 (s, 3H), 2.67-2.68 (d,  $J=4.89\text{Hz}$ , 1H), 2.05-2.12 (m, 1H), 1.95-2.03 (m, 1H), 1.77-1.88 (m, 3H), 1.69-1.72 (d,  $J=12.47\text{Hz}$ , 6H);  $^{13}\text{C}$  NMR ( $\text{CDCl}_3$ , 100MHz):  $\delta$  ppm 173.0, 171.6, 137.0, 135.0, 130.2, 124.0, 122.1, 62.2, 60.4, 49.3, 44.1, 31.2, 26.2, 26.1, 25.6, 24.4; MALDI-TOF-MS: 447.1573 ( $\text{M}+\text{H}$ )<sup>+</sup>, 469.1438 ( $\text{M}+\text{Na}$ )<sup>+</sup>, 485.1076 ( $\text{M}+\text{K}$ )<sup>+</sup>; Elemental analysis calculated for  $\text{C}_{17}\text{H}_{26}\text{N}_4\text{O}_6\text{S}_2$ : C, 45.73; H, 5.87; N, 12.55; Found: C, 45.49; H, 5.65; N, 12.16.

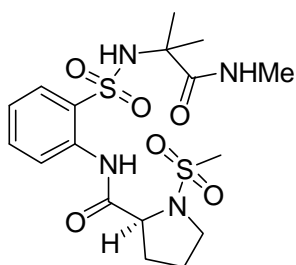
**Methyl(S)-2-methyl-2-((2-(1-(methylsulfonyl)pyrrolidine-2-carboxamido)phenyl)sulfonamido)propanoate 15**



Compound **15** was synthesized from compound **14**, following the synthetic procedure for **12**. Purified by column chromatography, (30:70 pet. ether/ethyl acetate,  $R_f$ : 0.5), white solid (95%), mp: 72-74°C;  $[\alpha]_D^{27}$ : -40.94° ( $c = 0.1$ ,  $\text{CHCl}_3$ ); IR ( $\text{CHCl}_3$ ,  $\nu$  ( $\text{cm}^{-1}$ ): 3332, 3020, 1732, 1620, 1522, 1436, 1216;  $^1\text{H}$  NMR

(CDCl<sub>3</sub>/200MHz):  $\delta$  ppm 10.09 (s, 1H), 8.24-8.28 (d,  $J=8.08$ Hz, 1H), 7.80-7.84 (d,  $J=7.96$ Hz, 1H), 7.48-7.55 (t,  $J=7.39$ Hz, 1H), 7.15-7.22 (t,  $J=7.64$ Hz, 1H), 6.56 (s, 1H), 4.34-4.40 (m, 1H), 4.02-4.13 (m, 1H), 3.42-3.69 (m, 3H) 3.37 (s, 3H), 3.08 (s, 3H), 2.21-2.39 (m, 3H), 1.31-1.42 (s, 6H); <sup>13</sup>C NMR (CDCl<sub>3</sub>, 100 MHz):  $\delta$  ppm 173.2, 170.6, 156.8, 134.3, 132.7, 131.5, 128.2, 124.0, 81.4, 61.9, 59.9, 58.0, 52.1, 47.4, 30.2, 28.3, 25.5, 25.2, 23.9; MALDI-TOF-MS: 448.1569 (M+H)<sup>+</sup>, 470.1021 (M+Na)<sup>+</sup>, 486.0770 (M+K)<sup>+</sup>; Elemental analysis calculated for C<sub>17</sub>H<sub>25</sub>N<sub>3</sub>O<sub>7</sub>S<sub>2</sub>: C, 45.63; H, 5.63; N, 9.39; Found: C, 45.42; H, 5.26; N, 9.72.

**(S)-N-(2-(N-(2-methyl-1-(methylamino)-1-oxopropan-2-yl)sulfamoyl)phenyl)-1-(methylsulfonyl)pyrrolidine-2-carboxamide 5**

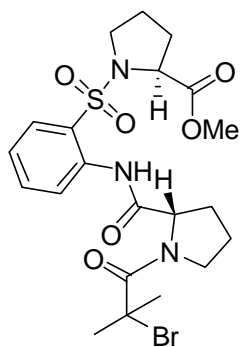


Compound **5** was prepared, from compound **16**, following the procedure for **4**. Purified by column chromatography, (05:95 methanol/dichloromethane, R<sub>f</sub>: 0.5) to furnish **5** as a white crystalline solid (96%). mp: 178-179°C; [ $\alpha$ ]<sub>D</sub><sup>26</sup>: -25.16° ( $c = 0.1$ , CHCl<sub>3</sub>); IR (CHCl<sub>3</sub>,  $\nu$  (cm<sup>-1</sup>): 3341, 3020, 1652, 1585, 1469,

1438, 1343, 1216; <sup>1</sup>H NMR (CDCl<sub>3</sub>/400MHz):  $\delta$  ppm 10.03 (s, 1H), 8.26-8.28 (d,  $J=8.28$ Hz, 1H), 7.90-7.93 (dd,  $J=7.78$ Hz,  $J=1.25$ Hz, 1H), 7.56-7.60 (m, 1H), 7.28-7.24 (t,  $J=7.65$ Hz, 1H), 6.56 (s, 1H), 7.45 (s, 1H), 4.29-4.33 (t,  $J=6.52$ Hz, 1H), 3.7-3.75 (m, 1H), 3.40-3.46 (m, 1H), 3.05 (s, 3H), 2.66-2.68 (d,  $J=4.77$ Hz, 3H), 2.37-2.42 (m, 2H), 2.02-2.09 (m, 2H), 1.29-1.32 (d,  $J=12.55$ Hz, 6H); <sup>13</sup>C NMR (CDCl<sub>3</sub>, 100MHz):  $\delta$  ppm 173.9, 169.8, 134.3, 133.8, 130.7, 129.4, 124.7, 123.2, 62.8, 60.2, 50.0, 53.0, 35.0, 31.6, 26.5, 25.0; MALDI-TOF-MS: 447.1363 (M+H)<sup>+</sup>, 469.1172 (M+Na)<sup>+</sup>, 485.0930 (M+K)<sup>+</sup>; Elemental analysis calculated for C<sub>17</sub>H<sub>26</sub>N<sub>4</sub>O<sub>6</sub>S<sub>2</sub>: C, 45.73; H, 5.87; N, 12.55; Found: C, 45.48; H, 5.59; N, 12.17.

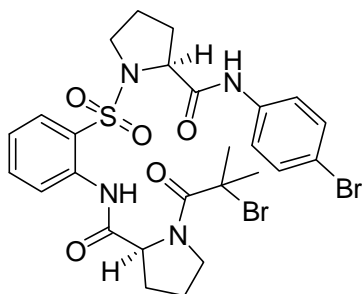
**Methyl ((2-((S)-1-(2-bromo-2-methylpropanoyl)pyrrolidine-2-carboxamido)phenyl)sulfonyl)-L-prolinate 26**

Compound **8** (0.2, 0.42mmol) was subjected to <sup>t</sup>Boc deprotection using TFA (2mL) in DCM (2mL). The reaction mixture was evaporated and the residue was neutralized with NaHCO<sub>3</sub> solution, followed by extraction using DCM (3 x 2mL) and evaporation to yield the free amine. To a solution of free amine in CHCl<sub>3</sub> (5mL), Et<sub>3</sub>N (0.18mL, 0.13g, 1.245mmoles) was added, followed by 2-bromo 2-methyl propanoyl bromide (0.06mL,



0.105g, 0.457mmol). After 12 hours, the reaction mixture was diluted with DCM (2mL) and the organic layer was washed with saturated solutions of sodium bicarbonate (4mL), potassium bisulphate (4mL), water (4mL) and saturated NaCl solution (4mL). The organic layer was dried over anhydrous Na<sub>2</sub>SO<sub>4</sub> solution and evaporated under reduced pressure to obtain the crude product which was purified by column chromatography, (30:70 pet. ether/ethyl acetate, R<sub>f</sub>: 0.5) to afford **26** as a white solid which was later crystallized from a solution of ethylacetate and pet-ether (2.05g, 93%). mp: 117-121°C; [α]<sub>D</sub><sup>26</sup>: -236° (*c* = 0.1, CHCl<sub>3</sub>); IR (CHCl<sub>3</sub>, ν (cm<sup>-1</sup>): 3341, 3019, 1744, 1700, 1631, 1589, 1529, 1436, 1336, 1215; <sup>1</sup>H NMR (CDCl<sub>3</sub>/400MHz): 9.85 (s, 1H), 8.52-8.54 (d, *J*=8.28, 1H), 7.87-7.89 (d, *J*=8.03, 1H), 7.53-7.57 (t, *J*=7.78, 1H), 7.17-7.21 (t, *J*=7.65, 1H), 4.76 (s, 1H), 4.40-4.43 (m, 1H), 4.27 (s, 1H), 3.83-3.90 (m, 1H) 3.72 (s, 3H), 2.25-2.34 (m, 1H), 2.08-2.2 (m, 3H), 2.05 (s, 3H), 1.98 (s, 3H), 1.82-2.00 (m, 3H); <sup>13</sup>C NMR (CDCl<sub>3</sub>,105MHz): δ ppm 172.4, 170.9, 169.8, 136.6, 134.3, 129.6, 125.2, 123.6, 123.2, 63.7, 59.6, 57.6, 52.6, 49.7, 48.7, 32.6, 30.8, 30.5, 28.7, 24.6; MALDI-TOF-MS: 552.1608 (M+Na)<sup>+</sup>, 568.1909 (M+K)<sup>+</sup>; Elemental analysis calculated for C<sub>21</sub>H<sub>28</sub>BrN<sub>3</sub>O<sub>6</sub>S: C, 47.55; H, 5.32; N, 7.92; Found: C, 46.73; H, 5.97; N, 7.24.

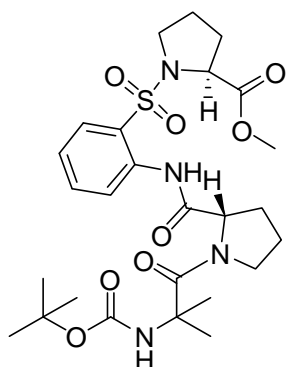
**(S)-1-(2-bromo-2-methylpropanoyl)-N-(2-(((S)-2-((4-bromophenyl)carbamoyl)pyrrolidin-1-yl)sulfonyl)phenyl)pyrrolidine-2-carboxamide**  
**25**



Compound **25** was synthesized from compound **10**, following the synthetic procedure for compound **26**. Purified by column chromatography, (75:25 ethyl acetate/pet. ether, R<sub>f</sub>: 0.5), white crystalline solid (97%), mp: 176-180°C; [α]<sub>D</sub><sup>27</sup>: -200.74° (*c* = 0.1, CHCl<sub>3</sub>); IR (CHCl<sub>3</sub>, ν (cm<sup>-1</sup>): 3345, 3022, 2890, 1698, 1651, 1590, 1546, 1371, 1216; <sup>1</sup>H NMR (CDCl<sub>3</sub>/200MHz): δ ppm 9.98 (s, 1H), 8.76 (s, 1H), 8.40-8.44 (d, *J*=7.96, 1H), 7.83-7.87 (d, *J*=7.96, 1H), 7.50-7.57 (t, *J*=7.51, 1H), 7.40 (s, 4H), 7.18-7.26 (m, 1H), 4.57-4.59 (m, 1H), 4.26-4.36 (m, 2H), 3.68-3.90 (m, 2H), 3.43-3.57 (m, 2H), 1.72-2.31 (m, 13H); <sup>13</sup>C NMR (CDCl<sub>3</sub>,50MHz): δ ppm 170.6, 170.4, 168.9, 136.5, 134.7, 131.7, 124.1, 121.6, 64.3, 62.2, 57.3, 49.8, 32.3, 30.4, 28.7, 24.3; MALDI-

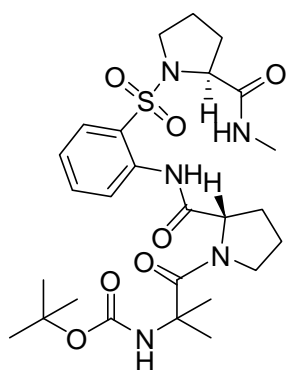
TOF-MS: 671.2068 (M+H)<sup>+</sup>, 691.0135 (M+Na)<sup>+</sup>, 708.9841 (M+K)<sup>+</sup>; Elemental analysis calculated for C<sub>26</sub>H<sub>30</sub>Br<sub>2</sub>N<sub>4</sub>O<sub>5</sub>S: C, 46.58; H, 4.51; N, 8.36; Found: C, 46.24; H, 4.36; N, 8.78.

**Methyl ((2-((S)-1-(2-((tert-butoxycarbonyl)amino)-2-methylpropanoyl)pyrrolidine-2-carboxamido)phenyl)sulfonyl)-L-prolinate 22**



Compound **8** (2, 4.12mmols) was subjected to 'boc deprotection using TFA (5mL) in DCM (5mL). The reaction mixture was evaporated and the residue was neutralized with NaHCO<sub>3</sub> solution, followed by extraction using DCM (5 x 2mL) and evaporation to yield the free amine. The free amine was then subjected to coupling reaction, following the procedure for **1**. Purified by column chromatography, (25:75 pet. ether/ethyl acetate, R<sub>f</sub>: 0.5) to afford **22** as a white solid which was later crystallized from a solution of ethyl acetate and pet-ether (2.28, 97%). mp: 149-153°C; [α]<sub>D</sub><sup>25</sup>: -238° (c = 0.1, CHCl<sub>3</sub>); IR (CHCl<sub>3</sub>, ν (cm<sup>-1</sup>): 3330, 3019, 1745, 1708, 1634, 1584, 1524, 1437, 1338, 1215; <sup>1</sup>H NMR (CDCl<sub>3</sub>/200MHz): δ ppm 9.80 (s, 1H), 8.44-8.48 (d, J=8.21, 1H), 7.86-8.12 (m, 1H), 7.62-7.81 (m, 1H), 7.51-7.58 (m, 1H), 7.29-7.44 (m, 1H), 7.15-7.23 (t, J=7.58, 1H), 5.01-5.23 (m, 1H), 4.78 (s, 1H), 4.22-4.50 (m, 1H), 3.72 (s, 3H), 3.32-3.38 (t, J=6.57, 2H), 1.84-2.22 (m, 10H), 1.53 (s, 6H), 1.42 (s, 9H); <sup>13</sup>C NMR (CDCl<sub>3</sub>, 50MHz): δ ppm 172.5, 171.3, 136.7, 134.2, 129.5, 125.3, 123.6, 123.4, 63.3, 59.5, 56.7, 52.5, 48.7, 48.2, 38.5, 30.8, 28.2, 24.6; MALDI-TOF-MS: 566.4657 (M)<sup>+</sup>, 589.2203 (M+Na)<sup>+</sup>, 605.1953 (M+K)<sup>+</sup>; Elemental analysis calculated for C<sub>26</sub>H<sub>38</sub>N<sub>4</sub>O<sub>8</sub>S: C, 55.11; H, 6.76; N, 9.89; Found: C, 56.24; H, 6.11; N, 9.23.

**Tert-butyl (2-methyl-1-((S)-2-((2-(((S)-2-(methylcarbamoyl)pyrrolidin-1-yl)sulfonyl)phenyl)carbamoyl)pyrrolidin-1-yl)-1-oxopropan-2-yl)carbamate 23**

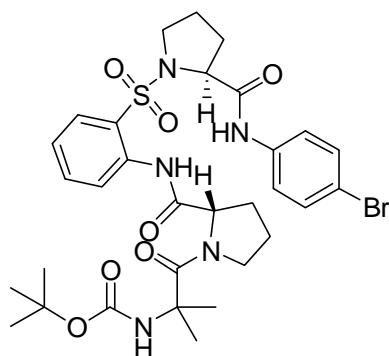


Compound **22** (0.5, 8.83mmols) was amidated using saturated methanolic methylamine (5mL). After 3 hours, the reaction mixture was evaporated under reduced pressure to obtain crude product which was purified by column chromatography, (05:95 methanol/ethyl acetate, R<sub>f</sub>: 0.5) to afford **24** as a white crystalline solid (0.4, 80%), crystallized from a solution of chloroform and



methanol. mp: 192-194°C;  $[\alpha]_{\text{D}}^{27}$ : -203° ( $c = 0.1$ ,  $\text{CHCl}_3$ ); IR ( $\text{CHCl}_3$ ,  $\nu$  ( $\text{cm}^{-1}$ ): 3343, 3019, 1709, 1634, 1586, 1531, 1439, 1339, 1216;  $^1\text{H}$  NMR ( $\text{CDCl}_3/200\text{MHz}$ ):  $\delta$  ppm 9.90 (s, 1H), 8.39-8.43 (d,  $J=7.63$ , 1H), 7.79-7.83 (m, 1H), 7.51-7.59 (t,  $J=7.58$ , 1H), 7.17-7.24 (t,  $J=7.64$ , 1H), 7.05 (s, 1H), 5.04 (s, 1H), 4.62 (s, 1H), 4.19-4.22 (d,  $J=5.19$ , 1H), 3.76-3.79 (m, 2H), 3.37-3.53 (m, 1H), 2.7-2.72 (m, 3H), 1.79-2.22<sub>rotamer</sub> (m, 9H), 1.5 (s, 6H), 1.42 (s, 9H);  $^{13}\text{C}$  NMR ( $\text{CDCl}_3, 125\text{MHz}$ ):  $\delta$  ppm 172.9, 171.3, 136.7, 134.4, 129.8, 124.0, 123.1, 63.7, 61.9, 49.5, 48.2, 30.6, 28.2, 26.2, 24.2; MALDI-TOF-MS: 567.3377 ( $\text{M}+2\text{H}$ )<sup>+</sup>, 588.2561 ( $\text{M}+\text{Na}$ )<sup>+</sup>, 604.2314 ( $\text{M}+\text{K}$ )<sup>+</sup>; Elemental analysis calculated for  $\text{C}_{26}\text{H}_{39}\text{N}_5\text{O}_7\text{S}$ : C, 55.20; H, 6.95; N, 12.38; Found: C, 54.18; H, 6.34; N, 11.86.

**Tert-butyl (1-((S)-2-((2-(((S)-2-((4-bromophenyl)carbamoyl)pyrrolidin-1-yl)sulfonyl)phenyl)carbamoyl)pyrrolidin-1-yl)-2-methyl-1-oxopropan-2-yl)carbamate 24**

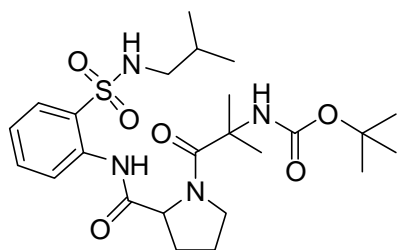


Compound **24** was synthesized from compound **22**, following the procedure for **1**. Purified by column chromatography, (25:75 ethyl acetate/pet. ether,  $R_f$ : 0.5) white crystalline solid (92%). mp: 216-220°C;  $[\alpha]_{\text{D}}^{26}$ : -248° ( $c = 0.1$ ,  $\text{CHCl}_3$ ); IR ( $\text{CHCl}_3$ ,  $\nu$  ( $\text{cm}^{-1}$ ): 3019, 1696, 1562, 1521, 1427;  $^1\text{H}$  NMR ( $\text{CDCl}_3/200\text{MHz}$ ): 9.93 (s, 1H), 8.93 (s, 1H), 8.31 (bs, 1H), 7.85-7.87 (d,  $J=8.07$ , 1H), 7.48-7.52 (t,  $J=7.70$ , 1H), 7.39 (m, 4H), 7.16-7.24 (t,  $J=7.71$ , 1H), 4.95 (s, 1H), 4.64 (s, 1H), 4.39-4.41 (m, 1H), 3.80 (m, 2H), 3.71-3.73 (m, 1H), 3.5-3.52 (m, 1H), 2.09-2.17 (m, 6H), 1.95-1.98 (s, 4H), 1.79 (m, 3H), 1.50 (s, 6H), 1.42 (s, 9H);  $^{13}\text{C}$  NMR ( $\text{CDCl}_3$ , 50 MHz):  $\delta$  ppm 172.9, 171.3, 136.7, 134.4, 129.8, 124.0, 123.1, 63.7, 61.9, 56.6, 49.5, 48.2, 30.6, 28.5, 28.2, 26.2, 24.2; MALDI-TOF-MS: 728.2606 ( $\text{M}+\text{Na}$ )<sup>+</sup>, 744.2314 ( $\text{M}+\text{K}$ )<sup>+</sup>; Elemental analysis calculated for  $\text{C}_{31}\text{H}_{40}\text{BrN}_5\text{O}_7\text{S}$ : C, 52.69; H, 5.71; N, 9.91; Found: C, 52.17; H, 5.94; N, 9.12.

**Tert-butyl (1-(2-((2-(N-isobutylsulfamoyl)phenyl)carbamoyl)pyrrolidin-1-yl)-2-methyl-1-oxopropan-2-yl)carbamate 17**

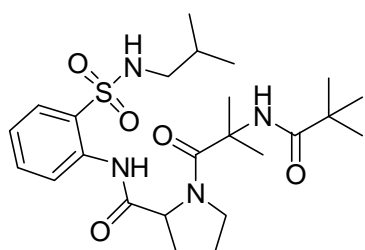
Compound **17** was synthesized from compound **12**, following the procedure for **2**

Purified by column chromatography, (30:70 pet. ether/ethyl acetate,  $R_f$ : 0.5), white solid (87%). mp: 78-79°C;  $[\alpha]_{\text{D}}^{25}$ : -70° ( $c = 0.1$ ,  $\text{CHCl}_3$ ); IR ( $\text{CHCl}_3$ ,  $\nu$  ( $\text{cm}^{-1}$ ): 3324, 3019,



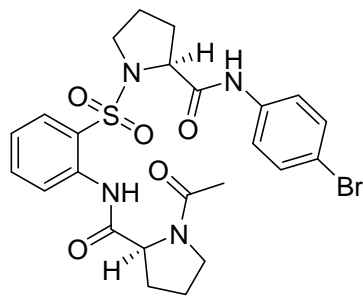
1696, 1648, 1618, 1618, 1482, 1425, 1341, 1215;  $^1\text{H}$  NMR ( $\text{CDCl}_3/200\text{MHz}$ ):  $\delta$  ppm 9.20 (s, 1H), 7.86-7.95 (m, 2H), 7.48-1.56 (m, 1H), 7.18-7.26 (m, 1H), 6.75 (s, 1H), 4.99 (s, 1H), 4.51 (s, 1H), 4.10-4.21 (m, 1H), 3.84-3.96 (m, 1H), 3.61-3.77 (m, 1H), 2.55-2.62 (m, 2H), 2.12-2.24 (m, 3H), 1.85-2.02 (m, 3H), 1.60-1.77 (m, 2H), 1.52 (s, 3H), 1.40-1.41<sub>rotamer</sub> (s, 9H), 1.21-1.28 (t,  $J=7.13$ , 1H), 0.80-0.86 (t,  $J=5.43$ , 6H);  $^{13}\text{C}$  NMR ( $\text{CDCl}_3, 50\text{MHz}$ ):  $\delta$  ppm 174.1, 170.8, 154.2, 134.3, 133.0, 130.2, 129.1, 125.1, 124.3, 64.0, 60.8, 56.9, 50.5, 48.4, 38.5, 28.6, 28.3, 28.1, 26.0, 25.0, 19.9, 19.8, 14.0; MALDI-TOF-MS: 533.2400 ( $\text{M}+\text{Na}$ ) $^+$ , 549.2123 ( $\text{M}+\text{K}$ ) $^+$ ; Elemental analysis calculated for  $\text{C}_{24}\text{H}_{38}\text{N}_4\text{O}_6\text{S}$ : C, 56.45; H, 7.50; N, 10.97; Found: C, 55.82; H, 7.70; N, 10.14.

**Tert-butyl (1-(2-((2-(N-isobutylsulfonyl)phenyl)carbamoyl)pyrrolidin-1-yl)-2-methyl-1-oxopropan-2-yl)carbamate 21**



Compound **21** was synthesized from **17** following the procedure for **2** using pivaloyl chloride as the acylating agent. Purified by column chromatography, (35:65 pet. ether/ethyl acetate,  $R_f$ : 0.5), white crystalline solid (95%). mp: 203-205°C;  $[\alpha]_D^{26}$ : -75° ( $c = 0.1$ ,  $\text{CHCl}_3$ ); IR ( $\text{CHCl}_3$ ,  $\nu$  ( $\text{cm}^{-1}$ ): 3324, 3020, 1648, 1618, 1618, 1482, 1425, 1341, 1215;  $^1\text{H}$  NMR ( $\text{CDCl}_3/500\text{MHz}$ ):  $\delta$  ppm 9.17 (s, 1H), 7.99-8.00 (d,  $J=7.93$ , 1H), 7.88-7.90 (d,  $J=7.63$ , 1H), 7.53-1.56 (t,  $J=7.63$ , 1H), 7.22-1.25 (t,  $J=7.47$ , 1H), 6.64-6.66 (t,  $J=5.03$ , 1H), 6.16 (s, 1H), 4.56-4.59 (m, 1H), 3.63-3.68 (m, 1H), 2.65-2.70 (m, 1H), 2.52-2.57 (m, 1H), 2.09-2.18 (m, 2H), 2.56-2.67 (m, 2H), 1.91-1.96 (m, 1H), 1.74 (m, 1H), 1.66-1.68 (m, 1H), 1.62 (s, 6H), 1.2 (s, 9H), 0.82-0.84 (m, 6H);  $^{13}\text{C}$  NMR ( $\text{CDCl}_3, 125\text{MHz}$ ):  $\delta$  ppm 177.6, 174.5, 170.7, 134.4, 133.1, 129.9, 125.1, 124.3, 64.0, 57.4, 50.5, 48.5, 39.0, 28.7, 28.2, 27.5, 25.9, 25.0, 24.8, 19.8; MALDI-TOF-MS: 517.2815 ( $\text{M}+\text{Na}$ ) $^+$ , 533.2591 ( $\text{M}+\text{K}$ ) $^+$ ; Elemental analysis calculated for  $\text{C}_{24}\text{H}_{38}\text{N}_4\text{O}_5\text{S}$ : C, 58.28; H, 7.74; N, 11.33; Found: C, 58.87; H, 7.16; N, 10.89.

**(S)-1-(acetyl)-N-(2-(((S)-2-((4-bromophenyl)carbamoyl)pyrrolidin-1-yl)sulfonyl)phenyl)pyrrolidine-2-carboxamide 19**



Compound **19** was synthesized from compound **10** using acetyl chloride as acylating agent, following the synthetic procedure for compound **26**. Purified by column chromatography, (75:25 ethyl acetate/pet. ether,  $R_f$ : 0.5), white (92%), mp: 84.2-86.2°C;  $[\alpha]_D^{27}$ : -193.64° ( $c = 0.1$ ,  $\text{CHCl}_3$ ); IR ( $\text{CHCl}_3$ ,  $\nu$  ( $\text{cm}^{-1}$ ): 3343, 3021, 2890, 1698, 1651, 1590, 1546, 1371, 1216;  $^1\text{H}$  NMR ( $\text{CDCl}_3/200\text{MHz}$ ):  $\delta$  ppm 10.13 (s, 1H), 9.48 (s, 1H), 8.61-8.58 (d,  $J=8.34$ , 1H), 7.85-7.90 (m, 1H), 7.48-7.60 (m, 3H), 7.36-7.41 (d,  $J=8.84$ , 2H), 7.18-7.25 (t,  $J=7.64$ , 1H), 4.62-4.68 (m, 1H), 4.28-4.32 (m, 1H), 3.50-3.81 (m, 4H), 2.26-2.38 (m, 1H), 2.19 (s, 3H), 1.89-2.11 (m, 5H), 1.63-1.02 (m, 2H);  $^{13}\text{C}$  NMR ( $\text{CDCl}_3$ , 50MHz):  $\delta$  ppm 172.2, 170.1, 169.3, 137.1, 136.1, 134.8, 131.6, 130.1, 123.9, 123.8, 121.8, 121.5, 116.7, 62.3, 61.7, 48.9, 48.2, 30.5, 30.0, 24.5, 24.3, 22.4; LC-MS: 585.00 ( $\text{M}+\text{Na}^+$ ), 601.10 ( $\text{M}+\text{K}^+$ ); Elemental analysis calculated for  $\text{C}_{24}\text{H}_{27}\text{BrN}_4\text{O}_5\text{S}$ : C, 51.16; H, 4.83; N, 9.94; Found: C, 49.24; H, 4.36; N, 9.58.

### 3.16 Single crystal X-ray crystallographic data.

Crystal data for the compounds were collected at  $T = 293$  K, on SMART APEX CCD Single crystal X-ray diffractometer using Mo KR radiation ( $\lambda$ ) 0.7107 Å. The structures were solved by direct methods using SHELXTL. All the data were corrected for Lorentz polarization and absorption effects. SHELX-97 (ShelxTL) was used for structure solution and full matrix least-squares refinement on  $F^2$ . Hydrogen atoms were included in the refinement in the riding mode. The refinements were carried out using SHELXL-97. For reference, see: G. M. Sheldrick, SHELX-97 program for crystal structure solution and refinement, University of Gottingen, Germany, 1997.

**Compound 1:** Single crystals of **1** were grown by slow evaporation of the solution mixture of ethylacetate and pet.ether. Colorless needle crystal of size 0.64 x 0.19 x 0.13  $\text{mm}^3$ , was used for data collection, Temperature = 297(2)K, Wave length = 0.71073 Å Quadrant data acquisition, Total scans = 4,  $F(000) = 1064$ ,  $\theta$  range = 2.19° to 25.49°, completeness to  $\theta$  of 24.99° is 100 %, Goodness-of-fit on  $F^2 = 1.018$ ,  $\text{C}_{21}\text{H}_{32}\text{N}_4\text{O}_6\text{S}_2$ ,  $M = 500.63$ . Crystals belong to Monoclinic, space group  $C2$ ,  $a = 18.6244(11)$ ,  $b = 8.4267(4)$ ,  $c = 16.0611(8)$  Å,  $\alpha = 90$ ,  $\beta = 93.118(5)$ ,  $\gamma = 90$ , 2516.9(2) Å<sup>3</sup>,  $Z = 4$ ,  $D_c = 1.321$  g/cc,  $\mu$  (Mo-K $\alpha$ ) = 0.254  $\text{mm}^{-1}$ , 4429 total reflections, 4052 unique [ $I > 2s(I)$ ], R value 0.0430,  $wR2 = 0.1171$ .

**Compound 2:** Single crystals of **2** were grown by slow evaporation of the solution mixture of methanol and dichloromethane. Colorless needle crystal of size 0.65 x 0.33 x 0.29 mm<sup>3</sup>, was used for data collection, Temperature = 296(2)K, Wave length = 0.71073 Å Quadrant data acquisition, F(000) = 616,  $\theta$  range = 2.36° to 30.42°, completeness to  $\theta$  is 95 %, Goodness-of-fit on F2 = 0.993, C<sub>23</sub>H<sub>27</sub>BrN<sub>4</sub>O<sub>6</sub>S<sub>2</sub>, M = 599.53. Crystals belong to Monoclinic, space group P21, a = 8.1060(12), b = 10.5928(16), c = 14.983(2) Å,  $\alpha$  = 90,  $\beta$  = 96.273(8),  $\gamma$  = 90, V = 1278.8(3) Å<sup>3</sup>, Z = 2, Dc = 1.557 g/cc,  $\mu$  (Mo-K $\alpha$ ) = 1.817 mm<sup>-1</sup>, 7389 total reflections, 5331 unique reflections, R value 0.0355, wR2 = 0.0875.

**Compound 3:** Single crystals of **3** were grown by slow evaporation of the solution mixture of ethyl acetate and pet. ether. Colorless block crystal of size 0.25 x 0.23 x 0.15 mm<sup>3</sup>, was used for data collection, Temperature = 90(2)K, Wave length = 0.71073 Å Quadrant data acquisition, F(000) = 1256,  $\theta$  range = 1.71° to 28.78°, completeness to  $\theta$  is 97 %, Goodness-of-fit on F2 = 1.166, C<sub>27</sub>H<sub>33</sub>BrN<sub>4</sub>O<sub>5</sub>S<sub>2</sub>, M = 605.54. Crystals belong to Orthorhombic, space group P212121, a = 15.7937(18), b = 26.446(3), c = 6.6869(8) Å,  $\alpha$  =  $\beta$  =  $\gamma$  = 90°, V = 2793.0(5) Å<sup>3</sup>, Z = 4, Dc = 1.440g/cc,  $\mu$  (Mo-K $\alpha$ ) = 1.590 mm<sup>-1</sup>, 7025 total reflections, 6264 unique reflections, R value 0.0921, wR2 = 0.1902.

**Compound 4:** Single crystals of **4** were grown by slow evaporation of the solution mixture of methanol and dichloromethane. Colorless plate crystal of size 0.47 x 0.31 x 0.05 mm<sup>3</sup>, was used for data collection, Temperature = 297(2)K, Wave length = 0.71073 Å Quadrant data acquisition, F(000) = 472,  $\theta$  range = 1.65° to 30°, completeness to  $\theta$  is 87 %, Goodness-of-fit on F2 = 1.027, C<sub>17</sub>H<sub>26</sub>N<sub>4</sub>O<sub>6</sub>S<sub>2</sub>, M = 446.54. Crystals belong to Monoclinic, space group P21, a = 7.7425(4), b = 10.0108(6), c = 13.8284(8) Å,  $\alpha$  = 90,  $\beta$  = 102.033(3),  $\gamma$  = 90, V = 1048.27(10) Å<sup>3</sup>, Z = 2, Dc = 1.415 g/cc,  $\mu$  (Mo-K $\alpha$ ) = 0.296 mm<sup>-1</sup>, 5303 total reflections, 4805 unique reflections, R value 0.0317, wR2 = 0.0819.

**Compound 5:** Single crystals of **5** were grown by slow evaporation of the solution mixture of methanol. Colorless prism crystal of size 0.70 x 0.42 x 0.28 mm<sup>3</sup>, was used for data collection, Temperature = 297(2)K, Wave length = 0.71073 Å Quadrant data acquisition, F(000) = 944,  $\theta$  range = 1.38° to 25°, completeness to  $\theta$  is 79 %, Goodness-of-fit on F2 = 1.042, C<sub>17</sub>H<sub>26</sub>N<sub>4</sub>O<sub>6</sub>S<sub>2</sub>, M = 446.54. Crystals belong to Orthorhombic, space group P212121, a = 9.5807(5), b = 14.7622(8), c = 14.7867(8) Å,  $\alpha$  =  $\beta$  =  $\gamma$  = 90°, V =

2091.32(19) Å<sup>3</sup>, Z = 4, Dc = 1.418 g/cc,  $\mu$  (Mo-K $\alpha$ ) = 0.296 mm<sup>-1</sup>, 2902 total reflections, 2703 unique reflections, R value 0.0277, wR2 = 0.0750.

**Compound 21:** Single crystals of **21** were grown by slow evaporation of the solution mixture of ethyl acetate and pet. ether. Colorless block crystal of size 0.23 x 0.21 x 0.18 mm<sup>3</sup>, was used for data collection, Temperature = 90(2) K, Wave length = 0.71073 Å Quadrant data acquisition, F(000) = 1064,  $\theta$  range = 2.25° to 28.30°, completeness to  $\theta$  is 90 %, Goodness-of-fit on F2 = 1.039, C<sub>24</sub>H<sub>38</sub>N<sub>4</sub>O<sub>5</sub>S, M = 494.64. Crystals belong to Orthorhombic, space group P212121, a = 8.6678(13), b = 16.756(3), c = 18.108(3) Å,  $\alpha = \beta = \gamma = 90$ , V = 2629.9(7) Å<sup>3</sup>, Z = 4, Dc = 1.249 g/cc,  $\mu$  (Mo-K $\alpha$ ) = 0.163 mm<sup>-1</sup>, 5915 total reflections, 4381 unique reflections, R value 0.0656, wR2 = 0.1699.

**Compound 22:** Single crystals of **22** were grown by slow evaporation of the solution mixture of methanol. Colorless plate crystal of size 0.42 x 0.23 x 0.06 mm<sup>3</sup>, was used for data collection, Temperature = 297(2) K, Wave length = 0.71073 Å Quadrant data acquisition, F(000) = 1208,  $\theta$  range = 1.75° to 25°, completeness to  $\theta$  is 100 %, Goodness-of-fit on F2 = 1.020, C<sub>26</sub>H<sub>38</sub>N<sub>4</sub>O<sub>8</sub>S, M = 566.66. Crystals belong to Orthorhombic, space group P212121, a = 8.3154(3), b = 12.1959(6), c = 29.2255(14) Å,  $\alpha = \beta = \gamma = 90$ , V = 2963.9(2) Å<sup>3</sup>, Z = 4, Dc = 1.270 g/cc,  $\mu$  (Mo-K $\alpha$ ) = 0.161 mm<sup>-1</sup>, 5221 total reflections, 3946 unique reflections, R value 0.0435, wR2 = 0.1033.

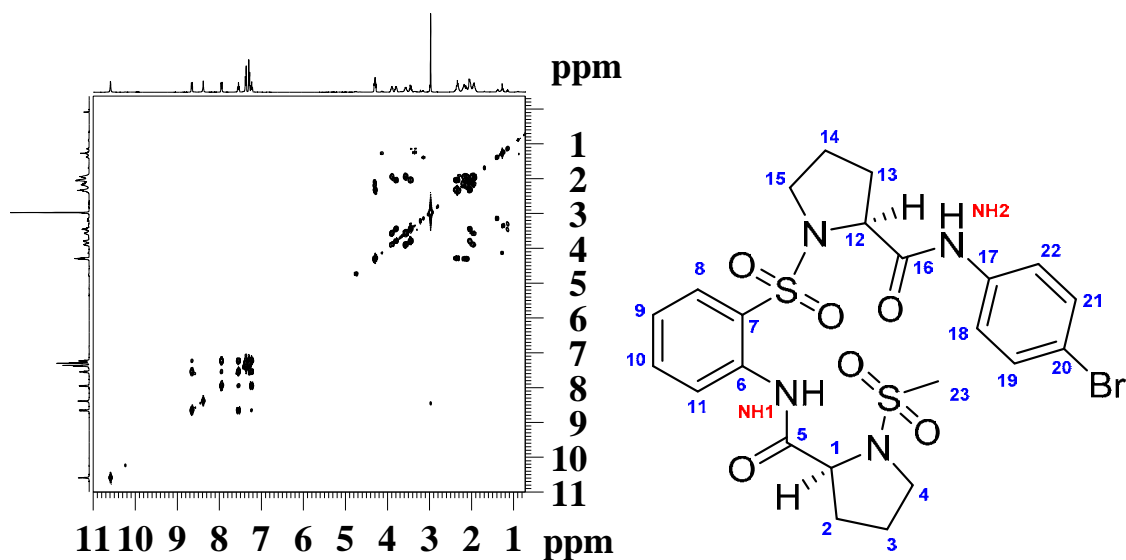
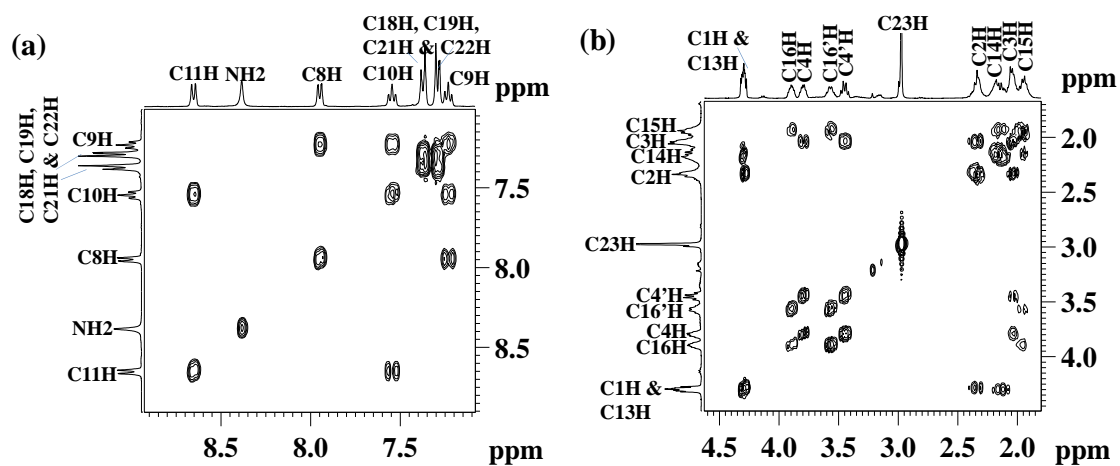
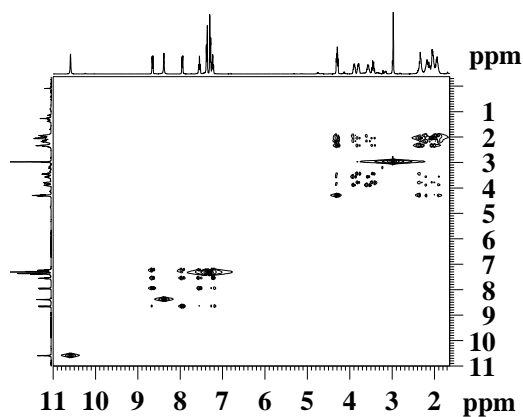
**Compound 23:** Single crystals of **23** were grown by slow evaporation of the solution mixture of methanol. Colorless square crystal of size 0.33 x 0.31 x 0.28 mm<sup>3</sup>, was used for data collection, Temperature = 297(2) K, Wave length = 0.71073 Å Quadrant data acquisition, F(000) = 1208.0,  $\theta$  range = 1.36° to 25°, completeness to  $\theta$  is 100 %, Goodness-of-fit on F2 = 1.027, C<sub>26</sub>H<sub>39</sub>N<sub>5</sub>O<sub>7</sub>S, M = 565.68. Crystals belong to Orthorhombic, space group P212121, a = 8.3677(7), b = 12.1053(7), c = 29.8655(18) Å,  $\alpha = \beta = \gamma = 90$ , V = 3025.2(4) Å<sup>3</sup>, Z = 4, Dc = 1.242 g/cc,  $\mu$  (Mo-K $\alpha$ ) = 0.156 mm<sup>-1</sup>, 5337 total reflections, 3611 unique reflections, R value 0.0874, wR2 = 0.1489.

**Compound 24:** Single crystals of **24** were grown by slow evaporation of the solution mixture of methanol and chloroform. Colorless plate crystal of size 0.29 x 0.21 x 0.06 mm<sup>3</sup>, was used for data collection, Temperature = 297(2) K, Wave length = 0.71073 Å Quadrant data acquisition, F(000) = 1472,  $\theta$  range = 1.73° to 24.990°, completeness to  $\theta$  is 100 %, Goodness-of-fit on F2 = 1.002, C<sub>31</sub>H<sub>40</sub>BrN<sub>5</sub>O<sub>7</sub>S, M = 706.65. Crystals belong to

Orthorhombic, space group P212121,  $a = 6.7431(4)$ ,  $b = 16.1961(7)$ ,  $c = 30.9899(13)$  Å,  $\alpha = \beta = \gamma = 90$ ,  $V = 3384.5(3)$  Å<sup>3</sup>,  $Z = 4$ ,  $D_c = 1.387$  g/cc,  $\mu$  (Mo-K $\alpha$ ) = 1.328 mm<sup>-1</sup>, 5914 total reflections, 3651 unique reflections, R value 0.0480, wR2 = 0.1082.

**Compound 25:** Single crystals of **25** were grown by slow evaporation of the solution mixture of methanol and chloroform. Colorless needle crystal of size 0.87 x 0.27 x 0.18 mm<sup>3</sup>, was used for data collection, Temperature = 297(2) K, Wave length = 0.71073 Å Quadrant data acquisition,  $F(000) = 1360$ ,  $\theta$  range = 1.74° to 24.990°, completeness to  $\theta$  is 100 %, Goodness-of-fit on  $F^2 = 1.036$ ,  $C_{26}H_{30}Br_2N_4O_5S$ ,  $M = 670.42$ . Crystals belong to Orthorhombic, space group P212121,  $a = 6.8326(4)$ ,  $b = 15.9014(9)$ ,  $c = 26.5246(14)$  Å,  $\alpha = \beta = \gamma = 90$ ,  $V = 2881.8(3)$  Å<sup>3</sup>,  $Z = 4$ ,  $D_c = 1.545$  g/cc,  $\mu$  (Mo-K $\alpha$ ) = 2.927 mm<sup>-1</sup>, 5056 total reflections, 3608 unique reflections, R value 0.0453, wR2 = 0.1214.

## 3.17 Spectra of compounds.

Figure 1: COSY spectra of **2** (500MHz, CDCl<sub>3</sub>)Figure 2: Partial COSY spectrum of **2** (500MHz, CDCl<sub>3</sub>); (a) aromatic (b) aliphatic regions.Figure 3: TOCSY spectrum of **2** (500MHz, CDCl<sub>3</sub>)

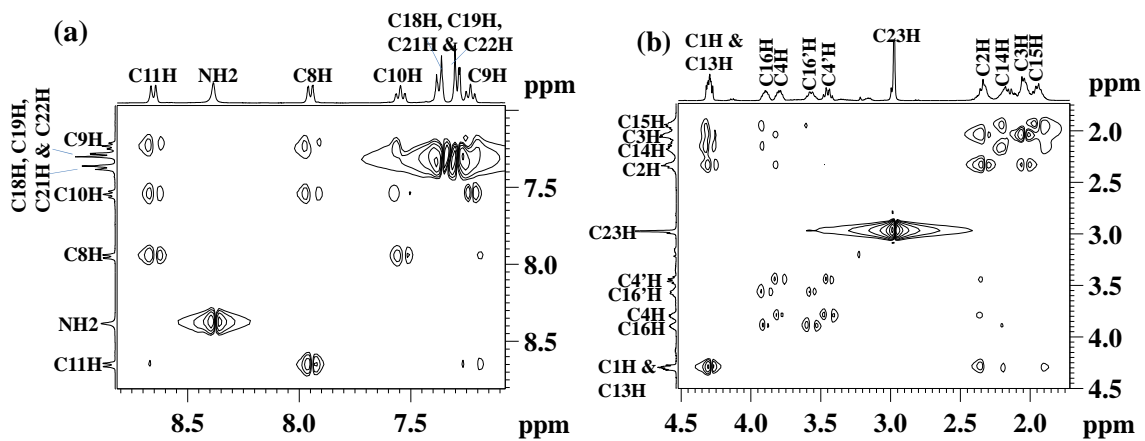


Figure 4: Partial TOCSY of **2** (500MHz, CDCl<sub>3</sub>); (a) aromatic (b) aliphatic regions.

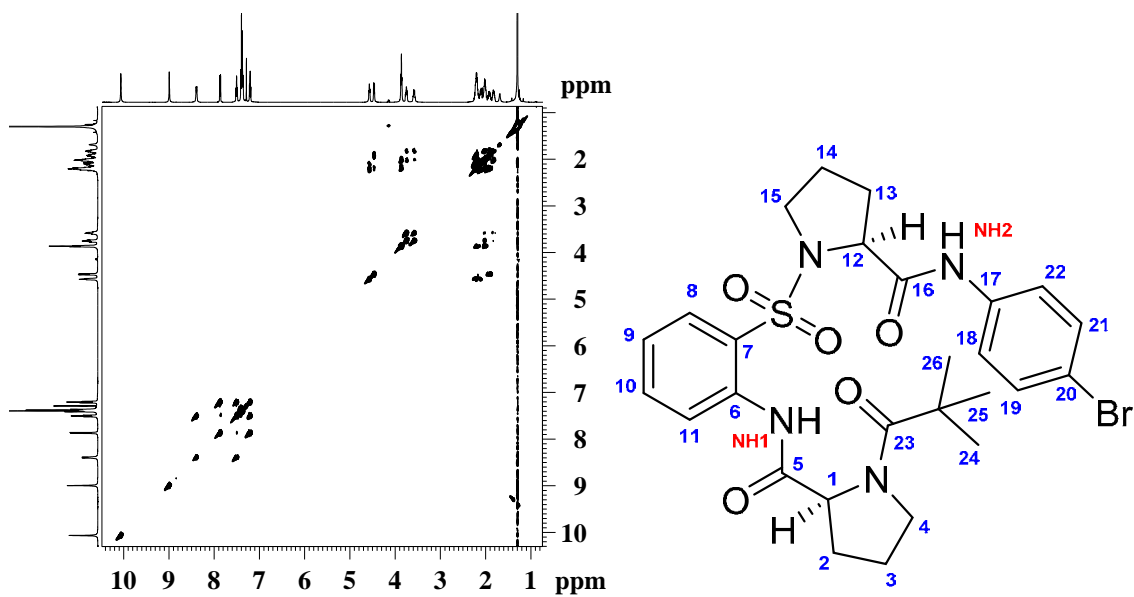


Figure 5: COSY spectrum of **3** (500MHz, CDCl<sub>3</sub>).

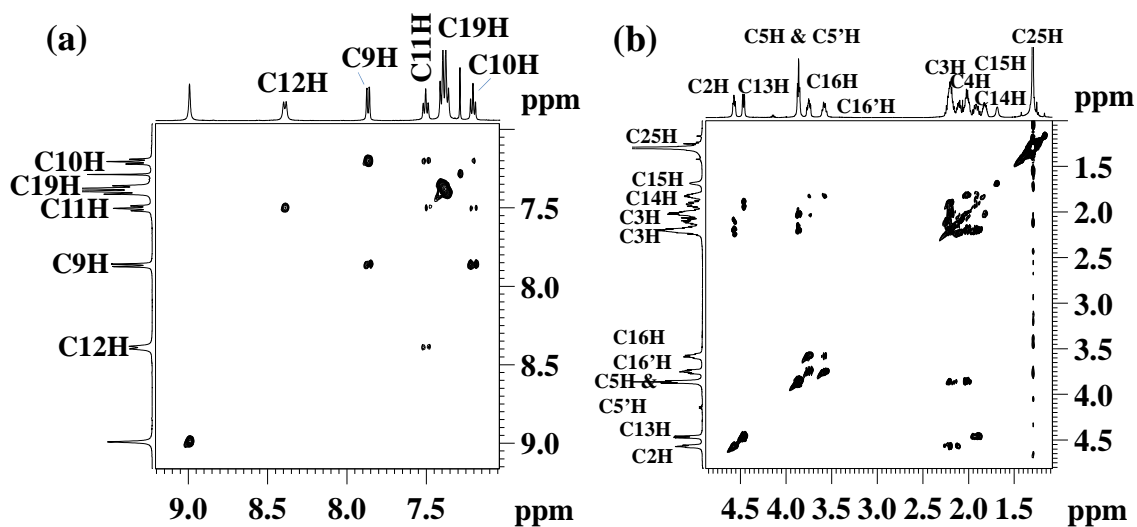


Figure 6: Partial COSY of **3** (500MHz, CDCl<sub>3</sub>); (a) aromatic & (b) aliphatic regions.



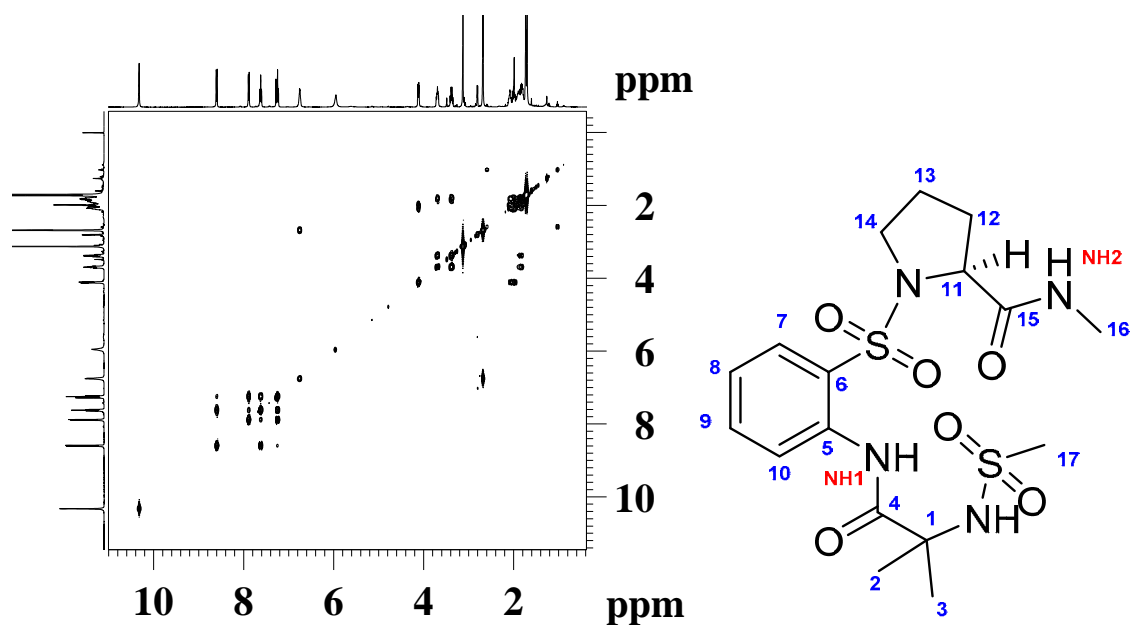


Figure 7: Molecular structure of compound 4.

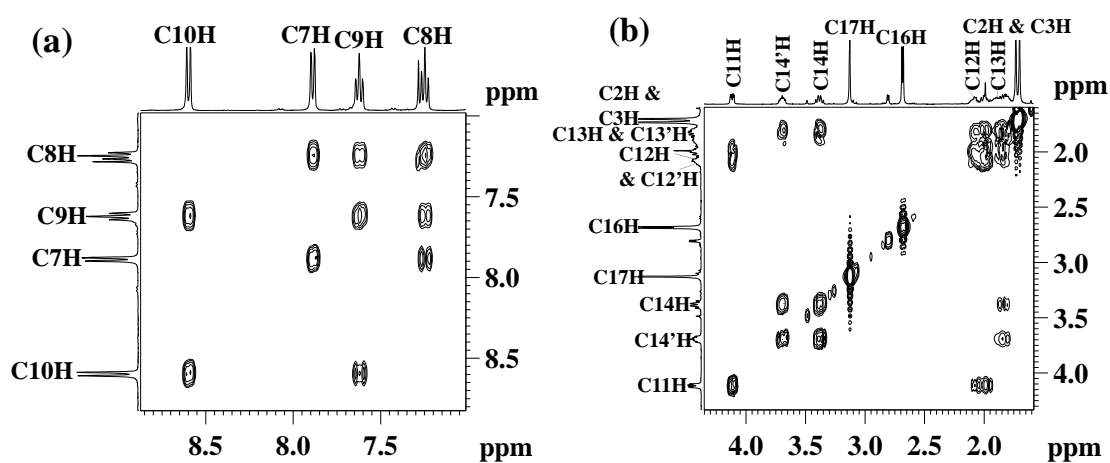


Figure 8: Partial COSY of 4 (500MHz, CDCl<sub>3</sub>); (a) aromatic and (b) aliphatic regions.

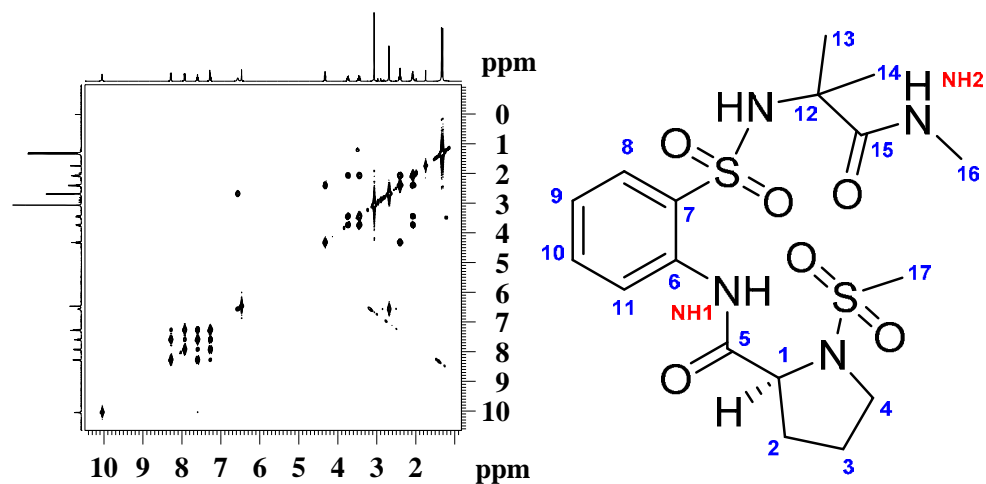


Figure 9: COSY spectrum of 5 (500MHz, CDCl<sub>3</sub>).

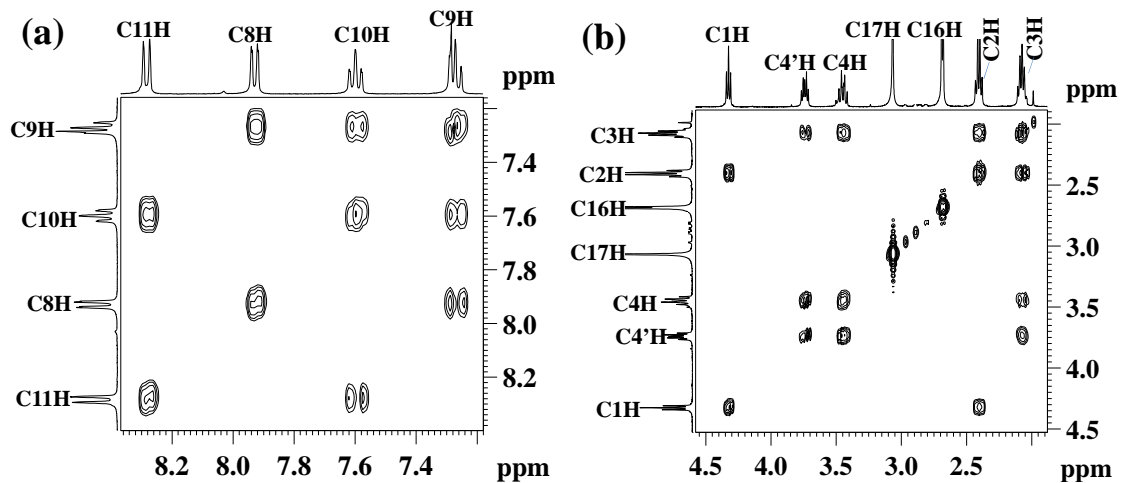


Figure 10: Partial COSY spectrum of **5** (500MHz, CDCl<sub>3</sub>); (a) aromatic and (b) aliphatic regions.

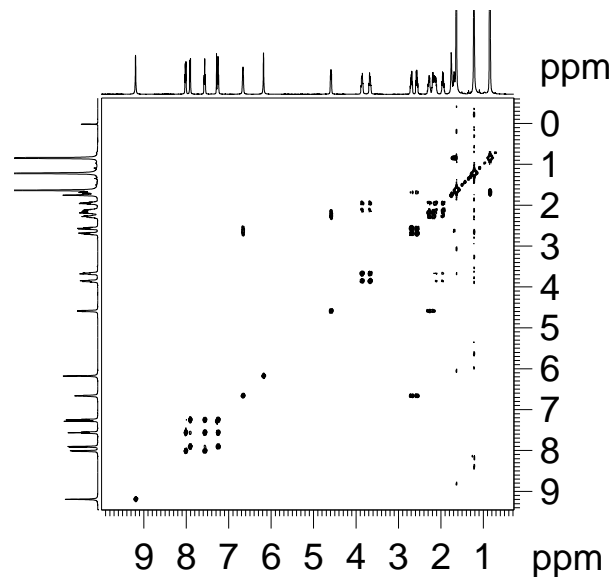


Figure 11: 2D COSY Spectrum of **21**

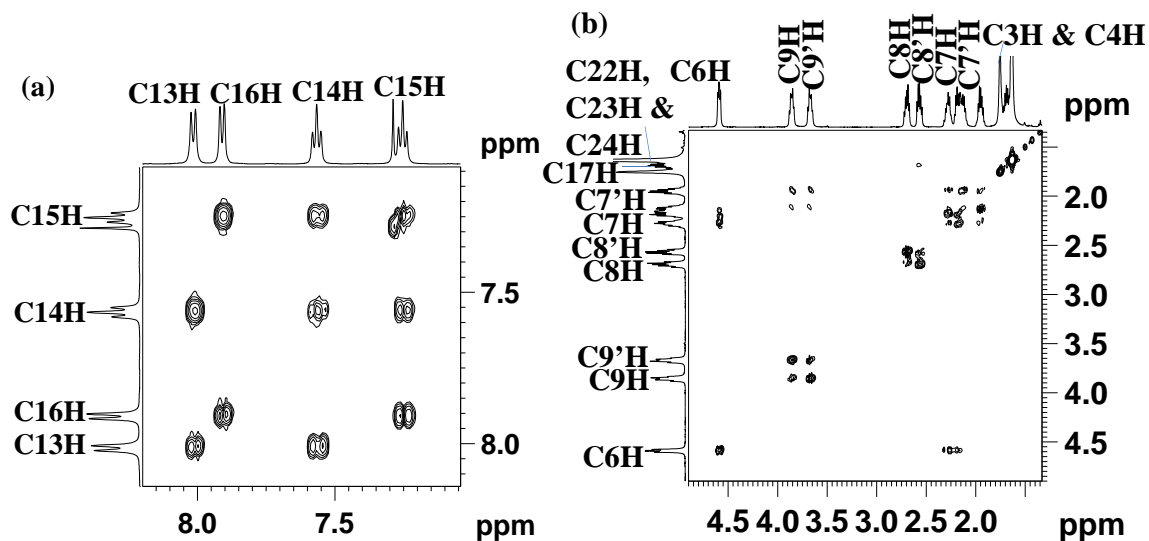


Figure 12: Partial COSY spectrum of **21**; (a) aromatic and (b) aliphatic regions.

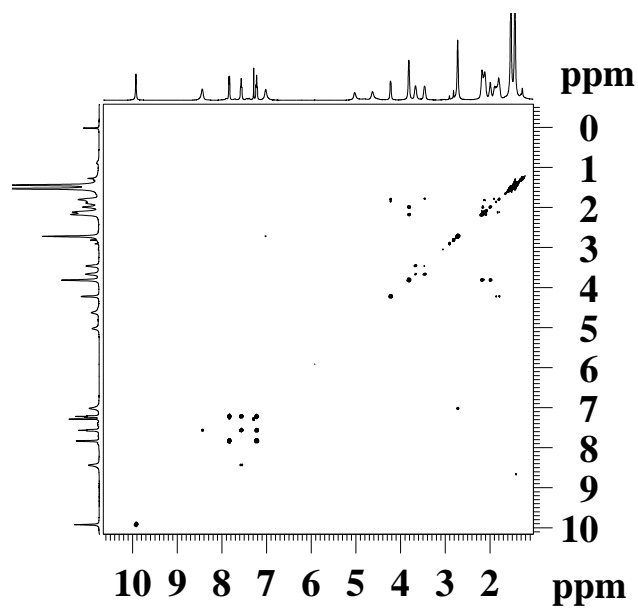


Figure 13: 2D COSY spectrum of 22.

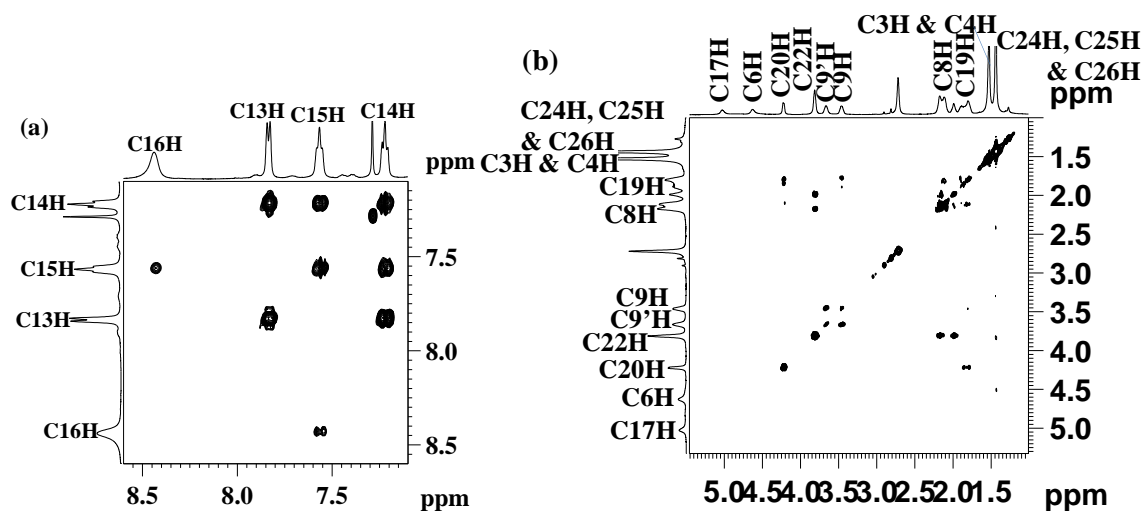


Figure 14: Partial COSY spectrum of 22; (a) aromatic and (b) aliphatic regions.

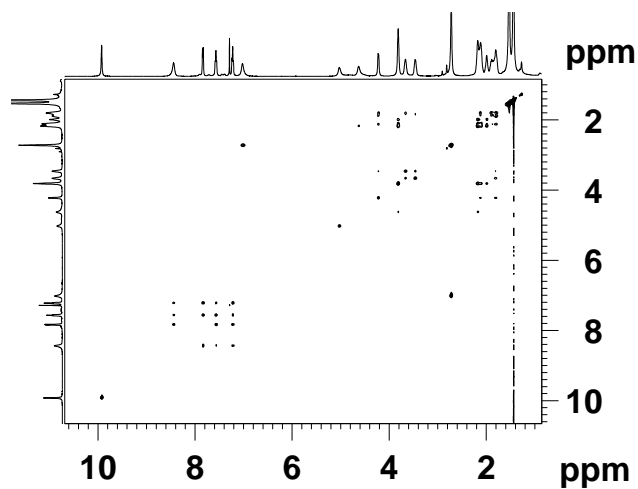


Figure 15: 2D TOCSY spectrum of 22.

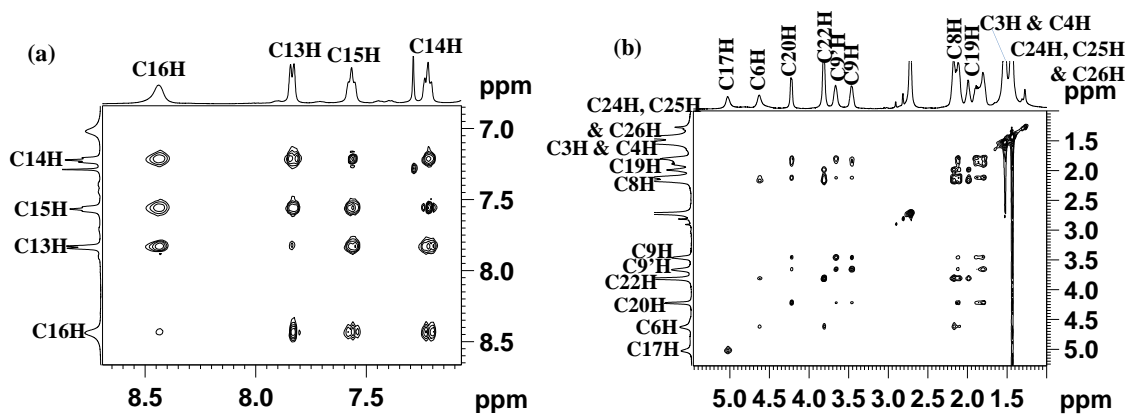


Figure 16: Partial TOCSY spectrum of 22; (a) aromatic and (b) aliphatic regions.

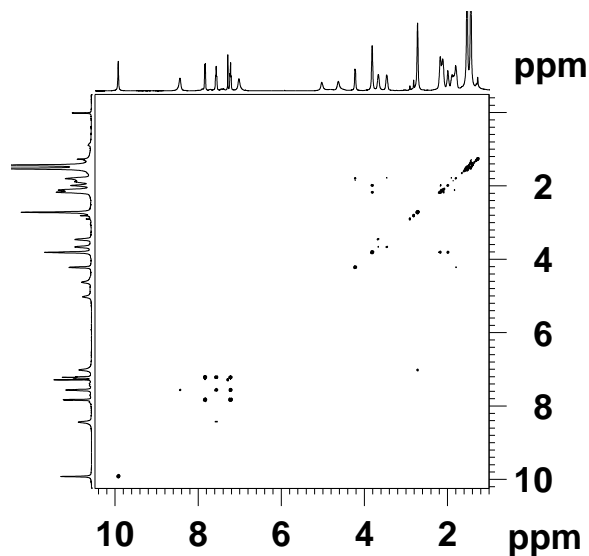


Figure 17: 2D COSY spectrum of 23.

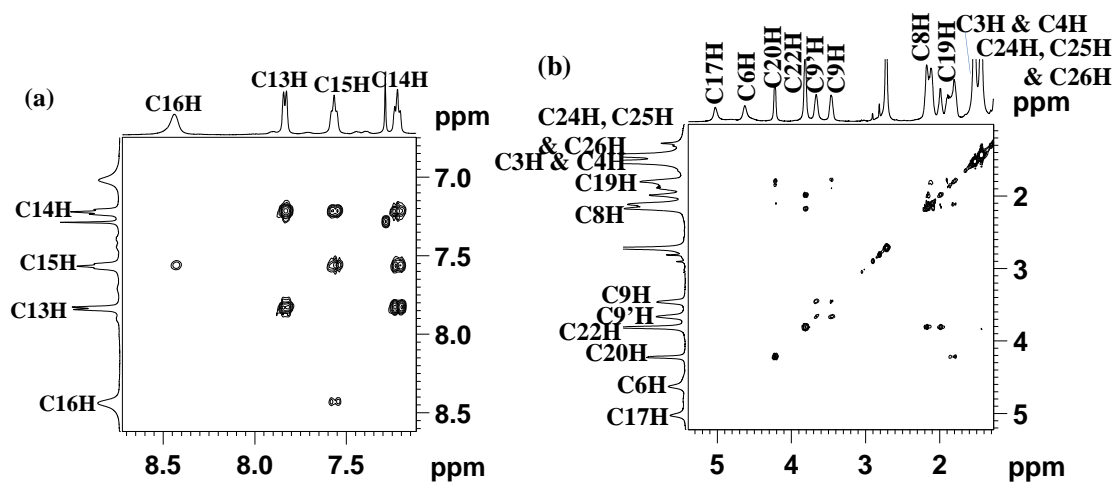


Figure 18: Partial COSY spectrum of 23; (a) aromatic and (b) aliphatic regions.

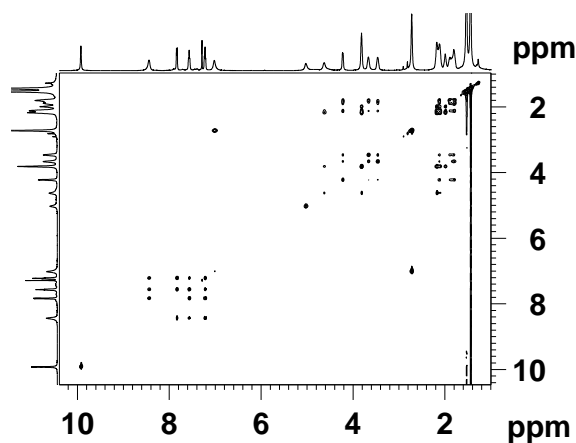


Figure 19: 2D TOCSY spectrum of 23.

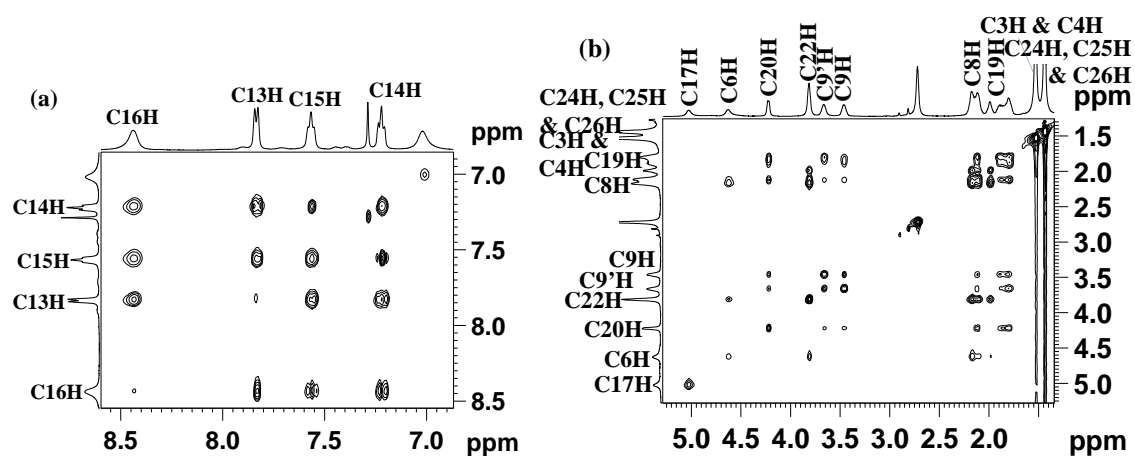


Figure 20: Partial TOCSY spectrum of 23; (a) aromatic and (b) aliphatic regions.

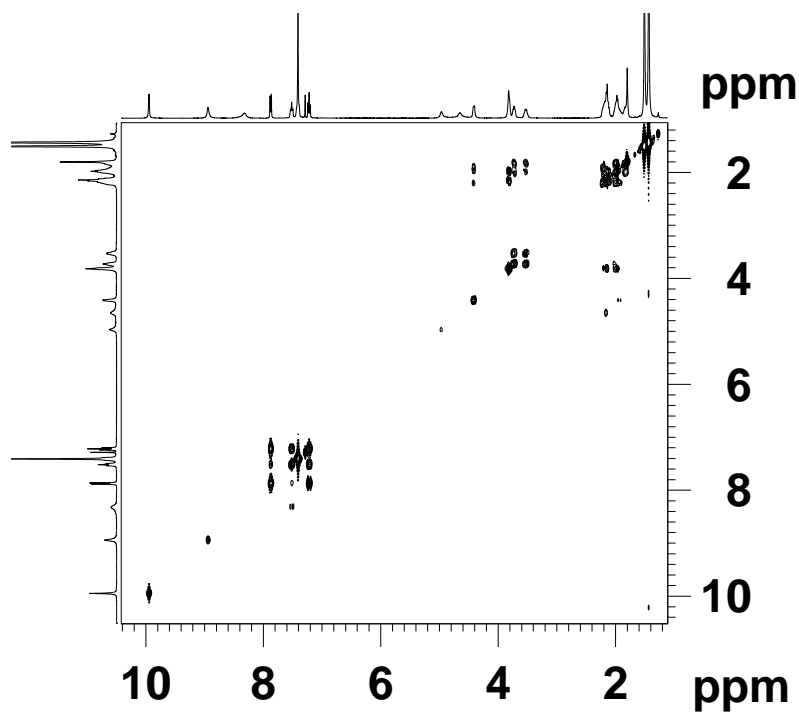


Figure 21: 2D COSY spectrum of 24.

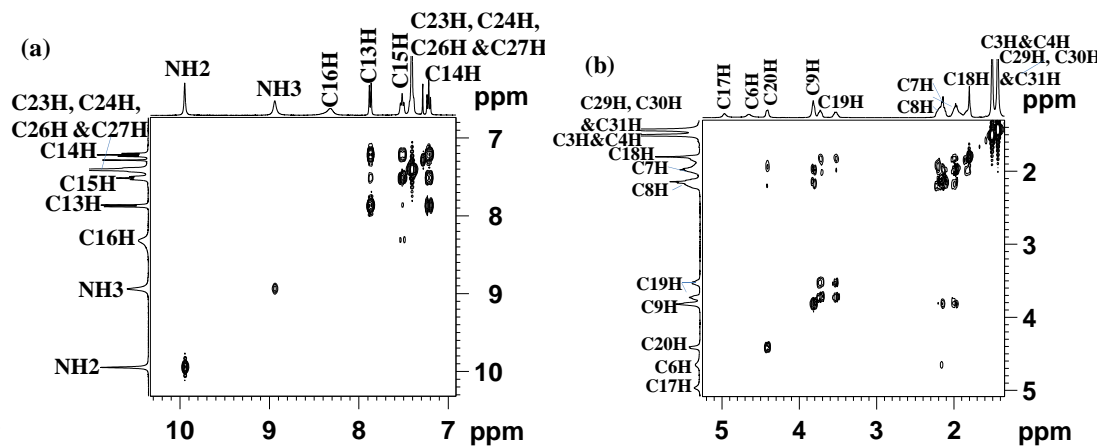


Figure 22: Partial COSY spectrum of **24**; (a) aromatic and (b) aliphatic regions.

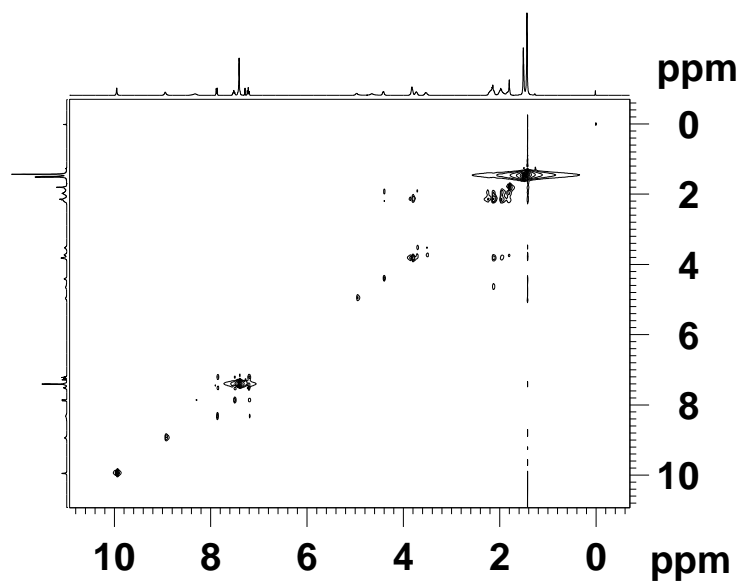


Figure 23: 2D TOCSY spectrum of **24**.

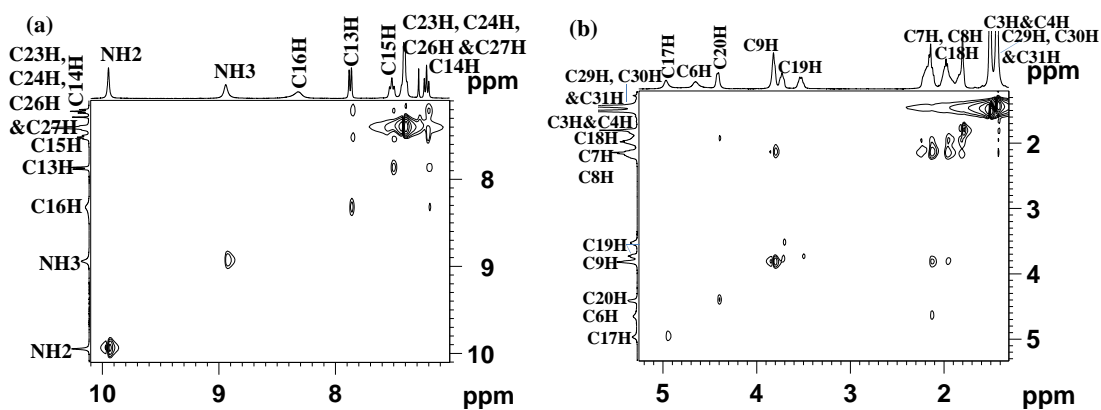


Figure 24: Partial TOCSY spectrum of **24**; (a) aromatic and (b) aliphatic regions.

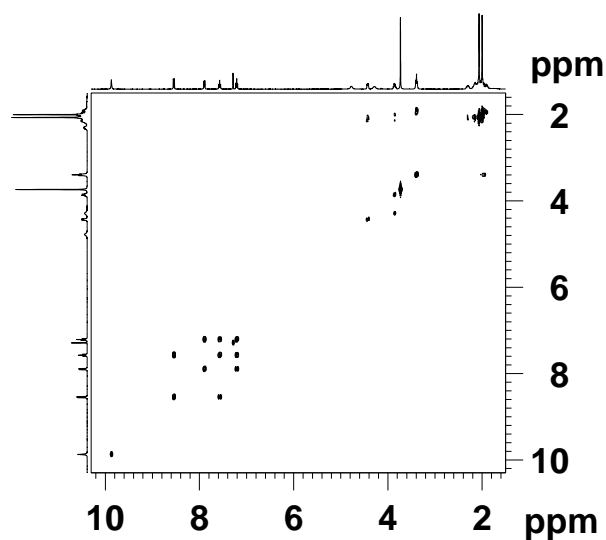


Figure 25: 2D COSY spectrum of 26.

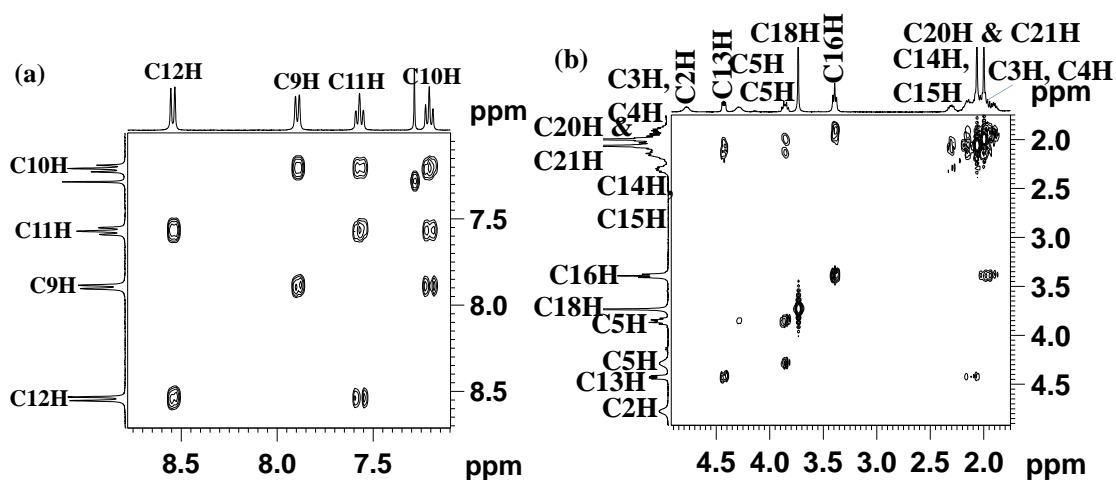
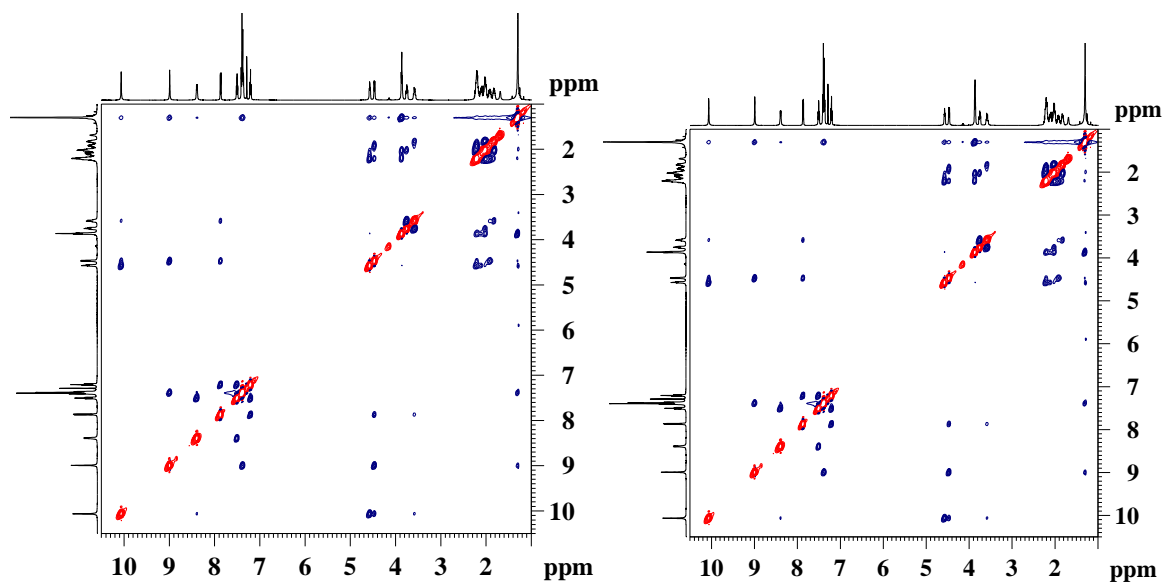


Figure 26: Partial COSY spectrum of 26; (a) aromatic and (b) aliphatic regions.

Figure 27: NOESY spectra of amide 2 (400MHz, CDCl<sub>3</sub>) and amide 3 (400MHz, CDCl<sub>3</sub>) respectively.

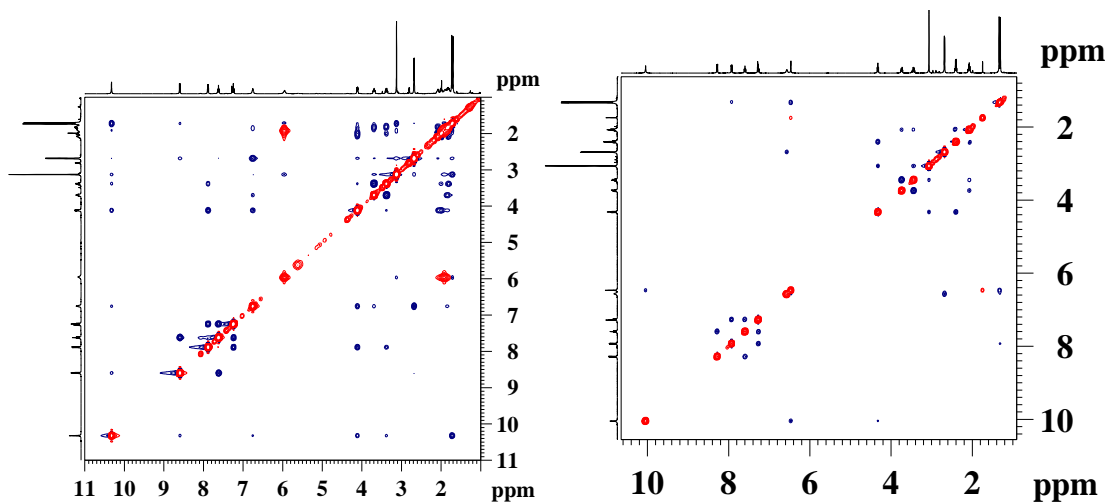


Figure 28: NOESY spectra of amide 4 (400MHz, CDCl<sub>3</sub>) and amide 5 (400MHz, CDCl<sub>3</sub>) respectively.

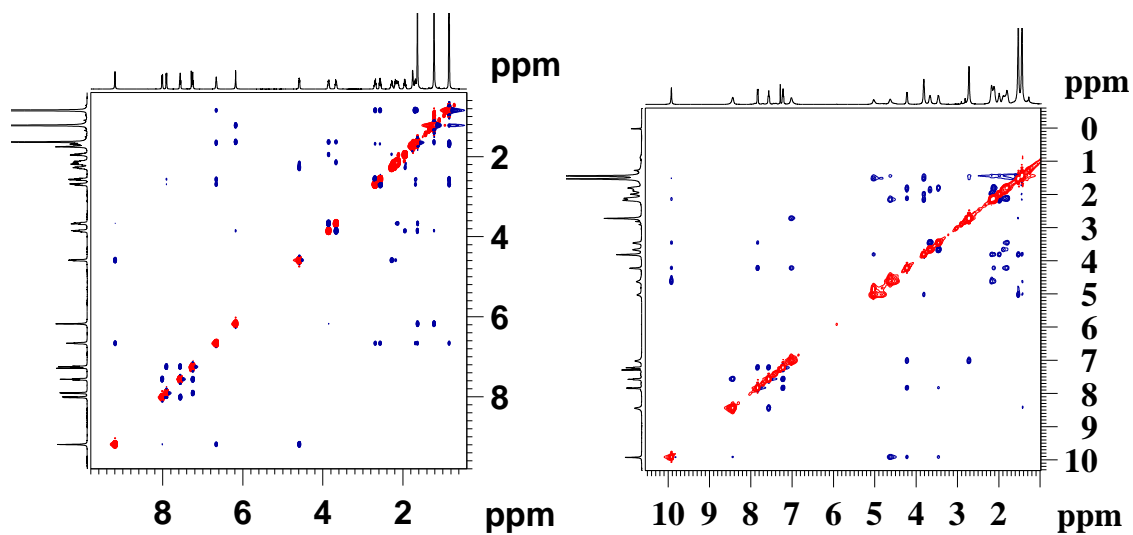


Figure 29: NOESY spectra of amide 21 (400MHz, CDCl<sub>3</sub>) and amide 22 (400MHz, CDCl<sub>3</sub>) respectively.

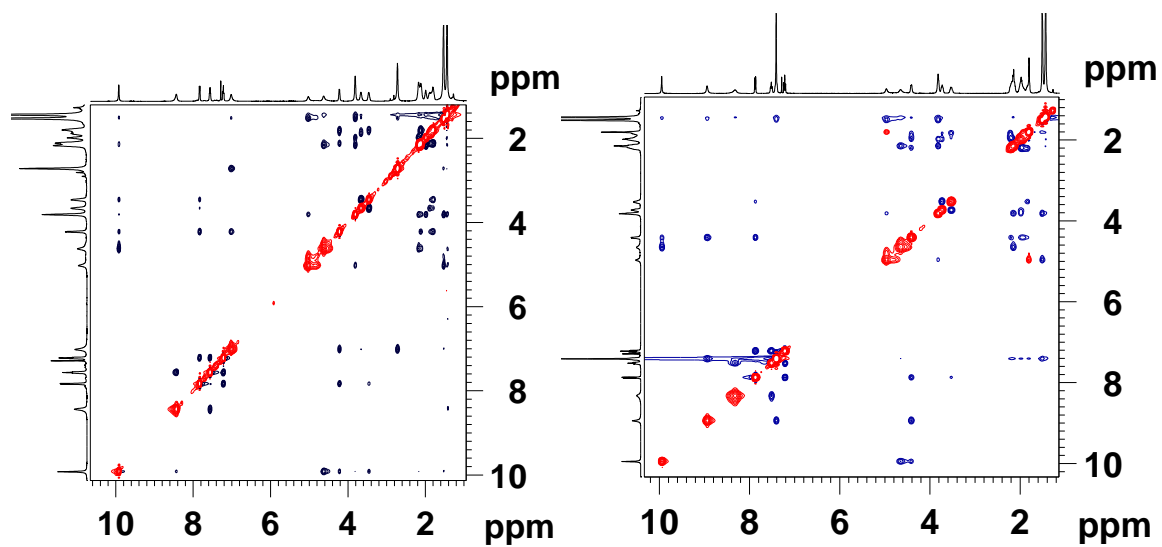


Figure 30: NOESY spectra of amide 24 (400MHz, CDCl<sub>3</sub>) and amide 23 (400MHz, CDCl<sub>3</sub>) respectively.



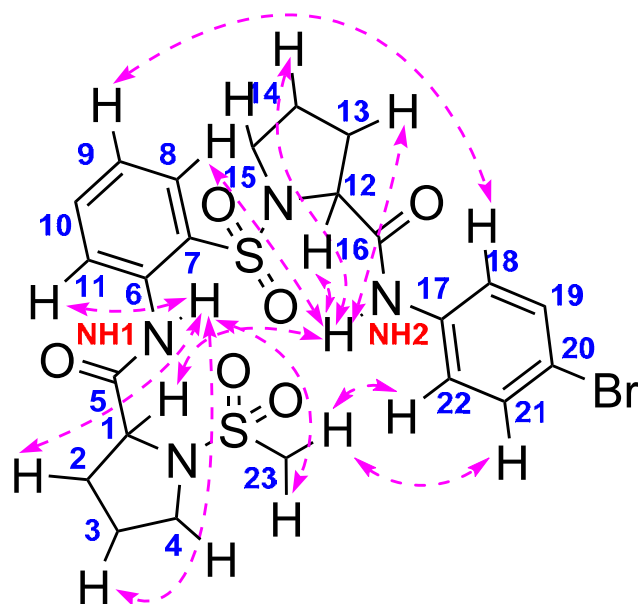
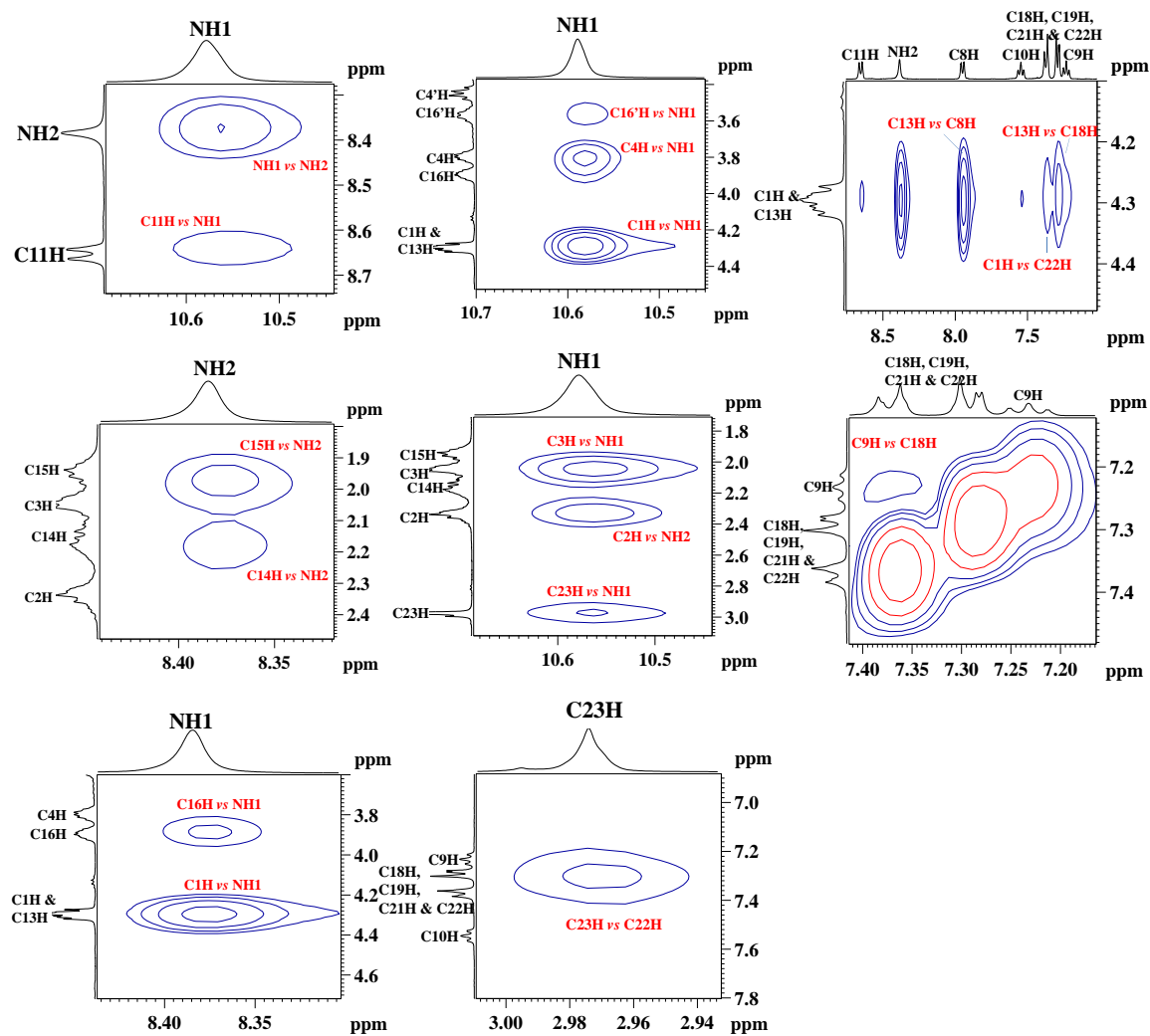
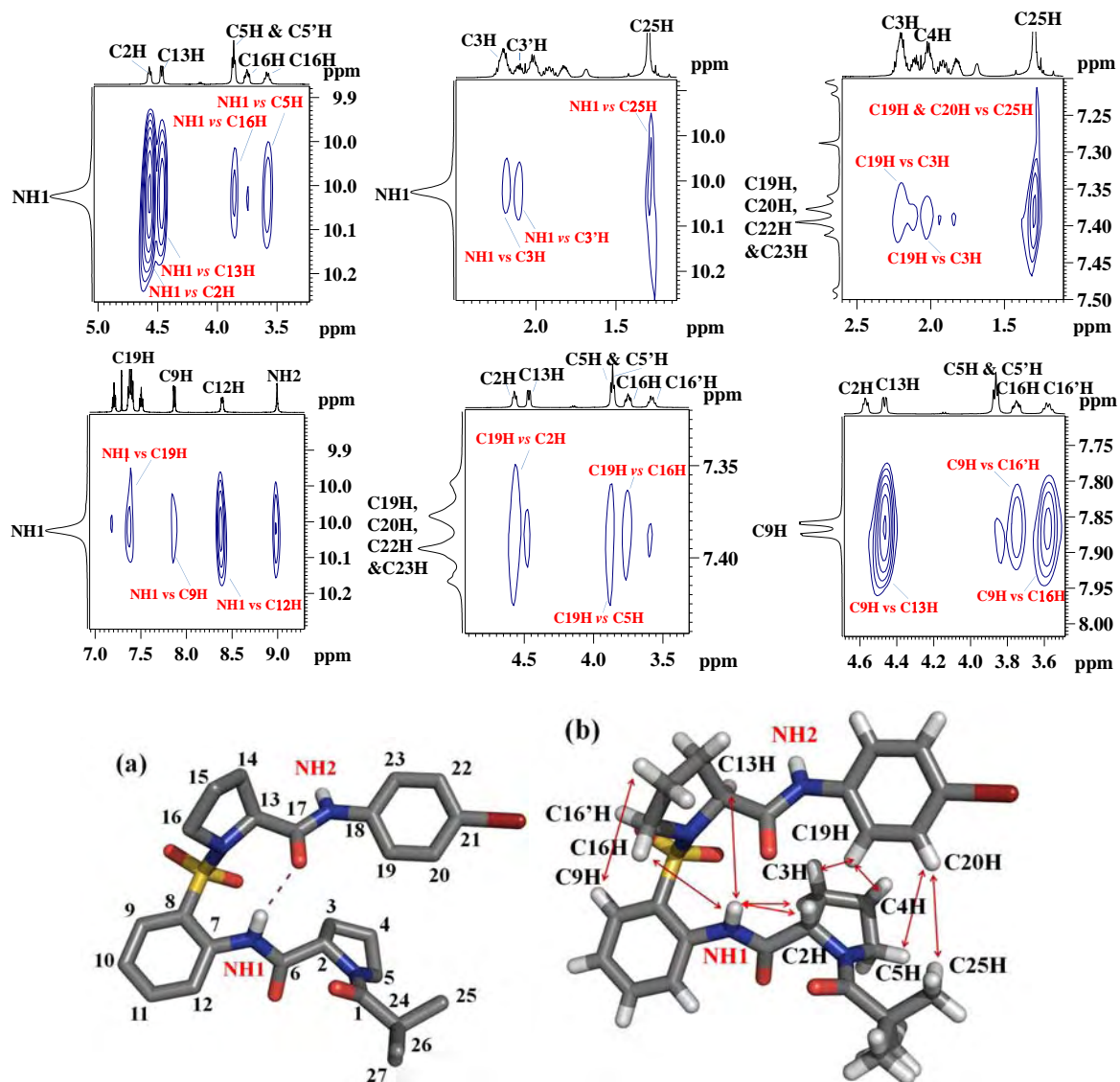
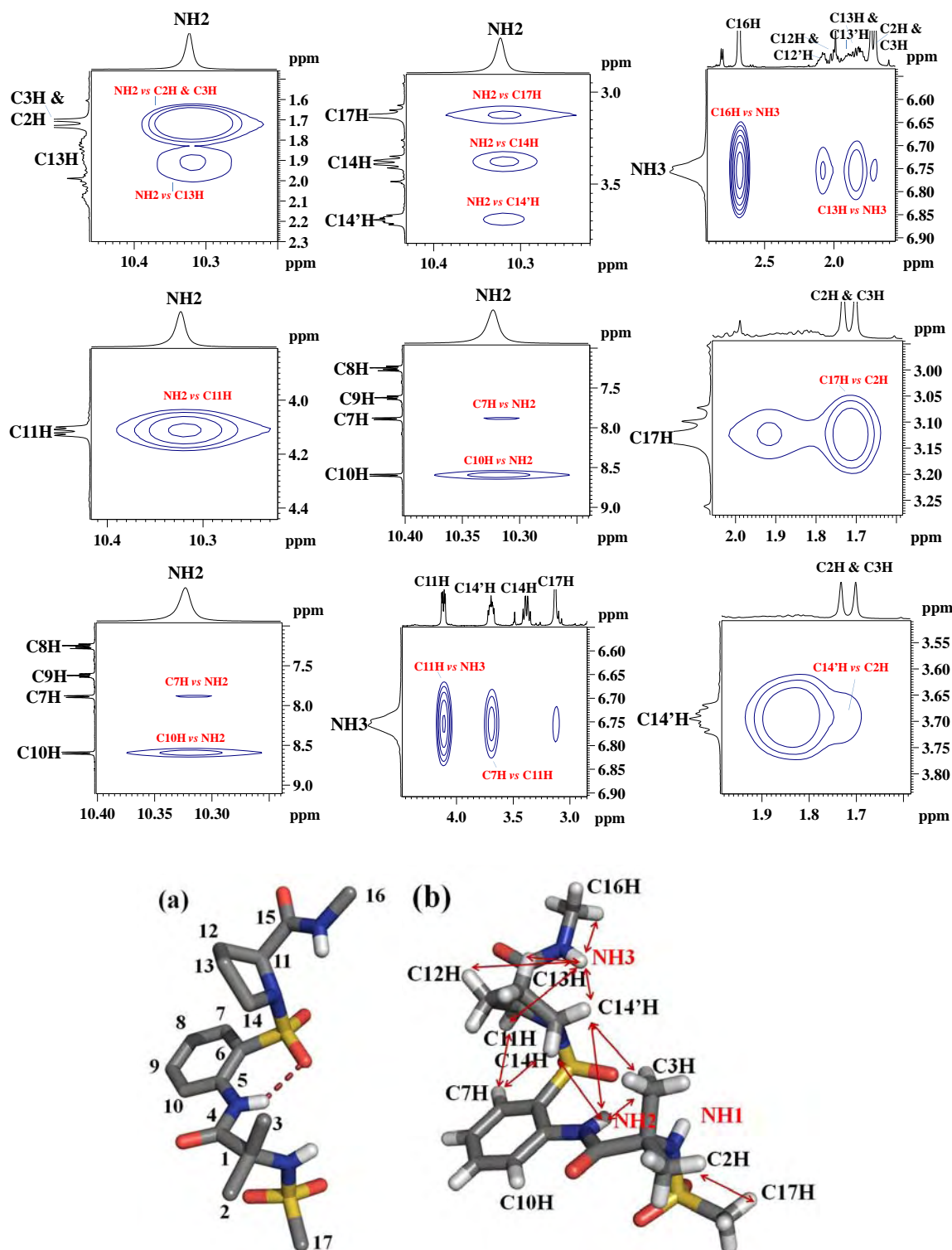


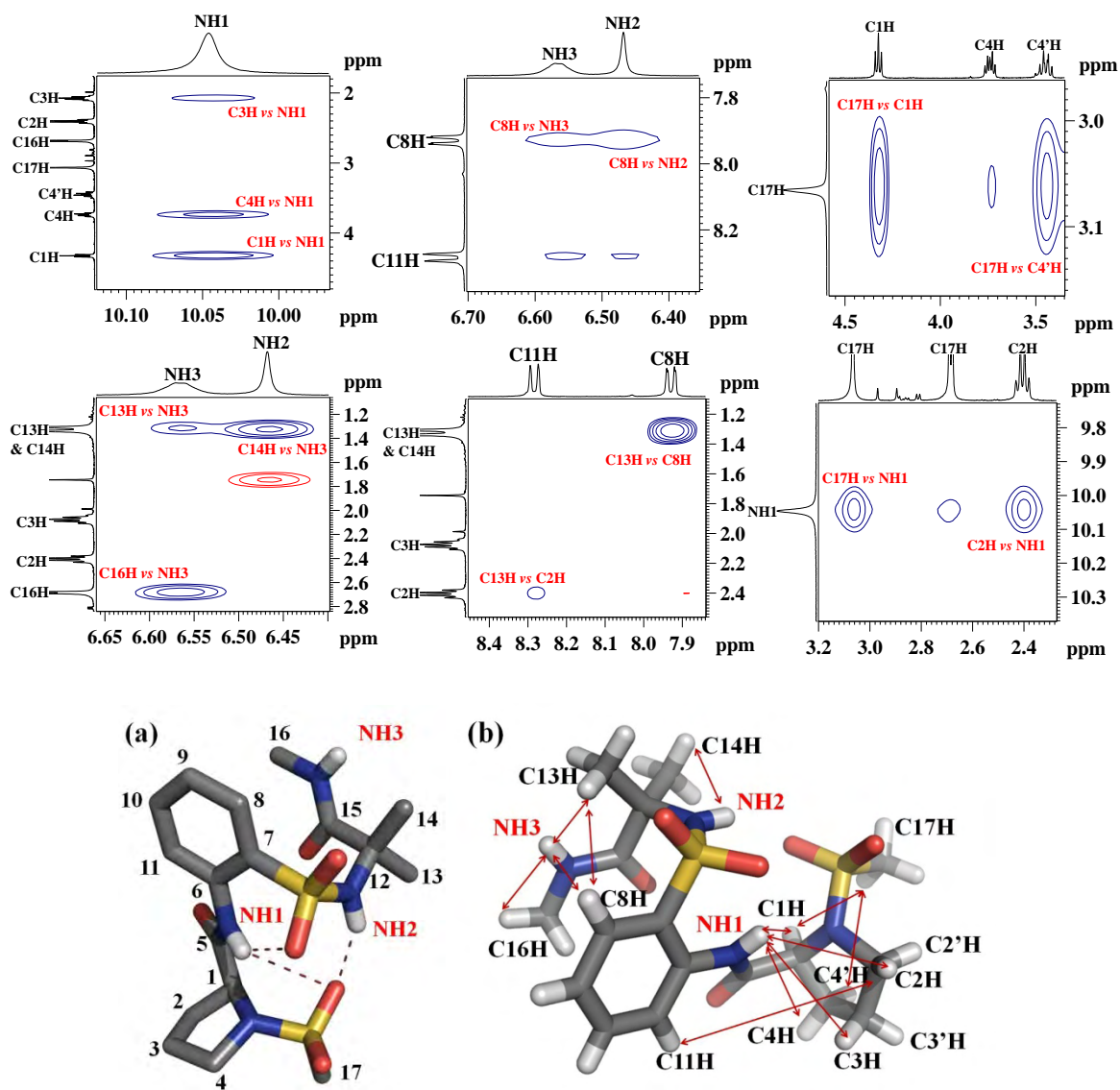
Figure 31: Partial 2D NOESY extracts of **2** (500MHz, CDCl<sub>3</sub>).



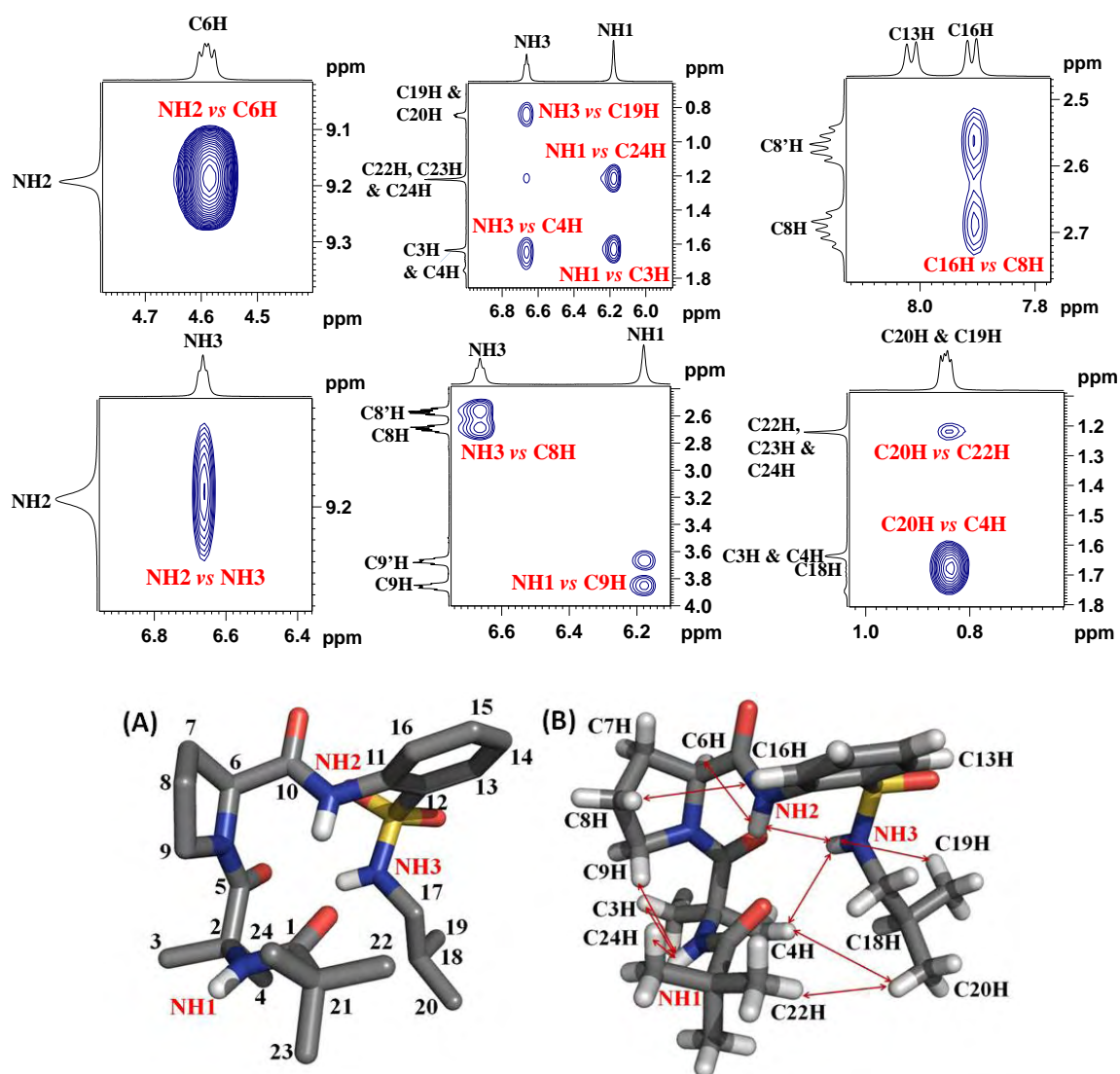
**Figure 32:** Partial 2D NOESY extracts of **3** (500MHz,  $\text{CDCl}_3$ ) - PyMOL rendered crystal structures of **3** with numbering (a) and showing NOE interactions (b).



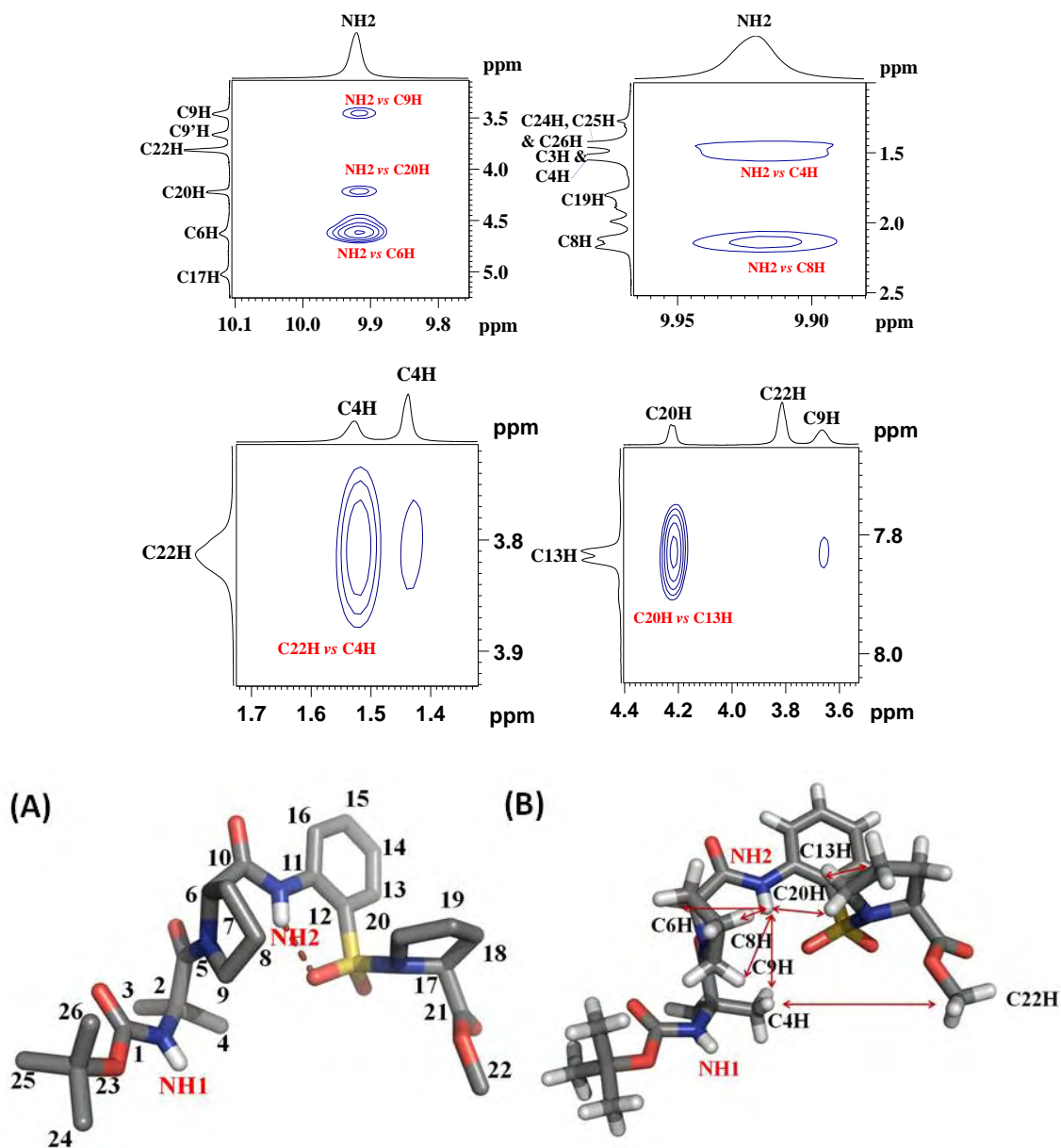
**Figure 33:** Partial 2D NOESY extracts of 4 (500MHz, CDCl<sub>3</sub>) - PyMOL rendered crystal structures of 4; with numbering (a) and NOE interactions (b).



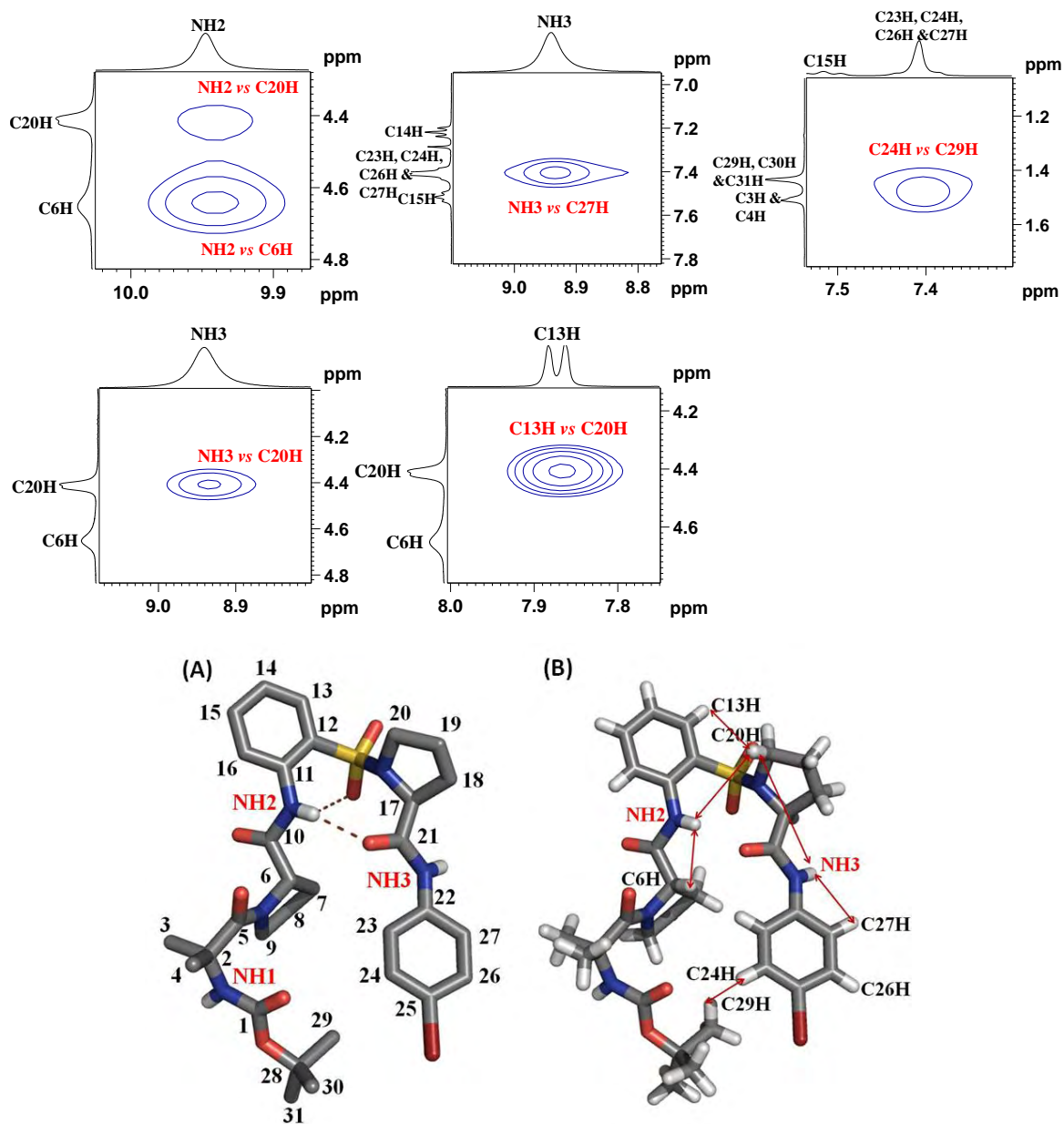
**Figure 34:** Partial 2D NOESY extracts of **5** (500MHz, CDCl<sub>3</sub>) - PyMOL rendered crystal structures of **5**; with numbering (a) and with NOE interactions (b).



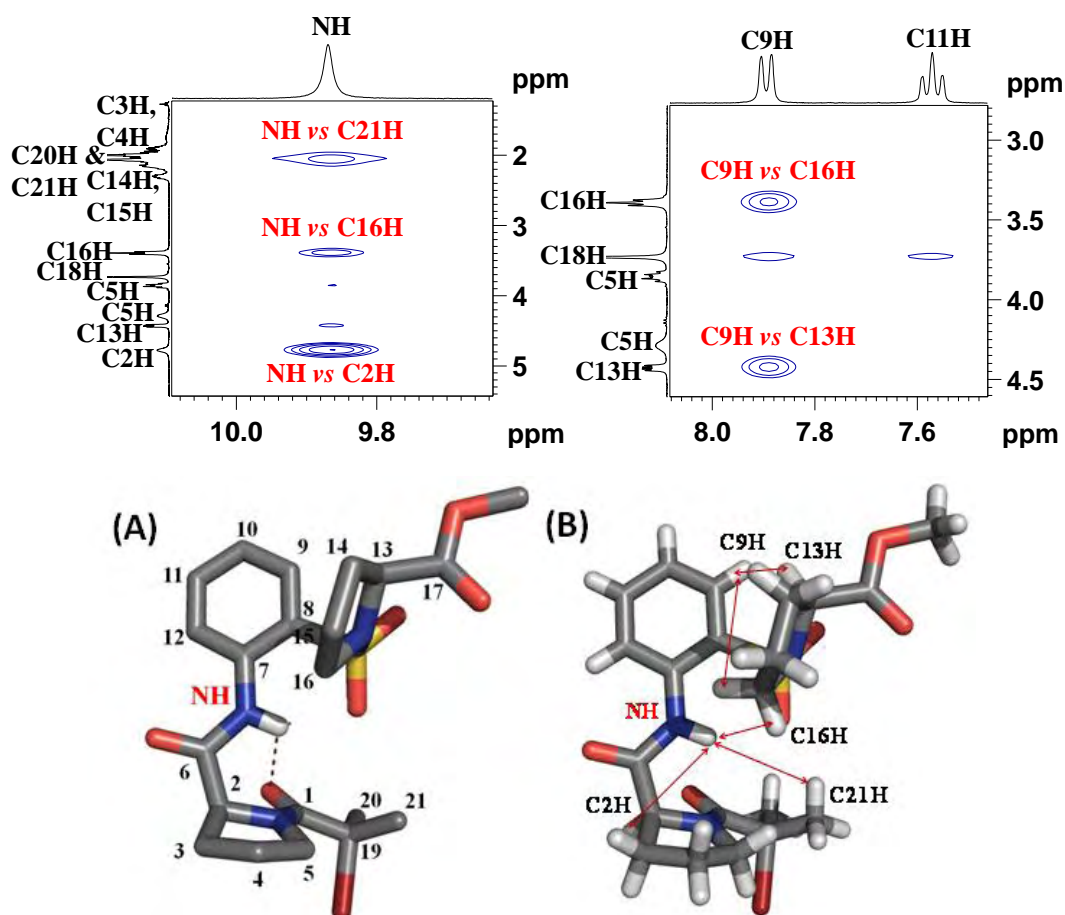
**Figure 35:** Partial 2D NOESY extracts of **21** (500MHz,  $\text{CDCl}_3$ ) - PyMOL rendered crystal structures of **21**; with numbering (A) and NOE interactions (B).



**Figure 36:** Partial 2D NOESY extracts of **22** (500MHz,  $\text{CDCl}_3$ ) - PyMOL rendered crystal structures of **22**; with numbering (A) and NOE interactions (B).



**Figure 37:** Partial 2D NOESY extracts of **24** (500MHz, CDCl<sub>3</sub>) - PyMOL rendered crystal structures of **24**; with numbering (A) and NOE interactions (B).

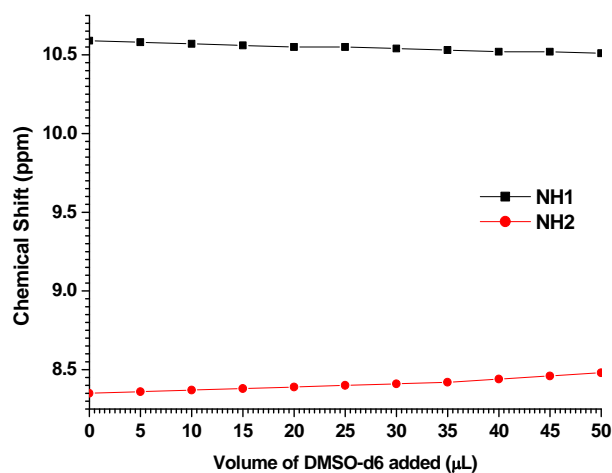


**Figure 38:** Partial 2D NOESY extracts of **26** (500MHz, CDCl<sub>3</sub>). - PyMOL rendered crystal structures of **26**; with numbering (A) and NOE interactions (B).

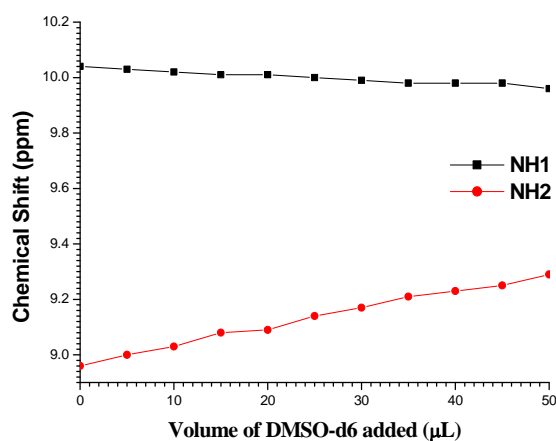


**Table 1:** NMR DMSO-*d*<sub>6</sub> titration studies of **2** (5mM, 400MHz, CDCl<sub>3</sub>).

No:	V <sub>DMSO-d6</sub> (in μ lit)	δNH1	δNH2
1	0	10.59	8.35
2	5	10.58	8.36
3	10	10.57	8.37
4	15	10.56	8.38
5	20	10.55	8.39
6	25	10.55	8.40
7	30	10.54	8.41
8	35	10.53	8.42
9	40	10.52	8.44
10	45	10.52	8.46
11	50	10.51	8.48

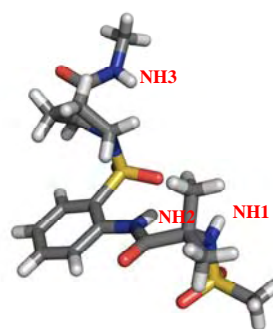
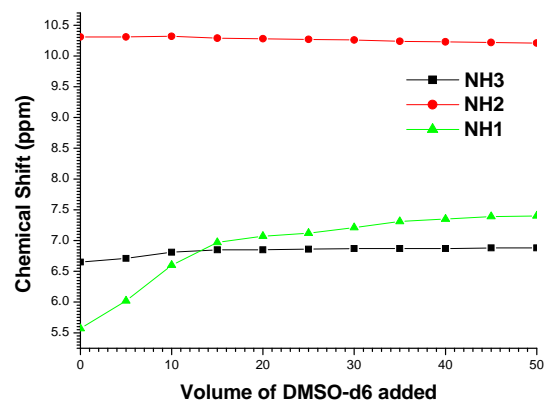
**Table 2:** NMR DMSO-*d*<sub>6</sub> titration studies of **3** (5mM, 400MHz, CDCl<sub>3</sub>).

No:	V <sub>DMSO-d6</sub> (in μ lit)	δNH1	δNH2
1	0	10.04	8.96
2	5	10.03	9.00
3	10	10.02	9.03
4	15	10.01	9.08
5	20	10.01	9.09
6	25	10.0	9.14
7	30	9.99	9.17
8	35	9.98	9.21
9	40	9.98	9.23
10	45	9.98	9.25
11	50	9.96	9.29

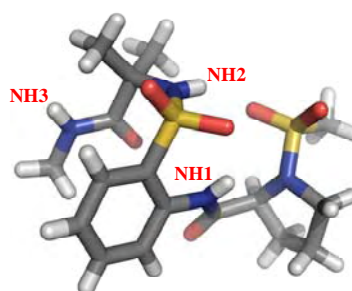
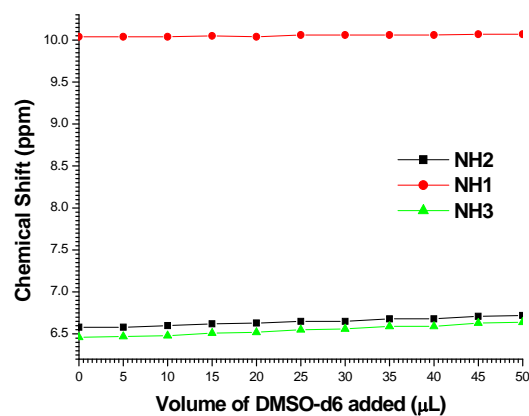


**Table 3:** NMR DMSO- $d_6$  titration studies of **4** (5mM, 400MHz,  $CDCl_3$ ).

No:	$V_{DMSO-d_6}$ (in $\mu$ lit)	$\delta_{NH3}$	$\delta_{NH2}$	$\delta_{NH1}$
1	0	6.65	10.31	5.57
2	5	6.71	10.31	6.02
3	10	6.81	10.32	6.60
4	15	6.85	10.29	6.97
5	20	6.85	10.28	7.07
6	25	6.86	10.27	7.12
7	30	6.87	10.26	7.21
8	35	6.87	10.24	7.31
9	40	6.87	10.23	7.35
10	45	6.88	10.22	7.39
11	50	6.88	10.21	7.40

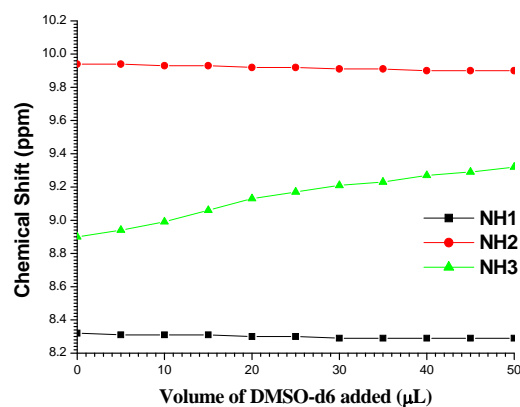
**Table 4:** NMR DMSO- $d_6$  titration studies of **5** (5mM, 400MHz,  $CDCl_3$ ).

No:	$V_{DMSO-d_6}$ (in $\mu$ lit)	$\delta_{NH2}$	$\delta_{NH1}$	$\delta_{NH3}$
1	0	10.04	6.46	6.58
2	5	10.04	6.47	6.58
3	10	10.04	6.48	6.60
4	15	10.05	6.51	6.62
5	20	10.04	6.52	6.63
6	25	10.06	6.55	6.65
7	30	10.06	6.56	6.65
8	35	10.06	6.59	6.68
9	40	10.06	6.59	6.68
10	45	10.07	6.63	6.71
11	50	10.07	6.64	6.72

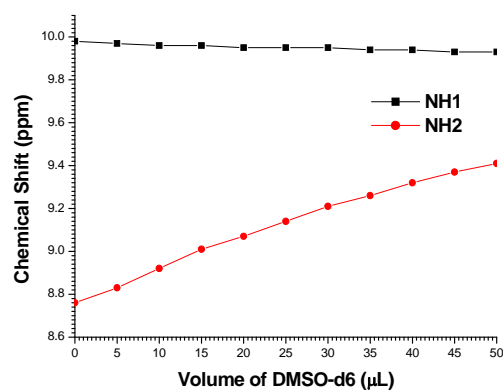


**Table 5:** NMR DMSO- $d_6$  titration studies of **24** (5mM, 400MHz,  $CDCl_3$ ).

No:	$V_{DMSO-d_6}$ (in $\mu$ lit)	$\delta_{NH1}$	$\delta_{NH2}$	$\delta_{NH3}$
1	0	8.32	9.94	8.9
2	5	8.31	9.94	8.94
3	10	8.31	9.93	8.99
4	15	8.31	9.93	9.06
5	20	8.30	9.92	9.13
6	25	8.30	9.92	9.17
7	30	8.29	9.91	9.21
8	35	8.29	9.91	9.23
9	40	8.29	9.90	9.27
10	45	8.29	9.90	9.29
11	50	8.29	9.90	9.32

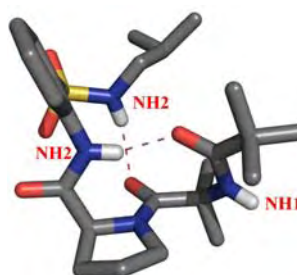
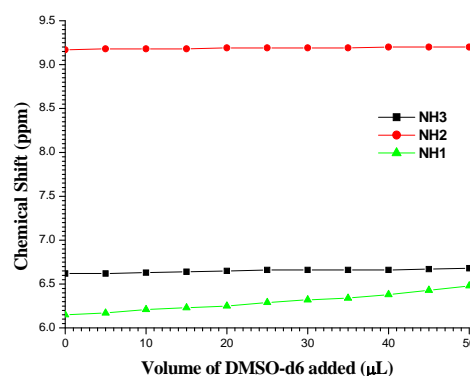
**Table 6:** NMR DMSO- $d_6$  titration studies of **25** (5mM, 400MHz,  $CDCl_3$ ).

No:	$V_{DMSO-d_6}$ (in $\mu$ lit)	$\delta_{NH1}$	$\delta_{NH2}$
1	0	9.98	8.76
2	5	9.97	8.83
3	10	9.96	8.92
4	15	9.96	9.01
5	20	9.95	9.07
6	25	9.95	9.14
7	30	9.95	9.21
8	35	9.94	9.26
9	40	9.94	9.32
10	45	9.93	9.37
11	50	9.93	9.41

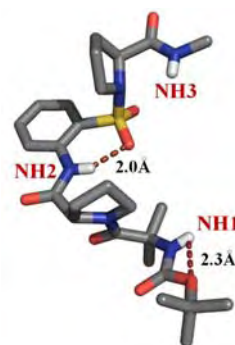
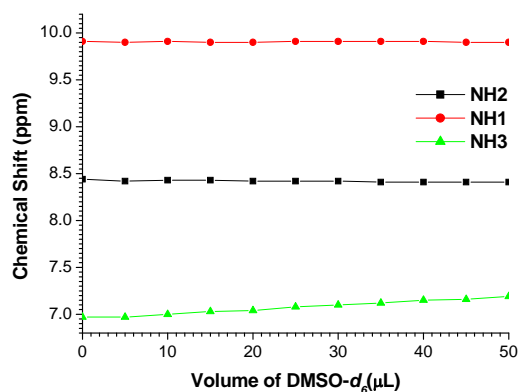


**Table 7:** NMR DMSO-*d*<sub>6</sub> titration studies of **21** (5mM, 400MHz, CDCl<sub>3</sub>).

No:	V <sub>DMSO-d6</sub> (in μ lit)	δNH3	δNH2	δNH1
1	0	6.62	9.17	6.15
2	5	6.62	9.18	6.17
3	10	6.63	9.18	6.21
4	15	6.64	9.18	6.23
5	20	6.65	9.19	6.25
6	25	6.66	9.19	6.29
7	30	6.66	9.19	6.32
8	35	6.66	9.19	6.34
9	40	6.66	9.20	6.38
10	45	6.67	9.20	6.43
11	50	6.68	9.20	6.48

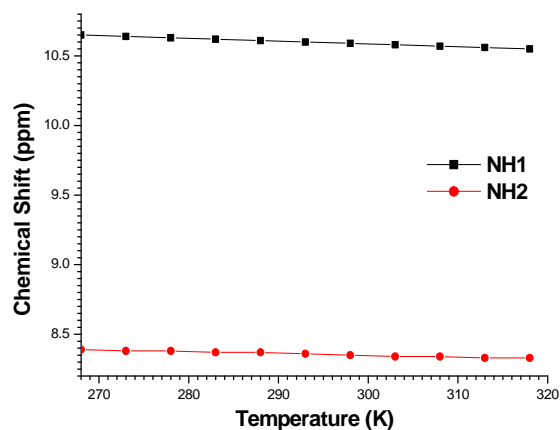
**Table 8:** NMR DMSO-*d*<sub>6</sub> titration studies of **23** (5mM, 400MHz, CDCl<sub>3</sub>).

No:	V <sub>DMSO-d6</sub> (in μ lit)	δNH1	δNH2	δNH3
1	0	8.44	9.91	6.97
2	5	8.42	9.90	6.97
3	10	8.43	9.91	7.00
4	15	8.43	9.90	7.03
5	20	8.42	9.90	7.04
6	25	8.42	9.91	7.08
7	30	8.42	9.91	7.10
8	35	8.41	9.91	7.12
9	40	8.41	9.91	7.15
10	45	8.41	9.90	7.16
11	50	8.41	9.90	7.19

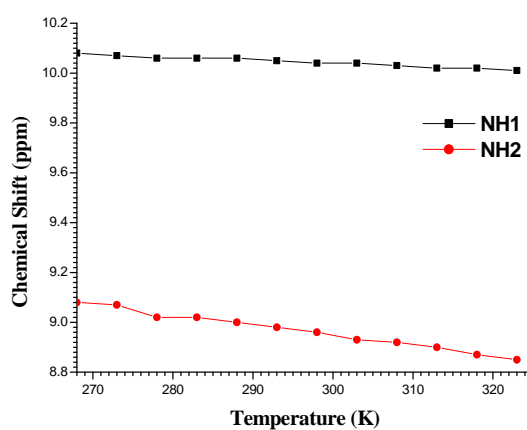


**Table 9:** NMR variable temperature studies of **2** (5mM, 400MHz, CDCl<sub>3</sub>).

No:	Temperature (K)	δNH1	δNH2
1	268	10.65	8.39
2	273	10.64	8.38
3	278	10.63	8.38
4	283	10.62	8.37
5	288	10.61	8.37
6	293	10.60	8.36
7	298	10.59	8.35
8	303	10.58	8.34
9	308	10.57	8.34
10	313	10.56	8.33
11	318	10.55	8.33
12	323	10.54	8.32

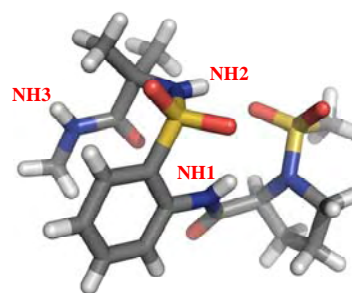
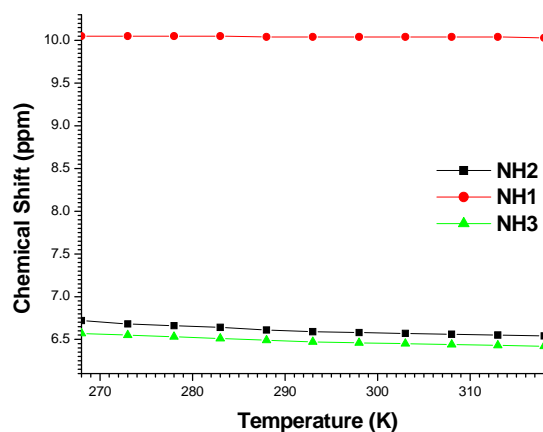
**Table 10:** NMR variable temperature studies of **3** (5mM, 400MHz, CDCl<sub>3</sub>).

No:	Temperature (K)	δNH1	δNH2
1	268	10.08	9.08
2	273	10.07	9.07
3	278	10.06	9.02
4	283	10.06	9.02
5	288	10.06	9.00
6	293	10.05	8.98
7	298	10.04	8.96
8	303	10.04	8.93
9	308	10.03	8.92
10	313	10.02	8.90
11	318	10.02	8.87
12	323	10.01	8.85

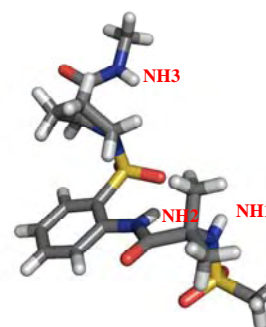
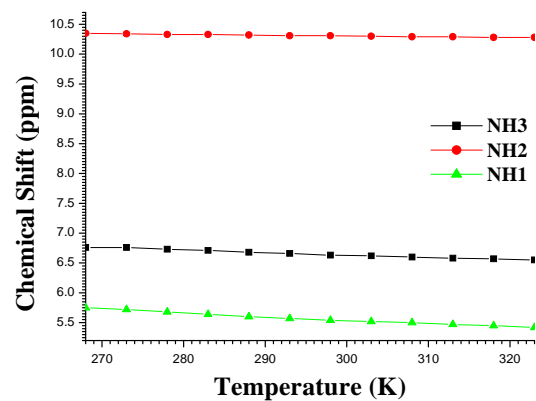


**Table 11:** NMR variable temperature studies of **5** (5mM, 400MHz, CDCl<sub>3</sub>).

No:	Temperature (K)	$\delta$ NH2	$\delta$ NH1	$\delta$ NH3
1	268	6.72	10.05	6.57
2	273	6.68	10.05	6.55
3	278	6.66	10.05	6.53
4	283	6.64	10.05	6.51
5	288	6.61	10.04	6.49
6	293	6.59	10.04	6.47
7	298	6.58	10.04	6.46
8	303	6.57	10.04	6.45
9	308	6.56	10.04	6.44
10	313	6.55	10.04	6.43
11	318	6.54	10.03	6.42
12	323	6.53	10.03	6.40

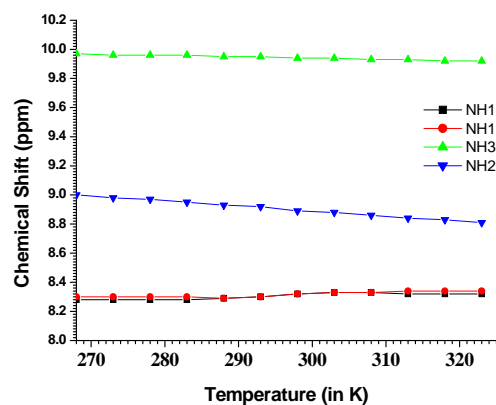
**Table 12:** NMR variable temperature studies of **4** (5mM, 400MHz, CDCl<sub>3</sub>).

No:	Temperature (K)	$\delta$ NH3	$\delta$ NH2	$\delta$ NH1
1	268	6.76	10.35	5.75
2	273	6.76	10.34	5.72
3	278	6.73	10.33	5.68
4	283	6.71	10.33	5.64
5	288	6.68	10.32	5.60
6	293	6.66	10.31	5.57
7	298	6.63	10.31	5.54
8	303	6.62	10.30	5.52
9	308	6.60	10.29	5.50
10	313	6.58	10.29	5.47
11	318	6.57	10.28	5.45
12	323	6.55	10.28	5.42



**Table 13:** NMR variable temperature studies of **24** (5mM, 400MHz, CDCl<sub>3</sub>).

No:	Temperature (K)	$\delta$ NH1	$\delta$ NH2	$\delta$ NH3
1	268	8.28, 8.30	9.97	9.00
2	273	8.28, 8.30	9.96	8.98
3	278	8.28, 8.30	9.96	8.97
4	283	8.28, 8.30	9.96	8.95
5	288	8.29	9.95	8.93
6	293	8.30	9.95	8.92
7	298	8.32	9.94	8.89
8	303	8.33	9.94	8.88
9	308	8.33	9.93	8.86
10	313	8.32, 8.34	9.93	8.84
11	318	8.32, 8.34	9.92	8.83
12	323	8.32, 8.34	9.92	8.81

**Table 14:** NMR variable temperature studies of **21** (5mM, 400MHz, CDCl<sub>3</sub>).

No:	Temperature (K)	$\delta$ NH3	$\delta$ NH2	$\delta$ NH1
1	268	6.74	9.18	6.16
2	273	6.71	9.17	6.16
3	278	6.69	9.17	6.16
4	283	6.67	9.17	6.15
5	288	6.65	9.17	6.15
6	293	6.64	9.17	6.15
7	298	6.62	9.17	6.15
8	303	6.61	9.18	6.16
9	308	6.59	9.17	6.15
10	313	6.57	9.17	6.15
11	318	6.56	9.18	6.14
12	323	6.55	9.17	6.14

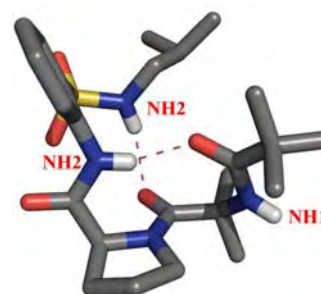
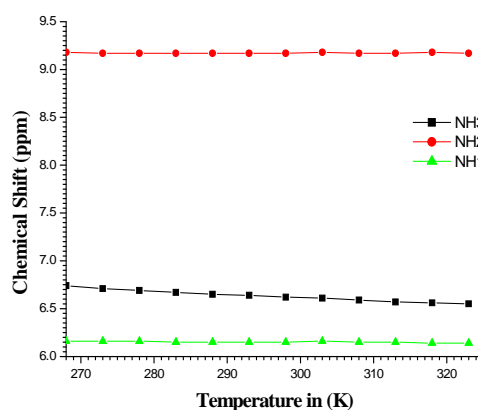
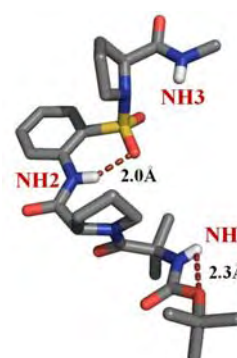
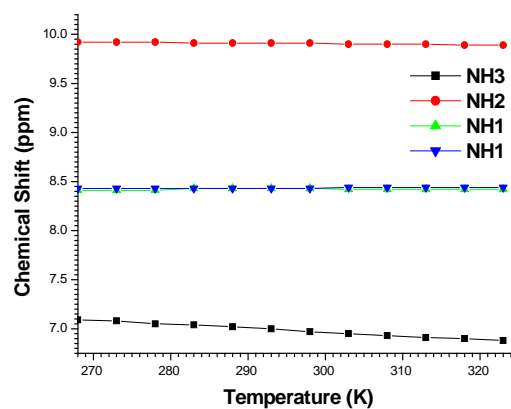


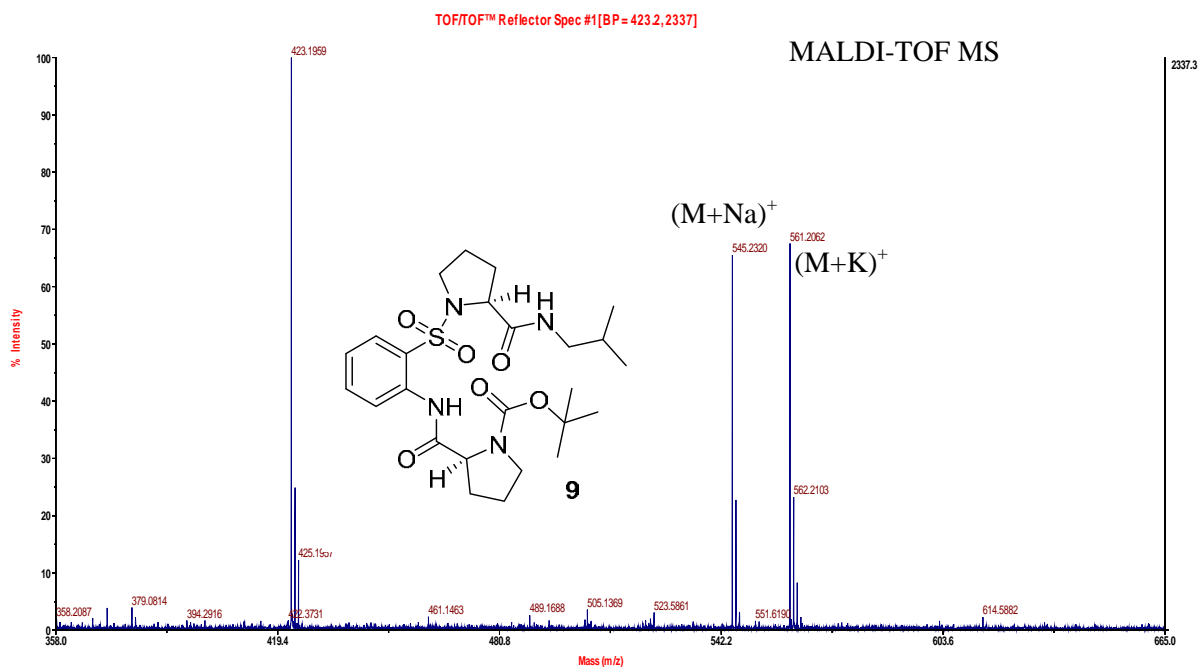
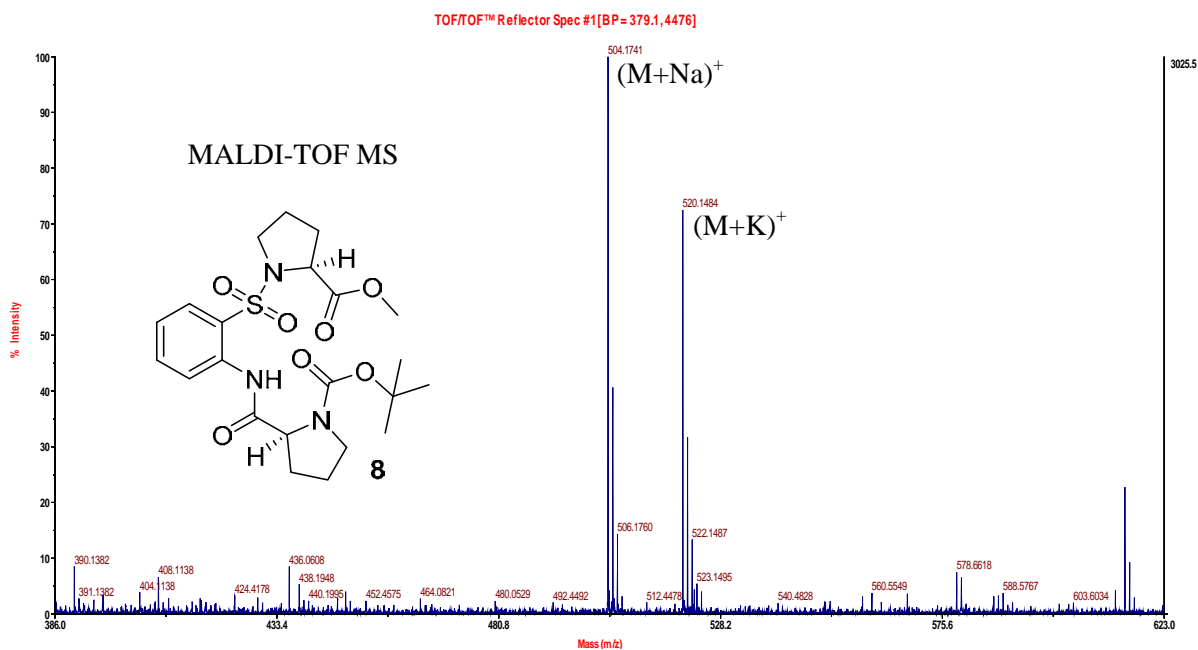
**Table 15:** NMR variable temperature studies of **23** (5mM, 400MHz, CDCl<sub>3</sub>).

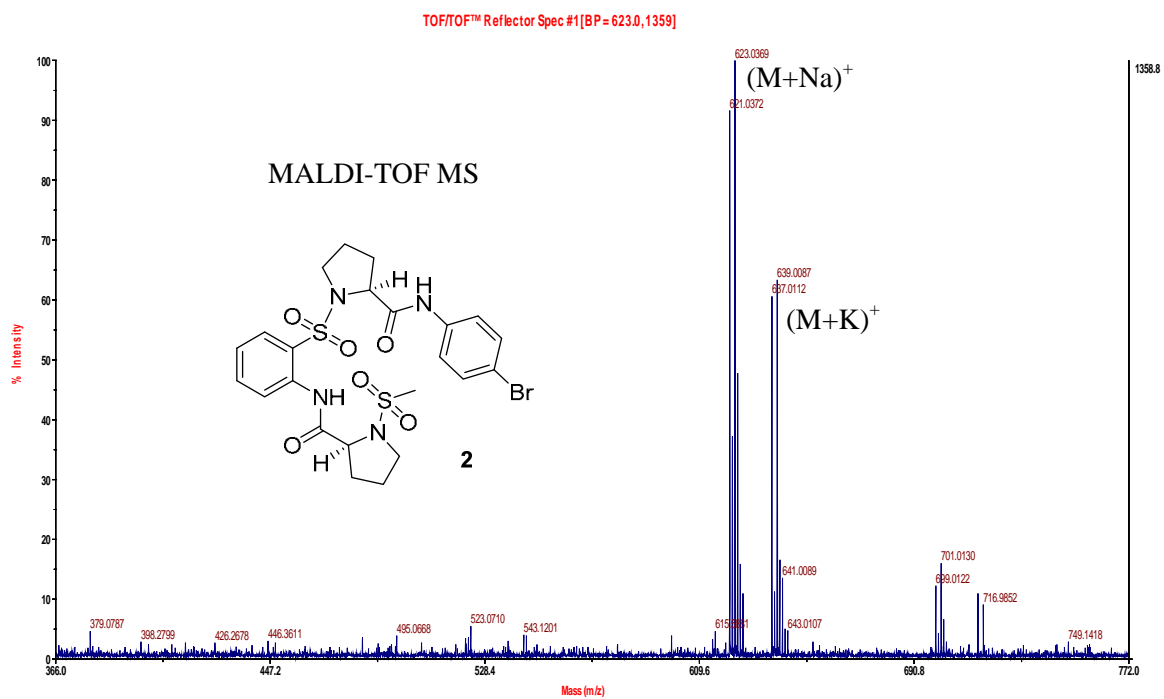
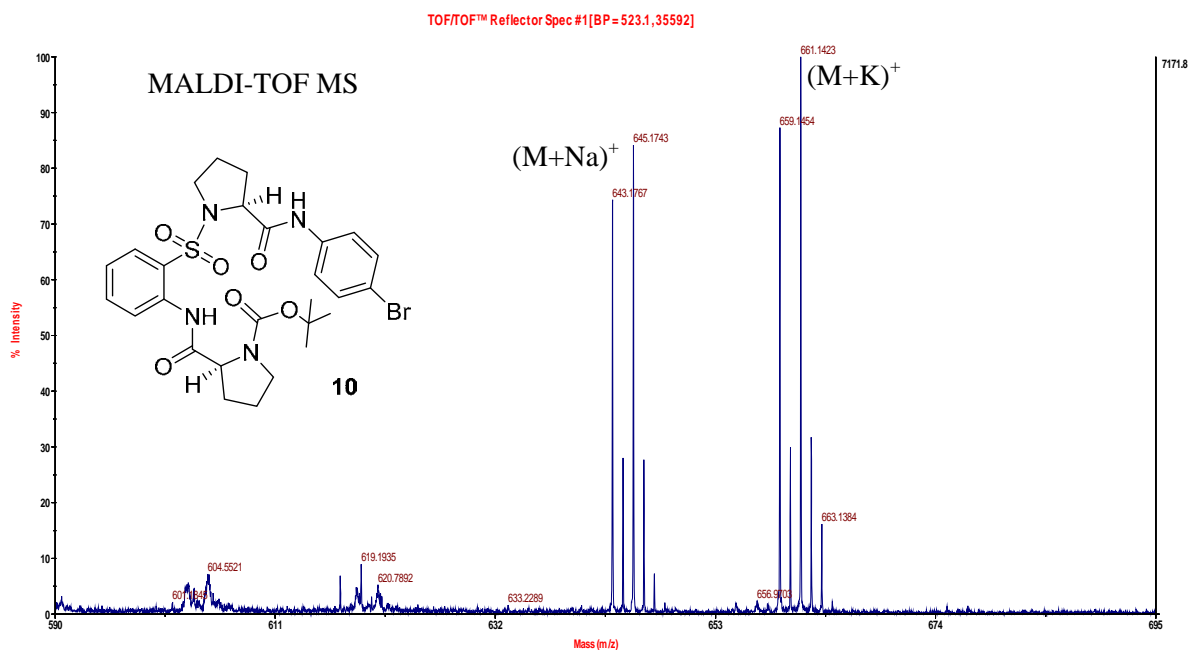
No:	Temperature (K)	$\delta$ NH3	$\delta$ NH2	$\delta$ NH1
1	268	7.09	9.92	8.41-8.43
2	273	7.08	9.92	8.41-8.43
3	278	7.05	9.92	8.41-8.43
4	283	7.04	9.91	8.43
5	288	7.02	9.91	8.43
6	293	7.00	9.91	8.43
7	298	6.97	9.91	8.43
8	303	6.95	9.90	8.42-8.44
9	308	6.93	9.90	8.42-8.44
10	313	6.91	9.90	8.42-8.44
11	318	6.90	9.89	8.42-8.44
12	323	6.88	9.89	8.42-8.44

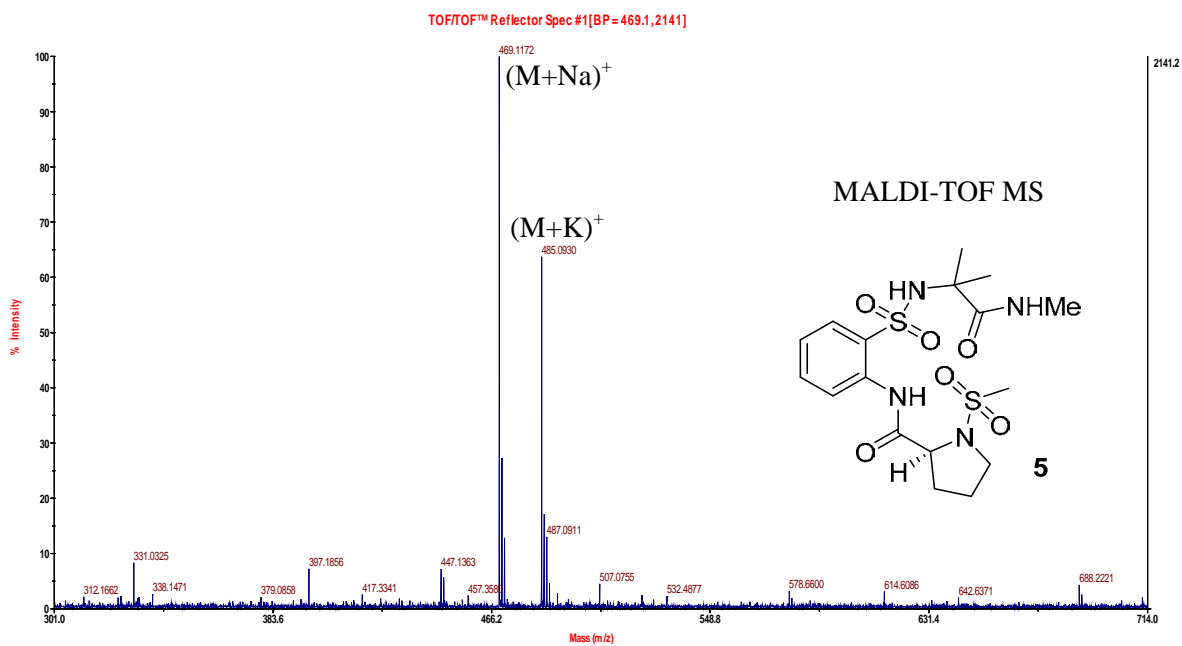
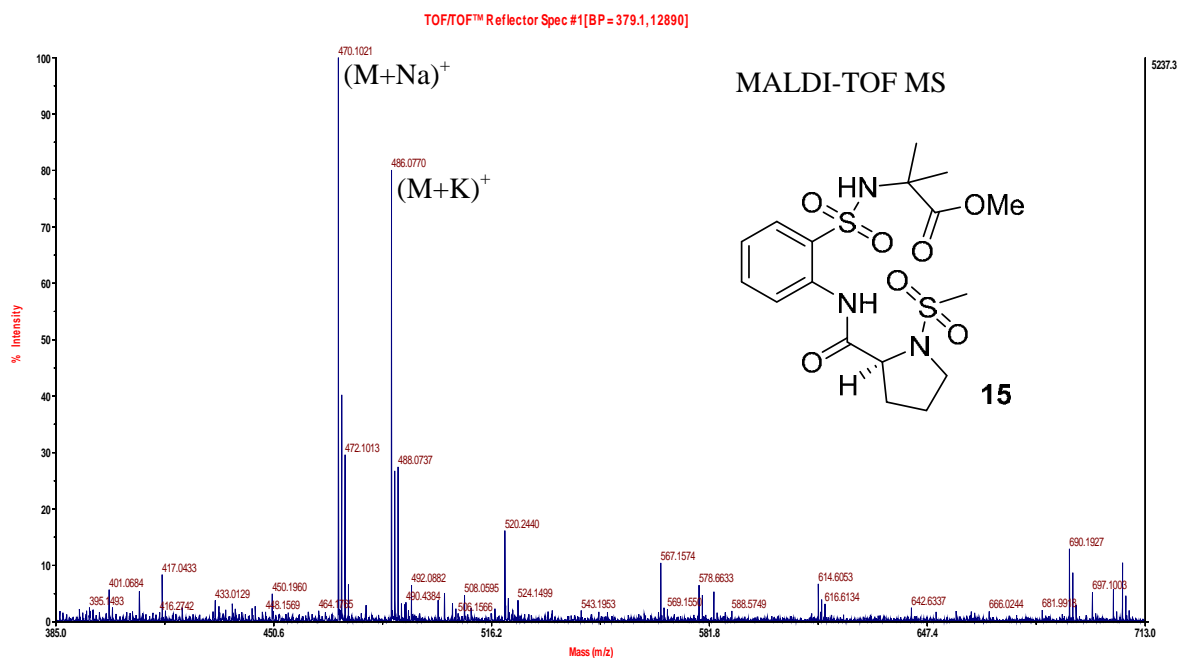


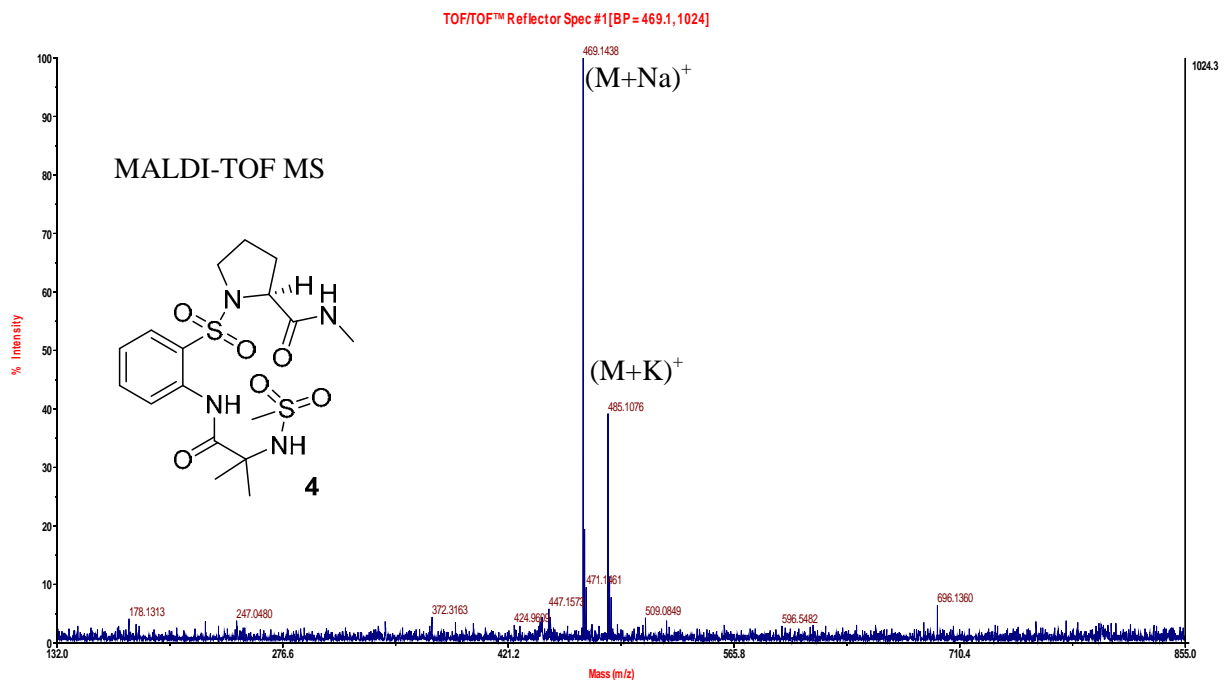
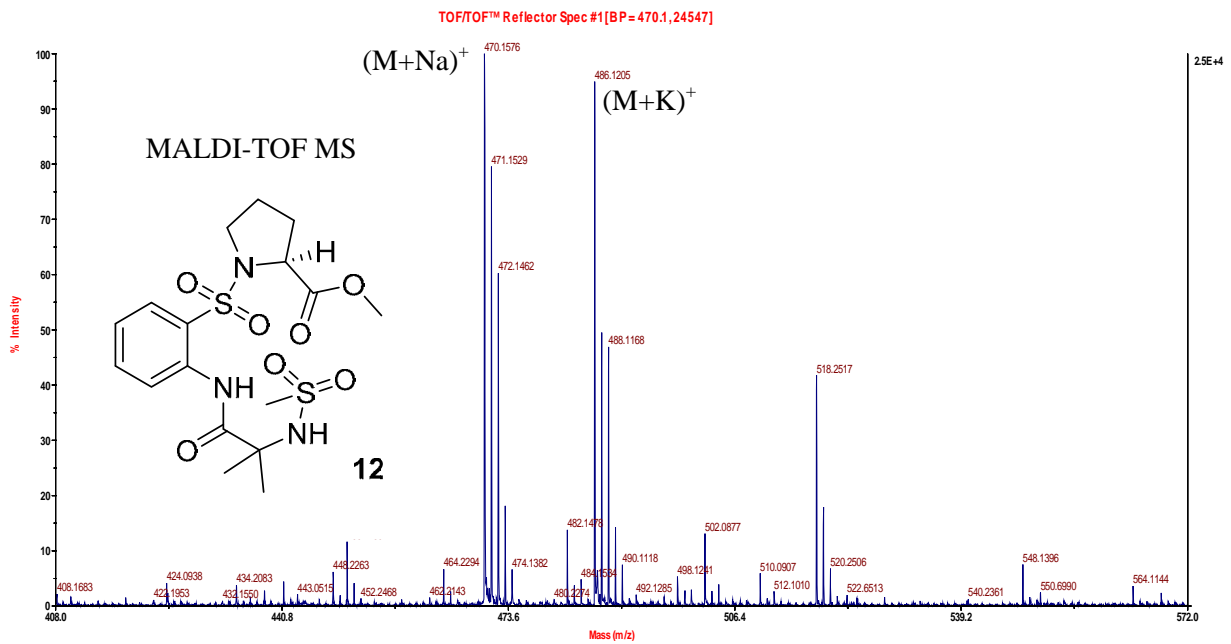
**NOTE:** Broad/Multiple set of signals seen are due to rotamer formation at the N-terminus (N-<sup>t</sup>BOC effect, *Chem. -Eur. J.*, 2008, 14, 6192)

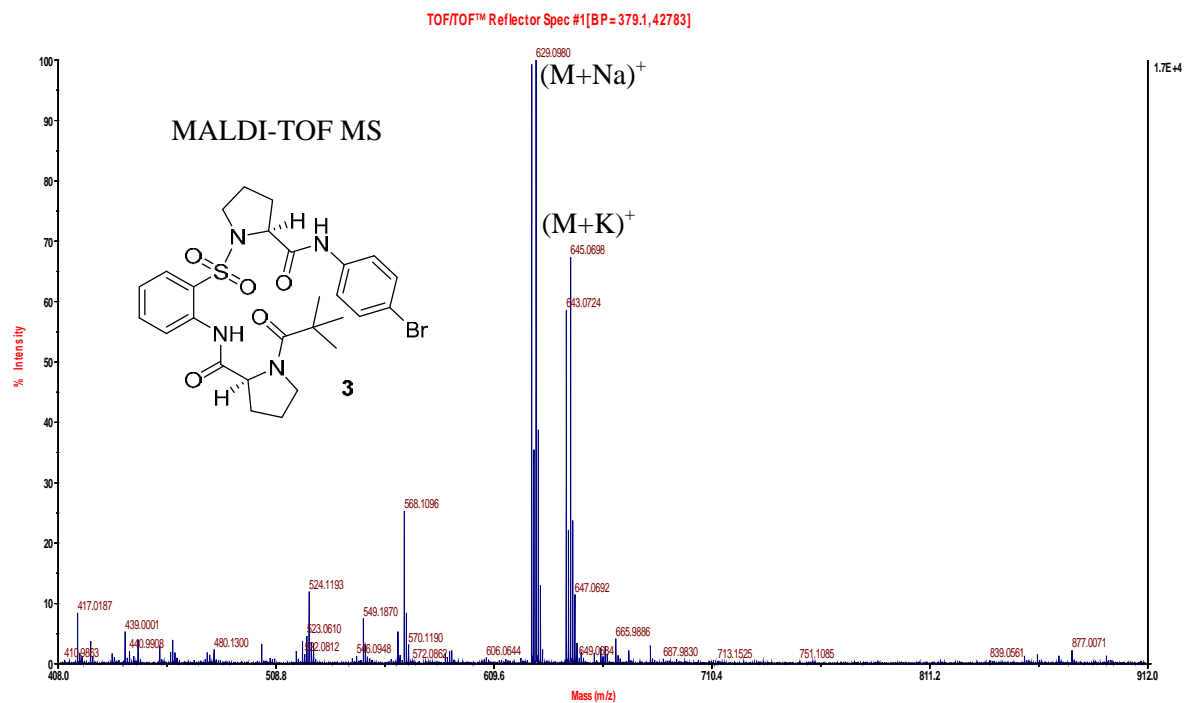
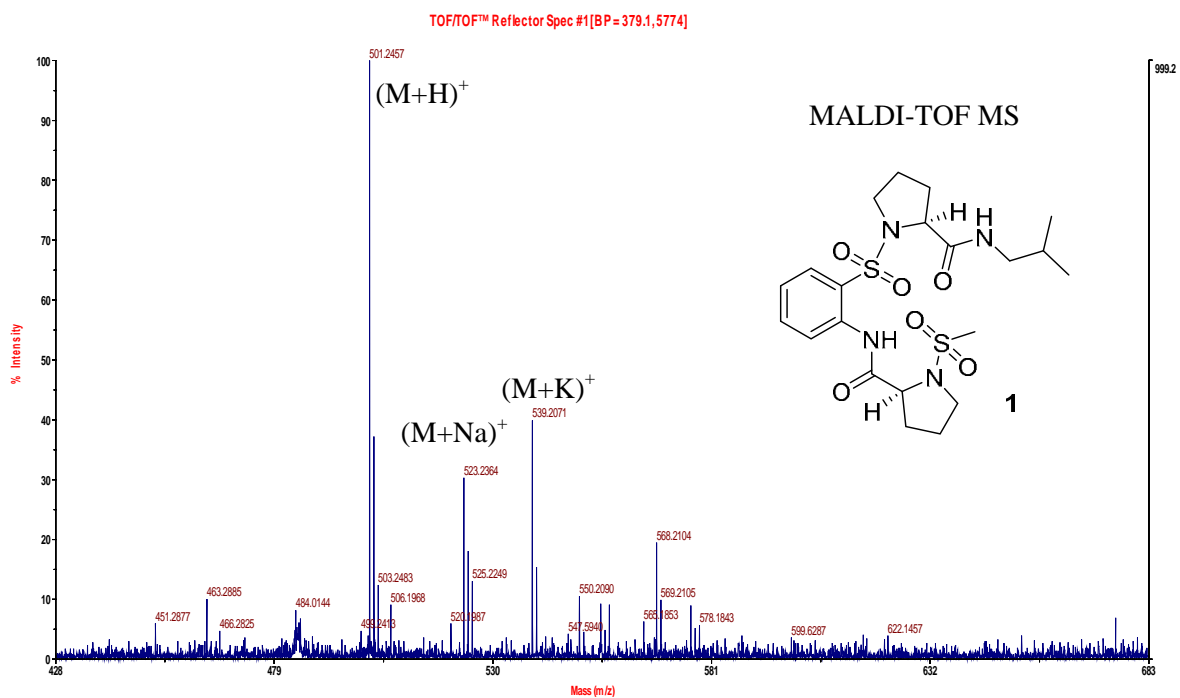


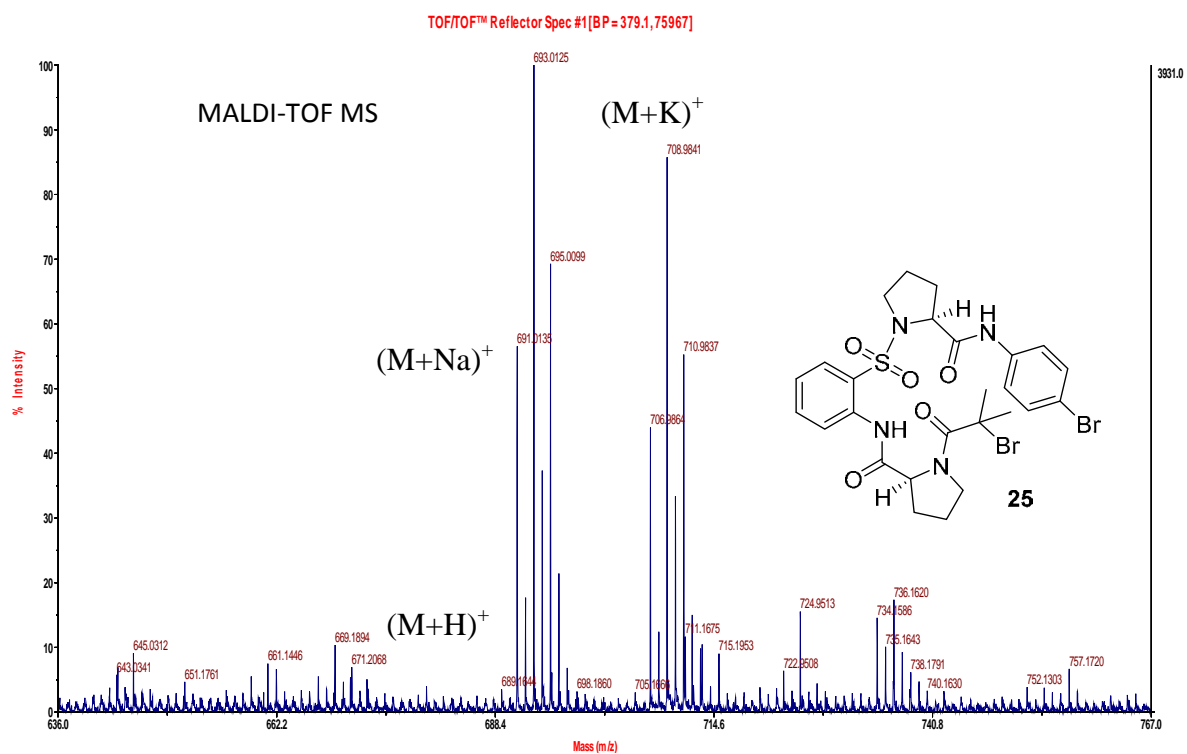
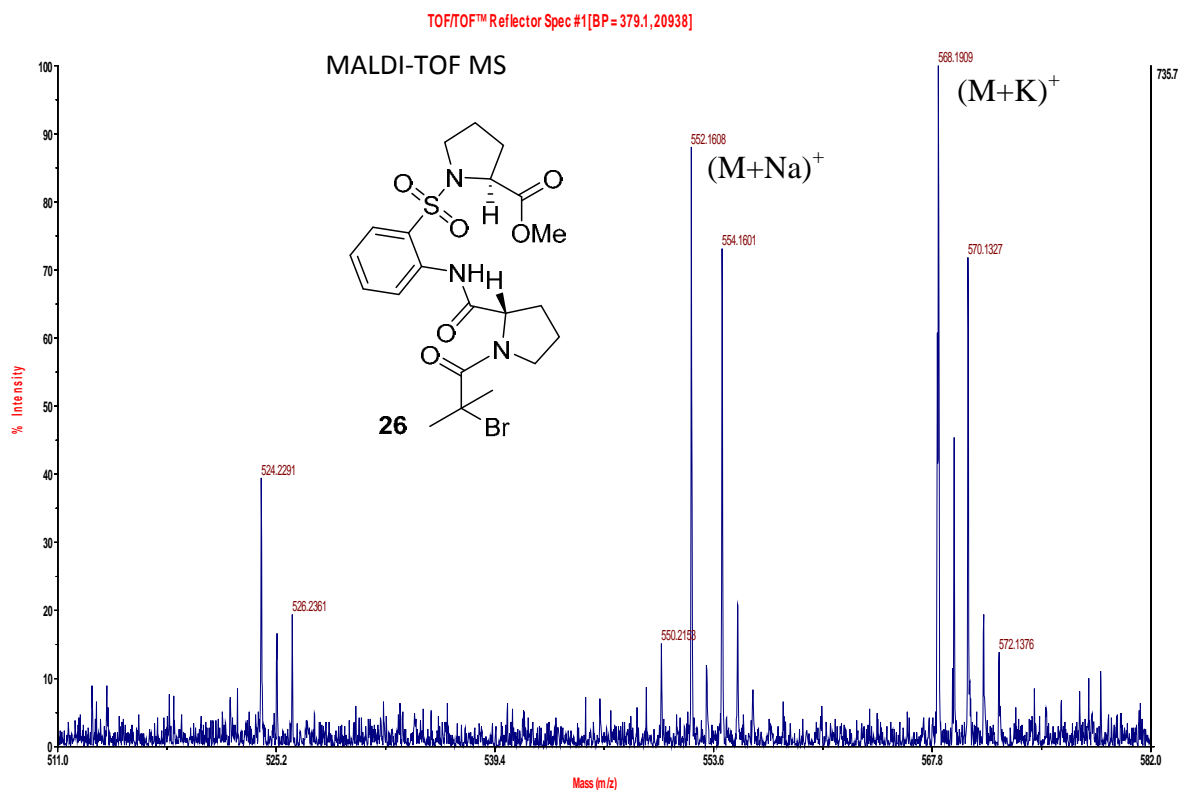


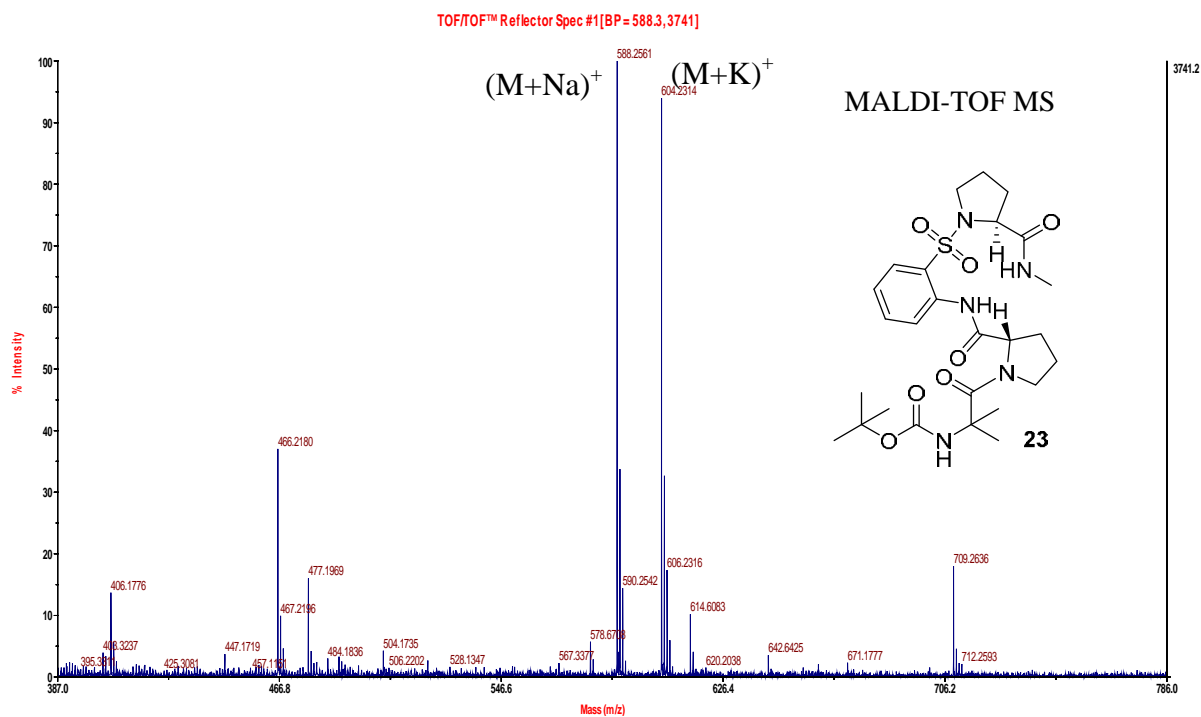
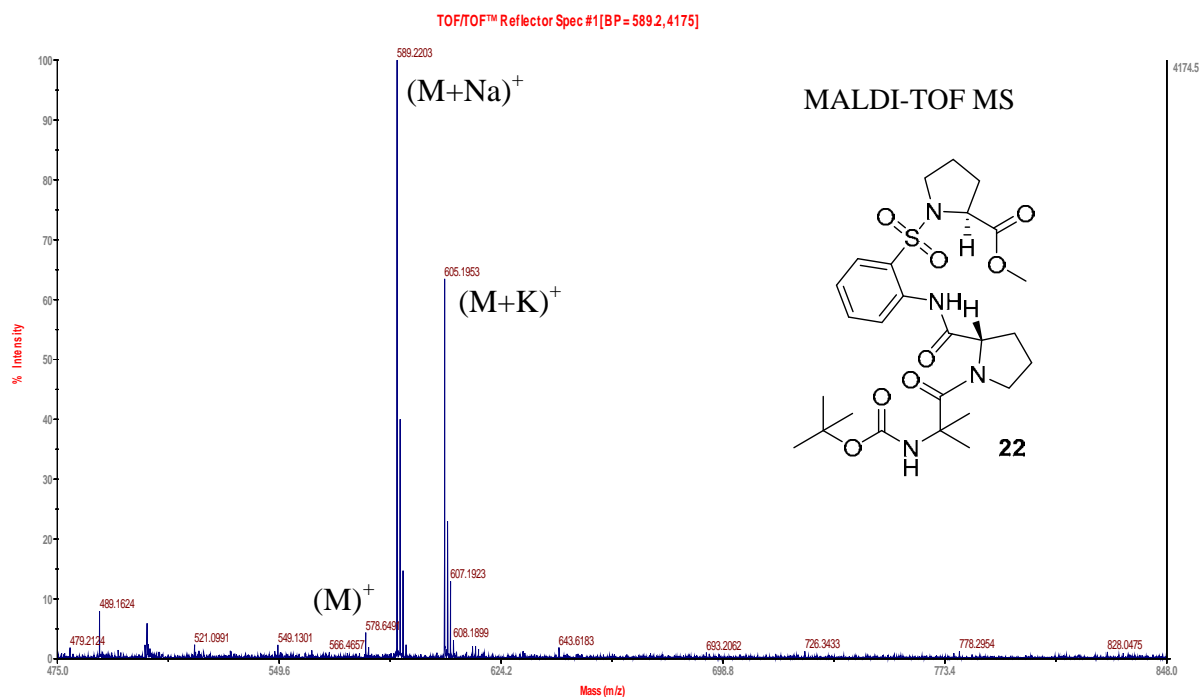


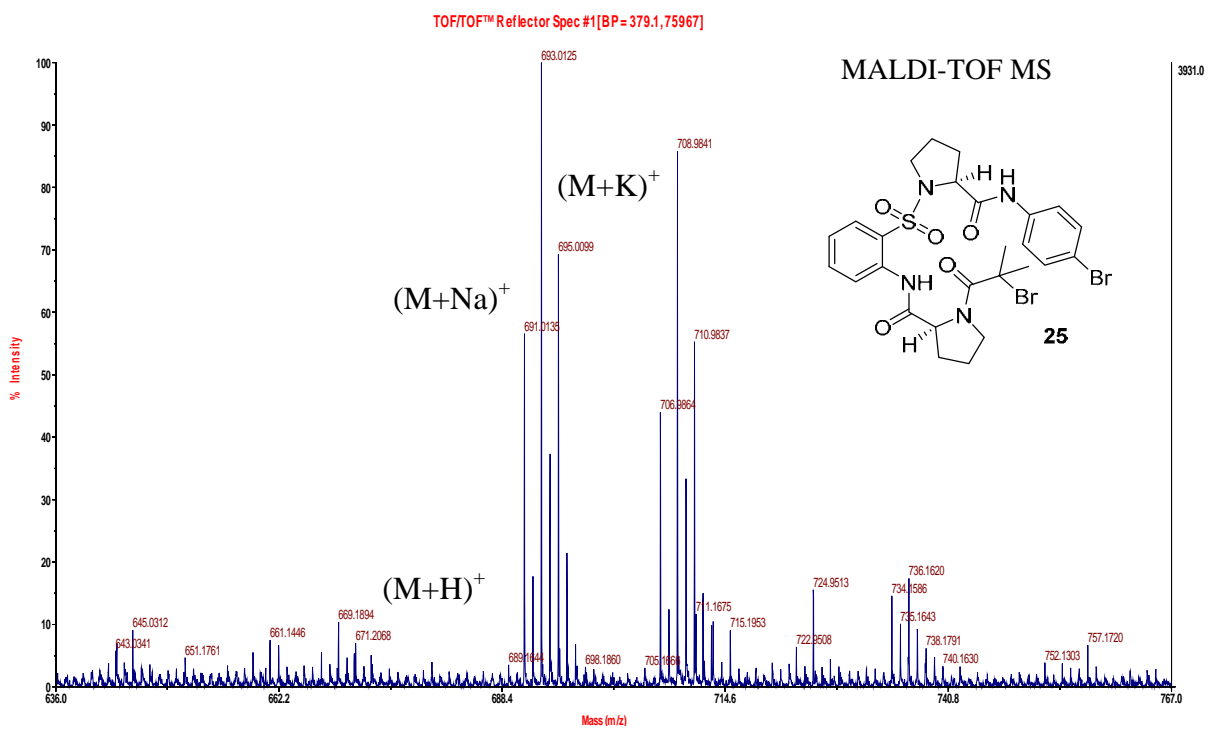
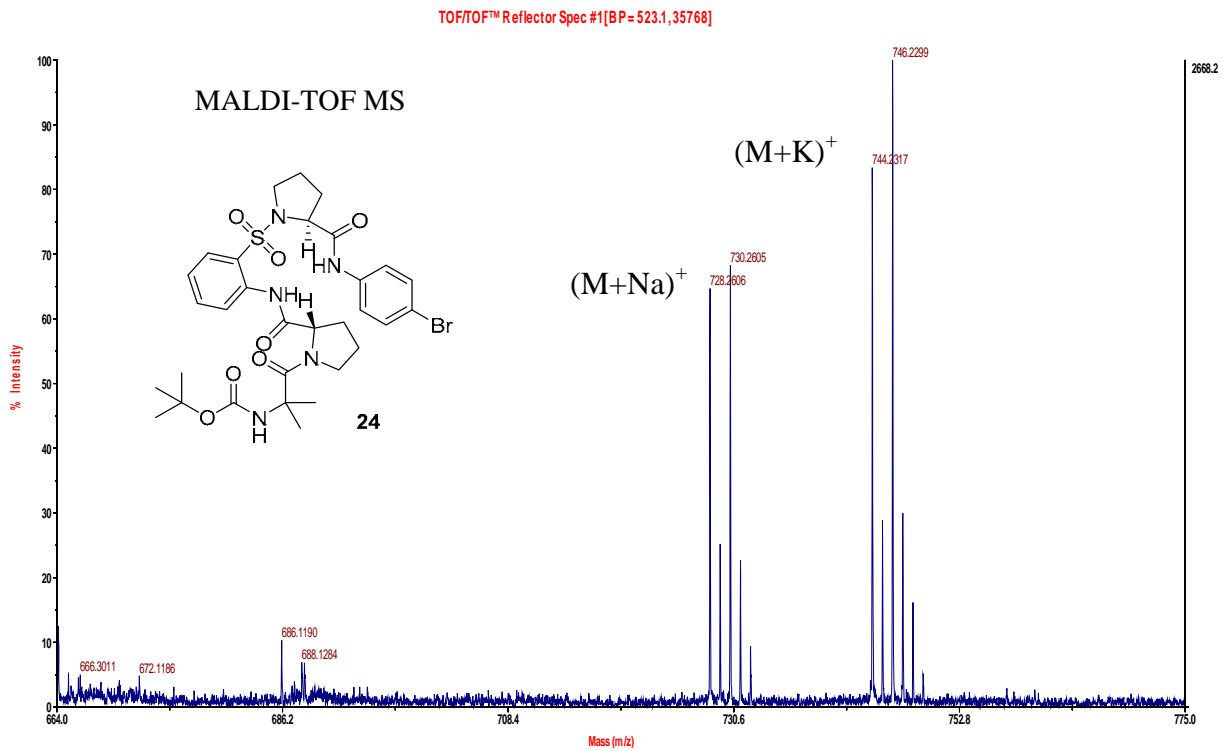




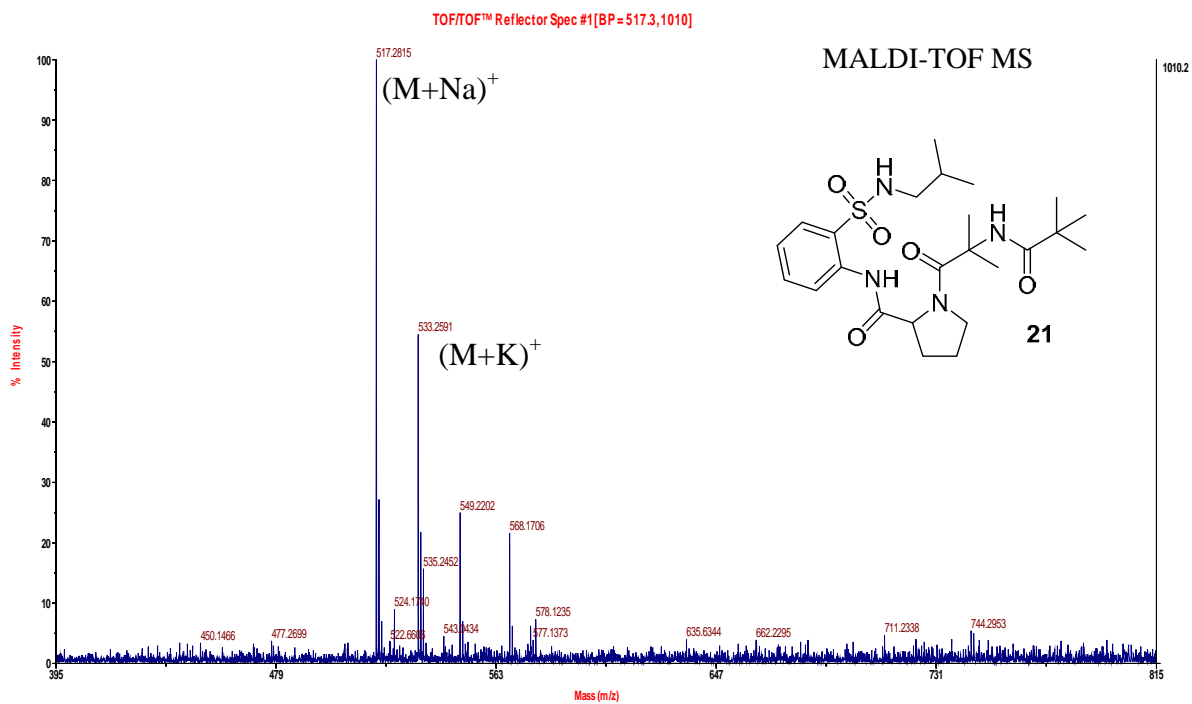
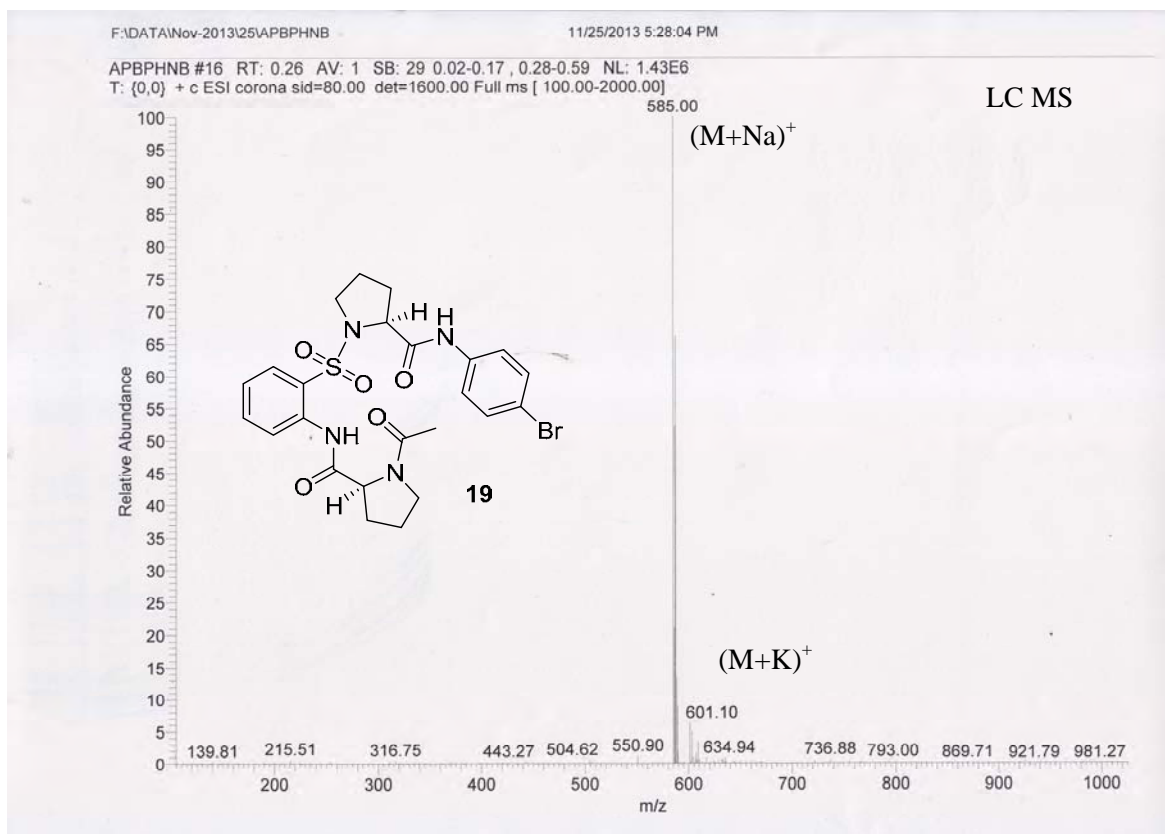




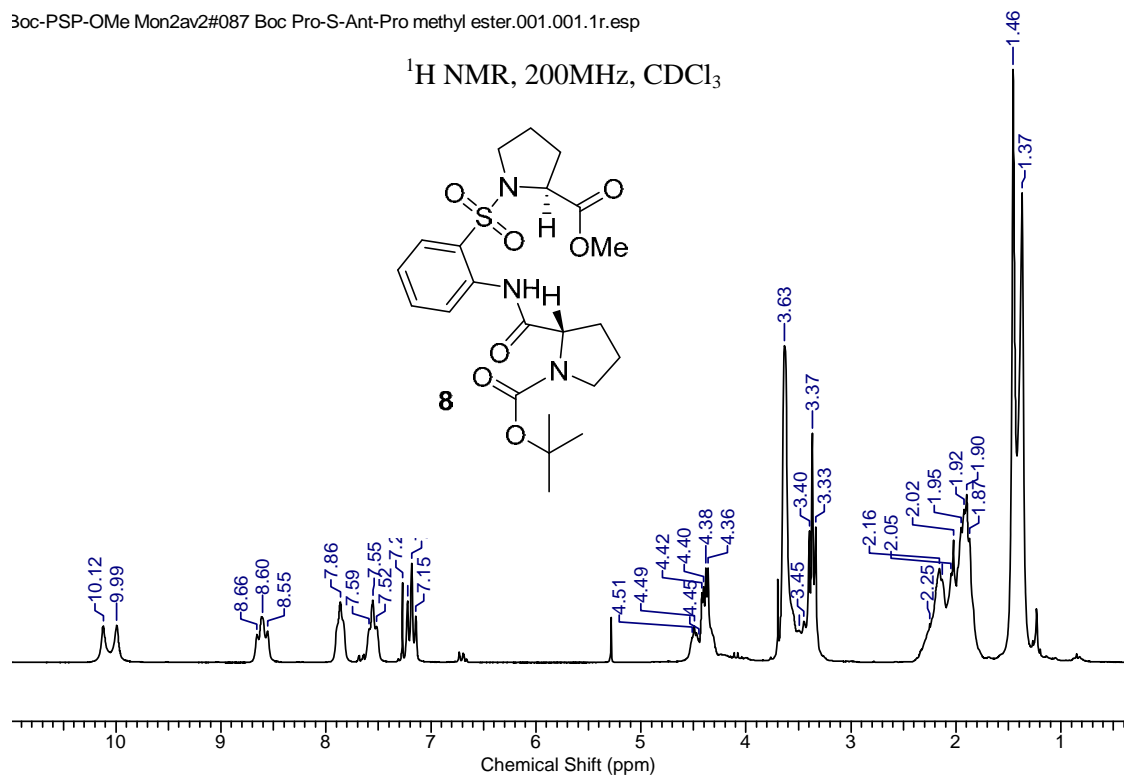
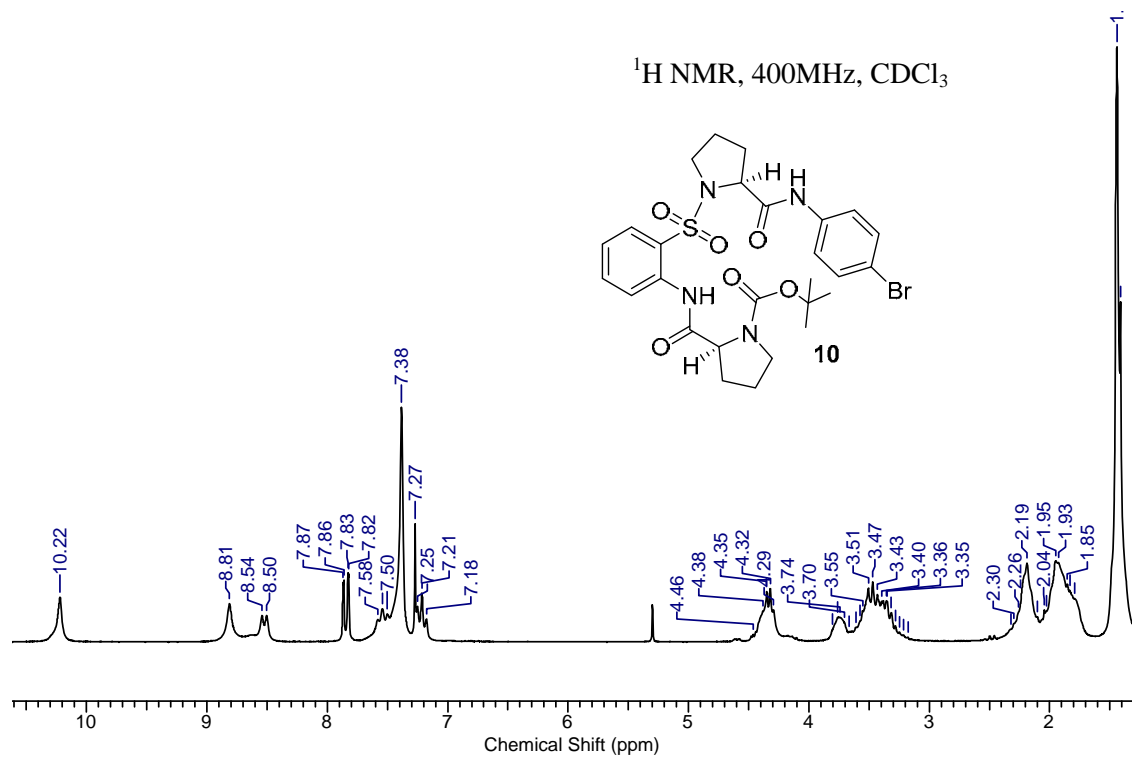




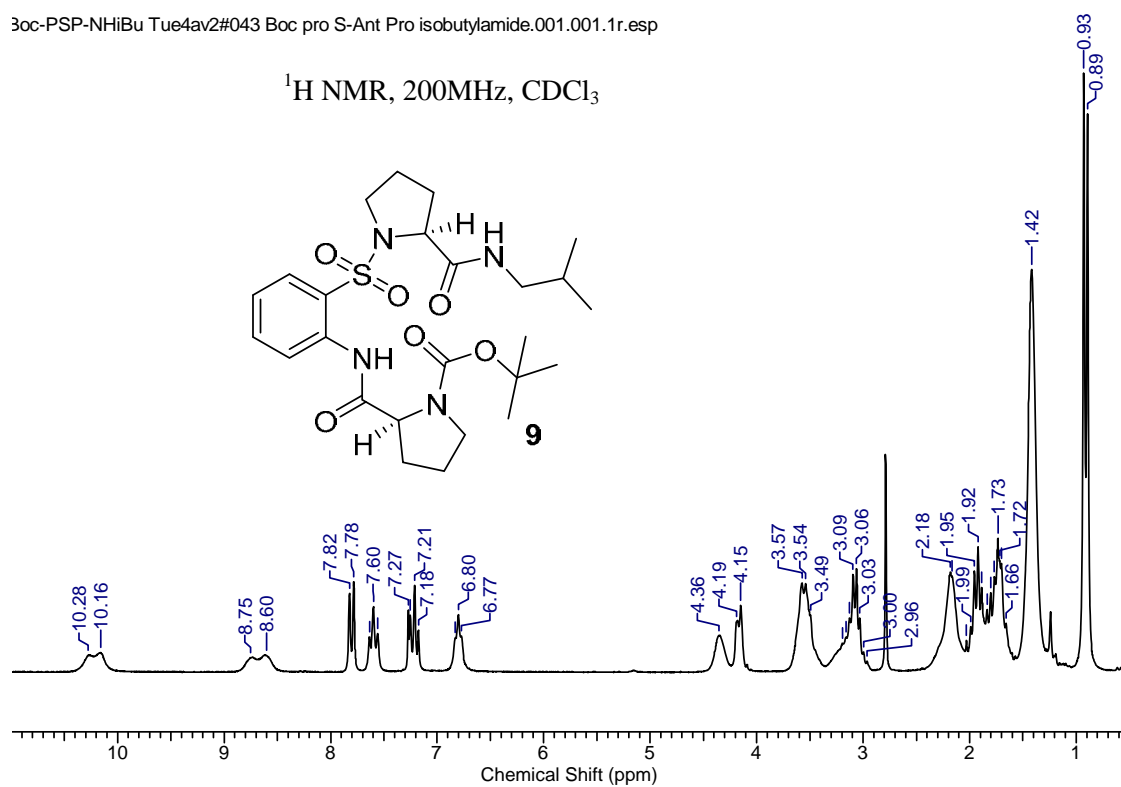




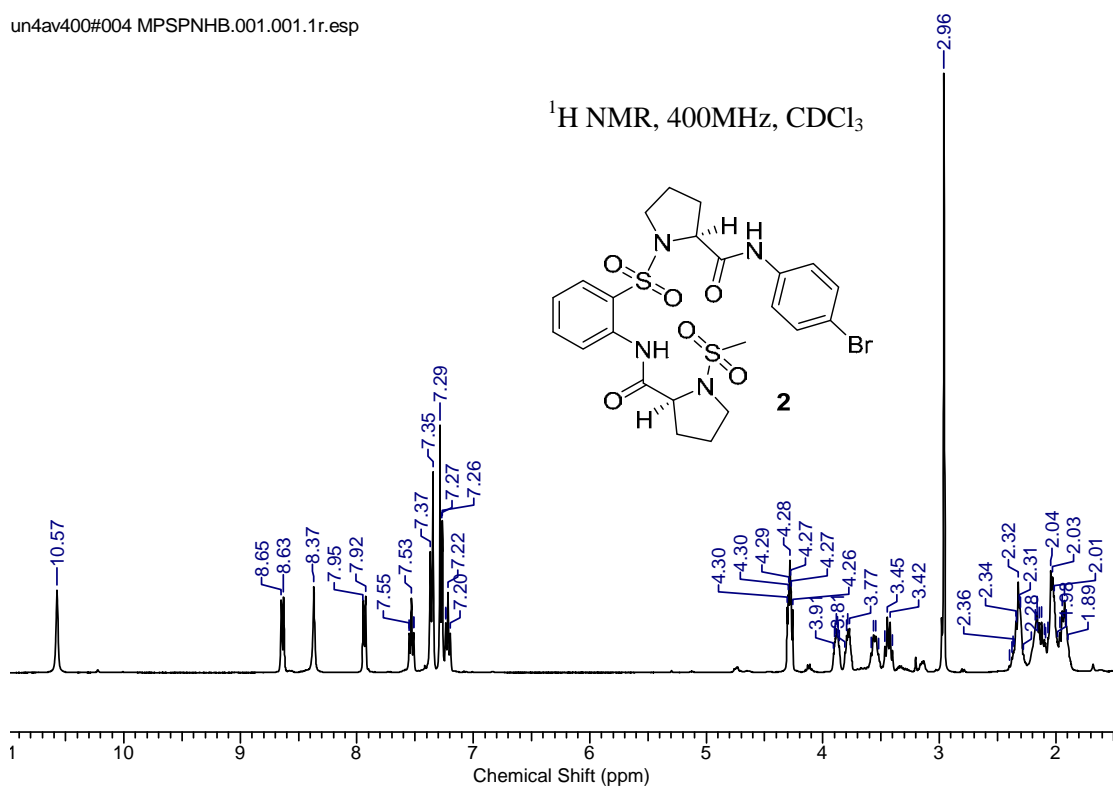
3oc-PSP-OMe Mon2av2#087 Boc Pro-S-Ant-Pro methyl ester.001.001.1r.esp

 $^1\text{H}$  NMR, 200MHz,  $\text{CDCl}_3$  $^1\text{H}$  NMR, 400MHz,  $\text{CDCl}_3$ 

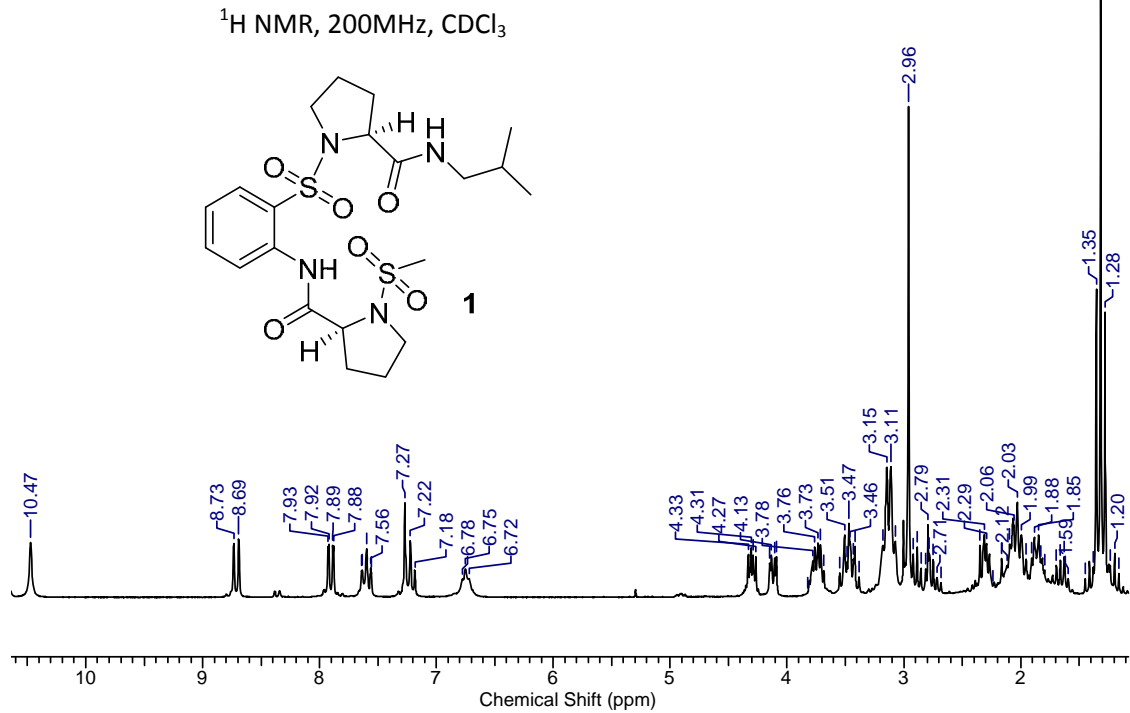
3oc-PSP-NHiBu Tue4av2#043 Boc pro S-Ant Pro isobutylamide.001.001.1r.esp

 $^1\text{H}$  NMR, 200MHz,  $\text{CDCl}_3$ 

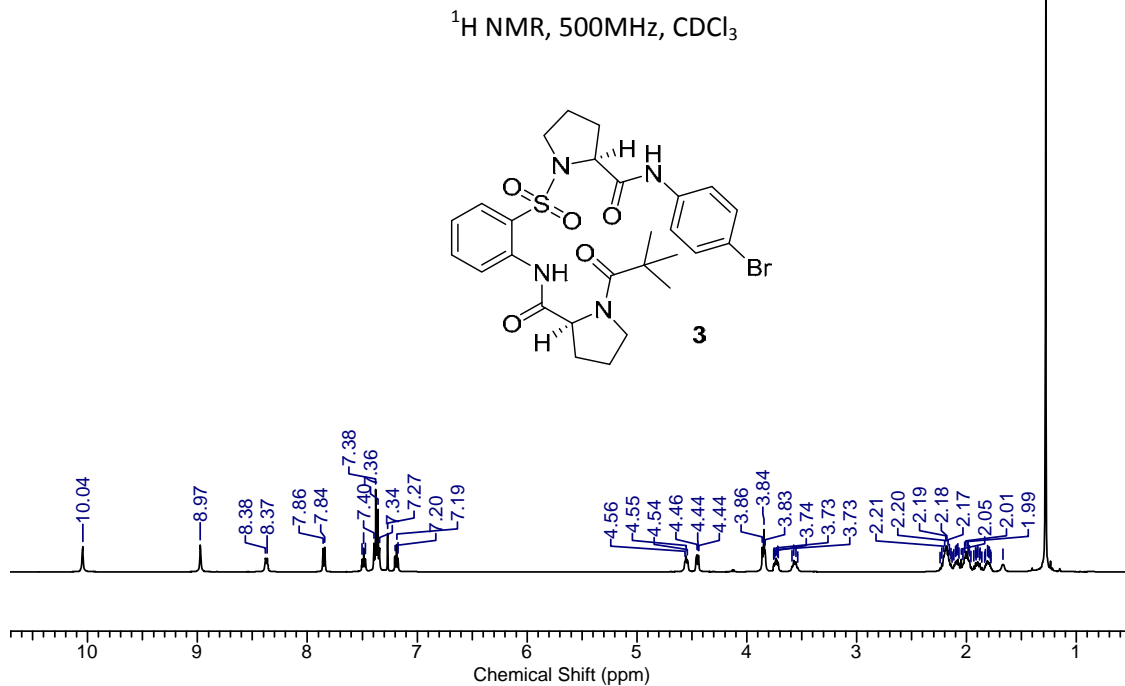
un4av400#004 MPSPNHB.001.001.1r.esp

 $^1\text{H}$  NMR, 400MHz,  $\text{CDCl}_3$ 

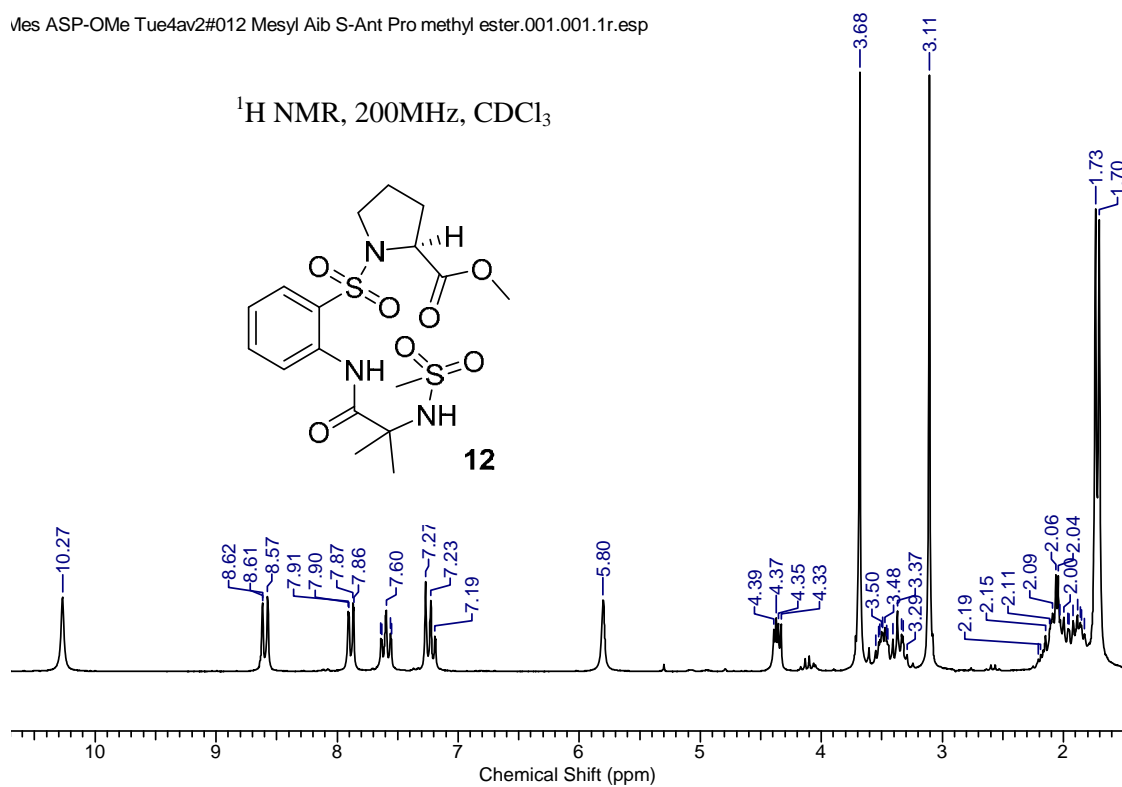
Mes-PSP-NHiBu Thu4av2#068 Mesyl Pro S-Ant Pro isobutylamide.001.001.1r.esp



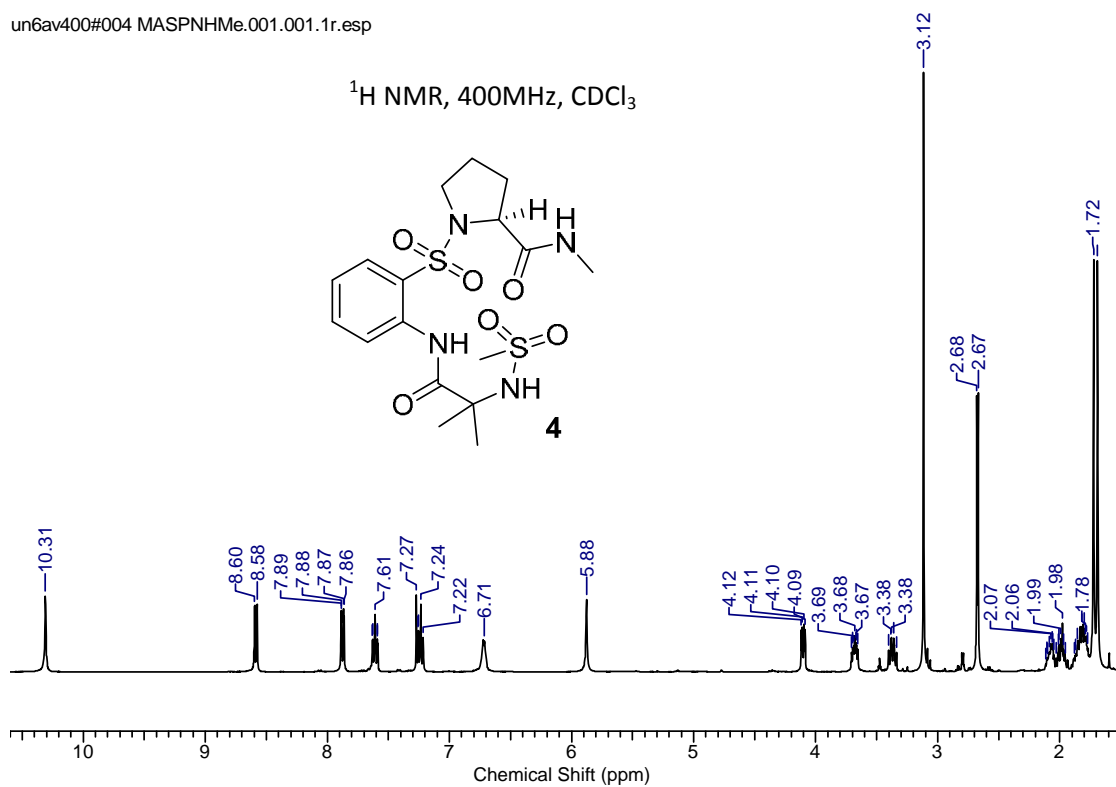
ri3av500#004.001.001.1r.esp



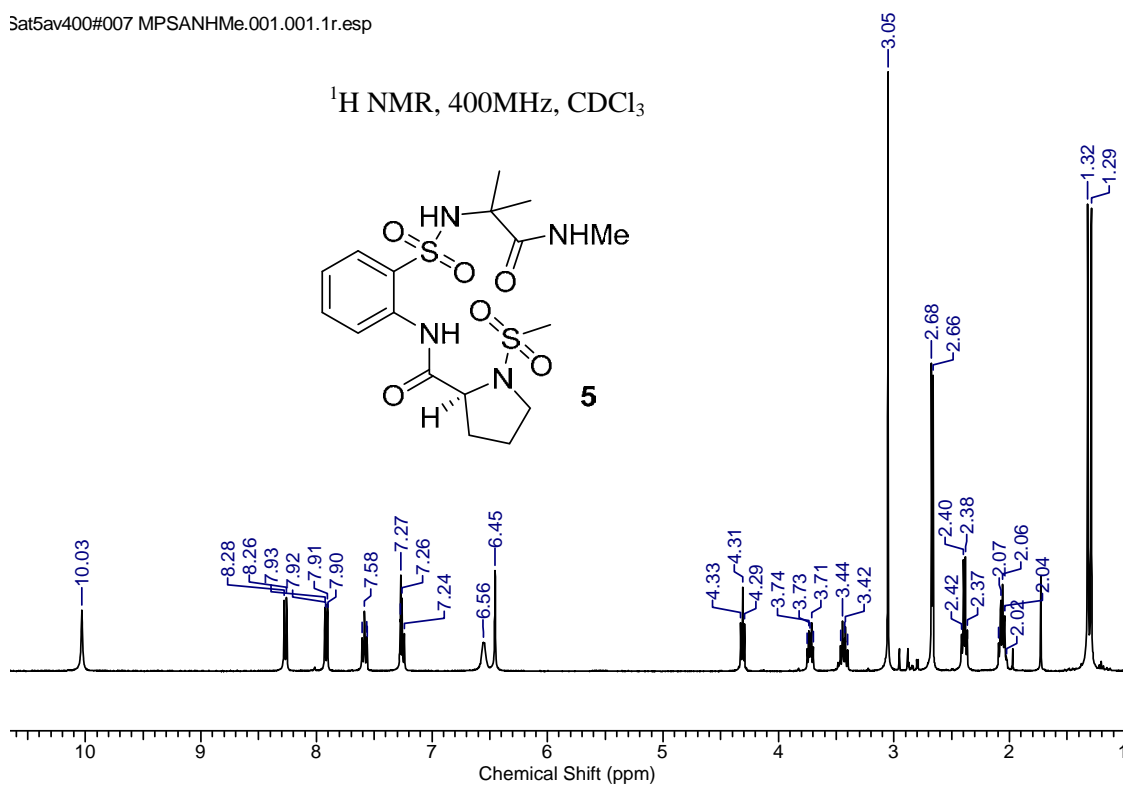
Mes ASP-OMe Tue4av2#012 Mesyl Aib S-Ant Pro methyl ester.001.001.1r.esp

 $^1\text{H}$  NMR, 200MHz,  $\text{CDCl}_3$ 

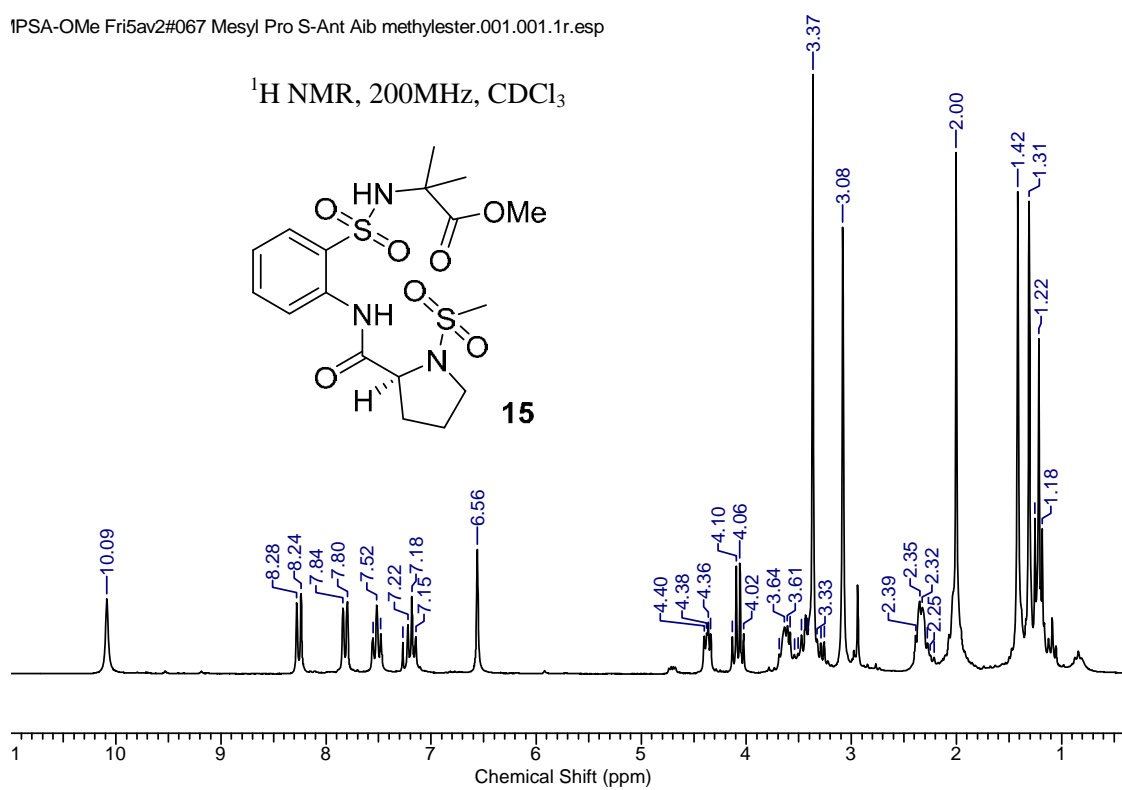
un6av400#004 MASPnHMe.001.001.1r.esp

 $^1\text{H}$  NMR, 400MHz,  $\text{CDCl}_3$ 

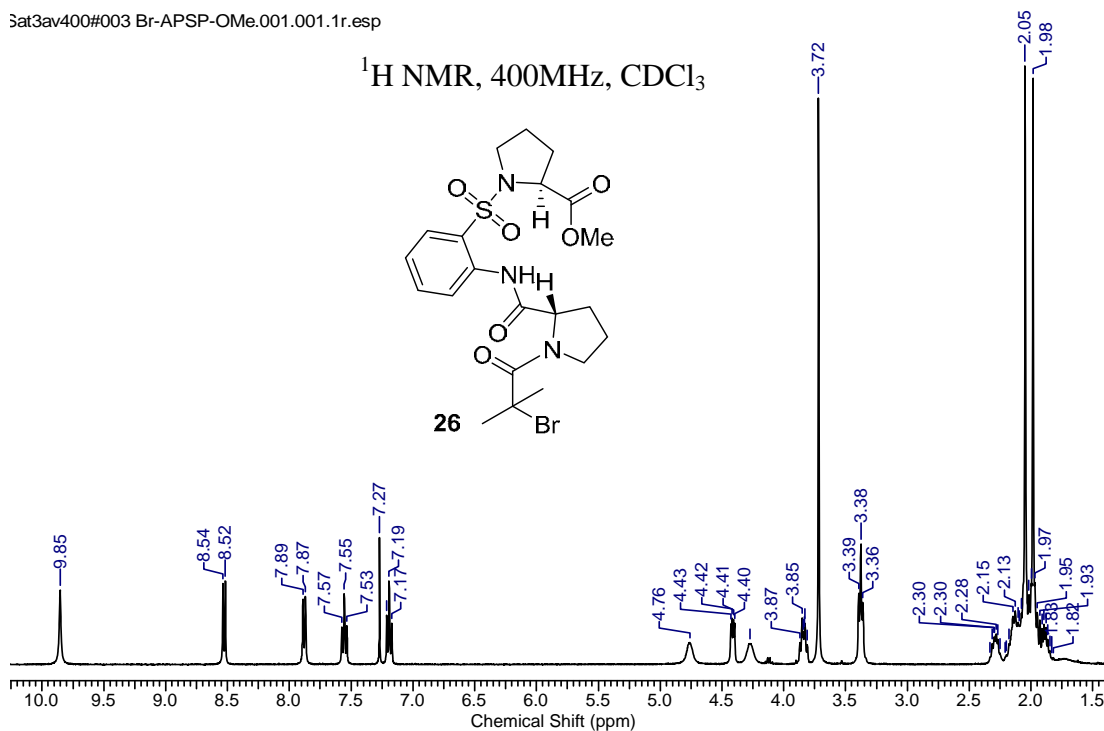
Sat5av400#007 MPSANHMe.001.001.1r.esp

 $^1\text{H}$  NMR, 400MHz,  $\text{CDCl}_3$ 

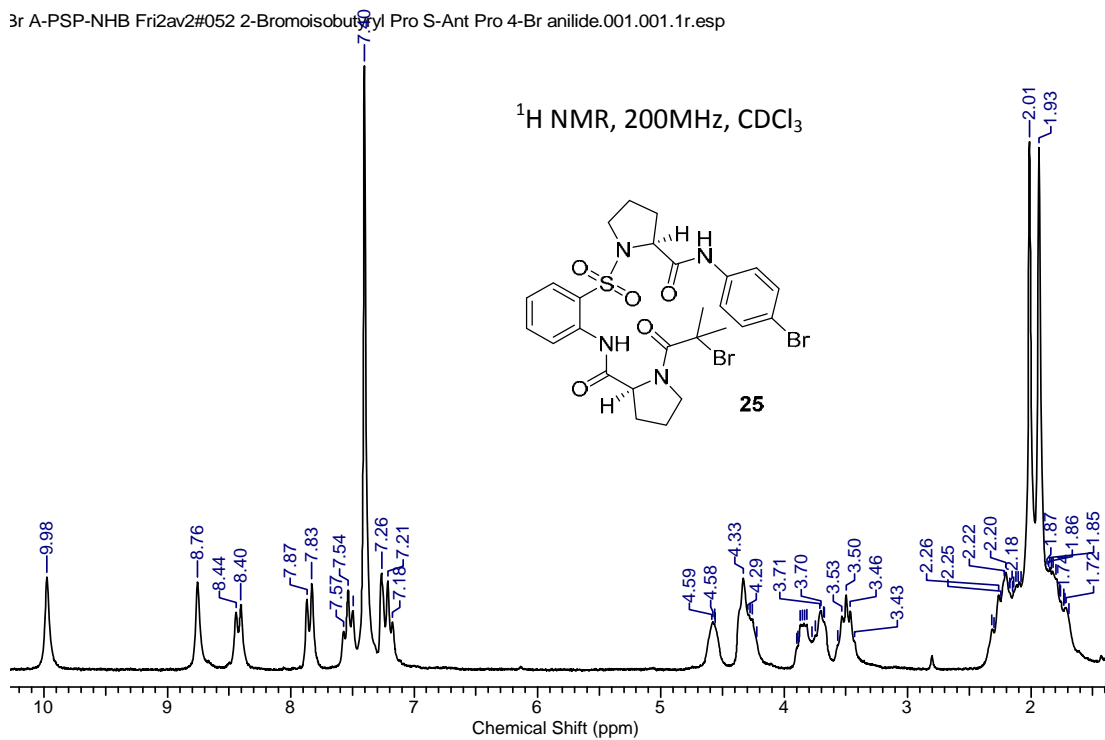
IPSA-OMe Fri5av2#067 Mesyl Pro S-Ant Aib methylester.001.001.1r.esp

 $^1\text{H}$  NMR, 200MHz,  $\text{CDCl}_3$ 

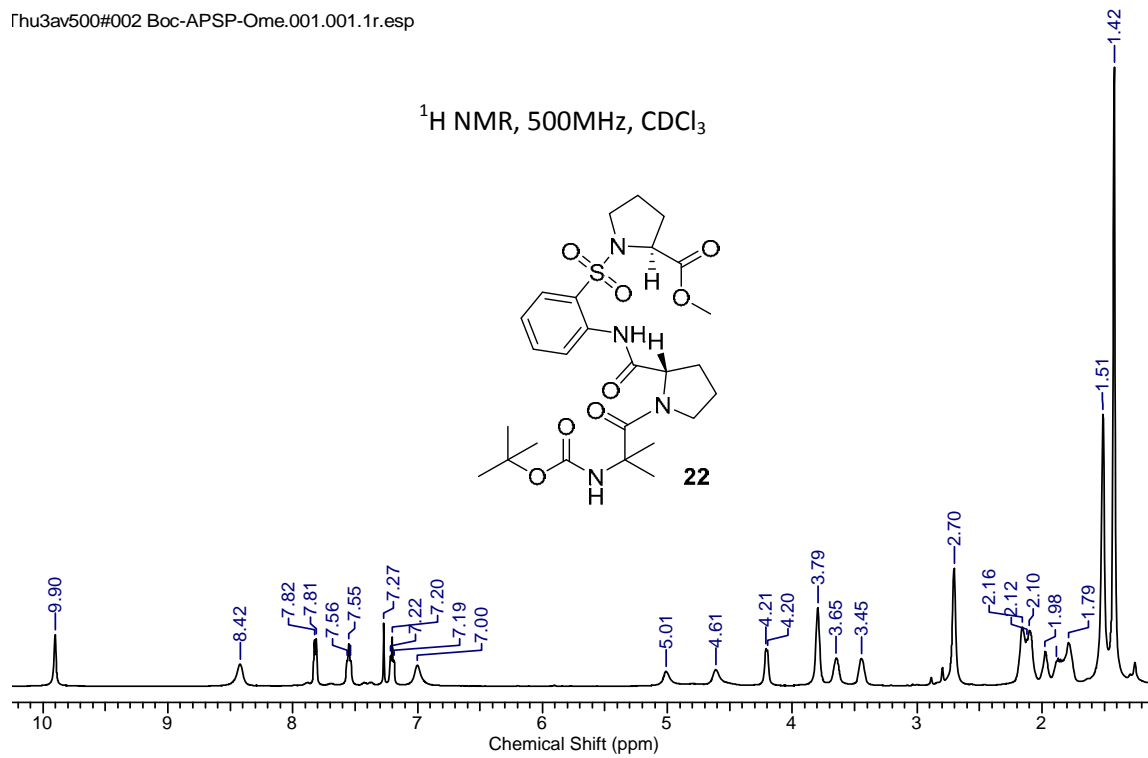
3at3av400#003 Br-APSP-OMe.001.001.1r.esp



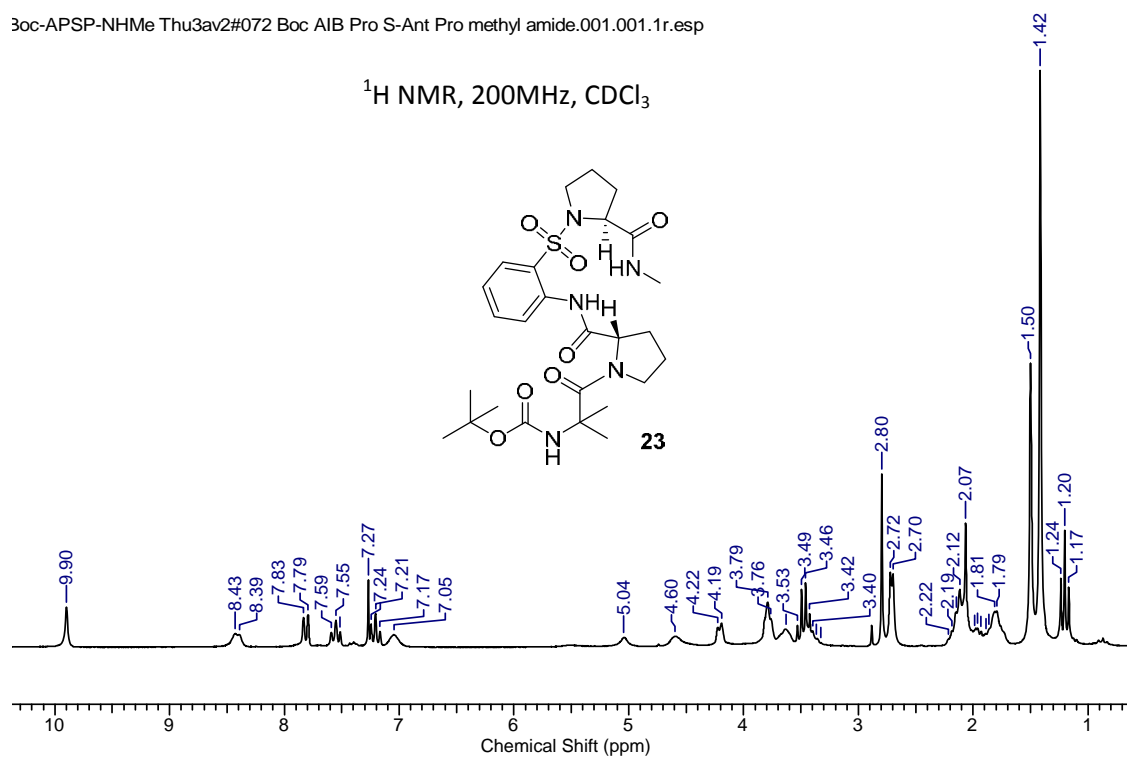
3r A-PSP-NHB Fri2av2#052 2-Bromoisobutyl Pro S-Ant Pro 4-Br anilide.001.001.1r.esp



Thu3av500#002 Boc-APSP-Ome.001.001.1r.esp

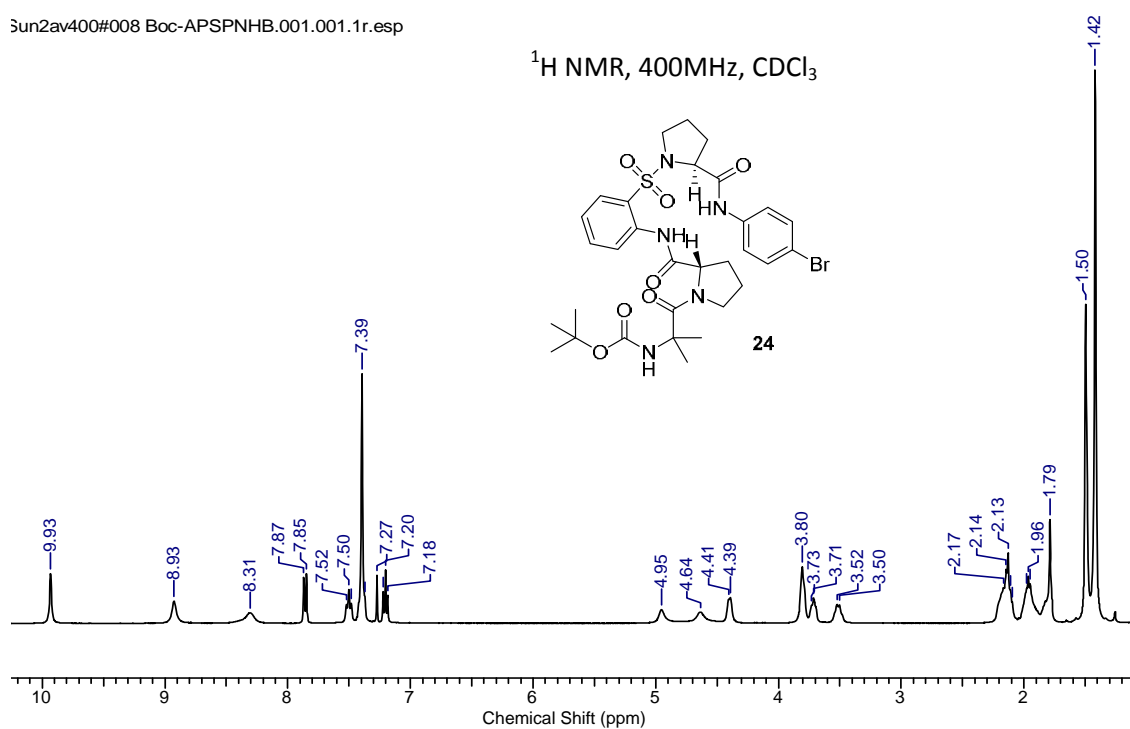
 $^1\text{H}$  NMR, 500MHz,  $\text{CDCl}_3$ 

3oc-APSP-NHMe Thu3av2#072 Boc AIB Pro S-Ant Pro methyl amide.001.001.1r.esp

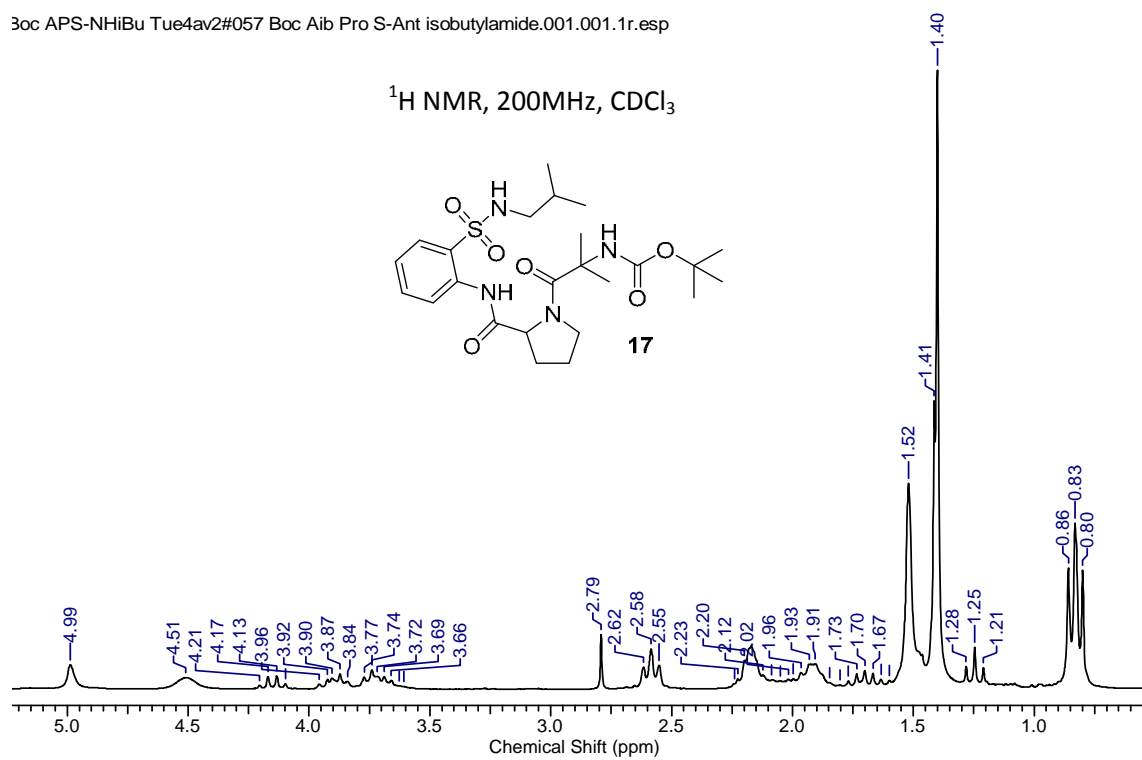
 $^1\text{H}$  NMR, 200MHz,  $\text{CDCl}_3$ 



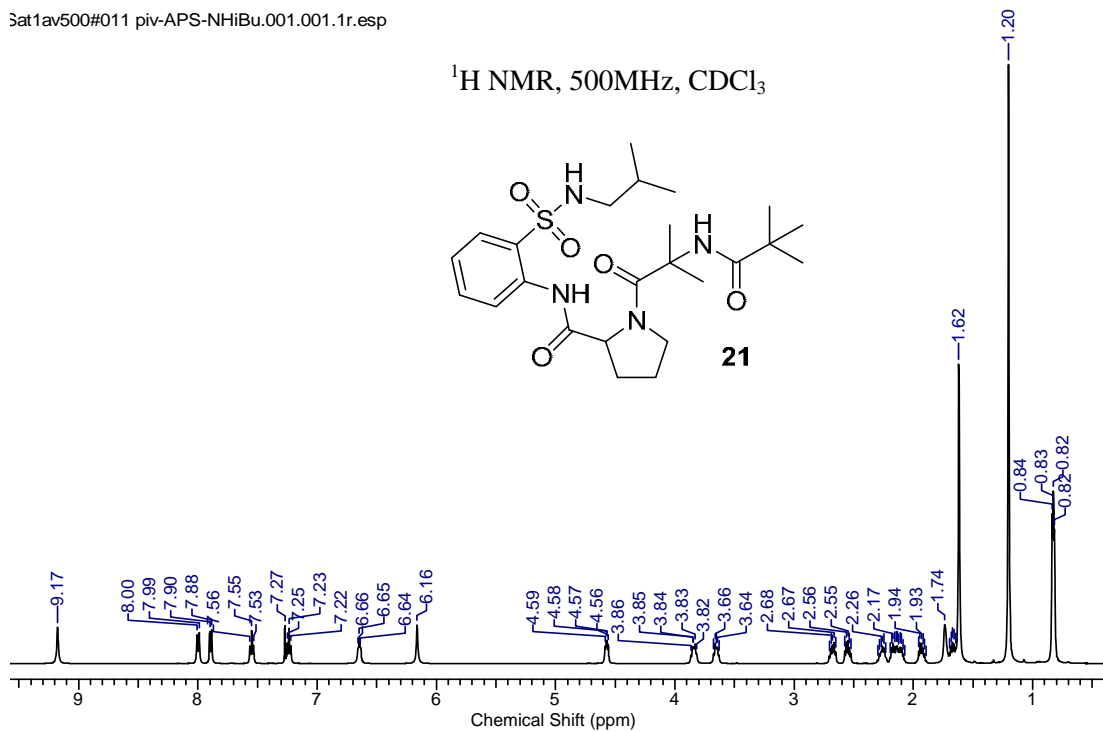
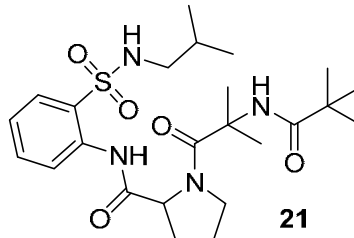
Sun2av400#008 Boc-APSPNHB.001.001.1r.esp

 $^1\text{H}$  NMR, 400MHz,  $\text{CDCl}_3$ 

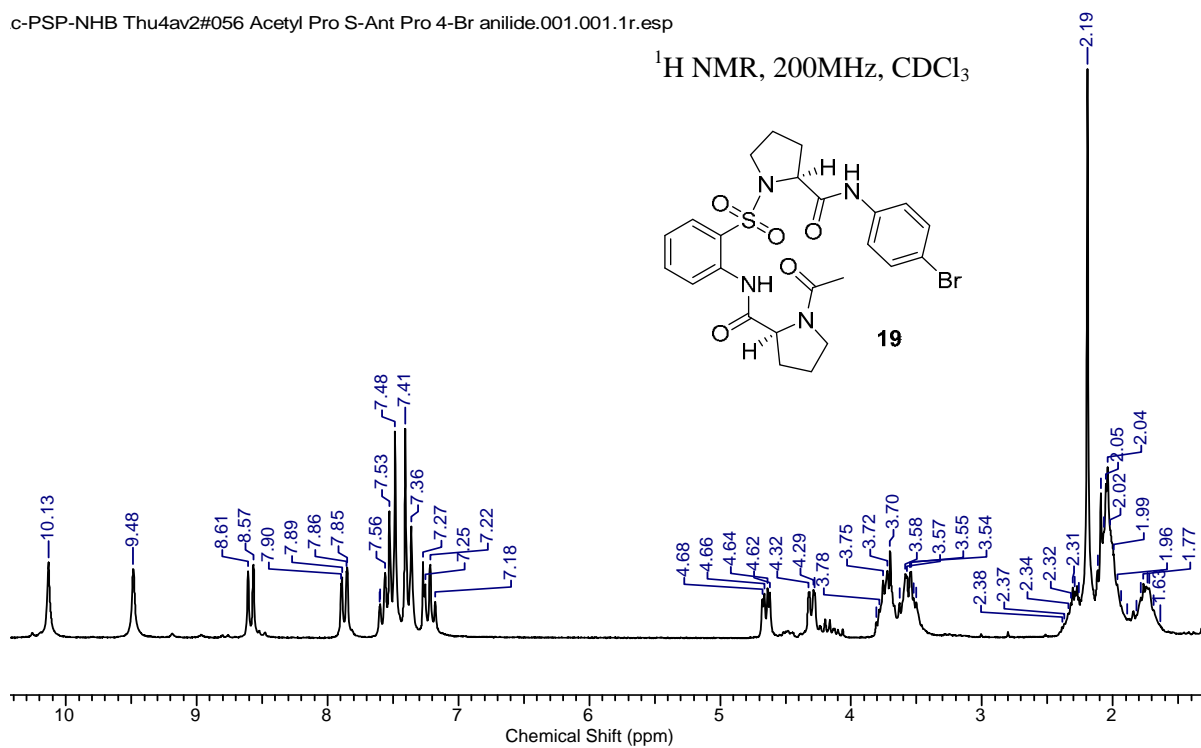
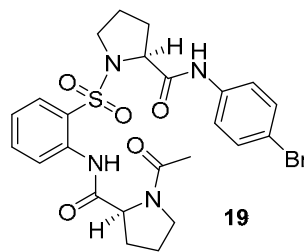
3oc APS-NHiBu Tue4av2#057 Boc Aib Pro S-Ant isobutylamide.001.001.1r.esp

 $^1\text{H}$  NMR, 200MHz,  $\text{CDCl}_3$ 

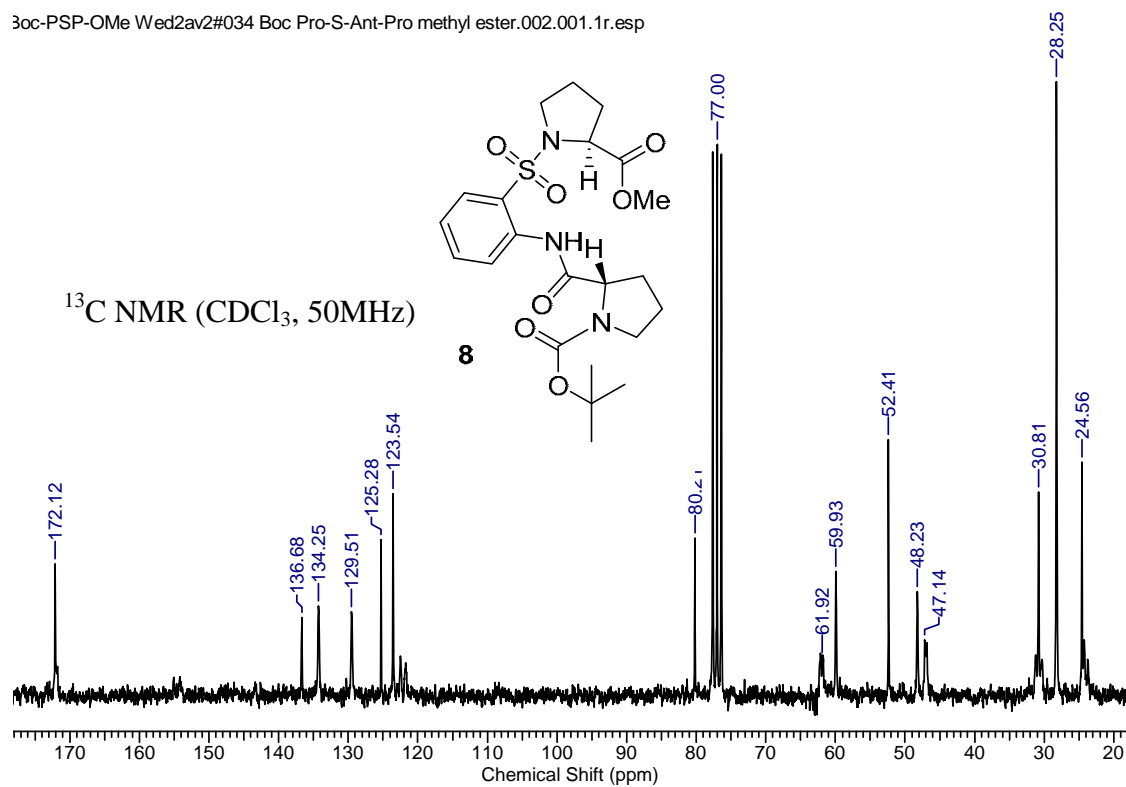
Sat1av500#011 piv-APS-NHiBu.001.001.1r.esp

 $^1\text{H}$  NMR, 500MHz,  $\text{CDCl}_3$ 

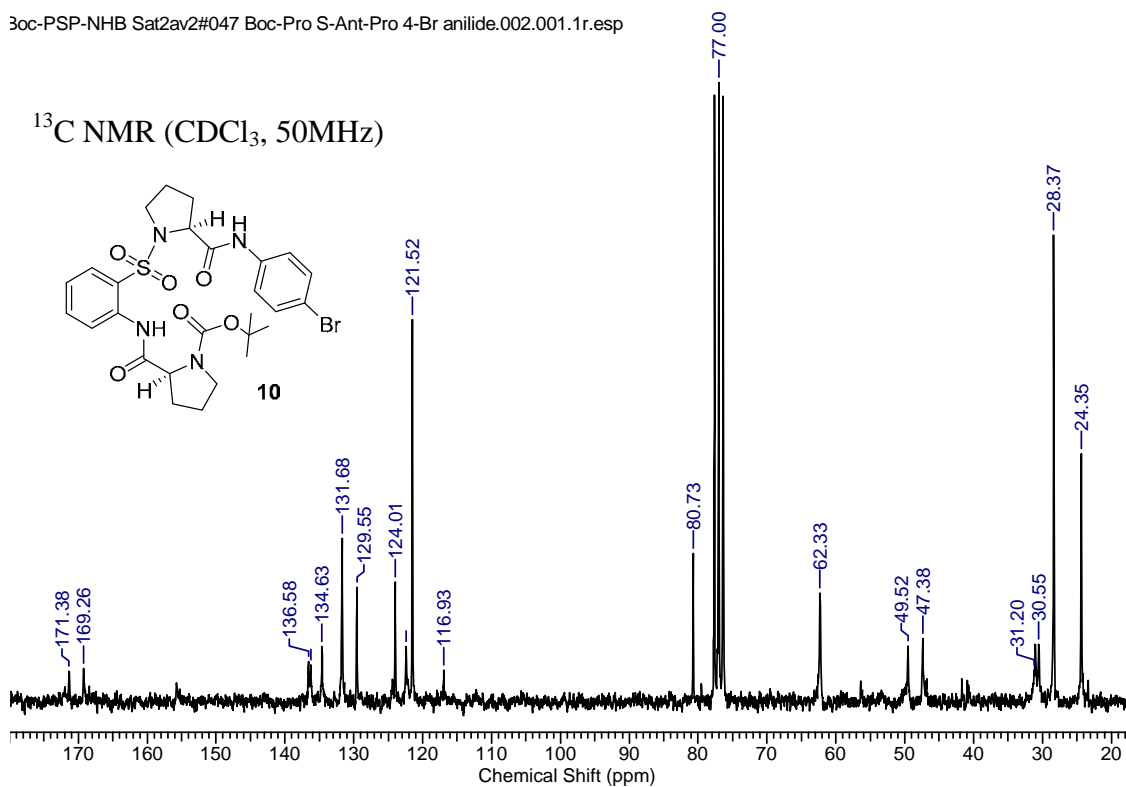
c-PSP-NHB Thu4av2#056 Acetyl Pro S-Ant Pro 4-Br anilide.001.001.1r.esp

 $^1\text{H}$  NMR, 200MHz,  $\text{CDCl}_3$ 

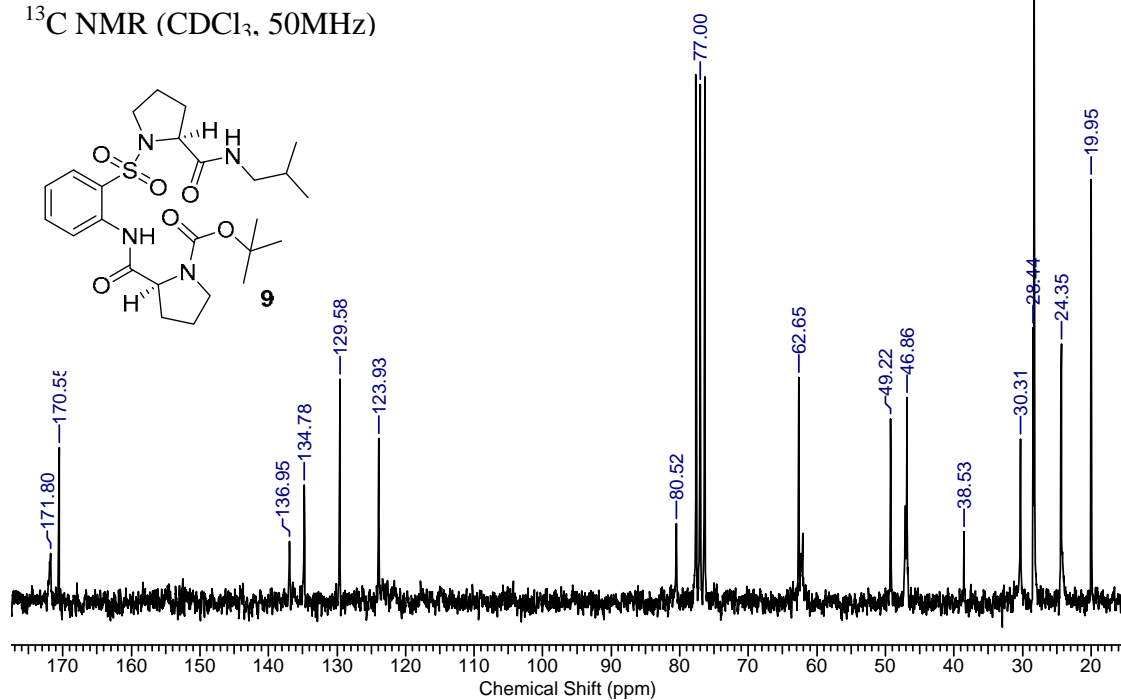
3oc-PSP-OMe Wed2av2#034 Boc-Pro-S-Ant-Pro methyl ester.002.001.1r.esp



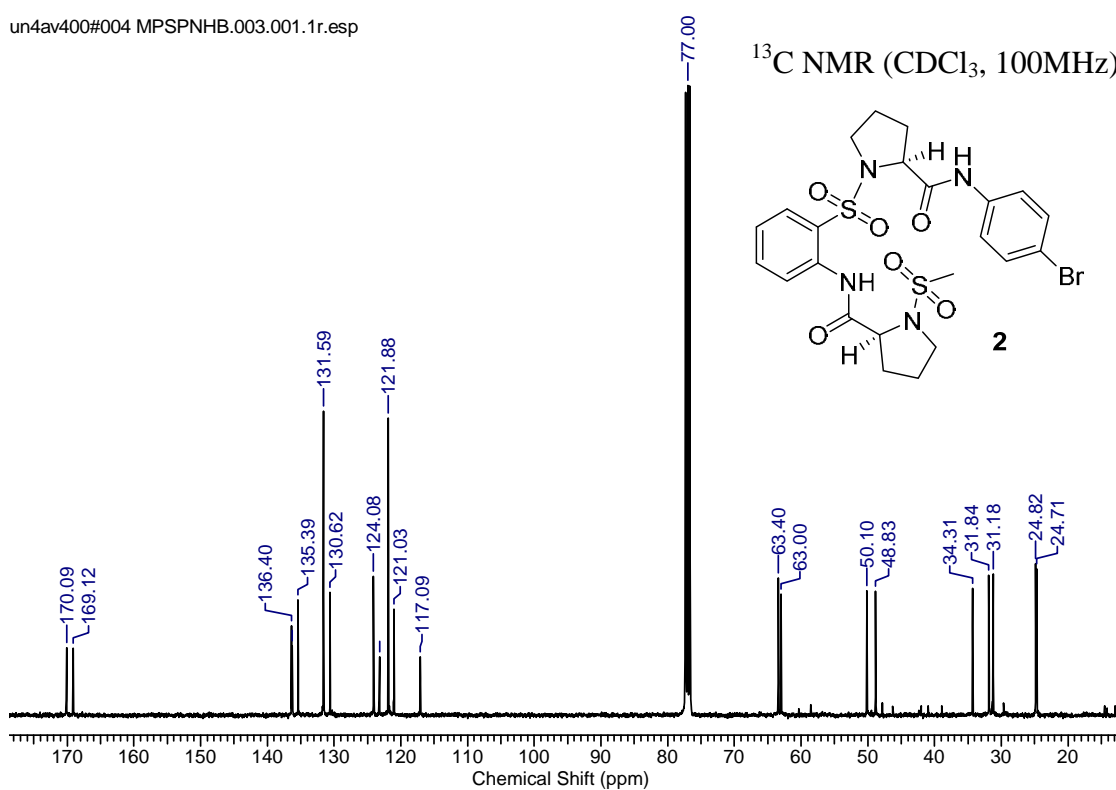
3oc-PSP-NHB Sat2av2#047 Boc-Pro S-Ant-Pro 4-Br anilide.002.001.1r.esp



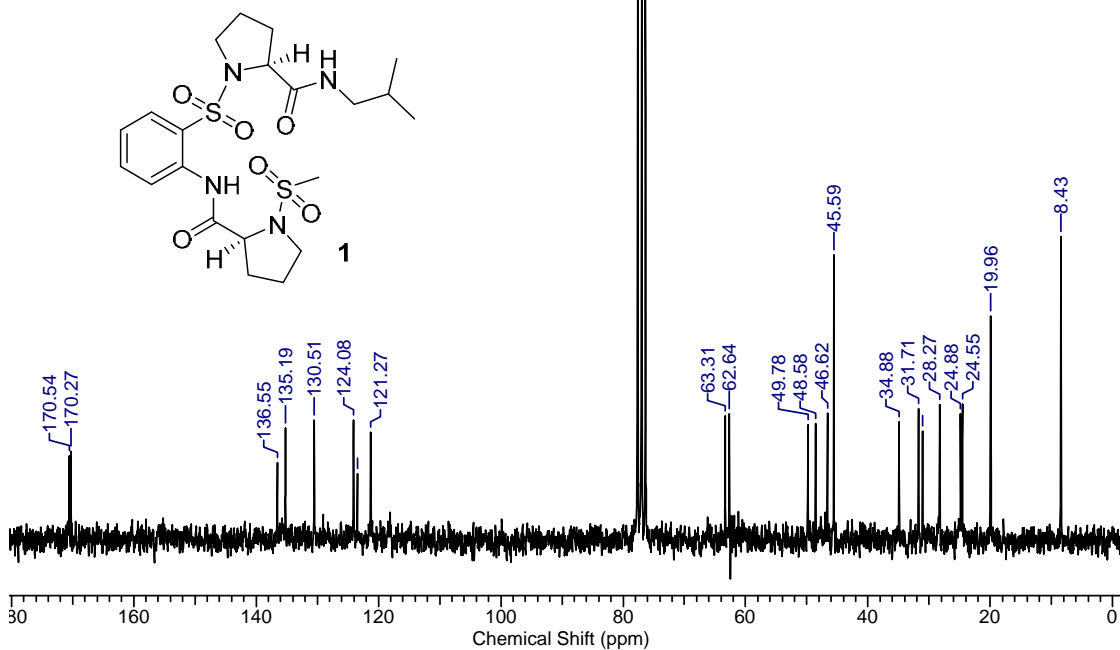
3oc-PSP-NHiBu Sat4av2#048 Boc Pro S-Ant Pro isobutylamide.002.001.1r.esp

 $^{13}\text{C}$  NMR ( $\text{CDCl}_3$ , 50MHz)

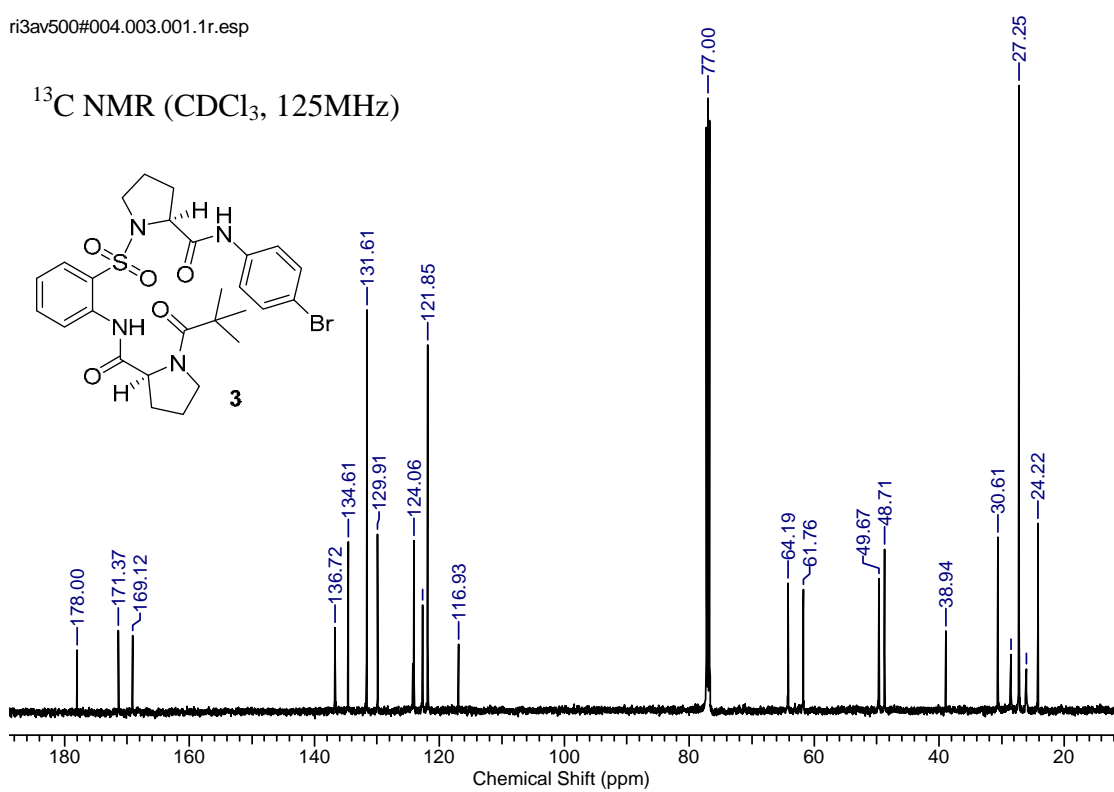
un4av400#004 MPSPNHB.003.001.1r.esp

 $^{13}\text{C}$  NMR ( $\text{CDCl}_3$ , 100MHz)

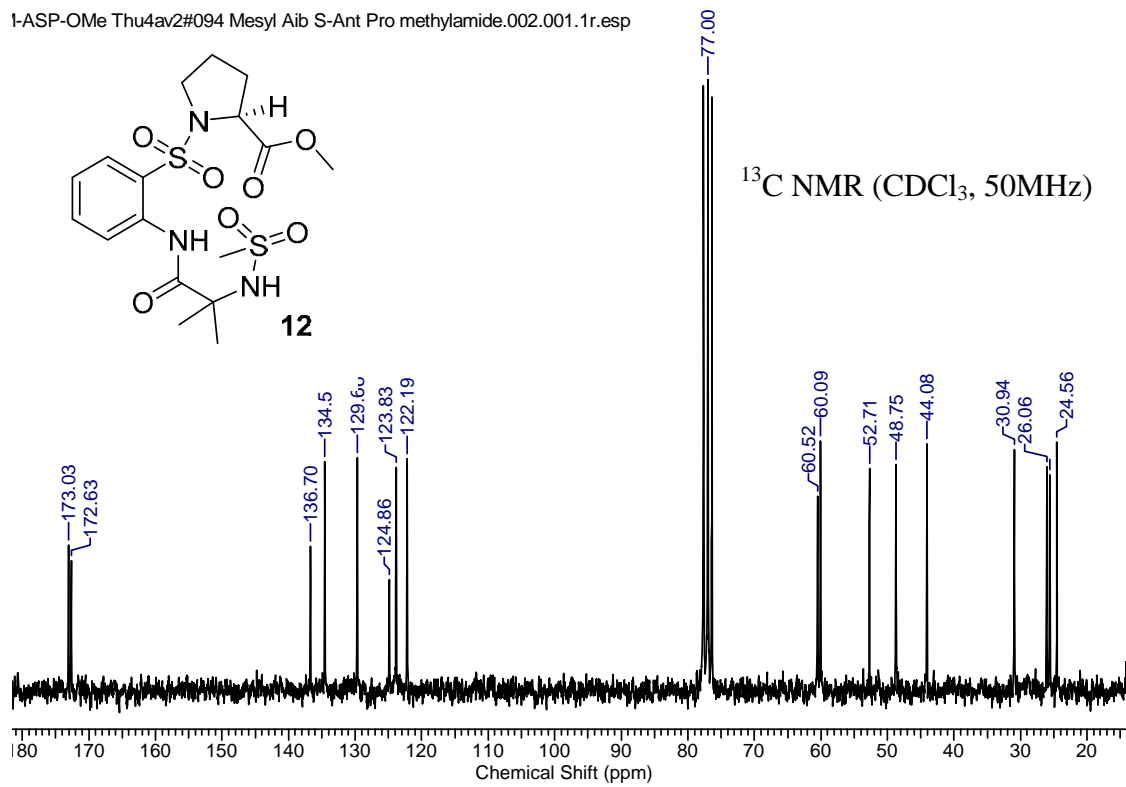
les-PSP-NHiBu Sat4av2#064 Mesyl Pro S-Ant Pro isobutylamide.002.001.1r.esp

 $^{13}\text{C}$  NMR ( $\text{CDCl}_3$ , 50MHz)

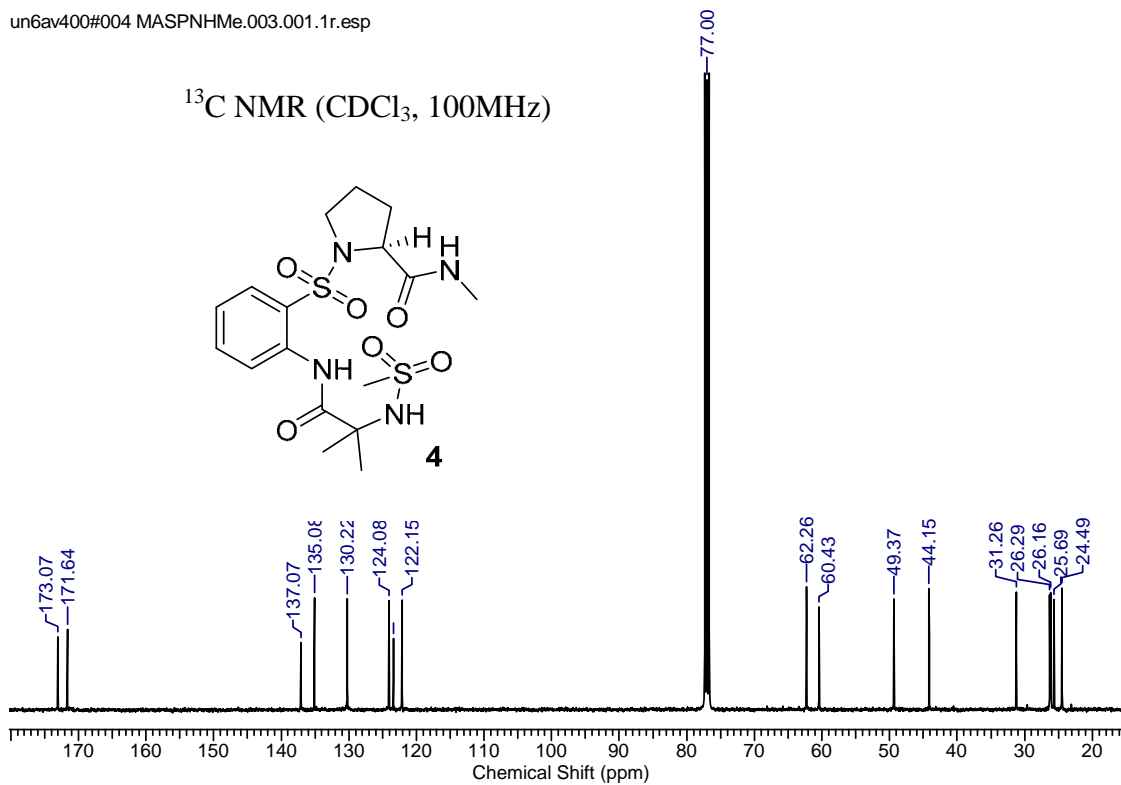
ri3av500#004.003.001.1r.esp

 $^{13}\text{C}$  NMR ( $\text{CDCl}_3$ , 125MHz)

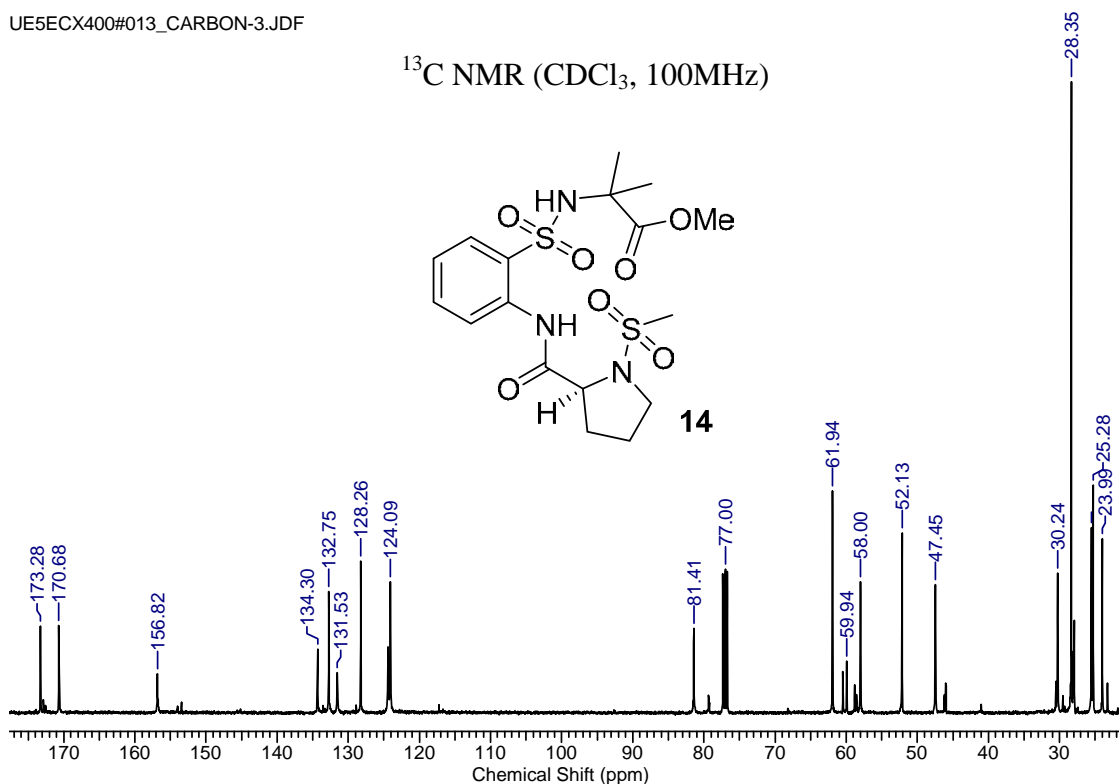
I-ASP-OMe Thu4av2#094 Mesyl Aib S-Ant Pro methylamide.002.001.1r.esp



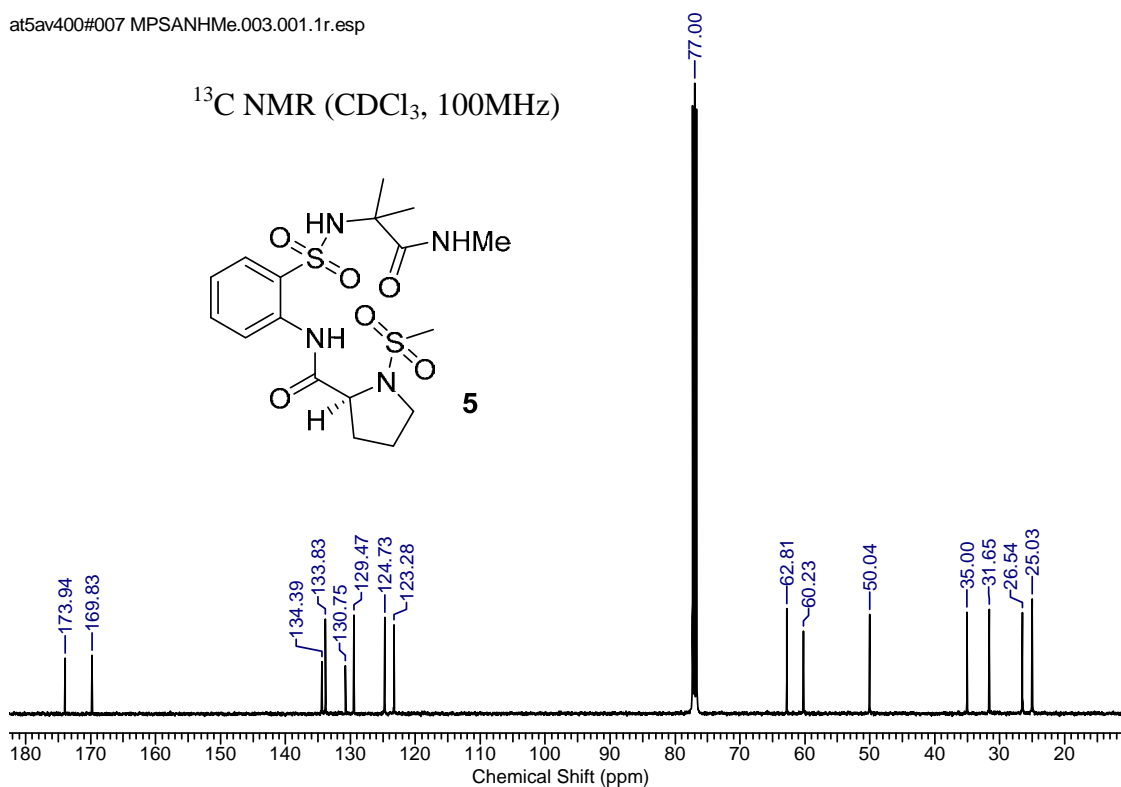
un6av400#004 MASPnHMe.003.001.1r.esp



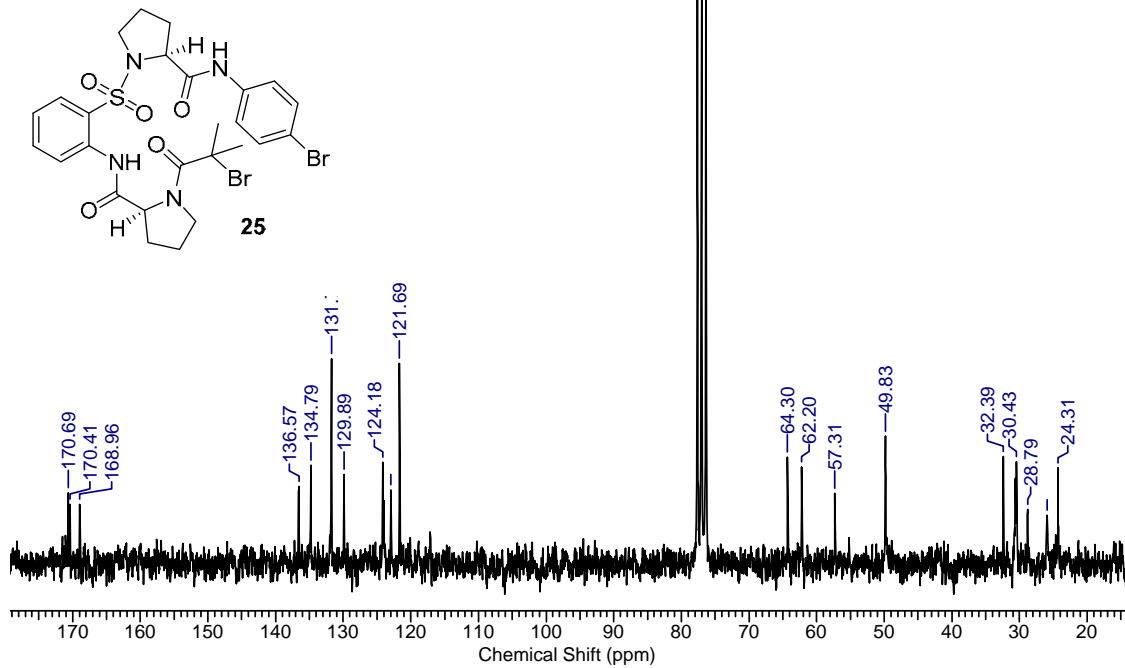
UE5ECX400#013\_CARBO-3.JDF

 $^{13}\text{C}$  NMR ( $\text{CDCl}_3$ , 100MHz)

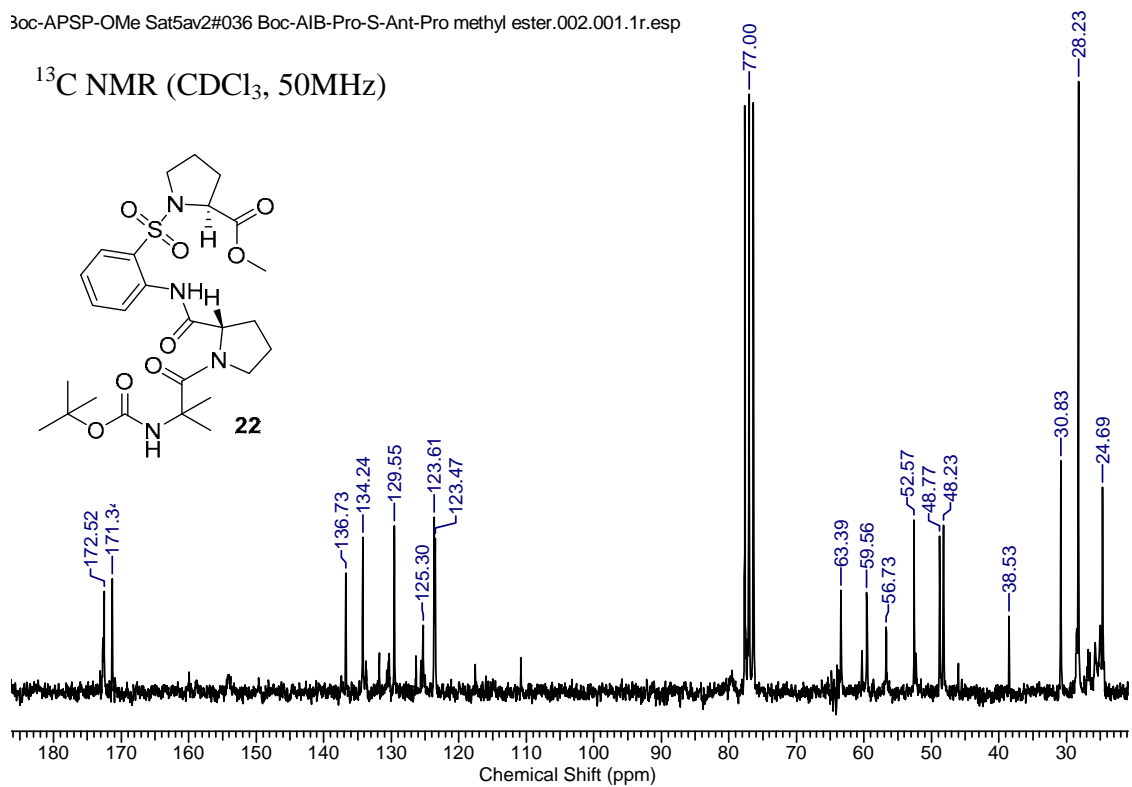
at5av400#007 MPSANHMe.003.001.1r.esp

 $^{13}\text{C}$  NMR ( $\text{CDCl}_3$ , 100MHz)

3r A-PSP-NHB Mon3av2#113 2-Bromopropionyl Pro S-Ant Pro 4-Br anilide.002.001.03.esp

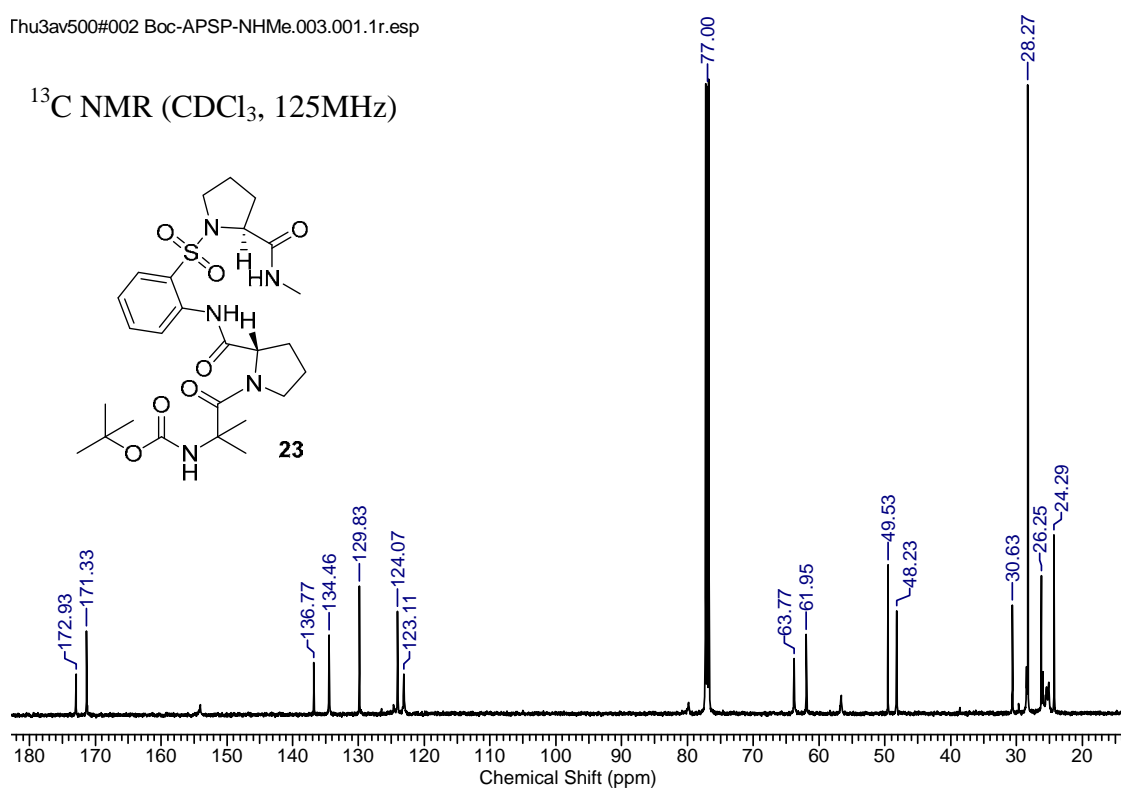
 $^{13}\text{C}$  NMR ( $\text{CDCl}_3$ , 50MHz)

3oc-APSP-OMe Sat5av2#036 Boc-AIB-Pro-S-Ant-Pro methyl ester.002.001.1r.esp

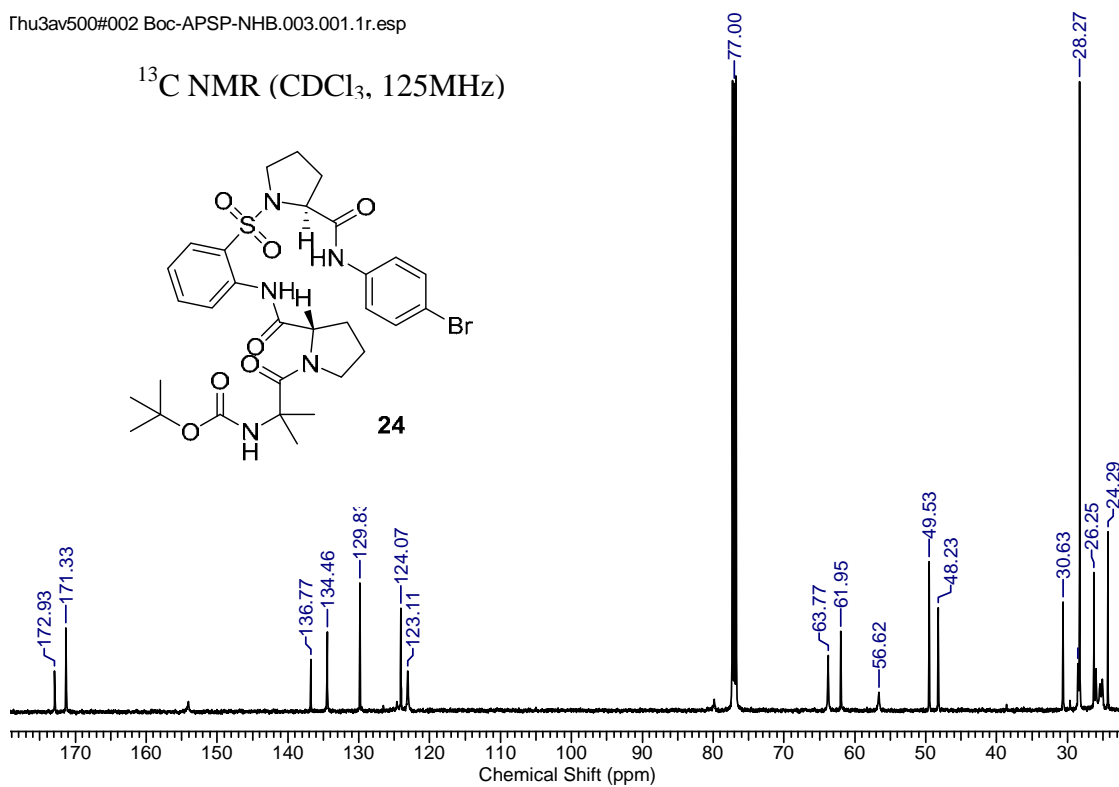
 $^{13}\text{C}$  NMR ( $\text{CDCl}_3$ , 50MHz)



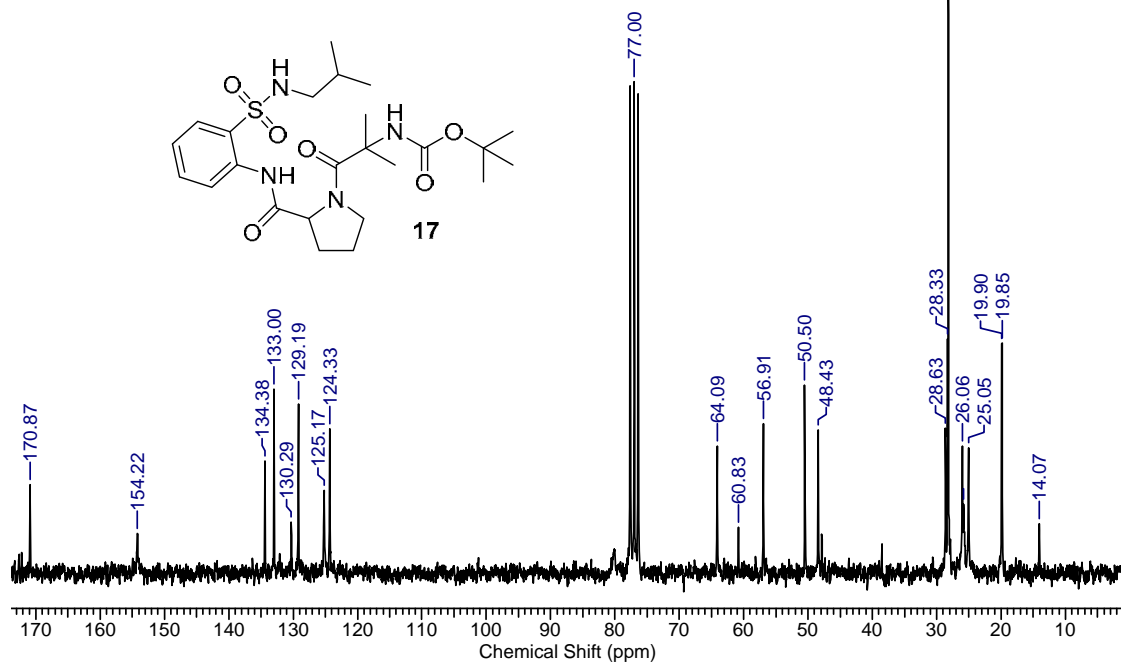
Thu3av500#002 Boc-APSP-NHMe.003.001.1r.esp

 $^{13}\text{C}$  NMR ( $\text{CDCl}_3$ , 125MHz)

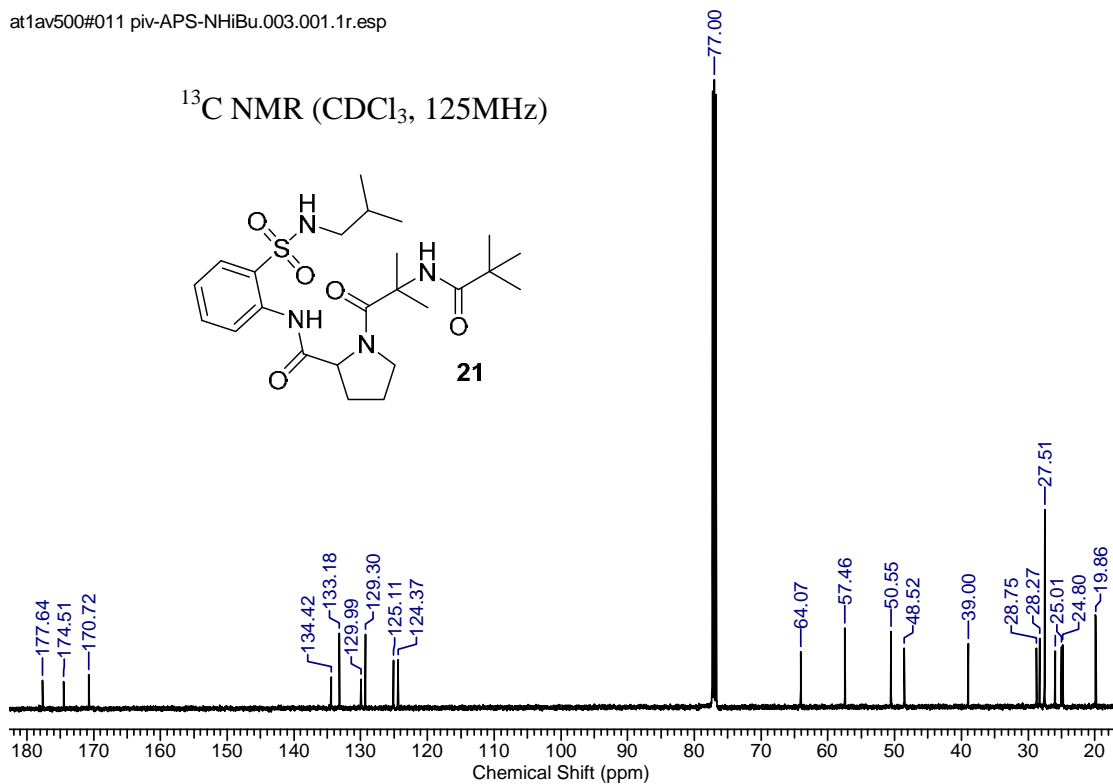
Thu3av500#002 Boc-APSP-NHB.003.001.1r.esp

 $^{13}\text{C}$  NMR ( $\text{CDCl}_3$ , 125MHz)

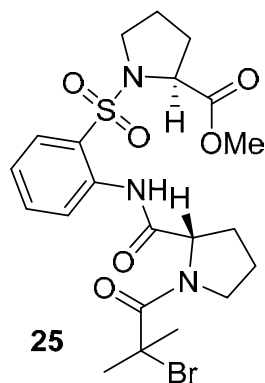
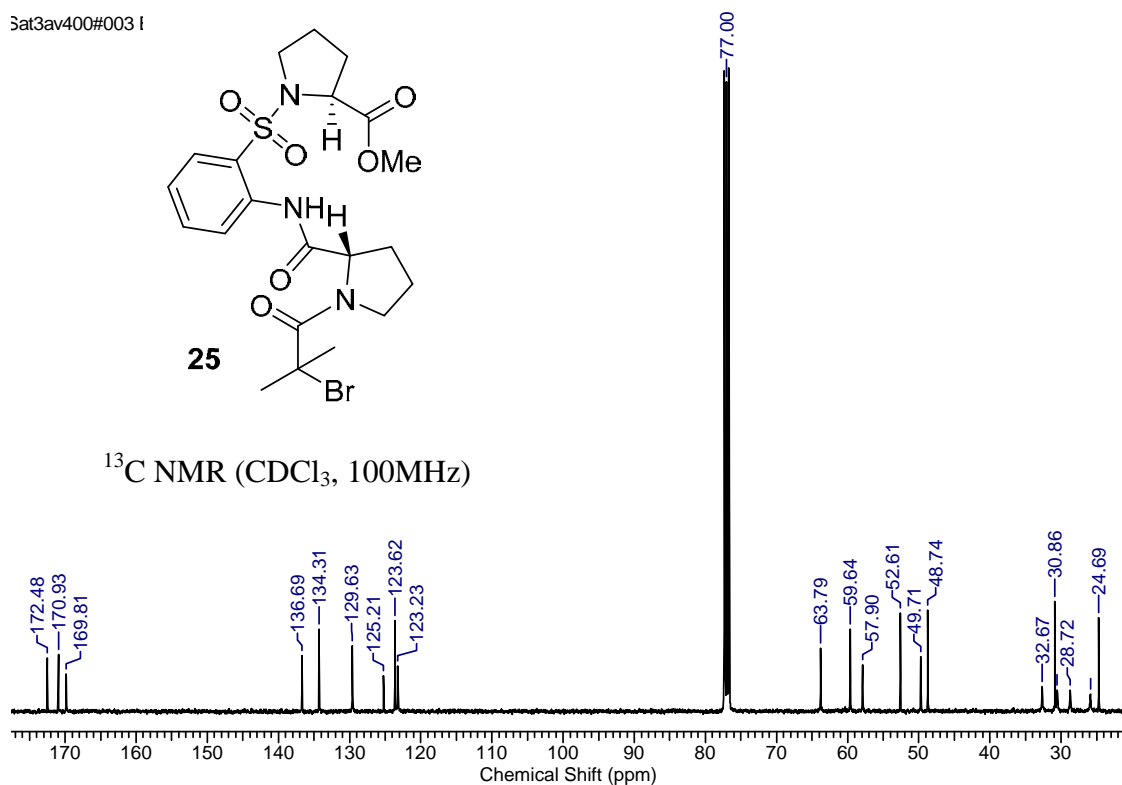
3oc-APS-NHiBu Thu4av2#138 Boc Aib Pro S-Ant isobutyl amide.002.001.1r.esp

 $^{13}\text{C}$  NMR ( $\text{CDCl}_3$ , 50MHz)

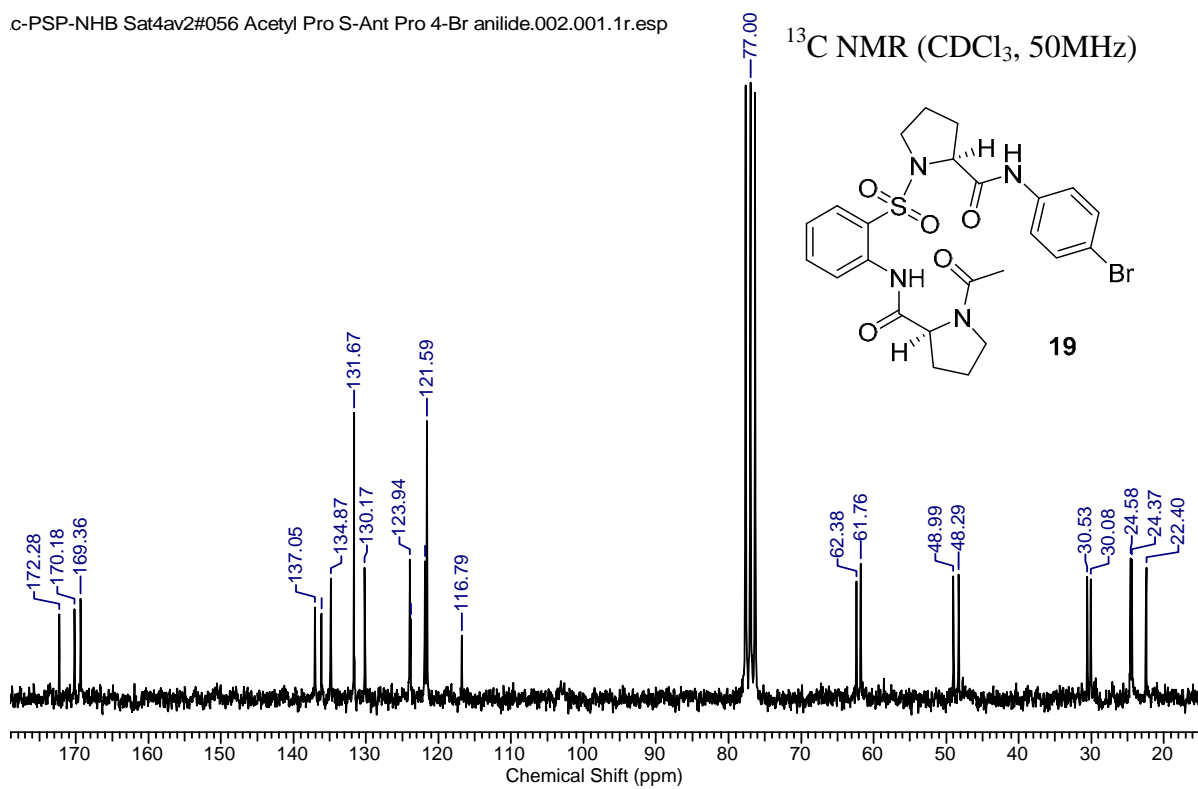
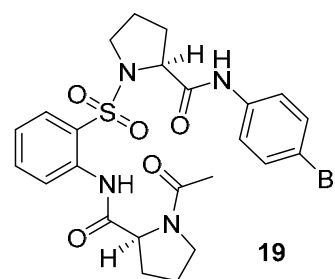
at1av500#011 piv-APS-NHiBu.003.001.1r.esp

 $^{13}\text{C}$  NMR ( $\text{CDCl}_3$ , 125MHz)

Sat3av400#003 f

 $^{13}\text{C}$  NMR ( $\text{CDCl}_3$ , 100MHz)

c-PSP-NHB Sat4av2#056 Acetyl Pro S-Ant Pro 4-Br anilide.002.001.1r.esp

 $^{13}\text{C}$  NMR ( $\text{CDCl}_3$ , 50MHz)

### 3.18 References

- (1) Howard, E. I.; Sanishvili, R.; Cachau, R. E.; Mitschler, A.; Chevrier, B.; Barth, P.; Lamour, V.; Zandt, M. V.; Sibley, E.; Bon, C.; Moras, D.; Schneider, T. R.; Joachimiak, A.; Podjarny, A. *PROTEINS: Structure, Function, and Bioinformatics*, **2004**, *55*, 792.
- (2) Frieden, E. *J. Chem. Educ.* **1975**, *52*, 754.
- (3) Wilcken, R.; Liu, X.; Zimmermann, M. O.; Rutherford, T. J.; Fersht, A. R.; Joerger, A. C.; Boeckler, F. M. *J. Am. Chem. Soc.* **2012**, *134*, 6810.
- (4) Rasmussen, S. G. F.; Choi, H.-J.; Rosenbaum, D. M.; Kobilka, T. S.; Thian, F. S.; Edwards, P. C.; Burghammer, M.; Ratnala, V. R. P.; Sanishvili, R.; Fischetti, R. F.; Schertler, G. F. X.; Weis, W. I.; Kobilka, B. K. *Nature* **2007**, *450*, 383.
- (5) Rosenbaum, D. M.; Cherezov, V.; Hanson, M. A.; Rasmussen, S. G. F.; Thian, F. S.; Kobilka, T. S.; Choi, H.-J.; Yao, X.-J.; Weis, W. I.; Stevens, R. C.; Kobilka, B. K. *Science* **2007**, *318*, 1266.
- (6) Lohse, M.; Benovic, J.; Codina, J.; Caron, M.; Lefkowitz, R. *Science* **1990**, *248*, 1547.
- (7) Blakeney, J. S.; Reid, R. C.; Le, G. T.; Fairlie, D. P. *Chem. Rev.* **2007**, *107*, 2960.
- (8) Whitby, L. R.; Ando, Y.; Setola, V.; Vogt, P. K.; Roth, B. L.; Boger, D. L. *J. Am. Chem. Soc.* **2011**, *133*, 10184.
- (9) Pierce, K. L.; Premont, R. T.; Lefkowitz, R. J. *Nat Rev Mol Cell Biol* **2002**, *3*, 639.
- (10) Raimondi, F.; Seeber, M.; De Benedetti, P. G.; Fanelli, F. *J. Am. Chem. Soc.* **2008**, *130*, 4310.
- (11) Nonaka, H.; Fujishima, S.-h.; Uchinomiya, S.-h.; Ojida, A.; Hamachi, I. *J. Am. Chem. Soc.* **2010**, *132*, 9301.
- (12) Catoire, L. J.; Damian, M.; Giusti, F.; Martin, A.; Heijenoort, C. v.; Popot, J.-L.; Guittet, É.; Banères, J.-L. *J. Am. Chem. Soc.* **2010**, *132*, 9049.
- (13) Engel, S.; Skoumbourdis, A. P.; Childress, J.; Neumann, S.; Deschamps, J. R.; Thomas, C. J.; Colson, A.-O.; Costanzi, S.; Gershengorn, M. C. *J. Am. Chem. Soc.* **2008**, *130*, 5115.
- (14) Wacker, D.; Fenalti, G.; Brown, M. A.; Katritch, V.; Abagyan, R.; Cherezov, V.; Stevens, R. C. *J. Am. Chem. Soc.* **2010**, *132*, 11443.
- (15) Heitz, A.; Avrutina, O.; Le-Nguyen, D.; Diederichsen, U.; Hernandez, J.-F.; Gracy, J.; Kolmar, H.; Chiche, L. *BMC Struct. Biol.* **2008**, *8*, 54.
- (16) Gracy, J.; Le-Nguyen, D.; Gelly, J.; Kaas, Q.; Heitz, A.; Chiche, L. *Nucleic Acids Res* **2008**, *36*, D314

- (17) Craik, D.; Daly, N.; Bond, T.; Waine, C. *J. Mol. Biol.* **1999**, *294*, 1327
- (18) Knappe, T. A.; Manzenrieder, F.; Mas-Moruno, C.; Linne, U.; Sasse, F.; Kessler, H.; Xie, X.; Marahiel, M. A. *Angew. Chem., Int. Ed.* **2011**, *50*, 8714.
- (19) Terlau, H.; Olivera, B. M. *Physiol. Rev.* **2004**, *84*, 41.
- (20) Adams, D. J.; Alewood, P. F.; Craik, D. J.; Drinkwater, R. D.; Lewis, R. J. *Drug Dev. Res.* **1999**, *46*, 219.
- (21) Hirschmann, R.; Nicolaou, K. C.; Pietranico, S.; Salvino, J.; Leahy, E. M.; Sprengeler, P. A.; Furst, G.; Smith, A. B.; Strader, C. D.; Cascieri, M. A.; Candelore, M. R.; Donaldson, C.; Vale, W.; Maechler, L. *J. Am. Chem. Soc.* **1992**, *114*, 9217.
- (22) Hirschmann, R.; Nicolaou, K. C.; Pietranico, S.; Leahy, E. M.; Salvino, J.; Arison, B.; Cichy, M. A.; Spoons, P. G.; Shakespeare, W. C.; Sprengeler, P. A.; Hamley, P.; Smith, A. B.; Reisine, T.; Raynor, K.; Maechler, L.; Donaldson, C.; Vale, W.; Freidinger, R. M.; Cascieri, M. R.; Strader, C. D. *J. Am. Chem. Soc.* **1993**, *115*, 12550.
- (23) Smith, A. B.; Hirschmann, R.; Pasternak, A.; Guzman, M. C.; Yokoyama, A.; Sprengler, P. A.; Drake, P. L.; Emini, E. A.; Schleif, W. A. *J. Am. Chem. Soc.* **1995**, *117*, 11113.
- (24) Smith, A. B.; Benowitz, A. B.; Guzman, M. C.; Sprengeler, P. A.; Hirschmann, R. *J. Am. Chem. Soc.* **1998**, *120*, 12704.
- (25) Smith, A. B.; Favor, D. A.; Sprengler, P. A.; Guzman, M. C.; Carroll, P. J.; Furst, G. T.; Hirschmann, R. *Bioorg. Med. Chem.* **1999**, *7*, 9.
- (26) Abell, A. D.; Gardiner, J. *J. Org. Chem.* **1999**, *64*, 9668.
- (27) Benedetti, F.; Berti, F.; Norbedo, S. *J. Org. Chem.* **2002**, *67*, 8635.
- (28) Guarna, A.; Guidi, A.; Machetti, F.; Menchi, G.; Occhiato, E. G.; Scarpi, D.; Sisi, S.; Trabocchi, A. *J. Org. Chem.* **1999**, *64*, 7347.
- (29) Uehling, D. E.; Donaldson, K. H.; Deaton, D. N.; Hyman, C. E.; Sugg, E. E.; Barrett, D. G.; Hughes, R. G.; Reitter, B.; Adkison, K. K.; Lancaster, M. E.; Lee, F.; Hart, R.; Paulik, M. A.; Sherman, B. W.; True, T.; Cowan, C. *J. Med. Chem.* **2001**, *45*, 567.
- (30) Hanessian, S.; Yun, H.; Hou, Y.; Tintelnot-Blomley, M. *J. Org. Chem.* **2005**, *70*, 6746.
- (31) Göschke, R.; Stutz, S.; Rasetti, V.; Cohen, N.-C.; Rahuel, J.; Rigollier, P.; Baum, H.-P.; Forgiarini, P.; Schnell, C. R.; Wagner, T.; Gruetter, M. G.; Fuhrer, W.; Schilling, W.; Cumin, F.; Wood, J. M.; Maibaum, J. *J. Med. Chem.* **2007**, *50*, 4818.
- (32) Roy, A.; Sanjayan, G. *J. Tetrahedron Lett.* **2012**, *53*, 3361.

- (33) Kale, S. S.; Chavan, S. T.; Sabharwal, S. G.; Puranik, V. G.; Sanjayan, G. J. *Org. Biomol. Chem.* **2011**, *9*, 7300.
- (34) Ramesh, V. V. E.; Puranik, V. G.; Sanjayan, G. J. *Tetrahedron: Asymmetry* **2012**, *23*, 1400.
- (35) Kuemin, M.; Engel, J.; Wennemers, H. *J. Pept. Sc.* **2010**, *16*, 596.
- (36) Chatterjee, S.; Vasudev, P. G.; Raghothama, S.; Ramakrishnan, C.; Shamala, N.; Balaram, P. *J. Am. Chem. Soc.* **2009**, *131*, 5956.
- (37) Chatterjee, B.; Saha, I.; Raghothama, S.; Aravinda, S.; Rai, R.; Shamala, N.; Balaram, P. *Chem. Eur. J.* **2008**, *14*, 6192.
- (38) Espinosa, J. F.; Gellman, S. H. *Angew. Chem., Int. Ed.* **2000**, *39*, 2330.
- (39) Langenhan, J. M.; Guzei, I. A.; Gellman, S. H. *Angew. Chem., Int. Ed.* **2003**, *42*, 2402.
- (40) Freire, F.; Fisk, J. D.; Peoples, A. J.; Ivancic, M.; Guzei, I. A.; Gellman, S. H. *J. Am. Chem. Soc.* **2008**, *130*, 7839.
- (41) Chorev, M.; Goodman, M. *Trends Biotechnol.* **1995**, *13*, 438.
- (42) Weeden, T.; Stefano, J.; Duan, S.; Edling, A.; Hou, L.; Chuang, W.-L.; Perricone, M. A.; Pan, C.; Dzuris, J. L. *J. Pept. Sci.* **2011**, *17*, 47.
- (43) Taylor, M.; Moore, S.; Mayes, J.; Parkin, E.; Beeg, M.; Canovi, M.; Gobbi, M.; Mann, D. M. A.; Allsop, D. *Biochemistry* **2010**, *49*, 3261.
- (44) Thorat, V. H.; Ingole, T. S.; Vijayadas, K. N.; Nair, R. V.; Kale, S. S.; Ramesh, V. V. E.; Davis, H. C.; Prabhakaran, P.; Gonnade, R. G.; Gawade, R. L.; Puranik, V. G.; Rajamohanam, P. R.; Sanjayan, G. J. *Eur. J. Org. Chem.* **2013**, *2013*, 3529.
- (45) Prabhakaran, P.; Kale, S. S.; Puranik, V. G.; Rajamohanam, P. R.; Chetina, O.; Howard, J. A. K.; Hofmann, H.-J.; Sanjayan, G. J. *J. Am. Chem. Soc.* **2008**, *130*, 17743.
- (46) Vijayadas, K. N.; Davis, H. C.; Kotmale, A. S.; Gawade, R. L.; Puranik, V. G.; Rajamohanam, P. R.; Sanjayan, G. J. *Chem. Commun.* **2012**, *48*, 9747.
- (47) Kale, S. S.; Priya, G.; Kotmale, A. S.; Gawade, R. L.; Puranik, V. G.; Rajamohanam, P. R.; Sanjayan, G. J. *Chem. Commun.* **2013**, *49*, 2222.
- (48) Mandelkern, L. *Poly-L-proline*, in *Poly- $\omega$ -AminoAcids: Protein Models for Conformational Studies*; Ed: G. D. Fasman, M. Dekker: New York, NY, 1967, p 675-724.
- (49) Toniolo, C.; Crisma, M.; Formaggio, F.; Peggion, C. *Biopolymers* **2002**, *60*, 396.
- (50) Antonello, S.; Formaggio, F.; Moretto, A.; Toniolo, C.; Maran, F. *J. Am. Chem. Soc.* **2003**, *125*, 2874.

(51) Srinivas, D.; Gonnade, R.; Ravindranathan, S.; Sanjayan, G. J. *J. Org. Chem.* **2007**, *72*, 7022.

(52) Ramesh, V. V. E.; Kale, S. S.; Kotmale, A. S.; Gawade, R. L.; Puranik, V. G.; Rajamohanam, P. R.; Sanjayan, G. J. *Org. Lett.* **2013**, *15*, 1504.